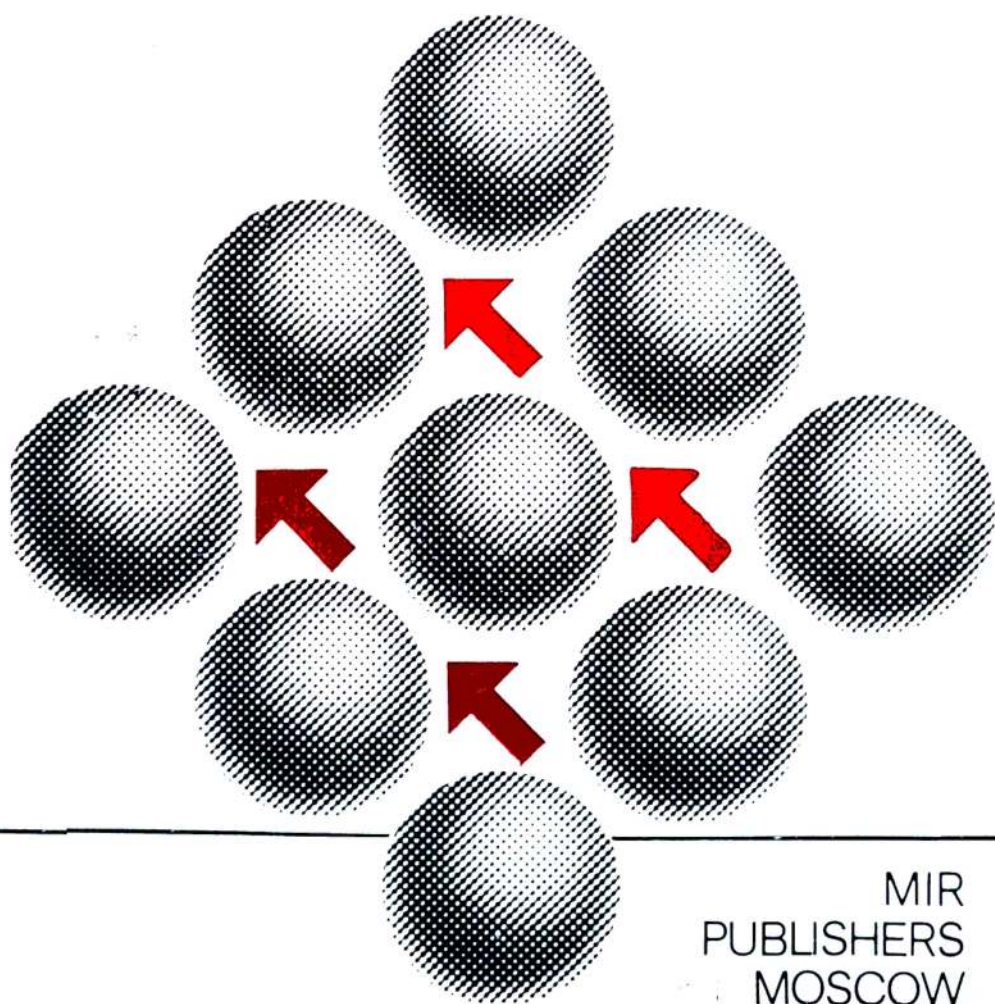


PHYSICS OF MAGNETIC SEMICONDUCTORS

E.L.NAGAEV



MIR
PUBLISHERS
MOSCOW

The book contains a theory of and experimental data on the semiconducting compounds of transition and rare-earth elements. Peculiar to magnetic semiconductors is the extremely strong influence exercised by their magnetic properties on their electrical and optical properties, and vice versa, the conduction electrons can have a significant effect on the magnetic properties. For this reason magnetic semiconductors display a number of unique properties as compared to nonmagnetic semiconductors and magnetic nonsemiconducting materials. For instance, their band-gap is strongly dependent on magnetization, and the type of magnetic ordering in them can be altered by varying charge carrier concentration. New types of carrier states are possible in magnetic semiconductors when the conduction electrons create a region of a normally-unstable phase in the crystal (e.g. the ferromagnetic phase in an antiferromagnet) and then stabilize it by their autolocalization in it. Especially interesting is the manifestation of such a heterophase auto-

(Continued on back flap)

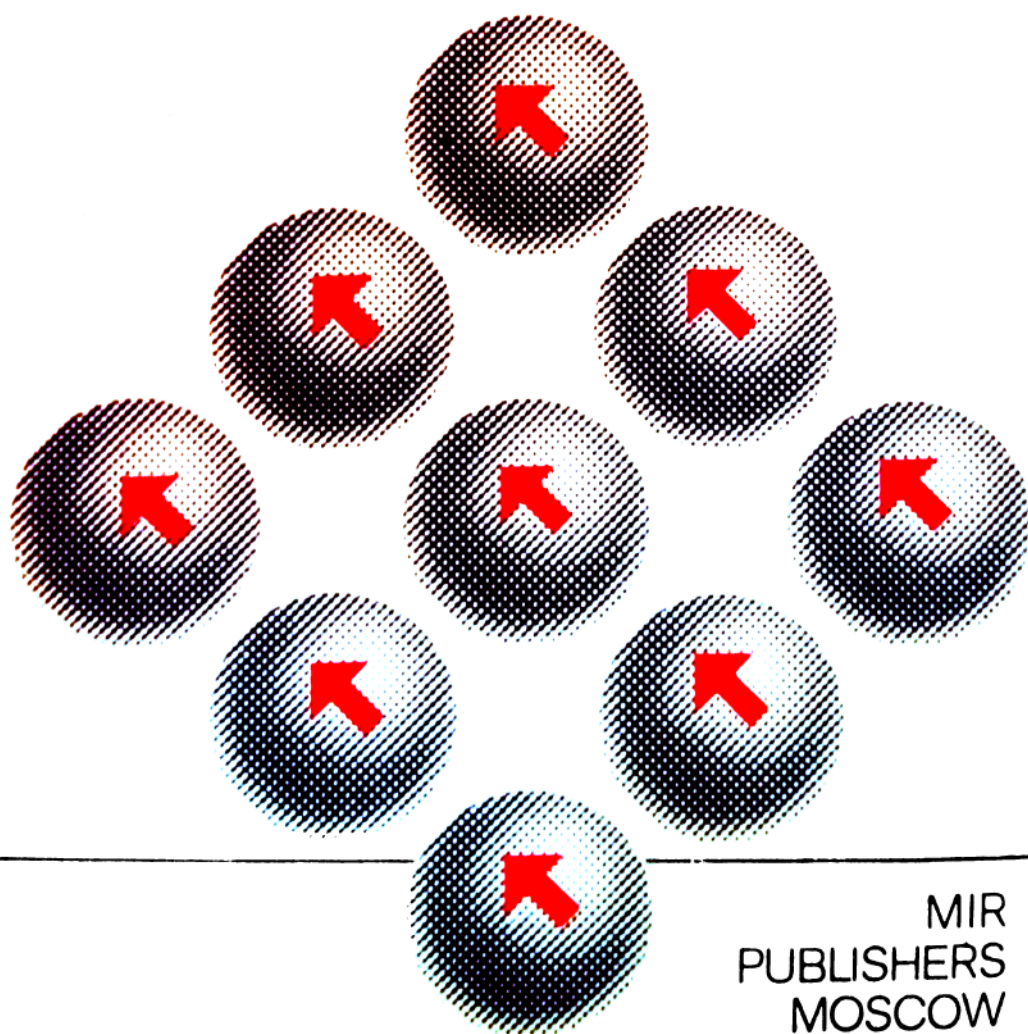
MIR
PUBLISHERS
MOSCOW

(Continued from front flap)

localization in degenerate semiconductors which results in magnetically-heterogeneous states of uniform crystals, and in the phase transitions of the insulator-metal type induced by a magnetic field or by temperature variations. The superposition of charge density and spin density waves is also possible in such semiconductors. At small charge carrier concentrations some magnetic semiconductors almost behave like ideal Heisenberg magnets, and their critical properties serve as test for the modern theory of phase transitions. Several general aspects of physics of magnetic phenomena (indirect exchange, singlet magnetism, etc.) and some aspects of the physics of semiconductors and materials exhibiting the insulator-metal phase transition are also dealt with in the book.

MIR
PUBLISHERS
MOSCOW

The author Edward Leonovich Nagaev was born in 1934 and graduated from Moscow University in 1956. At present Professor Nagaev, D.Sc. (Phys.-Math.), is the head of a laboratory at the All-Union Research Institute of Current Sources. Working on the theory of magnetic semiconductors since 1960, he now has over 100 papers and 4 reviews to his credit. His results dealing with the heterophase autolocalization of charge carriers in magnetic semiconductors have been recognized by the USSR Academy of Sciences as being some of the most significant scientific discoveries made in the USSR. In addition to magnetic semiconductors, Prof. Nagaev is interested in surface phenomena, in thermoelectricity and in the phase transitions in magnetic materials.



MIR
PUBLISHERS
MOSCOW

PHYSICS OF MAGNETIC SEMICONDUCTORS

E.L. NAGAEV



Э. Л. НАГАЕВ

**ФИЗИКА
МАГНИТНЫХ
ПОЛУПРОВОДНИКОВ**

**Издательство «Наука»
Москва**

PHYSICS OF MAGNETIC SEMICONDUCTORS

E.L.NAGAEV

Translated from the
Russian by
M. SAMOKHVALOV
Translation edited by
the author

MIR
PUBLISHERS
MOSCOW

First published 1983
Revised from the revised 1979 Russian edition

На английском языке

© English translation Mir Publishers, 1983

CONTENTS

Introduction. Basic Concepts	7
Chapter 1. The Nature of the Semiconducting State and the Semiconductor-metal Phase Transition	21
1.1. Energy-band Theory	21
1.2. Crystals with Imperfections	23
1.3. Polaron States in Ionic Crystals	26
1.4. The Method of Canonical Transformation in the Theory of the Polaron	32
1.5. Electron-electron Interaction	34
1.6. The Insulator-metal Phase Transition	39
1.7. Heavily-doped Semiconductors	49
Chapter 2. Magnetic Properties of Insulating Crystals	53
2.1. The Heisenberg Hamiltonian	53
2.2. Magnetic Interactions in Real Materials and Non-Heisenberg Hamiltonians	54
2.3. Magnetic Ordering and Effect on It of a Magnetic Field	60
2.4. Magnons and Low-temperature Magnetization of Ferromagnets	66
2.5. High-temperature and Critical Properties of Ferromagnets	68
2.6. Magnon Spectrum and Magnetic Disordering in an Antiferromagnet	74
2.7. "Order-order" and "Order-disorder" Phase Transitions of the First Kind	78
2.8. Experimental Data on Magnetic Semiconductors	83
Chapter 3. Conducting Magnetic Systems. The Vonsovsky Model	96
3.1. The Vonsovsky Model and Its Application to Magnetic Semiconductors	96
3.2. The Effect of Magnetic Ordering on the Energy of Charge Carriers	101
3.3. Indirect Exchange via Conduction Electrons in Magnetic Crystals	105
3.4. Superexchange in Magnetic Insulators	111
3.5. The c - l Model Hamiltonian in Case of Narrow Conduction Bands	116
Chapter 4. Nondegenerate Ferromagnetic Semiconductors	128
4.1. Energy Spectrum of Charge Carriers in Narrow-conduction-band Semiconductors	128
4.2. Energy Spectrum of Charge Carriers in Wide-band Semiconductors in the Spin-wave Approximation	133
4.3. Charge-carrier-energy Spectrum in Wide-conduction-band Semiconductors in the Vicinity of the Curie Point and in the Paramagnetic Region	139
4.4. Charge Carrier Scattering by Fluctuations of the Magnetic Moment	147
4.5. Effect of Imperfections on the Electric Properties of Ferromagnetic Semiconductors	157
4.6. Optical Properties (Experiment)	167
4.7. Conductivity and Photoconductivity (Experiment)	180

Chapter 5. Nondegenerate Antiferromagnetic and Magnetoexcitonic Semiconductors and Self-trapped Carrier States	188
5.1. Free and Quasi-oscillator States of Charge Carriers in Antiferromagnetic Semiconductors	188
5.2. Ferron States of Free Carriers	193
5.3. Localized Ferrons and Their Influence on Magnetic Properties of Antiferromagnets	206
5.4. Electrical and Optical Properties of Antiferromagnetic Semiconductors (Experiment)	212
5.5. Exciton Polarons and Transferons in Magnetoexcitonic Semiconductors	222
5.6. Ferrons in Magnetic Systems with Easily Variable Atomic Moments	226
Chapter 6. Indirect Exchange in Magnetic Semiconductors	231
6.1. Indirect Exchange in Ferromagnetic Semiconductors	231
6.2. Heavily-doped Antiferromagnetic Semiconductors	241
6.3. Photoferromagnetism	256
6.4. Subsurface Magnetism	263
6.5. The Effect of Electroactive Imperfections on the Magnetic Properties of Semiconductors and the Temperature-induced Shift of Donor Levels	267
Chapter 7. Collective Ferron States and Electrical Properties of Degenerate Semiconductors	280
7.1. Magnetoelectric Effect in Degenerate Semiconductors	280
7.2. Electric Field Response Functions of an Antiferromagnet at $T = 0$	285
7.3. Electric Field Response Function of Ferromagnets in the Spin-wave Region	289
7.4. Screened Potential and Instability of Uniform State of Magnetic Semiconductors	295
7.5. Nonuniform States of Antiferromagnetic and Magnetoexcitonic Semiconductors	305
7.6. Nonuniform States of Heisenberg and Singlet Ferromagnetic Semiconductors, and the Metal-insulator Phase Transition	327
7.7. Transport Phenomena in Degenerate Magnetic Semiconductors	336
Appendices	347
Appendix I. Spinpolaron Hamiltonian in the General Case	347
Appendix II. Spontaneous Hall and Faraday Effects	354
Appendix III. Effect of Indirect Exchange on Helicoidal Ordering and on the Structure of Domain Walls in Ferromagnets	364
References	372
Abbreviations for Soviet Journals	385
Index	386

INTRODUCTION. BASIC CONCEPTS

This introduction aims to provide a general presentation of the electrical, optical and magnetic properties of those transition-metal or rare-earth compounds that are known as magnetic semiconductors (MS)*. It should be made clear at once, however, that the term "magnetic semiconductor" is only accurate for the electric properties of those materials that are always greatly affected by a magnetic order. As far as the magnetic properties are concerned, conduction electrons influence them noticeably only when the electron density becomes large enough and so the same materials (e.g. EuO, EuS), considered from the point of view of their magnetic properties, are often classified as magnetic insulators. On the other hand, some highly imperfect crystals that are actually degenerate semiconductors are numbered among the magnetic metals (e.g. GdN, HoN). In the wider sense of this term, MS also include the ferrites, but these are not specially discussed in this book, although several theoretical results contained herein are also applicable to ferrites. Detailed information about the properties of ferrites may be found in [389].

Magnetic semiconductors possess a number of unique properties. For instance, their magnetoresistivity and spontaneous Faraday rotation of the polarization plane of light are by several orders of magnitude greater than those of magnetic metals. Some of their properties are even unparalleled in other materials, for example, a giant red shift of the optical absorption edge and photoconductivity threshold when magnetic semiconductors are magnetized.

It was for magnetic semiconductors that the novel physical phenomenon of heterophase autolocalization of conduction electrons** was first predicted and experimentally detected. The essence of this phe-

* The following abbreviations are used throughout: FM for ferromagnetic, FIM for ferrimagnetic, AF for antiferromagnetic, CAF for canted antiferromagnetic, and PM for paramagnetic; MS, FMS and AFS for magnetic, ferromagnetic and antiferromagnetic semiconductors, respectively.

** The concept of the heterophase autolocalization of electrons was first formulated and argued in papers [194, 195] by the author of this book. Papers by N. Mott [278], M.A. Krivoglaz [426], T. Kasuya [204-208] containing similar results appeared considerably later. The author was also the first to prove the possibility of a collective heterophase autolocalization in degenerate semiconductors [197, 46].

nomenon in nondegenerate semiconductors is that a conduction electron creates in the crystal a region of a phase that is normally unstable but then stabilizes the phase by being localized within the region. The result is the production of a new type of quasi-particle. For instance, in a nondegenerate antiferromagnetic semiconductor the electron may become self-trapped inside a ferromagnetic micro-region.

In degenerate semiconductors a collective heterophase autolocalization of charge carriers is also possible. The result is a new type of state where a homogeneous crystal splits up into alternating regions of normally stable and normally unstable phases with all the electrons assembling in the latter. For instance, an AF crystal splits up into FM and AF regions with all the electrons concentrating in the FM phase. Such a state could be interpreted as a superposition of very high-amplitude charge-density and spin-density waves. In principle, the structures that result from the superposition of relatively low-amplitude charge-density and spin-density waves are also possible in degenerate semiconductors, such structures being similar to the "incommensurate" structures that are observed earlier in low-dimensional nonmagnetic materials.

MAGNETIC AND SEMICONDUCTING PROPERTIES

All sorts of magnetic orderings are possible in MS. Antiferromagnetic semiconductors have been known long ago, and there is a large number of them. However, not a single ferromagnetic semiconductor had been discovered until 1960; indeed, an opinion had been voiced that ferromagnetic and semiconducting properties were incompatible. However, after Tsubokawa [10] succeeded in producing the first FMS, CrBr_3 , thus proving their existence, other FMS soon followed and at present their number is close to 100. Of the magnetic semiconductors the chalcogenides of europium (the FMS's: EuO , EuS and the AFS's: EuTe , EuSe) as well as the chrome chalcogenide spinels (the FMS's: CdCr_2Se_4 , HgCr_2Se_4 etc.) attracted the most attention from scientists.

The electrical properties of low-doped AFS are qualitatively similar to those of nonmagnetic semiconductors: their conductivity grows exponentially with the temperature. A long-standing assumption has been that it is small polarons which act as the charge carriers in many of them, e.g. in NiO . These move across the crystal by hopping from one atom to another, the directions of successive hops being uncorrelated. This is the radical difference between the hopping and band mechanisms of motion. The mobility of small polarons, in contrast to that of electrons, grows exponentially with the temperature. However, a necessary condition for the existence of small polarons is that the width of the conduction or the valence band be

small compared to the lattice polarization energy by an electron at rest. This is a very stringent condition, and, as is shown by analysis, is not fulfilled in any of the magnetic semiconductors known at present. If this condition is not fulfilled, a polaron existing in the crystal must be a large one for which the quasi-momentum is a well-defined quantum number, and the only difference between it and the usual band electron, from the viewpoint of its mechanism of motion, would be a somewhat larger effective mass. For this reason polaron effects would not bring about a qualitative change in the electric properties of magnetic semiconductors compared with nonmagnetic ones.

However, a sharp difference between the properties of FMS and of nonmagnetic semiconductors becomes apparent immediately. It manifests itself first and foremost in the so-called giant red shift of the optical absorption edge, which takes place as the temperature is lowered starting already in the paramagnetic region [85]. The decrease in the width of the optical gap with decreasing temperature amounts to 0.5 eV for some FMS's. In nonmagnetic semiconductors the shift is a blue one and is several orders of magnitude smaller. At a fixed temperature, the red shift can be induced by an external magnetic field, this being the case not only with FMS's, but with AFS's as well. This is unambiguous proof that the red shift is caused by the magnetization of the crystal.

On the other hand, the resistivity of nondegenerate FMS's frequently does not decrease monotonically with the temperature, as is the case with nonmagnetic semiconductors, but displays a sharp peak in the region of the Curie point T_c . Its relative height depends on the density of defects and may be several orders of magnitude high. The resistivity drops with increasing magnetic field, an especially drastic reduction occurring in the magnitude of the resistivity peak. The magnetoresistance in this region exceeds that of nonmagnetic semiconductors by several orders of magnitude, an additional difference being that in case of magnetic semiconductors the magnetic field does not raise, but on the contrary, reduces the magnetoresistance. These results are clear proof of a strong interaction between the charge carriers and the subsystem of magnetically ordered spins in MS.

MAGNETIC SEMICONDUCTOR MODEL AND SPINPOLARONS

Most of the principal properties of MS are in the majority of cases satisfactorily described by the *s-d* (or *s-f*) Vonsovsky model. This model, which for the sake of generality is referred to below as the *c-l* model, presumes that the crystal contains magnetic ions with nonzero spins of *d*- or of *f*-shells ("*l*-spins"). An exchange interaction occurs between the localized *l*-spins of these ions which establishes a magnet-

ic ordering of some type in the crystal, and, in the majority of cases, these interactions may be described by the Heisenberg Hamiltonian.

In addition to the localized electrons of partially-filled shells, the crystal also contains delocalized conduction electrons ("c-electrons") and holes. In the simplest case these electrons occupy states in an s-type band and c-l exchange interaction takes place between the c-electrons and the l-spins. It is this interaction that is responsible for the dependence of the charge carrier states on the ordering of the l-spins.

Such a model is, for example, directly applicable to the chalcogenides of Eu where the c-band states are constructed from the 6s- and 5d-type states, but the l-spins are f-type. However, in some materials the c-band states may be constructed from the same atomic states as the l-states. For example, in the FMS CdCr_2Se_4 the Cr ions are normally in the Cr^{3+} state. The appearance of a conduction electron in the crystal means that one on the ions becomes Cr^{2+} . In an ideal crystal, all the Cr ions are equivalent, and so each Cr ion must have the same probability to be in the Cr^{2+} state. In this case the motion of a c-electron in the crystal takes place as a result of the recharge reaction $\text{Cr}^{2+} + \text{Cr}^{3+} \rightarrow \text{Cr}^{3+} + \text{Cr}^{2+}$.

In terms of the c-l model, this situation corresponds to such a strong c-l exchange that the conduction-electron spin combines with the spin of the ion, to which at that moment it belongs, to form a single spin. For an ionic l-spin equal to S , the total spin is equal to $S + 1/2$ or $S - 1/2$, depending on whether the c-l exchange integral A is positive or negative. Following the transition of the c-electron to another atom, the spin of the c-electron combines with the l-spin of the new atom to form a single spin [69]. Hence, the motion of a charge carrier in the crystal is equivalent to the motion of an "irregular" spin $S \pm 1/2$. In contrast to a conventional band electron, this quasi-particle, termed a spinpolaron in [70]*, cannot be assigned a definite spin projection. The precondition for its existence is that width W of the c-band is small compared to the c-l exchange energy AS . However, spinpolaron effects can also appear in the opposite limit $W \gg AS$.

It should be emphasized that combining the c-electron spin with the l-spin into a single spin does not mean that the spinpolaron wanders about the crystal in random walks. For instance, in an FMS at $T \ll T_c$ one may introduce the concept of a quasi-momentum for the spinpolaron, i.e. it moves in accordance with the band mecha-

* To avoid misunderstanding, it should be noted that some authors apply the term "spinpolaron" to quite different states. In [69], where the two-atom problem is treated, the term "double exchange" is used but this is inadequate for many-atom systems.

nism. At $T \geq T_c$ it is no longer possible to introduce a quasi-momentum for the spinpolaron, however, in this case its mobility is not temperature-activated.

RED SHIFT AND CONDUCTION ELECTRONS IN THE VICINITY OF THE CURIE POINT

Within the framework of the c - l model it is possible to provide a satisfactory explanation for the red shift of the absorption edge in an FMS. Should the c - l exchange interaction be considered using the perturbation theory, the shift in the energy of an electron having a spin projection σ would be equal in the first order in AS/W , to $(-A\sigma\mathfrak{M})$, where \mathfrak{M} is the crystal magnetic moment per atom. Hence, if the electron spin projection is such that $A\sigma$ is positive, the electron energy will decrease as the magnetization is increased. This is equivalent to a reduction in the width of the gap in the energy spectrum.

Thus result is only a crudely qualitative. A more detailed consideration proves that the electron energy is nonanalytic in the c - l exchange, i.e. that the energy cannot be expanded in powers of AS/W . This means that generally it is impossible to apply the perturbation theory in AS/W . The physical explanation for this is that the electron energy is not in fact determined by the long-range, but by the short-range magnetic order. To be persuaded of this, consider the well-known expression for the electron energy in a crystal with a helicoidal magnetic ordering (3.2.6), the energy being accurately determinable at $T = 0$ in the limit of classically large spins S . The expression reveals that the c - l exchange shift in the energy of an electron at the bottom of the conduction band, in case of a large period of the helicoidal structure, practically coincides with the appropriate quantity in a ferromagnet, which is equal to $(-|A|S/2)$. At the same time, whereas the average of the crystal moment per atom \mathfrak{M} in the ferromagnetic state is indeed S , for the helicoid $\mathfrak{M} = 0$. The physical explanation is based on the fact that, because of a slow variation of the direction of the local moment in space, the spin of the conduction electron has ample time to arrange itself in accordance with the local moment and will always point in its direction, as is the case of a ferromagnet. In fact, this is a sort of a spinpolaron state.

The inapplicability of the perturbation theory for the c - l exchange manifests itself especially strongly in the vicinity of the Curie point T_c where the direction of the local moment also varies slowly in space, although there is, in contrast to the helicoid, no periodicity in the directions of the spins. Calculations in [93] demonstrate that the c - l shift remains rather large at the Curie point being of the order of $|AS|^{4/3}W^{-1/3}$, i.e. much larger than A^2S^2/W one would obtain from the perturbation theory. This result explains why a sub-

stantial red shift of the absorption edge takes place with falling temperature even before the Curie point is reached.

The red shift of the absorption edge is also obtained for spinpolarons appearing in the limit of very strong c - l coupling $W \gg AS$. In this case the red shift is not determined by the c - l exchange integral A , but by the width of the conduction band W , i.e. it retains a reasonable value even as $AS \rightarrow \infty$. The temperature dependence of the spinpolaron spectrum makes itself manifest by the narrowing of its energy band with growing temperature.

One interesting and, as yet, unresolved problem in FMS physics is whether the c -electrons experience maximum scattering by spin fluctuations in the vicinity of T_c . Neutrons are well known to display such a maximum, but the electrons in perfect specimens of FM metals do not. The situation in an FMS is much more complicated than in metals, since not only is the mobility of the c -electrons temperature-dependent in the FMS, but so too is their density. The latter in impurity semiconductors often has a minimum in the vicinity of T_c and in this background it would not have been easy to discover a mobility minimum, even if one had been present. At the same time it has not been possible to study an FMS with intrinsic conductivity in the region of T_c .

As yet, it has not been possible to arrive at definite conclusions about the existence of a maximum in the scattering of c -electrons by critical fluctuations of the magnetization purely from theoretical considerations. By now numerous papers have accumulated in which the mobility is calculated in the Born approximation in the c - l exchange, with various approximations being used for the spin correlation functions. But the authors fail to take into account that this approximation is inapplicable in the vicinity of T_c (see Sec. 4.4) and for this reason the respective results may not be regarded as reliable. On the other hand, a procedure, which takes account of the realignment of the c -electron spins parallel to the local moment and which thus goes beyond the limits set by the Born approximation, enables only an estimate of the relaxation time in the vicinity of T_c to be obtained. Still, this estimate shows the mobility minimum in the vicinity of T_c is either shallow or completely nonexistent. This result agrees with the experimental data on the photoconductivity of perfect FMS crystals: its minimum in the region of T_c is either nonexistent or very shallow.

INDIRECT EXCHANGE VIA CONDUCTION ELECTRONS IN MAGNETIC SEMICONDUCTORS

As has already been discussed in the previous section, the appearance of the FM ordering shifts the bottom of the conduction band downwards and because the establishment of an FM ordering reduces the

electron energy to its minimum, the conduction electrons strive to establish this ordering. Of course, to make it possible for the charge carriers to influence the magnetic order in a crystal, their density must be sufficiently large. This condition is met in degenerate semiconductors, and an indirect exchange in them via the conduction electrons can play an important part. At the same time, there are too few conduction electrons in nondegenerate semiconductors to affect their magnetic properties appreciably. The important part played by indirect exchange via conduction electrons can be surmised from the experimental fact that the Curie temperature of the heavily-doped FMS EuO may be twice as high as that of undoped crystals.

Numerous authors have attempted to describe the indirect exchange in magnetic semiconductors with the conventional Ruderman-Kittel-Kasuya-Yosida (RKKY) theory. It should be stressed that this theory is unable in fact to provide an adequate description of the properties of magnetic semiconductors. Indeed, a condition for its applicability is the smallness of the c - l exchange energy in comparison with the Fermi energy μ of the conduction electrons. In typical conditions, because of relatively small densities of charge carriers in degenerate semiconductors ($\sim 10^{18}$ to 10^{20} cm^{-3}), their Fermi energy is smaller than AS even for $AS \ll W$. Certainly the inequality $AS \ll \mu$ cannot be fulfilled at all in the opposite limiting case $AS \ll W$. There is an important corollary to the fact that the RKKY theory is inapplicable to MS: the indirect exchange in them cannot be described with the Heisenberg Hamiltonian, which is obtained in the RKKY theory in the second order in c - l exchange. However, even for $AS \ll W$ it is impossible to construct an effective magnetic Hamiltonian for an MS that would be valid at all temperatures. Still, it is possible to analyze the properties of those materials in various temperature ranges, and this analysis proves that they differ greatly from those of Heisenberg magnetic systems.

This difference probably makes itself most clearly manifest in the properties of a degenerate AFS. The indirect exchange via conduction electrons strives to establish an FM ordering, since this ordering would reduce the electron energy to its minimum. Should this indirect exchange be of the Heisenberg type, as the electron density reaches a certain value n_A , there would be an abrupt change in the type of magnetic ordering from AF to FM. However, because of the non-Heisenberg nature of the indirect exchange, there is an interval of densities $[n_A, n_F]$ such that for $n < n_A$ the AF ordering is the stable one, and for $n > n_F$ the FM ordering is stable, neither ordering being stable inside the interval. Probably for $n_A < n < n_F$ there is an intermediate state between FM and AF. The canted antiferromagnetic ordering (CAF), in which the magnetic moments of two equivalent sublattices of the crystal are not directed exactly opposite, but make an arbitrary angle with one another, could serve this

purpose. The result is that the crystal possesses spontaneous magnetization, and the energy of such a state inside the $[n_A, n_F]$ interval is lower than that of the collinear FM and AF*.

However, an analysis of the magnon spectrum of such a structure demonstrates that even the conditions of its stability against small short-wave fluctuations can only be met inside a much narrower density interval. Naturally, it is much more difficult to meet the conditions of stability against fluctuations of great amplitudes. Accordingly, there are at present no grounds for the conclusion that such a structure is possible in an MS. Experiment, too, has failed to substantiate its existence (the claims by several authors that experiments have proved its existence in a number of magnetic semiconductors have turned out to be erroneous).

The non-Heisenberg nature of the indirect exchange makes itself manifest in the essentially nonlinear magnetization vs. external magnetic field curve for a degenerate AFS with $n < n_A$. In an undoped Heisenberg antiferromagnet this function is linear, but as the electron density rises, the magnetic susceptibility in weak fields grows tending to infinity as n_A is approached. However, in strong fields the susceptibility becomes equal to that of an undoped specimen in the $W \gg AS$ limit.

The non-Heisenberg nature of the indirect exchange in a degenerate FMS results in their Curie temperature T_c being lower than the paramagnetic Curie point θ had both parameters coincided in the undoped semiconductor. At relatively low densities n , the shift in $(\theta - T_c)$ caused by indirect exchange is not large. For a very large n , when the inequality $\mu \gg AS$ begins to be valid, and the system is turning into a Heisenberg one, the shift is also small. Hence, the difference $(\theta - T_c)$ should pass through a maximum, and this has been observed in experiment. The magnon spectra in a degenerate MS differ sharply from those following from the RKKY theory.

The indirect exchange in an MS can be varied by an external action. This may be the application of an external electric field, which would increase the charge-carrier density in the surface layer of a degenerate semiconductor that has a thickness of the order of the screening length. The field intensifies indirect FM exchange in such a layer. Specifically, it is possible to establish ferromagnetic ordering on the surface of an AFS by applying a sufficiently strong electric field.

This is an example of a magnetoelectric effect in a degenerate MS. A weak magnetoelectric effect is also possible in magnetic insulators in case of certain special types of crystal symmetry. In degenerate semiconductors this effect is not connected with crystal symmetry,

* The idea that a CAF could exist in MS has been suggested in [74], but an erroneous result $n_A = 0$ was obtained in the paper.

but on the other hand the electric-field-induced magnetization can appear in only a relatively small portion of the crystal, whereas in an insulator the electric field magnetizes the whole crystal at once. An intensified FM indirect exchange in the subsurface layer results in the appearance of a specific branch, different from conventional surface magnons in the magnon spectrum. The magnetoelectric effect in subsurface layers has not, as yet, been studied experimentally.

Another external action, which may affect the magnetic properties of a semiconductor, is illumination. The absorption of light results in the generation of charge carriers and should it prove possible to create densities of photoelectrons $\sim 10^{18} \text{ cm}^{-3}$ or higher, indirect exchange via photoelectrons could make itself felt. This, probably, explains the rise by $\sim 0.1 \text{ K}$ of the Curie point of EuS when the crystal is illuminated by a laser [407]. The light-induced FM-PM phase transition displays some specific features that clearly distinguish it from a conventional phase transition taking place in equilibrium conditions [563]. Not only does light raise the Curie point, but it can also transform a phase transition of the second kind into a phase transition of the first kind.

To make such a transformation possible, the frequency of the light should be quite close to the optical absorption edge. If on the other hand the phase transition retains its continuous nature under illumination, it will no longer be possible to speak of singularities in the derivatives of thermodynamic potentials at the Curie point. One clearly defined physical quantity will in this case be the production of entropy per unit time, and there are singularities in its derivatives with respect to the temperature, the frequency and the intensity of light (in the mean field approximation they display discontinuities).

HETEROPHASE AUTOLOCALIZATION OF CHARGE CARRIERS IN ANTIFERROMAGNETIC SYSTEMS

The preceding section dealt with the effects on the magnetic ordering of the conduction electrons moving freely in the crystal. Those effects are, naturally, of a cooperative nature, since a single electron on its own cannot change the state of a macroscopic crystal. Still, this electron may cause a local change in magnetic ordering provided its motion is limited to the small region of the crystal where ordering has changed.

This can occur in an AFS [194, 195]. A conduction electron can set up an FM microregion of radius R , equal to several lattice parameters a in an AFS. Evidently, the change in the type of magnetic ordering will bring about a rise in the energy of exchange interaction between localized moments inside this region.

But to make up for this, there will be a drop in the energy of c - l exchange for $W \gg AS$ by $AS/2$, if the direction of the electron spin inside the ferromagnetic region is chosen properly. For $W \ll AS$ the conduction band inside the ferromagnetic region will expand, and its bottom will sink as a result. Hence, for all AS/W the ferromagnetic region acts as a potential well for the electron. If its radius is large enough, it will contain discrete levels, i.e. the electron energy will drop on account of its localization inside the ferromagnetic region. This drop may exceed the energy of l - l interaction spent to create the region, since in many AFS the l - l energy per atom is several orders of magnitude less than the depth of the potential well. In this case the ground state of the AF crystal + the conduction electron system will not correspond to a free electron at the bottom of the conduction band, but to an electron localized inside a ferromagnetic region whose radius R will be determined by the minimum energy of the system under consideration.

In an ideal crystal this ferromagnetic region may be anywhere, because all the atoms in the crystal are equivalent. The electron together with the ferromagnetic region that has been created by it and has trapped it constitutes a new quasi-particle named a ferron*.

The phenomenon of an electron self-trapping is specially interesting in heavily-doped AFS [197, 46]. Conventional heavily-doped semiconductors have metallic-type conductivity, and their conduction electrons are, naturally, distributed uniformly throughout the crystal. The situation is different in an AFS: their conduction electrons are concentrated inside the ferromagnetic regions of the crystal, which they themselves have created. At relatively low electron densities n (but, obviously above the density n_c at which the donor electrons are delocalized) the mass of the crystal retains its AF properties, with the FM portion taking the shape of small FM droplets distributed throughout the crystal. High-conductivity FM droplets are separated by AF interlayers, which behave like insulators, because the AF portions of the crystal have been drained of conduction electrons, having all crossed over to the FM portion of the crystal. Thus the crystal as a whole does not behave like a metal, but rather it behaves like an insulator, despite being highly doped.

The growth in the total electron density n is accompanied by the growth both in the number of electrons in each FM droplet and in the number and size of the droplets. Finally, at a certain density n_p the highly conductive FM droplets begin to touch each other. As n is increased further, the mass of the crystal becomes FM with isolated AF droplets distributed within it. Starting from the density n_p at which the FM droplets make contact, the system becomes highly

* In earlier papers [194, 195] the term used was "magnetic polaron".

conductive with the electrons now able to move freely from one end of the crystal to another along the FM portion, by-passing the insulating AF droplets, i.e. the percolation of the electron fluid begins. Hence, at densities exceeding n_p the electric properties of a heavily-doped AFS are similar to those of a conventional heavily-doped semiconductor.

It is quite extraordinary that in the case just considered a homogeneous crystal exists in an inhomogeneous state with alternating FM and AF regions over a wide temperature range. Normally, a homogeneous crystal, at a constant pressure, should remain in a homogeneous state everywhere except at the point of the phase transition of the first kind between different states, if such a point exists. The term "collective ferron state" may be applied to the inhomogeneous state of a heavily-doped AFS, because it appears as a result of the simultaneous autolocalization of all the conduction electrons in the crystal. The inhomogeneous two-phase state of a degenerate AFS is an alternative to the homogeneous state intermediate between the AF and the FM states, e.g. to the CAF state whose instability has already been mentioned above.

Like the individual ferrons discussed above, collective ferrons can be destroyed by an external magnetic field or by higher temperatures. At densities below n_p the ferron destruction should result in an abrupt transition of the crystal from an insulating to a high-conductivity state (the insulator-metal phase transition). Indeed, if the crystal as a whole goes over to the FM state, under the influence of a magnetic field, the conduction electrons that were previously trapped inside FM droplets, isolated from each other, will spread across the entire crystal, filling in regions which had been in the insulating AF state before the magnetic field was applied. This will make every part of the crystal highly conducting. A rise in temperature, that destroys the magnetic order, also results in a conductivity jump since in the absence of magnetic ordering the entire crystal is homogeneous, the conduction electrons being distributed uniformly throughout the crystal. At densities exceeding n_p , when the mass of the crystal is in the FM state and is in a highly conductive state, the destruction of ferrons by a magnetic field or by rising temperatures only results in a relatively small drop in the resistance of the crystal.

The first experimental proof of the existence of ferrons was obtained in [6] for the nondegenerate AFS EuSe and EuTe, the charge carriers having been generated by light. The experimental results [315] have fully substantiated the theoretical results concerning the collective ferron states in an AFS as applied to EuSe, both the highly conductive and the insulating AF-FM state having been observed. The destruction of the latter by a magnetic field of ~ 10 kOe resulted in a rise in conductivity by 10 orders of magnitude, and the same occurs for a rise in the temperature.

HETEROPHASE AUTOLOCALIZATION AND MAGNETOELECTRIC INSTABILITY IN FERROMAGNETIC SEMICONDUCTORS

The fact that ferrons are stable in an AFS at sufficiently high temperatures justifies the conclusion that, in principle, they can exist in an FMS at temperatures at which the FM ordering has to a considerable degree been destroyed. In this case the region with a higher degree of FM order will act as a potential well for the conduction electrons, and those may localize themselves in those regions which are thermodynamically favoured. Von Molnar and Methessel [162] were the first to suggest the possibility of trapping conduction electrons by magnetization fluctuations, but they failed to mention the possibility of autolocalization. Autolocalization of electrons in an FMS has been studied in [426, 204] on the assumption that the energy of a delocalized electron is determined by the long-range order.

However, the conditions for the appearance of ferrons in an FMS have been demonstrated by analysis to be much more stringent than in an AFS. To some degree this is the outcome of the circumstance that the energy of a delocalized electron is no longer determined by the long-range but by the short-range order. The latter on the other hand remains quite large, even higher than T_c , a considerable red shift of the absorption edge in the PM region being the proof. For this reason a delocalized electron in the vicinity of T_c still gains considerably in c - l exchange energy, and this prevents it from being localized in a region with a higher FM order. In particular, according to current estimates the self-trapping of charge carriers is impossible in important materials such as EuO and EuS.

As to collective ferron states in a highly degenerate FMS, it follows from the analysis of the stability of the homogeneous FM state against small electron-density fluctuations that a rise in temperature may result in a transition of the system to an inhomogeneous state. The cause of such a transition is the magnetoelectric instability of the system: a local increase in the electron density intensifies the indirect exchange via conduction electrons inside the fluctuation. At finite temperatures, this increases the degree of FM order and consequently lowers the electron energy, thus favouring further growth of the fluctuation [52].

In cases when the phase transition from the homogeneous to the heterogeneous state is of the second kind, the inhomogeneous state above the transition point may be treated as a superposition of charge-density and spin-density waves. The wavelength of both wave types is identical and generally incommensurate with the lattice parameter. However, the phase transition may also be of the first kind. There is, as yet, no reliable information about the structure of the inhomogeneous state for this case.

The numerous peculiarities of an FMS are due to the interaction between the donor electrons and the magnetic subsystem. A c -electron on a donor level may be regarded as a ferron localized in the vicinity of the donor. In contrast to free ferrons, such localized ferrons always exist: the Coulomb potential of the imperfection always produces a localized electron level, and for $T \neq 0$ the degree of local FM order in the vicinity of an ionized donor is always higher than the average magnetization of the crystal, since the localized c -electron carries out an indirect exchange between the l -spins. Naturally, localized ferrons exist in AFS as well, and in both AFS and FMS they may greatly increase the crystal magnetic susceptibility [195, 88].

The existence of localized ferrons may explain the resistivity peak in nondegenerate FMS. Indeed, since the degree of an FM order in the vicinity of a donor is higher, the depth of the donor level will grow with the temperature at $T < T_c$, and this may result in a drop in carrier density with temperature as T_c is approached. However, at $T > T_c$ the level depth will drop because of the destruction of the local magnetic order around the donor atom, and then the carrier density will again grow with the temperature.

This temperature dependence of the depth of the donor level may eventually explain the extremely interesting effect that has been observed in EuO. Specimens containing oxygen vacancies which behaved at $T \rightarrow 0$ like degenerate semiconductors abruptly jump over into the insulating state with a rise in temperature and thus their conductivity dropped by 15-17 orders of magnitude [109]. This effect has been explained in [196, 90] as the result of the collective autolocalization of conduction electrons in a system with fluctuations of the electrostatic potential. A crude qualitative explanation of the effect is that the radius of the electron orbit is reduced due to an increase in the depth of the localized level with the temperature rise. The result is a smaller overlap of the orbits of neighbouring donors, and the transition of their electrons from the delocalized to the localized states. It should be pointed out that an explanation of this effect based on the formation of "bound magnetic polarons" (i.e. localized ferrons) is occasionally encountered in literature but is not quite correct because it takes no account of the cooperative nature of the phenomenon.

In a highly degenerate FMS, the magnetoelectric effect results in a specific dependence of the carrier mobility on their density and on the temperature. The screening of the Coulomb potential of the imperfection by the charge carriers raises their density in the vicinity of the imperfection and thereby intensifies the indirect exchange in this location. The result is the appearance of an excess magnetic moment in the vicinity of the imperfection, and the scattering of the carriers by the imperfections will now not only be due to the spatial

fluctuations of their electrostatic potential, but also to the fluctuations in magnetization caused by the former. At sufficiently low temperatures, the latter grow with the temperature, and accordingly the scattering by the imperfections imitates the scattering by magnons. As the carrier density grows scattering by the magnetization fluctuations loses its importance with the result that the carrier mobility will grow with their density at the given temperature.

In conclusion it is worth pointing out that ferron-type states are possible in magnetic systems of other types as well, e.g. in singlet magnetic systems with both AF and FM ordering. In singlet ferromagnets these are even possible at $T = 0$. There are experimental data to support this possibility in the degenerate singlet FMS HoN. Ferrons can exist also in magnetoexciton semiconductors.

SOME GENERAL PROBLEMS OF PHYSICS OF MAGNETICS AND ELECTROCONDUCTIVITY

As has been already pointed out, in some cases MS do not exhibit any connection between their magnetic and electrical properties. For instance, perfect crystals of EuO, EuS and EuTe behaving like insulators at low temperatures are the only known almost ideal Heisenberg magnetic systems. Thus the experimental investigations of their critical properties are vital for the physics of phase transitions and results from some such investigations are compiled in this book.

One of the most important problems in the physics of phase transitions is the origin of the order-order and order-disorder phase transitions of the first kind, also treated here. An alternative to the fluctuation theory is stated, according to which these kinds of phase transitions are caused by multispin or biquadratic superexchange interactions between l -spins. This theory has made it possible to predict a new type of order-disorder phase transitions which have been termed order-improper disorder transitions [447, 442]. For this kind of phase transitions the type of the short-range order above the transition point differs from the type of the long-range order below it (e.g. FM short-range order and AF long-range order). Their existence is supported by experimental data on EuSe.

Concerning the electrical properties special attention is paid to the Mott transition and to the temperature- or pressure-induced metal-insulator phase transitions which occur mostly in transition-metal and rare-earth compounds. These transitions are not connected with changes in magnetic ordering; indeed, most materials which display them are not magnetically-ordered at all. These general problems in the physics of magnetism and electroconductivity are stated in Chapters 1 and 2 which also serve as a reference for the physics of semiconductors and magnetic systems.

THE NATURE OF THE SEMICONDUCTING STATE AND THE SEMICONDUCTOR-METAL PHASE TRANSITION

1.1. ENERGY-BAND THEORY

Many of the properties of semiconductors and metals are described by the energy-band theory. However, rigidly applying it to some materials, particularly magnetic semiconductors, results not only in quantitative, but also in crude qualitative errors. Still, some of the band concepts can be applied to MS as well and so we should start our account of MS theory by presenting the fundamental postulates of the standard band theory and those of its results that we will use later. Finally, the limits to the theory's applicability will be established later in the chapter.

Band theory is based on three fundamental assumptions: (1) the crystal structure is ideally periodic, (2) the motion of the atoms constituting the crystal exercises a negligible effect on the state of its electrons, and so all the atoms may be presumed to remain in their equilibrium position and (3) the effect of all other electrons on the electron can be accounted for by introducing some effective potential that is a function of the average electron density. The position of other electrons has no effect whatsoever on the probability that an electron is present at a specified point. In other words, there are no electron correlation effects, and the electrons feel only their average fields (the mean-field approximation).

All these physical assumptions are mathematically equivalent to the statement that each electron moves in an ideally periodic field that has the symmetry of the crystal lattice.

However, as will be demonstrated in Sec. 1.5, this is in fact only true for elementary excitations, conduction electrons and holes, but not for the actual particles which made up the crystal.

The band theory Hamiltonian in the simplest case can be written as

$$H_B = B \sum a_{g\sigma}^* a_{g+\Delta\sigma} = \sum E_{\mathbf{k}} a_{\mathbf{k}\sigma}^* a_{\mathbf{k}\sigma}, \quad (1.1.1)$$

$$E_{\mathbf{k}} = zB\gamma_{\mathbf{k}}, \quad \gamma_{\mathbf{k}} = \frac{1}{z} \sum_{\Delta} e^{i\mathbf{k} \cdot \Delta}, \quad (1.1.2)$$

where $a_{\mathbf{k}\sigma}^*$, $a_{\mathbf{k}\sigma}$ are the creation and annihilation operators of an electron in the Bloch state, i.e. with a quasi-momentum \mathbf{k} and a spin

projection σ , and $a_{g\sigma}^*$, $a_{g\sigma}$ are electron operators in the "lattice site" representation which are related to the operators in the "momentum" representation by

$$a_{g\sigma}^* = \frac{1}{\sqrt{N}} \sum_{\mathbf{k}} e^{i\mathbf{k} \cdot \mathbf{g}} a_{\mathbf{k}\sigma}^*, \quad a_{g\sigma} = \frac{1}{\sqrt{N}} \sum_{\mathbf{k}} e^{-i\mathbf{k} \cdot \mathbf{g}} a_{\mathbf{k}\sigma}. \quad (1.1.3)$$

Further: lattice sites are numbered by stating their coordinates $\mathbf{g} = (g_x, g_y, g_z)$, N is the total number of elementary cells in the crystal; Δ is a vector connecting a lattice site to its nearest neighbour; and z is the coordination number. In (1.1.1) and below, when the summation indices are not stated, this means that the summation is performed over the complete set of indices.

The Hamiltonian (1.1.1) only accounts for the electron states within one energy band, its index having been omitted for the sake of simplicity. The energy is measured from the band centre.

Strictly speaking, the nearest-neighbour approximation used to write down the Hamiltonian (1.1.1) is only valid for narrow bands. However, even for energy bands of arbitrary widths, it enables general qualitative regularities to be established and order-of-magnitude estimates to be obtained. In case the effects being considered are not associated with a definite crystal structure, to make the discussion clearer the lattice is assumed to be of the simple cubic type ($z = 6$, $|\Delta| = a$, where a is the lattice parameter).

The Hamiltonian of the (1.1.1) type is valid also in cases when the charge carriers are not conduction electrons, but holes (the hole creation operator is the annihilation operator of an electron in the corresponding state, and vice versa). All the statements made below concerning electrons can be easily generalized to include holes.

As will be seen from (1.1.1), if the quasi-momentum only varies within the first Brillouin zone, the energy will vary between the limits $-z|B|$ and $z|B|$, i.e. an energy band with width $W = 2z|B|$ is formed. The minimum energy of a moving electron turns out to be lower than that of an electron bound to a specific atom by the amount $z|B|$. Hence, the translational motion of the electron in the crystal reduces its minimum energy. The physical reason for this will be clear if it is remembered that the localization of the electron around one particular atom is similar to the localization of a free electron in a limited region of space, which, according to the uncertainty principle, raises its energy.

Expanding (1.1.1) to get an expression for the energy in the vicinity of the band minimum (for $B < 0$ it coincides with the centre of the Brillouin zone $\mathbf{k} = 0$) leads to the usual quadratic dispersion law. The difference between this and the corresponding expression for a free electron is that an effective electron mass m^* is substituted

for the true electron mass m_0 .*

$$E(\mathbf{k}) = -z |B| + \frac{\mathbf{k}^2}{2m^*}, \quad (1.1.4)$$

$$\frac{1}{m^*} = \frac{Wa^2}{6} = -2Ba^2. \quad (1.1.5)$$

Results similar to (1.1.4-5) are also obtained for other crystal structures (see, for example [214]). In particular, the formula that connects the effective mass with the conduction band width W will be valid for the important case of a face-centered cubic lattice, if $a_{\text{eff}} = a/\sqrt{2}$ is substituted for the lattice parameter a .

1.2. CRYSTALS WITH IMPERFECTIONS

The presence of imperfections in a crystal introduces radical changes to the nature of the electron-energy spectrum since, in addition to the allowed energy bands, discrete levels appear within the gaps between the bands. The states corresponding to these levels are those in which the electrons are localized near the imperfections. If the density of the imperfections is small, they may be considered mutually independently. An analysis of the changes in the crystal spectrum, introduced by an imperfection, is handicapped by the absence of a precise expression for the imperfection potential $V(\mathbf{r})$. However, in some cases that are important in practice it is sufficient only to know the long-range behaviour of $V(\mathbf{r})$ and this is the case for charged imperfections, if the radius of the impurity state a_B is large as compared with the lattice parameter a .

On the other hand, according to (1.1.4), the continuous-medium approximation, in which the effect of the crystal field is accounted for by substituting an effective electron mass m^* for the true electron mass m_0 , is valid for electrons whose wavelength is large compared to a . It is to be expected, therefore, that the state of an electron trapped by a positively-charged imperfection can, if its orbital radius is large, be described by the Schrödinger equation of the form

$$\left\{ -\frac{1}{2m^*} \Delta - \frac{e^2}{\epsilon_0 r} - E \right\} \psi(\mathbf{r}) = 0, \quad (1.2.1)$$

where ϵ_0 is the static dielectric constant of the crystal, and the energy E is measured from the bottom of the conduction band. Obviously, the only difference between this equation and the one for a hydrogen atom is that the mass and the charge have been renormalized ($m_0 \rightarrow m^*$, $e \rightarrow e/\sqrt{\epsilon_0}$), and thus we may write the result right away,

* We employ a system of units in which $\hbar = 1$, and the temperature and the magnetic field have energy dimensions ($k_B T \rightarrow T$, $2\mu_B H \rightarrow H$, where k_B is the Boltzmann constant, and μ_B is the Bohr magneton).

the expressions for the ground state energy E_d and for the Bohr orbit radius a_B being:

$$E_d = -\frac{m^* e^4}{2\epsilon_0^2} = -\frac{e^2}{2a_B \epsilon_0}, \quad a_B = \frac{\epsilon_0}{m^* e^2}. \quad (1.2.2)$$

The following reasoning is used to justify this approach, which has become known as the effective mass method [60]. Suppose that the potential $V(\mathbf{r})$ changes in space so slowly that $V(\mathbf{r})$ can be presumed to remain constant inside an elementary cell. In this case the potential matrix elements may be regarded as diagonal in the quasi-atomic Wannier functions $\varphi_g(\mathbf{r})$ which are localized inside an elementary cell with the corresponding number g . The function $\varphi_g(\mathbf{r})$ is a wave packet constructed from the band functions $\varphi_k(\mathbf{r})$ using the same law (1.1.3) used to construct the operators $a_{g\sigma}^*$ from the operators $a_{k\sigma}^*$. Accordingly, the Hamiltonian H_d of a crystal containing an imperfection can be written as:

$$H_d = B \sum a_{g\Delta}^* a_g + \sum V(g) a_g^* a_g \equiv \sum E_v a_v^* a_v. \quad (1.2.3)$$

It can be reduced to a diagonal form by the canonical transformation

$$a_v = \sum_g \psi_v(g) a_g \quad (1.2.4)$$

(the spin indices have been omitted).

The equation for the transformation coefficients $\psi_v(g)$ is obtained by writing down the equations of motion for the operator a_v

$$i \frac{da_v}{dt} = [a_v, H_d] = E_v a_v. \quad (1.2.5)$$

Substituting expression (1.2.4) into (1.2.5), we obtain:

$$[E_v - V(g)] \psi(g) = B \sum_{\Delta} \psi(g + \Delta). \quad (1.2.6)$$

When an orbit has a large enough radius so that $\psi(g)$ changes little over the distance of the lattice parameter, $\psi(g + \Delta)$ in (1.2.6) can be formally expanded into a series in Δ ($|\Delta| = a$) thus:

$\psi(g_x, g_y, g_z \pm a)$

$$= \left[1 \pm a \frac{\partial}{\partial g_z} + \frac{a^2}{2} \frac{\partial^2}{\partial g_z^2} \right] \psi(g_x, g_y, g_z) + \dots \quad (1.2.7)$$

If g is considered as a continuous variable, we can reduce equation (1.2.6) to the form (1.2.4) if $V(r) = -e^2/\epsilon_0 r$ and the relationships for the effective mass (1.1.5) is taken into account.

Knowing the density of the imperfections N_d and the depths of their levels, we can find the number of electrons that have gone from the donor levels to the conduction band. However, already at this point it turns out that accounting for those electron-electron interactions in

the mean field approximation used in the band theory method leads to serious errors. Actually, to take account of the correlation between the electrons, we shall have to go beyond the limits set by the band theory. Indeed, if this correlation is ignored, every donor level can be occupied by two electrons with opposite spins but Coulomb repulsion between the electrons prevents two electrons simultaneously occupying a donor level for a hydrogen-like donor. In fact there is only one electron on every donor level in the ground state, the number of occupied donor levels falling with rising temperature. For this reason donor levels statistics should be devised that accounts for the repulsion between the electrons [214]. The result is that the average number n_d of electrons occupying a donor level is expressed by a formula which differs greatly from the usual Fermi distribution function

$$n_d = \left\{ 1 + \frac{1}{2} \exp \left(\frac{E_d - \mu}{T} \right) \right\}^{-1} \quad (1.2.8)$$

(μ is the electron chemical potential).

The number of electrons in the conduction band is expressed in terms of the Fermi distribution function $n(E)$ and the density of states $g_e(E)$ with the aid of the expression

$$\begin{aligned} n &= 2 \sum_{\mathbf{k}} n(E_{\mathbf{k}}) = \int n(E) g_e(E) dE, \\ g_e(E) &= 2 \sum_{\mathbf{k}} \delta(E - E_{\mathbf{k}}). \end{aligned} \quad (1.2.9)$$

Using (1.2.9), we can obtain the following for the electron density of states (for a crystal of unit volume):

$$g_e(E) = \frac{2}{(2\pi)^3} \int d\mathbf{k} \delta \left(E - \frac{\hbar^2 \mathbf{k}^2}{2m^*} \right) = \frac{(m^*)^{3/2} (2E)^{1/2}}{\pi^2}. \quad (1.2.10)$$

For $|\mu| \gg T$, the electrons in the conduction band are nondegenerate, and their concentration is given by the expression

$$n = \int_0^\infty dE g_e(E) \exp \left\{ \frac{\mu - E}{T} \right\} = e^{\mu/T} N_{\text{eff}}, \quad N_{\text{eff}} = \frac{(2\pi m^* T)^{3/2}}{4\pi^2}. \quad (1.2.11)$$

The chemical potential of an impurity semiconductor can be found since the number of electrons in the conduction band is equal to the number of holes on donor atoms, whence we obtain for $|E_d - \mu| \gg T$ in accordance with (1.2.8):

$$n = \sqrt{\frac{N_d N_{\text{eff}}}{2}} \exp \left(-\frac{|E_d|}{2T} \right). \quad (1.2.12)$$

All these results are true only if the average distance between the donors $N_d^{-1/3}$ greatly exceeds the radius of the impurity state a_B .

For $N_d^{-1/3} \leq a_B$ the problem turns essentially into a many-electron one and shall be discussed in Sec. 1.7.

In addition to ideally (or almost ideally) periodic crystals, semiconducting properties are also displayed by systems not possessing a translational symmetry, such as glasses and liquids. There are no

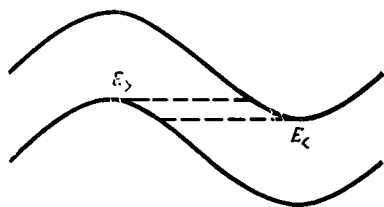


Fig. 1.1. Localization of a conduction electron owing to potential fluctuations

discrete levels in the energy spectra of amorphous systems. However, the continuity of the spectrum is no guarantee that the corresponding states are extended ones. For instance, in the one-dimensional case, if a function $V(g)$ (1.2.6) varies slowly with the atomic coordinates and lies inside an interval $[V_<, V_>]$, the system will have *a priori* no extended states for $V_> - V_< > W = 2|B|$. Indeed, in this

case the minimum electron energy in the region of the highest potential hump $E_> = V_> - |B|$ will be higher than the maximum energy $E_< = V_< + |B|$ in the region of the deepest potential well. Accordingly, electrons with an energy less than $E_>$ will be unable to get over the potential hump, and those with an energy above $E_<$ over the potential well (Fig. 1.1).

The situation in the three-dimensional case turns out to be more complicated, for an isolated potential hump, irrespective of its height, cannot, by itself, turn the system into an insulating one. Anderson [296] has obtained that in the three-dimensional case there will be no extended states if the amplitude of the fluctuations of the potential $V(g)$ exceeds $5W$ (obviously the numerical coefficient in this relationship should be considered with reservations). The established term for the capture of charge carriers by the spatial fluctuations of a random potential is Anderson localization.

In the case of smaller fluctuations, one would expect some of the states to be extended and the others localized. There is supposed to be a sharp boundary between the extended and the localized states at which the mobility changes abruptly from zero to a finite value (the mobility edge) [278]. At finite temperatures, the motion of a carrier, in the region of localized states (inside the so-called mobility gap), is possible by thermally activated hopping.

1.3. POLARON STATES IN IONIC CRYSTALS

In crystals with covalent bonds the assumption that atomic oscillations around equilibrium positions exercise only a negligible effect on the state of charge carriers is justified. However, in ionic crystals the displacement of ions from their equilibrium positions results in

the appearance of electric fields that can affect the state of conduction electrons very much. In these conditions conventional band theory ceases to be valid and the conduction electron goes over to a state termed the polaron state [281, 60]. The physics of these states is best understood in the case of the so-called small polaron [284]. If an immobile point charge is placed inside an ionic crystal, it will polarize the lattice with a resultant drop in its energy. The same happens if a band electron is localized inside an elementary cell of the crystal. This decrease in the energy of the system due to the lattice polarization E_p should be compared to the increase in the electron energy due to its localization, which according to Sec. 1.1 is equal to $W/2$. If the former greatly exceeds the latter, then the energy of the localized electron state will be lower than that of the band state, and accordingly there is a polaron state instead of a band state. The electron will be localized in the potential well it sets up itself by polarizing the lattice.

The lattice polarization energy can be estimated from the following considerations. The polarization of an ionic crystal \mathcal{P} , induced by an external field, is made up from the polarization of the electron shells of ions \mathcal{P}_e and the polarization due to the displacement of the ions from their equilibrium positions \mathcal{P}_i . The former polarization takes place irrespective of the charge-carrier state, that is whether it is localized or moves freely over the crystal. Accordingly, this need not be taken into account in an estimate of the potential well depth (it has already been accounted for in the crystal lattice potential). On the other hand, crystal polarization is expressed in terms of the static dielectric constant ϵ_0 and the electric induction \mathcal{D} by the relationship

$$\mathcal{P} = \frac{\epsilon_0 - 1}{4\pi\epsilon_0} \mathcal{D}, \quad (1.3.1)$$

and the electronic polarization \mathcal{P}_e , by a similar relationship in which the place of ϵ_0 is taken by the high-frequency dielectric constant ϵ_∞ (ionic polarization does not contribute to the last constant because slow ions are unable to follow a quickly changing field). The energy of interaction between the dipole moment of the lattice and the field set up by the electron must be also accounted for and is equal to $(-\mathcal{P}_i \cdot \mathcal{D}/2)$ [264]. Then expressing $\mathcal{P}_i = \mathcal{P} - \mathcal{P}_e$ in terms of \mathcal{D} using (1.3.1) we obtain the following for the energy of lattice polarization by the electron field

$$E_P^s = -\frac{e^2}{8\pi\epsilon^*} \int \frac{d^3r}{r^4} \simeq -\frac{e^2}{2\epsilon^*a_P}, \quad \frac{1}{\epsilon^*} = \frac{1}{\epsilon_\infty} - \frac{1}{\epsilon_0}, \quad (1.3.2)$$

where a_P is a characteristic length of the order of the lattice parameter at which the integration should be cut off (the physical reason for this is that ions displaced by the field of an electron are located at distances equal to or exceeding a).

If the electron moves to a neighbouring cell, the ion equilibrium positions change, but the lattice polarization energy E_p^s would remain the same, and this makes electron transitions from atom to atom possible. As the electron moves in the crystal, the induced lattice polarization must move with it. Hence, the polaron is a quasi-particle but of a more complex nature than a band electron. At $T=0$, when the thermal oscillations of the ions do not perturb the crystal translational symmetry, a well-defined quasi-momentum can be attributed to the polaron, and its energy spectrum is given by a band with a dispersion law of the type (1.1.1), but with a width W_p that should be much less than that of the electron band W . Indeed, because the motion of an electron from atom to atom is handicapped by the necessity to "drag" along the lattice polarization, the mean lifetime of a polaron on an atom τ is much longer than that of a band electron. But the bandwidth is determined by the speed of a quasi-particle moving in the crystal, since, by the uncertainty relation, it must be of the order of $1/\tau$. As was demonstrated in [284],

$$W_p = W \exp(-\tilde{\alpha}), \quad \tilde{\alpha} = |E_p^s|/\omega. \quad (1.3.3)$$

For typical values of the parameters: $\epsilon_0 = 10$; $\epsilon_\infty \approx 3$; $a_p \sim 5 \text{ \AA}$, the value of E_p^s (1.3.2) is 0.3 eV, and thus the small polaron is possible only for electron bands whose width does not exceed 0.1 eV, i.e. when, according to formula (1.1.5), the electron effective mass m^* is equal to several dozen true electron masses m_0 . A typical optical phonon frequency of 0.03 eV and $E_p^s \approx 0.3 \text{ eV}$ yield an electron-phonon coupling constant $\tilde{\alpha}$ of 10. Hence, according to (1.3.3), the polaron bandwidth W_p is 4 orders of magnitude less than the width of the electron band W and so a band with a width less than 10^{-5} eV can only exist in ideally perfect crystals. In a real crystal and in the presence of imperfections, Anderson localization of small polarons must take place (see Sec. 1.2); the polaron effective mass, as determined by formula (1.1.5) for such a bandwidth, must be greater than the mass of the heaviest atom.

At $T > \omega$ a small polaron can move by temperature-activated hopping. When impurity-potential fluctuations are small in comparison with E_p^s , the activation energy E_u of the mobility u should be of the order of magnitude of the energy E_p^s required to free an electron from the polaron potential well (including quantum effects E_u is equal to $E_p^s/2$ [55-58]). An exponential growth in the mobility of charge carriers, with the temperature as described, is possible only for very small u not exceeding 10^{-2} to $10^{-1} \text{ cm}^2/\text{V}\cdot\text{s}$. The conditions for the existence of small polarons having larger mobilities are not met.

Ionic crystals with wide conduction bands $W \gg E_p^s$ have different types of polaron states. These are determined by the magnitude of the

coupling constant between the electrons and the optical phonons

$$\alpha = \frac{e^2 (2m^*\omega)^{1/2}}{2\omega\epsilon^*\hbar^{3/2}} \sim \tilde{\alpha} \sqrt{\frac{\omega}{W}}. \quad (1.3.4)$$

The state that materializes when $\alpha \gg 1$ (starting in practice from $\alpha \sim 10$) is the one first considered by Pekar [60] and subsequently by Bogolyubov [283] and Tyablikov [284]. It is distinguished from the considered above because the radius of the localized state of the electron self-trapped by the lattice polarization is large compared to the lattice parameter (the large polaron).

In the opposite limiting case of a weak electron-optical phonon coupling ($\alpha < 1$) it no longer makes sense to talk about the localization of the electron in the potential well created by itself, despite the fact that in this case, too, the electron moves about the crystal dragging the lattice polarization. The energy of the polaron ground state and its effective mass m_p^* are equal [262] (see Sec. 1.4), respectively, to:

$$E_p = -\alpha\omega, \quad m_p^* = m^* \left(1 - \frac{\alpha}{6}\right)^{-1}. \quad (1.3.5)$$

For real crystals, the region of maximum interest is that of intermediate α 's. In the absence of the small parameters in this region, some kind of a variational method must be employed. The most successful method has proved to be one due to Feynman [282] which reproduces both limits $\alpha < 1$ and $\alpha \gg 1$ well, and for $\alpha \sim 1$ produces the lowest polaron energies ever obtained.

It is not possible to obtain an analytical expression for the polaron parameters in the region $\alpha \sim 1$, and so results can only be obtained with the help of numerical methods [285]. It follows from them that the expressions (1.3.5) are actually valid for α close to 6.

Having made these preliminary remarks, let us proceed to the polaron problem in magnetic semiconductors. The coupling constant in transition-metal and rare-earth compounds may be expected to be lower than in alkaline-haloid crystals having α in the range of 4.8-6.4 [290], since the part played by the ionic bond in the former is less than in the latter. To estimate it, we can use the experimental data for EuS: $\epsilon_0 = 11.4$; $\epsilon_\infty = 5.0$; $\omega = 267 \text{ cm}^{-1}$, and for EuSe: $\epsilon_0 = 9.4$; $\epsilon_\infty = 5.0$; $\omega = 182 \text{ cm}^{-1}$ [291]. Then putting $m^* = m_0$, we obtain, according to formula (1.3.4): $\alpha = 2$ for EuS and $\alpha = 2.5$ for EuSe. Hence, in these materials the drop in the electron energy caused by the polaron effect amounts, in accordance with formulae (1.3.5), to 0.06 eV, and the effective mass grows by 30-40%. In chrome spinels the polaron effects are still less pronounced. According to [500], $\epsilon_0 = 14.2$, and $\epsilon_\infty = 11.0$ for CdCr_2Se_4 at 300 K and $\epsilon_0 =$

$=14.9$, and $\epsilon_\infty = 11.3$ at 80 K. Hence, the quantity ϵ^* (1.3.2), to which the polarization energy is inversely proportional, in CdCr_2Se_4 is 5.2 times greater than in EuS. Data on CdCr_2S_4 [501] support the contention that the polaron effects in materials of this class are small.

A property peculiar to transition-metal compounds is their ability to have narrow d -type energy bands formed from the states of partially-filled cation shells. For this reason such materials should be regarded as most favourable for small polarons. However, the conditions for their materialization, $|E_p| \gg W$, are too stringent to permit small polarons becoming a typical phenomenon, and if these polarons are possible at all, they would be the exception and not the rule.

It should be kept in mind that experimental observations of small polarons are only possible in perfect crystals. In crystals containing imperfections, there may also be a mechanism for conductivity via impurity levels which would result in an exponential growth in mobility with temperature. Suppose, that the semiconductor contains both donor and acceptor impurities and so some electrons went over from the donors to the acceptors. Typically, an electron on a donor level more closely resembles a large polaron, the radius both of the potential well and of the electron orbit exceeding the lattice parameter [604]. When an electron goes over from an occupied donor level to a vacant neighbouring level, the lattice polarization goes with it. In contrast to the small polaron, the displacement of polarization in this case does not correspond to an electron transition to a neighbouring atom, but to the transition of the centre of the electron cloud from one atom to another. For a classical above-the-barrier transition, the energy required is of the order of the energy of lattice polarization by the electron localized on the donor, i.e. in typical conditions ~ 0.1 eV. The mobility may become activated also as a result of a difference in the depths of neighbouring donor levels caused by the spatial fluctuations of the potential of the other imperfections which are randomly distributed in the crystal.

The possibility that one or other impurity conductivity mechanism will imitate the temperature dependence of mobility of small polarons is probably the cause of the conflicting experimental data concerning their existence in a number of transition-metal compounds. Studies which provide a basis for some conclusion about the exponential growth of the mobility with temperature have been performed on imperfect crystals. For instance, according to [59], the hole mobility in NiO doped with Li is very low and grows exponentially with the temperature. At the same time, an exponential temperature dependence of the mobility has not been detected in other experiments with NiO, and rather high values have been obtained for

it—of the order of $10\text{--}100\text{ cm}^2\text{V}\cdot\text{s}$ [61, 63, 156]. According to [63], the effective mass of the hole polaron in NiO is $1.5 m_0$, and the coupling constant α is 1.6. Experimental data on electric properties of NiO obtained earlier are presented in the review [61].

From the point of view of the theory, the existence of small polarons in NiO seems unlikely. A high Néel temperature $T_N = 520\text{ K} \approx 0.05\text{ eV}$ is proof of not too small an overlap of d -shells of neighbouring cations. At the same time, the Néel temperature T_N is always small as compared to the bandwidth W , since W is a quantity of the first order of magnitude in the overlap of d -orbitals of the neighbouring cations, whereas T_N is a quantity of the second order in it (Sec. 2.1). Hence, in this case W must amount to at least several tenths of an electron-volt. Bearing in mind that the lattice polarization energy E_p^* does not exceed several tenths of an eV, one is bound to conclude that the condition for the existence of the small polaron $|E_p^*| \gg W$ in NiO can hardly be met.

The analysis of experimental data carried out in Secs. 4.6 and 5.3 indeed demonstrates that the typical width of the d -band in transition-element compounds is $\sim 1\text{ eV}$, and accordingly there are no small polarons in them. It should, however, be kept in mind that smaller widths of the d -band are not prohibited, and in principle materials with conditions favourable for the existence of small polarons are feasible. Experimental data obtained with slightly reduced rutile TiO_2 are interpreted as suggesting the existence of small polarons [292].

An additional principal difficulty involved in the analysis of the data on narrow-band semiconductors is worth mentioning. The standard expression for the Hall constant obtained within the framework of the band theory cannot be valid for small polarons. Attempts to calculate the Hall constant for them on the basis of the states of a single band cannot yield reliable results since the use of a complete set of functions is of principal importance for such calculations. (There is no such difficulty for calculating the mobility of the small polaron because the energy conservation law limits consideration to the states of a single band.) The use of incomplete sets of functions is, probably, the root of the sharp difference between results for the Hall constant for the small polaron calculated by different authors.

If the energy of interaction of the conduction electron in an MS with the lattice polarization is compared to that with the magnetic moments (see Sec. 3.1), we would find that the former is typically smaller than the latter. Except in the hypothetical case of small polarons, polaron effects cannot by themselves significantly affect the state and the nature of electron motion in the crystal, and in any case they cannot determine any specific property of an MS.

1.4. THE METHOD OF CANONICAL TRANSFORMATION IN THE THEORY OF THE POLARON

From the point of view of mathematics, the polaron problem is an extremely interesting one. Very elegant methods have been developed for its solution which have been applied subsequently to other problems of physics.

The electron's Hamiltonian in an ionic crystal has the form [60, 262] (for a unit volume):

$$\begin{aligned} H &= H_B + H_i + H_{ph}, \\ H_B &= \sum E_{\mathbf{k}} a_{\mathbf{k}}^* a_{\mathbf{k}}, \quad H_{ph} = \omega \sum b_{\mathbf{q}}^* b_{\mathbf{q}}, \\ H_i &= - \sum c_{\mathbf{q}} (b_{\mathbf{q}} a_{\mathbf{k}+\mathbf{q}}^* a_{\mathbf{k}} - b_{\mathbf{q}}^* a_{\mathbf{k}-\mathbf{q}}^* a_{\mathbf{k}}), \\ c_{\mathbf{q}} &= \frac{ie}{q} \sqrt{\frac{2\pi\omega}{\epsilon^* \Omega}} = \frac{ic}{q} \quad (\Omega = 1), \end{aligned} \quad (1.4.1)$$

where H_B and H_{ph} are the free electron and the longitudinal optical-phonon Hamiltonians, respectively, and H_i is their interaction Hamiltonian. A single-band model is used for the electrons, and accordingly the band index has been dropped. The spin index has also been omitted because the interaction with the lattice polarization preserves the electron spin. The frequency of the optical phonons ω is presumed to be independent of their quasi-momentum \mathbf{q} .

For small c , a canonical transformation of the Hamiltonian (1.4.1) is performed to eliminate the electron-phonon interaction to the first order of magnitudes in c [293]. If the unitary operator that performs this transformation is put in the form $\exp(U)$, where the operator U is of the order of c , the transformed Hamiltonian, up to terms of the order of c^2 , would assume the form

$$\tilde{H} = e^U H e^{-U} = H + [U, H] + \frac{1}{2} [U [U, H]]. \quad (1.4.2)$$

It follows from

$$H_i + [U, H_B + H_{ph}] = 0 \quad (1.4.3)$$

that the terms in \tilde{H} (1.4.2) linear in c vanish.

In the respective order the transformed Hamiltonian is of the form

$$\tilde{H} = H_B + H_{ph} + \frac{1}{2} [U, H_i]. \quad (1.4.4)$$

The operator U is determined from the condition (1.4.3), and we obtain

$$U = - \sum \frac{c_{\mathbf{q}}}{E_{\mathbf{k}-\mathbf{q}} - E_{\mathbf{k}} - \omega} (b_{\mathbf{q}} a_{\mathbf{k}-\mathbf{q}}^* a_{\mathbf{k}} - a_{\mathbf{k}-\mathbf{q}}^* a_{\mathbf{k}} b_{\mathbf{q}}^*). \quad (1.4.5)$$

By substituting (1.4.5) into (1.4.4), we obtain

$$\begin{aligned} \tilde{H} = \sum (E_{\mathbf{k}} + \Delta E_{\mathbf{k}}) a_{\mathbf{k}}^* a_{\mathbf{k}} + \omega \sum b_{\mathbf{q}}^* b_{\mathbf{q}} \\ + \frac{1}{2} \sum_{\mathbf{q}} \frac{|c_{\mathbf{q}}|^2 (a_{\mathbf{k}+\mathbf{q}}^* a_{\mathbf{k}+\mathbf{q}} - a_{\mathbf{k}}^* a_{\mathbf{k}})}{E_{\mathbf{k}+\mathbf{q}} - E_{\mathbf{k}} - \omega} b_{\mathbf{q}}^* b_{\mathbf{q}}, \end{aligned} \quad (1.4.6)$$

where we make use of the notation

$$\Delta E_{\mathbf{k}} = \sum_{\mathbf{q}} \frac{|c_{\mathbf{q}}|^2}{E_{\mathbf{k}} - E_{\mathbf{k}+\mathbf{q}} - \omega}. \quad (1.4.7)$$

We have omitted off-diagonal components in the last term of the Hamiltonian (1.4.6) since their contribution to the physical quantities is only of the order of c^4 . Terms of the type $a^* a^* a a$ have been set to zero owing to the condition of the single-electron problem.

The interaction with the optical phonons will be seen from expressions (1.4.6, 7) to shift the charge-carrier energy. Such a shift takes place also at $T = 0$ when the average numbers of phonons are equal to zero. It is just that shift that determines the gain in the carrier energy owing to the polarization of the lattice. The computation of $\Delta E_{\mathbf{k}}$ on the assumption of a simple quadratic dispersion law for bare electron energy $E_{\mathbf{k}} = k^2/2m^*$ for $E_{\mathbf{k}} < \omega$ yields just the results (1.3.5).

The following circumstances should be emphasized. The Hamiltonian \tilde{H} (1.4.6) features new fermion operators. In contrast to bare fermion operators in the Hamiltonian H (1.4.1), the new fermion operators have the meaning not of electron, but of polaron operators, i.e. they describe the motion of a complex consisting of an electron and of lattice polarization induced by it. The motion of the polarization together with the electron means that the equilibrium position of optical phonons are displaced in the wake of an electron. Just such phonons are described by new boson operators in (1.4.6), and they are the true elementary excitations since the degree of excitation of oscillations in a crystal is independent of the equilibrium position of its ions. (Recall that the normal coordinate of oscillations is proportional to the sum of the phonon creation and annihilation operators. Correspondingly, their displacements are also mutually proportional.)

To be sure that the equilibrium positions of the phonons indeed follow in the wake of the electron, we should compare the transformed operators $\tilde{b}_{\mathbf{q}}$ of bare phonons whose equilibrium positions are independent of the electron and the new operators $b_{\mathbf{q}}$ corresponding to the true phonons. According to (1.4.2, 5) and (1.1.3) in the first

order in c

$$\tilde{b}_q = b_q + [U, b_q] = b_q - \sum F_q(g, g-f) a_q^\dagger a_f, \\ F_q(g, g-f) = \frac{1}{N} \sum_k \frac{c_q}{E_{k-q} - E_k - \omega} \exp\{-ik \cdot (g-f) + iq \cdot g\}. \quad (1.4.8)$$

If we for the sake of clarity assume the conduction band to be very narrow ($W \ll \omega$), $F(g, g-f)$ will be nonzero only for $g=f$. $F(g, 0)$ is obviously the displacement of the equilibrium positions of the true ("dressed") phonons with respect to the bare when the electron is located on the g -atom (the same result has been obtained in [58] under the assumption of the small polaron being energetically favoured, i.e. $W \ll E_P$, but without the assumption of c being small).

A doubtless advantage of the canonical-transformation method is the opportunity to effect a direct transition to elementary excitation operators of a more complex nature than the bare band electron. However, there is an essential drawback to the method: if the processes of electron scattering by the phonons can take place, the energy denominators in \tilde{H} (1.4.6) may vanish. Formulae (1.4.6, 7) provide no answers to the question what should be done in this case. An answer can be obtained by employing a more powerful and universal method of Green's functions [64, 295]: an infinitesimal quantity η should be added to the energy denominators, and the formula should be applied

$$\frac{1}{x-i\eta} = \mathbf{P} \frac{1}{x} - i\pi\delta(x), \quad (1.4.9)$$

where \mathbf{P} means that the corresponding integrals should be taken in the sense of their principal value.

Thus, strictly speaking, the canonical transformation method is applicable only at sufficiently low temperatures $T \ll \omega$ when the last term in \tilde{H} can be neglected, and when the polarons occupy states with an energy below ω .

1.5. ELECTRON-ELECTRON INTERACTION

There is a wide class of systems applied to which the standard band theory yields results not only quantitatively but even qualitatively erroneous. In particular, MS, i.e. nonmetallic compounds of the transition and rare-earth elements, belong to such systems. Since they contain ions with partially filled d - and f -shells, from the point of view of the band theory d - and f -bands partially filled with electrons should form in them, i.e. such materials should exhibit metallic properties. The cause of such an erroneous conclusion is that the

band theory takes no account of the correlations between the electrons, which play a very important part in MS. The following section will be dedicated to the study of such correlations.

If we choose an appropriate system of Wannier functions as the basis functions, we can write down the Hamiltonian of the system under consideration in the single-band approximation with account of the electron-electron interaction in the form:

$$H = B \sum a_{g\sigma}^* a_{g+\Delta\sigma} + \frac{1}{2} \sum \mathfrak{U}(g_1 g_2 | g_3 g_4) a_{g_1\sigma_1}^* a_{g_2\sigma_2}^* a_{g_3\sigma_3} a_{g_4\sigma_4}, \quad (1.5.1)$$

where $\mathfrak{U}(g_1 g_2 | g_3 g_4)$ is the matrix element of Coulomb interaction $\mathfrak{U}(\mathbf{r}_1 - \mathbf{r}_2)$. The band is assumed to be nondegenerate (the Wannier functions are of the *s*-type)

$$\mathfrak{U}(g_1 g_2 | g_3 g_4) = \int d\mathbf{r}_1 d\mathbf{r}_2 \varphi_{g_1}^*(\mathbf{r}_1) \varphi_{g_2}^*(\mathbf{r}_2) \mathfrak{U}(\mathbf{r}_1 - \mathbf{r}_2) \varphi_{g_3}(\mathbf{r}_1) \varphi_{g_4}(\mathbf{r}_2).$$

But even in such a form the Hamiltonian turns out to be extremely complicated. Thus, in cases when the long-range nature of the Coulomb forces is of no essential importance, frequently use is made of the Hubbard model [43] in which the interaction between the electrons has been simplified to the utmost with only the repulsion between the electrons located on the same atom being taken into account

$$H_H = B \sum a_{g\sigma}^* a_{g+\Delta\sigma} + \mathfrak{U} \sum \hat{n}_{g\uparrow} \hat{n}_{g\downarrow} = H_B + H_{\mathfrak{U}}, \quad (1.5.2)$$

$$\hat{n}_{g\sigma} = a_{g\sigma}^* a_{g\sigma}.$$

It would be instructive to start with the investigation of the effects of a weak electron-electron interaction when the number of electrons n is less than $2N$, and the system behaves like a metal (N is the number of atoms). If in the zeroth approximation ($n - m$) electrons have a spin projection of $-1/2$ and occupy states with the quasi-momenta $\mathbf{k}_1, \dots, \mathbf{k}_{n-m}$, and m electrons have spin projections of $+1/2$ and occupy states with the quasi-momenta $\mathbf{p}_1, \dots, \mathbf{p}_m$, then in the first approximation in $H_{\mathfrak{U}}$ (1.5.2) the electron-electron interaction results in correction to the energy

$$\Delta E = \frac{\mathfrak{U}}{N} \sum n_{\mathbf{k}\uparrow} \sum n_{\mathbf{k}\downarrow} |0\rangle = \frac{\mathfrak{U}}{N} m(n - m), \quad (1.5.3)$$

where $|0\rangle$ is the vacuum electron function, $n_{\mathbf{k}\sigma}$ is the occupation number of the (\mathbf{k}, σ) state. When calculating (1.5.3) we have made the transition to the quasi-momentum representation in the Hamiltonian $H_{\mathfrak{U}}$.

The single-electron energy, which takes account of the electron-electron interaction, can be formally defined as the derivative of the

total energy $E\{n\}$ of the system with respect to the occupation number of the respective state $n_{k\sigma}$ as it has been done in Landau's theory of the Fermi liquid. Then we obtain with account taken of (1.5.3) (the symbol $\{n\}$ denotes the set of numbers $n_{k\sigma}$):

$$\tilde{E}_{k\sigma}\{n\} = \frac{\delta E}{\delta n_{k\sigma}} = E_{k\sigma} + \frac{un_{k-\sigma}}{N}, \quad n_{\sigma} = \sum_k n_{k\sigma}. \quad (1.5.4)$$

There is no sense in talking of $\tilde{E}_{k\sigma}$ as of a real energy possessed by the electron, as the total energy of the system is not equal to the sum of the energies $\tilde{E}_{k\sigma}$. Expression (1.5.4) yields the change in the energy of the system resulting from the addition to (or the subtraction from) it of an electron, and it is exactly in this sense that we can speak of the single-electron energy in the presence of the electron-electron interaction.

In systems with a constant number of electrons, the quantities $\tilde{E}_{k\sigma}$ play an exceptionally important part. In many cases important for practice, there is no need to know the absolute value of the energy of the system. It is enough to know only by what amount it exceeds the energy of the ground state. As a rule, only weakly excited states present any interest in solid-state physics. To describe them, modern physics makes use of the concept of elementary excitations. As applied to a metal, it is formulated as follows. In the ground state of the system the electrons occupy the lowest levels with quasi-momenta below the Fermi quasi-momentum k_F . The excitation of the system consists in the transition of the electron from a state below the Fermi surface having a quasi-momentum $k_{<} < k_F$ to a state lying above it and having a quasi-momentum $k_{>} > k_F$. According to what has been said above, the change in the energy in the result of the transition is equal to

$$\Delta E(k_{>}, k_{<}) = \tilde{E}_{k_{>}, \sigma} - \tilde{E}_{k_{<}, \sigma} \equiv \tilde{E}_{k_{>}, \sigma} + (-\tilde{E}_{k_{<}, \sigma}), \quad (1.5.5)$$

where the energies $\tilde{E}_{k\sigma} = \delta E / \delta n_{k\sigma}$ have been calculated for values of $n_{k\sigma}$ corresponding to the ground state. Such a transition is equivalent to the generation of two Fermi elementary excitations: of an electron above the Fermi surface and of a hole below it. With account taken of the fact that the signs of the energies of the electron and of the hole are opposite, the energy of the excited state (1.5.5) will be the sum of the energies of both elementary excitations. In the same way, the energies of a greater number of pairs of elementary excitations will be additive, if their number is small as compared with the total number of electrons n . Evidently, not only a hole below the Fermi surface will be a quasi-particle that represents the state of

the entire electron ensemble, but an electron above it as well, since its energy depends on the occupation number of other states.

As is seen from (1.5.4), to the first approximation in $U/W \ll 1$ the single-electron energy depends only on the occupation numbers $n_{k\sigma}$, i.e. on the mean field of other electrons. Thus, the conditions for the validity of the band theory are met. But this is not the case for higher approximations where the correlations between electrons become important. In real metals the parameter U/W is of the order of unity, which precludes using the band theory for electrons below the Fermi surface. But it is valid for the electrons and holes appearing in the result of the crystal excitation that, provided their number is small, indeed move independently of each other. The same is true of semiconductors: strictly speaking the energy-band theory is not applicable to the valence band, but adequately describes the electrons in the conduction band and holes in the valence band. In contrast to a metal where the excitation energy may be arbitrarily small ($\Delta E(k_+, k_-) \rightarrow 0$ for $k_+ \rightarrow k_F$, $k_- \rightarrow k_F$), in a semiconductor the excited electrons and holes are separated by an energy gap from the ground state.

The above discussion enables us to establish the fact that the band theory in a crystal is a theory of elementary excitations characterized by a definite quasi-momentum and by a corresponding energy $\tilde{E}_{k\sigma}$. It should, however, be emphasized that in this version, too, the band theory is not universal. As will be demonstrated below, in case of a sufficiently strong electron-electron interaction, the nature of the spectrum of the system considered changes radically as compared to the band spectrum, and it is no longer possible to introduce elementary excitations described by a definite quasi-momentum. The latter statement is not in contradiction with the periodicity of the crystal structure. The quasi-momentum in the single-electron approach appears as a result of the fact that the Hamiltonian is invariant with respect to the translation of the electron by a lattice parameter. But in the presence of electron-electron interaction the Hamiltonian of the system does not possess such a property of symmetry: it is invariant only with respect to a simultaneous translation by a lattice parameter of all the electrons in the crystal.

Now we shall be interested in the limit of a very strong repulsion $U \gg W$. In this case we should choose H_U as the zeroth-approximation Hamiltonian in (1.5.2). Its eigenfunctions differ radically from those of the band Hamiltonian H_B : whereas the corresponding electron states for H_B are extended over the entire crystal, eigenstates H_U are those in which every electron is localized on a definite atom. The energy to the zeroth approximation in W/U will evidently be given by the expression ($n_{g\sigma}$ are the occupation numbers of

states (g, σ)):

$$E_{\mathbb{U}} = \mathbb{U} \sum n_{g\uparrow} n_{g\downarrow}. \quad (1.5.6)$$

Of special interest is the case when the number of electrons is equal to that of the atoms N . The minimum energy for $N = n$ is attained when there is one electron on every atom ($E_{\mathbb{U}} = 0$). The excitation of the system consists in the transfer of an electron to another atom in the result of which an atom without an electron (a "hole") and an atom with two electrons (a "pair") are produced. The minimum excitation energy is equal to the large parameter of the problem \mathbb{U} .

Acted upon by the Hamiltonian H_B , the ground state of necessity goes over to an excited state with one vacant atom (a "hole") and two electrons on its nearest neighbour (a "pair"). At the same time the action of H_B on an excited state does not necessarily result in the appearance of a new hole and a pair: this operator can also transfer a surplus electron or a hole to a neighbouring atom without changing the zeroth-approximation energy.

The transitions of a surplus electron or of a hole from atom to atom are tantamount, as in the conventional band theory, to the charge transport over the crystal. However, in contrast to the band theory, definite quasi-momenta cannot generally be attributed to such quasi-particles, since in case of an arbitrary orientation of spins of electrons located on other atoms the system is not invariant with respect to translations of quasi-particles by a distance equal to a multiple of the lattice parameter (it is invariant only if the spins of all atoms are similarly oriented). Still, the main feature of the band spectrum is retained in this case as well: the ground state is separated by an energy gap from the continuous spectrum represented by a superposition of the "hole" and the "pair" spectra. In fact, the energy-band pattern of such a system at finite temperatures is rather of the type of amorphous semiconductors than of the crystalline. The band edges should in this case be spread, since owing to the randomness of the direction of spins of electrons on different atoms effects of the type of the Anderson localization of charge carriers (Sec. 1.2) are possible. Besides, autolocalized carrier states with lower energies than those of mobile charge carriers (Secs. 5.1 and 5.2) are also possible. More highly excited states are extended, i.e. the mobility gap is wider than the gap in the energy spectrum.

Whereas the conductive character of the excited states is quite evident, on account of the spin degeneracy of the zeroth-order ground state there may be doubts as to whether it may be a conductive one, too [212]. We could cite qualitative arguments to support the contention that it is an insulating state by considering the screening of an external electric field. The conducting state is characterized

by the fact of the field inside the bulk being zero, because charges whose field compensates the external field are produced on the surface of the specimen. Hence, should the state be a conducting one, the holes would have been drawn away from the pairs to a macroscopic distance (the specimen length) no matter how small the external field. If one constructs the ground-state wave function in the absence of an external field with the help of the perturbation theory in B/U , he will have to include in it states associated with virtual holes and pairs. However, they turn out to be closely-spaced, because the operator H_B transfers the electron to a neighbouring atom (e.g. in the first order in W/U the pair and the hole occupy neighbouring atoms, in the n th order of the perturbation theory the separation between them does not exceed na). A weak field should negligibly perturb the crystal ground state, and for this reason should be unable to cause a macroscopic separation of the virtual pairs and holes. Accordingly, a system, which for $U \ll W$ behaves like a metal, should for $U \gg W$ behave like an insulator.

In [213] the insulating nature of the ground state of such a system has been proved rigorously by means of calculations of the current. Similar results follow from [212] where the current has been calculated in the third order in W/U and in the nearest-neighbour approximation*.

1.6. THE INSULATOR-METAL PHASE TRANSITION

Impurity Semiconductors. The Hubbard model discussed in Sec. 1.5 enables an important conclusion to be drawn. Since for $W \gg U$ a crystal containing equal numbers of electrons and atoms behaves like a metal and for $W \ll U$ —like an insulator, the increase in W/U in the region of $W \sim U$ should be accompanied by a transition of the material from the insulating to the conducting state. Unfortunately, the analysis of the transition character involves great mathematical difficulties, since for $W \sim U$ there is no small parameter in the Hubbard Hamiltonian (1.5.2). Despite the fact that very much has been written on the subject, the problem can by no means be regarded as solved. It is still not clear, whether the transition should take place abruptly or smoothly. It is also possible that in case of the actual interaction between the electrons, which

* The expression for the current in the third order in W/U was regarded by the authors of [212] themselves as a proof that this state is a conducting one. However, a nonzero current is obtained only if the overlapping of orbits of more distant neighbours is taken into account. At the same time this overlapping is of a higher order of smallness than the overlapping of orbits of the nearest neighbours, and because of that its taking into account goes beyond the limits of accuracy of calculations accepted in [212].

is of a long-range character, the transition will be of a different type than in the case of the short-range Hubbard interaction.

Usually one assumes that some light on the properties of such a transition is thrown by Mott's consideration of the stability of the conducting state of an electron system in the Coulomb field of ionized atoms, e.g. of donors in a heavily-doped semiconductor [278]. If the electron Fermi energy is high as compared with the mean energy of electrostatic interaction between the electrons and the donor atoms, the electrons can be regarded in the zeroth approximation as free, and they will screen the donor Coulomb potential as stipulated by the law (1.7.11) (see below). As is well known a potential well of a finite radius that represents a screened Coulomb potential does not always contain discrete levels. The conducting state owes its very existence to this fact: the donor screened potential is too weak to capture an electron. However, as the number of electrons (and the equal number of donors) drops, the screening length r_s grows in accordance with formula (1.7.12). Starting from some critical value of the length r_s , a discrete level appears in the potential well, i.e. delocalized electron states become absolutely unstable, and the electrons tend to become localized each on its particular donor atom. Hence, the transition from the conducting to the insulating state should be an abrupt one. The critical density is determined by the condition for the appearance of a discrete level in the well:

$$\frac{a_B}{r_s} \simeq 1.19, \quad (1.6.1)$$

or, if formula (1.2.2) is taken into account

$$n^{1/3}a_B = C \simeq 0.25. \quad (1.6.2)$$

Comparison with experiment demonstrates a good agreement of this criterion with experimental data on the delocalization of electrons of donors in germanium and silicon [278]. Unfortunately, this much-cited argument cannot be accepted as good proof, as the criterion (1.6.1, 2) has been obtained from expression (1.7.12) valid only in the opposite limiting case $n^{1/3}a_B \gg 1$. Moreover, there are certain doubts whether Mott's arguments are correct, since they lead to an erroneous conclusion that two- and one-dimensional systems should always be insulating even if they are ideally ordered. This fault seems to stem from Mott treating the one-centre problem instead of the initial many-centre one, the equivalence of both being by no means self-evident. For this reason the criterion (1.6.1, 2) should rather be regarded as an empirical one.

We could try to clarify the problem of the nature of the insulator-metal transition by analyzing experimental data. However, if the transition takes place in a disordered system of the type of impurity

atoms in heavily-doped semiconductors, the effect will be complicated by the randomness of the impurity distribution. Even if the transition would take place abruptly in an ordered system, it may take place smoothly in a disordered one, since the transition criteria will not be satisfied simultaneously for different atomic groups, and the Anderson localization contributes to this. It has been established in studies of the transition of doped germanium and silicon to the conducting state that the transition, although continuous, is a very sharp one. Thus, according to [298], the conductivity-activation energy ΔE of phosphorus-doped silicon vanishes with the growth of phosphorus density at $n_c = 3.7 \times 10^{18} \text{ cm}^{-3}$, with the conductivity becoming a metallic one. On the insulating side ΔE grows steeply with the decrease in n from the critical value n_c in accordance with the law $(n_c - n)^{3/4}$. A proof that the insulator-metal phase transition in the Si : P system is a very steep one has also been obtained by measuring its resistivity in [564].

For continuous transitions of the type of phase transitions of the second kind quite common are exponents less than or close to unity, so that results [298] probably indicate, together with those of [564], that in an ordered system the transition would be an abrupt one. It is still not quite clear whether the transition is accompanied by the formation of an impurity band separated by a gap (or by a pseudo-gap) from the conduction band followed by a subsequent merger of the former with the latter at greater n 's, or whether there is no gap between the bands at all $n > n_c$. In Mott's opinion [278], there are experimental indications in favour of the former version.

It is interesting to note that a very sharp transition from the insulating to the conducting state has been observed in the course of variation of the component ratio in metal-inert gas films of the Cu-Ar type, despite the fact that such systems are strongly disordered [299]. However, this result is questioned in [300] where it has been established that in kindred Rb-Kr and Cs-Xe systems the transition takes place smoothly.

Transitions under Pressure and Mixed-valency Materials. Important information may be gained from studies of the insulator-metal transition in magnetic semiconductors under pressure when it takes place without changes in the crystal structure. Normally, very high pressures are required for this (~ 1 Mbar for NiO [304], 300 kbar for EuO [305]), but in some materials relatively low pressures do the job, and this facilitates detailed studies of the effect. An abrupt drop in resistivity with increasing pressure has been observed in SmS at $T = 300$ K when the pressure reached 6.5 kbar (Fig. 1.2 [301]). The jump in the resistivity was relatively small: about five times, this being possibly due to a small gap width in the semiconducting state (0.06 eV [308]). A pressure increase to 6.5 kbar reduces the crystal volume by about 12%. Hence, the conductivity jump may be

associated with the increasing overlapping of the orbits of neighbouring atoms resulting in the delocalization of localized f -electrons. The existence of a resistivity hysteresis (the reverse transition takes place at $p < 1$ kbar) proves that at pressures below 6.5 kbar the high-conductivity state can exist as a metastable one.

However, in isomorphous compounds SmSe and SmTe the transition to the conducting state at 300 K took place continuously, terminating

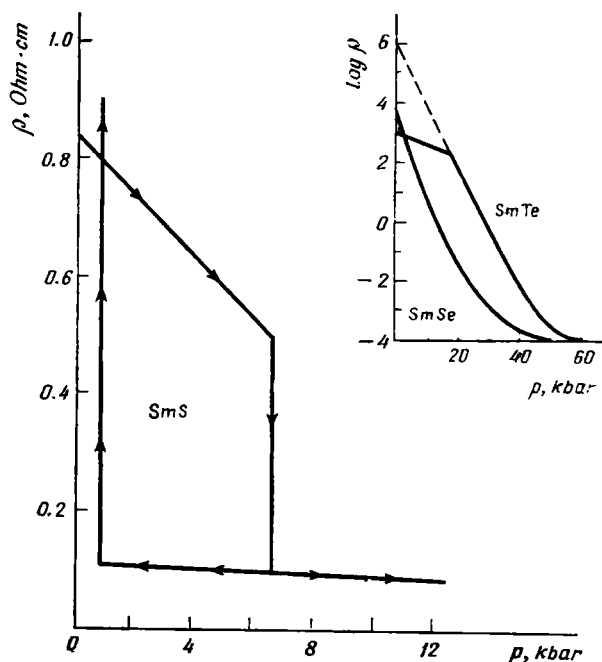


Fig. 1.2. Resistivity vs. pressure for SmS at 300 K. Insert: same for SmSe and SmTe [301]

at pressures of the order of 50 to 60 kbar with a change in conductivity by seven orders of magnitude. It may be presumed that such a difference in behaviour of samarium chalcogenides is due to the insulator-metal phase-coexistence curve on the phase diagram in the p - T plane terminating with a critical point (T_{cr} , p_{cr}). If the transition under pressure takes place at a temperature below T_{cr} , the coexistence curve will be intersected by the line of transition I , and the conductivity should experience a jump. If on the other hand the temperature is above T_{cr} , the concept of different phases becomes meaningless, and the resistivity changes along the line II continuously with the pressure (Fig. 1.3). The existence of a critical point for

SmS has already been proved, with the corresponding critical temperature being $T_{cr} = 800$ K [306]. Since the measurements in [301] were carried out at $T = 300$ K, the condition $T < T_{cr}$ for SmS has been satisfied, but it is possible that this was not the case for other samarium chalcogenides.

A behaviour qualitatively similar to that of SmS has been observed in the studies of V_2O_3 in which the transition from the insulating to the conducting state at 4.2 K took place at a pressure of 26 kbar with the reverse transition taking place at 23 kbar [302].

Judging by all those experimental data, it seems more probable that the transition from the insulating to the conducting state caused by an increase in overlapping of orbits of neighbouring atoms takes place abruptly. At a certain degree of overlapping, the energy terms corresponding to the conducting and to the insulating state may be expected to intersect.

Very little is known about the nature of the conducting state in the vicinity of the insulator-metal transition point. Probably, it is quite different from that described by the band theory. For instance, it has been established that the transition of Sm chalcogenides to the conducting state is accompanied by the delocalization of only one f -electron at every Sm ion, and even this is incomplete: whereas in the insulating phase the Sm ions are in a doubly charged state, in the conducting state they oscillate between the doubly and the triply charged state. Accordingly, Sm behaves like a chemical element with a valency of between 2 and 3. According to data presented in the review [289], it is equal to 2.7, although some authors are of the opinion that valency fluctuations in mixed-valency compounds are much less, e.g. according to [400], the valency of Sm is 2.85.

An additional point to be made is that in mixed-valency materials, as in transition metals of the platinum type, the proportionality factor between the electron specific heat and the temperature is abnormally great: it is by 1-2 orders of magnitude greater than in simple metals of the sodium type [289]. In terms of the band theory, it may be said to be proportional to the density of states on the Fermi surface, i.e. the latter should be abnormally great. The absence of magnetic ordering in mixed-valency materials, despite the fact that they contain Sm^{3+} ions with a nonzero moment, and that delocalized electrons should carry out indirect exchange between the ions,

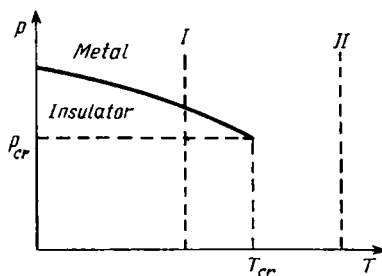


Fig. 1.3. A critical point on the insulator-metal coexistence curve: I, region of abrupt transition; II, region of gradual transition

should also be regarded as an anomaly. By the absence of a magnetic ordering such materials also resemble platinum [601].

Transition-metal Compounds. There is another important aspect of the problem of the insulator-metal transition worth considering: there are several materials, which at low temperatures behave like insulators, but at higher temperatures go over to the metallic conductivity state. Practically all of them belong to compounds of transition or rare-earth elements and should accordingly be classified

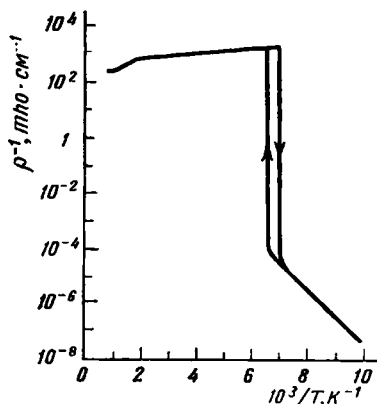


Fig. 1.4. Conductivity vs. temperature for V_2O_3 [278]

as magnetic semiconductors. However, many of them do not exhibit any magnetic ordering at all either in the metallic or the insulating state (e.g. VO_2 , Ti_2O_3 , despite the fact that the V^{4+} and Ti^{3+} ions have each one d -electron, i.e. their spin is nonzero). In the materials in which magnetic ordering can be detected, it appears as a rule at temperatures much below the insulator-metal transition point T_m (e.g. in V_4O_7 with $T_m = 250$ K the antiferromagnetic ordering sets in at 40 K). There are exceptions to this rule. For instance, in V_2O_3 the transition to the insulating state at 150 K is accompanied by the appearance of an antiferromagnetic

ordering with small sublattice moments*.

In some materials a change in the spin state of the transition-element ions takes place below the insulator-metal transition point, e.g. in $LaCoO_3$ with $T_m = 1210$ K the Co^{3+} ion goes over from the state with the $S = 1$ spin to the zero-spin state [252, 253].

In the majority of cases the insulator-metal phase transitions are of the first kind. The magnitude of the conductivity at temperatures below T_m , as in conventional semiconductors, is strongly dependent on the degree of the crystal imperfection. This causes the conductivity jump at the transition point to vary from specimen to specimen. In any case, it may be as high as 7 orders of magnitude (V_2O_3 , see Fig. 1.4 taken from [278]).

Such phase transitions are accompanied by small lattice deformations. Normally, the lattice symmetry is lower in the insulating phase than in the conducting. For instance, a doubling of the lattice parameter is observed in VO_2 when it goes over to the insulating state. In some materials, e.g. in titanium oxides, the lattice symmet-

* All data, unless specified, are cited from the review [427], see also [571].

ry remains unaltered following the transition to the insulating state, but the lattice parameter grows. Pressure can both raise the transition temperature (VO_2) and lower it (V_2O_3).

There are also materials in which the insulator-metal phase transition belongs to the second kind. Thus, in the spectrum of $\text{Cd}_2\text{Os}_2\text{O}_7$ at 200 K there appears a gap between the valence and the conduction band, which as the temperature lowers becomes as wide as $\simeq 0.07$ eV [307].

In materials that display a phase transition of the first kind the gap closes abruptly. In the insulating phase the gap may be quite wide (0.6-0.7 eV in VO_2). However, in magnetite (Fe_3O_4) with $T_m = 119$ K the gap in the optical absorption spectrum does not close [287].

Obviously, the transition in magnetite is of a more complex character than in kindred materials. It has been presumed formerly that such a transition constitutes simply an order-disorder transition in the $\text{Fe}^{2+}\text{-Fe}^{3+}$ ionic system (Verwey mechanism). However, recent research had demonstrated that a very important part in the transition is played by the deformation of the lattice resulting in a change in its symmetry [165, 221]. Besides, the transition turned out to be a many-stage one extending over an entire temperature interval [103].

Theories of the Insulator-metal Transition. In the absence of information about the ground state of a system of strongly interacting electrons it is impossible to construct a consistent theory of insulator-metal transitions. Several mechanisms for the insulator-metal transition have been suggested, but all of them are still at best hypothetical, and neither can explain the variety of phenomena taking place in the course of insulator-metal transitions. Such mechanisms may be subdivided into two groups: (1) the insulator-metal phase transition is an intrinsic one, i.e. it is due first and foremost to a change in the state of the electrons, the changes in other physical quantities (e.g. of the lattice parameters) being a follow-up; (2) the phase transition is an improper one, i.e. it constitutes a phenomenon accompanying another phase transition induced by a change in some other parameter.

First to be classified as belonging to the first group should be the exciton insulator model [278]. It postulates a small overlapping of the conduction and the valence band whose extrema lie at different points of a Brillouin zone. Hence, at $T = 0$ the conduction band will contain a number of electrons from the valence band, and the valence band will contain an equal number of holes. Such a crystal should behave as a semimetal, were it not for the Coulomb attraction of the electrons to the holes. The latter results in the formation of excitons (to be more exact, of a coherent state of electron-hole pairs similar to the state of electron pairs in a superconductor). To free an electron or a hole from the exciton condensate, energy has to

be spent. This means that a gap has appeared in the crystal energy spectrum, which in the absence of Coulomb interaction between the electrons and holes would be gapless. When the crystal is heated, the excitons dissociate, and the crystal goes over to the conducting state. In a simple isotropic band model, the insulator-metal phase transition is always of the second kind, but with adequate anisotropy it may become a first kind one [104].

In principle, the exciton model allows antiferromagnetic ordering, if the dominant part is played by triplet excitons with antiparallel spins of the electrons and holes [12]. This fact gives grounds for hopes that it will be possible to describe the properties of V_2O_3 in terms of it.

It has been suggested in [96] that the insulating state is produced from the metallic as a result of the crystal-lattice deformation. If its period is doubled, a gap appears in the centre of the conduction band, with the lower part of the band moving downwards and the upper part upwards. In case the numbers of electrons and of atoms are equal, only the lower subband is filled, and accordingly the doubling of the lattice period should reduce the electron energy. On the other hand the deformation of the lattice increases its elastic strain energy. The equilibrium value of the deformation parameter is determined from the condition that the total energy of the system made up of the sum of the elastic-strain and the electron energy be minimum. However, estimates [427] show a gain in the energy due to lattice deformation being possible only for unrealistically small conduction-band widths (<0.1 eV). This casts doubts on the principal idea of the paper [96].

Strictly speaking, the models described above from the outset are applicable only to crystals without partially filled d - or f -shells in the insulating state, whereas in fact such shells are typical of materials displaying the insulator-metal transition. An attempt to overcome this drawback was made in [65]. There it was presumed that the energy spectrum of the crystal consists of d -type (or f -type) atomic levels and a conduction band. In the ground state all electrons occupy atomic levels, with the conduction band being empty. As temperature rises, the electrons begin to go over to the conduction band, the transition being facilitated by the Coulomb attraction between the electrons and the holes remaining on atomic levels, which lowers the conduction-band bottom. In case of a sufficiently great number of carriers the result can be the disappearance of the gap in the energy spectrum. No account is taken of the electron-hole pairing, since in contrast to an exciton dielectric there are no electrons and holes at $T = 0$, and at finite temperatures the excitons dissociate. Other assumptions made in [65] are less obvious: (1) the interaction between the charge carriers of the same sign is accounted for only by the prohibition of their joint occupation of the same atom and (2)

the conduction-band width is presumed to be negligibly small as compared to the other energy parameters.

All the models described above that allow an intrinsic insulator-metal transition presume the gap to be narrow at $T = 0$, and accordingly the change in the resistivity following the transition should be relatively small. It is easier to explain a large jump, if the transition is presumed to be an improper one. In particular, an improper insulator-metal transition can take place in the result of polymorphic transformations of crystals (of course, they are not always accompanied by changes in the conductivity type). The cause of polymorphic transformations is a more rapid decline with growing temperature of the free energy F_1 of that structural modification, which is unstable at $T = 0$, with the result that starting from some temperature F_1 becomes less than the free energy F_0 of the modification stable at $T = 0$.

In many cases the temperature dependence of the free energy is determined by its phonon part F_{ph} :

$$F_{ph} = T \sum_k \ln (1 - e^{-\omega_k/T}). \quad (1.6.3)$$

At a specified temperature F_{ph} is the lower the lower the phonon frequencies ω_k . Because of that a polymorphic transformation can be stimulated by lattice softening in the high-temperature phase. (This statement should not be taken to mean that in the high-temperature phase there must always be a "soft" mode whose frequency tends to zero as the transition point is approached. It may be enough for the Debye temperature of the high-temperature phase to be lower than that of the low-temperature phase.) The proof of the feasibility of the mechanism described above is that the phonons in the metallic phase of VO_2 are "softer" than in the insulating phase [303]. However, such mechanism can hardly be a universal one. Thus, there are as yet no reasons to suppose that it operates in magnetite where the energy of optical phonons is practically unaffected by the transition [288].

In principle, a situation is possible when the insulator-metal transition is occasioned entirely or in part by the imperfections of the crystal lattice. To begin with, imperfections can facilitate polymorphic transformation. Their presence raises the crystal entropy. If in the result of a phase transition the lattice softens, the formation of imperfections in it is facilitated. Hence, the density of imperfections in the high-temperature phase should be higher than in the low-temperature one, this additionally decreasing the difference $F_1 - F_0$. The contribution of the imperfections to the free energy of V_nO_m -type compounds can be quite noticeable, since in cases when different valence states of the cations are possible, the number

of such imperfections as vacancies can be quite great (such materials display a tendency to form nonstoichiometric structures).

On the other hand, an abrupt rise in the number of imperfections in the course of a phase transition of the first kind can itself result in the transition of the crystal to the conducting state, even though such transition does not result in a radical reconstruction of the electron states of the crystal as a whole. Indeed, in many cases the imperfections behave as donors and acceptors (e.g. oxygen vacancies in VO are doubly charged donors). If the number of imperfections in the low-temperature phase is small, and the condition for the delocalization of their electrons (1.6.2) is not met, the conductivity in this phase will normally be of the semiconducting type. However, following the transition to the high-temperature phase, the density of imperfections may grow so much that their electrons will be delocalized, and the crystal will turn into a degenerate semiconductor with a metallic-type conductivity. The delocalization can also be caused by an increase in the radius of the impurity state, if for some reason or other such an increase takes place.

However, a polymorphic transformation is not a necessary condition for the delocalization of donor electrons: a normal smooth rise in the number of imperfections with the temperature may prove enough. In that case starting from some temperature, the Mott criterion (1.6.2) will be fulfilled, and the crystal will become conducting without a substantial change in its general state [406].

It is most probable that the insulator-metal transition due to the delocalization of imperfection electrons will take place at high temperatures. The possibility of such a mechanism in Fe_3O_4 follows from the existence of an energy band gap in the metallic phase, although this is not the only possible interpretation of this fact.

A mechanism for the insulator-metal transition based on the idea, that, because of interaction between the Frenkel excitons and the optical phonons, the exciton mode becomes unstable at high temperatures, has been suggested in [210]. The electrons on the other hand are supposed to interact strongly with the excitons, so that a jump in the exciton density following the disappearance of the gap in their spectrum results in a jump in the charge-carrier density that can be arbitrarily high. The model employed in [210] is oversimplified. Nevertheless, it is to be expected that the sound idea on which [210] is based will be substantiated by calculations on more realistic models as well.

Another variant of the electron-exciton mechanism has been discussed in [318]. There it was presumed that the transition takes place in the result of closing of the gap separating the valence band constructed of anionic p -orbits and the conduction band constructed of cationic s -orbits. At the same time the delocalization of the electrons of the internal partially-filled d - (or f -) shells of cations does not

take place in the course of the transition to the metallic state. The cause of the gap closing is the exchange interaction between the electrons and the Frenkel excitons that are born on cations as a result of the change in the state of their d -electrons. This interaction in turn decreases the exciton frequency, i.e. the growth in the number of conduction electrons is accompanied by a growth in the number of excitons, and vice versa. Depending on the parameters of the system, the phase transition may be both of the first and the second kind.

The transition of degenerate FMS and AFS to the insulating state is discussed in Chapter 7.

1.7. HEAVILY-DOPED SEMICONDUCTORS

In case of high donor density n when the mean separation between neighbouring imperfection $n^{-1/3}$ is small as compared with the Bohr radius a_B , great overlapping of orbits of neighbouring donor atoms brings about the delocalization of their electrons. The electron wave functions get extended over the entire crystal, and the donor levels become spread out and form an impurity band that merges with the conduction band. The physical reason for this is that the potential of positively charged imperfections causes the conduction band to move downwards, the donor level thus rising above its bottom. As a result the donor electrons occupy the states inside the conduction band, with the crystal conductivity type changing from the semiconducting to metallic. In respect to their carrier concentrations, the heavily-doped semiconductors correspond to the semimetals. However, they differ from the conventional semimetals in that their structure is highly imperfect, because of the random distribution of donors in the crystal, and that they have charge carriers of only one sign (in semimetals the numbers of electrons and of holes are equal).

The Fermi energy μ of carriers measured from the bottom of the conduction band is determined by the equality easily obtained from (1.2.10)

$$\mu = \frac{(3\pi^2 n)^{2/3}}{2m^*}. \quad (1.7.1)$$

If the spins of the electrons are completely polarized, their Fermi energy μ_F is $2^{2/3}$ times μ (1.7.1).

Making use of expressions (1.7.1) and (1.2.2), one may easily establish the equivalence of the criterion of heavy doping

$$a_B n^{1/3} > 1 \quad (1.7.2)$$

and of the inequality

$$\mu \gg \frac{e^2 n^{1/3}}{\epsilon_0}. \quad (1.7.3)$$

The latter has an obvious physical meaning: the Fermi energy is great as compared with the average energy of Coulomb interaction between the electrons or between the electrons and the donors. It follows from (1.7.3) that the conduction electrons on the Fermi surface are rather insensitive to the electrostatic potential of the impurity.

For a correct description of the effect on the electron of the static electric field Φ_q , in particular, of the field of imperfections, one should determine the static dielectric function of the spatially homogeneous medium $\varepsilon(q)$, taking account of the spatial dispersion. By definition, a Fourier-transform Φ_q of a static external field potential is connected with a Fourier-transform φ_q of the potential acting on the electrons by means of the relationship

$$\varphi_q = \Phi_q / \varepsilon(q), \quad \varphi_q \equiv \varphi(q) = \int e^{iq \cdot r} \varphi(r) dr. \quad (1.7.4)$$

An expression for $\varepsilon(q)$ of a degenerate electron gas in the long-wave limit $q \rightarrow 0$ can be easily obtained by means of a self-consistent procedure. If a field $\varphi(r)$, a function of coordinates, acts on the electrons, in equilibrium conditions (i.e. in the absence of a current) the electrochemical potential will be constant throughout the crystal

$$\mu(r) + e\varphi(r) = \mu, \quad (1.7.5)$$

where μ is the zero-field chemical potential, and the local Fermi energy of the carriers $\mu(r) = \mu + \Delta\mu(r)$ is connected with their density at the same point $n(r)$ by means of relation (1.7.1). It is understood that a spatially nonuniform distribution of the electron density is caused by a spatially nonuniform field $\Phi(r)$.

Taking only the linear terms of expression (1.7.5) and going over to Fourier-transforms of the density and the potential, we obtain the relationship between them

$$n(q) = -\frac{3}{2} \frac{en}{\mu} \varphi_q = -e\varphi_q \frac{dn}{d\mu}. \quad (1.7.6)$$

The field φ_q acting on the electrons is made up of the field Φ_q and the field $\delta\varphi_q$ set up by the electrons redistributed by Φ_q . With account taken of (1.7.4) we obtain the relation

$$\delta\varphi_q = \left[1 - \frac{\varepsilon(q)}{\varepsilon_0} \right] \varphi_q. \quad (1.7.7)$$

The polarization potential of the electrons $\delta\varphi_q$ is connected with their density by means of Poisson's equation (this is what self-consistency amounts to)

$$q^2 \delta\varphi_q = \frac{4\pi e}{\varepsilon_0} n(q). \quad (1.7.8)$$

Taking account of (1.7.7) one can rewrite equation (1.7.8) in the form

$$n(\mathbf{q}) = -\frac{q^2}{4\pi e} [\varepsilon(\mathbf{q}) - \varepsilon_0] \varphi_{\mathbf{q}}. \quad (1.7.8')$$

Expressing $n(\mathbf{q})$ in formula (1.7.8') in terms of $\varphi_{\mathbf{q}}$ from (1.7.6), we obtain the following formulae for the dielectric function:

$$\frac{\varepsilon(\mathbf{q})}{\varepsilon_0} = 1 + \frac{\kappa^2}{q^2}, \quad (1.7.9)$$

$$\kappa^2 = \frac{6\pi e^2 n}{\varepsilon_0 \mu} = \frac{4\pi e^2}{\varepsilon_0} \frac{dn}{d\mu}. \quad (1.7.10)$$

For the Coulomb external potential, we obtain making use of expression (1.7.9)

$$\varphi(\mathbf{r}) = \frac{4\pi e}{\Omega} \sum \frac{e^{i\mathbf{q} \cdot \mathbf{r}}}{q^2 \varepsilon(\mathbf{q})} = \frac{4\pi e}{\Omega \varepsilon_0} \sum \frac{e^{i\mathbf{q} \cdot \mathbf{r}}}{q^2 + \kappa^2} = \frac{e}{\varepsilon_0 r} \exp(-\kappa r). \quad (1.7.11)$$

Hence, the meaning of κ in formulae (1.7.9, 11) is that of the inverse screening length r_s .

It follows from (1.7.1), (1.2.2) that the screening length $r_s = \kappa^{-1}$ can be represented in the form

$$r_s \simeq \frac{1}{2} \sqrt{\frac{1}{a_B n^{-1/3}}}. \quad (1.7.12)$$

In conditions when the inequality (1.7.2) is satisfied, the screening length exceeds the mean separation between the imperfections, but is small in comparison with the Bohr radius.

Although the spatial fluctuations of the electrostatic potential due to the random distribution of impurity atoms exercise little effect on the state of fast electrons in heavily-doped semiconductors, they exercise a very strong influence on the states of slow electrons. A fluctuating potential results in the spreading out of the conduction-band bottom, with the electron density-of-states tail appearing in the band gap. In the region of energies not too far from the conduction-band bottom the density-of-states tail energy dependence is described by the expression [297, 183, 184]:

$$g_{\bullet}(E) \sim \exp \left\{ -\frac{(E - E_c)^2}{E_f^2} \right\}, \quad (1.7.13)$$

$$E_f \sim \frac{e^2}{\varepsilon_0} n^{1/2} r_s^{1/6}. \quad (1.7.14)$$

The expression obtained for $\varepsilon(\mathbf{q})$ enables the conductivity σ of a heavily-doped semiconductor at temperatures not too high, when the dominant scattering mechanism is the scattering by charged donors, to be calculated. Since condition (1.7.3) is presumed to be satisfied, and since the scattering of electrons by imperfections is

elastic, standard results of the kinetic theory may be used for the conductivity:

$$\sigma = neu, \quad u = \frac{e\tau(\mu)}{m^*}. \quad (1.7.15)$$

The electron-relaxation transport time in case of scattering by imperfections τ , which enters the expression for the conductivity, is given by the formula

$$\tau^{-1}(E_{\mathbf{k}}) = \sum W_{\mathbf{k}\mathbf{k}'} \left(1 - \frac{\mathbf{k} \cdot \mathbf{k}'}{k^2}\right), \quad (1.7.16)$$

where $W_{\mathbf{k}\mathbf{k}'}$ is the probability of the electron transition per second from the state with a quasi-momentum \mathbf{k} to the state with a quasi-momentum \mathbf{k}' of the same length ($k = k'$). In the Born approximation it is given by the expression

$$W_{\mathbf{k}\mathbf{k}'} = 2\pi e^2 |\varphi(\mathbf{k} - \mathbf{k}')|^2 n \delta(E_{\mathbf{k}} - E_{\mathbf{k}'}), \quad (1.7.17)$$

where $\varphi(\mathbf{q})$ is a Fourier-transform of the screened potential of a charged imperfection (1.7.11). Because of the random distribution of the imperfections in the crystal, each of them scatters the electron independently of the others, and for this reason the electron scattering probability is proportional to the number of donors, which is equal to that of the electrons.

Substituting (1.7.17) into (1.7.16) and performing simple integrations, we obtain the Brooks-Herring formula:

$$\tau^{-1}(E_{\mathbf{k}}) = \frac{2\pi e^4 n m^*}{\epsilon_0^2 k^3} \left\{ \ln(1 + \eta) - \frac{\eta}{1 + \eta} \right\}, \quad (1.7.18)$$

where $\eta = 4k^2/\kappa^2$.

On the Fermi surface (i.e. for $k = k_F = \sqrt{2m^*\mu}$) the parameter η should be large. Indeed, since $k_F \simeq 3n^{1/3}$, it follows that

$$\eta(k_F) \simeq 36(n^{1/3}r_s)^2$$

and $r_s n^{1/3}$ in accordance with the condition for heavy doping should substantially exceed 1. Hence, up to logarithmic accuracy $\tau(\mu)$ (see (1.7.18)) grows with μ for constant n as $\mu^{3/2}$ (μ can be increased by polarizing the electron spins).

MAGNETIC PROPERTIES
OF INSULATING CRYSTALS

2.1. THE HEISENBERG HAMILTONIAN

A peculiar feature of magnetic insulators discussed in this chapter is the localization of each electron responsible for the crystal magnetic properties on the appropriate atom. Due to exchange interaction between the electrons belonging to the same atom, their spins unite to form a single spin S . In the simplest case the rotation of the atomic spin does not result in a change in the orbital state of its electrons. In that case the state of the atom will be completely determined by the direction of its spin, i.e. it can be described by means of a wave function containing only the spin variable. The expression for a wave function describing the state of the atom g with the spin projection S_g^z equal to m is as follows

$$|m\rangle = \delta(S_g^z, m), \quad (2.1.1)$$

where the delta-function of a discrete argument $\delta(k, l)$ is equal to 1 for $k = l$ and to 0 for $k \neq l$. Here S_g^z is a variable running through all the $2S + 1$ values allowed to it, and m is a fixed quantity having the meaning of an index of state.

The spin operators $S_\pm = S_x \pm iS_y$ acting on the wave function obey the commutation relations

$$S_g^+ S_g^- - S_g^- S_g^+ = 2S_g^z, \quad S_g^\pm S_g^z - S_g^z S_g^\pm = \mp S_g^\pm. \quad (2.1.2)$$

Applying them, one can easily obtain the formulae

$$S_g^+ \delta(S_g^z, m) = \sqrt{(S - m)(S + m + 1)} \delta(S_g^z, m + 1), \quad (2.1.3)$$

$$S_g^- \delta(S_g^z, m) = \sqrt{(S + m)(S - m + 1)} \delta(S_g^z, m - 1). \quad (2.1.4)$$

Typically, the interatomic magnetic interaction is of the exchange type, i.e. it is a function solely of the angle the atomic spins make with each other. The simplest Hamiltonian that describes this interaction is of the form

$$H = -\frac{1}{2} \sum_{g, f} J(g-f) (S_g \cdot S_f) - \sum_g (\mathcal{H} \cdot S_g), \quad (2.1.5)$$

where the external field \mathcal{H} is expressed in energy units, i.e. it has been multiplied by the double Bohr magneton.

Specifically, under the additional condition $n_{g\uparrow} + n_{g\downarrow} = 1$, the Heisenberg Hamiltonian (2.1.5) may be obtained directly from the Hamiltonian (1.5.1), if one puts $B = 0$ and makes use of the electron spin operator [212]

$$s_g^i = \sum_{\sigma\sigma'} (s^i)_{\sigma\sigma'} a_{g\sigma}^* a_{g\sigma'}, \quad (2.1.6)$$

where s^i are Pauli matrices:

$$s^x = \frac{1}{2} \begin{vmatrix} 0 & 1 \\ 1 & 0 \end{vmatrix}, \quad s^y = \frac{i}{2} \begin{vmatrix} 0 & -1 \\ 1 & 0 \end{vmatrix}, \quad s^z = \frac{1}{2} \begin{vmatrix} 1 & 0 \\ 0 & -1 \end{vmatrix}.$$

Hereby it can be established that the exchange integral $J(g-f)$ together with the quantity $\mathfrak{U}(f, g | g, f)$ in (1.5.1) is of the second order of magnitude in the overlapping of orbits of neighbouring atoms.

2.2. MAGNETIC INTERACTION IN REAL MATERIALS AND NON-HEISENBERG HAMILTONIANS

Small Crystal Fields. In Sec. 2.1 we discussed the most simplified model of a magnetic system.

In actual conditions the interaction between the magnetic moments frequently turns out to be more complex, and it is not always possible to describe it by means of the Heisenberg Hamiltonian (2.1.5). There are three reasons for this. Firstly, the Hamiltonian (2.1.5) does not take full account of the interaction between spins, even when they may be regarded as free in the sense that the spin rotation does not change the orbital state of the electrons in the magnetic atom. Secondly, strictly speaking the spins in a crystal are not completely free, since they are acted upon by the anisotropic electrostatic field of the crystal. Thirdly, the electron orbital angular momentum may contribute to the total atomic angular momentum in addition to the electron spins.

Let us begin with non-Heisenberg interaction of free spins. As there is no preferential direction in space, the Hamiltonian should be invariant under simultaneous rotation of all the spins. The Heisenberg Hamiltonian is just a particular instance of an isotropic exchange Hamiltonian, since the spin scalar products are rotationally symmetric. In the simplest case of a two-atom system the latter is represented by a 2st degree polynomial in the scalar product of the spins of the two atoms [370] (higher powers of the scalar product need not be included in it, because they are expressed in terms of the lower: e.g. for a spin $S = 1/2$, the product of two spin projections, according to (2.1.6), is expressed either in terms of the third projection or in terms of a unit matrix). The situation is still more complex

in many-atomic systems where, besides bispin terms (i.e. of the $(\mathbf{S}_1 \cdot \mathbf{S}_2)$ type), four-spin terms (i.e. of the $(\mathbf{S}_1 \cdot \mathbf{S}_2)(\mathbf{S}_3 \cdot \mathbf{S}_4)$ type) etc. appear in the Hamiltonian. Accordingly, in the general case the isotropic exchange Hamiltonian takes the form

$$H_M = - \sum_n \sum_l J_n(\mathbf{r}_1, \dots, \mathbf{r}_{2n})(\mathbf{S}_{l_1} \cdot \mathbf{S}_{l_2}) \dots (\mathbf{S}_{l_{2n-1}} \cdot \mathbf{S}_{l_{2n}}). \quad (2.2.1)$$

In most cases of practical importance the non-Heisenberg part of the Hamiltonian (2.2.1) is small as compared with the Heisenberg one. For instance, in the framework of the Hubbard model (1.5.2) that describes a magnetic insulator for $U \gg W$, the four-spin terms is of the order of $(W/U)^2$ with respect to the Heisenberg ones. However, in certain circumstances the non-Heisenberg terms may become comparable to the Heisenberg ones. For instance, such may be the case, if the Heisenberg exchange integral between nearest neighbours J_1 regarded as a function of the distance between them changes sign in the vicinity of the equilibrium distance, or if different mechanisms of Heisenberg exchange compensate one another. Non-Heisenberg terms appear also as a result of a finite compressibility of the lattice [442]. Indeed if one expands the Heisenberg exchange energy $J(R_1 - R_2)(\mathbf{S}_1 \cdot \mathbf{S}_2)$ in powers of displacement of atoms 1 and 2 from their equilibrium position up to linear term and then eliminates it like in Sec. 1.4 one obtains the term $\sim (\mathbf{S}_1 \cdot \mathbf{S}_2)^2$. Certainly materials with abnormally weak Heisenberg exchange should have abnormally low Curie points as compared with those of kindred compounds.

The magnetic Hamiltonian may have a structure greatly different from a Heisenberg one in case of a specific exchange mechanism between localized spins executed by means of delocalized electrons (conduction electrons etc.). Such a situation will be investigated in Chapter 6. It will be demonstrated in Sec. 4.5 that there are physical systems described by means of a radical Hamiltonian of the $\sqrt{\sum C_{gt}(\mathbf{S}_g \cdot \mathbf{S}_t)}$ type.

In addition to the isotropic interaction Hamiltonian of the $(\mathbf{S}_1 \cdot \mathbf{S}_2)^n$ type, which is independent of the relative directions of the spins $\mathbf{S}_1, \mathbf{S}_2$ and the vector \mathbf{r}_{12} connecting the atoms 1 and 2, one may use the last three vectors to construct an anisotropic Hamiltonian of the $(\mathbf{r}_{12} \cdot \mathbf{S}_1)(\mathbf{r}_{12} \cdot \mathbf{S}_2)$ type. Such an anisotropic term includes the Hamiltonian of the magnetic dipole-dipole interaction. As a rule, the energy of dipole-dipole interaction is by several orders of magnitude less than that of exchange interaction, and for this reason the dipole-dipole interaction practically does not affect the temperature of magnetic ordering. However, there are crystals with extremely low Curie points whose magnetic ordering is induced by dipole-dipole interactions. If the electrons of the partially filled shell have an orbital angular momentum, the coupling between it and the

shell spin may appreciably affect the properties of the magnet. Spin-orbit interaction is described by the Hamiltonian

$$H_{s0} = \frac{\mu_B}{m_0 c} \left\{ \sum_i ([\nabla_i V(\mathbf{r}_i) \times \mathbf{p}_i] \cdot \mathbf{s}_i) + 2e \sum_{i \neq j} r_{ij}^{-3} ([\mathbf{r}_{ij} \times \mathbf{p}_j] \cdot \mathbf{s}_i) \right\}, \quad (2.2.2)$$

where \mathbf{s}_i is the spin of the i th electron, $V(\mathbf{r}_i)$ is the field of all the charges in the crystal acting on this electron. The first term in (2.2.2) describes the interaction between the orbit and the spin of the same electron, the second term describing the interaction of the electron orbit with the spins of other electrons.

Since the relativistic spin-orbit interaction is much less intense than the interatomic exchange interaction, the magnitudes of the total electronic spin \mathbf{S} and of the total orbital angular momentum \mathbf{L} of the shell may be regarded as fixed. Only the directions of those vectors are subject to change. Accordingly, it is frequently much more convenient to use the simplified Hamiltonian H_{s0} acting on functions of L^2 and S^2

$$\tilde{H}_{s0} = \lambda (\mathbf{L} \cdot \mathbf{S}) \quad (2.2.3)$$

instead of the Hamiltonian (2.2.2). The spin-orbit coupling constant λ may be of any sign.

Spin-orbit coupling (2.2.3) partially removes the degeneracy with respect to the directions of the spin and the orbital momentum of the partially-filled-shell energy levels. Specifically, according to (2.2.3), only states with the same total angular momentum $\mathbf{J} = \mathbf{L} + \mathbf{S}$ have the same energy. The angular momentum may assume the values $J = |L + S|, \dots, |L - S|$. However, the degeneracy in the directions of the vector \mathbf{J} still remains.

The situation is the simplest in the case of ions with the zero orbital momentum L , i.e. in the absence of the multiplet splitting according to J values (e.g. the Eu^{2+} and Gd^{3+} ions in the ${}^8S_{7/2}$ state). The crystal field acts on the spins of the magnetic atoms mainly via spin-orbital coupling, which is nonexistent in ions with $L = 0$. For this reason the magnetic moments of such ions behave in the crystal like free spins.

The existence of a nonzero orbital angular momentum plays an especially important part in the magnetic properties of rare-earth ions. Typically, they have high values of the spin-orbit coupling constant λ (from 0.07 eV for Ce^{3+} to 0.35 eV for Yb^{3+} [366]). The effect of the crystal field on the states of the f -electrons is usually much less than that of the spin-orbit coupling, since this field is almost completely screened by the electrons of the outer shells. The energy of exchange interaction with neighbouring ions is also

low as compared with the spin-orbit energy. For this reason the state of the magnetic ions is determined first and foremost by their total angular momentum J . The degree in which spin-orbit coupling may affect the magnetic properties of the ions may be furnished from the following example. The Eu^{3+} ion with the spin $S = 3$ has the same value of the orbital angular momentum $L = 3$, and in the ground state the total angular momentum of this ion is zero. Thus, an ion with a nonzero spin turns out to be nonmagnetic.

If the effect of the crystal field on the f -electrons is much less than that of the interatomic exchange, it is in principle possible to construct a Hamiltonian of isotropic exchange interaction between the atoms in which the operators of the total angular momentum will stand in place of the spin operators. Considering the indirect exchange in magnetic metals, de Gennes [337] suggested that the Heisenberg Hamiltonian (2.1.5) could be generalized for the case $L \neq 0$ by replacing the spin S_i by its average projection on the total angular momentum vector \mathbf{J}_i equal to $(g_J - 1) \mathbf{J}_i$, where g_J is the Landé factor for the operator \mathbf{J}_i itself

$$H_M = -\frac{(g_J - 1)^2}{2} \sum \mathcal{J}(\mathbf{f} - \mathbf{g}) (\mathbf{J}_g \cdot \mathbf{J}_f), \quad (2.2.4)$$

$$g_J - 1 = \frac{(\mathbf{J} \cdot \mathbf{S})}{J^2} = \frac{J(J+1) - L(L+1) + S(S+1)}{2J(J+1)}. \quad (2.2.5)$$

References [338, 339] contain arguments in favour of the Hamiltonian (2.2.4, 5) as applied to magnetic metals and corrections to it, which in practice turn out to be rather great. The Hamiltonian (2.2.5) may also be used for insulators.

High Crystal Fields. In the opposite limiting case, when the splitting of electron levels in the crystal field, although small in comparison with the spacing between the components of a spin orbit multiplet, is great in comparison with the interatomic exchange energy, the crystal field radically changes the nature of the exchange interaction between magnetic atoms. The details of the picture depend on the crystal-field symmetry, on the sign of the spin-orbit coupling constant and on other factors. It takes, in particular, a quite different aspect in the case of ions with an even number of electrons in the f -shell and in the case of an odd number.

In the case of ions with an odd number of electrons, the crystal field, while removing the degeneracy in directions of the total momentum \mathbf{J} , leaves in accordance with Kramers theorem, the ion ground state at least doubly degenerate. If, for example, the ion ground state is doubly degenerate, it will behave in respect of the crystal magnetic ordering as an ion with the angular momentum of $1/2$ and not as one with the momentum of J . Thus, the crystal field reduces the effective moment of an ion with $J > 1/2$. The corresponding magnetic Hamiltonian differs from the Heisenberg one by a high degree of anisotropy.

The freezing of the moment makes itself still more manifest in atoms with an even number of electrons. In them the crystal field may turn the ion ground state into a singlet one, so that the average value of the moment in the ground state will turn zero. For example, the lowest spin-orbit-multiplet component of the Pr^{3+} ion with a $4f^2$ configuration is 3H_4 . In a field with a cubic symmetry its nine-fold degenerate level splits into a singlet Γ_1 , a triplet Γ_4 separated by a distance $\omega \sim 10^{-3}$ eV from the singlet, a doublet Γ_3 and a triplet Γ_5 lying above the singlet by $(12/7)\omega$ and $\sim 3\omega$, respectively [367]. If the splitting ω appreciably exceeds the energy of interatomic exchange, the crystal will have no detectable magnetic order, even though it contains ions with a nonzero total angular momentum J . Such a situation is, for example, typical of many chalcogenides of Pr and Tm [369]. If, however, the effect of interatomic exchange is comparable with that of the crystal field, it may be the cause of magnetic polarization of the ions, resulting in the establishment of a magnetic ordering in the crystal.

To illustrate the point, let us write out the wave functions of the ground state $|\Gamma_1\rangle$ and of the lower triplet state $|\Gamma_4\rangle$ in an explicit form expressing them in terms of $|J^z\rangle$ [368].

$$\begin{aligned} |\Gamma_1\rangle &= 0.4564 [|4\rangle + | -4\rangle] + 0.7638 |0\rangle, \\ |\Gamma_4^0\rangle &= 0.7071 [|4\rangle - | -4\rangle], \\ |\Gamma_4^\pm\rangle &= 0.3536 |\pm 3\rangle + 0.9354 |\mp 1\rangle. \end{aligned}$$

Obviously, all the function $|\Gamma_1\rangle$ and $|\Gamma_4^0\rangle$ will include the states $|4\rangle$ and $| -4\rangle$ with an equal weight, but in any linear combination of such functions describing the magnetic polarization the weights of states $|\pm 4\rangle$ will be different. By force of this, a nonvanishing value is obtained for the average value of J^z in the result of mixing of $|\Gamma_1\rangle$ with $|\Gamma_4^0\rangle$. Magnetic polarization may also increase the magnetization of a crystal with an odd number of f -electrons in its magnetic atoms.

Normally, when studying magnetic systems with a singlet ground state, one takes into account besides the ground state of an ion in the crystal field only the multiplet nearest to it. The transition of an ion to such a multiplet state may be interpreted as the creation on it of a specific Frenkel exciton. In this case the magnetic Hamiltonian may be represented in the form

$$\begin{aligned} H_M &= \omega \sum b_{gi}^* b_{gi} \\ &- \frac{1}{2} \sum \mathcal{K}(g-f) (\langle i | J_g | 0 \rangle \cdot \langle 0 | J_f | j \rangle) (b_{gi}^* + b_{gj}) (b_{if}^* + b_{ij}) \\ &- \frac{1}{2} \sum \mathcal{K}'(g-f) (\langle i | J_g | j \rangle \cdot \langle j' | J_f | i' \rangle) b_{gi}^* b_{gj} b_{if}^* b_{i'j'}, \quad (2.2.6) \end{aligned}$$

where b_{gi}^* , b_{gi} are Pauli operators of creation and annihilation of an exciton on the atom g , i is the index of the multiplet component (the Pauli operators corresponding to the same atom obey the Fermi-type commutation rules, those corresponding to different atoms obey Bose-type commutation rules with $b_{gi}^*b_{gi}^* = b_{gi}b_{gi} = 0$).

An inverse relationship is typical of ions with partially-filled d -shells: the effect of the crystal field on the electrons of partially-filled shells is much more pronounced than that of the spin-orbit coupling. Accordingly, the crystal field should be taken into account in the zeroth approximation, and the spin-orbit coupling as a small perturbation, so that it is no longer possible to classify the electron states according to the total angular momentum J .

If the interatomic exchange interaction is stronger than the interaction of the electrons with the crystal field, the spin of the partially filled shell of an ion in the crystal, as is the case of a free ion, will, in accordance with the Hund rule, assume the maximum value. (This rule follows from the intrashell exchange constant being positive.) The crystal field removes the degeneracy not in the directions of \mathbf{J} , but in the directions of the orbital angular momentum. For this reason, in contrast to the spin, the orbital momentum cannot assume an arbitrary position in space. In case of a complete removal of degeneracy, it does not contribute anything to the total crystal moment induced by an external magnetic field or of a spontaneous origin (the "freezing" of the orbital momentum). The absence of a contribution from the orbital momentum should result in the Landé g -factor (2.2.5) being equal to 2 as for $L = 0$. This, indeed, is quite true for many ions, e.g. Cr^{3+} , Mn^{2+} . However, for Fe^{3+} and Co^{2+} ions the Landé factor is equal to 1.89 and 1.54, respectively, this being an indication of an incomplete freezing of their orbital momentum (the data on the g -factor of $3d$ -element ions in paramagnetic salts is quoted from [42]).

In stronger crystal fields the splitting of the d - or f -levels is so great that it even exceeds the energy of exchange interaction between the electrons of a shell. In this case the Hund rule is satisfied only for each separate component of the split level: as the states of the lower component are filled, the total electron spin at first rises. However, after the electron number becomes equal to the multiplicity of the orbital degeneracy of the lower component, there will no longer be any energetical advantage for the subsequent electrons to occupy states with an equal spin projection in the higher component. They remain in the lower component, but with an opposite spin, despite the fact that this results in a loss in the energy of exchange between the electrons belonging to the shell. When the electron number is twice the multiplicity of the orbital degeneracy of the component, the spin of the electrons belonging to it vanishes. Accordingly, de-

spite the fact that a d - or an f -shell is only partially filled, its spin may be zero.

Such, for example, is the situation in LaCoO_3 where the five-fold degenerate d -level splits into triple- and double-degenerate components, and six d -electrons of the Co^{3+} ion fill the lower triple-degenerate component, thus giving the ion a zero spin [252, 253]. No matter whether the Hund rule for the spin of an ion in the crystal is valid or not, in the absence of the spin-orbital and the dipole-dipole interaction between the magnetic ions there would be only an isotropic exchange interaction. The effect of the crystal field is to produce in the magnetic Hamiltonian a small anisotropic term obtained from the Hamiltonian (2.2.2) with the aid of the perturbation theory.

If there is an axis in the crystal along which the orientation of the spins is most energetically favoured (an "easy axis"), the magnetic anisotropy is conveniently described in terms of the effective magnetic field \vec{H}_A directed along this axis (in an antiferromagnet the anisotropy fields of two of its sublattices are presumed to point in opposite directions).

2.3. MAGNETIC ORDERING AND EFFECT ON IT OF A MAGNETIC FIELD

Heisenberg Magnetic Systems. Below we shall analyze possible types of magnetic ordering in Heisenberg magnetic systems built of identical atoms in identical crystallographic positions. It will be convenient to make use of the method of approximate secondary quantization [215]. The energy of the ground state in this method is calculated by substituting classical vectors for the spin operators in the Hamiltonian (2.1.5) with its subsequent minimization with respect to the direction cosines of the spin vectors. Such a procedure automatically determines the type of magnetic ordering as well.

The situation is the simplest when the exchange integral $J(f)$ is positive for all f 's. Then the energy minimum is attained in the case of FM ordering, this state being a precise eigenstate of the Hamiltonian (2.1.5). The problem becomes appreciably more complicated, if at least some of $J(f)$ are negative.

It would be reasonable to start the discussion with the case of a uniaxial crystal. We shall presume the exchange integral for atoms lying in the same plane perpendicular to the crystal axis to be positive, so that there is a ferromagnetic ordering in each such plane. Only the interaction of an atom with its nearest and next-nearest neighbours along the crystal axis will be taken into account, and the moments of the nearest-neighbouring FM sheets will be presumed to make an angle θ with each other (correspondingly, the angle the moments of next neighbours make with one another will be equal to 2θ) (Fig. 2.1). Such a structure is described by the heli-

coid vector \mathbf{q} pointing in the direction of the screw axis:

$$\begin{aligned} S_g^x &= S \cos qg_z, \\ S_g^y &= S \sin qg_z, \\ S_g^z &= 0 \quad (qa = \theta). \end{aligned} \quad (2.3.1)$$

The expression for the crystal energy as a function of the angle θ will be, with account taken of the Hamiltonian (2.1.5) and relations (2.3.1),

$$E = -N_l S^2 (\gamma_1 \cos \theta + \gamma_2 \cos 2\theta) + \text{const}, \quad (2.3.2)$$

where N_l is the number of layers, γ_1 is the integral of exchange with the nearest neighbour along the crystal axis and γ_2 —with the next neighbour. Differentiating the energy (2.3.2) with respect to θ , we find that both the FM ($\theta = 0$) and the AF ($\theta = \pi$) ordering satisfy the condition for its extremum. In addition the interval $|\gamma_1| < 4|\gamma_2|$ contains the solution

$$\cos \theta = -\gamma_1/4\gamma_2, \quad (2.3.3)$$

that corresponds to the helicoidal ordering of the spins with the moments of FM layers forming a spiral. Its period is determined solely by the ratio γ_1/γ_2 , i.e. in general it is incommensurate with the translational period along the crystal axis. The helicoidal ordering is more energetically favoured than the FM or the AF if γ_2 is negative*.

In case the conditions $\gamma_2 < 0$, $|\gamma_1| < 4|\gamma_2|$ are not satisfied, FM ordering will be established for positive γ_1 and AF ordering—for negative γ_2 .

It turns out that various types of AF ordering are possible in isotropic systems. For instance, staggered AF ordering with the spin of every atom opposite to those of its nearest neighbours (Fig. 2.2a) is not the only one possible in a simple cubic lattice, but such order-

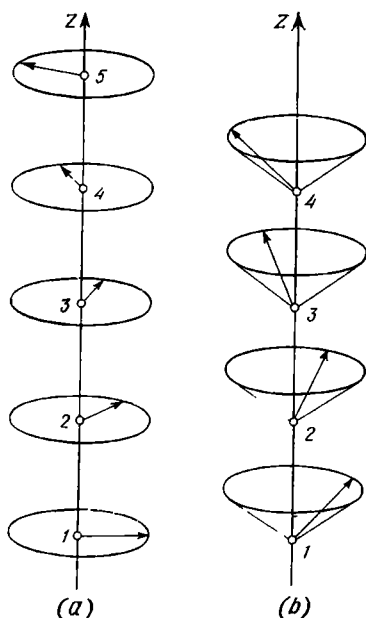


Fig. 2.1. Helicoidal ordering: (a) simple spiral; (b) ferromagnetic spiral

* A helicoidal ordering with a very large period may also be the result of deformation of the ferromagnetic structure by the forces of magnetic anisotropy [343].

ing in which FM sheets are formed in planes normal to the face diagonals [011] (Fig. 2.2b) as well [217]. The conditions for which the magnetic structure of Fig. 2.2b is more energetically favoured than that of Fig. 2.2a are easily found. If the integrals of exchange with 6 nearest and 12 next-nearest neighbours are negative, the energies of these structures are given by the expressions

$$E_a = -\frac{NS^2}{2} [6 |J_1| - 12 |J_2|] \quad \text{for } 2.2a, \quad (2.3.4a)$$

$$E_b = -\frac{NS^2}{2} [2 |J_1| - 4 |J_2|] \quad \text{for } 2.2b. \quad (2.3.4b)$$

Hence, E_b will be lower than E_a , if the exchange with the next neighbours is strong enough so that $|J_2| > \frac{|J_1|}{2}$. In other cases (including that of $J_2 > 0$) ordering of the type of Fig. 2.2a will take place.

The situation turns out to be still more complicated when magnetic atoms form a face-centred cubic lattice (crystals with the

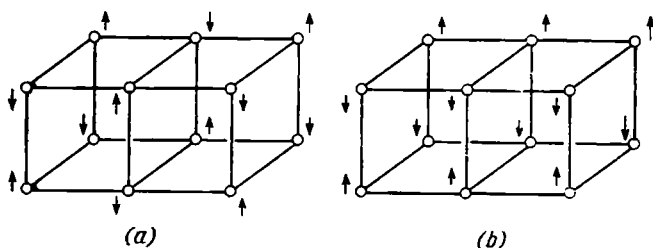


Fig. 2.2. Types of antiferromagnetic ordering in a simple cubic lattice consisting of magnetic atoms

NaCl structure). In such a lattice every atom has $z_1 = 12$ nearest neighbours along the face diagonals and $z_2 = 6$ next neighbours along the edges (Fig. 2.3). The essential point is that two nearest neighbours of an atom can themselves be nearest neighbours. This precludes the possibility of staggered ordering. Three different types of ordering are allowed as shown in Fig. 2.3, *a-c* [218]. Fig. 2.3a depicts the ordering in which FM atomic layers are formed in planes normal to one of the cube edges, with the moments of adjacent layers pointing in opposite directions (this is an analog of the ordering in a uniaxial crystal analyzed above). With such an ordering, the number of pairs of nearest neighbours with antiparallel spins is at its maximum (being equal to 8).

The second type corresponds to a magnetic structure, which can be represented as a set of four independent AF simple cubic lattices.

The ordering depicted in Fig. 2.3*b* features a system of FM planes orthogonal to the body diagonals [111], with the moments of nearest-neighbouring layers being antiparallel. Every atom has nearest neighbours with spins pointing up equal in number to those with spins pointing down, but the spins of next-nearest neighbours are all opposite to those of the given atom.

Next the third type of ordering (Fig. 2.3*c*) features an orientation of the spins of nearest neighbours similar to that of the first type, but the spins of next neighbours are oriented differently. Other types of ordering are also possible in principle, but they have not been observed in experiment.

In a magnetic field an AF acquires a nonzero magnetic moment. If the magnetic anisotropy can be neglected, the magnetization vector $\mathbf{m} = (\mathcal{M}_1 + \mathcal{M}_2)/2S$ will always point in the direction of the field \mathcal{H} and at right angles to the antiferromagnetism vector $\mathbf{I} = (\mathcal{M}_1 - \mathcal{M}_2)/2S$, where \mathcal{M}_1 and \mathcal{M}_2 are magnetic moments per atom of the sublattices (Fig. 2.4). In the nearest-neighbour approximation the energy of the system per atom is written down in the form $(\theta_1 - \theta_2 - \theta)$:

$$E = -\frac{\mathcal{Y}S}{2} \cos 2\theta - \mathcal{H}S \cos \theta, \quad \mathcal{Y} = z\mathcal{J}_1 S. \quad (2.3.5)$$

Minimizing the energy with respect to the angle θ , we obtain from (2.3.5) for the crystal moment

$$\mathcal{M} = S \cos \theta = \frac{\mathcal{H}S}{2|\mathcal{Y}|} \equiv \frac{\mathcal{H}S}{\mathcal{H}'_F}, \quad (2.3.6)$$

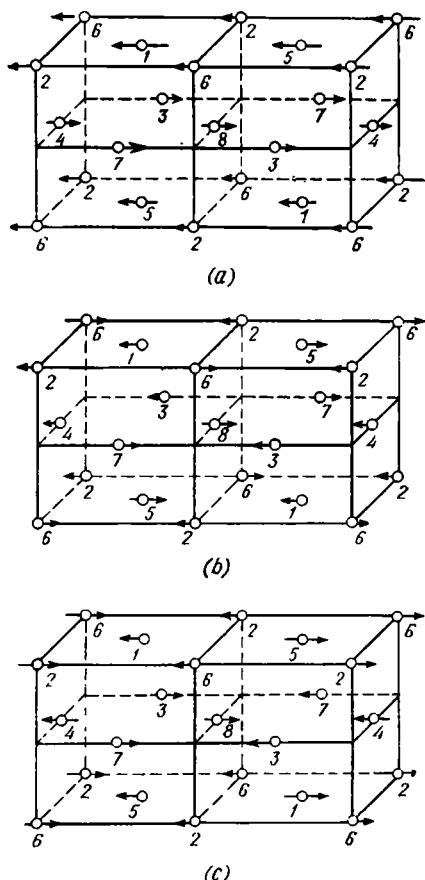


Fig. 2.3. Types of antiferromagnetic ordering in a face-centred cubic lattice consisting of magnetic atoms

where H_s is the magnetic saturation field (at which moments of both sublattices become parallel to each other).

Expression (2.3.6) remains valid in the case of a sufficiently weak anisotropy of the "easy plane" type as well, but an anisotropy of the "easy axis" type drastically changes the magnetic behaviour of the crystal. In a field normal to the crystal axis the moment grows with an increase in the field intensity in full agreement with formula (2.3.6). But in a field parallel to the axis the magnetization appears only in sufficiently strong fields $H \sim \sqrt{K_A} | \Psi | S$ where K_A is the field of anisotropy (Fig. 2.5). The situation depicted in Fig. 2.5

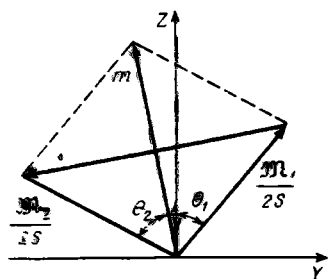


Fig. 2.4. Magnetic structure of an antiferromagnet in a magnetic field

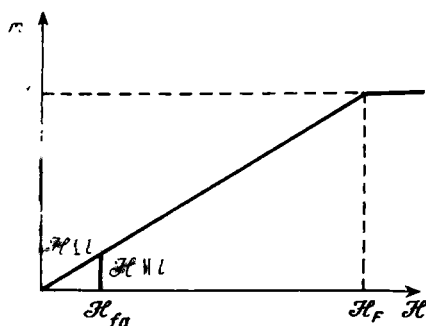


Fig. 2.5. Magnetization vs. magnetic field for an antiferromagnet

corresponds to an abrupt rotation of the AF vector through $\pi/2$. However, in some cases a continuous change in the direction of the vector from one parallel to the crystal axis to one at right angles to it with the field varying inside a narrow interval $\sim \sqrt{K_A} | \Psi | S$ around H_{fa} takes place instead of an abrupt change [216]. It is essential that the spin-flop field (i.e. of reorientation of moments in AF) H_{fa} for $| \Psi | S \gg K_A$ is $\sim \sqrt{K_A} | \Psi | S$, K_A times the field of reorientation in FM H_{fa} , which is of the order of magnitude of $\sqrt{K_A}$.

There is a group of AF in which the spin-flop field coincides with the magnetic saturation field H_F , i.e. the AF magnetization in a growing field at first remains zero to be followed by an abrupt transition of the crystal to the FM state when the critical field is reached (actually, of the order to thousands or tens of thousands oersteds). The term for such materials is *metamagnets*. Metamagnets are usually layered crystals with weak exchange interaction between the layers. Because of that the effective field of magnetic anisotropy in them exceeds the effective field of the interlayer exchange interaction [42].

Anisotropic AF with special symmetry properties that have a small magnetic moment even in the absence of a magnetic field are also

known. This moment is due to relativistic spin-spin interactions [219, 220].

Singlet Magnets. In instances discussed above the part played by exchange interaction was reduced to orienting the permanent moments of magnetic atoms in a definite way. A principally novel type of a magnetic system as compared to those discussed above is that of crystals having a singlet ground state. In such crystals exchange interaction not only orients the atomic moments, but is itself the cause of their very existence. Atomic moments are induced by exchange interaction of the atoms with one another irrespective of the sign of the exchange integral \mathcal{K} in the Hamiltonian (2.2.6), provided the intensity of the exchange interaction exceeds some critical value. Accordingly, the induced moments may both be FM and AF ordered. To be definite, below we shall consider the case of FM ordering.

The analysis of the ground state of a singlet magnet will be carried out in the self-consistent field approximation frequently used in problems concerning Heisenberg magnetic systems at finite temperatures (Secs. 2.5 and 2.6). In this approximation the interaction of the moment of a magnetic atom with FM ordered moments of other atoms is described with the aid of the mean field of the latter, which points like the magnetization in the direction of the z-axis:

$$\mathcal{H}_{MF} = c^2 \mathcal{K} \langle b \div b^* \rangle_0, \quad \mathcal{K} = \sum_g \mathcal{K}(g), \quad c = \langle \Gamma_4^0 | J^z | \Gamma_1 \rangle \quad (2.3.7)$$

(for the sake of simplicity, the exchange integral \mathcal{K}' has been put equal to zero). Here $\langle \dots \rangle_0$ is the symbol denoting averaging over the ground state. The average value of exciton operators entering (2.3.7) itself must be found from the subsequent solution of the problem by means of the self-consistency procedure. With account taken of (2.3.7), the Hamiltonian (2.2.6) can be replaced by the approximate single-atomic one

$$H_{MF} = \omega b^* b - \mathcal{H}_{MF} (b^* + b) \quad (2.3.8)$$

(the atomic number and the multiplet index for the exciton operators have been dropped, because the structure of the Hamiltonian H_{MF} is identical for all atoms, and because the ground state $|\Gamma_1\rangle$ mixes only with the component $j=0$ of the multiplet $|\Gamma_4^j\rangle$, which has a nonzero matrix element $\langle \Gamma_4^0 | J^z | \Gamma_1 \rangle$).

Taking into account that the exciton operators are of the Pauli type, we express the eigenfunction of the Hamiltonian (2.3.8) in terms of the vacuum function $|0\rangle$ in the form

$$\Phi_0 = (\mathcal{X} + \mathcal{Y} b^*) |0\rangle. \quad (2.3.9)$$

It follows immediately from formulae (2.3.7-9) that

$$E = \frac{\omega}{2} \pm \sqrt{\frac{\omega^2}{4} + c^4 \mathcal{K}^2 \langle b + b^* \rangle_0^2}, \quad (2.3.10)$$

$$\mathcal{X} = -\mathcal{H}_{MF} \mathcal{Y} / E, \quad \mathcal{X}^2 + \mathcal{Y}^2 = 1.$$

According to (2.3.9), $\langle b + b^* \rangle_0$ equals $2\mathcal{X}\mathcal{Y}$, and the coefficients \mathcal{X} and \mathcal{Y} are themselves expressed with the aid of formula (2.3.10) in terms of the average value of the exciton operators. In the result we obtain

$$\langle J^z \rangle_0 = c \langle b^* + b \rangle_0 = c \left(1 - \frac{\omega^2}{4c^4 \mathcal{K}^2} \right)^{1/2}. \quad (2.3.11)$$

It follows from formula (2.3.11) that a solution with FM ordering exists only if the exchange integral \mathcal{K} exceeds the critical value $\mathcal{K}_c = \omega/2c^2$. Otherwise the crystal will be in a nonmagnetic state. A similar result can be obtained for AF ordering, as well. In the nearest-neighbour approximation it coincides with (2.3.10, 11).

2.4. MAGNONS AND LOW-TEMPERATURE MAGNETIZATION OF FERROMAGNETS

At sufficiently low temperatures the state of a ferromagnet can be described in terms of its elementary excitations of magnons.

To describe magnons, Bose operators b_g^* , b_g of creation and annihilation of spin deviation on an atom are introduced instead of the spin-deviation operators S_g^\pm , the connection between operators of both types being given by Holstein-Primakoff relations (see, for instance, [215, 203]):

$$S_g^+ = \sqrt{2S} \varphi(\hat{m}_g) b_g, \quad S_g^- = \sqrt{2S} b_g^* \varphi(\hat{m}_g), \\ S_g^z = S - \hat{m}_g, \quad (2.4.1)$$

$$\hat{m}_g = b_g^* b_g, \quad \varphi(\hat{m}_g) = \left(1 - \frac{\hat{m}_g}{2S} \right)^{1/2}.$$

In the lowest order in $\hat{m}/2S$ the Hamiltonian (2.1.5) transformed with the aid of formulae (2.4.1) assumes the form, if the field \mathcal{H} points in the direction of the crystal moment:

$$H_M = S \sum \mathcal{Y}(\mathbf{h}) (b_g^* b_g - b_g^* b_{g+\mathbf{h}}) + \mathcal{H} \sum b_g^* b_g. \quad (2.4.2)$$

The spin-wave Hamiltonian (2.4.2) can be precisely diagonalized by a Fourier-transformation of magnon operators

$$b_q^* = \frac{1}{\sqrt{N}} \sum_{\mathbf{g}} e^{-i\mathbf{q} \cdot \mathbf{g}} b_g^* \quad (2.4.3)$$

and by a transformation conjugate to it (N is the number of magnetic atoms):

$$H_M = \sum_{\mathbf{q}} \omega_{\mathbf{q}} b_{\mathbf{q}}^* b_{\mathbf{q}},$$

$$\omega_{\mathbf{q}} = \mathcal{Y}_0 - \mathcal{Y}_{\mathbf{q}} + \mathcal{H}, \quad \mathcal{Y}_{\mathbf{q}} = S \sum_{\mathbf{h}} \mathcal{J}(\mathbf{h}) e^{i\mathbf{q} \cdot \mathbf{h}}. \quad (2.4.4)$$

Specifically, in the nearest-neighbour approximation

$$\mathcal{Y}_{\mathbf{q}} = \mathcal{Y} \gamma_{\mathbf{q}}, \quad \mathcal{Y} = \mathcal{J} S z, \quad \gamma_{\mathbf{q}} = \frac{1}{z} \sum_{\Delta} e^{i\mathbf{q} \cdot \Delta}. \quad (2.4.4')$$

Hence, in the spin-wave approximation the excited FM state is described in terms of noninteracting quasi-particles, magnons, whose state is characterized by quasi-momenta \mathbf{q} . As in the case of electrons, only quasi-momenta lying inside the first Brillouin zone ought to be considered. The similarity with the electrons becomes still greater at low temperatures $T \ll \mathcal{Y}$, when only magnons with $q \ll \pi a$ are of any importance, and for this reason their energy $\omega_{\mathbf{q}}$ can be expanded in \mathbf{q} and only the quadratic terms be retained ($\mathcal{H} = 0$):

$$\omega_{\mathbf{q}} = \frac{q^2}{2M}, \quad \frac{1}{2M} = \mathcal{J} S^2 a^2. \quad (2.4.5)$$

The quantity M the expression for which in (2.4.5) has been written in the nearest-neighbour approximation may naturally be termed *magnon effective mass*.

The average number of Bose quasi-particles, magnons, $m_{\mathbf{q}} = \langle b_{\mathbf{q}}^* b_{\mathbf{q}} \rangle$ is given by a standard distribution function

$$m_{\mathbf{q}} = \left[\exp \left(\frac{\omega_{\mathbf{q}}}{T} \right) - 1 \right]^{-1}. \quad (2.4.6)$$

Hence, the average crystal magnetization per atom is

$$\mathfrak{M} = \langle S^z \rangle = S - \frac{1}{N} \sum_{\mathbf{q}} m_{\mathbf{q}} = S - m(T). \quad (2.4.7)$$

Making use of formulae (2.4.5-7), we obtain that for $T \ll \mathcal{Y}_0$, when $\exp(-\omega_{\mathbf{q}}/T)$ can be regarded as small, and the distribution function of $m_{\mathbf{q}}$ can be expanded in it, the expression for demagnetization will be

$$m(T) \simeq \frac{a^3}{(2\pi)^3} \int_{-\infty}^{\infty} d\mathbf{q} \sum_{n=1}^{\infty} \exp \left(- \frac{\mathbf{q}^2 n}{2MT} \right) - \left(\frac{TM a^2}{2\pi} \right)^{3/2} \sum_{n=1}^{\infty} n^{-3/2}. \quad (2.4.8)$$

Hence, in this region demagnetization grows with the temperature as $T^{3/2}$.

If the atomic spin is large ($2S \gg 1$), the region of applicability of the spin-wave approximation extends to $T > \mathcal{Y}_0$. Since in this case the magnon distribution function is approximately equal to T/ω_q , demagnetization in this region will be proportional to the temperature. Specifically, in the nearest-neighbour approximation (2.4.4') we obtain for it

$$m(T) = \frac{T}{\mathcal{Y}N} \sum_q \frac{1}{1-\gamma_q} \simeq \frac{1.5T}{\mathcal{Y}} \quad (2.4.8a)$$

(for the Watson integral, which enters formula (2.4.8), we have quoted the result from the book [54]).

As the temperature rises, the interaction between the magnons becomes essential. To account for it in the framework of a perturbation theory in $\hat{m}/2S$, we should retain the terms of the first order in $\hat{m}/2S$ in the expression for the $\varphi(\hat{m})$ function, which enters the Holstein-Primakoff transformation (2.4.1). This will cause terms of the b^*b^*bb type describing the magnon anharmonism to appear in the magnon Hamiltonian obtained from (2.1.5) with the aid of (2.4.1):

$$\begin{aligned} H_{mm} = & -\frac{1}{8SN} \sum [\mathcal{Y}(q_1 - q_3) + \mathcal{Y}(q_1 - q_4) - \mathcal{Y}(q_2 - q_3) \\ & + \mathcal{Y}(q_2 - q_4) - \mathcal{Y}(q_1) - \mathcal{Y}(q_2) - \mathcal{Y}(q_3) - \mathcal{Y}(q_4)] \\ & \times \mathcal{D}(q_1 + q_2, q_3 + q_4) b_{q_1}^* b_{q_3}^* b_{q_2} b_{q_4}, \end{aligned} \quad (2.4.9)$$

where $\mathcal{D}(q + k, k)$ expresses the quasi-momentum conservation law: it is equal to 1 when q is zero or to the reciprocal lattice vector (i.e. $\frac{q \cdot \Delta}{2\pi} = 0, \pm 1, \dots$), and vanishes in all other cases.

From Hamiltonian (2.4.9) we can obtain a correction to the magnon frequency ω_q due to the interaction between the magnons. Defining in a way similar to Sec. 1.5 the renormalized magnon frequency $\hat{\omega}_q$, we obtain, taking into account (2.4.4, 4'):

$$\begin{aligned} \tilde{\omega}_q &= \omega_q + \frac{\delta}{\delta m_q} \langle H_{mm} \rangle = \tilde{\mathcal{Y}}(1 - \gamma_q), \\ \tilde{\mathcal{Y}} &= \mathcal{Y} \left[1 - \frac{1}{NS} \sum_k (1 - \gamma_k) m_k \right], \end{aligned} \quad (2.4.10)$$

where angular brackets mean averaging over the temperature.

2.5. HIGH-TEMPERATURE AND CRITICAL PROPERTIES OF FERROMAGNETS

Self-consistent Field Approximation. In the range of temperatures where the spin-wave approximation is inapplicable, the self-consistent field approximation proves very useful, as it qualitatively cor-

rectly reproduces the temperature dependence of magnetization and in many cases of practical importance provides quantitative agreement with experiment as well. Its basic physical idea is quite simple. If a periodic field $\mathcal{H}_g = \mathbf{h}e^{i\mathbf{q} \cdot \mathbf{r}}$ is applied to the crystal, the Hamiltonian (2.1.5) will take the form

$$H_q = \frac{1}{2} \sum_i J(\mathbf{g} - \mathbf{f}) \langle \mathbf{S}_g \rangle \langle \mathbf{S}_f \rangle - \sum_i \mathbf{S}_g \cdot \mathcal{H}_e(\mathbf{g}) + \delta H,$$

$$\mathcal{H}_e(\mathbf{g}) = \mathcal{H}_g + \sum_i J(\mathbf{g} - \mathbf{f}) \langle \mathbf{S}_f \rangle, \quad (2.5.1)$$

$$\delta H = -\frac{1}{2} \sum_i J(\mathbf{f} - \mathbf{g}) (\mathbf{S}_g - \langle \mathbf{S}_g \rangle) \cdot (\mathbf{S}_f - \langle \mathbf{S}_f \rangle),$$

where $\langle \mathbf{S}_g \rangle$ is the average spin at the specified temperature. The term δH in (2.5.1) describes the fluctuations of the spins about their central positions. The fluctuations being of variable signs, when summed over the atoms they will be mutually compensated the more the greater the radius of the exchange interaction (in the limit of an infinite radius the compensation would have been complete). The gist of the self-consistent-field method is that the fluctuating terms in formula (2.5.1) are neglected. Then the mean spin projection will be determined in the same way as for an isolated atom in an external field \mathcal{H}_e . For $q = 0$ we obtain for the magnetization per atom \mathfrak{M}

$$\mathfrak{M} = T \frac{d}{d\mathcal{H}_e} \ln Z_S = S B_S \left(\frac{S \mathcal{H}_e}{T} \right),$$

$$Z_S = \sum_{m=-S}^S \exp \left\{ \frac{m \mathcal{H}_e}{T} \right\} = \sinh \left\{ (2S+1) \frac{\mathcal{H}_e}{2T} \right\} \left\{ \sinh \frac{\mathcal{H}_e}{2T} \right\}^{-1},$$

$$B_S(x) = \frac{2S+1}{2S} \coth \left(\frac{2S+1}{2S} x \right) - \frac{1}{2S} \coth \frac{x}{2S}, \quad (2.5.2)$$

where B_S denotes the Brillouin function. The self-consistency manifests itself in the magnetization dependence of the field \mathcal{H}_e (2.5.1) in equation (2.5.2) determining the average magnetization.

First of all, the self-consistent field approximation predicts the existence of a critical point T_c above which the magnetization for $\mathcal{H} = 0$ vanishes, but is nonzero below that point

$$T_c = \frac{\mathcal{H}_0(S+1)}{3}. \quad (2.5.3)$$

Spontaneous magnetization for small $T_c - T$ grows with this difference according to the law: $\mathfrak{M} \sim \sqrt{T_c - T}$.

In the absence of a long-range FM order in a crystal ($\mathfrak{M} = 0$) there still remains a short-range order. The part of the quantitative characteristic of the short-range order is played by the binary spin

correlation function $\langle S_0^\alpha S_g^\beta \rangle$ ($\alpha, \beta = x, y, z$). Its Fourier-transform can be rigorously expressed in terms of the magnetic susceptibility in an infinitesimal field. One can easily obtain the relationship between them, if he, making use of (2.5.4), writes the ordinary thermodynamical average for the Fourier-transform of the spin projection S_q^α and next differentiates it with respect to h^β putting then $h = 0$:

$$\begin{aligned}\chi^{\alpha\beta}(\mathbf{q}) &= \frac{1}{\sqrt{N}} \frac{\partial \langle S_q^\alpha \rangle_h}{\partial h^\beta} \\ &= \frac{1}{T} [\langle S_q^\alpha S_{-q}^\beta \rangle - \langle S_q^\alpha \rangle \langle S_{-q}^\beta \rangle],\end{aligned}\quad (2.5.4)$$

$$\mathbf{S}_p = \frac{1}{\sqrt{N}} \sum_{\mathbf{g}} S_{\mathbf{g}} e^{-i\mathbf{p} \cdot \mathbf{g}}. \quad (2.5.5)$$

Above the Curie point there is no preferred direction in the crystal, and for this reason the magnetic susceptibility tensor is a diagonal one with equal components. In order to compute $\chi(\mathbf{q})$ approximately, one writes the expression for $\langle S_g^\alpha \rangle_h$ in the first order in \mathcal{H}_e/T and goes over to the Fourier-transforms of the spin $\langle S_q^\alpha \rangle_h$. Differentiating $\langle S_q^\alpha \rangle_h$ with respect to h , one obtains

$$\chi(\mathbf{q}) = \frac{S(S+1)}{3(T-\theta_q)}, \quad \theta_q = \frac{\mathcal{Y}_q(S+1)}{3}. \quad (2.5.6)$$

For $q = 0$ the result (2.5.6) expresses the Curie-Weiss law ($\chi \equiv \chi(0)$). In the mean field approximation just used the PM Curie point $\theta \equiv \theta_0$ coincides with the true Curie point T_c (2.5.3).

Making use of expressions (2.5.4) and (2.5.6) and expanding \mathcal{Y}_q in q , one obtains the following result for the binary spin correlation function at great separations:

$$\langle S_q^\alpha S_{-q}^\beta \rangle \simeq \frac{S(S+1)}{3r_1^2} \frac{\delta_{\alpha\beta}}{(\kappa^2 + q^2)}, \quad (2.5.7)$$

$$\langle \mathbf{S}_0 \cdot \mathbf{S}_l \rangle = \frac{1}{N} \sum_{\mathbf{q}} \langle \mathbf{S}_q \cdot \mathbf{S}_{-q} \rangle e^{i\mathbf{q} \cdot \mathbf{l}} = c e^{-\kappa l / f},$$

where the following notations have been introduced

$$r_1^2 = \frac{1}{6} \sum_{\mathbf{l}} \mathcal{Y}(\mathbf{l}) f^2 / \sum_{\mathbf{l}} \mathcal{Y}(\mathbf{l}),$$

$$\kappa^2 = r_1^{-2} \left| 1 - \frac{T_c}{T} \right|, \quad c = \frac{S(S+1)a^3}{4\pi r_1^2}.$$

According to (2.5.7), the correlation length $r_{\text{cor}} = \kappa^{-1}$ has a discontinuity at the Curie point of the $|T - T_c|^{-1/2}$ type.

At temperatures below T_c in a field $\mathbf{h} \parallel \mathbf{z}$ the expression for the longitudinal correlation function $\langle S_q^z S_{-q}^z \rangle$ for $q \neq 0$ coincides with

(2.5.7) in which $2\kappa^2$ has been substituted for κ^2 . The transverse correlation function for $q=0$, same as χ_{\perp} , must diverge at $\mathcal{H} \rightarrow 0$, since in an ideally isotropic medium an infinitesimal field $\mathbf{h} \perp \mathbf{z}$ can change the orientation of the spontaneous moment to one orthogonal to the original.

The limits of applicability of the self-consistent field theory for $T < T_c$ are determined by the condition that the fluctuations of magnetization in a volume with linear dimensions of the order of the correlation length be small as compared with its average value M [340, 341]. Comparing the square of the fluctuation amplitude expressed in terms of the two-spin correlation function with the square of magnetization, we obtain a criterion resembling one obtained otherwise in [81]:

$$1 \gg |\tau| \gg \frac{1}{(40\pi)^2} \frac{[2S^2 + 2S + 1]}{S(S-1)} \left(\frac{a}{r_1} \right)^6 \equiv \tau_{SF}, \quad (2.5.8)$$

$$\tau = \frac{T - T_c}{T_c}.$$

The parameter r_1 will be seen from formula (2.5.7) to be almost equal to the radius of exchange interaction. Hence, the region of applicability of the self-consistent field theory expands rapidly as the latter grows. This region, probably, exists even in the nearest-neighbour approximation ($r_1 = a^2/6$). According to formula (2.5.8), the condition for this is that $|\tau|$ exceeds 0.1. This agrees with the estimate $|\tau| > 1/2$ contained in [342]. If the inequality (2.5.8) is replaced by an opposite one, the part played by the fluctuations becomes so great that it would be quite unreasonable to ignore them, and this is what causes the self-consistent field method to break down.

High- and Low-temperature Expansions. In the case of interaction between nearest neighbours, a much more reliable information about the phase transition is to be gained from the method of high-temperature expansions. It enables any physical quantity at temperatures above T_c to be represented in the form of a series in the powers of the inverse temperature $\beta = 1/T$, and the behaviour of this quantity in the vicinity of T_c to be reproduced [344]. The magnetic susceptibility χ can be calculated, if the statistical sum

$$Z = \text{Sp} \{ e^{-\beta H} \} = \text{Sp} \{ 1 \} + \beta \text{Sp} \{ H \} + \frac{\beta^2}{2} \text{Sp} \{ H^2 \} + \dots \quad (2.5.9)$$

is known with the aid of the relationship

$$\chi \equiv \chi(0) = - \frac{\partial^2 F}{\partial \mathcal{H}^2}, \quad F = -T \ln Z.$$

In addition to the numerous coefficients of the series representing χ that have to be known, it is also necessary to make an assumption

concerning the type of the singularity of the magnetic susceptibility at the critical point. It is presumed to be of the $\chi(T) \sim (T - T_c)^{-\gamma}$ kind. Extrapolation of the series to the Curie point yields [54, 345, 344] for the Heisenberg magnet irrespective of the magnitude of the spin and of the lattice type a critical exponent $\gamma = 4/3$ instead of $\gamma = 1$ obtained in the mean field approximation (2.5.6). The critical temperature is, according to [54], given by the expression

$$T_c \simeq 0.026 \left(1 - \frac{1}{z}\right) \left[11(S+1) - \frac{1}{S}\right] \mathcal{J}, \quad (2.5.10)$$

this being some 30 to 50% less than the value (2.5.3) obtained with the self-consistent field approximation.

If only two terms of the high-temperature expansion are retained, the formula for χ will assume the form of the Curie-Weiss law (2.5.6) with the same parameters as in the self-consistent field theory. This is proof of the validity at sufficiently high temperatures of the self-consistent field approximation for a small radius of interaction as well, i.e. of the decline of the critical exponent with rising temperature (γ tends to 1).

The Curie point can also be evaluated with the aid of the method of low-temperature expansions of magnetization. In its simplest version it can be formulated as follows: expression (2.4.7) is presumed to be valid at the Curie point T_c as well. Accordingly, we put in it $\mathfrak{M} = 0$. For the magnon distribution function we use the high-temperature approximation $m_q(T_c) \simeq T_c \tilde{\omega}_q(T_c)$, where $\tilde{\omega}_q(T)$ is the magnon frequency with the magnon anharmonism being taken into account. Accordingly, the Curie temperature will be determined by the expression

$$T_c \simeq S \left[\frac{1}{N} \sum_q \frac{1}{\tilde{\omega}_q(T_c)} \right]^{-1}. \quad (2.5.11)$$

Once we substitute the unrenormalized frequency $\omega_q(0)$ (2.4.4, 4') into (2.5.11), we will obtain a T_c double that found with the self-consistent field approximation (2.5.3). However, already the inclusion of the first temperature-dependent correction to ω_q (expression (2.4.10) with magnon occupation numbers $m_q = T_c \omega_q(0)$) yields an estimate $T_c \simeq 0.39 \mathcal{J}S$.

Phenomenological Theories. Results equivalent to those of the self-consistent field theory can be obtained from the phenomenological theory of phase transitions developed by Landau [246] and first applied to FM by Vonsovsky [347, 348]. Landau postulated that the Gibbs free energy can be expanded in the vicinity of the Curie point in the powers of the order parameter whose part in FM is

played by the magnetization \mathfrak{M} (average moment per atom $\langle S_z^i \rangle$).

$$\Phi = \Phi_0 + N \left[\frac{\mathcal{A}\mathfrak{M}^2}{2} + \frac{\mathcal{B}\mathfrak{M}^4}{4} - \mathfrak{M}\mathcal{H} \right]. \quad (2.5.12)$$

The circumstance that expansion (2.5.12) for $\mathcal{H} = 0$ contains only even powers of the magnetization is the consequence of the invariance of the free energy under the magnetization inversion in the absence of an external magnetic field \mathcal{H} . The equilibrium value of the magnetization \mathfrak{M} determined from the condition

$$\frac{\partial \Phi}{\partial \mathfrak{M}} = 0 \quad (2.5.13)$$

is presumed to be sufficiently small. The coefficients \mathcal{A} and \mathcal{B} are pressure- and temperature-dependent. For \mathfrak{M} to vanish above the transition point T_c and to be nonzero below T_c , it suffices to presume that in the vicinity of T_c the coefficient \mathcal{A} can be written down in the form

$$\mathcal{A} = \alpha\tau, \quad \tau = (T - T_c)/T_c, \quad \alpha > 0. \quad (2.5.14)$$

For the phase transition to be of the second kind, it is necessary (but not sufficient) for the coefficient \mathcal{B} to be positive at the point T_c .

For the zero field we obtain from (2.5.12-14) that at $T > T_c$ the equilibrium value of \mathfrak{M} vanishes, and at $T < T_c$ the magnetization $\mathfrak{M} \sim |\tau|^{1/2}$. For a nonzero field, the Curie-Weiss law (2.5.6) is obtained for the magnetic susceptibility at $T > T_c$.

Another phenomenological theory, which became known as *scaling theory* [349-351], has been proposed for the region where Landau theory is inapplicable. It is founded on the universality hypothesis. In the region of large fluctuations the correlation length r_{cor} exceeds any linear dimension that characterizes the interaction forces acting between the particles in a system. In such a situation it would be natural to expect that details of behaviour of interatomic forces are unessential for the description of the behaviour of the fluctuation ensemble, and because of this the interaction length cannot be a characteristic of the fluctuations. In principle, in addition to the correlation length r_{cor} that characterizes the fluctuations, we can also introduce the quantity R_c representing the dimensions of the region inside which the fluctuations of temperature are of the order of $|T - T_c|$. The fundamental assumption of the scaling theory may be formulated as that of equality of r_{cor} and R_c resulting in the appearance of one and only length r_{cor} characterizing the fluctuations at the given temperature. Should this length be accepted as a unit, the fluctuation picture will be universal for all values of $T - T_c$. This assumption enables the relationships between critical exponents that characterize the behaviour of various quantities in the vicinity of T_c to be established. The following notations are

used for them: in the zero field

$$\begin{aligned} C &\sim |\tau|^{-\alpha}, \quad \chi \sim |\tau|^{-\gamma}, \quad \mathfrak{M} \sim |\tau|^{\beta} \quad (\tau < 0), \\ r_{\text{cor}} &\sim |\tau|^{-\nu}, \quad \langle S_0 \cdot S_r \rangle \sim r^{-1-\eta} \quad \text{for } r \ll r_{\text{cor}} \end{aligned} \quad (2.5.15)$$

(C is the specific heat).

In a strong field

$$C \sim |\mathcal{H}|^{-\varepsilon}, \quad \chi \sim \mathcal{H}^{1/\delta-1}, \quad \mathfrak{M} \sim \mathcal{H}^{1/\delta}, \quad r_{\text{cor}} \sim \mathcal{H}^{-\mu}.$$

The exponents α and η equal to zero at temperatures at which the self-consistent field theory is applicable may be supposed to remain small for $|\tau| < \tau_{SF}$ (2.5.8) as well. In particular, it has as yet not been possible to establish in experiments on the scattering of light, of neutrons etc. that the index η is nonzero. For the index α , experiments yield the upper estimate of $\alpha \leq 0.15$. With account taken of the smallness of the exponents α and η , it is possible to find the remaining exponents from the scaling relation:

$$\beta \simeq 1/3, \quad \gamma = 4/3, \quad \delta = 5, \quad \nu = 2/3. \quad (2.5.16)$$

Specifically, the value of the exponent γ thus obtained coincides with that found with the aid of high-temperature expansions.

2.6. MAGNON SPECTRUM AND MAGNETIC DISORDERING IN AN ANTIFERROMAGNET

Let us now turn to the discussion of the magnon spectrum of an AF. We shall consider the staggered ordering (Fig. 2.2a). It would be reasonable to introduce a separate coordinate system for each sublattice so that their Z axes would be directed along the sublattice moments, i.e. would be opposite to one another. For example, the coordinate system for the sublattice II (spins down) can be obtained from that for the sublattice I (spins up) by rotating the latter through the angle π about the X axis. In the result the X axes in both coordinate systems will coincide, with the Y and Z axes pointing in opposite directions:

$$x_I = x_{II}, \quad y_I = -y_{II}, \quad z_I = -z_{II}. \quad (2.6.1)$$

Holstein-Primakoff relations (2.4.1) with $\varphi(\hat{m}) = 1$ are used to effect the transformation from the spin projection operators in each sublattice. The expression for the Hamiltonian (2.1.5) is conveniently rewritten by introducing the variable-sign factor $e^{i\Pi \cdot \mathbf{g}}$, which assumes the value $+1$ for atoms of the first sublattice and -1 for atoms of the second, as well as projection operators $P_+(\mathbf{g})$ and $P_-(\mathbf{g})$ on sublattices I and II :

$$P_{\pm}(\mathbf{g}) = \frac{1}{2} [1 \pm e^{i\Pi \cdot \mathbf{g}}], \quad \Pi \equiv \left(\frac{\pi}{a}, \frac{\pi}{a}, \frac{\pi}{a} \right) \quad (2.6.2)$$

(e.g. $P_+ = 1$ on the atoms of the first sublattice and 0 on those of the second). With their help the spin projections in the common coordinate system are expressed as follows

$$S_g^z = e^{i\pi \cdot g} (S - b_g^* b_g), \quad (2.6.3)$$

$$\begin{aligned} S_g^+ &= \sqrt{2S} [b_g P_+(g) + b_g^* P_-(g)], \\ S_g^- &= \sqrt{2S} [b_g^* P_+(g) + b_g P_-(g)]. \end{aligned} \quad (2.6.4)$$

Substituting expressions (2.5.3, 4) into the Heisenberg Hamiltonian (2.1.5), we obtain the following result (terms of the fourth and higher orders in magnon operators have been omitted):

$$\begin{aligned} H &= -\frac{N}{2} \mathcal{Y}_\Pi S^2 + \sum \mathcal{B}_q b_q^* b_q - \frac{1}{2} \sum \mathcal{C}_q (b_q^* b_{-q}^* + b_{-q} b_q), \\ \mathcal{B}_q &= \mathcal{Y}_\Pi - \frac{1}{2} (\mathcal{Y}_q + \mathcal{Y}_{\Pi+q}), \quad \mathcal{C}_q = \frac{1}{2} (\mathcal{Y}_q - \mathcal{Y}_{\Pi+q}), \end{aligned} \quad (2.6.5)$$

where the Fourier-transforms of the magnon operators and of the exchange integral are given by expressions (2.4.3, 4).

The last term of (2.6.5) contains the products of two creation and two annihilation operators. Their presence is the consequence of the circumstance that the classical AF state in which the spins in one sublattice point precisely up and in the other precisely down is not the true ground state of the system. However, the ground state of an antiferromagnet usually differs slightly from the classical: the difference between S and the average projection of the spin of an atom on the direction of the moment of its sublattice in the nearest-neighbour approximation is of the order of the inverse coordination number z^{-1} [215]. Should the ground state differ greatly from the classical AF, it would not be possible to leave just the quadratic terms in the Hamiltonian (2.6.5).

We shall have to introduce new Bose operators β_q, β_q^* representing a mixture of the former creation and annihilation operators [215]:

$$b_q = u_q \beta_q + v_q \beta_{-q}^*, \quad b_{-q}^* = u_q \beta_{-q}^* + v_q \beta_q, \quad (2.6.6)$$

which diagonalize the Hamiltonian (2.6.5):

$$H = \text{const} + \sum \omega_q \beta_q^* \beta_q. \quad (2.6.7)$$

To find the coefficients of transformation (2.6.6), we write down motion equations for the operators b_q

$$i \frac{db_q}{dt} = [b_q, H] = \mathcal{B}_q b_q - \mathcal{C}_q b_{-q}^*. \quad (2.6.8)$$

Next we substitute relations (2.6.6) into both the left-hand and the right-hand side of equations (2.6.8) and take into account that the

equation of motion for the "correct" magnon operator β_q , according to (2.6.7), should be of the form

$$i \frac{d\beta_q}{dt} = \omega_q \beta_q. \quad (2.6.9)$$

Equating to zero the coefficients multiplying the β_q and β_q^* operators, we obtain from (2.6.8, 6, 9) a set of two equations whose resolvability conditions yield the magnon frequencies ω_q :

$$\begin{aligned} u_q (\mathcal{R}_q - \omega_q) - \mathcal{C}_q v_q &= 0, \\ -\mathcal{C}_q u_q + (\mathcal{R}_q + \omega_q) v_q &= 0, \end{aligned} \quad (2.6.10)$$

i.e. the frequency, with account taken of the definition of the quantities \mathcal{R}_q and \mathcal{C}_q (2.6.5), will be given by the expressions

$$\omega_q = \sqrt{\mathcal{R}_q^2 - \mathcal{C}_q^2} = \sqrt{(\mathcal{Y}_\Pi - \mathcal{J}_q)(\mathcal{Y}_\Pi - \mathcal{Y}_{\Pi-q})}. \quad (2.6.11)$$

The Néel point can be found in the self-consistent field approximation from expression (2.5.6) for the magnetic susceptibility with account taken of its spatial dispersion. It follows from expression (2.1.5) for $\mathcal{E} = 0$ that an ordering with such a wave vector q will be established that the Fourier-transform of the exchange integral \mathcal{Y}_q will be at its maximum, since this satisfies the condition for its minimum energy. In accordance with it the denominator of expression (2.5.6) vanishes first for the same value of q when the critical temperature is approached from the high-temperature side. Hence, the Néel point for any kind of helicoidal ordering including the AF will be given by the expression

$$T_N = \mathcal{Y}_q \frac{(S+1)}{3}. \quad (2.6.12)$$

Specifically, for a simple cubic lattice in the nearest-neighbour approximation (AF ordering of the staggered type, Fig. 2.2a) T_N will be given by the expression

$$T_N = \mathcal{Y}_\Pi \frac{(S+1)}{3} = 2 |\mathcal{J}| (S+1). \quad (2.6.13)$$

A similar but more laborious analysis carried out for a face-centred cubic lattice of magnetic atoms yields the following expressions for the Néel point of structures depicted in Fig. 2.3, *a-c.* respectively [218]:

$$\begin{aligned} T_N^{(a)} &= \frac{S(S+1)}{3} (6\mathcal{J}_2 - 4\mathcal{J}_1), \\ T_N^{(b)} &= -2S(S+1)\mathcal{J}_2, \\ T_N^{(c)} &= \frac{S(S+1)}{3} (-4\mathcal{J}_1 + 2\mathcal{J}_2). \end{aligned} \quad (2.6.14)$$

Spatially-uniform susceptibility $\chi(0)$ above the Néel point is given by the same expression as for FM, i.e. the Curie-Weiss law

is also valid for AF, but the PM Curie point θ for them is negative. In particular, in the nearest-neighbour approximation for a simple cubic lattice $\theta = -T_N$.

From the fact that θ is negative it follows that there is no discontinuity in the magnetic susceptibility of AF at the Néel point, i.e. its behaviour is substantially different from that of FM. Still, at the Néel point it may display singularities of another type (Fig. 2.6). Indeed, it follows from formula

(2.5.6) that the magnetic susceptibility in the paramagnetic region decreases with rising temperature. In case of a uniaxial crystal, below the Curie point one should distinguish between the susceptibilities $\chi_{||}$ and χ_{\perp} with respect to a field parallel and perpendicular to the crystal axis, respectively. It follows from the analysis made in Sec. 2.3 that in case of an "easy" axis the former is zero in weak fields, the latter being of a finite value (Fig. 2.5). Because of that, the "parallel" susceptibility displays a sharp maximum at the Néel point, with its derivative changing its sign abruptly. At the same time it follows from formulae (2.3.6), (2.5.6) and (2.6.13) that the "perpendicular" susceptibility retains the same value at $T = 0$ as at the Néel point.

Since in case of a helicoidal ordering with an arbitrary vector \mathbf{q} the inequality $\chi_{\mathbf{q}} > \chi_0$ should also be valid, the spatially-uniform susceptibility should be finite at the Néel point as well. In this case the PM Curie point will be proportional to

$$\theta \sim \chi_0 = 2(\mathcal{J}_1 + \mathcal{J}_2) + z_{||}\mathcal{J}_{||}, \quad (2.6.15)$$

where $z_{||}$ is the number of nearest neighbours in a ferromagnetic plane, $\mathcal{J}_{||}$ is the integral of exchange between them which should be positive. In compliance with condition (2.3.3), the exchange integral \mathcal{J}_2 is negative, and its modulus exceeds $\mathcal{J}_1/4$. It follows from formulae (2.3.3) and (2.6.15) that the PM Curie temperature in case of a helicoidal ordering is *a priori* positive for $\cos qa \geq 1/4$ and for all values of q including π/a (FM planes with alternating moment directions), if $\mathcal{J}_{||}$ exceeds \mathcal{J}_2 .

A theory of critical phenomena similar to one presented in Sec. 2.5 of this chapter can be formulated for AF as well. The order parameter that vanishes at the Néel point is the magnetization of sublattices.

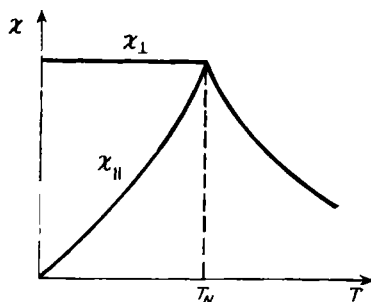


Fig. 2.6. Magnetic susceptibility vs. temperature for a uniaxial anti-ferromagnet

2.7. "ORDER-ORDER" AND "ORDER-DISORDER" PHASE TRANSITIONS OF THE FIRST KIND

Some magnetic systems as the temperature rises display phase transitions of the first kind between various magnetic structures, and sometimes even successions of such transitions (see, for example, [442]). They cannot be explained within the framework of the conventional Heisenberg model. This model is also unable to explain why the order-disorder phase transition in a number of magnetic systems is of the first kind. Kittel [243] suggested an explanation for the FM-AF-type phase transition based on the change of sign of the Heisenberg exchange integral following the thermal expansion of the lattice. This theory could in principle be true only for high-temperature phase transitions. A more universal mechanism of phase transitions of the first kind is purely a magnetic one: they are a result of substantial difference of the exchange interaction in such magnetic systems from the Heisenberg type (see Sec. 2.2).

Fundamental properties of non-Heisenberg magnetic systems can be established, if one considers the simplest models in which one of the following Hamiltonians is added to the Heisenberg Hamiltonian (2.1.5) (designated \mathcal{H}_1):

a biquadratic exchange Hamiltonian

$$\mathcal{H}_2 = -\frac{1}{2} \sum \mathcal{K}_2(g, f) (S_g \cdot S_f)^2, \quad (2.7.1)$$

a three-spin exchange Hamiltonian

$$\mathcal{H}_3 = -\frac{1}{2} \sum \mathcal{K}_3(g, f, h) (S_g \cdot S_h) (S_h \cdot S_f). \quad (2.7.2)$$

or a four-spin exchange Hamiltonian

$$\mathcal{H}_4 = -\frac{1}{2} \sum \mathcal{K}_4(g, f, h, k) (S_g \cdot S_f) (S_h \cdot S_k). \quad (2.7.3)$$

No index in any of the expressions (2.7.1-3) coincides with another.

With the addition of any one of the Hamiltonians (2.7.1-3) to the Hamiltonian \mathcal{H}_1 the respective model acquires principally novel properties as compared to those of the Heisenberg model. Thus, on account of a different dependence of the Heisenberg and the non-Heisenberg exchange interaction on the angle between neighbouring spins, a canted antiferromagnetic ordering becomes possible when the moments of two equivalent sublattices make an angle other than π [39, 40].

The easiest way to convince ourselves that a non-Heisenberg exchange can cause phase transitions between different magnetic structures is to consider the Hamiltonian $\mathcal{H}_1 + \mathcal{H}_4$ with competing

Heisenberg and four-spin exchanges, each trying to establish a different type of magnetic ordering. In this case, because of different temperature dependences of such interactions, the low-temperature properties may be determined by one and the high-temperature properties by the other exchange interaction.

Imagine, for example, that the four-spin AF interaction is stronger than the FM Heisenberg interaction. In that case at $T = 0$ an AF ordering should be established in the crystal. However, as temperature rises the effect of the four-spin exchange on the magnetic ordering diminishes more rapidly than that of the Heisenberg exchange. This follows from the fact that the contribution of the Heisenberg exchange to the mean field is proportional to $\langle S^z \rangle$, whereas that of the four-spin exchange to $\langle S^z \rangle^3$. Accordingly, the AF ordering loses its stability, and in the result is succeeded by the FM [442]. A similar result has also been obtained for the Hamiltonian $\mathcal{H}_1 + \mathcal{H}_3$ in [447].

Both these models display an additional interesting property:

they behave as isotropic metamagnets. Namely, in the temperature range where AF ordering is stable an increase in the external magnetic field brings about an abrupt increase in the magnetization of the crystal [39, 447]. The magnetization jump in a field is usually attributed to strongly anisotropic interaction between the spins (e.g. an Ising one). Hence, non-Heisenberg exchange leads to an alternative explanation for this effect: because of the competition between the former and the Heisenberg interaction, the energy of the system may have two closely-spaced energy minima at relative magnetization values of $M = 0$ and $M = S$, with the latter being displaced downwards by the magnetic field (Fig. 2.7).

More complex models employing non-Heisenberg exchange enable a succession ("cascade") of phase transitions to be obtained instead of one. For instance, a model was discussed in [447] that enabled the cascade of phase transitions observed in the AF EuSe (Fig. 2.8) to be reproduced. In this model the crystal was presumed to consist of planes with a strong Heisenberg FM exchange in them, the Heisenberg exchange between the atoms lying in neighbouring planes being relatively weak. Accordingly, additional factors such as Heisenberg exchange between the atoms of next-neighbouring planes, three-spin interaction (2.7.2) in which the nearest neighbours, g and f atoms, belong to neighbouring planes and biquadratic exchange

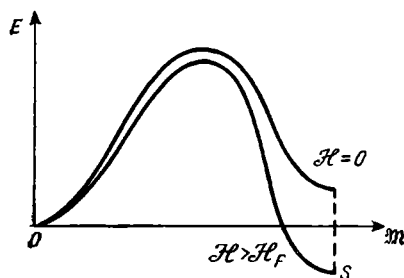


Fig. 2.7. Energy diagram of an isotropic metamagnet

between those atoms that stabilizes collinear structures are taken into account.

Phase transitions are due to a temperature dependence of the three-spin exchange different from that of the Heisenberg exchange. To draw a roughly qualitative picture of the phenomenon, let us introduce an effective integral of the exchange between an atom and its neighbour lying in an adjacent plane $\tilde{J}_1 = J_1 - 2z_L K_3 \langle (S^z)^2 \rangle$, where J_1 and K_3 are appropriate exchange constants from the

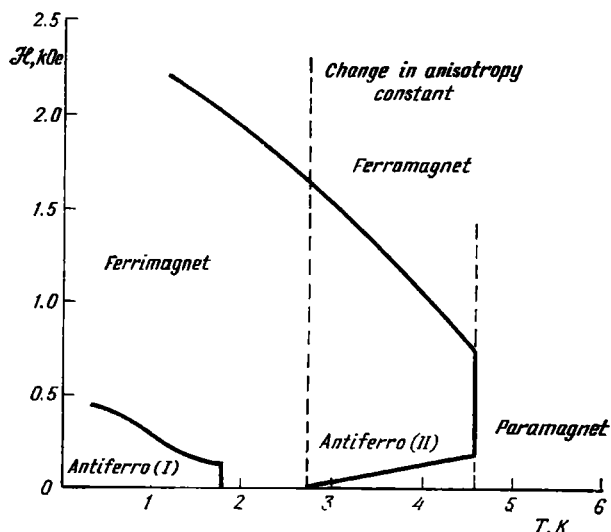


Fig. 2.8. Phase diagram of europium selenide [6]

Hamiltonians \mathcal{H}_1 (2.1.5) and \mathcal{H}_3 (2.7.2), z_L is the number of nearest neighbours of the specified atom lying in a FM plane (the factor 2 appears as a result of summation over the h-atoms whose spin twice enters (2.7.2)). We shall presume that $J_1 > 0$, $K_3 < 0$, with \tilde{J}_1 being negative at $T = 0$. If the exchange integral J_2 between the atom and its nearest neighbour from the adjacent FM plane is negative as well, the type of the structure will depend on the ratio between \tilde{J}_1 and J_2 : in case of $|\tilde{J}_1| > |J_2|$ a usual two-sublattice AF structure of the $\uparrow\downarrow$ type, where the arrows designate the moments of FM planes, is established. At the same time if the inequality is of the opposite sign, a four-sublattice AF structure of the $\uparrow\uparrow\downarrow\downarrow$ type impossible within the Heisenberg model framework should be established (but for the biquadratic exchange, the ordering would be of the helicoidal type).

Suppose at $T = 0$ the inequality $|\tilde{J}_1| > |\tilde{J}_2|$ is satisfied, but in the case being considered $|\tilde{J}_1|$ decreases with rising temperature owing to a decrease in $\langle (S^z)^2 \rangle$. Because of that, above a certain temperature the sign of this inequality may be reversed, i.e. the $\uparrow\downarrow$ type structure must change to the $\uparrow\uparrow\downarrow$ type. A more rigorous analysis in which the free energies of various spin structures calculated in the self-consistent field approximation have been compared has demonstrated [447] that a "ferrimagnetic" three-sublattice structure of the $\uparrow\uparrow\downarrow$ type should appear between two AF structures $\uparrow\downarrow$ and $\uparrow\uparrow\downarrow$ in accordance with what has been observed experimentally in EuSe (see Sec. 2.8).

As to "order-disorder" phase transitions, all non-Heisenberg interactions considered here may transform these transitions from the continuous into the abrupt [39, 442, 444-447]. This can be explained with the aid of the effective exchange integral \tilde{J}_1 introduced above. Suppose, both the Heisenberg and the three-spin exchange tend to establish FM ordering. The quantity \tilde{J}_1 decreases in magnitude with decreasing magnetization because of a decrease in $\langle (S^z)^2 \rangle$. But a decrease in \tilde{J}_1 in turn leads to a decrease in the magnetization, i.e. there is a positive feedback between them. The latter brings about the change in the type of the transition as the ratio between the non-Heisenberg and the Heisenberg exchange reaches a certain critical value.

The problem of the character of short-range order above the transition point merits special discussion, because such properties of the crystal as, for instance, the electrical and the optical are determined by the short-range order. The short-range order above the transition point is usually assumed to be the remnants of the long-range order that existed below the transition point. Actually, with a non-Heisenberg exchange this is not always the case. For a more precise description of the nature of the phase transition, it is necessary to find out the relationship between the long-range order wave vector Q_{L0} below the transition point and the short-range order wave vector Q_{S0} above it. The former is the vector of the reciprocal magnetic lattice, the latter is the value of q at which the susceptibility $\chi(q)$ attains its maximum. The phase transitions in which Q_{S0} is equal to Q_{L0} have been termed "order-proper disorder" phase transitions. In case Q_{S0} and Q_{L0} are not equal, the term is "order-improper disorder" phase transitions [442].

Transitions from AF long-range order to FM short-range order with $Q_{L0} = \left(\frac{\pi}{a}, \frac{\pi}{a}, \frac{\pi}{a} \right)$ and $Q_{S0} = (0, 0, 0)$ may serve as an example of the "order-improper disorder" phase transitions. In the result an isotropic AF turns out to have a positive paramagnetic

Curie point θ . Such a situation is impossible in a Heisenberg magnetic system, but is quite real in magnetic systems with a three-spin or a four-spin exchange [447, 442]. In essence, the phase transition being considered is similar to the "AF-FM" transition, and qualitative considerations cited above remain in force in its case. However, the transition temperature turns out to be so high that the long-range FM ordering above the transition point is destroyed, and only the short-range FM ordering remains. However, generally Q_{S0} and Q_{L0} are incommensurate.

The fluctuation theory of phase transitions (see, for instance, [469]) can serve as an alternative to the non-Heisenberg exchange in explaining the origin of phase transitions of the first kind. The corner-stone of the theory, the idea that the phenomena in the vicinity of the critical point are determined by large-scale fluctuations, is treated mathematically with the aid of the renormalization-group technique. The appropriate R_s transformations correspond to the assembling of spins into larger blocks consisting of s^3 original blocks and to a simultaneous s -fold change in the scale. The set of parameters determining the effective Hamiltonian of the system generally changes following every transformation. The set remaining invariant is termed the fixed point in the parameter space. The characteristics of a phase transition of the second kind are determined from the behaviour of the system in the vicinity of the fixed point.

While Heisenberg ferromagnets always have a stable fixed point, antiferromagnets of a definite symmetry have no such point. This fact has been interpreted in [377-379] as proof that the phase transition in such materials is an abrupt one. However, this hypothesis has as yet failed to be substantiated by experiment (see Sec. 2.8). Moreover, the properties of the AF NdSn_3 studied in [470] forced the authors to the conclusion that the absence of a stable fixed point does not necessarily entail an abruptness of the phase transition. It may just as well correspond to some anomalies of a continuous phase transition.

On the other hand at least some materials exhibiting a phase transition of the first kind whose symmetry does not allow the fixed point for the effective Hamiltonian are characterized by a strong non-Heisenberg exchange, which may be the true cause of the discontinuous phase transition (e.g. Mn compounds, see Sec. 2.8). Moreover, many magnetic structures, which do not possess a fixed point, are impossible within the framework of the Heisenberg models. We may point to the important example of the four-sublattice AF structure discussed above, which materializes in isotropic magnetic systems EuSe and in the nuclear antiferromagnetic solid ^3He [442]. The absence of a stable fixed point for it has been proved in [606], but this is only the consequence of the non-Heisenberg exchange acting in this case that the authors of [606] failed to recognize.

2.8. EXPERIMENTAL DATA ON MAGNETIC SEMICONDUCTORS

Ferromagnets. The first FMS CrBr_3 (Table I) has been synthesized only in 1960 [10], this being an answer to the question as to the compatibility of the semiconducting and FM properties. Shortly afterwards FM crystals EuO [11] have been synthesized, which attract great attention of explorers on account of the simplicity of their crystallographic structure (cubic, of the NaCl-type) and of the absence of an orbital angular momentum of electrons of partially-filled f -shells of the Eu^{++} ions (those f -shells are in $^8S_{7/2}$ states with $L = 0$, $S = J = 7/2$). It should be added, that according to [233] the magnetic dipole-dipole energy of ferromagnetically-ordered spins in a cubic lattice is zero. Those are the reasons for the crystallographic anisotropy of such crystals to be quite small, and for the crystals to be almost ideal Heisenberg magnets. EuS crystals possess similar properties. According to [223, 224], the anisotropy field in EuO is equal to 190 Oe, that in EuS being less than 30 Oe, the effective exchange field \mathcal{H}_0 in them being of the order of 10^6 Oe ($T_c = 69$ K and 16 K, respectively). Anisotropy constants of EuO have also been measured in [37].

The magnetic ions in EuO and EuS form a face-centred cubic lattice. The current opinion is that only the exchange with 12 nearest and 6 next-nearest neighbours plays an essential part. In that case the two unknown exchange integrals \mathcal{J}_1 and \mathcal{J}_2 can be found from the PM Curie point θ (2.5.6) and, for example, from the temperature dependence of magnetization in the spin-wave region (2.4.8) determined experimentally or from other data (see [9]). The following values have been obtained: $\mathcal{J}_1 = 1.26$ K, $\mathcal{J}_2 = -0.14$ K for EuO and $\mathcal{J}_1 = 0.40$ K and $\mathcal{J}_2 = -0.16$ K for EuS . It is worth pointing out that the interpretation of experimental data with the aid of the self-consistent field theory should, according to what was said in Sec. 2.5, lead to errors amounting to 30-50%.

Despite difficulties of neutronographic studies of Eu compounds resulting from their high neutron absorption, the authors of [417] succeeded in determining the exchange integrals from data on inelastic scattering of neutrons in the spin-wave region by employing crystals of EuO and EuS containing only the ^{153}Eu isotope. The results in the notations used in this book are as follows: for EuO $\mathcal{J}_1 = 1.212$ K, $\mathcal{J}_2 = 0.238$ K, for EuS $\mathcal{J}_1 = 0.472$ K, $\mathcal{J}_2 = -0.236$ K. Somewhat different values of exchange integrals for EuS have been obtained with the same method in [458]. Both the magnetostriction [452, 456] and the variation of T_c with the temperature [453-455] were studied in EuO and EuS . It has been established that the value of $d \ln T_c / d \ln V$ (V is the volume) amounts to -6 for EuO and to -5.5 for EuS . According to [294] a weak exchange interaction in EuO is observable even at distances achieving 5 lattice constants.

Ferromagnetic Semiconductors

Table I

No.	Material	Crystal structure	T_c , K	θ_c , K	Cell moment M_0 in μ_B	References
1	CrBr ₃	Trigonal symmetry with vacancies	37	~ 37	3.85	[10]
2	EuO	NaCl, $a = 5.441 \text{ \AA}$	66.8	76	6.8	[6, 11]
3	EuS	NaCl, $a = 5.968 \text{ \AA}$	16.3	19	6.87	[6]
4	Eu ₁₁ S ₈		8	4		[18, 19, 23, 24]
5	Eu ₁₃ P ₂	Ba ₃ P ₂ structure, $a = 9.026 \text{ \AA}$	25	33	6.8	[22]
6	Eu ₃ As ₂	Ba ₃ P ₂ structure, $a = 9.225 \text{ \AA}$	18	23	7.03	
7	Eu ₂ SiO ₄	Monocline (ferroelastic) $T > 165 \text{ K}$ and monocline orthorhomb $T < 165 \text{ K}$	5.4 7 9	7 9	7 7	[26-28] [27] [27-30] [387] [9]
8	Eu ₂ SiO ₄	Th ₃ P ₄	84.5-97	135	5.15-5.55	
9	Eu ₃ SiO ₅	Spinel, $a = 10.244 \text{ \AA}$	130-142	190	5.4 6	[9]
10	Eu ₂ S ₄	Spinel, $a = 10.755 \text{ \AA}$	106 120	192 200	5.4 5.64	[9]
11	CdCr ₂ S ₄	Spinel, $a = 10.753 \text{ \AA}$	< 4.4	0 25		[9]
12	CdCr ₂ Se ₄	Spinel, $a = 10.416 \text{ \AA}$	274	345	5.25	[9]
13	HgCr ₂ Se ₄	Spinel, $a = 11.125 \text{ \AA}$	204	4.4	4.10	[9]
14	CuCrTiS ₄	Spinel, $a = 11.125 \text{ \AA}$	3.5			[25]
15	CuCr ₂ Se ₃ Br	C_{3h} symmetry group with axes $c = 3.56 \text{ \AA}$, $a = 6.24 \text{ \AA}$	2.5	4.2		[25]
16	CuCr ₂ Te ₃ I	Perovskite	8.9		1	[31-33]
17	Dy(OH) ₃	Volume-centred tetragonal	2.85			[210, 328]
18	Ho(OH) ₃	Volume-centred tetragonal	2.53			[210]
19	(CH ₃ NH ₃) ₂ CuCl ₂	Volume-centred tetragonal	3.91			[210]
20	LiTbF ₄	Volume-centred tetragonal	2.2			[365]
21	DyF ₃	Volume-centred tetragonal	7.2	69	6.6	[6]
22	TbF ₃	NaCl	3.8			[387, 497]
23	GdCl ₃	Th ₃ P ₄	24			[451]
24	GdN ₂	»	22.5			[451]
25	Eu ₃ S ₄	»	20			[451]
26	Eu ₄ P ₂ S	»	38			[498]
27	Eu ₄ P ₂ Se	Perovskite	50-60			[457]
28	Eu ₄ As ₂ S	Layered				
29	EuLiH ₃					
30	M ₂ CrCl ₄ (M = Rb, K, Cs)					

Very valuable information can be gained from the measurement of critical exponents of EuO and EuS, since owing to the small anisotropy such crystals are up to a very high degree of accuracy described by the Heisenberg model, and an agreement with the experimental results is a criterion of adequacy of any theory of critical phenomena in Heisenberg magnets. Magnetic resonance measurements have demonstrated that in the temperature range $0.1 > |\tau| > 0.01$ where $\tau = (T - T_c)/T_c$ the temperature dependence of the magnetization of EuS is described by formula (2.5.15) with $\beta = 1/3$. Neutronographic methods have yielded for the exponent in EuO and EuS the value 0.36 [418]. This is in good agreement with the scaling estimate (2.5.16).

The values of the exponent γ for the susceptibility (2.5.15) cited by various authors differ slightly. Experiments on critical neutron scattering in EuO and EuS yield for the index γ the values of 1.387 and 1.399 and for the correlation-length exponent ν the values of 0.681 and 0.702, respectively [225, 418]. Susceptibility measurements demonstrate [35] that in the immediate vicinity of T_c the exponent γ in EuO is equal to 1.30. As the temperature rises, starting from $\tau = 0.05$ this index decreases rapidly approaching the value $\gamma = 1$ obtained with the self-consistent field theory. However, γ still exceeds this value by 20% even at $\tau = 0.1$. (The authors of [35] interpret their results as proof of the positive sign of the exchange integral J_2 , with $J_2 = (0.5 \pm 0.2) J_1$, this contradicting the results of other authors.) Studies of the Faraday effect in EuO yield $\gamma = 1.30$, this value remaining unchanged in the interval $0 < \tau < 0.1$ [36], [374] (in [374] it has also been obtained that $\beta = 0.37$).

In [226, 227] an opinion has been expressed proceeding from the analysis of the specific heat of EuO that at $|\tau| \sim 0.02$ the crossover from the Heisenberg critical behaviour to that for which the dipole-dipole Hamiltonian is responsible takes place.

According to [459], the critical exponents of specific heat of EuS on both sides of T_c are equal to $\alpha = \alpha' = -0.13$. Those values prove the dipole forces in EuS to be stronger than in EuO. Spin dynamics in EuO in the vicinity of T_c has been studied in [460] by means of the electron-spin resonance method and in [461] by means of inelastic neutron scattering. According to [461], above T_c magnetic excitations change from Lorenz peaks in the centre of the Brillouin zone to well defined magnons near the zone edge. Thus, specific magnons due to the existence of a short-range order above T_c ("paramagnons") have been discovered in the PM region in EuO.

Reference [419] reports the results of studies of spin dynamics in EuO close to T_c . It also presents experimental proof of the theory of temperature renormalization of magnon frequencies discussed in Sec. 2.4.

The authors of [448, 449] have used a sophisticated method of inel-

astic scattering of light to study magnetostatic magnons in EuO and EuS (the term magnetostatic applies to ultra-long-wave magnons whose frequency is determined by magnetic anisotropy). The existence of both bulk and surface magnons in those materials has been established. Numerous magnetostatic modes have been observed in [462].

Another important group of FMS is composed of chrome spinels of which CdCr_2S_4 and CdCr_2Se_4 have been studied most extensively. Their crystallographic structure is much more complex than that of EuO and EuS, and because of that they are less suitable for testing physical theories. But to make up for this they have much higher Curie points. For $\text{CuCr}_2\text{Te}_3\text{I}$ it lies even in the range of room temperatures, and this is very valuable from the point of view of their practical applications. Out of papers dealing with their magnetic properties in the vicinity of T_c [463-465] containing the results of studies of resonance phenomena are worthy of mention. It should be noted that in [357] two nearby specific heat peaks have been discovered in CdCr_2S_4 . They are interpreted in [357] as proof of the abrupt nature of the FM-PM phase transition.

Recently highly anisotropic FM with very low Curie points have been discovered (e.g. $\text{Dy}(\text{OH})_3$, $\text{Ho}(\text{OH})_3$) in which FM ordering is either completely or partly the result of spin dipole-dipole interaction. According to [33], the sharply anisotropic compound $(\text{CH}_3\text{NH}_3)_2\text{CuCl}_2$ in the immediate vicinity of T_c behaves like a three-dimensional magnet, but already 1 K above T_c ($\tau \simeq 0.25$) its behaviour corresponds to that of a two-dimensional system.

Table I includes GdN and EuB_6 crystals, too. Such materials can be synthesized only with an imperfect stoichiometry. Accordingly, it is not clear whether their ferromagnetism is due to charge carriers (the part played by charge carriers will be discussed in Sec. 6.1). GdN single crystals in which the charge-carrier density is negligible display in weak fields a temperature peak of χ , this being probably proof of their antiferromagnetic nature [6]. A similar conclusion was arrived at in [526, 594] where the result $T_N = 40$ K has been cited.

According to [450], EuB_6 is a degenerate FMS with $T_c = 13.7$ K and an abnormally strong pressure dependence of T_c : a pressure of 1 kbar raises its T_c by 4%. A similar conclusion was made in [514] where the result $T_c = 12.5$ K has been cited, as well as in [552]. The alloy $\text{EuS}_{1-x}\text{Se}_x$ one of whose components is an FM and the other an AF deserves special mention. However, the alloy turns FM already at $x \simeq 0.87$, behaving like a mixture of two FM's with different intensities of exchange interaction [466].

Antiferromagnets. In contrast to FM, most AF are semiconductors or insulators. The known AFS are much more numerous than FMS- and only those with most interesting electrical and magnetic proper,

Table II

Antiferromagnetic Semiconductors

No.	Material	Crystal structure	Ordering type	T_N , K	θ_p , K	Cell moment M_0 in μ_B	References
1	EuTe	NaCl, $a = 6.598 \text{ \AA}$	MnO	9.58	-6		[4]
2	EuSe	NaCl, $a = 6.435 \text{ \AA}$		4.6	9	6.7	[2-7]
3	Eu ₃ O ₄	Rhombohedral structure (r.s.) $a = 10.40$, $b = 12.45$, $c = 3.51 \text{ \AA}$	Spins form FM chains in direction of C -axis. Moments of neighbouring chains directed against each other	5.3	7	7.8	[13, 14]
4	EuLa ₂ O ₄	r.s., $a = 9.49$, $b = 11.69$, $c = 3.65 \text{ \AA}$		7.5	4	7	[15]
5	EuGd ₂ O ₄	r.s., $a = 10.09$, $b = 12.11$, $c = 3.53 \text{ \AA}$		4.5	2	13.3	[15]
6	Gd ₂ Se ₃	Th ₃ P ₄ with vacancies		6	-10	7.75	[8, 9]
7	MnO	NaCl	\parallel to ferromagnetic (111) plane	122	-610	5.0	[16]
8	MnSe	NaCl	MnO	173	-360	5.0	[16]
9	NiO	NaCl	MnO	520	-2600	2.0	[16]
10	CoO	NaCl	\parallel [001]	291	-320	3.8	[16]

Table 11 (continued)

No.	Material	Crystal structure	Ordering type	T_N , K	θ_p , K	Cell moment M_0 in μ_B	References
11	MnTe	Hexagonal	\perp [001]	323	-715	5.0	[16]
12	MnTe ₂	Face-centred cubic	\parallel to ferromagnetic (001) plane	80	-520	5.0	[16]
13	LaMnO ₃	Orthorhombic symmetry	Ordering with alternating FM planes	100	-500	3.9	[16]
14	CuFeS ₂	Tetragonal	\parallel [001]	825			[16]
15	CoCl ₂	Trigonal	Ferromagnetic layers connected antiparallel	25	-37	3.1	[16]
16	NiCl ₂	Trigonal	CoCl ₂	50	-75	—	[16]
17	ZnCr ₂ S ₄	Spinel	A weak ferromagnet	18	18		[9]
18	HgCr ₂ S ₄	Spinel	Helicoidal with rotation angle $\varphi = 22^\circ$ at 4.2 K and $\varphi = 10^\circ$ at 30 K	60	137 142	5.35 5.46	[9, 161]
19	ZnCr ₂ Se ₄	Spinel	Helicoidal with φ at 4.2 K	20	-115		[9, 211]
20	α -Pr ₂ S ₃	Spinel		2.48			[375]
21	γ -Pr ₂ Se ₃	Spinel		1			[375]
22	TmSe	Spinel		1.8-2.8			[375]

ties are represented in Table II. Information about other AFS can be found in the book [16].

A large group of AFS consists of transition metal compounds in which magnetic ions form a face-centred cubic lattice. The majority of them (such materials with a NaCl structure as MnO, MnSe, NiO etc.) have an antiferromagnetic ordering of the type depicted in Fig. 2.3b. Ordering of the type shown in Fig. 2.3a is peculiar to MnTe₂ and of the type shown in Fig. 2.3c to MnS.

A NaCl structure is also the property of EuTe and EuSe crystals, which are isoelectronic with FMS EuO and EuS. Of them EuTe behaves like an ordinary Heisenberg antiferromagnet with an ordering as shown in Fig. 2.3b. Estimates of exchange integrals in EuTe from the experimentally determined Néel point and paramagnetic Curie point with the aid of formulae (2.6.14) and (2.5.6) yield the values $J_1 = 0.20$ K, $J_2 = -0.42$ K [38]. Such values provide for the energetically most favoured ordering of the type shown in Fig. 2.3b which exists in EuTe in reality (according to formula (2.6.14), a higher T_N corresponds to it). But they have been obtained in the self-consistent field approximation and hence are not very accurate.

Reference [467] reports the results of research on AF resonance in EuTe and [468] on the critical exponents for the specific heat. On both sides of T_N they are equal to 0.08 ± 0.06 . Within the framework of existing theories, these values correspond to lower crystal symmetries than the cubic, and by reason of this assumptions have been made in [468] concerning the existence in EuTe in the vicinity of T_N of uniaxial stresses.

Magnetic ordering in EuSe, which displays complex and unusual properties, has been studied in [2-7, 471-474] with the aid of various experimental methods including neutronographic ones and NMR. The results have been summed up in a phase diagram (Fig. 2.8): all magnetic structures actually encountered in EuSe can be represented as a set of FM (111) planes whose moments are either parallel or antiparallel to one another.

For $H = 0$, at the Néel point 4.6 K a transition from the PM to the AF state with an unusual structure takes place: the FM planes form four equivalent sublattices ordered as $\uparrow\uparrow\downarrow\downarrow$. On cooling down to 2.8 K this ordering goes over abruptly to the "ferrimagnetic" (FIM) state with a nonzero, but an unsaturated magnetic moment. This state is presumed to be a two-phase one: one phase is of the ordinary AF MnO-type, i.e. of the $\uparrow\downarrow$ type, and the other—a magnetized three-sublattice one of the $\uparrow\uparrow\downarrow$ FIM-type. The relationship between volumes of these phases is 5 : 13. Because of that the resulting moment per Eu²⁺ ion is equal not to $7 \mu_B$, but only to $1.68 \mu_B$. The results of magnetic and dilatometric studies demonstrate [71] that at 1.8 K a complete phase transition to an AF state other than

the $\uparrow\uparrow\downarrow$ state takes place. Judging by the fact, that, according to neutronographic data [2], in the immediate vicinity of the transition point (1.9 K) the FIM-state $\uparrow\uparrow\downarrow$ coexists with the AF $\uparrow\downarrow$ state, the latter is exactly the AF state that should materialize below the transition point. An additional proof that below 1.8 K the AF ordering is of the MnO-type has been obtained in [472]: after the temperature has sunk below 1.8 K the Faraday rotation spectra of EuSe assume the same form as that of EuTe, which has the magnetic structure of MnO.

In the regions of stability of AF states a weak magnetic field transforms the crystal at first into the FIM and subsequently into the FM state. The anisotropy field in EuSe amounts only to 100 Oe [9], i.e. this material constitutes a unique example of an isotropic metamagnet. Studies of the Mössbauer effect [471] have demonstrated that the "order-disorder" phase transition at 4.6 K is of the first kind, this being in agreement with experimental data obtained from NMR [473]. The $\uparrow\uparrow\downarrow$ phase can be stabilized by substituting less than 1% of S for Se [538], and the $\uparrow\downarrow$ phase by substituting Te for Se [537]. Then the magnetic polymorphism disappears.

It should be remarked that the phase diagram in Fig. 2.8. probably, simplifies the behaviour of EuSe in magnetic fields. According to [474], below T_N in a field of 4 kOe the temperature derivatives of the anisotropy constants display anomalies incompatible with a complete FM ordering. At 1.3 K the magnetization does not attain saturation even at $\mathcal{H} = 19$ kOe [474]. According to [473], in case of cyclic variations of either the field or the temperature the magnetic phase transitions display a hysteresis. Some intermediate phase lies between the FIM and the FM phase.

If one compares experimental data obtained by different authors, he will probably find indications as to the existence in EuSe of an "order-improper disorder" phase transition. According to [471], the long-range order in EuSe in contrast to other chalcogenides disappears abruptly. In the PM-state θ in EuSe is positive ($\theta = 9$ K), this pointing to an FM short-range order.

The quantity θ in EuSe being positive has been presumed in [471] to be due to donor imperfections in the vicinity of which FM ordering is established (localized ferrons (see Sec. 5.3)). With such a possibility in mind, let us cite additional proof in favour of the FM short-range order in the PM region being a property of regular EuSe crystals. Firstly, Mössbauer effect spectra demonstrate that an FM short-range order appears above the AF-PM transition point [471]. Should it be associated with the above-mentioned imperfections, it would also be detectable at all temperatures below T_N . Secondly, in the PM region a very pronounced red shift of the optical absorption edge E_g is observed when the temperature is lowered, this shift stopping abruptly below T_N (Fig. 4.2).

The giant red shift E_J is typical of FMS. In them it takes place both above and below T_c and is the result of FM ordering established at lower temperatures, at first of the short-range order and subsequently of the long-range order type (Secs. 4.1-4.3). It is also observed in crystals with a helicoidal ordering, if the helicoid period is very great, and for this reason local ordering is practically of the FM-type (e.g. in HgCr_2S_4 , Fig. 5.9). At the same time in isotropic AF the red shift both above and below T_N was not observed. On the contrary, they display a small blue shift. Specifically, there is no red shift in the two-sublattice antiferromagnet EuTe (Fig. 5.7), whereas in FMS EuO and EuS it is very large (Figs. 4.2, 4.3).

The following fact proves that the red shift in EuSe above T_N is associated with the FM short-range order: a magnetic field that establishes an FM order intensifies the red shift (Fig. 4.2). A calculation shows (Sec. 5.4) that a weak red shift should occur as the four-sublattice AF ordering is established. It is too small to explain optical properties of EuSe above T_N . But it may explain the experimental fact that the position of the absorption edge itself changes little after the transition.

On the other hand, this may be the result of the coexistence of the AF and the PM phase below T_N caused by stresses present in the crystal. A strong influence of stresses on the states of EuSe is the consequence of a strong pressure dependence of its magnetic properties: a pressure of 1 kbar reduces the Néel point by as much as one degree [405]. In any case, if the red shift above T_N had been caused by the short-range four-sublattice AF order, it would have grown abruptly after an abrupt appearance of the corresponding long-range order at T_N contrary to the experiment.

The data cited above are naturally inadequate to establish the short-range-order wave vector \mathbf{Q}_{S0} in EuSe : it can be determined only with the aid of neutronographic studies. However, from the similarity between the properties of EuSe in the PM region and the behaviour in this region of FM crystals \mathbf{Q}_{S0} may be expected to be sufficiently small.

All the anomalous properties of EuSe (a cascade of "order-order" phase transitions, non-Heisenberg magnetic structures, metamagnetism, the possibility of "order-improper disorder" phase transitions of the first kind) are satisfactorily described by a model with non-Heisenberg exchange (Sec. 2.7). Its applicability follows not only from the abnormally low ordering temperature of EuSe as compared with that of other Eu chalcogenides, but also from the very strong pressure dependence of exchange parameters (i.e. the dependence on crystal volume) mentioned above, which also enhances the part played by non-Heisenberg exchange.

An attempt to explain the properties of EuSe was made earlier in [595-597]. There the coupling between FM (111) planes has been

presumed to be mainly of the dipole-dipole type, and lattice deformations associated with the type of ordering have been explicitly taken into account. However, this model has been unable to explain both the magnetic polymorphism and the abrupt AF-PM phase transition.

The Eu_3O_4 crystal is also metamagnetic [13, 14]. It is highly anisotropic and in certain aspects may be regarded as quasi-one-dimensional. The ions Eu^{++} in an elementary cell are arranged along the c -axis, forming spin chains pointing in this direction. The spins of neighbouring chains are antiparallel to one another. In a field of ~ 2 kOe pointing in the direction of the c -axis all the chains are oriented parallel to one another. The EuLu_2O_4 and EuGd_2O_4 crystals belong to the same type [15].

Out of chrome spinels included in Table II, HgCr_2S_4 and ZnCr_2Se_4 display helicoidal ordering. It has been established that in the former the spin rotation angle decreases markedly with rising temperature [161]. At $T < 25$ K the HgCr_2S_4 spinel is metamagnetic.

Table II contains several semiconducting compounds of Pr and Tm which are magnetic systems with a singlet ground state. We would also like to mention some materials presently classified as Pauli paramagnets: FeS, TiSe, TiS, TiTe (see [602, 603]). Specifically one should mention the metamagnet TmSe belonging to the mixed valency materials [375, 614-616]. Whereas at higher temperatures it behaves like a metal, it becomes semiconducting at $T \rightarrow 0$ [615]. Of the semiconducting Tm compounds, interest attaches to $\text{Tm}_{0.5}\text{Eu}_{0.5}\text{Se}$ in which the moments of Eu ions are antiparallel to those of Tm ions. The spontaneous magnetization results from the difference between their magnitudes, the Curie point of this ferromagnet being 18.5 K [612, 613].

As has been already stated in Sec. 2.7, the existing theory of critical phenomena predicts that in AF crystals with certain types of symmetry the destruction of the magnetic order must take place abruptly. Among them crystals with the MnO-type symmetry have been studied most extensively. However, there are still no reliable experimental data to support the theory. The only material of this group in which the abrupt disappearance of the magnetic order has been reliably verified by experiment is MnO itself. According to [251], at the transition point the magnetic order parameter changes from the value that amounts to 60% of the maximum to zero. However, the conclusion arrived at in [251] concerning the discontinuity only in magnetic properties following the AF-PM phase transition in MnO has been questioned in [423]: it has been established that simultaneously with the reduction in the magnetic scattering of neutrons at the presumed phase transition point, a decrease in the nuclear scattering comparable with the former in magnitude takes place. Hence, at this point not only a pronounced change in the state of

the magnetic subsystem takes place, but some substantial change in the state of the lattice as well. At the same time the magnetic phase transition of the first kind predicted by the fluctuation theory (Sec. 2.7) is not connected with any changes in the state of the lattice. In this case such a transition may be the result of the dependence of the exchange integral on the lattice parameters which leads to a non-Heisenberg exchange (see Sec. 2.6).

According to [376], a small (~ 5 kbar) uniaxial stress applied to a MnO crystal turns the magnetic transition in it into a continuous one. At this stress the Néel point is equal to 133.5 K and the critical index of sublattice magnetization $\beta = 0.3$. An almost equal value of β has been obtained for NiO, which has the symmetry of MnO [114, 234]. By investigating optical birefringence, the authors of [234] have obtained $\beta = 0.325$. An AF-PM phase transition of the first kind has been discovered in MnS_2 [397].

There is experimental evidence that the phase transition in MnSe is possibly also of the first kind [515]. On the other hand the intensity of biquadratic exchange between the Mn^{2+} ions in Mn compounds is known to be comparable to the intensity of the Heisenberg exchange [475, 476]. One can perhaps explain the discontinuity of phase transitions in Mn compounds without invoking the fluctuation theory (see Sec. 2.7).

Spin Glasses. Quite recently semiconducting glasses have been discovered and studied. The term spin glasses is understood to apply to magnetic systems in which the average spin of every atom is non-zero, but there is no order in the directions of the spins. Such a situation is possible, if, for example, the signs of the exchange integrals fluctuate randomly, a precondition for this being the absence of crystallographic ordering in the magnetic material. Spin glasses can also be obtained by introducing imperfections, e.g. nonmagnetic impurities [477-479] into antiferromagnets. In a wider sense of this word nonferromagnetic materials containing clusters with FM ordering caused by spatial fluctuations of the material composition (e.g. fluctuations of the components of an alloy) are also classified as spin glasses.

A feature distinguishing spin glasses is the magnetic susceptibility peak at a certain temperature T_f termed freezing temperature. It becomes sharper as the magnetic field is reduced, and in an alternating field moves to the high-temperature side. This peak is not accompanied by any singularities of specific heat or of electric conductivity (see, for example, [496]). The magnitude of magnetization in an external field below T_f depends on whether cooling proceeded in a magnetic field or without one: in the former case it will be higher ("thermoremanence").

The theory of spin glasses is still in a rudimentary state. It is even not clear whether the spin-glass state is a thermodynamically

equilibrium one. Such facts as the frequency dependence of T_f and thermoremanence speak in favour of it being a nonequilibrium state. Moreover, there is evidence that such experimental results as the height of the peak of χ depend on the duration of the observation [605].

It has been repeatedly stated (e.g. in [481, 549-551]) that the properties of spin glasses in which FM clusters are produced can be explained in terms of the superparamagnetism theory [482]. According to this theory, at low temperatures the directions of the cluster moments in the crystal remain frozen by the anisotropy field, and for this reason the susceptibility χ is small. As temperature rises their defreezing takes place, and their contribution to the total susceptibility of the crystal grows. On the other hand at high temperatures the contribution of the clusters to the susceptibility should diminish with the rise in temperature according to the Curie-Weiss law. Hence, a maximum of χ should be observable in weak fields, but there should be no maximum in strong fields that defreeze the moments at $T \rightarrow 0$. The difference between the magnetization when the specimen is cooled in a field and without a field can be explained by the existence of an activation barrier for cluster moments due to magnetic anisotropy. An alternative approach based on the treatment of the spin-glass state as an equilibrium cooperative phenomenon was first proposed in [607].

The first semiconducting material in which the existence of the spin-glass state has been definitely established was probably the solid solution $\text{Eu}_x\text{Sr}_{1-x}\text{S}$ with $x < 0.52$ [480, 523, 605], which at $x = 1$ is an FMS. Below T_f equal to 4 K there is in this material at $x \sim 0.5$ a strong small-angle neutron scattering, which suggests the existence of a short-range FM order. The fluctuations in the distribution of Eu and Sr over cation sites probably produce FM clusters in regions of enhanced density of the Eu^{2+} ions. Proof of this is the discovery in such glasses at lower temperatures of a red shift of the absorption edge typical of FMS [491] and calorimetric data [486]. But, according to [605], the cluster theory may be adequate only for very small x . At larger x interaction between clusters becomes essential.

However, spin glasses can be obtained when not only FMS, but AFS as well, are diluted by nonmagnetic ions (e.g. $\text{Hg}_{1-x}\text{Mn}_x\text{Te}$ with $x \sim 0.35$ [483], $\text{Cd}_{1-x}\text{Mn}_x\text{Te}$ [484]) and it is not clear to what extent the superparamagnetism theory is applicable to such materials. It is hardly applicable to manganese aluminium silicate whose spin-glass state is due to the topological disorder in the arrangement of Mn ions. Judging by the high negative PM Curie point (-100 K) and by the dependence of T_f on the field frequency, it is improbable that it contains FM clusters [488].

$\text{Eu}_{1-x}\text{Gd}_x\text{S}$ also possesses spin-glass properties [524], the explanation for this being the FM exchange between two Eu ions and AF

exchange between the Eu and Gd ions. The cause of the spin-glass state of several materials is fluctuations in the arrangement of non-magnetic ions. As example of the former is the spinel $\text{Ga}_{2/3}\text{Cr}_2\text{S}_4$ with $T_f \sim 4$ K in which the Ga atoms can occupy nonequivalent sites. Their fluctuating distribution causes the fluctuations of superexchange interaction between magnetic ions [489, 490]. FM interactions in this case are probably not quite compensated by AF interactions: $\theta = 10$ K is positive.

Spin-glass properties are also displayed by the $x\text{CuCr}_2\text{S}_4 - (1-x)\text{Ga}_{2/3}\text{Cr}_2\text{S}_4$ system with $x < 0.45$. For greater x it turns into an FM and simultaneously goes over from the insulating to the conducting state [490]. Thus, the spin-glass state is destroyed by indirect exchange via charge carriers. The situation here looks like a paradox from the point of view of conventional ideas about the origin of metallic spin glasses: the current opinion is that the changes of signs of their exchange integrals result from the indirect exchange via charge carriers (see Sec. 3.3).

There are also quasi-one-dimensional spin glasses, e.g. FeMgBO_4 in which nonmagnetic Mg ions interrupt chains of Fe ions, resulting in the establishment of local helicoidal ordering in every segment [521, 525].

CONDUCTING MAGNETIC SYSTEMS. THE VONSOVSKY MODEL

3.1. THE VONSOVSKY MODEL AND ITS APPLICATION TO MAGNETIC SEMICONDUCTORS

The problem discussed in Chapter 2 was actually one of the magnetic insulator. A crystal becomes a conductor when free electrons and holes appear in it. For the description of MS a very useful model is one that has been first proposed by S.V. Vonsovsky [42]. It presumes that all electrons in the crystal may be subdivided into the localized that form partially-filled ionic d - or f -shells and the delocalized occupying s -type states. Originally, it has been termed s - d model, but the author himself regards this term as inaccurate [42]. Since in this model the localized d - and f -electrons receive a perfectly identical treatment, and the delocalized electrons need not necessarily occupy s -type states, we shall use the symbol " l " to denote the former and the symbol " c " to denote the latter. Accordingly, we shall use the brief " c - l model" for the Vonsovsky model.

If the delocalized electrons can be described in the single-electron approximation, the Hamiltonian of the c - l model will be of the form

$$H = H_B + H_A + H_M. \quad (3.1.1)$$

Here H_B is the Hamiltonian of conduction electrons (1.1.1). The Hamiltonian of the magnetic subsystem is usually taken in the Heisenberg form (2.1.5), not necessarily in the nearest-neighbour approximation. Lastly, the Hamiltonian H_A describes the exchange between the conduction electrons and the spins of magnetic ions. In the single-band approximation it is written down in the form

$$H_A = -A \sum (S_g \cdot s)_{\sigma\sigma'} a_{g\sigma}^* a_{g\sigma'}, \quad (3.1.2)$$

where expression (2.1.6) is used for the c -spin operator, and $s_{\sigma\sigma'}$ are Pauli matrices. The structure of (3.1.2) will be understood better, if one notes that in the coordinate representation the energy of the exchange between a conduction electron localized at the moment on the f -ion and the magnetic g -ion is expressed in the form $-A (f - g) (S_g \cdot s)$, where s is the operator of the conduction-electron spin (higher powers of $(S_g \cdot s)$ cannot be part of this energy, because of the properties of the $1/2$ -spin cited in Sec. 2.2). Next, the exchange interaction is a short-range one. Accordingly, we may take into account only the c -electron interaction with the atom it

occupies, since in this case the exchange integral $A(0)$ is of the zeroth order in the overlap of the Wannier c -function with the wave functions of the partially-filled l -shell. If on the other hand the c -electron is on a neighbouring atom ($\mathbf{f} = \mathbf{g} - \Delta$), its exchange with the l -shell of the \mathbf{g} -atom will be of the second order in orbit overlap, the latter being small owing to the smallness of the radii of orbits of partially-filled shells. Since $A(\mathbf{f})$ has the properties of a δ -function, only the term with $A(0) \equiv A$ needs be taken into account in the c - l exchange energy. This very term is written in expression (3.1.2) in the secondary quantization representation.

In principle, the Hamiltonian of c - l exchange should also include multispin terms of the type of $(\mathbf{S}_f \cdot \mathbf{S}_g)(\mathbf{S}_g \cdot \mathbf{s})$, but they must be of a still higher order in orbit overlap, and for this reason are discarded.

Let us now discuss the applicability of the c - l model to MS. As a rule, they are constructed of cations with a nonzero spin and of nonmagnetic anions. The charge-carrier-energy spectrum in them consists of an electron and a hole band vacant at $T = 0$. In the simplest case the electron band (conduction band) is constructed of states of a type different from that of the states of the partially-filled shells (e.g. of s -type cation states). The hole band for its part is built of p -type anion states, and for this reason the orbital states of l -electrons do not change when a "conduction electron-hole" pair appears. In this case the applicability of the Hamiltonian (3.1.1) to charge carriers of both signs is self-evident. Since the electrons move from one magnetic cation to another, and the holes—from one nonmagnetic anion to another, the exchange between the l -spins and the conduction electrons should be much more intense than between the former and the holes. The Hamiltonian (3.1.1) can be easily generalized for cases when the interband c - l exchange matrix elements are of substantial importance (Sec. 3.4).

The basic assumption in the situation described above is that the electron transitions into the conduction band from partially-filled shells are not energetically favoured (in a roughly qualitative sense, the electron levels of partially-filled shells lie below the top of the valence band). However, this is not always the case, and the model should be generalized to include the case, when electrons of partially-filled shells, e.g. d -electrons, take part in the current. The energy spectrum of such a magnetic semiconductor is depicted in the form of an energy-band diagram (Fig. 3.1). It should at once be clear that it is just as pointless to speak of a d -band when each of the d -electrons is localized on its own atom and is unable to take part in the current as of a donor band in a nondegenerate nonmagnetic semiconductor. The d -band concept becomes meaningful when an additional electron appears on one of the magnetic cations, or one of the d -electrons formerly present on it disappears (the situation

here is quite different from the case of metals with delocalized d -electrons).

If before the arrival of an excess electron all the cations were in the M^{n+} state (e.g. Cr^{3+} in $CdCr_2Se_4$), the cation with an excess electron will be in the $M^{(n-1)+}$ state. Owing to the equivalence of all the cations in the crystal lattice, the excess electron can migrate over them by means of the reaction $M^{(n-1)+} + M^{n+} \rightarrow M^{n+} + M^{(n-1)+}$. In the result of its motion over the cations, its level

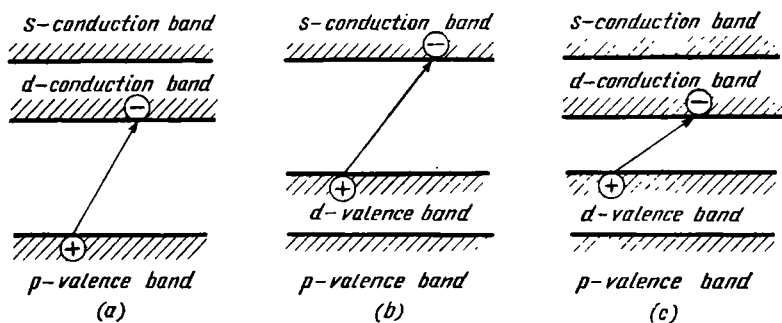


Fig. 3.1. Charge-carrier generation by electron transitions: (a) from the p -valence band to d -levels; (b) from a d -level to the s -conduction band; (c) between d -levels

broadens into a band depicted in Fig. 3.1a (" d -conduction band"). In addition the same figure depicts the " s -conduction band" constructed of states of outer cation shells and the " p -valence band" constructed of anion states. We would like to emphasize once again that the " d -conduction band" is not the band of M^{n+} ions, but the band of $M^{(n-1)+}$ ions, and in the absence of the latter it is vacant.

In the same way, if an electron has been removed from one of the cations M^{n+} , and the ion went over to the $M^{(n+1)+}$ state, its excess positive charge can move over the cations by means of the reaction $M^{(n+1)+} + M^{n+} \rightarrow M^{n+} + M^{(n+1)+}$. Hence, the $M^{(n+1)+}$ ion behaves like a hole, and a hole band should be introduced to correspond to it. However, in compliance with the traditions of a conventional band diagram, which makes use only of the electron states, Fig. 3.1b depicts instead of a hole band a " d -valence band", which is presumed to be completely filled when all ions are in the M^{n+} state.

Finally, a situation is possible when the d -states simultaneously form both the d -conduction band and the d -valence band (Fig. 3.1c). It comes about when one of the d -electrons of a M^{n+} ion goes over to another such ion (a reaction of the $M^{n+} + M^{n+} \rightarrow M^{(n-1)+} + M^{(n+1)+}$ -type). A particular case of such a reaction is the excitation of the "pair"- and "hole"-type carriers in the Hubbard model

(Sec. 1.5). All the three diagrams in Fig. 3.1 comply with the general rule formulated in Sec. 1.5: the energy-band diagram is inapplicable to the ground state of a system of interacting electrons (here when all cations are in the M^{n+} state), but is applicable to their excited states. The reader should also be reminded that because of strong electron-electron correlations, it is not always possible to attribute a definite quasi-momentum to the charge carriers, and the edges of their bands may be spread.

To describe the motion of a charge carrier over the states of partially-filled shells belonging to different cations, one should in principle apply directly the many-electron Hamiltonian (1.5.1) in which the width of the electron band W is presumed small as compared with the characteristic electron-electron interaction energy (the polar model of a metal of Shubin and Vonsovsky [42]). However, actually there is no need to turn to the polar model, which is more complicated than the c - l model. In this case, too, the motion of a charge carrier can be described within the framework of the c - l model. If, as in the Hamiltonian (1.5.1), the orbital degeneracy of electrons of partially-filled states is not taken into account, the spin of magnetic atoms S should be put equal to $1/2$, and the c - l exchange integral A should be assumed to be a very large negative quantity [45]. The same is true of H_H (1.5.2).

Indeed, in the zeroth approximation in W/AS we may discard the term H_B in the Hamiltonian (3.1.1). This fixes the conduction electron on one of the magnetic atoms, and owing to antiferromagnetic exchange interaction between the electron and the spin of the atom ($A < 0$), their spins combine to form a united spin equal to $S - 1/2$, i.e. to zero for $S = 1/2$. In the Hubbard model the situation is similar, since the spin of an "excess" electron playing the part of a charge carrier and the spin of another electron of the atom on which the excess electron is located point in opposite directions.

The Hamiltonian H_B causes the transfer of the charge carrier to a neighbouring atom. In both models the spin of the electron that changes place must be opposite to that of the atom to which it goes over. In the Hubbard model any one of two electrons can move to a neighbouring atom, whereas in the c - l model only the c -electron can do so. But on account of the electrons identity, this difference is only of a formal nature and is easily accounted for by an appropriate renormalization of the Bloch integral [45]. A rigorous proof of this statement will be given in the concluding part of Appendix I.

Thus, in principle conduction bands of the c - and the l -type are possible (actually, a partial hybridization of the states of those types takes place). The former is as a rule a wide one in the sense that the inequality $W \gg AS$ is satisfied for it. The latter is on the contrary narrow, with an opposite relationship between the band width W and the exchange energy AS . In future only the lower of

the conduction bands will be considered. The conduction bands in various materials will be classified only according to the parameter AS/W . The same will apply to holes.

Europium chalcogenides may serve as an example of materials with a wide conduction band. In them $AS \sim 0.5$ eV, and the effective mass of charge carriers is of the order of the free-electron mass m_0 . The width of the conduction band in the simplest case of a cosine dispersion law (1.1.1) is connected with m^* through relation (1.1.5), the same order of magnitude being retained in case of other dispersion laws as well. Hence, according to (1.1.5), for $a \sim 3.5 \times 10^{-8}$ cm the bandwidth in europium chalcogenides is of the order of 3.5 eV.

An example of an opposite situation is probably provided by conduction electrons in chalcogenide spinels and by holes in nickel oxide. An essential point to be made is that in narrow bands, which should be of the l -type, the magnitude of AS is much greater than in the wide ones: according to data presented in the book [54], the exchange energy inside the same partially-filled shells amounts to 1-10 eV, setting the scale for AS .

In case of strong crystal fields (Sec. 2.2), low-energy transitions inside partially-filled shells involving changes in their spin, but with the conservation of the number of l -electrons on every ion become possible (e.g. in LaCoO_3 the transitions of the Co ion from the state with a spin $S = 0$ to the state with a spin $S = 1$). Such transitions correspond to the creation of a Frenkel exciton on a magnetic ion. They cannot be described within the framework of the c - l model formulated above. The effect of Frenkel excitons on the state of charge carriers will be discussed in Chapter 5.

For rare-earth compounds in which the orbital momentum of magnetic atoms is nonzero, the c - l exchange model must in principle be modified. This applies both to the magnetic Hamiltonian H_M and to the c - l exchange Hamiltonian, which, in accordance with what has been said in Sec. 2.2, should be replaced by

$$H_A = -A(g_J - 1) \sum (\mathbf{J}_g \cdot \mathbf{s})_{\sigma\sigma'} a_{g\sigma}^* a_{g\sigma'}, \quad (3.1.3)$$

the latter being the mathematical equivalent of the Hamiltonian (3.1.2). If the crystal field is not strong enough to "freeze" the total ion angular momentum \mathbf{J} , the Hamiltonian H_M (2.2.4) will have the same structure as that of the Heisenberg Hamiltonian (2.1.5), and by force of this the only difference between the c - l model in this case and one discussed at the beginning of this section will be the notation used.

Substantial differences appear only in case of strong crystal fields, for instance, when magnetic systems with magnetic ions in the singlet ground state have to be described. The exchange interaction between the conduction electron and the l -electrons produces

their magnetic polarization and may even cause a complete "defreezing" of \mathbf{J} . The magnetic polarization is described in terms of excitons. However, the exciton Hamiltonian (2.2.6) may prove inadequate for the c - l model, since it takes account only of the lowest exciton states, whereas in case of a complete defreezing the exciton states should be taken into account.

3.2. THE EFFECT OF MAGNETIC ORDERING ON THE ENERGY OF CHARGE CARRIERS

The interaction between the charge carriers and the localized spins makes the carrier energy dependent on the magnetic ordering. If the interaction of the conduction electron with quantum objects (l -spins) is taken into account, its energy, in contrast to the energy of the complete "electron -- l -spins" system will no longer be a well-defined quantity. Below we shall take the term minimum electron energy δE_m to mean the difference $E_m - E_m^0$ between the minimum energies of the magnetic crystal containing and not containing a c -electron.

For positive values of the c - l exchange integral A in the Hamiltonian (3.1.2) it can be rigorously proved that the minimum electron energy is attained in case of the FM ordering. To this end we make use of the inequality

$$\delta E_m = (\psi, H\psi) - E_m^0 \geq E_m^A + E_m^B, \quad (3.2.1)$$

where E_m^A and E_m^B are the least eigenvalues of the Hamiltonians H_A and H_B , respectively. Inequality (3.2.1) follows from the circumstance that the eigenfunction ψ of the Hamiltonian H (3.1.1) is generally not an eigenfunction of the Hamiltonians H_A , H_B and H_M taken separately. There is an exception only in case of the FM ordering when the spin of the conduction electron also points in the direction of the spins of magnetic atoms. The wave function

$$\psi_{\mathbf{k}} = \frac{1}{\sqrt{N}} \sum \exp(i\mathbf{k} \cdot \mathbf{g}) a_{\mathbf{g}+}^* |0\rangle \prod_{\mathbf{f}} \delta(S_{\mathbf{f}}^z, S), \quad (3.2.2)$$

$$(a_{\mathbf{g}\sigma} | 0\rangle = 0)$$

is at the same time an eigenfunction of the Hamiltonians H_A , H_B and H_M and consequently of the complete Hamiltonian H , which is equal to their sum.

Should the electron wave vector \mathbf{k} in formula (3.2.2) be chosen so as to correspond to the bottom of the conduction band, in case of a positive c - l exchange integral A and a positive l - l exchange integral J minimum eigenvalues of each of the three Hamiltonians H_A , H_B and H_M will correspond to the state (3.2.2). Hence, in the case an equality sign should stand in formula (3.2.1). In case

of a magnetic ordering of any other type or in case of absence of any such ordering, formula (3.2.1) must contain an inequality sign, and this proves the above statement about the minimum value of the electron energy in case of the FM ordering.

For $A < 0$ it is not possible to prove a similar statement in a general form. However, concrete calculations presented below prove that it remains valid in this case as well.

The problem concerning the effects of magnetic ordering on the charge-carrier spectra can most easily be solved analytically when the spins of magnetic atoms can be presumed to remain stationary and not to change as the carrier moves over the crystal. Such an approach is justified for classically large spins ($2S \gg 1$).

In case of an ideally ordered crystal the problem of the electron spectrum thus formulated can be solved precisely [67, 92]. Below we shall consider the case of helicoidal ordering when the spin components are described by formulae (2.3.1). Substituting these formulae into the Hamiltonian (3.1.1), we are able to write down its electronic part in the form

$$H = \sum_{\mathbf{k}} E_{\mathbf{k}} a_{\mathbf{k}\sigma}^* a_{\mathbf{k}\sigma} - \frac{AS}{2} \sum_{\mathbf{k}} (a_{\mathbf{k}\uparrow}^* a_{\mathbf{k}-\mathbf{q}\downarrow} + a_{\mathbf{k}\downarrow}^* a_{\mathbf{k}+\mathbf{q}\uparrow}). \quad (3.2.3)$$

The spectrum of the Hamiltonian (3.2.3) is found with the aid of Bogolyubov's transformation, which mixes the operators $a_{\mathbf{k}\uparrow}$ and $a_{\mathbf{k}-\mathbf{q}\downarrow}^*$, or with the aid of the method of equations of motion for retarded Green's functions [64]

$$G_{\mathbf{k}\sigma, \mathbf{p}\sigma'} \equiv \langle \langle a_{\mathbf{k}\sigma} | a_{\mathbf{p}\sigma'}^* \rangle \rangle = -i [\langle a_{\mathbf{k}\sigma}(t) a_{\mathbf{p}\sigma'}^*(t) + a_{\mathbf{p}\sigma'}^* a_{\mathbf{k}\sigma}(t) \rangle] \theta(t), \quad (3.2.4)$$

$$a_{\mathbf{k}\sigma}(t) = \exp(iHt) a_{\mathbf{k}\sigma} \exp(-iHt),$$

$\theta(t) = 1$ for $t \geq 0$ and $\theta = 0$ for $t < 0$, the angular brackets symbolizing averaging over the temperature. For the Fourier-components

of Green's function $G(t) = \int_{-\infty}^{\infty} G(E) \exp(-iEt) \frac{dE}{2\pi}$ we obtain the

following equations:

$$(E - E_{\mathbf{k}}) \langle \langle a_{\mathbf{k}\uparrow} | a_{\mathbf{k}\uparrow}^* \rangle \rangle = 1 - \frac{AS}{2} \langle \langle a_{\mathbf{k}-\mathbf{q}\downarrow} | a_{\mathbf{k}\uparrow}^* \rangle \rangle, \quad (3.2.5)$$

$$(E - E_{\mathbf{k}-\mathbf{q}}) \langle \langle a_{\mathbf{k}-\mathbf{q}\downarrow} | a_{\mathbf{k}\uparrow}^* \rangle \rangle = -\frac{AS}{2} \langle \langle a_{\mathbf{k}\uparrow} | a_{\mathbf{k}\uparrow}^* \rangle \rangle.$$

Solving the set of equations (3.2.5), we obtain an expression for the poles of Green's functions that determine the electron spectrum:

$$E_{\mathbf{k}}^{(\pm)} = \frac{(E_{\mathbf{k}-\mathbf{q}} + E_{\mathbf{k}})}{2} \pm \frac{1}{2} \sqrt{(E_{\mathbf{k}} - E_{\mathbf{k}-\mathbf{q}})^2 + A^2 S^2}. \quad (3.2.6)$$

From it the electron energy spectrum for any helicoid vector \mathbf{q} will be seen to consist of two subbands. For $\mathbf{q} = 0$ (the FM ordering)

they appear in the result of Zeeman spin splitting of the electron spectrum in the mean field of the crystal, such splitting being proportional to the crystal magnetization. The splitting is equal in magnitude to AS . For $q \neq 0$ there is no magnetization of the crystal as a whole, but if the inequality $|E_{k+q} - E_k| \ll AS$ is satisfied, the splitting will be practically the same as in a ferromagnet. This splitting may be interpreted as the Zeeman effect caused by local magnetization of the crystal. As the electron moves over the crystal, its spin constantly aligns itself parallel or antiparallel to the local magnetic moment. (The term local moment implies the moment of a region of the crystal whose dimensions are $\leq q^{-1}$.)

In particular, in case of narrow bands $W \ll AS$ the inequality $|E_{k+q} - E_k| \ll AS$ is satisfied for all q 's including the largest. For these $q^{-1} \sim a$, and consequently the electron spin will always be parallel or antiparallel to the spin of the atom on which it is presently located. Since the orientation of the spins affects only the energy of translational motion, which is of the order of $W \ll AS$, the Zeeman splitting of the spectrum equal to AS exists in case of an arbitrary configuration of atomic spins and even in the total absence of a magnetic order. This remains valid for small spins as well (this problem is dealt with in more detail in Sec. 3.5).

The inequality $|E_{k+q} - E_k| \ll AS$ can be satisfied for any S in case of wide bands $W \gg AS$, too, provided q is sufficiently small. The fact that the Zeeman splitting in a helicoid is close to that in an FM means that the spin of the electron moving over the crystal, owing to slow changes in the direction of the local moment, has ample time to align itself along the latter. For greater q 's the inequality will be satisfied only in a portion of the k -space, the easier the smaller is k . However, a resonance between the E_k and the E_{k+q} states for large k 's is also possible (e.g. for a quadratic dispersion law in the vicinity of the surface $q^2 = -2(\mathbf{k} \cdot \mathbf{q})$).

If k and q are so great that the opposite inequality $|E_{k+q} - E_k| \gg AS$ is satisfied, the electron spin is unable to catch up with the local moment and retains its direction in space. Accordingly, the corrections to the electron spectrum due to the c - l exchange obtained from (3.2.6) will be not of the order of AS , but much smaller, i.e. of the order of A^2S^2/W .

To illustrate the structure of an electron spectrum described by formula (3.2.6), let us suppose that the helicoid vector points in the direction of the Z -axis, and that the unrenormalized dispersion law for the electrons is of the form:

$$E_k = 2B \cos k_z a + f(k_\perp) \quad (B < 0), \quad (3.2.7)$$

where $f(k_\perp)$ is an arbitrary function of transverse quasi-momentum components k_x, k_y . In this case formula (3.2.6) reduces to the follow-

ing expression:

$$E_{\mathbf{k}}^{\pm} = f(k_{\perp}) + 2B \left(\cos \frac{qa}{2} \right) (\cos pa) \pm \sqrt{4B^2 (\sin^2 pa) \left(\sin^2 \frac{qa}{2} \right) - \left(\frac{AS}{2} \right)^2}, \quad p = k_z - q/2. \quad (3.2.8)$$

The resonance condition will be seen from formula (3.2.8) to be satisfied for the values $p = 0$ ($k_z = q/2$) and $p = \frac{\pi}{a}$ ($k_z = q/2 - \pi/a$) irrespective of the value of k_{\perp} . In that case the Zeeman splitting should be precisely equal to AS , i.e. the electron spin aligns itself ideally along the local moment. The points $p = 0$ and $p = \pi/a$ themselves correspond to the extrema of the electron energy. Besides in a definite range of values of q , extrema at points p_1 determined by the equalities

$$\cos p_1 a = \pm \cos \frac{qa}{2} \sqrt{1 - \left(\frac{AS}{4B} \right)^2 \sin^2 \frac{qa}{2}} \quad (3.2.9)$$

are also possible (the order of signs in (3.2.9) corresponds to that in (3.2.8)).

For such q 's for which there are no extrema at points p_1 , the point $p = 0$ will correspond to the minimum of each subband E_p^+ and E_p^- , and the point $p = \pi/a$ to their maximum. Appearance of the extrema at the points p_1 changes the type of the extrema at the points $p = 0$ and $p = \pi/a$. For the lower subband, the extremum at a point p_1 is a minimum, so that both extrema $p = 0$ and $p = \pi/a$ turn into maxima. For the upper subband the opposite is true. In case of an AF ordering ($q = \pi/a$), the points p_1 correspond either to $k_z = 0$ or to $k_z = \pi/a$.

It follows from formulae (3.2.8, 9) and (1.1.5) that for $q < q_0$ the minimum energy of the electron in the crystal is given by the expression

$$E_{\min}(q) = E_{\min}(0) + 4|B| \sin^2 \frac{qa}{4}, \quad (3.2.10)$$

$$q_0 = \sqrt{2m^*AS}, \quad (3.2.11)$$

where $E_{\min}(0)$ is the minimum energy in case of the FM ordering. For reasons to be stated in Sec. 4.2, we shall term the wave number q_0 , which in future will play an important part, *spinpolaron vector*. For $|4B| \ll AS$, relation (3.2.10) is valid over the entire Brillouin zone.

Note in addition that expression (3.2.6) remains valid also in case of a staggered AF ordering whose corresponding wave vector is $\mathbf{q} = \Pi \equiv (\pi/a, \pi/a, \pi/a)$.

With account taken of the equality $E_{\mathbf{k}} = -E_{\Pi-\mathbf{k}}$, the minimum electron energy in an antiferromagnet will be given by the expression

$$E_{\min} = -\frac{1}{2} \sqrt{W^2 + A^2 S^2},$$

$$W = |E_{\Pi} - E_0| = 2 |E_0|. \quad (3.2.12)$$

3.3. INDIRECT EXCHANGE VIA CONDUCTION ELECTRONS IN MAGNETIC CRYSTALS

The *c-l* model of Vonsovsky described in Sec. 3.1 formed the cornerstone of the theory of magnetism of rare-earth metals developed by Ruderman and Kittel [235], Kasuya [237] and Yosida [236] (RKKY).

This theory is based on the following physical picture: magnetic ordering is in effect the ordering of localized spins same as in the Heisenberg model, the contribution of spins of *c*-electrons to the total moment of an FM crystal or to the moments of sublattices of an AF crystal being small in comparison to that of the *l*-electrons. However, it is the *c*-electrons that make magnetic ordering in a system of localized spins possible and determine its nature, since in the process of their motion in the crystal they transport the interaction between the *l*-spins. Such an interaction between localized spins via conduction electrons became known as *indirect exchange*.

From the point of view of its formalism, the RKKY theory corresponds to the second order of the perturbation theory in the parameter $AS\mu$, which is small in metals (the Fermi energy $\mu \sim 5$ eV, whereas $AS \sim 0.5$ eV). If we regard the *c-l* interaction as a perturbation, the electron energy in the zeroth approximation would be independent of the spin orientation. Accordingly, the numbers of electrons with spins pointing up and down should be equal. Interaction with the *l*-spins perturbs the electron distribution and makes the *c*-electron energy depend on the relative orientation of *l*-spins. This dependence means that there is an effective interaction between the *l*-spins via the *c*-electrons. It can be described by means of an **effective spin-dependent Hamiltonian**.

The Hamiltonian of the *c-l* model (3.1.1, 2) following the Fourier-transformation (1.1.3) in the absence of a direct exchange ($H_M = 0$) will be written down as follows

$$H = \sum E_{\mathbf{k}\sigma} a_{\mathbf{k}\sigma}^* a_{\mathbf{k}\sigma} - \frac{A}{V\bar{N}} \sum' (\mathbf{S}_{\mathbf{q}} \cdot \mathbf{s})_{\sigma\sigma'} a_{\mathbf{k}\sigma}^* a_{\mathbf{k}+\mathbf{q}, \sigma'} \equiv H_d + H_{nd}, \quad (3.3.1)$$

$$E_{\mathbf{k}0} = E_{\mathbf{k}} - A\sigma\mathfrak{M}, \quad \mathfrak{M} = S_0^z / \sqrt{N}, \quad \mathbf{S}_{\mathbf{q}} = \frac{1}{\sqrt{N}} \sum S_{\mathbf{q}} e^{-i(\mathbf{q} \cdot \mathbf{R})}.$$

The prime above the sum in the second term of (3.3.1) designated as H_{nd} means that it does not contain diagonal terms, which have been included in the zeroth-approximation Hamiltonian H_d (the first term in (3.3.1)).

In order to construct the magnetic Hamiltonian, it is advisable first to carry out a canonical transformation of the Hamiltonian (3.3.1) of the type carried out in Sec. 1.4 to eliminate in the first order in AS/μ all terms linear in spins. The formulae for it are similar to (1.4.2-4). Retaining in the transformed Hamiltonian only the terms diagonal in electron operators, this corresponding to the second order in AS/μ , we obtain

$$\tilde{H} = H_d + \frac{A^2}{2} \sum' \times \frac{(S_q \cdot s)_{\sigma\sigma'} (S_{-q} \cdot s)_{\sigma'\sigma} (a_{k\sigma}^* a_{k\sigma} - a_{k-q, \sigma'}^* a_{k+q, \sigma'})}{E_{k\sigma} - E_{k+q, \sigma'}}. \quad (3.3.2)$$

The eigenfunctions of the Hamiltonian (3.3.2) $\Phi(n, S^z)$ are represented in the form of a product of the wave function Φ_e , which depends solely on the electron occupation numbers $n_{k\sigma}$, and of the wave function of the magnetic subsystem Φ_M , which depends on the variables S_q^z . The electron occupation numbers enter Φ_M only as parameters

$$\Phi(n, S^z) = \Phi_e(n) \Phi_M(S^z | n), \quad (3.3.3)$$

$$\Phi_e = \prod_{q\sigma} \delta(n_{q\sigma}, n_{q\sigma}^0). \quad (3.3.4)$$

The choice of the electron wave function Φ_e in the form of (3.3.4) has been made on the grounds that each of the wave functions that enter the product over q and σ is an eigenfunction of an appropriate particle number operator $a_{q\sigma}^* a_{q\sigma}$ with the eigenvalue $n_{q\sigma}^0$:

$$a_{q\sigma}^* a_{q\sigma} \delta(n_{q\sigma}, n_{q\sigma}^0) = n_{q\sigma}^0 \delta(n_{q\sigma}, n_{q\sigma}^0) \quad (3.3.5)$$

(similar to (2.1.1), $n_{q\sigma}$ is a variable, $n_{q\sigma}^0$ is an index of state). Therefore after the substitution of Φ (3.3.3, 4) into the Schrödinger equation with the Hamiltonian (3.3.2), multiplication by Φ_e and summing up over the variables $n_{q\sigma}$, we obtain the Schrödinger equation for the wave function of the magnetic subsystem $\Phi_M(S^z | n)$ in the form

$$\begin{aligned} H_M(n^0) \Phi_M = E(n^0) \Phi_M, \quad H_M(n^0) &= (\Phi_e, \tilde{H} \Phi_e), \\ H_M(n^0) &= \sum E_{k\sigma} n_{k\sigma}^0 \\ &+ \frac{A^2}{2N} \sum \frac{(n_{k\sigma}^0 - n_{k+q, \sigma'}^0) (S_q \cdot s)_{\sigma\sigma'} (S_{-q} \cdot s)_{\sigma'\sigma}}{E_{k\sigma} - E_{k+q, \sigma'}} = H_{Md} + H_{Mnd}. \end{aligned} \quad (3.3.6)$$

Subsequent calculations are carried out for an electron gas in the ground state, i.e. thermal excitations in the electron system are neglected, this being justified by the fact that T is small as compared with μ .

Despite the fact that the contribution $(-A\sigma\mathfrak{M})$ of diagonal terms in the c - l exchange to the energy $E_{k\sigma}$ of an electron with a fixed spin direction is of the first order in AS/μ , their contribution H_{Md} to the total electron energy is only of the second order in this parameter. This follows from the fact that the c - l shift $(-A\sigma\mathfrak{M})$ changes sign with the change in the spin direction to the opposite, and that in the zeroth approximation the numbers of electrons with spins up and down are equal. To find H_{Md} , one has to take into account that in the presence of magnetization \mathfrak{M} these numbers will no longer be equal.

The Fermi energy shifts by the amount $\Delta\mu$ with respect to its value μ for $\mathfrak{M} = 0$. The correction $\Delta\mu$ can be found from the condition of total electron number being constant:

$$n = \sum_{k\sigma} \theta(\mu - E_k) = \sum_{k\sigma} \theta(\mu + \Delta\mu - E_k + A\sigma\mathfrak{M}), \quad (3.3.7)$$

where $\theta(\mu - E_k)$ is the Fermi distribution function for electrons at $T = 0$, n is their total number independent of the magnetization. According to (3.3.7), the shift of the Fermi energy is

$$\Delta\mu = -\frac{A^2\mathfrak{M}^2}{8} \frac{g'_e(\mu)}{g_e(\mu)}, \quad (3.3.8)$$

where the electron density of states g_e is given by expression (1.2.10), its definition leading to the equality $g_e(\mu) = dn/d\mu$. Then we obtain for H_{Md} taking into account equality (3.3.8)

$$H_{Md} = \sum E_{k\sigma} \theta(\mu + \Delta\mu - E_{k\sigma}) = \sum E_k \theta(\mu - E_k) - \frac{A^2\mathfrak{M}^2}{8} g_e(\mu). \quad (3.3.9)$$

The second term H_{Mnd} in the expression for the magnetic Hamiltonian $H_M(n^0)$ (3.3.6) after the substitution of E_k for $E_{k\sigma}$ is transformed with the aid of the equality

$$\sum_{\sigma\sigma'} (\mathbf{S}_q \cdot \mathbf{s})_{\sigma\sigma'} (\mathbf{S}_{-q} \cdot \mathbf{s})_{\sigma'\sigma} = \frac{1}{2} (\mathbf{S}_q \cdot \mathbf{S}_{-q}). \quad (3.3.10)$$

Combining expressions (3.3.6, 9, 10), we obtain the following final result for the spin-dependent part of the electron energy:

$$H_M = -\frac{1}{2} \sum_q \mathcal{J}_{\text{eff}}(\mathbf{q}) (\mathbf{S}_q \cdot \mathbf{S}_{-q}), \quad (3.3.11)$$

$$\mathcal{J}_{\text{eff}}(\mathbf{q}) = -\frac{A^2}{2N} \sum_k \frac{n_k - n_{k+q}}{E_k - E_{k+q}}, \quad n_k = \theta(\mu - E_k), \quad (3.3.12)$$

the term with $\mathbf{q} = 0$ being included is the sum over \mathbf{q} in (3.3.11).

The Hamiltonian (3.3.11) that describes the dependence of the electron energy on the spin configuration has the form of the Heisenberg Hamiltonian (2.1.5), i.e. it is quadratic in spins. This is a corollary of the circumstance that the original c - l exchange Hamiltonian H_A (3.1.2) is linear in spins of magnetic atoms, and the Hamiltonian H_M (3.3.11) is obtained in the second order of the perturbation theory in H_A .

The Hamiltonian (3.3.11) may be rewritten in the form (2.1.5). Making use of the quadratic dispersion law for the electron energy, we can write the effective indirect-exchange integral in the form

$$J_{\text{eff}}(\mathbf{f}) = \frac{1}{N} \sum_{\mathbf{q}} J_{\text{eff}}(\mathbf{q}) e^{i(\mathbf{q} \cdot \mathbf{f})} = \frac{9\pi}{2} \frac{A^2}{\mu} \left(\frac{n}{N} \right)^2 F(2k_F f), \quad (3.3.13)$$

where for $x \gg 1$

$$\mathcal{F}(x) = \frac{x \cos x - \sin x}{x^3}, \quad k_F = \sqrt{2m^* \mu}.$$

Hence for great distances between the atoms $R \gg k_F^{-1}$ the indirect-exchange integral diminishes as R^3 , oscillating. This result follows from the fact that the Fourier-component

$$J_{\text{eff}}(\mathbf{q}) = \frac{J_{\text{eff}}(\mathbf{q})}{S} = \frac{3}{8} \frac{nA^2}{N\mu} \left[1 + \frac{4k_F^2 - q^2}{4k_F q} \ln \left| \frac{2k_F + q}{2k_F - q} \right| \right] \quad (3.3.14)$$

displays the so-called Kohn singularity: $dJ_{\text{eff}}(q)/dq$ diverges logarithmically at $q = 2k_F$. In cases when the Fermi surface is not defined clearly enough (e.g. the electrons are scattered intensively by the impurities, so that their quasi-momentum is no more their exact quantum number) the Kohn singularity of $J_{\text{eff}}(\mathbf{q})$ vanishes. Because of that, a slow oscillating long-range decline of $J_{\text{eff}}(\mathbf{f})$ is replaced by a more rapid one*. The long-range indirect-exchange interaction plays a decisive role in the establishment of a magnetic ordering in rare-earth metals, since the direct exchange between the f -electrons of neighbouring atoms is very weak owing to a small overlap of their orbits (the radius of the latter is very small: ~ 0.3 - 0.4 Å [9], with the separation between the nearest neighbours being ~ 3 - 5 Å).

* The Kohn singularity possibly vanishes also in pure crystals at elevated temperatures, if the conduction electrons are scattered intensively enough by fluctuations of magnetization. In this case one has to take into account the temperature dependence of the effective exchange integral in (3.3.11), despite the fact that this corresponds formally to a higher approximation in the c - l exchange than one employed in the RKKY theory. A finite exchange length at $T \neq 0$ is obtained not only on account of attenuation of the electron Bloch states, but also on account of smoothing of the step-like distribution function $n_{\mathbf{k}}$ with temperature rising. The latter factor apparently affects the exchange much less than the former: if it were not for the damping, this length would be very great, of the order of $\mu\lambda/T$.

As has been stated in Chapter 2, if the system can be described by means of the Heisenberg Hamiltonian, the magnetic structure established in it will be that to which the maximum value of the Fourier-component $J_{\text{eff}}(\mathbf{q})$ corresponds. The quantities $J_{\text{eff}}(\mathbf{q})$ (3.3.12) should be calculated with account taken of the actual structure of the Fermi surface, which as a rule is very complicated in rare-earth metals. The indirect exchange may result both in the FM and in the AF orderings. In principle, it may result also in a helicoidal ordering, but, according to Dzyaloshinsky [92], in this case it cannot be generally described with the aid of the RKKY theory based on the perturbation theory in AS/μ .

This is due to the circumstance that in fact the electron energy is nonanalytic in AS/μ on account of the contribution to it of the resonance regions of the \mathbf{k} -space $(E_{\mathbf{k}+\mathbf{q}} - E_{\mathbf{k}}) < AS$ where \mathbf{q} is the wave vector of the structure. In cases when the Fermi surface is not of a very complex shape this nonanalyticity makes itself manifest only in terms of higher orders in AS/μ than those taken into account in the RKKY theory. For this reason the RKKY theory remains valid for materials with relatively simple Fermi surfaces. However, in case of a Fermi surface of a complex shape this nonanalyticity may make itself manifest in the leading terms, and in such cases the RKKY theory cannot be applied.

To illustrate the point, let us calculate the electron energy for the case of antiferromagnetic ordering when the number of electrons is equal to that of atoms (in the absence of c - l exchange the electrons would occupy a half of the Brillouin zone). In addition to an isotropic crystal, we shall consider a strongly anisotropic one, which for the sake of simplicity will be represented by a one-dimensional model. In both cases we shall presume the electron spectrum to be described by the simple cosine dispersion law (1.1.1).

Making use of formula (3.2.6), one can calculate the electron energy in the one-dimensional case with account taken of the c - l exchange. The electrons occupy all states with quasi-momenta lying in the $[-\frac{\pi}{2a}; \frac{\pi}{2a}]$ range. Their total energy is given by the expression (for a chain of unit length):

$$\begin{aligned}
 E_1 &= -\frac{2}{\pi} |B| \int_0^{\pi/2a} dk \sqrt{\alpha_1^2 + \cos^2 ka} \\
 &= -\frac{2|B|}{\pi a} \sqrt{1 + \alpha_1^2} \mathcal{E}\left(\sqrt{\frac{1}{1 + \alpha_1^2}}\right), \quad (3.3.15) \\
 \alpha_1 &= \frac{AS}{4|B|},
 \end{aligned}$$

where \mathcal{E} is the complete elliptical integral of the second kind. Expanding it into a series, we obtain:

$$E_1 = -\frac{2|B|}{\pi a} \left[1 - \frac{\alpha_1^2}{2} \ln |\alpha_1| \right] + O(\alpha_1^2). \quad (3.3.16)$$

The singularity in (3.3.16) is associated with the momenta $k \approx \pi/2a$, this being easily verified by the expansion of $\cos ka$ in (3.3.15) in a series around $k_F = \pi/2a$. Hence, the contribution of electrons with $k \sim k_F$ for which the condition of resonance $|E_k - E_{(\pi/a) - k}| < AS$ is satisfied makes the electron energy non-analytic in the small parameter α_1 . The electron energy given by formula (3.3.16) is lower than one obtained with the RKKY theory in which the c - l energy shift is proportional to α_1^2 (in accordance with formulae (3.3.11, 12), it is equal to $J_{eH}(\pi/a) S^2/a$).

Similar calculations carried out for an isotropic three-dimensional case demonstrate that the energy becomes unanalytic in α_1 only in the order $\alpha_1^4 \ln |\alpha_1|$, this being the result of the density of states vanishing on the Fermi surface. It follows hence that the RKKY theory is valid, but that corrections to it cannot be calculated in the following order in c - l exchange as several authors tried to do.

As has already been discussed, a substantial gain in energy (3.3.16) as compared with that computed with the aid of the RKKY theory in the one-dimensional case is the result of the helicoid vector \mathbf{q} coinciding with the Fermi surface diameter. Dzyaloshinsky has demonstrated [92] that in the three-dimensional case, too, if the Fermi surface is anisotropic, a helicoidal ordering with a wave vector \mathbf{q} almost equal to the extremal diameter of the Fermi surface tends to be established in a metal.

Strictly speaking, even if the RKKY theory is valid at $T = 0$, it cannot be applied in the vicinity of the Curie point. Indeed, the zeroth-approximation states in the RKKY theory, which fundamentally regards the c - l exchange as a perturbation, are Bloch functions with a fixed projection of the c -electron spin. But, following formulae (4.3.2, 2a), the attenuation of such states due to c - l exchange becomes infinite at the Curie point, so that the perturbation theory in the c - l exchange becomes meaningless. As was pointed out already, even far from T_c where the damping caused by c - l exchange is small, but finite, it substantially modifies the results obtained with the RKKY theory by making the c - l exchange length finite.

It should not be forgotten that the RKKY theory based on the concept of free electrons serves as a model theory for actual metals. Indeed, on account of a strong electron-electron interaction (inequality (1.7.3) is not satisfied in metals, because in them $\epsilon_0 = 1$) there are no adequate grounds to describe the electrons of a metal as free ones. Nevertheless, such a treatment of the electrons still remains meaningful, because it reproduces the physical aspects qualitatively

correctly. Moreover, for small quasi-momenta it can be regarded quantitatively correct too, because in this case, according to (3.3.12), only the electron states close to the Fermi surface are of any importance, and the RKKY theory can be reformulated in terms of elementary excitations (of electrons above the Fermi surface and of holes below it).

The RKKY theory is generally inapplicable to magnetic semiconductors, since the condition $\mu \gg AS$ is not met in them. However, if $M = 0$, and $W \gg AS$, some results of this theory are valid for semiconductors as well (for more detailed discussion, see Secs. 6.1, 6.2).

3.4. SUPEREXCHANGE IN MAGNETIC INSULATORS

In magnetic insulators the direct exchange between the magnetic atoms is weak, because such atoms are separated from each other by nonmagnetic atoms, and by force of it the overlap of l -orbits of neighbouring atoms is small. Kramers [240] suggested that the strong exchange interaction between the magnetic atoms observed experimentally is the result of the part played in it by nonmagnetic atoms. In terms of the c - l model the exchange via the electrons of nonmagnetic atoms can be interpreted as an indirect exchange via the electrons of the completely filled valence band. Below we shall use the term *superexchange* to describe it.

Qualitatively, superexchange is caused by the generation of virtual conduction electrons and holes in the result of their exchange interaction with one of the magnetic atoms and by their subsequent annihilation in the result of exchange interaction with another magnetic atom. The contribution of such processes to the electron energy depends on the mutual orientation of spins of these atoms.

First we shall present the theory of superexchange for the case of wide electron and hole bands [238]. The Hamiltonian of the c - l model, which takes into account interband transitions, but does not take into account the intraband c - l exchange, can be written in the form

$$\begin{aligned} H &= H_0 + H_{cv}, \\ H_0 &= \sum E_{\mathbf{k}} a_{\mathbf{k}\sigma}^* a_{\mathbf{k}\sigma} + \sum K_{\mathbf{k}} c_{\mathbf{k}\sigma}^* c_{\mathbf{k}\sigma}, \\ H_{cv} &= -\frac{D}{\sqrt{N}} \sum (\mathbf{S}_{\mathbf{q}} \cdot \mathbf{s})_{\sigma\sigma'} (a_{\mathbf{k}\sigma}^* c_{\mathbf{k}+\mathbf{q}, \sigma'}^* + c_{\mathbf{k}\sigma} a_{\mathbf{k}+\mathbf{q}, \sigma}), \end{aligned} \quad (3.4.1)$$

where $a_{\mathbf{k}\sigma}^*$, $a_{\mathbf{k}\sigma}$ and $c_{\mathbf{k}\sigma}^*$, $c_{\mathbf{k}\sigma}$ are the creation and the annihilation operators of conduction electrons and holes, respectively. To elucidate the structure of (3.4.1), it should be pointed out that, after the transformation from the hole operators to those of the valence

band electrons has been performed (the hole creation operator is the electron annihilation operator, and vice versa), the c - l exchange Hamiltonian H_{cl} would have assumed a form similar to (3.1.2). In other words, the existence of c - l exchange terms occasioning the creation or the annihilation of an electron-hole pair is a direct consequence of the usual exchange interaction between the electrons.

The interband c - l exchange integral D is supposed to be small in comparison with the width of the band-gap E_g , and the intraband c - l exchange integrals A_e and A_h are supposed to be small in comparison with the widths of the electron W_e and the hole W_h band, respectively. The latter proposition enables us to omit the intraband exchange terms from the Hamiltonian (3.4.1) altogether. Indeed, in an intrinsic semiconductor there is no indirect exchange via real charge carriers, but there is an indirect exchange via virtual carriers generated in the result of an interband exchange. For the latter to be operational, it suffices that the interband exchange integral be nonzero, i.e. the superexchange appears already in the zeroth approximation in A_e and A_h , and for this reason the inclusion of the intraband exchange would yield only small corrections.

Since there are no diagonal terms in the interband exchange Hamiltonian, the effective Hamiltonian is obtained from the Hamiltonian (3.4.1) by means of the canonical transformation of the type of (1.4.2-4), which eliminates from the Hamiltonian (3.4.1) terms linear in D . The operator \mathcal{U} is defined by the equation

$$\mathcal{U} = \frac{D}{\sqrt{N}} \sum_{\mathbf{k}} \frac{1}{E_{\mathbf{k}} + K_{\mathbf{k}+\mathbf{q}}} [(\mathbf{S}_{\mathbf{q}} \cdot \mathbf{S})_{\sigma\sigma'} a_{\mathbf{k}\sigma}^* c_{\mathbf{k}+\mathbf{q}, \sigma'}^* - (\mathbf{S}_{-\mathbf{q}} \cdot \mathbf{S})_{\sigma\sigma'} c_{\mathbf{k}-\mathbf{q}, \sigma} a_{\mathbf{k}\sigma}]. \quad (3.4.2)$$

Neglecting the numbers of excited electrons and holes in comparison with the number of magnetic atoms, we obtain from formulae (1.4.2-4) and (3.4.1, 2), taking into account relation (3.3.10), the magnetic Hamiltonian of the form (3.3.11) with the effective exchange integral

$$\mathcal{J}_{\text{eff}}(\mathbf{q}) = \frac{D^2}{2N} \sum_{\mathbf{k}} \frac{1}{E_{\mathbf{k}} + K_{\mathbf{k}+\mathbf{q}}}. \quad (3.4.3)$$

The magnetic structure that provides for the minimum energy of the system depends on the value of \mathbf{q} for which the exchange integral $\mathcal{J}_{\text{eff}}(\mathbf{q})$ attains its maximum. If the maximum is attained for $\mathbf{q} = 0$ (the minima of conduction and the hole bands lie at the same point in the \mathbf{k} -space), the ferromagnetic ordering will be the most energetically favoured one. If on the other hand one of the minima lies at the centre of the Brillouin zone, and the other on its boundary at point $\Pi = \left(\frac{\pi}{a}, \frac{\pi}{a}, \frac{\pi}{a}\right)$, $\mathcal{J}_{\text{eff}}(\Pi)$ will be at its maximum, and the antiferromagnetic ordering will be the most favoured one.

It follows from formula (3.4.3) that, if the electron or the hole band is very narrow, i.e. if E_k or K_k is independent of the quasi-momentum \mathbf{k} , $J_{\text{eff}}(\mathbf{q})$ will no longer depend on \mathbf{q} . But this means that there is no exchange interaction between l -spins, since the Fourier-transform $J_{\text{eff}}(\mathbf{f})$ of the exchange integral $J_{\text{eff}}(\mathbf{q})$ (see (3.3.13)) is proportional to $\delta(\mathbf{f}, 0)$. It follows hence that in case of narrow bands the exchange integral should be proportional to the width of the carrier energy band. However, formula (3.4.3) is inadequate to cover this case, since it takes no account of the intraband c - l exchange, which plays an important part in the case of narrow ($AS \gg W$) bands.

Below we intend to analyze the superexchange in a magnetic semiconductor with a narrow conduction band [239]. The hole band is as before presumed to be wide, so that we may take no account of the intraband hole c - l exchange. In the Hamiltonian of the system we conveniently make use of the site representation for the electrons and of the momentum representation for the holes:

$$\begin{aligned} H &= H_0 + H_{cv} + H_B, \\ H_0 &= \sum K_p c_{p\sigma}^* c_{p\sigma} + E_c \sum a_{g\sigma}^* a_{g\sigma} - A \sum (\mathbf{S}_g \cdot \mathbf{s})_{\sigma\sigma'} a_{g\sigma}^* a_{g\sigma'}, \\ H_{cv} &= -\frac{D}{\sqrt{N}} \sum e^{-i(\mathbf{q} \cdot \mathbf{a})} (\mathbf{S}_g \cdot \mathbf{s})_{\sigma\sigma'} [a_{g\sigma}^* c_{q\sigma'}^* + c_{-q\sigma}^* a_{g\sigma'}], \end{aligned} \quad (3.4.4)$$

where E_c is the energy corresponding to the centre of the conduction band.

The terms H_{cv} (3.4.4) and H_B (1.1.1) will be treated below as perturbations. As has already been stated, the effective exchange Hamiltonian should be proportional to B . But on the other hand, for H_B to yield a nonzero result, there should be electrons in the conduction band. Virtual electron transitions from the valence to the conduction band are caused by the interband Hamiltonian H_{cv} . Accordingly, we must first find the wave function of the ground state of the system with account taken of the perturbation H_{cv} and use it to compute the average value of the Hamiltonian H_B .

In compliance with the standard perturbation theory, the first-order correction $|1\rangle$ to the vacuum wave function $|0\rangle$ for the electrons and holes is given by the expression

$$|1\rangle = \sum_m \frac{|m\rangle \langle m| H_{cv} |0\rangle}{E_m - E_0} \equiv (H_0 - E_0)^{-1} H_{cv} |0\rangle, \quad (3.4.5)$$

where $|m\rangle$ and E_m are eigenfunctions and eigenvalues of the Hamiltonian H_0 (3.4.4), respectively, and E_0 is the energy of its ground state. $|1\rangle$ is calculated by expanding the energy denominator ($H_0 -$

$-E_0)^{-1}$ in a power series in $A(E_c + K_p)^{-1}$:

$$|1\rangle = -\frac{D}{A\sqrt{N}} \sum_{\mathbf{p}} e^{-i(\mathbf{p}\cdot\mathbf{g})} \left\{ \sum_{n=0}^{\infty} \left(\frac{A}{E_c + K_p} \right)^{n+1} \right. \\ \times (S_{\mathbf{g}} \cdot \mathbf{s})_{\mu_1 \mu'_1} a_{\mathbf{g}\mu_1}^* a_{\mathbf{g}\mu'_1} \dots (S_{\mathbf{g}} \cdot \mathbf{s})_{\mu_n \mu'_n} a_{\mathbf{g}\mu_n}^* a_{\mathbf{g}\mu'_n} \left. \right\} \\ \times (S_{\mathbf{g}} \cdot \mathbf{s})_{\sigma\sigma'} a_{\mathbf{g}\sigma}^* c_{\mathbf{p}\sigma'}^* |0\rangle. \quad (3.4.6)$$

When writing equation (3.4.6), we took account of the fact that all terms of the type $a_{\mathbf{f}\tau}^* a_{\mathbf{f}\tau'}$ with $\mathbf{f} \neq \mathbf{g}$ and $c_{\mathbf{q}\tau}^* c_{\mathbf{q}\tau'}$ with $\mathbf{q} \neq \mathbf{p}$ do not contribute anything owing to the property of the vacuum wave function $c_{\mathbf{q}\tau} |0\rangle = a_{\mathbf{f}\tau} |0\rangle = 0$. The disappearance of such terms is the result of the circumstance that the Hamiltonian H_0 conserves the hole quasi-momentum and the number g of the site on which the electron is localized.

Next, to obtain a nonzero resultant effect of a sequence of electron operators acting on the vacuum wave function, the equalities $\mu'_n = \sigma$, $\mu'_{n-1} = \mu_n$, \dots , $\mu'_1 = \mu_2$ must be satisfied. Taking this condition into account when summing in formula (3.4.6) over intermediate spin indices and assembling the series obtained anew into a geometric progression, we obtain

$$|1\rangle = -\frac{D}{A\sqrt{N}} \sum_{\mathbf{p}} e^{-i(\mathbf{p}\cdot\mathbf{g})} \sum_{n=1}^{\infty} \left(\frac{A}{E_c + K_p} \right)^{n+1} [(S_{\mathbf{g}} \cdot \mathbf{s})^{n+1}]_{\sigma\sigma'} a_{\mathbf{g}\sigma}^* c_{\mathbf{p}\sigma'}^* |0\rangle \\ = -\frac{D}{\sqrt{N}} \sum_{\mathbf{p}} e^{-i(\mathbf{p}\cdot\mathbf{g})} \left[\frac{(S_{\mathbf{g}} \cdot \mathbf{s})}{E_c + K_p - A(S_{\mathbf{g}} \cdot \mathbf{s})} \right]_{\sigma\sigma'} a_{\mathbf{g}\sigma}^* c_{\mathbf{p}\sigma'}^* |0\rangle \\ = -\frac{D}{\sqrt{N}} \sum_{\mathbf{p}} e^{-i(\mathbf{p}\cdot\mathbf{g})} [x_{\mathbf{p}} + y_{\mathbf{p}} (S_{\mathbf{g}} \cdot \mathbf{s})]_{\sigma\sigma'} a_{\mathbf{g}\sigma}^* c_{\mathbf{p}\sigma'}^* |0\rangle \quad (3.4.7)$$

(we do not present here explicit expressions for the coefficients $x_{\mathbf{p}}$ and $y_{\mathbf{p}}$, because they are too cumbersome). The last equality in (3.4.7) is based on the proposition that any function of the operator $(S_{\mathbf{g}} \cdot \mathbf{s})$ can be represented as a linear function of this operator. Indeed, two operators having identical eigenfunctions and eigenvalues are equivalent. The operator $(S_{\mathbf{g}} \cdot \mathbf{s})$ has only two eigenvalues corresponding to the parallel and the antiparallel orientations of the spins $S_{\mathbf{g}}$ and \mathbf{s} , all functions of $(S_{\mathbf{g}} \cdot \mathbf{s})$ have the same number of eigenvalues. Eigenvalues of an arbitrary function of $(S_{\mathbf{g}} \cdot \mathbf{s})$ and of a linear function of $(S_{\mathbf{g}} \cdot \mathbf{s})$ can be made equal by an appropriate choice of coefficients of the linear function: they should be determined from the condition of equality of both functions calculated for arguments coinciding with the eigenvalues of the $(S_{\mathbf{g}} \cdot \mathbf{s})$ operator. The latter are determined by squaring the operator of the total spin of the

electron and the atom $\mathbf{T}_g = \mathbf{S}_g + \mathbf{s}$:

$$2(\mathbf{S}_g \cdot \mathbf{s}) = \mathbf{T}_g^2 - \mathbf{S}_g^2 - \mathbf{s}^2. \quad (3.4.8)$$

In states with definite values of the squares of momenta \mathbf{L} their operators in (3.4.8) can be replaced by their eigenvalues $L(L+1)$, the total momentum T_g being, in accordance with the momentum summation rule, equal to $S+1/2$ or $S-1/2$. Then we obtain from (3.4.8) the following expressions for the eigenvalues of $(\mathbf{S}_g \cdot \mathbf{s})$:

$$\begin{aligned} (\mathbf{S}_g \cdot \mathbf{s}) &= \frac{S}{2} \quad \text{for} \quad T_g = S + 1/2, \\ (\mathbf{S}_g \cdot \mathbf{s}) &= -\frac{S+1}{2} \quad \text{for} \quad T_g = S - 1/2. \end{aligned} \quad (3.4.9)$$

The effective magnetic Hamiltonian H_M has the meaning of a correction to the energy of the ground state of the electrons that is a function of directions of l -spins, i.e. in this case the expression for it will be $\langle 1 | H_B | 1 \rangle$. Making use of formulae (3.4.7, 9) and (3.3.10), we obtain after having found the explicit form of the coefficients x_p and y_p :

$$\begin{aligned} H_M &= -\frac{\tilde{J}}{2} \sum (\mathbf{S}_g \cdot \mathbf{S}_{g+\Delta}), \quad (3.4.10) \\ \tilde{J} &= \frac{BD^2}{N} \sum_q \frac{(K_q + E_c)^2 \gamma_q}{\left[K_q + E_c - \frac{AS}{2} \right]^2 \left[K_q + E_c + \frac{A(S+1)}{2} \right]^2}, \\ \gamma_q &= \frac{1}{z} \sum_{\Delta} e^{iq \cdot \Delta} \end{aligned}$$

Formula (3.4.10) takes into account that, according to (3.1.2) and (3.4.9), the c - l exchange causes the energy of the conduction electron to shift by $AS/2$ or by $-\frac{|A|}{2}(S+1)$. The sign of the exchange integral \tilde{J} is in this case determined by that of the Bloch integral B .

An interesting point is that in contrast to the indirect exchange, the superexchange turns out to be short-range. In the case of narrow bands (3.4.10) it is nonzero only for nearest neighbours, although in the case of wide bands (3.4.3) its length may be greater.

The above approach provides a sufficiently simple and at the same time mathematically rigorous description of the superexchange. Some papers dealing with the superexchange (e.g. well-known papers of Anderson [618]) ignore the c - l model, and this makes construction of a consistent theory very difficult (a critical review of such papers is presented in [42]). The final result of all such papers obtained with a varying degree of rigour is a Heisenberg Hamiltonian, but

the form of the exchange integral is very sensitive to the details of the model employed.

It is hardly probable that reliable numerical computation of the exchange integrals could be carried out. This is in essence not a physical, but a quantum-chemical problem. At the same time the successes of quantum chemistry in the field of numerical computations are quite modest: even the available solution of the problem of such a simple system as the hydrogen molecule is not very precise.

For its part, the problem of calculating exchange integrals in a crystal is much more intricate.

At the same time, all calculations of superexchange cited in [42] lead to qualitative conclusions similar to those that follow from formulae (3.4.3) and (3.4.10): (1) the superexchange integral may both be positive and negative, (2) it decreases in magnitude as the gap in the electron spectrum widens. There is probably no sense in complicating the existing superexchange calculation in order to obtain immediately the contributions to it of various mechanisms described in [42]. It would be more reasonable to regard the exchange integrals as phenomenological parameters possessing qualitative properties cited above.

3.5. THE c - l MODEL HAMILTONIAN IN CASE OF NARROW CONDUCTION BANDS

Classical Spins. The Hamiltonian of the c - l model in the form of (3.1.1, 2) is convenient when for some reason or other the Hamiltonian H_A can be regarded as a perturbation. If on the other hand the interaction energy AS is great as compared with the width of the conduction band, the nondiagonal structure of the Hamiltonian in the c - l exchange makes operations with it much more difficult. Accordingly, it would be desirable to reconstruct the Hamiltonian to make it diagonal in the c - l exchange.

In case of classically large spins of magnetic atoms this is achieved by introducing a local coordinate system, such that the axis the projection of the c -electron spin onto which has a definite value would coincide with the spin of the atom occupied by the c -electron at the moment. Then the energy of an electron with the spin projection τ would in the zeroth approximation in W/AS be equal to $(-A\tau S)$ irrespective of the direction of spins of magnetic atoms in the crystal. As the energy AS is very great, it is usually enough to consider the electron states with a lower c - l exchange energy $\left(-\frac{|A|S}{2}\right)$.

The dependence of the c -electron energy on the orientation of the spins of magnetic atoms appears when the terms of the first order in W are taken into account. Qualitatively, its origin can be under-

stood as follows. The term H_B in the Hamiltonian (3.1.1) transfers the c -electron from one atom to another, retaining the direction of the electron spin in space. Should the spin of the atom that receives the c -electron be parallel to that of the atom vacated by the electron, the exchange energy of the c -electron with the magnetic atom ($-|A|S/2$) would not change and would remain at its minimum. Hence, there are no obstacles for the electron transition when the spins of the magnetic atoms are parallel. However, if the spins of the magnetic atoms are antiparallel, a transition of the c -electron to a neighbouring atom would result in its spin being oriented in the energetically-unfavoured direction with respect to the atomic spin, i.e. its energy would grow by a very large amount $|A|S$. Because of this such transitions are forbidden in the first approximation in W/AS .

On the other hand, if a transition is forbidden, and the electron is localized on one of the atoms, in accordance with the uncertainty principle, its energy will be higher than if it were able to go over to other atoms. On account of this the electron energy is at its minimum when the spins of all atoms are parallel. As will be demonstrated below, the dependence of the electron energy on the orientation of spins of magnetic atoms can be described with the aid of the effective Bloch integral, which depends on the direction of the spins in space.

The transition to a local frame of reference whose Z_g axis coincides with the spin of the atom g must be accompanied by such a transformation of the electron operators that the electron states would be characterized by the projections of the spin \uparrow and \downarrow on the Z_g axis instead of the spin projections $\sigma = \pm 1/2$ in the laboratory frame of reference.

The corresponding canonical transformation in the general case is of the form

$$\begin{aligned} a_{g, 1/2}^* &= e^{-i\delta_g} \cos \gamma_g a_{g\uparrow}^* + e^{-i\beta_g} \sin \gamma_g a_{g\downarrow}^*, \\ a_{g, -1/2}^* &= e^{i\gamma_g} \sin \gamma_g a_{g\uparrow}^* + e^{-i\mu_g} \cos \gamma_g a_{g\downarrow}^*, \end{aligned} \quad (3.5.1)$$

where the phase angles are connected by relationship that guarantees that the transformation is always unitary:

$$\delta_g - \beta_g = \gamma_g - \mu_g \div \pi.$$

The coefficients of the transformation (3.5.1) must obviously be expressed in terms of Cayley-Klein parameters. Here it is more convenient to make use, instead of Euler angles, of the angles that determine the direction of the vector S_g in the laboratory frame of reference (the polar angle θ_g and the longitude φ_g). The explicit form of the coefficients of the transformation (3.5.1) can be found from the following conditions: (1) from the invariance of the scalar product

of the atomic and the c -electron spin under rotation of the frame of reference; (2) from the requirement that the operators $a_{g, 1/2}^*$, $a_{g, -1/2}^*$ change signs following a rotation through the angle 2π , same as the spin wave functions do, because the latter can be represented in the form $a_{g\sigma}^* |0\rangle$. In the result we obtain

$$\gamma_g = \frac{\theta_g}{2}, \quad \delta_g = u_g - \frac{\varphi_g}{2}, \quad \beta_g = \pi - u_g - \frac{\varphi_g}{2},$$

$$\nu_g = \pi - \beta_g, \quad \mu_g = -\delta_g. \quad (3.5.2)$$

The quantity u_g without loss of generality can be put equal to zero, since it can always be eliminated by means of a canonical transformation that changes the phase of electron operators.

Substituting expressions (3.5.1, 2) into the Hamiltonian (3.1.1, 2), we obtain

$$H = H_{\uparrow} + H_{\downarrow} + H_{\uparrow\downarrow},$$

$$H_{\uparrow} = -\frac{AS}{2} \sum a_{g\uparrow}^* a_{g\uparrow} + B \sum \cos \frac{\theta_{g, g+\Delta}}{2} e^{i\gamma_{g, g+\Delta}} a_{g\uparrow}^* a_{g+\Delta\uparrow},$$

$$H_{\downarrow} = \frac{AS}{2} \sum a_{g\downarrow}^* a_{g\downarrow} + B \sum \cos \frac{\theta_{g, g+\Delta}}{2} e^{-i\gamma_{g, g+\Delta}} a_{g\downarrow}^* a_{g+\Delta\downarrow},$$

$$H_{\uparrow\downarrow} = -iB \sum \sin \frac{\theta_{g, g+\Delta}}{2} [e^{-i\mu_{g, g+\Delta}} a_{g\uparrow}^* a_{g+\Delta\downarrow} - e^{i\mu_{g, g+\Delta}} a_{g\downarrow}^* a_{g+\Delta\uparrow}],$$

where $\theta_{g, g+\Delta}$ is the angle between the spins of the g and the $g + \Delta$ atom,

$\cos \theta_{g, g+\Delta} = \cos \theta_g \cos \theta_{g+\Delta} + \sin \theta_g \sin \theta_{g+\Delta} \cos(\varphi_g - \varphi_{g+\Delta})$,
and the expressions for the phases are

$$\gamma_{g, g+\Delta} = \arctan \left\{ \frac{\cos \eta_{g, g+\Delta}}{\cos \xi_{g, g+\Delta}} \tan \zeta_{g, g+\Delta} \right\},$$

$$\mu_{g, g+\Delta} = \arctan \left\{ \frac{\sin \eta_{g, g+\Delta}}{\sin \xi_{g, g+\Delta}} \tan \zeta_{g, g+\Delta} \right\},$$

$$\zeta_{g, g+\Delta} = \frac{\varphi_g - \varphi_{g+\Delta}}{2}, \quad \eta_{g, g+\Delta} = \frac{\theta_g + \theta_{g+\Delta}}{2}, \quad \xi_{g, g+\Delta} = \frac{\theta_g - \theta_{g+\Delta}}{2}.$$

The Hamiltonian in the form (3.5.3) is suitable for constructing a perturbation theory in WAS . In the first approximation we may discard the term $H_{\uparrow\downarrow}$ in expression (3.5.3), and then the Hamiltonian will split up into two independent Hamiltonians H_{\uparrow} and H_{\downarrow} .

A similar problem for a system of two atoms for $A > 0$ has earlier been considered in [69], which tried to present arguments in favour of Zener's idea that electron transitions between two magnetic atoms bring about ferromagnetic ordering of their spins ("double

exchange" [68]). It has been demonstrated in [69] that the spectrum of such a system in the main approximation in B/A for a given angle between the atomic spins θ consists of two levels with the energies

$$E_{\pm} = \pm B \cos \frac{\theta}{2} \quad (3.5.5)$$

(the constant $(-AS/2)$ has been dropped). This result is immediately obtainable from the Hamiltonian H_+ , which in the case of two atoms numbered 1 and 2 with account taken of the equality $\gamma_{12} = -\gamma_{21} = \gamma$ that follows from (3.5.4), is of the form

$$H_+ = -\frac{AS}{2} (a_{1\uparrow}^* a_{1\uparrow} + a_{2\uparrow}^* a_{2\uparrow}) + B \cos \frac{\theta}{2} [e^{i\gamma} a_{1\uparrow}^* a_{2\uparrow} + e^{-i\gamma} a_{2\uparrow}^* a_{1\uparrow}] \quad (3.5.6)$$

and can be diagonalized by the canonical transformation of the operators

$$a_{\pm\uparrow} = \frac{1}{\sqrt{2}} (a_{1\uparrow} \pm \tilde{a}_{2\uparrow}), \quad \tilde{a}_{2\uparrow} = e^{i\gamma} a_{2\uparrow}. \quad (3.5.7)$$

The energy of the ground state of the system irrespective of the sign of the hopping integral B will be seen from formula (3.5.5) to be the less the smaller the angle θ , i.e. the electron transitions, indeed, tend to establish a ferromagnetic spin ordering.

De Gennes [74] attempted to generalize the result (3.5.5) for the case of an arbitrary number of magnetic atoms by postulating for it an H_+ -type Hamiltonian (3.5.3) with all $\gamma_{\mathbf{g}, \mathbf{g}+\Delta} = 0$. In case of two atoms the presence of a phase multiplier $\exp(\pm i\gamma)$ in (3.5.6) is inessential, for it can be eliminated from the Hamiltonian (3.5.6) by means of the canonical transformation (3.5.7) that shifts the phase of the electron operator $a_{2\uparrow}$. From the physical point of view, the independence of the energy (3.5.5) of the phase γ follows from the fact that this phase determines the spin orientation with respect to the laboratory frame of reference, whereas the energy of a closed "two atoms - an electron" system is independent of the orientation of its total spin in space.

For three and more atoms, there is generally no canonical transformation that would eliminate the phases γ : rotation of spins of any two atoms through equal angles changes the energy of the system, since it depends on the orientation of those two spins with respect to the spins of other magnetic atoms, too. Accordingly, it is not permissible to discard the quantities $\gamma_{\mathbf{g}, \mathbf{g}+\Delta}$ in the Hamiltonian (3.5.3). There is an exception when all the spins are parallel to the same plane ($\varphi_{\mathbf{g}} = \text{const}$), but this is possible only at $T = 0$. Those factors determine the conditions of applicability of the de Gennes Hamiltonian.

As will be demonstrated in the following item, another limitation of the applicability of the Hamiltonian (3.5.3) is that for $\theta_g, g-\Delta = \pi$ it is accurate not up to $1/2S$, but only up to $1/\sqrt{2S}$. Since in actual conditions the spin S does not exceed 9/2, the latter quantity turns out to be of the order of unity, and the use of (3.5.3) for antiferromagnetic ordering may lead to serious errors (see Sec. 6.2).

Eigenfunctions of the c - l Exchange Hamiltonian. To construct an effective Hamiltonian for the c - l model in the quantum case, one should in advance find the eigenfunctions $\psi_{\mathbf{g}m}^{\pm}$ of the c - l exchange Hamiltonian (3.1.2), where \mathbf{g} is the atom on which the electron is localized, M is the value of the projection of the total angular momentum \mathbf{T}_g of the atom and the c -electron on an arbitrary axis Z whose magnitude is $S + 1/2$ or $S - 1/2$. The signs \pm in the notation for the wave function correspond to these two possibilities. The only difference between the eigenvalues (3.1.2) and expressions (3.4.9) is in the factor $(-A)$. Each of the energy levels is degenerate in the direction of the total spin \mathbf{T}_g .

We may conveniently use the spin functions corresponding to definite values of their z -projections as the basis functions: the functions (2.1.1) $\delta(S_g^z, m)$ for the atomic spin ($m = -S, -S + 1, \dots, S - 1, S$) and $a_{g\sigma}^* |0\rangle$ for the c -electron spin ($\sigma = \pm 1/2$), where $|0\rangle$ is the vacuum electron wave function. Let us begin with the case of the total spin $T_z = S + 1/2$. For the maximum total-spin projection $M = S + 1/2$, the atomic and the electron spins are parallel and also have maximum values (the projection of the former is S and of the latter $1/2$). For this reason the eigenfunction of such a state is simply

$$\psi_{\mathbf{g}, S+1/2}^+ = \delta(S_g^z, S) a_{g\uparrow}^* |0\rangle. \quad (3.5.8)$$

A similar expression can be written for $M = -S - 1/2$.

If the spin projection M is not equal to $\pm(S + 1/2)$, there are two possibilities corresponding to a state with a specified value of M : (1) the projection m of the atomic spin is equal to $M - 1/2$ and of the electron spin to $1/2$ (the state $\delta(S_g^z, M - 1/2) a_{g\uparrow}^* |0\rangle$); (2) the projection m of the atomic spin is equal to $M + 1/2$ and of the electron spin to $-1/2$ (the state $\delta(S_g^z, M + 1/2) a_{g\downarrow}^* |0\rangle$). Since the Hamiltonian (3.1.2) does not conserve the individual spin projections of the electron and the atom, but only their total spin projection, its eigenstate must be a linear combination of the two states:

$$\psi_{\mathbf{g}M}^+ = \{x\delta(S_g^z, M - 1/2) a_{g\uparrow}^* + y\delta(S_g^z, M + 1/2) a_{g\downarrow}^*\} |0\rangle. \quad (3.5.9)$$

The coefficients of this linear combination can be found from simple geometric considerations. The state (3.5.9) is depicted in the figure with the big arrow denoting the atomic spin and the small one the

c-electron spin

$$\equiv \cos \frac{\theta}{2} \left\{ \begin{array}{c} \uparrow s \\ S \text{ along } Z' \\ m = M - \frac{1}{2} \end{array} \right\} + \sin \frac{\theta}{2} \left\{ \begin{array}{c} \downarrow s \\ S \text{ along } Z' \\ m = M + \frac{1}{2} \end{array} \right\}$$

Since the total atomic spin is equal to $S = 1/2$, both spins point in the same direction. If the total spin projection is equal to M , the Z' axis in the direction of which the atomic and the electron spins point will be deflected from the Z -axis by an angle θ such that

$$\cos \theta = \frac{M}{S + 1/2}. \quad (3.5.10)$$

In that case the coefficients x_+ and y_+ in expression (3.5.9) should be equal to $\cos(\theta/2)$ and $\sin(\theta/2)$, respectively. This follows from the general rules of spinor transformation [75] and can also be obtained by simple reasoning. Indeed, the average electron spin projection on the Z -axis is equal to

$$\overline{S^z} = (1/2) \cos \theta.$$

But on the other hand, according to formula (3.5.9), it is equal to

$$\overline{S^z} = 1/2 (x_+^2 - y_+^2),$$

since x_+^2 and y_+^2 are the probabilities of the values $\sigma = \pm 1/2$, respectively. Taking also into account the normalization condition

$$x_+^2 + y_+^2 = 1,$$

we obtain

$$x_+^2 = \cos^2 \frac{\theta}{2}, \quad y_+^2 = \sin^2 \frac{\theta}{2}. \quad (3.5.11)$$

The choice of the coefficients x_+ and y_+ of the same sign is enforced by the condition that the energy

$$E_A = (\psi_{gM}^+, H_A \psi_{gM}^+) = -\frac{AS}{2},$$

which for $A > 0$ is the energy of the ground state, be minimum. Making use of the familiar trigonometric relations, we can rewrite formula (3.5.9), taking account of relations (3.5.10, 11), in the form

$$\psi_{gM}^+ = \left\{ \sqrt{\frac{S+M+1/2}{2S+1}} \delta(S_g^z, M-1/2) a_{g\uparrow}^* + \sqrt{\frac{S-M-1/2}{2S-1}} \delta(S_g^z, M+1/2) a_{g\downarrow}^* \right\} |0\rangle. \quad (3.5.12)$$

One can obtain the expression for $\psi_{\vec{g}M}^-$ with the aid of formula (3.5.12), if he takes into account that it, too, must have the structure of (3.5.9). The coefficients of the linear combination of x_- and y_- can be found from the condition of orthogonality of $\psi_{\vec{g}M}^+$ and $\psi_{\vec{g}M}^-$ together with the normalization condition. This yields: $y_- = \cos(\theta/2)$, $x_- = -\sin(\theta/2)$, i.e.

$$\psi_{\vec{g}M}^- = \left\{ \sqrt{\frac{S+M+1/2}{2S+1}} \delta(S_{\vec{g}}, M+1/2) a_{\vec{g}\downarrow}^* - \sqrt{\frac{S-M+1/2}{2S-1}} \delta(S_{\vec{g}}, M-1/2) a_{\vec{g}\uparrow}^* \right\} |0\rangle. \quad (3.5.13)$$

It can be easily ascertained with the aid of relations (2.1.3, 4) that (3.5.12) and (3.5.13) are eigenfunctions of the Hamiltonian H_A (3.1.2).

Spin-wave Approximation. In the quantum analysis of spins it would be reasonable to start constructing the Hamiltonian for the simplest case, that of ferromagnetic semiconductors. In the zeroth approximation in W/AS every electron is fixed on some atom, and the system resides in eigenstates of the c - l exchange Hamiltonian. This means that the spins of an atom and of the electron occupying it form a united spin equal to $S - 1/2$ for $A > 0$ and to $S + 1/2$ for $A < 0$. In the first approximation in W/AS the electron is able to migrate from atom to atom, so that the spin of each atom is no longer a fixed quantity, being dependent on whether the atom is occupied by an electron or vacant.

In its turn, strong coupling of the electron with the spins of magnetic atoms means that in this case not an ordinary band electron serves as a charge carrier, but a quasi-particle of a more complicated nature for which the term "spinpolaron" has been suggested in [70]*.

In this section we intend to construct a spinpolaron Hamiltonian for the case when the spin configuration of magnetic atoms is close to the perfect FM, and when the spin-wave approximation is applicable. Of principal importance is the circumstance that in this case it is senseless to speak of magnetic ordering of just the intrinsic magnetic-atom spins. Of physical meaning is the moment of the entire system including the moments of the conduction electrons. Hence, we are dealing here with magnetic ordering in a system with variable atomic spins.

The ideal FM ordering should be understood here to mean that the total moment of the entire system is at its maximum. Qualitatively, it means that the spins of all atoms point in the same direction, no matter whether there are electrons on them or not, and that the

* The terminology in magnetic semiconductor physics is, as yet, not firmly established, and several authors use the term "spinpolaron" to designate states of a totally different type termed "ferrons" in this book.

transitions of c -electrons from atom to atom just change the lengths of their spin vectors without changing their directions (this is equivalent to the motion of "irregular" $S \pm 1/2$ spins in the crystal).

The presence of a magnon in such a system means that a spin deviation wave propagates along the crystal whose specific property is that its motion takes place against the background of "irregular" $S \pm 1/2$ spins moving in the crystal. The passage of a wave across an atom, no matter whether it bears an extra electron or not, results equally in the decrease in its spin projection by unity. Such magnons remind one of phonons discussed in Sec. 1.4, which constitute the displacements of atoms from their equilibrium positions in the lattice polarized by a conduction electron. They are introduced invariantly with respect to the specific equilibrium positions of atoms, which are displaced adiabatically following the motion of the electron.

The variability of the spin of a magnetic atom makes it impossible to introduce magnon operators with the aid of the Holstein-Primakoff relations (2.4.1), and for this reason the operator of creation of a magnon on an atom is defined simply as one that changes the projection of the atomic spin from its maximum value to one less unity, and the magnon operator of annihilation as a conjugate operator, both obeying the Bose commutation rules. Such a definition, being invariant with respect to the magnitude of the atomic spin, may be used in case of variable-magnitude spins as well.

The spinpolaron Hamiltonian is constructed by expanding it in powers of magnon operators*. With account taken of the fact that the system conserves the number of magnons, this expansion should be of the form (to be definite, we consider the case $A > 0$)

$$H = H_0 + H_2 + O(b^*b^*bb),$$

$$H_0 = B \sum \alpha_{g, >}^* \alpha_{g+\Delta, >} - \frac{AS}{2} \sum \alpha_{g, >}^* \alpha_{g, >}, \quad (3.5.14)$$

$$H_2 = B \sum \{ \mathcal{X} (b_g^* b_g - b_{g+\Delta}^* b_{g-\Delta}) - \mathcal{Y} b_g^* b_{g+\Delta} + \mathcal{Z} b_{g+\Delta}^* b_g \} \alpha_{g, >}^* \alpha_{g+\Delta, >},$$

where $\alpha_{g, >}^*$, $\alpha_{g, >}$ and b_g^* , b_g are the operators of the creation and annihilation of a spinpolaron and a magnon on the atom g , respectively (the sign $>$ means that $A > 0$); \mathcal{X} , \mathcal{Y} , \mathcal{Z} are unknown coefficients (the spinpolaron operators are not the same as the electron ones, but also obey the Fermi commutation rules).

The Hamiltonian H_0 in (3.5.14) corresponds to an ideal FM ordering when the spinpolaron moves like an ordinary band electron. It includes the c - l exchange energy obtained in the zeroth approxi-

* Since the Hamiltonian H_A (3.1.2) is nonlinear in magnon operators (2.4.1), the true magnon operators cannot be introduced by means of a canonical transformation of the type (1.4.2).

ation in WAS , which does not change as the spinpolaron moves from atom to atom and is independent of the relative orientation of atomic spins. For this reason the term H_2 quadratic in magnon operators must be associated with the transitions of the spinpolaron from atom to atom. This means that, as H_B in (3.1.1), its structure must correspond to the nearest-neighbour approximation. At the same time it must not contain terms of the $\alpha_g^* \alpha_g b_{g+\Delta}^* b_{g+\Delta}$ type that retain the spinpolaron position unchanged. On account of the condition $J \ll B$, we may neglect the changes introduced into the Hamiltonian H_M in (3.1.1) by the presence of a spinpolaron.

To find the coefficients \mathcal{X} , \mathcal{Y} , \mathcal{Z} , we consider the eigenstate of a system containing one magnon. Its wave function can be represented in form

$$\Phi = \sum c_{gh} \alpha_g^* b_h^* |v\rangle, \quad (3.5.15)$$

where $|v\rangle$ is the vacuum wave function for the spinpolaron and the magnon. By substituting (3.5.15) into (3.5.14), we obtain the Schrödinger equation for the spinpolaron in the following form:

$$\begin{aligned} B \sum_{\Delta} c_{g+\Delta, h} + B\mathcal{X} \sum_{\Delta} c_{hh} \delta(g+\Delta, h) \\ + B\mathcal{Z} \sum_{\Delta} c_{h, h+\Delta} \delta(h+\Delta, g) = \left(E + \frac{AS}{2}\right) c_{gh} \quad (g \neq h), \quad (3.5.16) \\ B(1+\mathcal{X}) \sum_{\Delta} c_{g+\Delta, g} + B\mathcal{Y} \sum_{\Delta} c_{g-\Delta, g+\Delta} = \left(E + \frac{AS}{2}\right) c_{gg}. \end{aligned}$$

Equation (3.5.16) corresponds to the adiabatic approximation: because of the condition $J \ll B$, the motion of the magnon caused by terms entering H_M is not taken into account.

On the other hand the same state can be described by directly applying the Hamiltonian (3.1.1). If an atom does not bear an extra electron, its wave function will be simply $\delta(S_g^z, S)$ for an undeflected atomic spin, and $\delta(S_g^z, S-1)$ for an atomic spin deflected from the direction of the total moment of the crystal. If the atom bears an extra electron, its wave function will be $\psi_{g, S+1/2}^*$ (3.5.8) for an undeflected atomic spin, and $\psi_{g, S-1/2}^*$ (3.5.12) for a deflected spin. In that case the wave function of the system can be represented in the form

$$\begin{aligned} \psi = \sum_{g \neq h} c_{gh} \alpha_g^* |0\rangle \delta(S_h^z, S-1) \prod_{t \neq h} \delta(S_t^z, S) \\ + \sum c_{gg} \psi_{g, S-1/2}^* \prod_{t \neq g} \delta(S_t^z, S), \quad (3.5.17) \end{aligned}$$

where $|0\rangle$ is the electron vacuum wave function.

Substituting expansion (3.5.17) into the Schrödinger equation with the Hamiltonian (3.1.1), we obtain a result, which will coincide with (3.5.16), if we put

$$H_{>} = -\frac{AS}{2} \sum \alpha_{\mathbf{g},>}^* \alpha_{\mathbf{g},>} + B \sum \alpha_{\mathbf{g},>}^* \alpha_{\mathbf{g}+\Delta,>} - B \sum \left\{ \frac{b_{\mathbf{g}}^* b_{\mathbf{g}-\Delta}}{2S-1} - \left(1 - \sqrt{\frac{2S}{2S-1}} \right) (b_{\mathbf{g}}^* b_{\mathbf{g}} + b_{\mathbf{g}+\Delta}^* b_{\mathbf{g}+\Delta}) \right\} \times \alpha_{\mathbf{g},>}^* \alpha_{\mathbf{g}+\Delta,>} \quad (3.5.18a)$$

In the same way for $A < 0$ we obtain

$$H_{<} = \frac{A(S+1)}{2} \sum \alpha_{\mathbf{g},<}^* \alpha_{\mathbf{g},<} + \frac{2SB}{2S+1} \sum \alpha_{\mathbf{g},<}^* \alpha_{\mathbf{g}+\Delta,<} - \frac{B}{2S-1} \sum \left\{ b_{\mathbf{g}+\Delta}^* b_{\mathbf{g}} - 2S \left(1 - \sqrt{1 - \frac{1}{2S}} \right) \times (b_{\mathbf{g}}^* b_{\mathbf{g}} + b_{\mathbf{g}+\Delta}^* b_{\mathbf{g}+\Delta}) \right\} \alpha_{\mathbf{g},<}^* \alpha_{\mathbf{g}+\Delta,<} \quad (3.5.18b)$$

The case of an AFS can be considered similarly. Since magnons of two types are possible in an AFS, those of one type increasing and those of the other decreasing the moment of the crystal (Sec. 2.6)), the projection of the total crystal moment cannot be expressed in terms of the total number of magnons, and for this reason this number does not constitute a conserving quantity.

The term $\sim B$, which does not contain magnon operators, is in this case absent, since in compliance with (3.5.3), the electron transitions from atom to atom not accompanied by changes in their spins are forbidden for $\theta_{\mathbf{g}}, \mathbf{g}+\Delta = \pi$. Because of that the expansion of the spinpolaron kinetic energy in magnon operators starts right with linear terms:

$$H_{>} = -\frac{AS}{2} \sum \alpha_{\mathbf{g},>}^* \alpha_{\mathbf{g},>} + \frac{iB}{\sqrt{2S-1}} \sum e^{i\Pi \cdot \mathbf{g}} (b_{\mathbf{g}+\Delta} + b_{\mathbf{g}}^*) \alpha_{\mathbf{g},>}^* \alpha_{\mathbf{g}+\Delta,>} \quad (3.5.19a)$$

$$H_{<} = \frac{A(S+1)}{2} \sum \alpha_{\mathbf{g},<}^* \alpha_{\mathbf{g},<} + \frac{iB \sqrt{2S}}{2S+1} \sum e^{i\Pi \cdot \mathbf{g}} (b_{\mathbf{g}+\Delta}^* + b_{\mathbf{g}}) \alpha_{\mathbf{g},<}^* \alpha_{\mathbf{g}+\Delta,<} \quad (3.5.19b)$$

where $b_{\mathbf{g}}^*, b_{\mathbf{g}}$ are operators of deviation of spins from directions corresponding to staggered AF ordering of Fig. 2.2a.

The following considerations will throw light on the structure of expressions (3.5.19a, b). For $A > 0$ with the electron occupying the atom $\mathbf{g} + \Delta$ its spin will be parallel to that of the atom. In case

the AF state of the crystal is not disturbed, for a total atomic spin $T_{g+\Delta} = S + 1/2$, its projection will be at its maximum equal to $S + 1/2$. The electron goes over to a neighbouring atom g . After the transition the projection of the spin of the g -atom in the laboratory frame of reference will be equal to $(-S - 1/2)$ with the total spin magnitude $S + 1/2$. And this means that a magnon has been created on the g -atom, i.e. that the Hamiltonian must include a term of the form of $b_{g\Delta}^* \alpha_{g\Delta, >}^* \alpha_{g\Delta, >}$ and one conjugate to it. The matrix element corresponding to such a process is $(\delta(S_{g+\Delta}^z, S) \times \psi_{g_0-S+1/2}^+ H_B \psi_{g+\Delta, S+1/2}^+ \delta(S_g^z, -S))$, which, if formula (3.5.12) is taken into account, yields the factor $(2S - 1)^{-1/2}$ that renormalizes the hopping integral B .

Consider now a pair of neighbouring atoms with antiparallel spins one of which bears an extra electron for $A < 0$. The transition of an electron from the $g + \Delta$ -atom to the g -atom may be interpreted as the transition of a hole from the g -atom to the $g - \Delta$. In the process the spin of the g -atom equal to S should be regarded as the sum of the spin of the atom bearing the extra electron $T_g = (S - 1/2)$ and of the hole spin parallel to it. If we take into account that before the transition of the hole the spin of the $g + \Delta$ -atom was equal to $S - 1/2$, and that the spin of the hole is antiparallel to it we shall obtain that after the transition of the hole the spin of $g + \Delta$ -atom will grow to S , and its projection will diminish by $1/2$, i.e. it will be equal to $(S - 1)$. Hence, after the arrival of a hole, i.e. after the departure of the electron, a magnon will be created on the $g + \Delta$ -atom. Accordingly, the Hamiltonian should include a term of the form $b_{g+\Delta}^* \alpha_{g\Delta, <}^* \alpha_{g\Delta, <}$ and one conjugate to it. The matrix element corresponding to such a process is $(\delta(S_{g+\Delta}^z, S - 1) \times \psi_{g_0-S+1/2}^+ H_B \psi_{g+\Delta, S-1/2}^+ \delta(S_g^z, S))$ and this, according to (3.5.13), yields a renormalizing factor equal to $1/2S(2S + 1)^{-1}$. A more detailed deduction of the Hamiltonians (3.5.19a and b) is contained in [76].

For $S \rightarrow \infty$ the kinetic energy of spinpolarons in the Hamiltonians (3.5.19a, b) diminishes as $1/\sqrt{2S}$. Hence, the picture of classical spins in which the transitions of the electron from atom to atom in the first order in W/AS are forbidden in case of an AF ordering is accurate only in the limit $1/\sqrt{2S} \rightarrow 0$ and not up to the usual accuracy of the classical approximation of $1/2S \ll 1$. If the inequality $2S \gg 1$ can be satisfied for realistic spin magnitudes, $1/\sqrt{2S}$ will not exceed 3, i.e. the use of the classical spin picture to describe the motion of the electron in narrow-band AFS's may result in serious errors.

A Hamiltonian of a more general form similar to one deduced in the spin-wave approximation can also be constructed for arbitrary

spin configurations [70-72]. The most difficult point in the description of the system, the variable magnitude of atomic spins, can be overcome by the formal introduction of spins of equal magnitude for all atoms, with the actual difference between vacant atoms and ones occupied by extra electrons being accounted for by the structure of the Hamiltonian (see Appendix I). In the limit $S \rightarrow \infty$ this Hamiltonian reduces to (3.5.4).

NONDEGENERATE FERROMAGNETIC SEMICONDUCTORS

4.1. ENERGY SPECTRUM OF CHARGE CARRIERS IN NARROW-CONDUCTION-BAND SEMICONDUCTORS

Owing to a strong interaction of the charge carriers with the spins of magnetic atoms, their state in MS generally differs appreciably from that of band electrons moving in a stationary field of periodically arranged atoms. The exact solution to the problem of the conduction-electron state within the framework of the c - l model can be obtained only at $T = 0$. Two different cases are possible. If the total spin of the crystal and the conduction electron assumes its maximum value, then the conduction-electron spin projection is preserved, and the state of the electron is described by the conventional band theory. Much more complicated is the case when the total spin of the system is 1 less than its maximum value. Then the c -electron spin projection is no longer preserved. Formally an exact solution for this case was first obtained in [9]; the charge carrier is a quasi-particle consisting of an electron and a bound bare magnon (i.e. the wave of l -spin deviations).

Unfortunately, no physical conclusions were drawn in [9] from the result obtained. Virtually the same solution was obtained also in [77], and its detailed analysis was carried out in both limiting cases $W \gg AS$ and $W \ll AS$. In particular, results obtained earlier in [70] for $W \ll AS$ were confirmed in [77]. Further investigation of this problem was carried out in [619]. Having in mind that the solution obtained in [9, 77, 619] for arbitrary W/AS is valid only at $T = 0$ and is rather cumbersome, only limiting cases $W \gg AS$ and $W \ll AS$ will be considered in what follows. In both cases dressed magnons (i.e. waves not only of l -spins, but also of c -electron spin deviations) will be introduced instead of bare magnons used in [9, 77, 619].

The interaction with the magnetic subsystem exercises an especially strong influence on the electrons occupying a narrow band $W \ll AS$. It has already been pointed out in Sec. 3.5 that in this case the spin of the conduction electron is rigidly tied to the spin of the atom it occupies at the moment, so that a united spin equal to $S + 1/2$ for $A > 0$ and to $S - 1/2$ for $A < 0$ is formed. Thus, the motion of a conduction electron in a crystal is equivalent to the motion of an "irregular" spin $S \pm 1/2$ in a lattice of "regular" spins S . Such a particle was termed spinpolaron [70, 71].

The spinpolaron carrier states in transition element compounds may be expected to become a reality when the energy bands of the compounds are of the d -type and by force of that narrow. For example, in CdCr_2Se_4 the appearance of a conduction electron amounts to the transition of one of the normal Cr^{3+} ions into the Cr^{2+} -state in the result of the reaction $\text{Cr}^{3+} + e \rightarrow \text{Cr}^{2+}$. However, despite the frequently expressed opinion, this does not mean that the electron e is localized. Since all the Cr^{3+} ions are equivalent, it moves from one Cr^{3+} ion to another by means of the recharge reaction $\text{Cr}^{2+} + \text{Cr}^{3+} \rightarrow \text{Cr}^{3+} - \text{Cr}^{2+}$. The motion of the electron in the crystal causes an energy band to be formed. According to estimates of Sec. 4.6, its width may reach ~ 1.0 eV, and this may be compatible with the inequality $W \ll AS^*$.

Let us discuss first of all the state of the carrier at $T = 0$ when the spins of all magnetic atoms are parallel. If $A > 0$, the c -electron spin will be parallel to that of atom g it occupies. The electron motion in the crystal is described by means of the Hamiltonian H_B (1.1.1). The transitions of the electron from atom to atom must, as seen from the structure of H_B , take place without changes in its spin projection. Hence, following the transition of the electron to a neighbouring atom, the electron spin turns out to be parallel to the spin of this atom, too, i.e. the gain in the c - l exchange energy remains maximum (equal to $AS/2$). It follows hence that exchange interaction with magnetic atoms has no effect on the electron motion in the crystal. Its energy spectrum will, as before, be determined by expression (1.1.1), the only difference being its downward shift by the amount $AS/2$ owing to the c - l exchange.

If on the other hand $A < 0$, the effect of exchange interaction with the spins on carrier motion in the crystal will make itself manifest already at $T = 0$. The distinction of this case from the preceding one consists in the c -electron spin projection having no definite value: according to (3.5.13), for $M = S - 1/2$ it is with the probability of $|y_-|^2 = \frac{2S}{2S-1}$ equal to $-1/2$ and with the probability of $|x_-|^2 = \frac{1}{2S-1}$ equal to $+1/2$. When $\sigma = 1/2$, the electron is unable to go over from the g -atom to the $g + \Delta$ -atom: the transition takes place without a change in the electron spin, and on the $g - \Delta$ -atom it would be parallel to the spin of this atom, this resulting in a very big increase in its energy $\sim AS$. Accordingly, the transition of the electron from the g to the $g - \Delta$ -atom is only possible when

* In some papers, e.g. [546, 547], attempts have been made to calculate the band spectrum of CdCr_2Se_4 . However, the calculations have been carried out as if the problem were one of the conventional band electrons moving in a stationary periodic potential, i.e. the spinpolaron effects have been neglected. Even with such a simplified approach, results obtained with different methods are widely different and thus cannot be treated as reliable.

$\sigma = -1/2$. Because of that the transition integral B appears to be reduced $|y_-|^2 = 2S/2S - 1$ times. The energy bandwidth of the mobile charged quasi-particle, the spinpolaron, is reduced as many times, and its effective mass is increased as many times as compared with the bare effective mass of the band electron. This result obtained first in [70] was confirmed in [77, 620].

The state of the carrier in this case resembles the polaron state in an ionic crystal, this justifying the use of the term "spinpolaron". Indeed, in the polaron state the electron moves over the crystal together with the lattice polarization it itself has created. This shifts its energy compared with the electron energy in an unpolarizable lattice downwards by the amount equal to the lattice polarization energy, its effective mass rising. In other words, the bottom of the polaron band lies below that of the electron band, but the former is narrower. Just this is the case for the spinpolaron band, too.

The above does not imply that the spinpolaron state is a specific property of the case $A < 0$. In the case $A > 0$ the spinpolaron state at $T = 0$ coincides with the band-electron state, but at finite temperatures they differ appreciably: namely, for $A > 0$ as for $A < 0$ the spinpolaron state enables maximum gain in the c - l exchange energy to be obtained, although at finite temperatures the width of the spinpolaron band turns out to be less than the width of the electron band $2z|B|$. This will be immediately evident from the Hamiltonian (3.5.3): the angles between the spins grow with rising temperature, and the effective integral for the electron transitions from atom to atom diminishes. Hence, as the temperature rises, the bottom of the spinpolaron band moves upwards, and the spinpolaron effective mass grows.

From the most general considerations it may be asserted that at ultra-low temperatures $T < T_c$ the energy shift will proceed with rising temperature at a slower rate than changes in the magnetization proportional to $T^{3/2}$ (2.4.8). Indeed, a rotation of all the spins through an identical angle will not change the carrier spectrum since space is presumed to be isotropic. On the other hand, the rotation of the moment of the crystal as a whole corresponds to the creation of magnons with zero quasi-momentum q . Accordingly, the energy of interaction between the spinpolarons and the magnons should vanish for $q \rightarrow 0$. As this energy is independent of the magnon direction of motion, its expansion in q should start with the term $\sim q^2$ proportional to the magnon frequency. Its mean value is proportional to the temperature T . The shift in the spinpolaron energy with the temperature is proportional to the product of their mean interaction energy with the magnons and of the average number of magnons (2.4.8), i.e. to $T^{5/2}$. For $2S \gg 1$ in the temperature range $\frac{1}{2} < T \ll \frac{1}{2}S$ when the spin-wave approximation is still valid, but short-wave magnons are predominant, their interaction energy with the

spinpolarons is weakly dependent on the temperature, and the shift in the spinpolaron spectrum should proceed according to the same linear law as the change in magnetization (Sec. 2.4).

At elevated temperatures when the FM ordering is destroyed, the crystal cannot even approximately be treated as a periodic structure, since the angles between neighbouring l -spins fluctuate. Since in disordered media the quasi-momentum concept becomes generally meaningless, the established method is to describe the carrier energy spectrum not by means of a dispersion law, but by means of a cruder characteristic, the density of states. Some of its moments about the band centre will be calculated below. It follows from their analysis that at high temperatures the density of states vs. energy dependence conforms to a law similar to one valid at $T = 0$ when the quasi-momentum is a good quantum number [72].

In the spin-wave region the spinpolaron Hamiltonian is given by expressions (3.5.18a) for $A > 0$ and by (3.5.18b) for $A < 0$. The first two terms in them describe spinpolarons that do not interact with magnons, i.e. at $T = 0$. If the spectrum of a free spinpolaron for $A > 0$ coincides with expression (1.1.1) displaced by $AS/2$, the expression for it for $A < 0$ will, in accordance with what has been said above about the spinpolaron renormalization of the Bloch integral, be

$$E_{\mathbf{k}} = \frac{A(S-1)}{2} - \frac{2S}{2S+1} z |B| \gamma_{\mathbf{k}}. \quad (4.1.1)$$

The analysis of the interaction of the spinpolaron with magnons is carried out in the limiting case of large spins by expanding the Hamiltonians (3.5.18) in the small parameter $(2S)^{-1}$. The results in the limiting case are practically independent of the sign of the c - l exchange integral A . To be definite, we shall consider the case $A > 0$. Following Fourier-transformation of the spinpolaron and the magnon operators of the type (1.1.3), the Hamiltonian (3.5.18a) in the momentum representation in the first approximation in $(2S)^{-1}$ assumes the form (the free magnon Hamiltonian (2.4.4) in the nearest-neighbour approximation has been added to it):

$$H = -\frac{AS}{2} \sum \alpha_{\mathbf{k}}^* \alpha_{\mathbf{k}} - zB \sum \gamma_{\mathbf{k}} \alpha_{\mathbf{k}}^* \alpha_{\mathbf{k}} - \sum \omega_{\mathbf{q}} b_{\mathbf{q}}^* b_{\mathbf{q}} + \frac{zB}{4SN} \sum (\gamma_{\mathbf{k}} + \gamma_{\mathbf{k}'} - 2\gamma_{\mathbf{q}+\mathbf{k}}) b_{\mathbf{q}}^* b_{\mathbf{q}'} \alpha_{\mathbf{k}}^* \alpha_{\mathbf{k}'} \mathcal{L}(\mathbf{q} + \mathbf{k}, \mathbf{q}' + \mathbf{k}'). \quad (4.1.2)$$

The symbol $\mathcal{L}(\mathbf{q}, \mathbf{k})$ expresses the quasi-momentum conservation law.

To obtain a correction to the spinpolaron energy of the first order in $(2S)^{-1}$, it suffices to take the diagonal part of the last term in expression (4.1.2) averaged over the magnons. In the first order in $(2S)^{-1}$ the destruction of ferromagnetic ordering does not change

the character of the dispersion law, resulting only in the renormalization of the Bloch integral

$$\begin{aligned}\tilde{E}_{\mathbf{k}} &= -\frac{AS}{2} + z\tilde{B}\gamma_{\mathbf{k}}, \\ \tilde{B} &= B \left\{ 1 - \frac{1}{2SN} \sum (1 - \gamma_{\mathbf{q}}) m_{\mathbf{q}} \right\}, \quad m_{\mathbf{q}} = \langle b_{\mathbf{q}}^* b_{\mathbf{q}} \rangle.\end{aligned}\quad (4.1.3)$$

It follows from expressions (4.1.3) and (2.4.6) that, indeed, the difference $(\tilde{B} - B)$ is proportional to $T^{3/2}$ at $T \ll \frac{1}{2}$ and to T at $\frac{1}{2} < T \ll \frac{1}{4}S$.

Now we shall analyze the temperature dependence of the charge carrier spectrum at higher temperatures, in the PM region starting from the vicinity of the Curie point T_c . In this region it is generally impossible to diagonalize the spinpolaron Hamiltonian (3.5.3) even approximately, and for this reason a very useful method of analysis is the method of moments, which does not require previous diagonalization of the Hamiltonian [72]. The latter are defined by expressions

$$\mathcal{M}_n = \frac{1}{N} \langle \text{Sp } H^n \rangle, \quad (4.1.4)$$

where $\langle \dots \rangle$ symbolizes averaging over the temperature.

Only even moments about the band centre will be seen from the structure of the Hamiltonian (3.5.3) to be nonzero, i.e. the energy band will be seen to be symmetrical about its centre. We obtain immediately from (3.5.3) and (4.1.4) for the square of relative dispersion

$$\mathcal{M}_2 = 6B_{\text{eff}}^2, \quad B_{\text{eff}}^2 = \frac{B^2}{2} \left[1 + \frac{\langle \mathbf{S}_0 \cdot \mathbf{S}_1 \rangle}{S^2} \right] \quad (4.1.5)$$

(the lattice is presumed to be a simple cubic one).

Calculating the fourth moment with account taken of the symmetry of the system, we obtain

$$\begin{aligned}\mathcal{M}_4 &= B^4 \left\{ \frac{39}{2} + 51 \frac{\langle \mathbf{S}_0 \cdot \mathbf{S}_1 \rangle}{S^2} + 3 \frac{\langle (\mathbf{S}_0 \cdot \mathbf{S}_1) (\mathbf{S}_1 \cdot \mathbf{S}_4) \rangle}{S^4} \right. \\ &\quad + 6 \frac{\langle (\mathbf{S}_1 \cdot \mathbf{S}_2) (\mathbf{S}_0 \cdot \mathbf{S}_3) \rangle}{S^4} + 12 \frac{\langle (\mathbf{S}_0 \cdot \mathbf{S}_1) (\mathbf{S}_0 \cdot \mathbf{S}_3) \rangle}{S^4} \\ &\quad \left. - 3 \frac{\langle (\mathbf{S}_1 \cdot \mathbf{S}_3) (\mathbf{S}_0 \cdot \mathbf{S}_2) \rangle}{S^4} + \frac{3}{2} \frac{\langle (\mathbf{S}_0 \cdot \mathbf{S}_1)^2 \rangle}{S^4} \right\}, \quad (4.1.6)\end{aligned}$$

where the following abbreviations of atomic coordinates have been introduced: $0 \equiv (0, 0, 0)$; $1 \equiv (1, 0, 0)$; $2 \equiv (1, 1, 0)$; $3 \equiv (0, 1, 0)$; $4 \equiv (2, 0, 0)$.

One may infer how the conduction band changes its form with the temperature from the ratio $r = \mathcal{M}_4^{1/4} / \mathcal{M}_2^{1/2}$. Calculations in the vicinity of the Curie point are carried out using the approximate equality

$\langle \mathbf{S}_0 \cdot \mathbf{S}_1 \rangle / S^2 = 1/3$ [241], other correlation functions except $\langle (\mathbf{S}_0 \cdot \mathbf{S}_1)^2 \rangle$ being presumed zeros. At $T \rightarrow \infty$ all the correlation functions are presumed zeros. At $T = 0$ all the correlation functions are obviously unities. For the above ratio we obtain from (4.1.5, 6).

$$\text{at } T = 0 \quad r_0 = 1.25;$$

$$\text{at } T = T_c \quad r_c = 1.23;$$

$$\text{at } T \gg T_c \quad r_\infty = 1.23.$$

The ratio r will be seen from the above estimates to change little with the temperature. This suggests that the density of states $g_0(E)$ obtained for a cosine dispersion law with the Bloch integral B_{eff} (4.1.5) may be close to the true density of states $g(E)$. In this case, as in the spin-wave region, the position of the bottom of the conduction band with respect to its centre will be given by the quantity $(-6 | B_{\text{eff}} |)$. Taking account of the value of the binary correlation function in the vicinity of T_c , we obtain that the temperature-induced shift of the conduction band bottom in the entire PM region constitutes 60% of that in the entire FM region.

It is worth pointing out that the problem of an electron in a narrow-band ferromagnetic system for $A < 0$ has been previously considered in [79], but because the c - l exchange has not been taken into account correctly, the results obtained have been erroneous: the c - l energy shift is less than $A(S - 1)/2$, and the carrier bandwidth at $T = 0$ is exponentially small, same as for a small polaron (1.3.3). Hence, the ground-state energy obtained in [79] exceeds (4.1.1), and this proves [79] to be in error. The authors of [620], using the coherent potential approximation, obtained that for $A < 0$ the carrier band width at $T \rightarrow \infty$ is $\sqrt{S+1}/\sqrt{2S+1}$ times less than $2z | B |$, which for $S \gg 1$ coincides with the result presented above.

4.2. ENERGY SPECTRUM OF CHARGE CARRIERS IN WIDE-BAND SEMICONDUCTORS IN THE SPIN-WAVE APPROXIMATION

Normal Intraband Exchange. Wide-conduction-band semiconductors ($W \gg AS$) include europium chalcogenides in which, according to Sec. 4.6, $AS \sim 0.5$ eV, $W \sim 5$ eV. This case appears at first glance to be a simpler problem than one considered in Sec. 4.1. Were we to use the perturbation theory, we would obtain in the first order for the electron energy the expression

$$E_{\mathbf{k}\sigma} = E_{\mathbf{k}} - A\mathfrak{M}\sigma, \quad (4.2.1)$$

where \mathfrak{M} is the mean projection of the atomic spin on the total magnetic moment of the system. Hence, up to the Curie point the electron spectrum should consist of two spin subbands displaced with

respect to each other by AM (Zeeman splitting in the mean field of the crystal). Actually, however, the situation turns out to be much more complicated: as has already been stated in Secs. 3.2, 3.3, the electron energy is nonanalytic in c - l exchange, i.e. it cannot be expanded in a series in ASW . In what manner the nonanalyticity manifests itself depends on the temperature.

Primarily we ought to discuss the interaction of the carriers with magnons in the spin-wave region. Same as in the case of narrow bands (Sec. 4.1), the electron spin takes part in the oscillations of the total moment of the system even though it is not so strongly coupled with the spin of the atom, which it occupies at the moment. By definition, a magnon is an elementary excitation that reduces the total spin projection by unity. The total spin projection is a conservative quantity (the c - l model Hamiltonian (3.1.1, 2) contains no terms capable of changing it). Accordingly, the Hamiltonian of the system should also conserve the total number of magnons, i.e. it should be quadratic in their operators b^* , b . Specifically, the electron magnon interaction Hamiltonian, just as (4.1.2), should have an a^*ab^*b structure.

Arguments presented in the preceding section concerning the energy of carrier interaction with extremely long-wave magnons tending to zero, being based only on the properties of symmetry, remain valid in this case as well. Accordingly, we may expect the conduction-band bottom to be shifted with the temperature at first in proportion to $T^{5/2}$ and finally, if the spins are large enough ($2S \gg 1$) in proportion to T . We may moreover insist that, contrary to (4.2.1), the temperature-induced shift at low temperatures is practically independent of the c - l exchange integral. Indeed, a spin wave corresponds to such a state of the crystal when the atomic spins form a periodic structure. In this sense the helicoidal ordering considered in Sec. 3.2 can be interpreted as a static spin wave. As discussed in the same section, for small wave vectors q of a periodic perturbation the electrons move so that their spins follow the direction of the local magnetic moment. This guarantees maximum gain in the c - l exchange energy. On account of this the increase in the electron energy due to the appearance of a spin wave with the wave vector q turns out to be proportional to Bq^2 and not to Aq^2 (see (3.2.10)).

Hence, for small q 's the electron behaves like a spinpolaron discussed in the preceding section. Moreover, it will be demonstrated below that in the wide-band case considered here the carrier spectrum will be the same as in the narrow-band case. However, the difference between a spinpolaron for $W \gg AS$ and one for $W \ll AS$ is that the former dissociates at some temperature T_0 when the short-wave magnons begin to play the predominant part, and the electron spin is no longer able to follow the rapid changes of the local magnetic moment in space. At $T > T_0$ the electron spin

may be presumed to retain its orientation in space approximately, i.e. expression (4.2.1) may be presumed to be valid for its energy.

However, even at $T > T_0$ the electron spin falls in with long-wave magnetization fluctuations. This results in appreciable corrections to formula (4.2.1) greatly exceeding those that would result from the perturbation theory in AS [89, 90]. Because of such corrections, the downward shift of the conduction band owing to the c - l exchange (" c - l shift") remains rather large even as T_c is approached.

In the spin-wave approximation in the main approximation in 1.2S, after Holstein-Primakoff relations (2.4.1) have been substituted into the c - l model Hamiltonian (3.1.1. 2), the latter assumes the form:

$$\begin{aligned} H &= H_0 + H_1 + H_2, \\ H_0 &= \sum E_{\mathbf{k}\sigma} a_{\mathbf{k}\sigma}^* a_{\mathbf{k}\sigma} + \sum \omega_{\mathbf{p}} b_{\mathbf{p}}^* b_{\mathbf{p}}, \\ H_1 &= A \sqrt{\frac{S}{2N}} \sum [a_{\mathbf{k}\uparrow}^* a_{\mathbf{k}+\mathbf{p}\downarrow} b_{\mathbf{p}}^* + a_{\mathbf{k}\downarrow}^* a_{\mathbf{k}-\mathbf{p}\uparrow} b_{\mathbf{p}}], \\ H_2 &= \frac{A}{N} \sum \sigma a_{\mathbf{k}\sigma}^* a_{\mathbf{k}'\sigma} b_{\mathbf{q}}^* b_{\mathbf{q}'} \mathcal{D}(\mathbf{q} + \mathbf{k}, \mathbf{q}' + \mathbf{k}'), \\ E_{\mathbf{k}\sigma} &= E_{\mathbf{k}} - AS\delta \end{aligned} \quad (4.2.2)$$

(we make use of the momentum representation).

The introduction of "true" magnons instead of l -spin-deviation operators $b_{\mathbf{q}}^*, b_{\mathbf{q}}$ (" l -magnons") is achieved by subjecting the Hamiltonian (4.2.2) to a canonical transformation of the type of (1.4.2-4), which eliminates from it all terms linear in l -magnons. Discarding very small terms $\sim \gamma S A$, we obtain for the operator \mathcal{H} :

$$\mathcal{H} = A \sqrt{\frac{S}{2N}} \sum \left[\frac{a_{\mathbf{k}\uparrow}^* a_{\mathbf{k}+\mathbf{q}\downarrow} b_{\mathbf{q}}^*}{E_{\mathbf{k}\uparrow} - E_{\mathbf{k}+\mathbf{q}\downarrow}} + \frac{a_{\mathbf{k}\downarrow}^* a_{\mathbf{k}-\mathbf{q}\uparrow} b_{\mathbf{q}}}{E_{\mathbf{k}\downarrow} - E_{\mathbf{k}-\mathbf{q}\uparrow}} \right]. \quad (4.2.3)$$

The transformed Hamiltonian is given by the expression

$$\begin{aligned} \tilde{H} &= H_0 + \sum \{C_{\mathbf{k}\mathbf{q}\mathbf{r}}^{\uparrow} a_{\mathbf{k}\uparrow}^* a_{\mathbf{k}-\mathbf{r}\uparrow} - C_{\mathbf{k}\mathbf{q}\mathbf{r}}^{\downarrow} a_{\mathbf{k}\downarrow}^* a_{\mathbf{k}-\mathbf{r}\downarrow}\} b_{\mathbf{q}}^* b_{\mathbf{q}+\mathbf{r}} + \sum \Delta E_{\mathbf{k}} a_{\mathbf{k}}^* a_{\mathbf{k}}, \\ C_{\mathbf{k}\mathbf{q}\mathbf{r}}^{\uparrow} &= C(\mathbf{k} + \mathbf{q}, \mathbf{k}) + C(\mathbf{k} + \mathbf{q}, \mathbf{k} - \mathbf{r}), \\ C_{\mathbf{k}\mathbf{q}\mathbf{r}}^{\downarrow} &= C(\mathbf{k} - \mathbf{r}, \mathbf{k} - \mathbf{q} - \mathbf{r}) + C(\mathbf{k}, \mathbf{k} - \mathbf{q} - \mathbf{r}), \\ C(\mathbf{k}, \mathbf{p}) &= \frac{A}{4N} \left[\frac{E_{\mathbf{k}} - E_{\mathbf{p}}}{AS + E_{\mathbf{k}} - E_{\mathbf{p}}} \right], \\ \Delta E_{\mathbf{k}} &= \frac{A^2 S}{2N} \sum_{\mathbf{q}} \frac{1}{E_{\mathbf{k}\downarrow} - E_{\mathbf{k}+\mathbf{q}\uparrow}}. \end{aligned} \quad (4.2.4)$$

In accordance with what has been said in Sec. 1.4 the use of the canonical transformation (1.4.2-4) is justified only for such states

for which the energy denominators in the expression for $C_{\mathbf{k}q\mathbf{r}}$ (4.2.4) do not vanish. Otherwise the energy conservation law will not prohibit electron transitions involving the emission or the absorption of an l -magnon. This brings about the appearance of electron and magnon damping that cannot be accounted for with the aid of the canonical transformation method. It follows from the form of the Hamiltonian (4.2.4) that, for example, for $A > 0$ electrons with the \uparrow spin projection will have no damping due to the one-magnon scattering, if their momentum k is smaller than $q_0 \equiv \sqrt{2m^*AS}$. The physical meaning of this result is quite simple: because of Zeeman splitting of the electron spectrum in the mean field of the FMS, the states with a \uparrow spin projection lie by the amount AS below those with a \downarrow spin projection. The creation or the annihilation of an l -magnon reverses the projection of the electron spin. But if the energy of the electron with a spin projection \uparrow is lower than the bottom of the subband with a \downarrow spin projection, the energy conservation law prohibits the reversal of its spin from \uparrow to \downarrow (recall that the energy of a magnon is several orders of magnitude less than AS , and for this reason is neglected in the expression for $C_{\mathbf{k}q\mathbf{r}}$). Such states near the conduction-band bottom are of essential importance for MS, and this is just why the Hamiltonian (4.2.4) is applicable to such materials.

Since the energy denominators in expression (4.2.4) contain AS , the ratio AS/W is not an expansion parameter in the perturbation theory developed above. The true expansion parameter is the inverse spin $1/S$. Indeed, whereas for $q \gg q_0$ the order of $C_{\mathbf{k}q\mathbf{r}}$ with respect to the electron kinetic energy $\sim W$ is $1/S$ (AS/W), for $q \rightarrow 0$ the small parameter AS/W vanishes from it (it is of the order of q^2a^2/S). The existence of the small parameter $1/S$ makes it possible to describe correctly effects nonanalytic in AS/W^* .

Let us discuss the meaning of the canonical transformation employed above. The transformed l -magnon creation operator $e^{\mathcal{U}}b_{\mathbf{q}}^*e^{-\mathcal{U}} \simeq b_{\mathbf{q}}^* + [\mathcal{U}, b_{\mathbf{q}}^*]$, according to (4.2.3), is distinguished from the new magnon operator $b_{\mathbf{q}}^*$ by the presence of a term with an $a_{\mathbf{k}\downarrow}^*a_{\mathbf{k}-\mathbf{q}\uparrow}$ structure describing the decrease in the spin projections of conduction electrons. Hence, the new operator $b_{\mathbf{q}}^*$ in (4.2.4), indeed, describes the contribution of conduction electrons to spin waves. Since the Hamiltonian (4.2.4) conserves the number of magnons, the magnon operators in it correspond to oscillations of the total magnetic moment of the system. On the other hand, new electron operators $a_{\mathbf{k}\uparrow}^*$, $a_{\mathbf{k}\downarrow}^*$ being expressed in terms of the old contain admixtures $a_{\mathbf{k}+\mathbf{q}\downarrow}^*b_{\mathbf{q}}$ and $a_{\mathbf{k}-\mathbf{q}\uparrow}^*b_{\mathbf{q}}^*$, respectively, i.e. do not conserve the electron spin projection. In effect, they are no longer electron, but spinpola-

* For $W \ll AS$ the Hamiltonian (4.2.4), (1.1.1) in the first order in W/AS coincides with (4.1.2).

ron operators, in the same way as in ionic crystals similarly transformed operators correspond to weak-binding polarons (Sec. 1.3).

The last term in (4.2.4) describes the decrease in the electron energy occasioned by the spinpolaron effect, i.e. by the creation and annihilation of virtual l -magnons in the result of their interaction with the conduction electron. Same as for $W \ll AS$, it takes place only for electrons with spins antiparallel to the crystal moment, i.e. for $A < 0$. For $A > 0$ the electron spin is parallel to the crystal moment, i.e. at $T = 0$ the electrons occupy eigenstates of the system corresponding to its minimum energy. Accordingly processes involving virtual magnons are impossible in this case. In the case considered here the renormalization of the energy of electrons having a \downarrow spin projection is of the order of $(1/S)(AS/W)^2$ and will accordingly be neglected.

The temperature-dependent charge-carrier spectrum in the first order in $1/S$ is, according to (4.2.4), given by the expression

$$\tilde{E}_{\mathbf{k}\uparrow} = E_{\mathbf{k}\uparrow} + \sum_{\mathbf{q}} m_{\mathbf{q}} C_{\mathbf{q}\mathbf{q}0}. \quad (4.2.5)$$

Taking into account formula (1.1.1), we obtain that, if the thermal momentum of the magnon is small as compared with q_0 and q_0^2/k , expression (4.2.5) will coincide with (4.1.3). Hence at $T < T_0 = = q_0^2/2M$ the electron spin indeed follows adiabatically the direction of the local moment ($q_0 = \sqrt{2m^*AS}$, M being the magnon effective mass (2.4.5)).

At $T \gg T_0$, when the typical magnon momenta are great as compared with q_0 , and the spinpolaron dissociates, expression (4.2.5) for $k \ll q_0$ is conveniently represented in two forms

$$\tilde{E}_{\mathbf{k}\uparrow} = E_{\mathbf{k}\uparrow} + \frac{A}{2} m(T) - \Delta E \equiv E_{\mathbf{k}} - \frac{A\mathfrak{M}}{2} - \Delta E, \quad (4.2.6)$$

$$m(T) = \frac{1}{N} \sum_{\mathbf{q}} m_{\mathbf{q}},$$

$$\Delta E = \frac{Aq_0^2}{2N} \sum_{\mathbf{q}} \frac{m_{\mathbf{q}}}{q_0^2 + 6(1 - \gamma_{\mathbf{q}})}. \quad (4.2.7)$$

According to (4.2.6), ΔE is the deviation of the electron energy from one given by formula (4.2.1). One may easily see that its order of magnitude with respect to the temperature-induced shift $(A/2)m(T)$ obtained from (4.2.1) is $\sqrt{AS/W}$. Indeed, the magnon distribution function $m_{\mathbf{q}}$ (2.4.6), if (2.4.5) is taken into account, for small q 's diverges as q^2 . Hence, the most important range of momenta in expression (4.2.7) is one with $q \leq q_0$, and the order of magnitude of ΔE at $T > T_c/S$ is that of $Am(T)q_0a$. In actual conditions AS/W

may be rather small (AS in compounds of rare-earth elements is ~ 0.5 eV, and $W \sim 5$ eV). However, the magnitude of $\sqrt{AS/W}$ is of the order of unity, i.e. the correction ΔE is quite important. Still, even if ΔE is taken into account, the temperature-induced energy shift in this temperature range remains proportional to variations of magnetization $m(T)$.

As T_c is approached \mathfrak{M} diminishes, and ΔE grows. Hence it will be obvious that, although the magnetization \mathfrak{M} vanishes at the critical point, the c - l shift in it remains sufficiently large. This is associated with the cut-off of electron interaction with long-wave magnons ($C_{kq0} \sim q^2$ in (4.2.5)) that can be interpreted as the conformity of the electron spin direction to long-wave magnetization fluctuations.

Abnormally Small Intraband Exchange. In case of the valence band being of a p -type, the c - l exchange in the conduction band is usually much more intense than the interband c - l exchange that is responsible for virtual transitions of the electrons from the valence to the conduction band and then the c - l exchange in the valence band. The reason for this is that the conduction electrons move mainly over magnetic cations, with the holes moving over nonmagnetic anions. Accordingly, the downward shift of the conduction band bottom as the temperature drops is tantamount to a similar decrease in the width of the band-gap E_g ("red shift" of the optical absorption edge). However there is a possibility that for some reason or other the c - l exchange in the conduction band will be small, and the dominant role will be played by the interband c - l exchange (e.g. if the conduction band is the result of hybridization of states with opposite signs of the integral of exchange with l -electrons). In such conditions the band-gap E_g can become wider with falling temperature, i.e. a "blue shift" of the absorption edge may be observable [384].

A qualitative explanation of this effect is as follows. The interaction between two energy terms is known to result in their mutual repulsion. Same as the intraband exchange, the interband c - l exchange is intensified when a magnetic order is established. This also intensifies the repulsion between the valence and the conduction band caused by it, thus widening the gap between them. Thus the interband exchange operates in the direction opposite to that of the intraband exchange.

In the main approximation in DW we need only take account of the terms with $q = 0$ in the Hamiltonian (3.4.1). Such a Hamiltonian is diagonalized by a transformation of the type (2.6.6), which mixes the electron creation and the hole annihilation operators. In the result we obtain a formula, which is an analogue of (4.2.1):

$$\tilde{E}_{\mathbf{k}}^{\pm} = \frac{E_{\mathbf{k}} - K_{\mathbf{k}}}{2} \pm \frac{1}{2} \sqrt{(E_{\mathbf{k}} - K_{\mathbf{k}})^2 + D^2 \mathfrak{M}^2}. \quad (4.2.8)$$

The quantity $\tilde{E}_{\mathbf{k}}$ has the meaning of the renormalized energy of the conduction electron, $\tilde{E}_{\mathbf{k}}$ same as before, for an electron in the valence band (correspondingly, $(-\tilde{E}_{\mathbf{k}})$ is the renormalized hole energy).

According to (3.4.3), superexchange via the valence band electrons results in the FM ordering when the minima of the induction and the hole band occur at the same point in the \mathbf{k} -space. Hence, the gap E_g is equal to the minimum value of the difference $\tilde{E}_{\mathbf{k}}^+ - \tilde{E}_{\mathbf{k}}^-$. If we take this into account, we obtain from formula (4.2.8) that the temperature dependence of the band-gap is expressed by the law

$$E_g(T) = \Delta \sqrt{1 + \frac{D^2 \gamma^2}{\Delta^2}}, \quad \Delta \equiv E_g(\infty). \quad (4.2.9)$$

It will be seen from formula (4.2.9) that the shift can be appreciable only for $|D|S \sim \Delta$. For the values of these parameters in the range 0.5-1 eV, it can be of the order of 0.1 eV. For a wide band-gap ($|D|S \ll \Delta$) the inequality $|D| > |A|$ is by no means a guarantee that the absorption edge shift will necessarily be blue.

It is interesting to note that the interband exchange, in contrast to the intraband one, does not cause the Zeeman splitting of the electron bands.

4.3. CHARGE-CARRIER-ENERGY SPECTRUM IN WIDE-CONDUCTION-BAND SEMICONDUCTORS IN THE VICINITY OF THE CURIE POINT AND IN THE PARAMAGNETIC REGION

Variational Procedure. It will be seen already from the results of the preceding section that the relative contribution of long-wave fluctuations of the magnetic moment to the electron energy rises as the Curie point is approached from the low-temperature side. After T_c has been passed the spontaneous magnetization of the crystal as a whole vanishes, but sufficiently large areas still retain a non-zero local magnetization (the correlation length becomes infinite at T_c). Since the direction of a fluctuating local moment slowly varies in space, the electron spin has ample time to fall in, just as it falls in with the local moment in a helicoid (Sec. 3.2). Accordingly, we may expect a substantial Zeeman splitting to take place even at $T \neq T_c$: two subbands correspond to a parallel and an antiparallel orientation of the electron spin with respect to the direction of the local magnetic moment.

Of course, in contrast to the helicoid, the local moment in the vicinity of T_c is less than S (per atom). Because of that the c - l shift of the electron energy in the vicinity of T_c turns out to be less than its value at $T = 0$ (i.e. $AS/2$). However, it should be substantially

greater than $A^2 S^2 / W$ obtained in [87, 95] from the perturbation theory. The c - l shift may be expected to be of the order of $AS (AS/W)^x$. The exponent x should not exceed $1/2$, since in the vicinity of T_c the part played by the long-wave fluctuations is even greater than in the spin-wave region, where x in the expression (4.2.7) for their contribution to the c - l exchange is equal to $1/2$. It will be demonstrated below that actually x is equal to $1/3$ in the vicinity of T_c [93, 94]. Even if the inequality $AS/W \ll 1$ were satisfied, the quantity $(AS/W)^{1/3}$ may be of the order of unity, e.g. for $W = 5$ eV, $AS = 0.5$ eV $(AS/W)^{1/3}$ is equal only to $1/2$. Owing to this the c - l shift in the vicinity of the Curie point turns out to be of the same order of magnitude as at $T = 0$.

At $T \gg T_c$ the correlation length is small, and because of that the perturbation theory in AS/W is applicable, i.e. the c - l shift turns out to be $\sim A^2 S^2 / W$. Hence, a strong upward shift of the conduction band bottom with rising temperature should not cease after the long-range ferromagnetic order has been destroyed. It continues also after T_c has been attained until the short-range order is destroyed.

It would be reasonable to start the analysis of the electron spectrum with the case of temperatures appreciably exceeding T_c . This will enable us to shed light on the conditions of applicability of the perturbation theory in the c - l exchange in the paramagnetic region. By using standard perturbation theory methods of the type used to obtain formulae (1.4.6-9), we obtain the following expression for the renormalized electron energy in the Born approximation:

$$\begin{aligned} \tilde{E}_{\mathbf{k}} &= E_{\mathbf{k}} + \mathcal{M}_{\mathbf{k}}, \\ \mathcal{M}_{\mathbf{k}} &= \frac{A^2}{4N} \sum_{\mathbf{q}} \frac{\langle \mathbf{S}_{\mathbf{q}} \cdot \mathbf{S}_{-\mathbf{q}} \rangle}{E_{\mathbf{k}} - E_{\mathbf{k}+\mathbf{q}} - i\eta} \quad (\eta \rightarrow 0). \end{aligned} \quad (4.3.1)$$

In the region where the mean field theory is applicable the asymptotic behaviour of the binary spin correlation function is described by the Ornstein-Zernicke formula (2.5.7). According to (2.5.15, 16), this formula may be taken as valid much nearer to T_c , but with a modified temperature dependence of the correlation length $\kappa^{-1} \sim (T - T_c)^{-2/3}$. From formulae (4.3.1) and (2.5.7) we obtain

$$\text{Im } \mathcal{M}_{\mathbf{k}} = \frac{A^2 S(S+1) m^* a^3}{32\pi v_1^2 k} \ln \left(1 + \frac{4k^2}{\kappa^2} \right). \quad (4.3.2)$$

For the perturbation theory to be applicable, the inequality must hold:

$$\frac{m^* \text{Im } \mathcal{M}_{\mathbf{k}}}{k^2} \ll 1. \quad (4.3.3)$$

The smallness of AS/W by itself will be seen from formulae (4.3.2, 3) to be insufficient for the condition (4.3.3) to be satisfied, since the damping diverges logarithmically for $\kappa \rightarrow 0$. Because of that as T_c is approached, inequality (4.3.3) is reversed the earlier the smaller is k , e.g. for $AS/W \sim 0.1$, $W \sim 4$ eV, $E \sim 0.01$ eV this takes place at $T - T_c \sim 0.1 T_c$.

But even if the condition that the Born approximation corrections to the electron energy (4.3.2, 3) be small is satisfied, this does not guarantee that the corrections of higher orders in AS/W will be small, since their singularities in κ are more pronounced. For instance, the first post-Born correction to the damping (4.3.2) obtained with the aid of Wick's theorem for four-spin correlation functions turns out to be of the order of

$$\left(\frac{AS}{W}\right)^2 \frac{1}{(\kappa^2 - 4k^2) \kappa a^3} \quad (4.3.2a)$$

with respect to it (numerical multipliers have been omitted). For the same reason the results of perturbation theory in AS/W can be regarded as quite reliable only for $\kappa a \sim 1$, i.e. for $T \gg T_c$.

To find the spectrum of conduction electrons in the vicinity of the Curie point, use is made of the variational procedure. The choice of the trial function is based on the following considerations. The electron energy is determined by the competition of two factors: of c - l exchange and translational energy. The latter is understood to mean the difference between the energy of an electron moving about the crystal and that of an electron localized on one of its atoms (a quantity of the order of magnitude of the bandwidth W (see Sec. 1.1)). Obviously, the maximum gain in the c - l exchange equal to $AS/2$ can be obtained, if the electron spin on every atom will be parallel to the atomic spin ($A > 0$). On the other hand, according to (3.5.3), the maximum gain in the translational energy $z|B| = W/2$ is obtained, if the electron retains the direction of its spin as it goes over from atom to atom. Near the Curie point the angles $\theta_{\mathbf{g}, \mathbf{g}+\Delta}$ between the spins of neighbouring atoms cannot be presumed small. If we take into account the inequality $W \gg AS$, it follows from (3.5.3), that the electron cannot go over from atom to atom so that its spin on every atom would be parallel to the atomic spin, for this would drastically cut the gain in the translational energy, making it equal to $(W/2) \cos \theta_{\mathbf{g}, \mathbf{g}+\Delta}$.

It will be evident from the above that the only thing the electron can do is to change the direction of its spin a little when going over from atom to atom. This condition can be met, if the electron spin on every atom is presumed to point in the direction of the total magnetic moment $\mathbf{M}_{\mathbf{g}}$ of some region with the given atom \mathbf{g} as its centre (this very direction is chosen as the $Z_{\mathbf{g}}$ -axis). If the radius of such a region R is large compared with the lattice parameter, the regions

corresponding to neighbouring atoms will overlap greatly, and because of that their moments \mathbf{M}_g and $\mathbf{M}_{g+\Delta}$ will differ little both in magnitude and in direction. This difference will obviously be the smaller the greater the radius R , so that the gain in translation energy increases with the growth in R .

As to the gain in the c - l exchange energy, the latter on the contrary diminishes as R grows. Indeed, the spin \mathbf{S}_g points in an arbitrary direction with respect to \mathbf{M}_g , but owing to correlations between the spins its mean projection on \mathbf{M}_g is positive. With the growth in R it should diminish on account of the correlations of \mathbf{S}_g with the atomic spins in the region becoming weaker with growing distance between the atoms. For its part, the gain in the c - l exchange energy is proportional to the projection of \mathbf{S}_g on \mathbf{M}_g , since the electron spin points in the direction of \mathbf{M}_g (A is presumed to be > 0).

Hence, R should play the part of a variational parameter. To avoid misunderstanding, we should like to emphasize that R generally need not necessarily be of the order of magnitude of the correlation length χ^{-1} . This is evident from the fact that even for $\chi^{-1} \rightarrow \infty$ the correlation functions diminish with the distance as $1/r$ (r is the distance between the atoms), and for this reason in the approximation $R \sim \chi^{-1}$ the gain in the c - l energy vanishes. As will be seen below, for $\chi^{-1} \rightarrow \infty$ the optimum value of R depends only on the ratio AS/W .

The Hamiltonian of the system for classically large spins ($2S \gg 1$) can conveniently be rewritten by introducing a separate frame of reference for every atom in which however the Z_g -axis would coincide not with the spin \mathbf{S}_g , but with the moment \mathbf{M}_g . Accordingly, the Hamiltonian should also contain a term off-diagonal in the c - l exchange, its terms corresponding to the translational electron energy (i.e. $\sim B$) retaining the same structure as in the Hamiltonian (3.5.3), since their form is independent of the orientation of the Z_g -axis with respect to the spin \mathbf{S}_g . Taking into account that the angles between the neighbouring regions $\theta_{g, g+\Delta}$ are small, we may write the Hamiltonian in the form

$$H = \sum_{\sigma} H_{\sigma} + H' + H_{\uparrow\downarrow},$$

$$H_{\sigma} = -A \sum_{\sigma} \sigma S_g^z a_{g\sigma}^* a_{g\sigma} + B \sum_{\sigma} \cos \frac{\theta_{g, g+\Delta}}{2} a_{g\sigma}^* a_{g-\Delta\sigma}, \quad (4.3.4)$$

$$H' = -\frac{A}{2} \sum (S_g^+ a_{g\downarrow}^* a_{g\uparrow} + S_g^- a_{g\uparrow}^* a_{g\downarrow}).$$

Here $a_{g\sigma}^*$, $a_{g\sigma}$ are the creation and annihilation operators of the conduction electron located on the g -atom having the spin projection σ on the Z_g -axis. The projections of the spins \mathbf{S}_g are written down in the same frame of reference. Next, θ_g and φ_g are the polar angle and

the longitude of a vector pointing along the Z_g -axis in the laboratory frame of reference. $\theta_{g, g+\Delta}$ is the angle between the Z_g - and the $Z_{g+\Delta}$ -axes. In writing down the Hamiltonian (4.3.4) in addition to expanding formulae (3.5.3) for H_+ and H_- in small differences ($\varphi_g - \varphi_{g+\Delta}$) and $(\theta_g - \theta_{g+\Delta})$ we have subjected the electron operators to a canonical transformation

$$a_{g\sigma}^* \exp\{i\sigma\varphi_g \cos \theta_g\} \rightarrow a_{g\sigma}^*, \quad (4.3.5)$$

so that the Hamiltonian (4.3.4) is accurate up to terms of the order of squares of these differences, inclusively.

In accordance with the condition that the electron spin follows the direction of the local moment adiabatically, the trial wave function for the conduction electron is chosen in the form of a plane wave with a fluctuating spin direction

$$\psi(\mathbf{k}, \sigma) = \frac{1}{V N} \sum_{\mathbf{g}} e^{i\mathbf{k} \cdot \mathbf{g}} a_{g\sigma}^* |0\rangle \quad (a_{g\sigma} |0\rangle \equiv 0). \quad (4.3.6)$$

The wave function (4.3.6) is an eigenfunction of the Hamiltonian

$$H_0^e = B \sum_{\mathbf{g}, \Delta} a_{g\sigma}^* a_{g+\Delta\sigma}, \quad (4.3.7)$$

obtained from H_e in the zeroth approximation in A and $\theta_{g, g+\Delta}$. Estimates of accuracy of approximation (4.3.6) will be presented below.

Making use of formulae (4.3.4, 6), we obtain the following expression for the electron energy:

$$\begin{aligned} \tilde{E}_{k\sigma} &= zB\gamma_{\mathbf{k}} \left(1 - \frac{\overline{P_{g, g+\Delta}}}{4} \right) - A\sigma \frac{\overline{S_{\mathbf{g}} \cdot \mathbf{M}_{\mathbf{g}}}}{M_{\mathbf{g}}}, \\ P_{g, g+\Delta} &= 1 - \frac{\mathbf{M}_{\mathbf{g}} \cdot \mathbf{M}_{\mathbf{g}+\Delta}}{M_{\mathbf{g}} M_{\mathbf{g}+\Delta}} \simeq \frac{1}{2} \left[1 - \frac{(\mathbf{M}_{\mathbf{g}} \cdot \mathbf{M}_{\mathbf{g}+\Delta})^2}{M_{\mathbf{g}}^2 M_{\mathbf{g}+\Delta}^2} \right]. \end{aligned} \quad (4.3.8)$$

The line above a symbol means averaging over all the atoms, this being the equivalent of calculating thermodynamic mean values of spin correlation functions. The radius of the region R should be determined from the condition that the energy of the conduction electron at the band bottom be minimum (for $A > 0$, $B < 0$ the corresponding values for the band bottom are $k \rightarrow 0$, $\sigma \rightarrow 1/2$).

In the method being discussed it is of principal importance that the mean values of spin correlation functions are calculated without taking account of the reciprocal effect on them of the conduction electron. Such an approach is quite natural when optical absorption spectra are calculated: according to the Franck-Condon principle, the

electron transitions from the valence to the conduction band take place with the coordinates of the slow subsystem with which the electron interacts, in this case the l -spin system (in the polaron theory, the ions [60]) remaining constant. The probability of a specific configuration of the slow subsystem is determined solely by the mutual interaction of l -spins, since such a configuration is established already before the electron has made its appearance.

In principle, large-scale magnetization fluctuations may trap the conduction electron. The greater the fluctuation the lower is the energy of the electron localized inside it. This causes the formation of the density-of-states tail below the conduction-band bottom, which should be termed the mobility edge to be more accurate. As the number of fluctuations rapidly decreases with rise in their magnitude, the tail falls off quickly inside the gap. The problem of the conduction-electron states bound to fluctuations will be discussed in more detail in Sec. 5.2.

The trial function (4.3.6) that describes delocalized states does not yield an absolute electron energy minimum, because the energy of states bound to fluctuations is lower than that of the delocalized. But the variational procedure is known to be applicable for excited states of a system, too, provided their trial wave function is orthogonal to the wave functions of lower-lying states. In this case this condition is met: function (4.3.6) is with asymptotic accuracy orthogonal to wave functions of localized states. The energies of delocalized states calculated with the aid of (4.3.6) turn out to be substantially lower than those obtained with other methods, and this is proof of the effectiveness of the above approach.

Energy Spectrum and Spontaneous Zeeman Splitting. To bring the calculation to its end, we must calculate the spin correlation functions in (4.3.8). First of all note that the average of a quotient in contrast to the average of a product, can, up to a good accuracy, be replaced by the ratio of average values, since high-amplitude fluctuations in the numerator are to a considerable degree compensated by similar fluctuations in the denominator. In that case the average values of spin operators in (4.3.8) will reduce to binary correlation functions, the condition $R \gg a$ enabling us to use only their long-wave asymptotic behaviour.

We shall confine ourselves to the discussion of temperatures so close to T_c that $\kappa R \ll 1$. In the zeroth order in κR the binary correlation function in the Ornstein-Zernicke approximation (2.5.7) is inversely proportional to the distance between the spins, its behaviour in the scaling theory being similar, if the small index η in (2.5.15) is discarded. The proportionality constant c should in both cases be of the order of aS ($S \rightarrow 1$), since on account of the exchange-interaction length being small the lattice parameter a is the only geometrical parameter of the system. Finally we obtain for the corre-

lation functions (4.3.8):

$$\begin{aligned} \langle \overline{\mathbf{S}_g \cdot \mathbf{M}_g} \rangle &= \langle \mathbf{S}_g \cdot \mathbf{M}_g \rangle \simeq \frac{c}{a^3} \int_0^R \frac{dr}{r} = \frac{3}{2} \frac{c\mathfrak{N}}{R}, \\ \overline{M^2} &\simeq \frac{c}{a^3} \int_0^R \frac{dr dr'}{|\mathbf{r} - \mathbf{r}'|} = \frac{6}{5} \frac{\mathfrak{N}^2 c}{R}, \\ \langle \overline{\mathbf{M}_0 \cdot \mathbf{M}_\Delta} \rangle &= \overline{M^2} - \frac{\mathfrak{N}^2 c a^2}{2R^2}, \quad \mathfrak{N} = \frac{4\pi}{3} \left(\frac{R}{a} \right)^3. \end{aligned} \quad (4.3.9)$$

Substituting formulae (4.3.9) into (4.3.8) and subsequently minimizing the energy with respect to R , we obtain the following expression for its optimum value:

$$R = \left[\frac{4|B|a^2}{A} \right]^{2/3} \left[\frac{2}{15c} \right]^{1/3}, \quad (4.3.10)$$

the expression for the electron spectrum being

$$\tilde{E}_{p\sigma} = 6B\gamma_p - \frac{A}{4} \sqrt{\frac{15c}{2R}} \left(2\sigma - \frac{\gamma_p}{4} \right). \quad (4.3.11)$$

Hence, the downward shift of the electron spectrum due to the c - l exchange E_{cl} (the second term in (4.3.11)) is, according to (4.3.10) and (4.3.11), of the order of AS (AS/W)^{1/3}. The same result has been obtained in [94] by summing graphs of all orders in AS of the single-electron Green's function corresponding to the conduction-band bottom (i.e. for $k = 0$). It is possible to carry out such summation up to a constant within the framework of the thermodynamic fluctuation theory. It is of essential importance that, whereas the c - l shift at $T > T_c$ in case of narrow bands is determined by short-range spin correlations, in case of wide bands it is determined chiefly by intermediate-range correlations ($R \sim a(W/AS)^{2/3}$).

The stability of the result obtained (4.3.11) with respect to the perturbation introduced by nonadiabatic terms of the Hamiltonian H' and H_1 in (4.3.4) can be checked by evaluating corrections due to them in the second order of the perturbation theory. The former turns out to be $\sim (AS/W)^{2/3}$, and the latter $\sim 1/z$ from the c - l exchange (4.3.11), the last result being the consequence of the fact that the quantities $\mu_{\mathbf{g}, \mathbf{g}+\Delta}$ (3.5.3, 4) are functions of the ratio of two small quantities $\varphi_{\mathbf{g}} - \varphi_{\mathbf{g}+\Delta}$ and $\theta_{\mathbf{g}} - \theta_{\mathbf{g}+\Delta}$ and because of that fluctuate perfectly at random [93]. Since there is Zeeman splitting, these terms in the Born approximation by themselves do not give rise to the damping of plane waves with a variable spin direction (4.3.6) for $\sigma = 1/2$.

Upper-bound estimates of the correction to the spectrum and of the damping due to the fluctuating portion $H_\sigma - H_\sigma^0$ of the Hamiltonian H_σ demonstrate that their order of magnitude does not exceed that of E_{cl} . Numerically, they should not exceed $0.3E_{cl}$. This is proof that the expression for the electron energy (4.3.11) is quite reasonable [93].

It would be interesting to note that the radius R (4.3.10) obtained from the condition of minimum energy (4.3.8) is almost equal to the value of R at which the damping of plane waves (4.3.6) vanishes for the spin orientation corresponding to the minimum energy. Hence, the condition that energy be minimum (4.3.8) simultaneously provides for a small damping as should be the case. The disappearance of the damping for $k \rightarrow 0$ is the outcome of the fact, that for $k \ll \kappa$ the electron feels the crystal as a homogeneous medium. The situation is quite similar in case of highly imperfect crystals when the electron wavelength is great as compared with characteristic dimensions of inhomogeneities of the medium [247].

Only short-wave magnetization fluctuations are of any importance in the temperature range $T \gg T_c$, and because of that the electron is no longer able to align its spin with the local moment. Accordingly, there will be no Zeeman splitting. To find the electron spectrum, we may use the Born approximation in ASW . Taking account of the disappearance of correlations between the l -spins at $T \rightarrow \infty$, we obtain from formula (4.3.1) [87]:

$$\tilde{E}_{k\sigma}(\infty) = E_k - \frac{A^2 S(S+1)}{4N} \sum_q \frac{1}{E_{k+q} - E_k - i\eta} \quad (\eta \rightarrow 0). \quad (4.3.12)$$

i.e. the shift in the electron energy owing to the c - l exchange is of the order of $A^2 S^2/W$. For a simple cosine dispersion law (1.1.1), the energy shift is equal to

$$\tilde{E}_{k\sigma}(\infty) - E_k \simeq -\frac{3A^2 S^2}{4W} \quad (T \rightarrow \infty). \quad (4.3.13)$$

(The contribution of the interaction with short-wave fluctuations to the c - l shift is of the order of $A^2 S^2/W$ near T_c as well. It is described by the term H' in the Hamiltonian (4.3.4).)

The result (4.3.11) obtained above that the energy shift at the Curie point is proportional to $A^{4,3}$ is not a specific feature of the Heisenberg exchange interaction. A similar result is obtained when the interaction between the magnetic moments is of the Ising type [380].

The validity of the $A^{4,3}$ -law is also substantiated by calculations employing graphical methods for a single-electron Green's function [380].

4.4. CHARGE CARRIER SCATTERING BY FLUCTUATIONS OF THE MAGNETIC MOMENT

Carrier Mobility Far from T_c . It would be expedient to start analyzing the carrier kinetics with the spin-wave region [70, 45, 142]. First of all, we would like to point out that the average spinpolaron velocity \mathbf{v}_k obeys the relationship $\mathbf{v}_k = \nabla_k \tilde{E}$. In the main approximation in 1/2S it can be easily checked by applying expression (4.2.5) for the energy and the canonical transformation (1.4.2), (4.2.3) for the velocity operator.

This circumstance enables the kinetics in the spin-wave region to be studied on the basis of the conventional Boltzmann equation for the charge carriers. The latter in the main approximation in (2S)⁻¹ is of the form

$$e(\mathcal{E} \cdot \mathbf{v}_k) \frac{\partial n_k}{\partial E} = 2\pi \sum \mathcal{M}_{kq|k'q'}^2 \times [f_{k'}(1+m_q)m_{q'} - f_k(1+m_{q'})m_q] \delta(E_k + \omega_q - E_{k'} - \omega_{q'}), \quad (4.4.1)$$

where n_k and f_k are the equilibrium and the nonequilibrium charge carrier distribution functions, m_q is the equilibrium magnon distribution function, and the matrix elements for the two-magnon carrier scattering $\mathcal{M}_{kq|k'q'}$ are obtained from the Hamiltonians (4.1.2) and (4.2.4). Here one has to keep in mind that the typical carrier momentum is small as compared to that of the magnon. The scattering of light electrons by heavy magnons may be presumed to be elastic. Indeed, at $T \ll \mathcal{Y}$ it follows from the energy and the momentum conservation laws that the energy transfer from the spinpolarons to the magnons is equal to

$$\Delta E = 4\mathcal{Y}S\mathbf{k} \cdot (\mathbf{q} + \mathbf{k}) a^2,$$

where \mathbf{k} and \mathbf{q} are the initial momenta of the spinpolaron and the magnon, respectively ($k \sim \sqrt{m^*T}$, $q \sim \sqrt{MT}$, $M^{-1} \sim \mathcal{Y}Sa^2$). Hence, ΔE turns out to be equal to $\sim \sqrt{\frac{m^*}{M}} T \ll T$. At $T > \mathcal{Y} = 6\mathcal{Y}S$ the scattering is elastic by definition. This enables the transport relaxation time (1.7.16) to be introduced. Keeping in mind that the scattering is isotropic, we obtain for it from (4.4.1), (4.1.2) and (4.2.4):

$$\tau_k^{-1} = \frac{9ka|B|}{2\pi\hbar S^2 N} \sum_q (1-\gamma_q)^2 m_q (1+m_q) = \frac{9ka|B|T^2 C_m}{2\pi\hbar (\mathcal{Y}S)^2} \quad (W \ll AS), \quad (4.4.2)$$

$$\tau_k^{-1} = \frac{ka^3 m^* A^2}{4\pi\hbar^3 N} \sum_q \frac{q^4}{(q_0^2 + q^2)^2} m_q (1+m_q) = \frac{2\pi n e^2 T \Gamma_0}{m^*} \quad (W \gg AS), \quad (4.4.3)$$

where $C_m(T)$ is the specific heat of magnons with the dispersion law (2.4.4, 4') for $\mathcal{H} = 0$. When writing out (4.4.2) we made use of the equality

$$m_q(1 + m_q) = \frac{T^2}{\omega_q} \frac{d}{dT} m_q. \quad (4.4.4)$$

Two points should be emphasized: (1) scattering by true magnons takes place in such a manner that their number is conserved, (2) the probability for a carrier to be scattered by long-wave magnons vanishes as q^4 tends to zero. Substantial decrease in scattering by long-wave magnons is reflected in the fact that infinitely long spin waves ($q \rightarrow 0$) do not exercise any effect on carrier motion. Indeed, they correspond to the rotation in space of the crystal moment as a whole, but the carrier spin always points in the direction of the crystal moment and by force of it also rotates when the crystal moment rotates. The carrier does not change its direction of motion, since such a spin wave does not disturb the periodic structure of the crystal. Earlier theories [125, 141] did not lead to a cut-off at small q 's, because they considered carrier scattering not by true, but by bare l -magnons.

Below the dissociation temperature of a wide-band spinpolaron both expressions (4.4.2, 3) yield the same result: the relaxation time is independent of the c - l exchange integral A and proportional to $T^{-7/2}$:

$$\tau_k^{-1} = \frac{Lka|B|}{(2S)^2\hbar} \left(\frac{T}{\mathcal{Y}S} \right)^{7/2}, \quad L = \frac{1}{(2\pi)^3} \int_0^\infty \frac{x^{5/2} dx}{e^x - 1} \simeq 1.3 \cdot 10^{-2}. \quad (4.4.5)$$

In case of narrow bands the conditions of its applicability are generally broader. They are expressed by the inequality $T \ll \mathcal{Y}$. In the region $T > \mathcal{Y}$ the relaxation time becomes less dependent on T ; it is proportional to T^{-2} :

$$\tau_k^{-1} = \frac{9ka|B|}{2\pi\hbar S^2} \left(\frac{T}{\mathcal{Y}} \right)^2 \quad (W \ll AS), \quad (4.4.6)$$

$$\tau_k^{-1} = \frac{9m^*a^2A^2k}{8\pi^2\hbar^3q_0} \left(\frac{T}{\mathcal{Y}} \right)^2 \quad (W \gg AS). \quad (4.4.7)$$

The result (4.4.3, 5, 7) obtained for wide bands is different from those of [125, 141] and others where the scattering probability was presumed to be proportional to A^2 in that it is in addition nonanalytic in A : at $T < T_0$, according to (4.4.5), it does not contain A at all, τ_k^{-1} at $T > \mathcal{Y}$ being proportional not to A^2 , but to $A^{3/2}$ (since (4.4.7) contains the momentum q_0).

To assess the conductivity of wide-conduction-band semiconductors in the PM region at $T \gg T_c$, one may use the perturbation theory in AS/W , since long-range spin correlations play no part in it

($\langle \mathbf{S}_q \cdot \mathbf{S}_{-q} \rangle \approx S(S+1)$). In the result one obtains [125, 141]:

$$\tau^{-1}(E_k) = \frac{A^2}{4\hbar N} \sum \langle \mathbf{S}_q \cdot \mathbf{S}_{-q} \rangle \frac{(\mathbf{k} \cdot \mathbf{q})}{k^2} \delta(E_k - E_{k-q}) \approx \frac{A^2 S^2}{8\hbar} g_e(E_k) a^3, \quad (4.4.8)$$

where $g_e(E)$ is the density of states (1.2.10). The conditions of applicability of expression (4.4.8) are determined by the inequality (4.3.3) for $\kappa^{-1} = a$.

The Boltzman equation cannot be employed in the case of narrow bands at high temperatures, and to calculate the conductivity one should make use of Kubo's formula [312]:

$$\rho^{-1} = \frac{1}{T} \int_0^\infty dt \langle e^{iHt} j_x e^{-iHt} j_x \rangle. \quad (4.4.9)$$

Here the angular brackets mean averaging over the temperature.

In the general case it is extremely difficult to decipher expression (4.4.9). Below we shall consider only the case of very high temperatures and very narrow energy bands $T \gg W \gg \frac{1}{2}S$, when it is possible to obtain from formula (4.4.9) an estimate for the conductivity without resorting to the direct calculation of the current-current correlation functions. In the main approximation in W, T unity can be substituted for the statistical operator $\exp(-H/T)$ in the expression for the average over the temperature. Next, on account of the condition $W \gg \frac{1}{2}S$ we may discard the terms $\sim \frac{1}{2}S$ in the evolution operator e^{iHt} . The c -l exchange energy will be seen from the structure of the Hamiltonian (3.5.3), (Ap. I.16) to enter the first approximation in W, AS only as an additive term. Hence, all the operators contained in expression (4.4.9) in the approximation used are functions of only one energy parameter, the Bloch integral B . All in all the following expression for the spinpolaron mobility can be obtained [45]:

$$u = \frac{e\tilde{\tau}}{m^*}, \quad \tilde{\tau} = \frac{\hbar c_u}{2T}, \quad (4.4.10)$$

where c_u is a dimensionless current-current correlation function entering (4.4.9). The magnitude of c_u is of the order of unity. By employing the approximate analytic continuation, the value of 0.96 has been obtained for it in [143, 73].

Hence, formally the expression for the mobility takes here the same form as in the conventional band theory, but the part of the relaxation time is played by a quantity inversely proportional to the thermal energy. An important point is that formula (4.4.10) is valid only for semiconductors with low carrier mobilities for which the conventional band theory is *a priori* inapplicable. For instance at

temperatures of ~ 1000 K it is applicable to materials in which the mobilities do not exceed $1 \text{ cm}^2/\text{V}\cdot\text{s}$. The result (4.4.10) is valid irrespective of the type of magnetic ordering existing at low temperatures and of the magnitude of the spin of magnetic atoms.

An interesting point is that we succeeded in obtaining the estimate (4.4.10) for the mobility, despite the obvious invalidity in this case of the concept of the carriers as of quasi-particles with definite quasi-momenta scattered by fluctuations of the magnetic moment density. The degree of the magnetic disorder is so large here that the system cannot be regarded as a periodical one and the mechanism of the charge carrier motion should be similar to that in semiconducting glasses.

A crude qualitative picture is that of a carrier travelling in the crystal at a variable speed: a relatively high one in microregions with an identical spin orientation and a relatively low one in microregions with sharp changes in the directions of spins inside them. In the former there should be a correlation between the directions of successive carrier transitions from atom to atom.

Transport Phenomena in the Vicinity of T_c . The most intricate problem is that of the behaviour of the resistivity ρ in the vicinity of T_c . At the first glance, charge carrier scattering by magnetization fluctuations in this region should also be maximum, just as neutron scattering. However, from the point of view of physics there is a drastic difference between neutron and electron scattering: the former moving through the crystal experience only one scattering act, whereas the collisions of the latter with l -spins are so frequent as to change radically the electron state: according to results of Sec. 4.3, the electron spin must fall in with the local atomic moment. Numerous experiments on pure FM metals demonstrate the absence of a resistivity ρ maximum at T_c , $d\rho/dT$ displaying a singularity of the specific heat type*. In contrast to metals, FMS as a rule display a resistivity peak at T_c . However, when analyzing such data, one should keep in mind that, because of T_c being low in all investigated FMS, direct measurements of resistivity are possible only in comparatively heavily doped specimens with impurity conduction whose behaviour may be quite different from that of perfect crystals. Judging by the photoconductivity of the most perfect crystals studied, they should have no peak in ρ (see Sec. 4.7). Sometimes attempts are being made to explain this peak as being the result of carrier trapping by magnetization fluctuations. Such an explanation appears to be unsatisfactory for the following reasons. For an ideal crystal, carrier trapping by fluctuations is only possible, if its Curie point lies below 10 K (Sec. 5.3). At the same time the resistivity peak is

* One exception is Gd, which displays a peak in ρ in the direction of the c -axis and a peak in $d\rho/dT$ in the directions of other axes.

observed also in crystals with $T_c \gg 10$ K, e.g. in EuO. The cause of a peak ρ in the vicinity of T_c in imperfect crystals is explained in the following section.

When formula (4.4.8) together with the Ornstein-Zernicke function (2.5.7) is used to calculate electron scattering by critical fluctuations in the vicinity of T_c [145], in disagreement with the experiment a result is obtained that there should always be maximum in electron scattering at T_c . Unsatisfactory results [145] obtained in the Born approximation are the outcome of the inapplicability of the perturbation theory in the c - l exchange in the presence of correlations between the spins, as pointed out in Sec. 4.3.

A better agreement with experiment is obtained, if the correlations between l -spins in formula (4.4.8) are cut off at the value of the electron mean free path. A justification for this is the incoherent scattering of the electron by spins separated by larger distances [146]. Already with the Ornstein-Zernicke correlation function such cut-off eliminates the peak in ρ and produces a peak in $d\rho/dT$ at T_c [381]. If on the other hand one describes short-range correlations instead of the Ornstein-Zernicke function with the aid of the expression for the binary correlation function (2.5.15) valid in the scaling region, $d\rho/dT$ will behave both sides of T_c as the specific heat [381-383]. According to [146], there should be still a resistivity peak above T_c . The fact that it has not been observed experimentally in metals has been explained in [146] by a simultaneous intensification of electron scattering by phonons with rising temperatures.

However, the method [146, 381-383, 492-495] has no reliable foundation, one reason being that it is by no means obvious that the Born approximation can be used as the initial. In particular in the case of semiconductors the following argument can be advanced against this method: the renormalized electron energy (4.3.1), because of the cut-off, should grow in the vicinity of the conduction-band bottom, whereas as the calculation accuracy improved it should diminish. On the other hand the substitution in formulae (4.3.1-3) of the mean free path L for the correlation length κ^{-1} for $\kappa^{-1} > L$ does not by itself guarantee small electron damping, since L is also great as compared with the lattice parameter.

On account of the inapplicability of the Born approximation established in Sec. 4.3, the paper [147] in which in this approximation a peak of electron scattering in semiconductors in the vicinity of T_c has been obtained must be regarded as controversial. At present the theory is unable to state definitely that such a peak actually exists.

The theory should be further developed to take account of the nonanalytic nature of scattering in ASW , and to this end it should go beyond the Born approximation. An example of such an approach is the approximation of plane waves with a fluctuating spin used in Sec. 4.3. It follows from results (4.4.3) that the alignment of the

spin with the direction of the local moment greatly diminishes the electron scattering by magnetization fluctuations at $T \ll T_c$. It seems natural to expect the same to happen at T_c . Indeed, as demonstrated in Sec. 4.3, this appreciably reduces to electron scattering by long-wave magnetization fluctuations, the result being a finite lifetime of elementary excitations at the critical point.

Note that, to evaluate the mobility, one need not take into account changes in the structure of the current operator resulting from the transformation (3.5.1, 2), since in the approximation (1.1.1) the current operator contains only the operators $a_{\mathbf{g}-\Delta}^\dagger a_{\mathbf{g}}$ corresponding to the nearest neighbours, the angles $\theta_{\mathbf{g}} - \theta_{\mathbf{g}+\Delta}$ and $\varphi_{\mathbf{g}} - \varphi_{\mathbf{g}+\Delta}$ being small. This makes it possible to use the conventional Boltzmann equation. The transport relaxation time $\tau_c(\mathbf{k}, \sigma)$ in the vicinity of T_c is determined by the conventional expression (see formulae (4.3.4, 6, 7), (1.7.16))

$$\tau_c^{-1}(\mathbf{k}, \sigma) = 2\pi \sum_{\mathbf{k}'} |T_{\mathbf{k}\mathbf{k}'}^{(\sigma)}|^{(2)} \left[1 - \frac{\mathbf{k} \cdot \mathbf{k}'}{k^2} \right] \delta(E_{\mathbf{k}\sigma} - E_{\mathbf{k}'\sigma}). \quad (4.4.11)$$

$$T_{\mathbf{k}\mathbf{k}'}^{(\sigma)} = \langle \mathbf{k}\sigma | H_\sigma - H_\sigma^0 | \mathbf{k}'\sigma \rangle.$$

Expression (4.4.11) contains multispin correlation functions about whose behaviour in the immediate vicinity of T_c we have practically no information at present. For this reason a rigorous calculation can be carried out only in the region of applicability of the mean field theory, when the long-wave components $S_{\mathbf{q}}$ with different \mathbf{q} 's are not connected with one another [246], i.e. when multispin correlation functions can, in accordance with Wick's theorem, be split up into binary ones. Outside the region of applicability such a splitting should overestimate singularities of higher correlation functions: actually, the growth of long-wave fluctuations as T_c is approached should be weakened by the kinematic interaction between different $S_{\mathbf{q}}$ entering the multispin correlation function. This interaction arising from the finite value of the spin of the magnetic atom remains unaccounted for in the mean field approximation. Accordingly, the results obtained below will in this case have the meaning of an upper estimate, too.

Confining ourselves to the energetically-favoured direction of the spin of the charge carriers and carrying out the calculations in exactly the same way as it has been done when formula (4.3.11) has been deduced, we obtain the upper estimate for the inverse relaxation time [93]:

$$\tau_c^{-1}(\mathbf{k}) < 0.04|B| \left(\frac{ASa}{|B|r_1} \right)^{4/3}. \quad (4.4.12)$$

This estimate gives no indication as to whether there is a maximum in the carrier scattering at T_c . However, in any case it is a

proof that it cannot be a very sharp one. It may not make itself felt at all, when other mechanisms of carrier scattering are taken into account, e.g. the scattering by phonons whose intensity rises continuously with the temperature.

For $AS = 0.5$ eV, $W = 12$ | B | = 5 eV, $r_1 \sim a$ the mobility at T_c , when only the scattering by critical fluctuations is taken into account, should amount, according to (4.4.12), to several tens $\text{cm}^2 \text{ V} \cdot \text{s}$, this being in agreement with experimental data for EuO depicted in Fig. 4.18.

We would like to point out a principal difficulty, which appears as we go beyond the Born approximation: we must have the presently unavailable information about higher spin correlation functions in the vicinity of the critical point. Accordingly, we can hardly hope to be able to develop an accurate kinetic theory in the vicinity of T_c and will have to count on estimates of the type (4.4.12).

Magnetoresistance. A specific feature of ferromagnetic semiconductors is their giant magnetoresistance exceeding by many orders of magnitude that of nonmagnetic semiconductors. In the latter the magnetoresistance is caused by the deformation of the orbital motion of charge carriers produced by the magnetic field \mathcal{H} : it deflects the carriers from moving in the direction of the electric field \mathcal{E} twisting them and hence increases the distance they travel between the electrodes. In case of the mean free path remaining constant this is tantamount to an increase in the number of scattering acts in the time the electron travels through the crystal, i.e. to a reduction of its mobility (positive magnetoresistance). The effect should be greatly dependent on the orientation of \mathcal{H} with respect to \mathcal{E} . Specifically, in an isotropic crystal with carriers of one type there should be no longitudinal magnetoresistance $\Delta\rho_{\parallel} \propto \rho (\mathcal{H} \parallel \mathcal{E})$, because the average Lorentz force acting on electrons moving in the direction of the field is zero. The transverse magnetoresistance $\Delta\rho_{\perp} \propto \rho (\mathcal{H} \perp \mathcal{E})$ for its part should for small \mathcal{H} be proportional to \mathcal{H}^2 , since \mathcal{H} is the only pseudovector in the system, and the only way to make a scalar out of it is to square it.

On the other hand the lengthening of the trajectory in a magnetic field is limited to acts of electron scattering, which interrupts the electron twisting, and for this reason the relative magnitude of the lengthening should be proportional to the ratio of the relaxation time τ to the period of the electron rotation in a Larmour orbit, i.e. $\Delta\rho_{\perp} \propto \rho$ should be of the order of $\left(\frac{e\hbar\tau}{m^*c}\right)^2$ [214]. For an effective mass of the electron almost equal to its true one and for carrier mobilities of $\lesssim 100 \text{ cm}^2 \text{ V} \cdot \text{s}$ this quantity is small up to fields of several hundred kOe.

High magnetoresistance and its opposite (negative) sign in FMS are due to different mechanisms. To begin with, the scattering of

carriers by magnetization fluctuations decreases in a magnetic field, which suppresses such fluctuations. The field also affects the carrier concentration in nondegenerate MS. This effect and its influence on magnetoresistance will be discussed in the following section.

In contrast to the orbital magnetoresistance described above, which depends on the mutual orientation of the magnetic field and the current, the magnetoresistance due to the suppression of spin fluctuations by the magnetic field is independent of its direction. In the spin-wave region the effect of the field on the carrier scattering can be easily found from formulae (4.4.2, 3) by shifting the magnon frequencies ω_q entering the Bose function m_q by the amount \mathcal{H} . In small fields the effect turns out to be linear in the field, since there is another pseudovector, the magnetization \mathbf{M} , and accordingly one may construct a scalar $(\mathbf{M} \cdot \mathbf{H})$ linear in the field. Evaluating the change in the relaxation time produced by the field $\Delta\tau$ ($\sim \mathcal{H}$), we obtain for $\mathcal{H} \ll \mathcal{Y}$

$$\frac{\Delta\tau(\mathcal{H})}{\tau} \sim \frac{\mathcal{H}}{\mathcal{Y}}. \quad (4.4.13)$$

Consider now the effect of the magnetic field on carrier scattering in the PM region for $W \gg AS$. Whereas in the absence of a field the electron spectrum is degenerate in the spin direction, the field causes a giant Zeeman splitting of magnitude $A\mathfrak{M}$, where $\mathfrak{M} = \chi \mathcal{H}$ is the field-induced magnetization (in accordance with formula (2.5.6), it is $AS/(T - \theta) \sim 10^2$ - 10^3 times the usual Zeeman splitting $\sim \mathcal{H}$). Because of that one has to introduce instead of one relaxation time various relaxation times $\tau_{\mathbf{k},0}$, $\tau_{\mathbf{k},2\sigma}$ for processes taking place without a change in the spin projection and with a change from σ to $(-\sigma)$, respectively:

$$\begin{aligned} \tau_{\mathbf{k},0}^{-1} &= \frac{A^2}{8} (R^2 - \mathfrak{M}^2) g_e(E_{\mathbf{k}}), \\ \tau_{\mathbf{k},2\sigma}^{-1} &\simeq \frac{A^2}{8} [S^2 - R^2] g_e(E_{\mathbf{k}} - 2\sigma A \mathfrak{M}) \theta(E_{\mathbf{k}} - 2\sigma A \mathfrak{M}), \end{aligned} \quad (4.4.14)$$

where $\theta(x) = 1$ for $x > 0$ and 0 for $x < 0$, $R^2 = \langle (S_g^z)^2 \rangle$.

Since at $T \gg T_c$ every l -spin scatters independently of the rest, and since because of the small length of the c - l exchange forces the scattering is isotropic, the linearized Boltzmann equation for the occupation numbers $f_{\mathbf{k}\sigma}$ will have in this case a very simple form [125, 141]:

$$e(\mathbf{g} \cdot \mathbf{v}_{\mathbf{k}}) \frac{\partial n_{\mathbf{k}\sigma}}{\partial E} = - \frac{f_{\mathbf{k}\sigma} - n_{\mathbf{k}\sigma}}{\tilde{\tau}_{\mathbf{k}\sigma}}, \quad \tilde{\tau}_{\mathbf{k}\sigma}^{-1} = \tau_{\mathbf{k},0}^{-1} + \tau_{\mathbf{k},2\sigma}^{-1}, \quad (4.4.15)$$

where $n_{\mathbf{k}\sigma}$ is the equilibrium value of $f_{\mathbf{k}\sigma}$. The scattering for the electrons from the lower subband whose energy lies below the bottom of the upper subband for $S \gg \mathfrak{M} \gg T, A$ will be seen from formu-

lae (4.4.14, 15) to be three times less intense than in the absence of a field (see formula (4.4.8)).

As to the transverse galvanomagnetic effect, in addition to the usual Hall effect proportional to $[\mathfrak{H} \times \mathbf{j}]$ (\mathfrak{H} is the magnetic induction, and \mathbf{j} is current density), there should in FM also be an anomalous Hall effect proportional to $[\mathbf{M} \times \mathbf{j}]$, where \mathbf{M} is the magnetization. The calculation presented in Appendix II shows the anomalous effect in not very dirty semiconductors to be much less intense than in metals and in typical conditions to be small compared with the normal [363]. The origin of this is as follows. The anomalous Hall effect is due to magnetization fluctuations, but in FMS their role is diminished, because of their averaging over the electron wavelength, which in FMS is much greater than in metals. Next, in nondegenerate semiconductors the dependence of the normal Hall voltage on the field \mathfrak{H} may be a substantially nonlinear one, because the electron concentration which enters the Hall constant $R \sim 1/nec$ may be appreciably field-dependent. This circumstance makes it difficult to subdivide the Hall voltage observed in experiment into the normal and the anomalous parts.

Kinetic problems also include one of calculating the wave-vector- and frequency-dependent dielectric function $\epsilon(q, \omega)$ [582]. The static dielectric constant ϵ_0 of a crystal is known to grow with the decrease in the band-gap width. That is why in FMS the red shift of the absorption edge in a magnetic field should result in a rise in ϵ_0 , the greater the greater the shift. Calculation of the absorption coefficient near the absorption edge in the spin-wave region shows light to generate not a bare electron, but an electron dressed on account of its interaction with magnons, i.e. a spinpolaron. Hence, the Franck-Condon principle, according to which the electron must go over to the conduction band in such a way that the state of the magnetic subsystem remains unchanged, is, strictly speaking, in this case violated. However, it holds when the frequency of light substantially exceeds that of the absorption edge. It should be stressed that violation of the Franck-Condon principle is a quantum effect absent for classically large l -spins (Sec. 4.3).

Thermoelectric Power. Let us now discuss thermoelectric phenomena. In nonmagnetic semiconductors the established practice is to subdivide the thermoelectric power into two parts: the diffusion thermopower, which would be generated in the absence of a phonon flux, and the phonon drag thermopower. If the relaxation time is a function of the energy of the type $(E - E_0)^{-p}$, the former will be equal in a nondegenerate semiconductor to

$$\alpha_0 \simeq \frac{|\mu - E_0|}{eT} + \frac{1}{e} \left(\frac{5}{2} - p \right), \quad (4.4.16)$$

where E_0 is the energy of the conduction band bottom.

The latter is appreciable in cases when the drift velocity of long-wave phonons capable of dragging the electrons along is high. This velocity is determined by scattering inside the phonon subsystem, which at temperatures much below the Debye temperature T_D is very weak and declines rapidly with decreasing temperature. In materials in which the momentum from the phonon subsystem is carried eventually by the imperfections, the phonon drag thermoelectric power grows as T^{-1} with decreasing temperature [353]. But in highly perfect crystals it grows as $\exp(aT_D/T)$, where $a \sim 1$, since the loss of momentum occurs due to Umklapp-processes inside the phonon subsystem [354]. Hence, at low temperatures the phonon drag thermoelectric power may substantially exceed the diffusion thermopower (4.4.16). The growth in the phonon drag thermopower is limited by phonon scattering at the boundaries of the specimen or by electrons. After the phonon-phonon scattering mechanism ceases to be the dominant one, the thermopower after passing through a maximum diminishes as the temperature continues to fall.

A feature peculiar to FMS when compared to nonmagnetic semiconductors is that in the former in addition to the phonon drag of electrons there may also be the magnon drag. However, estimates have shown the thermoelectric power of the magnon drag to remain small, despite the fact that at $T_c/S < T < T_c$ it rises with decreasing temperature. At $T \ll T_c/S$ it diminishes with decreasing temperature, because of interaction of electrons with long-wave phonons weakening which manifests itself in $\langle \tau \rangle^{-1}$ being proportional to T^2 for a degenerate and to T^4 for a nondegenerate semiconductor (see (4.4.5)). Hence, the magnon drag thermoelectric power should pass through a maximum at $T \sim T_c/S$ [150]. The estimate of the effect obtained in [150] shows that it is small enough and, thus, explains why it has not been observed in experiment.

Not only do the magnons drag the electrons poorly, they also obstruct the phonon drag by scattering long-wave phonons and thereby diminishing their average momentum along the temperature gradient. A magnetic field that suppresses magnons should cause the phonon drag thermoelectric power to grow. This effect is particularly large in highly perfect crystals if the momentum is carried away by means of Umklapp-processes among the magnons, i.e. when the Debye temperature T_D exceeds T_c/S . In that case, according to Sec. 1.8,

the thermoelectric power should be proportional to $e \frac{\Delta E_m}{T}$ with $\Delta E_m \sim \frac{T_c}{S}$. After the magnons have been suppressed, the momentum can be carried away only by means of Umklapp-processes between the phonons, i.e. the thermoelectric power becomes proportional to $e \frac{\Delta E_p}{T}$ with $\Delta E_p \sim T_D > \Delta E_m$ [150]. In other words, the magnetic field should increase the thermopower very strongly.

Strong Electric Fields. Up to now we have been dealing with the c - l exchange interactions of the charge carriers with magnetic order fluctuations. In certain cases of principal importance the interaction of l -spins with orbits of c -electrons can be described by the last term in the Hamiltonian (2.2.2) where s_i stands for the l -spin operator, and p_i for the c -electron momentum operator. In particular, it makes magnon generation by charge carriers accelerated by an external electric field possible [320, 356], whereas the c - l exchange interaction that conserves the total moment of the crystal is incapable of producing such an effect. However, the c - l exchange should be weak enough for the acceleration of the carriers by an electric field to be possible. Such a situation can be created in experiment for holes moving over the anions (Sec. 4.8). The interaction between electrons and magnons in strong fields has been studied also in [390, 431-433, 542, 543, 548, 598] where some interesting results have been obtained (PM resonance in FMS in a strong alternating electric field, generation of high-frequency magnons by nonequilibrium electrons etc.).

4.5. EFFECT OF IMPERFECTIONS ON ELECTRIC PROPERTIES OF FERROMAGNETIC SEMICONDUCTORS

Carrier Concentration. The width of the band-gap in FMS is as a rule great enough. Because of that their conductivity is typically of the impurity type. The presence of imperfections in the crystal spectrum produces donor and acceptor levels corresponding to localized states of c -electrons (to avoid misunderstanding, it should be emphasized that this does not mean that an electron goes over to an l -state: whereas each l -electron is localized on its atom, localized c -electrons are spread over a region measuring one or several lattice parameters around the impurity). Peculiarities of FMS are manifested in the temperature dependence of their impurity conductivity, which is much more intricate than that of conventional semiconductors. This is the outcome of the circumstance that with the rise in temperature the conduction band bottom E_c shifts upward according to a different law than that, which describes the shift of the donor level E_L . Indeed, the position of a level depends on the degree of magnetic order in the region over which the electron is spread. The energy of a localized c -electron is determined by the short-range magnetic order at distances on the scale of the radius of its orbit, whereas the energy of a delocalized c -electron is determined by magnetic order in a region of much larger dimensions. At finite temperatures the degree of the former is always higher than that of the latter, and because of that the upward shift of the conduction band from its position at $T = 0$ is greater than that of a local level cor-

responding to the same most energetically-favoured electron spin projection.

Actually, this difference is even greater, since a localized electron intensifies the FM coupling between magnetic atoms in the vicinity of the imperfection. The existence of such an indirect exchange between the magnetic atoms via a localized c -electron is a direct consequence of the fact that the electron energy is at its minimum in case of FM ordering. For this reason the c -electron strives to uphold it when the thermal motion of the spins tends to destroy it.

The c - l shift of a donor level remains large even at temperatures so high that the short-range order in the vicinity of a donor is completely destroyed. Indeed, the degree of short-range order in a region containing \mathfrak{N} atoms is expressed in terms of averaged spin scalar products by the relation

$$d_{\mathfrak{N}} = \frac{1}{\mathfrak{N}(\mathfrak{N}-1)S^2} \sum_{\mathbf{f} \neq \mathbf{g}}^{\mathfrak{N}} \langle \mathbf{S}_{\mathbf{g}} \cdot \mathbf{S}_{\mathbf{f}} \rangle. \quad (4.5.1)$$

At high temperatures when the spins are uncorrelated $\langle \mathbf{S}_{\mathbf{g}} \cdot \mathbf{S}_{\mathbf{f}} \rangle = \langle \mathbf{S}_{\mathbf{g}} \rangle \langle \mathbf{S}_{\mathbf{f}} \rangle = 0$. However, the moment $\mathcal{L}_{\mathfrak{N}}$ in this region (per atom) is nonzero, although the average value of its projection on an arbitrary direction is zero:

$$\langle \mathcal{L}_{\mathfrak{N}}^2 \rangle = \frac{1}{\mathfrak{N}^2} \sum_{\mathbf{g}, \mathbf{f}}^{\mathfrak{N}} \langle \mathbf{S}_{\mathbf{g}} \cdot \mathbf{S}_{\mathbf{f}} \rangle = \frac{S^2}{\mathfrak{N}} \left[1 + d_{\mathfrak{N}} \left(1 - \frac{1}{\mathfrak{N}} \right) \right]. \quad (4.5.2)$$

Hence, for $d_{\mathfrak{N}} \rightarrow 0$ the average fluctuating moment of the region is proportional to $1/\sqrt{\mathfrak{N}}$ in agreement with well-known results of the fluctuation theory. Despite the fact that the fluctuating moment $\mathcal{L}_{\mathfrak{N}}$ is oriented perfectly at random, the spin of an electron localized in this region for $W \gg AS$ can always point in the direction of the moment $\mathcal{L}_{\mathfrak{N}}$ fluctuating with it. This will produce a gain in the c - l exchange energy of the first order in AS/W :

$$E_{cl}(\mathfrak{N}) \simeq \frac{|A|S}{2\sqrt{\mathfrak{N}}}. \quad (4.5.3)$$

Actually, in this case we have the same alignment of the spin with the direction of the local moment as in the case of a free electron in the vicinity of the Curie point (Sec. 4.3), and here, too, there must be a spontaneous Zeeman spin splitting of the electron level, although the total crystal moment is zero. Of course, this makes sense only if the dimensions of the region in which the electron is localized and temperature are not too large, so that the inequality $E_{cl} \gg T$ is not violated. For a conduction electron \mathfrak{N} is a macroscopic quantity, and for it the c - l shift (4.5.3) vanishes.

The following physical picture emerges from what has been said above [116, 89, 90]. In the spin-wave region the temperature-induced shift of a localized energy level is much less than that of the conduction-band bottom, because the degree of the local FM order in the vicinity of a donor is much higher than the average over the crystal. Hence, the depth of the local level grows with rising temperature. At high temperatures $T \gg T_c$ the depth of a local level $E_d(T) = E_c(T) - \bar{E}_L(T)$ decreases with rising T , since the magnetic ordering averaged over the crystal has already been destroyed, and the energy of a free carrier is no longer temperature-dependent. For its part, the magnetic ordering in the vicinity of an imperfection continues to be disrupted so that the donor level rises.

However, the effective depth of a donor level $E_d(T)$ at very high temperatures exceeds $E_d(0)$ by the amount $E_{cl}(\mathfrak{N})$, which for localized states of small radii may be quite considerable. Suppose, for example, that an electron trapped by an impurity atom substituting the Eu^{++} ion in EuO is localized on its 12 nearest neighbours. Then (4.5.3) is as high as 1.3 of the maximum gain in the c - l exchange energy equal to $AS/2$. For the compounds being considered the latter amounts to 0.25–0.3 eV, so that at high temperatures the donor level lies 0.1 eV lower than at $T=0$. An analogous E_d vs. T dependence was suggested in [117, 111, 112] without explaining its physical origin.

The fact that the impurity-conductivity activation energy passes through a maximum in the region of T_c should produce singularities in its temperature dependence not present in case of an intrinsic conductivity when the activation energy changes with the temperature monotonously. Namely, at low temperatures the increase in the depth of a level $E_d(T)$ with the temperature may produce a resistivity minimum in the low-temperature region at a temperature at which the exponent in expression (1.2.12) attains its minimum value, i.e. when $\frac{d}{dT} \left(\frac{E_d}{T} \right) = 0$ [117, 111, 112, 90]. Above this temperature the carrier concentration diminishes with the temperature. The presence of a minimum in ρ automatically produces a resistivity maximum in the region of T_c , since at $T \gg T_c$ the concentration must of necessity grow, and ρ must fall with rising T (the activation energy diminishes with T).

The minimum in the carrier concentration in the region of T_c may be interpreted as the result of conduction electron trapping by regions of relatively high magnetization produced around imperfections when conduction electrons are localized on them (localized ferron states (Sec. 5.2)).

For $W \gg AS$ one easily obtains analytic expressions for the temperature dependence of the conduction-electron concentration [90]. In the spin-wave field the appropriate formula is (1.2.12) with $E_d =$

$E_c(T) - E_L(T)$ (the fact that at $T \ll T_c$ the electrons are practically all spin-polarized is irrelevant, since it does not change the ratio of the number of donor levels to the effective number of states in the conduction band that can be occupied by the electrons). The shift of a localized energy level in the spin-wave region will be shown in Sec. 6.6 to be negligible. Accordingly, the temperature dependence of the depth of the impurity level practically coincides with that of the conduction-band bottom as determined by formula (4.2.6).

At $T > T_c$ there is no FM ordering in a crystal as a whole, but the combined moment of atoms in the vicinity of nonionized donors may be large enough. This means that magnetic clusters with moments appreciably exceeding the atomic moment are produced around the imperfections. Since the magnitude of the cluster moment is greatly affected by its interaction with the electron, the concept of the energy of a localized electron is meaningless, and one should speak of the energy of the complete system consisting of the localized electron and of magnetic atoms forming the cluster. As to the free electrons, the concept of their energy remains meaningful, since the magnetic ordering in a crystal as a whole is practically unaffected by conduction electrons, because their concentration in a non-degenerate semiconductor is small. For its part, at $T \gg T_c$ the electron energy is practically independent of magnetization fluctuations. The expression for the renormalized electron energy $E_k(\infty)$ is (4.3.12), and in it the damping may be neglected (it is small in the vicinity of the conduction-band bottom).

We consider here the localized state of a c -electron when it with a probability of almost unity is located near z magnetic atoms constituting the first coordination sphere of the imperfection. Then the electron energy will be determined by the magnitude of the average moment of this atomic group \mathbf{K} . For $A > 0$ it is energetically-favoured that the electron spin point in the direction of \mathbf{K} and rotate together with \mathbf{K} when the latter changes its direction. Hence, the energy of a cluster having a moment \mathbf{K} and containing a conduction electron is in the first approximation in AS/W given by the expression

$$E_{\mathcal{K}} = E_L - \frac{A\mathcal{K}}{2} |\Psi(\Delta)|^2 \quad \left(|\Psi(\Delta)|^2 \simeq \frac{1}{z} \right), \quad (4.5.4)$$

where $\Psi(\Delta)$ is the electron wave function on a magnetic atom. It is presumed that $A\mathcal{K} > 2zT$, so that we need not take into account the state with the opposite orientation of the spin with respect to the cluster moment ($\mathbf{K} = \mathcal{K}$).

In order to develop the statistics of magnetic clusters, it is necessary to find the statistical weight of the given macroscopic state. It is equal to the product of the statistical weight of conduction electrons as given by the usual Fermi expression [246] and of the sta-

tistical weight of clusters

$$\Delta\Gamma_{cl} = \left[\frac{N_d!}{N!(N_d - N_L)!} \right] \left[\frac{N_L!}{\prod_{\mathcal{K}} N_{\mathcal{K}}!} \right] \times (2S+1)^{z(N_d - N_L)} \left[\prod_{\mathcal{K}} (2\mathcal{K}+1) f(K) \right]^{N_{\mathcal{K}}}, \quad N_L = \sum_{\mathcal{K}} N_{\mathcal{K}}, \quad (4.5.5)$$

where $N_{\mathcal{K}}$ is the number of clusters with the moment \mathcal{K} , and N_L is their total number. The first expression in brackets in (4.5.5) is the number of ways in which N_L nonionized donors can be chosen from their total number N_d , the second expression in brackets is the number of ways in which a state with the specified numbers \mathcal{K} can be produced on N_L imperfections, the third expression in brackets is the multiplicity of ionized, and the fourth that of nonionized clusters. A method for calculating the number of states $\mathcal{F}(\mathcal{K})$ with a specified moment \mathcal{K} , that a system of z spins each equal to S can have, was developed in [88].

Making use of the expression for the energy (4.5.4) and of the statistical weight (4.5.5), we construct the thermodynamic potential Ω

$$\Omega = F_c + \sum_{\mathcal{K}} E_{\mathcal{K}} N_{\mathcal{K}} - TS_{cl} - \mu N_d, \quad S_{cl} = \ln \Delta\Gamma_{cl}, \quad (4.5.6)$$

where F_c is the free energy of conduction electrons, S_{cl} is the entropy of clusters, μ is the chemical potential (the conduction electrons are supposed to appear only in the result of transitions from impurity levels). Minimizing expression (4.5.6) with respect to the occupation numbers of electron states in the conduction band and with respect to the numbers of clusters with a specified moment \mathcal{K} , we obtain for the former the usual Fermi distribution function and for the latter

$$n_{\mathcal{K}} = \frac{N_{\mathcal{K}}}{N_d} = \frac{p_{\mathcal{K}} e^{b\mathcal{K}}}{R(T)} \left\{ 1 + R^{-1} \exp \left(\frac{E_L - \mu}{T} \right) \right\}^{-1}, \quad (4.5.7)$$

where we have introduced the notation

$$p_{\mathcal{K}} = \frac{\mathcal{F}(\mathcal{K})(2\mathcal{K}+1)}{(2S+1)^z}, \quad b = \frac{A|\Psi(\Delta)|^2}{2T}, \quad R(T) = \sum_{\mathcal{K}} p_{\mathcal{K}} e^{b\mathcal{K}}. \quad (4.5.8)$$

The quantity $p_{\mathcal{K}}$ is the normalized weight of the cluster state having a specified \mathcal{K} , R plays the role of the statistical sum for the cluster bearing the conduction electron. For $A = 0$ it is equal to 1,

and the expression for $\sum_{\mathcal{K}} N_{\mathcal{K}} = N_L$ reduces to the usual Fermi distribution function, since here, in contrast to (1.2.8), only one electron spin projection has been taken into account.

Taking into account the absence of spin polarization for the conduction electrons, we obtain from the equality $n(T) = N_d - N_L$ for the number of electrons in the conduction band an analogue of formula (1.2.12):

$$n(T) = 2N_{\text{eff}} \exp \left\{ \frac{u - E_c(\infty)}{T} \right\} = \sqrt{\frac{2N_d N_{\text{eff}}}{R T}} \exp \left\{ \frac{E_L - E_c(\infty)}{2T} \right\}. \quad (4.5.9)$$

If $b \gg 1$, the behaviour of the sum for $R(T)$ (4.5.8) is determined by terms having maximum values of $\mathcal{K} = zS$, and then $R(T) \sim \sim \exp \left\{ \frac{AS}{2T} \right\}$. If on the other hand $b \ll 1$, the main contribution to $p_{\mathcal{K}}$ is that of values of \mathcal{K} bordering on $\mathcal{K}_0 \sim S/\sqrt{z}$ for which $p_{\mathcal{K}}$ is maximum. Accordingly, $R(T) \sim \exp \left\{ \frac{A\mathcal{K}_0}{2zT} \right\}$, and the activation energy in (4.5.9) as the temperature rises in the region $T > T_c$ decreases by $\sim \frac{A}{4} \left(S - \frac{\mathcal{K}_0}{z} \right)$.

An external magnetic field increases the degree of local FM order in the vicinity of an imperfection, thereby reducing the energy of the electron occupying a donor. But simultaneously it produces a long-range magnetic order, thus lowering the conduction-band bottom. The second effect is as a rule more pronounced, and by force of it a field increases the carrier concentration.

However, under certain special conditions the concentration in weak fields may be observed at first to diminish as the field grows and later to increase. In such cases the magnetoresistance of the crystal in weak fields will have a positive sign anomalous for MS, having normally a negative sign in strong fields [532] (cf. Sec. 4.5).

Energy Dependence of a Localized c -electron on l -spins. In this item we shall obtain a general expression for the c - l shift of an impurity level valid for any l -spin configuration and for any radius of the electron orbit. Taking into account the circumstance that the electron Hamiltonian in the Coulomb field of a donor (1.2.3) can be diagonalized with the aid of transformation (1.2.4) whose coefficients $\psi_{\nu}(\mathbf{g})$ are spin-independent, the complete electron Hamiltonian which includes in addition the c - l exchange term (3.1.2) can be written down in the form

$$H_d = \sum_{\nu} E_{\nu} a_{\nu\sigma}^* a_{\nu\sigma} - A \sum_{\nu} \psi_{\nu}^*(\mathbf{g}) \psi_{\mu}(\mathbf{g}) (\mathbf{S}_{\mathbf{g}} \cdot \mathbf{s})_{\sigma\sigma'} a_{\nu\sigma}^* a_{\mu\sigma'}. \quad (4.5.10)$$

In the first order in A in the Hamiltonian (4.5.10) we need only take into account terms diagonal in the orbital indices ν, μ . In this

approximation its eigenfunction is sought in the form

$$\Phi_v = [\varphi_v(S^z) a_{v\uparrow}^* + \chi_v(S^z) a_{v\downarrow}^*] |0\rangle_e, \quad (4.5.11)$$

where $|0\rangle_e$ is the electron vacuum function, (φ, χ) is the two-component wave function of l -spins. Making use of formulae (4.5.10, 11), we can represent the Schrödinger equation in the following form

$$\begin{aligned} \frac{A\mathcal{L}^+}{2} \varphi + \left(E_1 - \frac{A\mathcal{L}^z}{2}\right) \chi &= 0, \quad E_1 = E - E_v, \\ \left(E_1 + \frac{A\mathcal{L}^z}{2}\right) \varphi + \frac{A\mathcal{L}^-}{2} \chi &= 0, \\ \mathcal{L} &= \sum_{\mathbf{g}} w_{\mathbf{g}} \mathbf{S}_{\mathbf{g}}, \quad w_{\mathbf{g}} = |\psi_v(\mathbf{g})|^2. \end{aligned} \quad (4.5.12)$$

Consider first the case when the electron with an equal probability is located on any one of \mathfrak{N} atoms. Making use of the relations

$$\begin{aligned} S^- F(S^z) &= F(S^z + 1) S^-, \\ \mathcal{L}^- \mathcal{L}^+ &= \hat{\mathcal{L}}^2 - \mathcal{L}^z (\mathcal{L}^z + 1), \end{aligned}$$

the former following from the definition of the S^- operator, and the latter from relations (2.1.2), we obtain from (4.5.12)

$$\left(E_1 + \frac{A}{4\mathfrak{N}}\right)^2 \varphi = \left(\frac{A}{2\mathfrak{N}}\right)^2 \left(\hat{\mathcal{L}}^2 + \frac{1}{4}\right) \varphi.$$

Hence, we may introduce the magnetic Hamiltonian

$$H_{M1} = -\frac{A}{2\mathfrak{N}} \left[\frac{1}{2} \pm \sqrt{\hat{\mathcal{L}}^2 + \frac{1}{4}} \right], \quad (4.5.13)$$

whose eigenvalues E_1 provide the energy spectrum $E = E_v + E_1$ of the system being considered. One should only keep in mind that its eigenfunction φ is only one component of the two-component wave function of the magnetic subsystem (φ, χ) . This circumstance should be taken into account in calculating the average values of the spin operators [49].

If one fails to make the assumption that the probability $w_{\mathbf{g}} = \text{const}$ for all the \mathfrak{N} atoms, he will succeed in constructing the magnetic Hamiltonian only discarding terms $\sim w_2$, i.e. $\sim 1/\mathfrak{N}$ as compared with $2S$ (they appear as a result of commutation of \mathcal{L}^- and $\left(E_1 - \frac{A\mathcal{L}^z}{2}\right)^{-1}$ after the elimination of χ from the second equation of system (4.5.12)). Then the magnetic Hamiltonian will be given by the expression (the index v has been omitted)

$$H_{M1} = \pm \frac{A}{2} \sqrt{\sum_{\mathbf{g}, \mathbf{f}} w_{\mathbf{g}} w_{\mathbf{f}} (\mathbf{S}_{\mathbf{g}} \cdot \mathbf{S}_{\mathbf{f}})}. \quad (4.5.13a)$$

As has been demonstrated in [49], the calculation of Hamiltonian (4.5.13a) in the next order in A involves the renormalization of the probabilities

$$w_g \rightarrow w_g - \frac{A}{2} \sum_{\mu \neq \nu} |\psi_\nu(g)|^2 |\psi_\mu(g)|^2 (E_\nu - E_\mu)^{-1},$$

and the addition to it of the term H_{M2} having the usual Heisenberg structure

$$H_{M2} = \sum_{\lambda \neq \nu} \frac{\mathcal{L}_{\nu\lambda} \cdot \mathcal{L}_{\nu\lambda}^*}{E_\nu - E_\lambda}, \quad \mathcal{L}_{\nu\lambda} = \sum_g \psi_\nu^*(g) \psi_\lambda(g) \mathbf{S}_g. \quad (4.5.13b)$$

The non-Heisenberg term has the following physical meaning. It represents the energy of the coupling between the c -electron spin and the combined l -spin \mathcal{L} with their forming a united spin equal to $\mathcal{L} = 1/2$ or $\mathcal{L} = 1/2$. The two signs in expressions (4.5.13, 13a) correspond to those two possibilities—to a parallel and an antiparallel orientation of the c -electron spin with respect to the l -spin \mathcal{L} .

The smallness of AS as compared with the donor ionization energy E_d is a guarantee of applicability of the Hamiltonian (4.5.13). This condition is evidently sufficient, but not necessary: at $T \rightarrow 0$ the Hamiltonian (4.5.13) is a precise expression, and at $T \rightarrow \infty$ the Hamiltonian H_{M2} is small as compared with H_{M1} , provided the inequality

$$E_d \gg AS/\sqrt{\mathfrak{N}}$$

is satisfied.

Note that formula (4.5.13) together with the condition that at $T \rightarrow \infty$ there are no correlations between the spins immediately yields a high-temperature estimate of the c - l shift (4.5.3).

Carrier Scattering. The presence of magnetic imperfections may exercise an appreciable effect on carrier transport properties [144]. Suppose that in the crystal a magnetic atom has been replaced by an impurity atom whose ferromagnetic coupling with the neighbours is stronger than that of a "regular" magnetic atom. In that case, as the temperature rises, the short-range order near the impurity will be retained up to higher temperatures than the long-range order in the crystal as a whole. Thus a microregion with an anomalously high magnetic moment will be established around the impurity. The same physical picture is true for a nonionized donor.

The conduction electron owing to the c - l exchange interaction is scattered by spin fluctuations. At $T \gg T_c$ the l -spins remote from the impurity scatter the electron independently of one another. But the spins forming a cluster around the impurity, being strongly correlated, scatter coherently, and because of that the scattering in-

tensity rises sharply.* This is apparent already from Born's approximation: if N spins constituting the cluster scatter independently of one another, their total scattering probability will be proportional to the square of the momentum of one spin S^2 multiplied by the number of spins N in the cluster. If on the other hand they scatter as a united momentum NS , the scattering intensity will be proportional to its square, i.e. will be N times that of uncorrelated scattering. For a cluster of a 2-3 lattice parameters radius, N may be as high as several hundred.

Scattering by a cluster turns out to be still more intense in conditions when the Born approximation is inapplicable. In case of a favourable parameter ratio it may even become resonance scattering, i.e. gain additionally several orders of magnitude in intensity. The parameter that serves as a "fitting" parameter an appropriate choice of which produces resonance conditions is the cluster moment proportional to the difference between the short-range order parameter near the impurity and the long-range order parameters. This difference is a function of the temperature passing through a maximum in the region of the Curie point (at $T = 0$ the crystal is fully magnetized, and at $T \rightarrow \infty$ the short-range order near the impurity is also destroyed). Accordingly, resonance scattering conditions can be met (if they can be met at all) only in a short temperature interval in which maximum scattering should be observable. Evidently, the corresponding temperature does not necessarily coincide with T_c .

Possibly, the cluster will have such a large moment that it will be able to capture a conduction electron. If the original level depth is not great ($AS > E_d(0)$), the capture by a donor atom of a second electron may perceptibly affect the free carrier concentration.

The calculation carried out below is confined to the case of sufficiently high temperatures when there is practically no correlation between the spins at large distances from the impurity, being still rather great near the impurity. The scattering by spins remote from the impurities is calculated for $AS \ll W$ in the Born approximation. In this approximation it is simply summed with scattering by magnetic clusters according to the well-known Matthiessen rule. The probability of electron scattering by an individual cluster in case when the electron wavelength is great as compared with the cluster dimensions can be found without any limiting assumptions concerning the magnitude of AS , where M is the cluster moment assumed

* It does not follow from this reasoning that there must be a maximum in the electron scattering by magnetic-order fluctuations in the vicinity of T_c . There is a qualitative difference between the situation being considered here and one analyzed in Sec. 4.4: firstly, strong correlations between the l -spins exist only in the vicinity of imperfections distributed over the crystal perfectly at random. Secondly, the correlation length is in this case small as compared with the electron characteristic wavelength.

to exceed appreciably the atomic spin. The probability is expressed in terms of the electron correlation function with the aid of the relationship

$$W_{q\sigma, k\sigma'} = \lim_{t \rightarrow \infty} \frac{1}{t} |\langle a_{q\sigma}^*(t) a_{k\sigma'} \rangle|^2, \quad (4.5.14)$$

the latter in turn being connected with retarded Green's function (3.2.4) through the relationship [64]

$$\langle a_{q\sigma}^*(t) a_{k\sigma'} \rangle = \lim_{\delta \rightarrow 0} i \int_{-\infty}^{\infty} \frac{d\omega e^{i\omega t}}{e^{\omega/T} + 1} [\langle \langle a_{k\sigma'} | a_{q\sigma}^* \rangle \rangle_{\omega + i\delta} - \langle \langle a_{k\sigma'} | a_{q\sigma}^* \rangle \rangle_{\omega - i\delta}]. \quad (4.5.15)$$

Green's functions in formula (4.5.15) are calculated with the aid of the equations-of-motion method using Hamiltonian (3.1.1) involving only those l -spins, which enter the cluster. In what follows they will be treated as classical vectors. The cluster moment is conveniently chosen as the quantization axis for the conduction electron spin. If the cluster magnetization is nearly as high as the maximum, the equations of motion for Green's functions take the form

$$(E - E_k) \langle \langle a_{k\sigma} | a_{q\sigma}^* \rangle \rangle = \delta_{kq} - \frac{AS\sigma}{N} \sum_{\mathbf{k}'} \sum_{\mathbf{g}}^{\mathfrak{H}} e^{i(\mathbf{k}-\mathbf{k}') \cdot \mathbf{g}} \langle \langle a_{\mathbf{k}'\sigma} | a_{q\sigma}^* \rangle \rangle. \quad (4.5.16)$$

Since only the long-wave components of Green's functions are of any importance, we may put $\exp \{i(\mathbf{k} - \mathbf{k}') \cdot \mathbf{g}\}$ equal to 1 in the right-hand side of (4.5.16). Then the integral equation (4.5.16) is easily solved

$$\langle \langle a_{k\sigma} | a_{q\sigma}^* \rangle \rangle = - \frac{A\mathfrak{H}\sigma}{N(E - E_q)(E - E_k)(1 + A\mathfrak{H}\sigma G_0)}, \quad (4.5.17)$$

$$G_0 = \frac{1}{N} \sum_{\mathbf{p}} \frac{1}{E - E_{\mathbf{p}}}.$$

Taking account of the isotropic nature of scattering of long-wave electrons, we obtain the following expression for the relaxation time (1.7.16) by summing over both spin polarizations

$$1/\tau_{cl}(E) = \frac{\pi g_e(E) N_d A^2 \mathfrak{H}^2}{8N} \sum_{\sigma} |1 + A\mathfrak{H}\sigma G_0|^{-2}, \quad (4.5.18)$$

where N_d is the impurity density.

The bound states corresponding to the poles of the scattering amplitude, according to (4.5.18), are those with $\sigma = 1/2$ for $A > 0$ and

$\sigma = -1/2$ for $A < 0$. Comparing the probabilities of paramagnetic scattering (4.4.8) and of scattering by clusters (4.5.18) in the Born approximation, we obtain that the latter becomes predominant when $N_d > \mathfrak{N}^{-2}a^{-3}$, i.e. when the volume of the clusters $\mathfrak{N}a^3N_d$ exceeds the $1/\mathfrak{N}$ -th part of the crystal volume. For $\mathfrak{N} \gg 1$ this condition can be met for nondegenerate semiconductors as well.

In conclusion we would like to point out that conductivity directly via impurity atoms is also possible, if the semiconductor is a partially-compensated one. For instance, if an *n*-type semiconductor contains a small amount of an acceptor impurity, some of the donor electrons will be captured by the acceptors, which results in the appearance of vacant donors. Accordingly, electron hopping from a donor atom to another vacant one becomes possible. A property peculiar to MS is magnetic deceleration of charge carriers. It is due to the fact that the degree of FM order in the vicinity of a donor occupied by an electron is higher than in the vicinity of a vacant one. Because of that electron hopping from a donor to a neighbouring one results in an increase in its energy, and this requires activation [517]. The activation energy, same as the depth of an electron level, passes through a maximum at sufficiently high temperatures, the reasons being similar in both cases. Such a conductivity can be of any importance only if the donor levels are deep enough for the concentration of band electrons to be negligible.

4.6. OPTICAL PROPERTIES (EXPERIMENT)

The optical absorption spectra of typical FMS EuO and EuS at room temperature are depicted in Fig. 4.1 [6]. They display a clear-cut structure in general similar to that observed in nonmagnetic semiconductors. For example, the long-wave maxima resemble the absorption crest in the spectrum of germanium resulting from van Hove singularities in the interband density of states. The existence of several crests is typical also for lead chalcogenides whose structure is similar to that of europium chalcogenides [441].

Sometimes the narrow (~ 1 eV) long-wave crest in the spectra of EuO and EuS is interpreted in literature as proof that their conduction band is a narrow one, i.e. of the *d*-type. The analogy with germanium pointed out above indicates that there are no adequate grounds for such an interpretation. Moreover, estimates of the effective mass of conduction electrons obtained in this section from other experimental data indeed point to the existence of a wide conduction band in europium chalcogenides.

A noteworthy feature is the absence in Fig. 4.1 of absorption tails due to magnetization fluctuations. The latter constitute random-parameter potential wells for conduction electrons and therefore should result, same as imperfections, in the appearance of a finite den-

density of states inside the band-gap (see Secs. 1.2 and 4.3). Their density is apparently too small to make itself felt in absorption spectra.

All FMS display a giant shift of the absorption edge with the temperature, which exceeds by two or three orders of magnitude that in nonmagnetic semiconductors (in the latter it amounts to $\sim 10^{-5}$ eV/deg). As the temperature is lowered from high temperatures, this abnormally great shift begins even before the Curie point

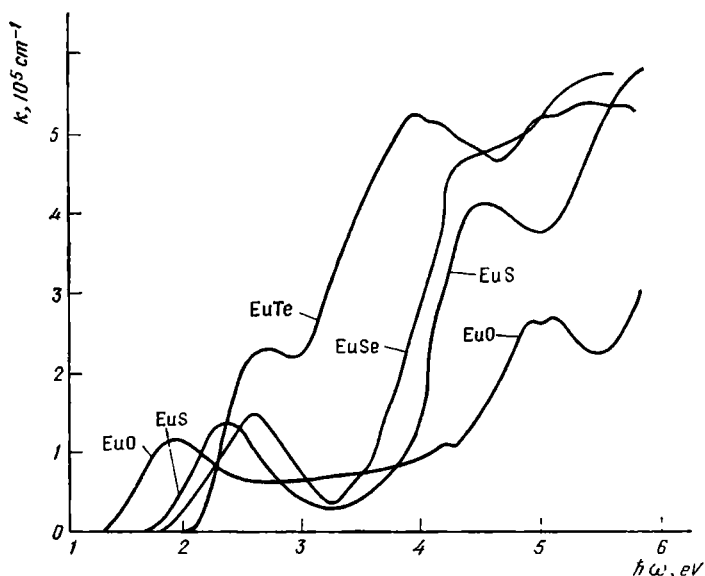


Fig. 4.1. Absorption coefficient k of Eu chalcogenides at 300 K [6]

is reached and continues down to the ultralow temperatures. Almost in all FMS the absorption edge E_g shifts in the long-wave direction as the temperature is lowered, i.e. in a direction opposite to that of the shift in nonmagnetic semiconductors (the red shift in FMS instead of the blue one in nonmagnetic semiconductors).

An external magnetic field shifts the absorption edge in the same direction as a decrease in the temperature, this effect being especially manifest in the vicinity of the Curie point. At very low and very high temperatures, the shift of the absorption edge caused by an external magnetic field disappears. All these regularities will be seen in Fig. 4.2 depicting the position of the absorption edge E_g in EuS [6]. Figure 4.3 illustrates the position of the absorption edge in EuO crystals as a function of the doping level [112]. The dependence of the absorption edge on the magnetic field in EuO is of the same type as in EuS. However, an anomaly is observable below T_c : fields

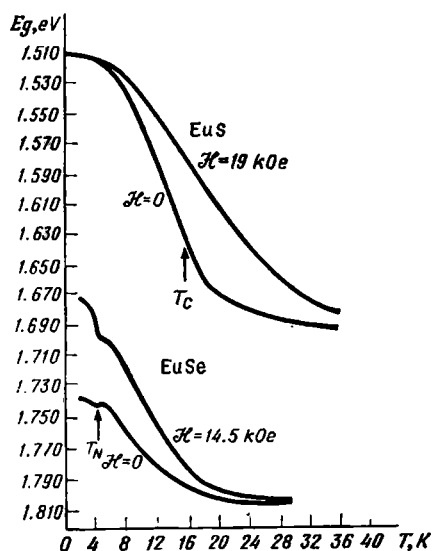


Fig. 4.2. Temperature-induced shift of optical absorption edge in EuS, EuSe [6]

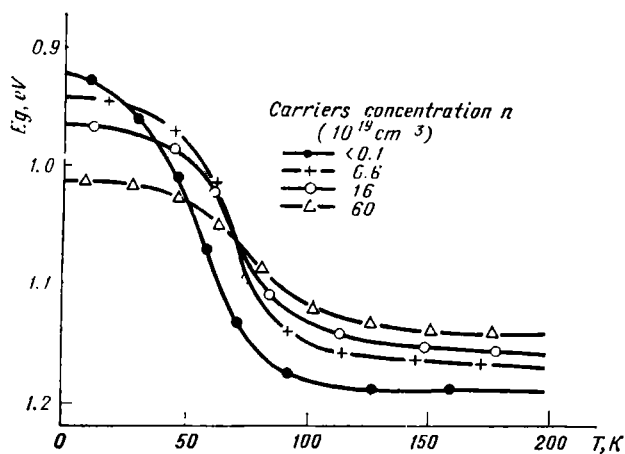


Fig. 4.3. Optical absorption edge vs. temperature for EuO crystals with different Gd concentrations (a nondegenerate crystal and degenerate crystals with electron concentrations of 6.6, 16 and $60 \times 10^{19} \text{ cm}^{-3}$) [112]

with intensities below 2 kOe shift slightly the edge in the blue direction (at 50 K by 0.02 eV). As the field is increased, the sign of the

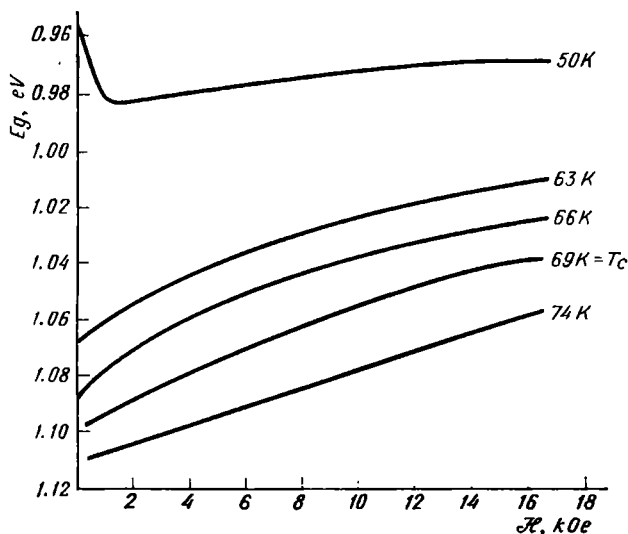


Fig. 4.4. Position of the optical absorption edge vs. magnetic field for EuO [6] shift is reversed. At temperatures above 63 K the field causes a monotonous shift in the red direction (Fig. 4.4 [6]).

Studies of the band-gap vs. pressure dependence in EuO have been reported in [507]. A sign reversal of dE_g/dP at the Curie point has been established. An attempt has been undertaken in [530, 503] to provide experimental and theoretical proof that $E_g(T)$ has an irregularity at T_c . However, this approach can hardly be a sensible one: in contrast to thermodynamical quantities, the absorption edge is not a clearly-defined quantity, because of density-of-states tails inside the band-gap appearing as a result of magnetization fluctuations. On the other hand, the theoretical analysis in [530, 503] is founded on the perturbation theory in the c - l

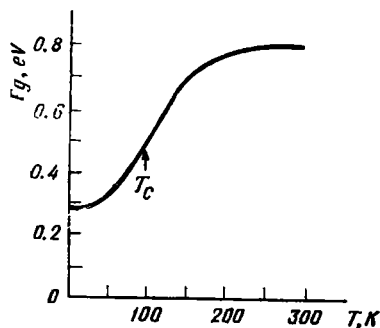


Fig. 4.5. Optical absorption edge of HgCr_2Se_4 vs. temperature [86]

exchange, and the latter cannot be used in the vicinity of T_c (see Sec. 4.3).

FM spinel chalcogenides display generally similar optical properties. The spinel HgCr_2Se_4 has the greatest red shift of all FMS:

it is as high as 0.5 eV with the optical band-gap diminishing by a factor of three [86] (Fig. 4.5).

The optical absorption edge of CdCr_2Se_4 and CdCr_2S_4 has been studied both in case of transmission and of diffuse reflection [322-325, 391]. At room temperature, the edge of the absorption band of CdCr_2Se_4 is located at 1.32 eV. As the temperature is lowered, the absorption edge moves towards higher energies reaching 1.35 eV at 190 K. As the temperature is lowered still further, a red shift becomes observable, which continues even below the Curie point (130 K). At 20 K the absorption edge reaches 1.16 eV. A red shift of the absorption edge is observed also when an external magnetic field that enhances the magnetic order is applied. The effect of the magnetic field is most pronounced in the vicinity of the Curie point, in the FM region it is somewhat smaller. Similar results were reported in [391] for the system $\text{CdCr}_2\text{Se}_{4-x}\text{S}_x$ (Fig. 4.6). As the pressure is increased, the optical gap width in CdCr_2Se_4 grows at a rate of $\sim 10^{-6}$ eV/bar [504].

The behaviour of the optical absorption edge in CdCr_2S_4 is markedly different from that in other FMS. The absorption edge in CdCr_2S_4 at room temperature is located at 1.57 eV, moving towards higher energies as the temperature is lowered. In the range from 300 K to 150 K the edge shifts linearly with the temperature to 1.63 eV. The behaviour of the optical absorption edge in CdCr_2S_4 below 150 K is more intricate. For instance, an anomalous variation of the shape of the absorption edge with a plateau between 1.6 and 1.7 eV is observed to take place, which is most pronounced in the vicinity of the Curie point (85 K). At lower temperatures the upper portion of the absorption edge shifts towards higher energies, whereas the less clearly defined lower portion displays a red shift. The application of an external magnetic field smoothly shifts the absorption edge towards higher energies, i.e. the field-induced shift coincides in direction with that induced by a decrease in the temperature. This effect is also most pronounced in the vicinity of the Curie point T_c . A complex behaviour of the absorption edge similar to one described above is also displayed by CdCr_2S_4 films [392] (Fig. 4.7).

All FMS studied display large spontaneous Faraday rotation θ . It is especially large in EuO and EuS . In EuO θ may be as high as 8.5×10^5 deg/cm for a wavelength of light of 0.61μ [100], i.e. exceeds by far the largest Faraday rotation discovered in metals. In EuS the spontaneous rotation is still larger (Fig. 4.8): at 8 K in the field of 11.5 kOe it is equal to 1.1×10^6 and 1.5×10^6 for the 2.1 eV and the 4.3 eV peaks, respectively. Extrapolating these values to complete saturation of magnetic ordering, we obtain for them 2×10^5 and 2.7×10^6 deg cm [101, 102]. The Faraday rotation is also large in spinel chalcogenides [392], e.g. in CdCr_2Se_4 (Fig. 4.9).

The above-mentioned materials typically have an exceptionally high Faraday quality Q . The latter is defined as the rotation angle per decibel of light intensity attenuation. In metals the Q is always

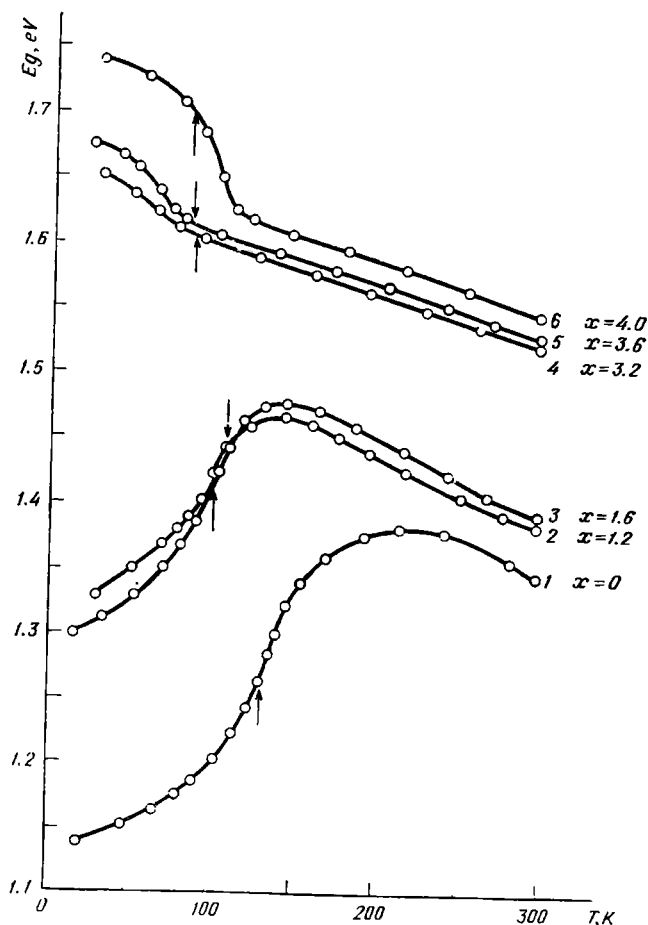


Fig. 4.6. Optical absorption edge vs. temperature for a $\text{CdCr}_2\text{Se}_{4-x}\text{S}_x$ system. The arrows indicate the positions of T_c [391]

less than 0.1 deg/dB , whereas in EuO a figure of $1.4 \times 10^4 \text{ deg/dB}$ at 2.5μ has been obtained. The highest Faraday Q is attained in the windows in the absorption spectrum of europium chalcogenides (e.g. EuO is transparent for light with a wavelength of 2.5μ , which cannot cause electron transitions from the valence to the conduction

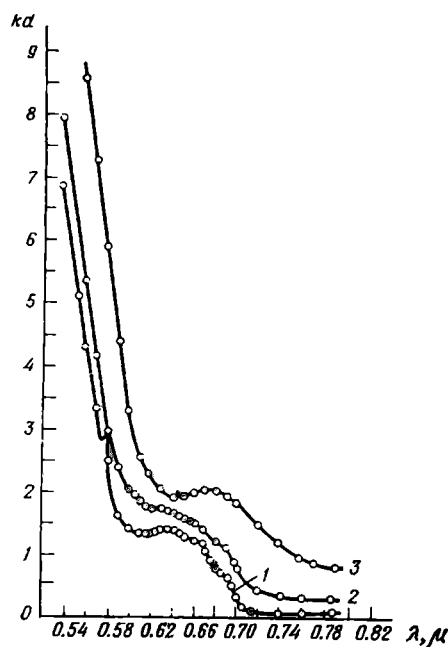


Fig. 4.7. Optical absorption (kd) of a $d \sim 0.5 \mu$ thick CdCr_2S_4 film at temperatures: 1, 20 K; 2, 80 K; 3, 300 K. Curves 2 and 3 have been raised by 0.5 and 0.8, respectively [392]

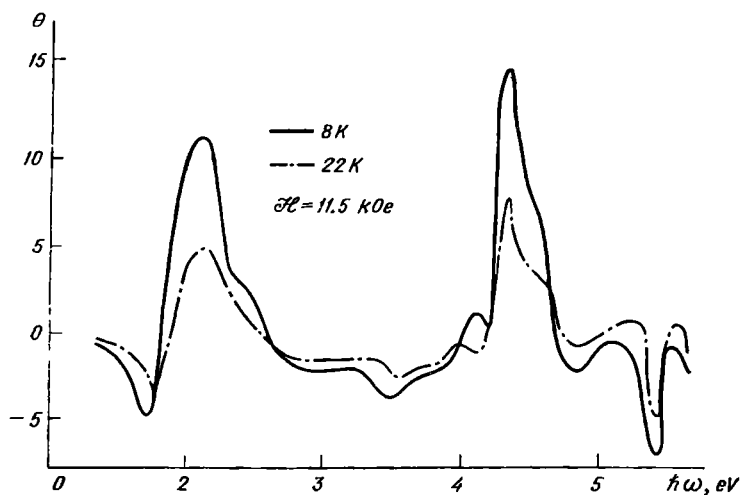


Fig. 4.8. Faraday rotation θ spectrum in EuS in a field $H = 11.5 \text{ kOe}$ at 8 K and 22 K (θ in 10^6 deg/cm) [101, 102]

band, since the width of the band-gap substantially exceeds the light frequency).

An interesting phenomenon has been discovered in studies of the Faraday rotation in EuO at room temperatures in ultrahigh magnetic fields: starting from 450 kOe the effect grows sharply in intensity,

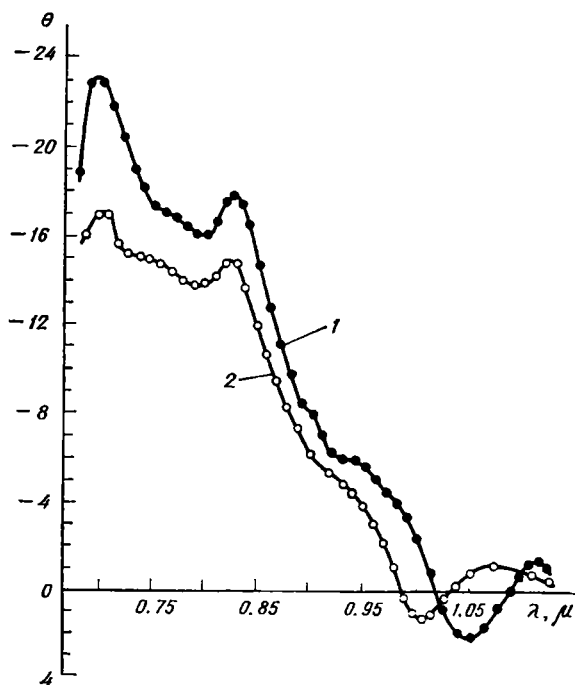


Fig. 4.9. Faraday rotation θ spectrum of a CdCr_2Se_4 film in a field of $H = 4$ kOe: 1, $T = 200$ K; 2, $T = 80$ K (θ in 10^4 deg/cm) [392]

attaining a record level of 3.7×10^7 deg cm for a wavelength of light $\lambda = 6328$ Å in the field of 800 kOe [358].

Other results of studies of optical properties of FMS worth mentioning include the discovery of doublets with frequencies 4.76 and 5.17 eV and 4.15 and 4.32 eV in thermoreflexion spectra of EuO and EuS, respectively, in ultraviolet region. As the temperature was lowered, the splitting of the doublet into a multiplet took place at the Curie point. In EuTe and EuSe in which such doublets have also been observed there was no such splitting of the doublets into multiplets at the Néel point [388]. The authors of [388] associate these doublets with exciton levels split by spin-orbital interaction. However, such an exciton is quite peculiar in that its frequency great-

ly exceeds the band-gap width (in the materials referred to the gap lies in the range of 1-2 eV). Accordingly, it can obviously not be interpreted as a Wannier-Mott exciton (a conduction electron and a hole bound by Coulomb interaction) whose level lies inside the band-gap.

Interesting results have been obtained in research on the luminescence of certain FMS. According to [387], the luminescence of Eu_3S_4 crystals decays rapidly as the temperature is lowered below the Curie point (3.8 K). It is also reduced by a not very strong field (~ 10 kOe), the effect of the field being noticeable up to 50 K. The spectral maximum of the luminescence displays a red shift discernible already at 50 K.

Data on the luminescence of EuO and EuS is presented in [6, 505]. According to [502], all monochalcogenides of Eu, both FM and AF, display an anti-Stokes shift of the frequency of luminescence. The luminescence of CdCr_2S_4 has been studied in [506].

Raman scattering of light greatly dependent on the degree of magnetic order is observable in FMS and AFS. An interesting point is that it has been discovered not only in CdCr_2Se_4 [436, 509] where it is allowed by the symmetry of the crystal lattice, but also in Eu chalcogenides where it is forbidden by the symmetry [434, 435]. In [437] an expression has been obtained for the intensity of Raman scattering in terms of spin correlation functions (see also [510, 511]). On the subject of inelastic scattering of light in Eu_3S_4 , an anomalous vibration mode has been discovered [512].

The absorption edge in FMS corresponds to electron transitions accompanied by conduction electron-hole pair generation. This follows from the fact that it is very close to the photoconductivity edge, which also experiences a similar giant red shift as the temperature is decreased. For the purpose of illustration, Fig. 4.10 depicts the spectral photoconductivity curve for $\text{CdCr}_2\text{Se}_4^*$. According to [6], a temperature shift of the photoconductivity maximum parallel to the shift of the absorption edge is also observable in EuO and EuS .

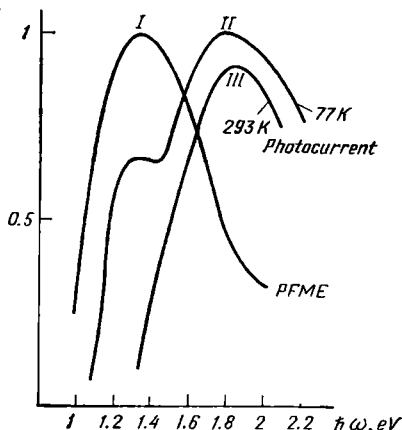


Fig. 4.10. Spectral curves of the photoferromagnetic effect at 77 K (curve I) and photoconductivity at 77 K (curve II) and at 293 K (curve III) of CdCr_2Se_4 . All in relative units

* The author is indebted to V.G. Veselago for supplying the figure.

The optical absorption edge corresponds to the long-wave shoulder of the photoconductivity peak at its middle height level.

It was suggested in [88, 517] that the optical absorption edge in Eu chalcogenides corresponds to the creation of a "magnetic exciton". It consists of a hole on an Eu ion and an extra electron moving over the nearest neighbours of this ion. But the creation of the magnetic exciton should not be accompanied by the appearance of the photoconductivity mentioned above. This means apparently that the magnetic exciton model is inadequate for FMS considered here. According to [499], the main features of the temperature dependence of HgCr_2Se_4 thermorefectance are also an evidence that the red shift in this material is caused by the temperature-dependent spin-subband splitting of the charge-carrier bands.

The statement is frequently encountered in the literature that the intrinsic absorption edge in Eu chalcogenides corresponds to the electron transitions from the f -levels to the conduction band. The results of numerical calculation of the energy spectra of such materials and data on their optical and photoelectrical properties presented in this and in the following sections are cited as arguments in support of this opinion. It should be pointed out that the accuracy of theoretical calculations is absolutely inadequate for an authentic picture to be obtained, and that the interpretation of the optical and the photoelectric spectra is ambiguous. Reliable conclusions as to the nature of the generated hole can be drawn from the intensity of the dependence of the hole conductivity on the crystal magnetization. In EuO this dependence is a weak one, and this means that the holes interact weakly with the f -spins. Hence, the valence band in such crystals is built not of cation f -orbits, but of anion p -orbits. The same is true of CdCr_2Se_4 (see Sec. 4.7) and of HgCr_2Se_4 (see Sec. 7.7).

The dependence of the optical gap width on the temperature and on the field proves that the positions of the minimum of the electron band and the maximum of the hole band are determined by the magnetic order. In some temperature range below the Curie point the same law governs the temperature dependences of the absorption edge and of the magnetization. However, an abnormally large shift of the edge takes place at T_c as well. This means that the carrier spectrum is determined not by the long-range order parameter (i.e. by the average magnetization of the crystal), but by some short-range order characteristics. Comparing the temperature dependence of the absorption edge in EuS with the nearest-neighbour correlation function, we see that it does not reproduce the gap width vs. T and \mathcal{H} dependence [6] either.

The experimental facts described above agree with theoretical results obtained in Secs. 4.1 and 4.2. It follows from them that the shift of the electron spectrum is proportional to that of the magneti-

zation only inside a certain temperature interval (see (4.1.3), (4.2.6)). At lower temperatures the spectrum shift is proportional to $T^{5/2}$, i.e. it occurs slower than that of magnetization. In Fig. 4.2 the corresponding temperatures are below 4 K.

An important part in the vicinity of T_c for $W \gg AS$ is played by spin correlations at intermediate distances $\sim a (WAS)^{2/3}$ (4.3.10). According to (4.3.11), their contribution makes the gain in the c - l exchange energy in the vicinity of T_c comparable to a similar gain at $T = 0$. Accordingly, the total shift of the conduction band bottom in FM and PM regions should also be comparable. The same conclusion can be drawn from the analysis carried out for the case of narrow bands $W \ll AS$. True, in the latter case it is impossible to define the position of the band bottom precisely, since it is greatly blurred by magnetization fluctuations, and one has to be content with analyzing the temperature dependence of the density of states moment (4.1.5). The latter is a function of the nearest-neighbour spin correlation function, but were the energy corresponding to the absorption edge defined more precisely, long-range correlations should also contribute to it. The shift of the edge in the PM region in EuS will be seen from Fig. 4.2 to be only twice smaller than in the FM region. In HgCr_2Se_4 (Fig. 4.5) the former even exceeds the latter.

As has already been stated in Sec. 4.2, if the holes move over nonmagnetic anions, the absorption edge shift is in typical conditions a red one. In a special case there is an exception when for some reason or other the interband exchange is the dominant factor. In such cases the shift is a blue one. In addition to such a true shift, a blue shift in the region of greater absorption combined with a red shift in the region of weak absorption is also possible in principle. Such a situation can materialize when the holes travel over l -shells of the cations. Suppose that the spins of all l -electrons on each cation are parallel. In case of complete FM ordering an l -electron can go over only to such a Zeeman subband of the conduction band in which the c -electron spin is parallel to the crystal moment, since the electron spin projection is conserved in an optical transition caused by the electric vector. This subband will be the lower one, if the c - l exchange integral A is positive, and the higher one, if A is negative. As the temperature rises, one of the subbands moves upwards and the other downwards (Fig. 4.11).

On the other hand the departure of an l -electron is tantamount to the arrival of a hole moving in a narrow energy band (see Sec. 3.1). It follows from results of Sec. 4.1 that the width of the hole band diminishes with rising temperature. Its minimum moves upwards accordingly (in terms of the single-electron theory this corresponds to a downward shift of the valence band maximum). The absorption edge corresponds to an electron transition resulting in the generation of an electron and a hole at the minima of corresponding bands. If

the l -electron goes over to the lower Zeeman subband ($A > 0$), both minima move upwards with rising temperature causing the energy of the absorption edge to increase (red shift with a decreasing temperature). If on the other hand the l -electron goes over to the higher Zeeman subband ($A < 0$), then the hole minimum moves upwards, and the electron minimum downwards. Accordingly, the absorption edge shift will be determined by the difference between these two shifts, i.e. it may both be red and blue. In the latter case at finite

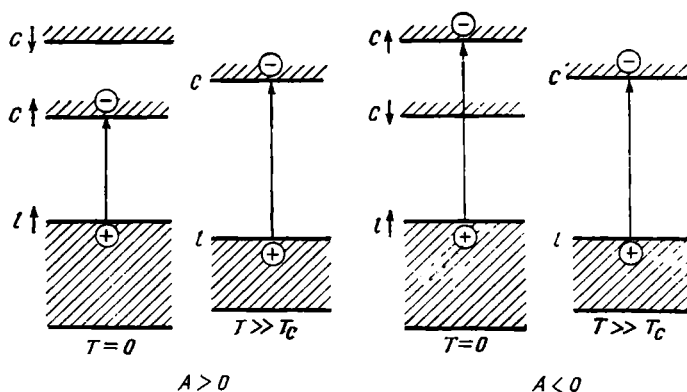


Fig. 4.11. Mechanisms of the red ($A > 0$) and the blue ($A < 0$) shift of the absorption edge with decreasing temperature. The symbols $c\uparrow$, $c\downarrow$ denote spin conduction subbands c . To obtain a clearer picture, the rise in the maximum of l -valence band with decreasing temperature in the case $A < 0$ is presumed to be negligibly small

temperatures there must also be a weak component with a red shift, because the appearance of reversed l -spins creates a possibility for the transition of l -electrons to the lower subband of the conduction band, i.e. strictly speaking, the blue shift in this case is an apparent one.

Unfortunately, from optical data of the kind reproduced in Fig. 4.7 it is difficult to draw an unambiguous conclusion as to whether the blue shift in CdCr_2Se_4 is a true or an apparent one. An indirect proof that it is a true one is the decrease in the PM Curie temperature following the doping of CdCr_2Se_4 with a donor impurity (see Sec. 6.5).

A small blue shift of the absorption edge in EuO in a weak field (Fig. 4.4) is probably associated with the circumstance that the crystal for some reason or other resides in a state of a nonuniform magnetization, which is destroyed by the field causing the regions of higher magnetization to disappear.

The data on the absorption edge shift in pure and heavily-doped semiconductors may be used to obtain an estimate for the effective

mass of the carriers. Such data borrowed from [112] are depicted in Fig. 4.3 for EuO. Since the holes in EuO are practically insensitive to crystal magnetization (see Sec. 4.7), this shift is equal to that of the conduction band. We shall not discuss here the exact position of the adsorption edge which may be strongly influenced by impurity atom clusters existing in EuO: Gd. The only thing that matters is the magnitude of the red shift. The electron transitions from the valence band take place only to such states of the conduction band that lie above the Fermi level, which rises with respect to the band bottom with the rise in concentration. On the other hand, the adsorption edge shifts with rising temperature the less the higher the carrier concentration. This may be explained as the result of a decrease in the degree of electron spin polarization with rising temperature that according to (1.7.1) causes their Fermi energy to diminish $2^{2/3}$ times that at $T = 0$ when the electrons are completely spin-polarized. Because of that the edge shift $\Delta E(n)$ should be the following function of the concentration*

$$\Delta E(n) = \Delta E(0) - \frac{(2^{2/3} - 1)(3\pi^2 n)^{2/3}}{2m^*}, \quad (4.6.1)$$

this enabling us to find the electron effective mass m^* from the shift vs. n dependence. The data reproduced in Fig. 4.3 when substituted into formula (4.6.1) yield for all the three concentrations of doping impurity the same effective mass of $0.9 m_0$, which strongly supports the adequacy of such a treatment. According to formula (1.4.5), the width of the conduction band corresponding to such an effective mass is $W \sim 3\text{--}4$ eV. It would be natural to assume EuO to be a wide-band semiconductor ($W \gg AS$). In that case $\Delta E(0)$ will be equal to $AS/2$, and its experimental value of 0.25 eV could substantiate the validity of such an assumption.

Unfortunately, there are no such data for other FMS, and solely on the basis of the magnitude of the red shift it is strictly speaking even impossible to determine whether the carrier band is a wide or a narrow one (according to results of Secs. 4.1, 4.2, the magnitude of the shift is determined by the smallest of the parameters AS , W , and because of that can be of the same order both for $AS \gg W$ and for $AS \ll W$). The relatively small c - l shift (~ 0.15 eV, Fig. 4.6) substantiates the assumption that the electron band in CdCr_2Se_4

* Here we do not take into account the downward shift of the conduction-band bottom with an increase in n . It can be shown that its only difference from μ (1.7.4) is the presence of a small factor < 0.1 . In compliance with the condition of heavy doping, we also do not take into account small corrections to μ (1.7.4) resulting from the interaction of the electrons with other electrons and the donors. Were we to assume following [112] that the ΔE vs. n dependence is due to the decrease in the c - l exchange integral caused by the screening by conduction electrons, the value of $\Delta E(n) - \Delta E(0)$ would be by several orders of magnitude

is a narrow one. To provide an explanation for it in the framework of a wide-band model, one would have to assume the exchange integral of conduction electrons with *d*-shell electrons to be of a quite unrealistic magnitude. The small width of the conduction band is also substantiated by electrical measurements data (Sec. 4.7), according to which the electron mobility in such materials is low and very sensitive to changes in the magnetic order, and the carrier concentration remains low even at very high doping levels. According to results of Sec. 4.1, the shift of the band bottom for $W \ll AS$ should be approximately equal to

$$\Delta E \simeq \frac{W}{2} (1 - 1/\sqrt{2}), \quad (4.6.2)$$

this yielding for $\Delta E \sim 0.15$ eV an estimated $W \sim 1$ eV for CdCr_2Se_4 . Since the exchange integral between electrons of the same *d*-shell can be as high as 10 eV [54], the inequality $W \ll AS$ is compatible with the above estimate.

4.7. CONDUCTIVITY AND PHOTOCONDUCTIVITY (EXPERIMENT)

Experimental data demonstrate that the electrical properties of FMS are similar to those of nonmagnetic semiconductors only in the temperature range $T \gg T_c$. In this temperature range the conductivity rises with the temperature according to an exponential law. As a rule, specimens with an intrinsic conductivity cannot be produced as yet. Thus, the conductivity activation energy is determined by the depth of impurity levels. It is an interesting point that in certain cases the depth of impurity levels in FMS is small. For instance, in EuO the impurity Gd creates donor levels whose depth at $T \gg T_c$ is 0.017 eV [112]. This is probably the result of a high dielectric constant ϵ_0 (according to [123], $\epsilon_0 = 23.9$). At the same time this means that the carrier effective mass m^* must not be very large. Estimated with the aid of the conventional formula for the energy of a hydrogen-like atom (1.2.2), it should be equal to 0.7 of the free electron mass m_0 , this being in fair agreement with estimates made on the basis of optical data in the end of the preceding section.

In the range of lower temperatures $T \leq T_c$ a nonmonotonous ρ vs. T dependence of the type depicted in Figs. 4.12 and 4.13 for In-doped $n\text{-CdCr}_2\text{Se}_4$ [107, 113] is peculiar to nondegenerate FMS: at very low temperatures the resistance falls, passes through a minimum at $T \ll T_c$, then through a maximum in the region of T_c , and only from then on does the usual exponential decline in the resistance with rising temperature begin. Similar results have been

obtained for EuO and EuS with not very high donor concentrations [109, 111, 112] (Fig. 4.14). As was demonstrated in Sec. 4.5, such a temperature dependence of resistivity is due to a nonmonotonous temperature dependence of the carrier concentration owing to a more rapid upward shift at $T < T_c$ of the conduction-band bottom than of the impurity level, with the impurity level again approaching the band bottom at $T > T_c$. Proof of it is the maximum of the Hall constant $R_0 = 1/nec$ in the vicinity of T_c in Fig. 4.12.

It will be seen from Fig. 4.12 that, in addition to conductivity, thermoelectric power also displays anomalous behaviour at $T \lesssim T_c$. Namely, it is nonmonotonous, whereas, according to (4.4.16), for a constant relaxation time exponent p it should together with the resistivity and the Hall constant pass through a maximum (dashed curve in Fig. 4.12). Indeed, the ρ and R_0 peaks in the region of T_c are due to the increase in the separation between the donor level and the conduction-band bottom owing to differences in their temperature dependences (Sec. 4.5). But with the growth in this separation the difference $E_0 - \mu$ in formula (4.4.16) should grow, too, since, according to formulae (1.2.11, 12), the Fermi level lies approximately midway between the conduction-band bottom and the donor level. A possible cause of this anomaly is the change in the dominant electron scattering mechanism in the vicinity of T_c resulting in an increase in the exponent p .

In many cases the behaviour of crystals having a hole conductivity proves to be quite different from that of crystals with an electron conductivity. For example, the resistivity of p -CdCr₂Se₄ declines monotonously with rising temperature and does not display a peak in the region of T_c [113] (Fig. 4.13). p -EuO behaves similarly [109]. The Hall mobility of holes $u_H = R_0 \rho^{-1}$ in CdCr₂Se₄ is by an order of magnitude higher than that of electrons: in the region of 160 K

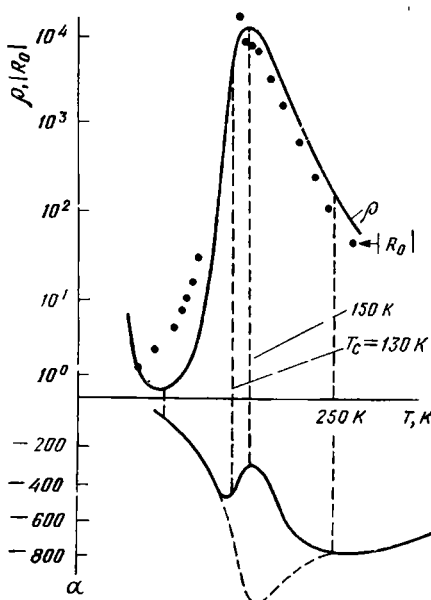


Fig. 4.12. Resistivity ρ (Ohm-cm), normal Hall effect constant R_0 (cm²/A·s) and thermoelectric power α (mV/deg) of CdCr₂Se₄ doped with In (a donor impurity). (Data on Cd_{0.99}In_{0.01}Cr₂Se₄ are presented in [107])

it is as high as 200 cm² V⁻¹ s. The properties of Cu-doped CdCr₂Se₄ have been studied in [375].

It should be pointed out that there is generally no unique solution for the problem of separating the contributions of the normal and the anomalous Hall effect to the total Hall voltage, and one has to resort to additional assumptions as to the properties of the two Hall constants R_0 and R_A . They are often assumed to be independent of

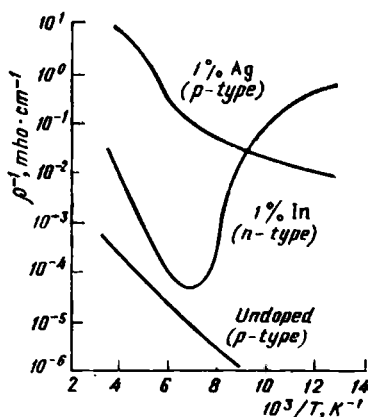


Fig. 4.13. Conductivity of In (*n*-type)- and Ag (*p*-type)-doped CdCr₂Se₄ [107, 113]

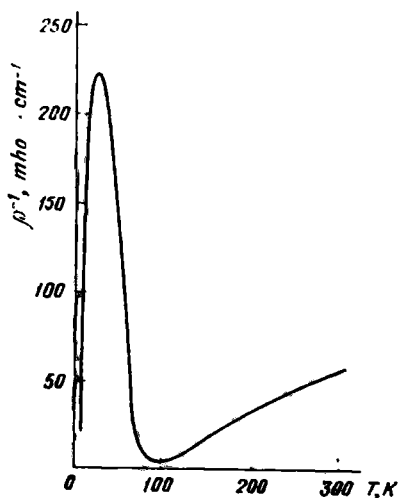


Fig. 4.14. Conductivity of Gd-doped EuO [111, 112]

the external field H . But in the case of FMS such an assumption is unjustified, because the magnetic field shifts the conduction-band bottom and can thereby change the carrier concentration.

Most reliable information about the Hall effect in FMS can be gained from studies of heavily doped specimens where carrier concentrations are independent both of the temperature and the magnetic field. Studies of heavily-doped EuO crystals at 4.2 K and 20 K have demonstrated that the Hall voltage in them is proportional to the magnetic induction B , i.e. that the anomalous Hall coefficient R_A in expression (Ap. 11.1) is zero. A detailed analysis of the experiments proves the inequality $R_0 \gg R_A H$ to be valid at reasonable fields at least to 55 K [121]. Similar results have been obtained for EuS [122]. The conclusion about the nonexistence of an anomalous Hall effect in EuO has also been drawn from direct experiments with photoelectrons [119]. The behaviour of the Hall voltage in *n*-CdCr₂Se₄

as a function of the magnetic field turns out to be essentially nonlinear, and it has not been possible to determine from it R_0 and R_A [113].

The absence of a noticeable spontaneous Hall effect in europium chalcogenides proves, firstly, that in FMS this effect is much less pronounced than in metals in which R_A may be 2 or 3 orders of magnitude greater than the normal constant R_0 . This fact is in accord with the theoretical results [363] (see Appendix II). Secondly, it possibly means that the spin-orbit coupling constant in Eu is very small. The small value of the magnetic anisotropy of such crystals leads to the same conclusion (Sec. 2.8).

These *n*-type crystals, which display a conductivity peak near the Curie point, also display a very high isotropic negative magnetoresistance dependent on the crystal doping level. It reaches a maximum in the region of T_c , where a field of ~ 10 kOe may reduce the resistance by a factor of 10 or more. As has been already stated in Sec. 4.4, the negative magnetoresistance is caused both by an increase in the carrier concentration owing to the conduction-band bottom approaching the donor level and by an increase in carrier mobility owing to a decrease in their scattering by magnetization fluctuations.

An unusual behaviour of the magnetoresistance discovered in In-doped or Se-deficient CdCr_2Se_4 crystals has been reported in [316, 361]. In the range from 80 K to 160 K ρ at first falls with an increase in \mathcal{H} , but then after having passed through a minimum at values of the field ~ 1 kOe it begins to grow. In the range 140-160 K ρ ($\%$) in fields of ~ 10 kOe even exceeds the original value $\rho(0)$ by 1-10%. At lower temperatures the magnetoresistance is always negative, and as a temperature function for a fixed \mathcal{H} reaches its maximum in the vicinity of T_c .

p-Type crystals display a substantially different behaviour in a magnetic field: their magnetoresistance is appreciably smaller and anisotropic. The transverse magnetoresistance of *p*- CdCr_2Se_4 is by 2 or 3 orders of magnitude less than that of *n*- CdCr_2Se_4 , below T_c it is negative, being positive above T_c as in the case of nonmagnetic semiconductors [118]. This together with the absence of a resistivity maximum in the vicinity of T_c justifies the assertion that the interaction of the holes with the spins of the magnetic atoms is much weaker than that of the electrons and is probably not the dominant mechanism of their scattering at $T \gg T_c$. The holes in CdCr_2Se_4 and EuO probably move mainly over nonmagnetic anions whereas the electrons move over magnetic cations. In other words, the hole band in such materials is constructed mainly from anionic *p*-orbits, which overlap little with cationic *d*-orbits, and this is the reason for a weak *p*-*d* exchange.

The fact that the interaction between the holes and the *d*-spins is weak makes their heating by strong electric fields possible. The

heating manifests itself in the field dependence of the longitudinal magnetoresistance discovered in $p\text{-CdCr}_2\text{Se}_4$ at $T < T_c$ [118]. As the electric field is increased, the magnetoresistance changes signs, becoming positive in the range of field intensities from 30 to 300 V/cm, being dependent on the orientation of both fields with respect to the crystallographic axes of the crystal (Fig. 4.15). Above $T_c = 130$ K the effect disappears (it is already absent at 135 K), i.e. it is due to the long-range order. [118] explains this effect as a result of amplification of magnons by hot holes. The fact that the effect is due

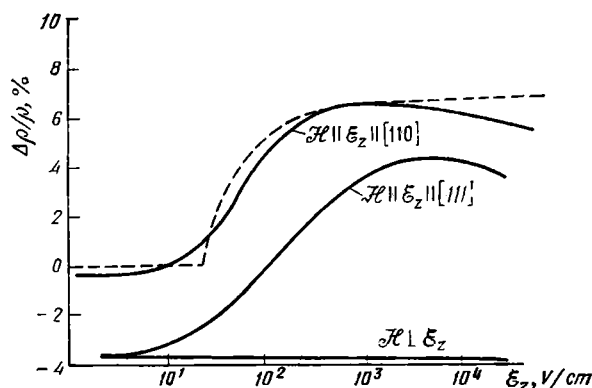


Fig. 4.15. Magnetoresistance vs. electric field for $p\text{-CdCr}_2\text{Se}_4$: $\text{Cd}_{1-x}\text{Ag}_x\text{Cr}_2\text{Se}_4$, $x = 0.004$, $T = 100$ K, $\mathcal{H} = 5$ kOe, $\rho = 6.7 \times 10^4$ Ohm·cm [118]

to long-range order is an argument in favour of the opinion that from the microscopic point of view long-range spin-orbital interaction is responsible for it, as has been suggested in theoretical papers [320] (see Sec. 4.4).

Influence of a strong electric field on ultrahigh-frequency radiation, absorption, magnetization and electroconductivity of CdCr_2Se_4 and EuO was discovered in [608-610] and explained by magnon heating.

The fact that it is impossible to investigate low-temperature electric properties of pure crystals makes it very important to study their photoelectric properties. Certainly, this involves a number of other problems, e.g. the problem of the intricate structure of the photosensitivity spectrum. For instance, the photosensitivity curve of CdCr_2Se_4 will be seen from Fig. 4.10 to display below T_c two maxima merging above T_c . In some specimens these peaks are more sharp and remain distinctly separate even at $T > T_c$. As the temperature rises, the long-wave narrow peak experiences a red shift, and the short-wave wide peak—a blue shift [136].

The photosensitivity spectra of EuO and EuS have a simple bell-shaped form [6], i.e. in their case the situation is simpler. Normally, photoconductivity is measured in the sensitivity maximum, which shifts with the temperature in the same way as the optical absorption edge [6]. The maximum sensitivity grows with the magnetic field, the effect being the more pronounced the closer the temperature to T_c . The salient features of the maximum sensitivity vs. temperature dependence described in different papers are different, the probable reason being the differences in the degree of imperfection of the crystals. Figure 4.16 depicts the maximum sensitivity of europium chalcogenides as a function of the temperature [6]. The photoconductivity minimum in EuO in the vicinity of T_c will be seen from it to be a very shallow one, whereas in EuS it is very sharp. According to [131-134], the minimum in EuO at T_c is practically nonexistent, the minimum in EuS being shallow and vanishing already in a weak magnetic field (Fig. 4.17). This probably indicates that even if the

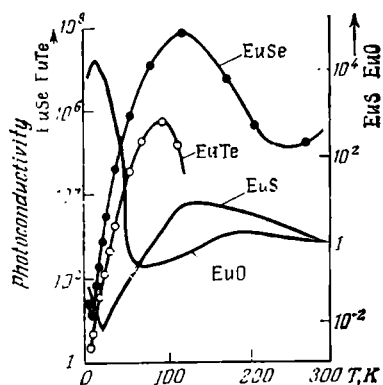


Fig. 4.16. Photoconductivity of europium chalcogenides in the spectral sensitivity maximum (in arbitrary units) [6]

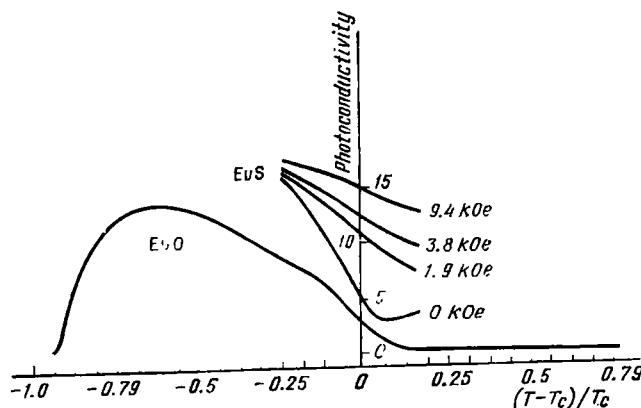


Fig. 4.17. Photoconductivity of EuO and EuS (in arbitrary units) [131-134]

mobility in pure crystals passes through a minimum at T_c , this minimum is a shallow one (Sec. 4.4). Figure 4.18 depicts the Hall mobility of the electrons in EuO [134]. Its value at $T = T_c$ agrees with

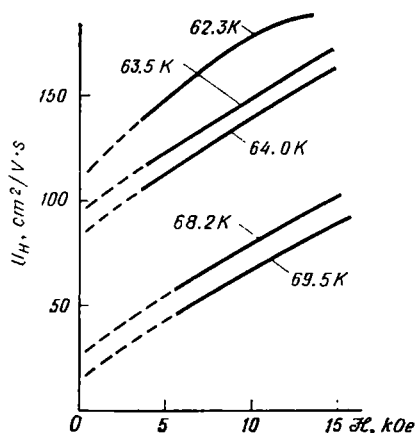


Fig. 4.18. Hall mobility of photoelectrons in EuO [134]

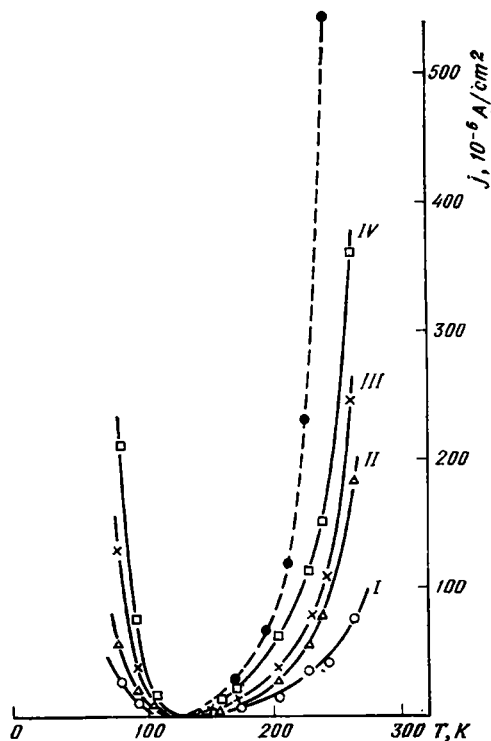


Fig. 4.19. Photoconductivity of $\text{CdCr}_2\text{Se}_4 + 1\% \text{ Ga}$ when illuminated with white light (dashed curve—dark current, other curves—photocurrent for incandescent lamp power of: I, 10 W; II, 40 W; III, 400 W; IV, 400 W) [138]

the value obtained from formula (4.4.12) for $AS \sim 0.5$ eV, $W \sim 3$ eV. An interesting point is that pure CdCr_2Se_4 crystals illuminated with light display a positive magnetoresistance, while at the same time the dark resistance in the fields studied (up to 15 kOe) experiences practically no change [249].

The photosensitivity of CdCr_2Se_4 rises sharply when it is doped with $\sim 1\%$ Ga, the impurity altering also the nature of the temperature dependence of the photocurrent [138]. Namely, if the impurity concentration is under 2% , the photosensitivity displays in the region of T_c a very sharp minimum practically vanishing at T_c (Fig. 4.19). If on the other hand the impurity concentration exceeds 2% , the photoconductivity below T_c is nonzero, but above T_c it is practically zero. The similarity of the temperature dependences of the photocurrent and the dark current (Fig. 4.12) justifies the opinion that charge carrier trapping by imperfections is responsible for their minima in the vicinity of T_c . As was already explained in this section on approaching T_c , the equilibrium carriers may be trapped back by ionized donors, which they had left for the conduction band. But the photoelectrons should be trapped by nonionized donors since the number of ionized donors is small as compared to that of the photoelectrons. In fact, the nonionized donors, according to what was said in Sec. 4.5, turn into electron traps at $T \approx T_c$, because microregions with an increased degree of ferromagnetic order form in the vicinity of the donors. A sharp photoconductivity minimum in the vicinity of T_c has also been discovered in highly imperfect EuO crystals [393].

The photoconductivity of CdCr_2Se_4 crystals containing less than 0.05% Ga or Ag-doped decreases monotonously by 3-4 orders of magnitude on cooling from 300 to 77 K. The photoconductivity activation energy diminishes after T_c has been passed [394]. Doping with Ag produces FM resonance anomalies in CdCr_2Se_4 [245]. In addition, a peculiar nonlinear resonance effect is observed in this material: a high-frequency field of ~ 1 -10 W power nonuniformly distributed over the specimen in conditions of FM resonance produces d.c. voltage of ~ 1 mV in the crystal [429, 438, 439]. Photoelectric properties of CdCr_2Se_4 have also been studied in [513].

NONDEGENERATE ANTIFERROMAGNETIC AND MAGNETOEXCITONIC SEMICONDUCTORS AND SELF-TRAPPED CARRIER STATES

5.1. FREE AND QUASI-OSCILLATOR STATES OF CHARGE CARRIERS IN ANTIFERROMAGNETIC SEMICONDUCTORS

In case of AF ordering, the energy of a conduction electron is appreciably higher than in case of FM ordering*. It follows from formula (3.2.12) that in former the gain in the electron energy due to the c - l exchange for $W \gg AS$ is of the order of $A^2 S^2 / W$, whereas in the latter it is equal to $AS/2$. In the opposite limit of narrow bands $W \ll AS$ the electron gains fully in the c - l exchange energy also in case of AF ordering, but on the other hand its band width turns out to be of the order of W^2/AS , i.e. in the limit $AS \rightarrow \infty$ it no longer can go over from atom to atom at all. In case of FM ordering its bandwidth is W , i.e. its minimum energy is $W/2$ lower than in case of AF ordering.

Formula (3.2.12) has been obtained under the assumption that the conduction electron does not affect the magnetic order in the crystal, i.e. AFS is regarded as an ideally-ordered two-component alloy. Actually the electron in the process of its motion about the crystal alters the magnetic order. It will be demonstrated below that in many cases this greatly reduces the energy of the system. Various mechanisms of conduction electron motion in the crystal are possible, which are accompanied by the disruption of AF ordering in the region where the electron is located. Accordingly, we may speak of different types of charge-carrier states in AFS. Which of them will materialize in a specific material will depend on its parameters. Obviously, at $T \rightarrow 0$ there should be a charge-carrier energy minimum to correspond to the materialized charge-carrier state.

One of the quantum numbers that may be used to classify the carrier state in an AFS at $T = 0$ is the total angular momentum of the crystal + conduction electron system. We shall study in this section a case when the appearance of a charge carrier in the crystal alters the total spin of the system only by an amount equal to the carrier spin (i.e. it turns equal to $1/2$ because of the AF crystal total spin being zero).

The carrier state is determined by the quantity AS/W and by the sign of the c - l exchange integral A . In case of wide bands $AS/W \ll 1$, we may take into account the interaction of the c -electrons with

* Materials with an abnormally weak intraband c - l exchange of the type discussed in Sec. 4.2 are not considered here.

the l -spins by making use of the perturbation theory. The part of the perturbation Hamiltonian is played by the c - l exchange Hamiltonian H_A (3.4.2) in which formulae (2.6.3) have been used to effect the transformation to spin deviation operators, and subsequently formula (2.6.6) has been used to effect the transformation to magnon creation and annihilation operators. The electron energy spectrum that one obtains by taking into account terms in the Hamiltonian H_A not containing magnon operators is given by expression (3.2.6) with $\mathbf{q} = \Pi$. These terms introduce essential changes into the nature of the spectrum only near the resonance values of \mathbf{k} for which $E_{\mathbf{k}} \simeq E_{\mathbf{k}-\Pi}$. However, this region of the \mathbf{k} -space is of no interest in case of semiconductors, since it corresponds to the centre of the conduction band. At the same time in the vicinity of its extrema the part played by these terms reduces to that of corrections $\sim A^2 S^2 / W$. This refers to the relative downward shift of the conduction band bottom and the growth in the carrier effective mass.

The terms of the Hamiltonian H_A linear in magnon operators resemble the Hamiltonian of interaction of the electrons with optical phonons (1.4.1). However, the coupling constant of the electron with long-wave magnons (an analogue of c_q), because of the small length of the c - l exchange interaction, has no singularities at small momenta \mathbf{q} . Accordingly, the "polaron shift" of the electron energy occasioned by its interaction with virtual magnons (an analogue of expression (1.4.7)) in the case being considered remains, in contrast to the polaron in the polar crystal, finite for $\omega \sim \gamma \rightarrow 0$ as well. If we take into account formulae (2.6.11), we will obtain for it the order $A^2 S / W$, i.e. $\sim 1/5$ from the shift due to AF ordering of stationary spins (3.2.6, 12). The term of electron-magnon interaction quadratic in magnons yields a shift of a still higher order in $1/S$.

In the case of helicoidal ordering the situation may be quite different, as has already been discussed in Sec. 3.2. Namely, if the helicoid vector \mathbf{q} is small in comparison with the spinpolaron vector \mathbf{q}_0 , the gain in the c - l exchange energy will be almost equal to $AS/2$ [163]. There will be a similar situation in the case of many-valley semiconductors, if the helicoid vector is almost equal to the separation between equivalent maxima of the conduction band in the \mathbf{k} -space [584].

If in the case $W \gg AS$ the effect of AF ordering on the carrier state is small, the interaction of the electron with the magnons playing an even smaller part, in the opposite limit of narrow bands $W \ll AS$ the latter will be of decisive importance for the nature of carrier motion in the crystal. The physical picture depends essentially on the sign of the c - l exchange integral A . It will be discussed in what follows.

The Case of a Negative c - l Exchange Integral. This case has been first analyzed in [157] within the framework of the Hubbard model,

and subsequently a more detailed analysis has been presented in [158, 159, 73] within the framework of the c - l exchange model (as has been already pointed out in Sec. 3.1, the Hubbard model in the semi-conducting limit corresponds to a particular case of the c - l model with $A < 0$, $S = 1/2$). The quantitative picture is best explained with the aid of the Hubbard model (Fig. 5.1).

Let the charge carrier (an excess electron) initially be located on the atom $(0,0)$, and the AF ordering in the crystal be undisturbed

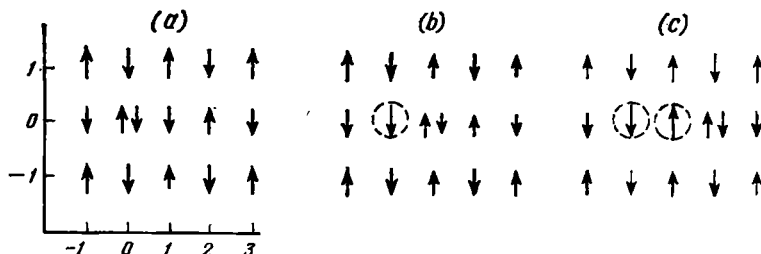


Fig. 5.1. A quasi-oscillator for $A < 0$

(Fig. 5.1a). One of the electrons can move from the $(0,0)$ -atom to the neighbouring $(1,0)$ -atom. This will be the electron whose spin is opposed to that of the $(1,0)$ -atom. In the result the spin of the $(0,0)$ -atom vacated by the excess electron will point in the direction opposite to that of the sublattice to which the atom belongs (it is encircled in Fig. 5.1b). In terms of the c - l model, a magnon has been created on the $(0,0)$ -atom. In the same way the transition of an excess electron from the $(1,0)$ -atom to the $(2,0)$ is accompanied by the reversal of the spin of the $(1,0)$ -atom (Fig. 5.1c). Each such reversal increases the energy of the system (the first by $(z-1) |J| S$, the second and the subsequent by $(z-2) |J| S$).

Hence, the spins of all atoms lying on the path of electron motion are reversed, the number of the reversed spins increasing as the number of steps in the path grows. The magnetic energy of the system grows proportionally. Return of the charge carrier along its path removes the reversed spins. This is equivalent to the existence of a quasi-elastic force tending to return the electron to the $(0,0)$ -atom. For this reason the electron must oscillate about the central $(0,0)$ -atom.

Such a state has been termed *quasi-oscillator state* [157]. This is a novel type of a carrier state distinguished from the polaron state by the degree of deformation of the periodic structure oscillating with the electron about the equilibrium position. Formally, this is a corollary of the absence in $H_{<}$ (3.5.19b) of the term $\sim \alpha_g^* \alpha_{g+\Delta}$ describing the motion of free spinpolarons, and of the nonlocality of the spin-

polaron-magnon interaction Hamiltonian (3.5.19b), i.e. of the presence in it of terms of the type of $b_{\mathbf{g}}^* - \Delta a_{\mathbf{g}}^* a_{\mathbf{g}+\Delta}$ off-diagonal in the electron coordinates. It is instructive to compare (3.5.19b) with the Hamiltonian of the electron-phonon interaction (1.4.1) which has the structure of the type of $b_{\mathbf{r}}^* a_{\mathbf{g}}^* a_{\mathbf{g}}$ in the site representation independently of the concrete form of quantities $c_{\mathbf{g}}$, i.e. it is diagonal in the electron coordinates. The nonlocality of the Hamiltonian (3.5.19b) obtained from the local Hamiltonian (3.1.1) is a consequence of its being valid only for certain ratios of the parameters of the problem, i.e. the set of eigenfunctions corresponding to it is incomplete.

As follows from (3.5.19b) the effective Bloch integral in this case is $B\sqrt{2S(2S-1)}$. Thus, for $|B| \gg |J|S^2$ the minimum energy of the quasi-oscillator when its centre remains at rest turns out to be close to $-W\sqrt{2S(2S-1)}$, i.e. comparable to the minimum band-state energy ($-W/2$). The minimum energy of the electron, obtained for fixed l -spins is appreciably higher: according to (3.2.12), it is of the order of $W^2/4S$. Various approximations were used in [73, 158, 159] to estimate the minimum quasi-oscillator energy more accurately.

If one takes into account zero-point oscillations of the spins of magnetic atoms and closed paths, he will find that it is possible for a quasi-oscillator to move about the crystal [158, 159]. However, the quasi-oscillator energy-band width is very small, being in typical conditions of the order of the magnon one.

After the paper [157] has been published, a similar problem has been analyzed within the framework of the Hubbard model in [97, 98, 160]. But only electron density-of-states moments have been calculated in them and no account taken of quasi-elastic forces appearing in the result of spin reversal along the path.

The Case of a Positive c - l Exchange Integral. The situation is completely different when $A > 0$. In this case, according to (3.5.19a) the transition of an electron to a neighbouring atom produces a spin deviation not on the atom vacated by the electron, but on the new host atom. Indeed, let the spin projection of atom I be S , and that of the neighbouring atom II be $(-S)$, and let the electron with $\sigma = 1/2$ initially be located on the atom I (Fig. 5.2a). Then the total spin of this atom equal to $S + 1/2$ will point precisely up. After an electron has gone over to atom II (Fig. 5.2b), the spin of atom I will as before point precisely up, the total spin of atom II deviating from the down direction: its magnitude being $S + 1/2$, its projection will be equal to $(-S + 1/2)$ owing to the conservation of the spin projection of the system in the course of an electron transition. In the course of a reverse transition the spin of the atom II returns to its former state. But it will return to its former state in exactly the same way, if the electron from atom II goes over not to atom I ,

but to another nearest neighbour whose spin is parallel to that of spin I . Thus, in a simplified form the mechanism of carrier motion in a crystal is as follows. On the atoms of sublattice I the electron spin is parallel to the sublattice moment. Its transition to an atom of sublattice II is accompanied by the creation in it of a magnon and by the disappearance of the magnon after the electron has returned

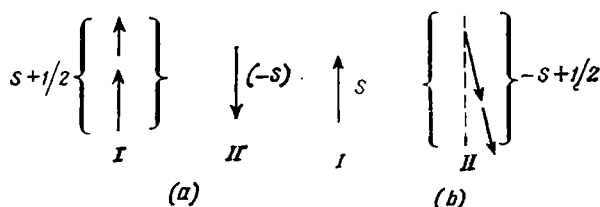


Fig. 5.2. A quasi-oscillator for $A > 0$

to sublattice I . The energy spent to create the magnon may be neglected on account of the condition $|J| S^2 \ll |B|$. Accordingly, the carrier energy spectrum with regard to (3.5.19a) will be given by a dispersion law of the form of (1.1.1), but with a $\sqrt{2S+1}$ -times narrower bandwidth:

$$E_{\mathbf{k}} \simeq \frac{zB\gamma_{\mathbf{k}}}{\sqrt{2S+1}}. \quad (5.1.1)$$

In a more accurate consideration one should take into account that besides transitions from atom II to atom I accompanied by the restoration of the spin, transitions in which the deviation of the spin on atom II is preserved and a spin deviation on atom I is induced are also possible. Such transitions result in the superposition on the carrier motion of oscillations similar to those in the case of $A < 0$. However, they play in this case a much less important part, increasing the carrier effective mass not more than by 25% [158, 159, 73]. The carrier spectrum is doubly-degenerate, since the electron spin may be parallel not to the moment of the sublattice I , but to that of the sublattice II .

Thus, on account of the magnons taking part in carrier motion in the crystal, the carrier spectrum turns out to be quite different from what it should have been in the assumption of static spins of magnetic atoms (i.e. from (3.2.6)). In particular, for $A > 0$ and for realistic spin values the effective mass of a quasi-particle (of a quasi-oscillator) is only $\sqrt{2S+1}$ times that of a band electron, the carrier ground state energy

$$E_{\min} = -\frac{AS}{2} - z|B|/\sqrt{2S+1} \quad (5.1.2)$$

being much lower than one would have obtained from (3.2.6), (3.2.12).

5.2. FERRON STATES OF FREE CARRIERS

In many instances states other than the quasi-oscillator ones described in Sec. 5.1, namely ferron states, prove to be more energetically favoured*. To explain their nature, one should first of all recall that, according to the results of Sec. 3.2, the conduction electrons tend to establish and maintain FM ordering in the crystal, because it guarantees the minimum electron energy. Accordingly, in an AFS with a high enough carrier concentration n an FM ordering should be established. However, in case the concentration is not high enough to turn the whole crystal into an FM, it is still possible to gain in the energy by making all the electrons concentrate in some part of the crystal, turning it into an FM. For instance, a single electron can establish an FM microregion and become self-trapped in it. The energy spent to reverse the l -spins is compensated by gains in the electron energy, since an FM microregion acts as a potential well for an electron in AFS**. In principle, an electron together with an FM region can move about the crystal, but in actual conditions the mobility of such a system is extraordinarily small, and it may be considered to be at rest (the total spin of an FM region is so great that it may be regarded as a classical object).

The complexes of the type "an electron + a microregion of another phase produced by the electron in the crystal" whose existence has originally been proved in [194, 195] constitute quasi-particles of quite a different type than the polaron. Such quasi-particles are destroyed at sufficiently high temperatures, but if the depth of the potential well is great enough, they can exist even in the PM region. Further analysis of electron autolocalization in ferromagnetic regions is the subject of [204-209, 426, 579-581, 583].

At sufficiently high temperatures FM microregions appear as a result of thermal fluctuations even in the absence of conduction electrons. The number of fluctuations capable of electron trapping may prove to be higher than the number of electrons. Because of that it is no longer necessary for an electron to create for itself a microregion of an FM phase, i.e. the localization of the electron in such fluctuations is of the same type as the Anderson localization in nonperiodic structures (see Sec. 1.2). The trapping of electrons by thermal fluctuations is possible not only in AFS, but also in FMS, Methfessel and von

* In the original papers [194, 195] an inappropriate term "magnetic polaron" has been used to describe such states.

** Worth mentioning is a special situation possible in anomalous FMS displaying a blue shift of the optical absorption edge (Sec. 4.2). The fact that in them the conduction band bottom sinks when FM ordering is destroyed creates a principal possibility for the appearance of "antiferron" states of the conduction electron. Characteristic of them is that condition electrons set up in an FMS regions with disrupted FM (e.g. AF) ordering and stabilize them by localizing themselves in them [384].

Molnar [162] being the first to draw attention to this point. We would like to point out that especially favourable conditions for this exist in quasi-two-dimensional and quasi-one-dimensional magnetic systems where thermal fluctuations are especially large. Thus, for example, in an Ising two-dimensional magnet the correlations between the spins at T_c diminish with increased separation between the spins R as $R^{-1/4}$, while at the same time in the three-dimensional case they diminish at a much greater rate as R^{-1} . As a rule, in isotropic three-dimensional crystals the autolocalization of carriers is

much more probable than their Anderson localization.

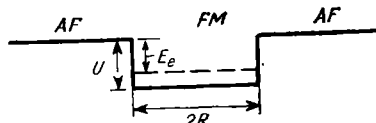


Fig. 5.3. Ferron state in an antiferromagnet

in this parameter. If we retain only the leading terms in ASW , we may regard the electron in an AF portion of the crystal as a normal band-electron. Inside an FM region the energy of an electron with a spin direction most energetically-favoured shifts downward as compared to that in an AFS by the amount $U = |A|S/2$. Hence, an FM region represents an AS 2-deep potential well for the conduction electron.

The greater the volume of the FM region the lower is the electron energy E_e of the electron trapped by it. But on the other hand the energy of the exchange between magnetic atoms grows with dimension of the FM region: the creation of the FM region inside an AFS requires an energy E_M proportional to its volume and to the integral \mathcal{J} of the exchange between the nearest neighbours. The electron ground state is obtained from the condition that the total energy of the system $E_e + E_M$ be minimum. It follows from symmetry considerations that for a specified volume of the FM region the electron level in the potential well E_e will lie lowest of all, if the region is spherically shaped (Fig. 5.3).

If the radius of the potential well R is large as compared to the lattice parameter, we may make use of the effective mass method (Sec. 1.2) to describe the electron state. In this approximation the electron energy is obtained from the well-known solution of the problem of an electron in a spherical potential well [75], the electron effective mass being substituted for its true mass. The expression for the ferron energy measured from the minimum energy of the system with the undisturbed AF ordering is as follows:

$$E(k) = -U + \frac{k^2}{2m^*} + \frac{4\pi}{3} D \left(\frac{R}{a} \right)^3, \quad (5.2.1)$$

where D is the l -spin interaction energy spent to reverse one spin. For a Heisenberg AFS $D = |\mathcal{Y}| S$. The parameter k is related to the radius by means of the usual expression [75] obtained from the matching condition for expressions for the electron wave function outside and inside the potential well at the boundary $|\mathbf{r}| = R$:

$$\begin{aligned} \frac{2}{\pi} k R_{\min} &= \sin kR, \quad \pi/2 < kR < \pi, \\ R_{\min} &= \frac{\pi}{2} [m^* AS]^{-1/2} = \frac{\pi}{2\sqrt{2}} q_0^{-1}, \end{aligned} \quad (5.2.1a)$$

where R_{\min} is the minimum radius of the potential well at which a level appears in it (it is almost equal to the inverse spinpolaron wave vector q_0^{-1} (Sec. 4.2), i.e. in actual conditions it certainly exceeds the lattice parameter). The equilibrium radius of the FM region is obtained from the condition that the total energy of the system be minimum (5.2.1), i.e. from the equation:

$$\frac{dE}{dR} = 0. \quad (5.2.2)$$

It must obviously exceed R_{\min} . Indeed, for $R = R_{\min}$ the electron level coincides with the conduction-band bottom, i.e. there is as yet no gain in the electron energy following the creation of an FM region, while at the same time a magnetic energy $\sim R_{\min}^3 D$ has already been spent to create it. The electron level must sink in the well to compensate for the magnetic energy. Hence, in the case $W \gg AS$ only large ferron states are possible.

Instead of seeking the total energy minimum (5.2.1) in R , it is technically more expedient to seek its minimum in k , taking account of the relationship existing between k and R (5.2.1a) and introducing the parameter $x = kR_{\min}$. Then the condition of the minimum will take the form:

$$\begin{aligned} \frac{1}{x} \frac{d}{dx} \mathcal{F}(x) &= -\frac{3a^5}{2\pi R_{\min}^5} \left| \frac{B}{D} \right|, \\ \mathcal{F}(x) &= \left[\frac{\pi - \arcsin \frac{2}{\pi} x}{x} \right]^3 = \left(\frac{R}{R_{\min}} \right)^3, \end{aligned} \quad (5.2.3)$$

where the values of $\arcsin \varphi$ should be taken for the first quarter (the effective mass is expressed in terms of the Bloch integral with the aid of (1.1.5)). Putting in expression (5.2.1) $E(R) < 0$ and making use of (5.2.3), one easily obtains the condition of stability of large ferron states:

$$\Phi(x) = \mathcal{F}(x) - \frac{x}{2} \frac{d}{dx} \mathcal{F}(x) \leq \frac{3}{4\pi} \frac{a^3 U}{R_{\min}^3 D}. \quad (5.2.4)$$

Since k diminishes with increasing R , $d\mathcal{F}/dx$ is negative, and the function $\Phi(x)$ in (5.2.4) is a positively determined one. Its minimum lies at the point $x_0 = 1.51$ and is equal to $\Phi(x_0) = \Phi_0 = 9.8$. Hence, for equation (5.2.4) to have a solution, the inequality [200] must be satisfied

$$D \leq D_c \equiv 0.2W \left(\frac{U}{W} \right)^{5/2}. \quad (5.2.5)$$

The solution of (5.2.1) can be obtained in an explicit form only for $R \gg R_{\min}$ ($x \ll 1$):

$$R = a \left[\frac{\pi}{2} \left| \frac{B}{D} \right| \right]^{1/5}, \quad E = -U - \frac{5}{3} \pi^{3/5} |B|^{3/5} D^{2/5}. \quad (5.2.6)$$

An interesting point is that, according to (5.2.6) the maximum gain in the c - l exchange energy equal to $AS/2$ is obtained already for small AS/W (AS does not enter the second term in the expression (5.2.6) for E). The situation in the case $R \gg q_0^{-1}$ is similar to that discussed in Sec. 3.2: if the local moment varies appreciably at distances long as compared with $q_0^{-1} \simeq R_{\min}$, the electron will gain fully in the c - l exchange energy even when the crystal has no mean moment.

If formula (2.6.13) is taken into account, it follows from equation (5.2.6) that for typical values of parameters $AS/2W \simeq 0.1$, $W \sim \sim 3$ eV ferrons can exist, at least, at $T \rightarrow 0$ in an AFS with $T_N \leq 10$ K, e.g. in EuTe. The radius of an FM region is equal to 2-3 lattice parameters, so that the ferron moment may be as high as several hundred atomic moments.

In metamagnets where the energy spent to establish an FM region is very small, ferron states of much larger radii are possible. An especially interesting situation exists in EuSe. In it in addition to an FM ordering requiring an energy of $D \sim 10^{-5}$ eV (per atom) the ferrimagnetic (FIM) ordering is also possible, the energy required for it being by an order of magnitude less (Fig. 2.5). In this case the ferrons have a more intricate structure: an FM sphere in the centre is enveloped in a FIM shell. The radius of the FM spheres for the parameters stated above, according to formula (5.2.6), will be equal to about ten lattice parameters [198]. Accordingly, the moment of such a complex ferron may be as high as several thousand atomic moments. Remembering that the spin of Eu^{++} is $7/2$, we obtain that the minimum carrier energy is attained when it induces in the AFS a moment four orders of magnitude greater than the electron spin*.

According to data depicted in Fig. 2.5, inside the interval 1.8-2.8 K the compound EuSe resides in the FIM state. The moment of

* A theory of ferrons in isotropic metamagnets with a strong volume dependence of the exchange integral discussed in Sec. 2.3 has been developed in [399]. For parameters corresponding to those of EuSe, an estimate close to one obtained in this section is obtained for the ferron radius.

the FIM phase corresponds to an atomic spin of 0.75 (Sec. 2.6). Accordingly, the c - l shift in it is five times smaller than in the FM phase, and autolocalization of an electron in an FM region inside a FIM phase is possible [198].

The ferrons are destroyed in strong magnetic fields, fields weaker than the magnetic saturation fields $\mathcal{H}_F = 2 | \mathcal{Y} |$ (2.3.6) being required for it. The ferron moment can naturally be presumed to align with the field, the vector of antiferromagnetism \mathbf{l} (Fig. 2.4) being orthogonal to it. The depth of the potential well diminishes in a field $(1 - \cos \theta)$ times, where θ is the angle between the field and the AFS sublattice moments as given by expression (2.3.6). At the same time the energy spent to create an FM microregion equal for $\mathcal{H} = 0$ to $D = | \mathcal{Y} | S$ per atom diminishes $(1 - \cos \theta)^2$ times. This follows from the circumstance that, according to formulae (2.3.5, 6), the energy of the AF ordering in the presence of a field diminishes by $| \mathcal{Y} | S \cos^2 \theta$, and of the FM ordering by $(\mathbf{S} \cdot \mathbf{H}) = (2 | \mathcal{Y} | S \cos \theta)$ (per atom). Substituting $D (1 - \cos \theta)^2$ for D and $U (1 - \cos \theta)$ for U into expression (5.2.5), we obtain the critical ferron dissociation field [200]

$$\mathcal{H}_c = \mathcal{H}_F \left[1 - \frac{25 D^2 W^3}{U^6} \right]. \quad (5.2.7)$$

The condition of stability of the ferron state for $\mathcal{H} = 0$ can be obtained from formula (5.2.7) by equating the ferron dissociation field to zero. The lower the ferron energy, the greater is the field required to destroy it. In metamagnets the ferron state is destroyed at fields at which an AF ordering abruptly turns into an FM one.

Less favourable are the conditions for the materialization of ferron states in highly anisotropic AFS with a layered ordering [198].

Ferrons at High Temperatures. As the temperature rises, the ferrons dissociate, the dissociation temperature possibly exceeding T_N . The ferron stability conditions at finite temperatures are obviously determined not by the condition that the energy of the system be minimum, but by the condition that its free energy be minimum. For $AS \ll W$ the results (5.2.5, 6) at $T = 0$ can be easily generalized for a PM region. To this end it is sufficient to substitute in them the loss in the free energy per atom F incurred in the creation of an FM microregion for the loss in the magnetic energy per atom D . To find F , one may conveniently make use of the familiar thermodynamic relationship connecting the free energy with the average energy $E_M(T)$ [246]:

$$E_M = - T^2 \frac{\partial}{\partial T} \left(\frac{F}{T} \right). \quad (5.2.8)$$

Integrating it in the limits from T to ∞ and taking into account that F tends to $-T \ln(2S + 1)$ at $T \rightarrow \infty$, we obtain

$$F(T) = -T \ln(2S + 1) + T \int_T^\infty \frac{E_M(\tau)}{\tau^2} d\tau. \quad (5.2.9)$$

According to (2.1.5), in the nearest neighbour approximation the energy per atom is given by the expression

$$E_M(T) = -\frac{J_z}{2} \langle \mathbf{S}_0 \cdot \mathbf{S}_\Delta \rangle. \quad (5.2.10)$$

According to formulae (5.2.9, 10), if the temperature dependence of the spin correlation function for nearest neighbours $\langle \mathbf{S}_0 \cdot \mathbf{S}_\Delta \rangle$ is known, this suffices to make the calculation of the free energy of an AFS possible. To evaluate the correlation function, we may make use of the high-temperature expansion method (Sec. 2.5):

$$\begin{aligned} \langle \mathbf{S}_0 \cdot \mathbf{S}_\Delta \rangle &= \text{Sp} \left\{ (\mathbf{S}_0 \cdot \mathbf{S}_\Delta) e^{-\frac{H_M}{T}} \right\} / \text{Sp} \left\{ e^{-\frac{H_M}{T}} \right\} \\ &\simeq -\frac{1}{T} \frac{\text{Sp} \{ (\mathbf{S}_0 \cdot \mathbf{S}_\Delta) H_M \}}{\text{Sp} 1} = -\frac{J_z S^2 (S+1)^2}{T}. \end{aligned} \quad (5.2.11)$$

The difference between the FM ordering energy and the free energy of the AFS at $T \gg T_N$ (5.2.9-11) should be substituted for D in formulae (5.2.5, 6):

$$\begin{aligned} D(T) &= -\frac{J_z S}{2} - F(T) \\ &= T \ln(2S + 1) + \frac{J_z^2 (S+1)^2}{4zT} - \frac{J_z S}{2}. \end{aligned} \quad (5.2.12)$$

Taking into account the expression for the Néel temperature (2.6.13), we obtain for the relationship connecting $D(T_N)$ with $D = | \chi | S$ the expression

$$D(T_N) = D \left[\frac{S+1}{3S} \ln(2S + 1) + \frac{S+1}{8S} + \frac{1}{2} \right], \quad (5.2.13)$$

i.e. $D(T_N)$ for $S = 7/2$ exceeds D by about 60%. As the temperature continues to rise, $D(T)$ continues to grow. For this reason the ferron state is no longer a thermodynamically favourable one. The ferron dissociation temperature is found by equating $D(T)$ to D_c in formula (5.2.5). For $W = 3$ eV, $1S/2W \sim 0.1$ and $T_N \simeq 10$ K (the parameters of EuTe) it should be close to T_N .

Ferron states are evidently possible not only in AFS, but in FMS at high temperatures as well, when the FM ordering is sufficiently disrupted. The most favourable conditions for electron trapping by fluctuations of magnetization can naturally be expected to exist in the region of the Curie point. However, one should keep in mind the

result obtained in Sec. 4.3: long-wave fluctuations especially prominent in the vicinity of the Curie point are unable to trap an electron, because its spin follows local magnetization variations. Such a spin adjustment results in a substantial gain in the c - l exchange energy comparable to that at $T = 0$ even without the electron self-trapping. Of course, this appreciably handicaps the autolocalization. Nevertheless, in principle, crystals may exist in which autolocalization would be thermodynamically favourable.

The appropriate criterion is established with the aid of formulae (5.2.5), (5.2.12) where U in formula (5.2.5) should be taken to mean the shift of the conduction-band bottom at the specified temperature with respect to its position at $T = 0$. The critical value D_c for which the existence of a ferron is possible will be seen from formula (5.2.5) to be very sensitive to U . If one assumes it in accordance with (4.2.4) to be equal to $4kT_c \approx 3R/2$, this will result in an appreciable overestimate of the ferron existence probability at T_c . For instance, U at the Curie point $T_c = 16$ K will be seen from experimental data on EuS (Fig. 4.2) to amount only to $2/3$ of $4kT_c$. Accordingly, the critical value D_c turns out to be $(3/2)^{1/2} \approx 1.5$ times less than one would have obtained from formula (4.2.4). Putting $W = 3$ eV, which value corresponds to an electron effective mass equal to the true mass, and taking for $U(T_c)$ the experimental value of 0.12 eV, we obtain $D_c = 2 \times 10^{-4}$ eV, whereas, if formulae (5.2.12) and (2.5.3) are taken into account, an order-of-magnitude larger value will be obtained for $D(T_c)$. For this reason the fluctuations of magnetization in EuS should hardly be expected to trap the electrons. This is still more true of EuO for which T_c lies substantially higher.

The same conclusion has been arrived at in [206] despite the fact that in it, as well as in [204-209, 426], (4.2.4) was used for the band bottom. For this reason, as has already been pointed out, the ferron existence probability has been overestimated in these papers. Even were we to put $U = 0.3$ eV, we would obtain that for the parameters presumed above the existence of ferrons may be possible only in crystals with $T_c \ll 5$ K. However, in contrast to results of [206] etc., the above consideration shows that the most favourable conditions for electron autolocalization exist not at the critical point, but above it in the range $T_c < T < 2T_c$ where not only the long-range, but also the short-range order is destroyed.

The trapping of electrons by fluctuations of magnetization has been suggested by von Molnar and Methfessel [462] as an explanation for the existence of a resistivity peak in FMS near the Curie point. However, as demonstrated by experimental data presented in Secs. 4.7 and 7.7, the behaviour of the resistivity in the vicinity of T_c is greatly influenced by the degree of crystal imperfection. The photoconductivity of EuS depends on the purity of the crystal and does not exhibit a noticeable minimum near T_c in pure crystals. There is similarly no

photoconductivity minimum in EuO (Figs. 4.16, 4.17) These data support the theoretical results obtained above, according to which no free carrier trapping by magnetization fluctuations takes place in EuS and EuO.

The case of electrons localized due to impurity of the potential differs from the case of free electrons very strongly. The localized state of an electron on a donor at finite temperatures differs from the state at $T = 0$ in that the degree of FM order around the donor is greater than on the average in the crystal. Accordingly, such a state may be regarded as a localized ferron state. The decrease in the carrier concentration as T_c is approached from the low-temperature side, which has been interpreted in Sec. 4.5 in terms of an increase in the depth of the local level is nothing but the transition of the electrons to localized ferron states which unlike free ferron states exist in any FMS at any temperature.

As to the AFS, there are experimental data in support of the existence of free ferrons in EuSe and EuTe (Sec. 5.4). The theory of localized ferrons in such materials will be developed in Sec. 5.3.

Since any two-dimensional potential well of arbitrarily small radius possesses at least one discrete energy level, the conditions for the existence of surface ferrons are much more favourable than for the existence of bulk ones, which are possible only at $R > R_{\max}$. If the crystal energy spectrum contains a surface conduction band lying below the bulk band, for parameters stated above the ferrons can be stable up to temperatures ~ 100 K, i.e. they may exist even in such high-temperature FMS as EuO [539]. In [545] ferrons in many-valley semiconductors have been studied where their structure is more complex than in single-valley semiconductors discussed above.

Ferrons in Narrow-band Semiconductors. If the inequality $AS \ll W$ is not satisfied, it is possible to consider the problem of ferron states correctly only for AFS at $T \ll T_N$, since we do not know anything about the states of free charge carriers in MS at high temperatures*. In some cases one is able even without a detailed calculation to conclude that free ferrons cannot form. This probably is the case with CdCr_2Se_4 : the red shift of the absorption edge that determines the depth of the potential well is small in it (~ 0.1 eV), T_c determining the energy required to create an FM region being on the contrary high (~ 0.01 eV).

Since the calculation results for $W \sim AS$ are very cumbersome, we shall present below the calculation of a ferron in AFS in the limit

* For a more detailed criticism of papers dealing with the calculation of ferrons in FMS with $AS \geq W$, see [73]. In particular in some of them too favourable conditions for the materialization of ferrons in FMS with $AS \gg W$ are obtained owing to an erroneous proposition that at $T > T_c$ the conduction band-width in FMS is infinitesimal. Actually, even at $T \rightarrow \infty$ it is only 30% smaller than at $T = 0$ (Sec. 4.1).

$W \ll AS$ [195]. Consider first the case $A > 0$. According to (5.1.1), an FM microregion constitutes a potential well for a charge carrier (a spinpolaron) of the depth

$$U = z |B| \left[1 - \frac{1}{\sqrt{2S+1}} \right], \quad (5.2.14)$$

the spinpolaron effective mass in the AF portion of the crystal being $\frac{1}{2S+1}$ times larger than in the FM portion. The peculiarity of the case of narrow bands consists in the possibility of the electron being trapped not only by an FM microregion, but by an individual atom whose spin is reversed with respect to the moments of its sublattice as well. In this case the effective mass approximation is unsuitable. On account of that we shall explain the calculation for the case $W \ll AS$ in more detail.

As before, we shall make use of the direct variational principle. When constructing a trial wave function, we presume the atomic spins of sublattice *II* in the microregion of radius R to be reversed with respect to the direction of the moment of their sublattice, i.e. to point in the direction of the moment of sublattice *I*. The spin of the c -electron is assumed to be parallel to the spins of atoms of sublattice *I* and atoms of sublattice *II* inside the FM region. But the electron transitions to atoms of sublattice *II* outside the FM region are accompanied with creation of magnons on them according to (3.5.19a). For this reason the trial function is chosen in the form

$$\psi = \left\{ \sum_{\mathbf{g}_1} \psi(\mathbf{g}_1) \alpha_{\mathbf{g}_1}^* + \sum_{|\mathbf{g}_2| \leq R} \psi(\mathbf{g}_2) \alpha_{\mathbf{g}_2}^* + \sum_{|\mathbf{g}_2| > R} \psi(\mathbf{g}_2) \alpha_{\mathbf{g}_2}^* b_{\mathbf{g}_2}^* \right\} |R\rangle, \quad (5.2.15)$$

where $|R\rangle$ is a wave function that plays the part of the vacuum wave function for a spinpolaron and for magnons and that corresponds to the above-mentioned spin configuration. The indices \mathbf{g}_1 and \mathbf{g}_2 denote atoms belonging to sublattices *I* and *II*, respectively. The possibility that the atomic states in the antiferromagnetic region can be limited to those with one l -spin deviation in sublattice *II* follows from the results [73, 158, 159] cited in the preceding section, according to which the states with a greater number of deviated spins per atom little affect the energy of the system.

In the FM microregion $|\mathbf{g}| < R$ the system is described by the Hamiltonian (3.5.18a) and outside it by the Hamiltonian (3.5.19a). Substituting the wave function (5.2.15) into the Hamiltonian of the system, we obtain the following equations for the coefficients $\psi(\mathbf{g})$ sought ($E_e(R)$ is the spinpolaron energy for a specified R):

$$(-E_e) \psi(\mathbf{g}) + B \sum_{\Delta} \psi(\mathbf{g} + \Delta) = 0, \quad (5.2.16)$$

$$(-E_e) \psi(\mathbf{g}) + \frac{B}{\sqrt{2S+1}} \sum_{\Delta} \psi(\mathbf{g} - \Delta) = 0. \quad (5.2.17)$$

The former of these sets of equations refers to the FM region, and the latter to the AF region. The condition $|B| \gg |J|S^2$ was taken into account when (5.2.17) was written.

For $R \gg a$ we can use the continuous-medium approximation. To this end we must regard the amplitudes $\psi(\mathbf{g}_1)$ and $\psi(\mathbf{g}_2)$ as components of spinor wave functions $\psi_1(\mathbf{r})$ and $\psi_2(\mathbf{r})$, respectively. The expansion of these functions into a Taylor series enables us to rewrite the sets (5.2.16, 17) in the form

$$(-E_e)\psi_i(\mathbf{r}) + B[z + a^2\Delta]\psi_j(\mathbf{r}) = 0 \quad (r < R), \quad (5.2.18)$$

$$(-E_e)\psi_i(\mathbf{r}) + \frac{B}{\sqrt{2S+1}}[z + a^2\Delta]\psi_j(\mathbf{r}) = 0 \\ (r > R), \quad i, j = 1, 2 \quad (i \neq j). \quad (5.2.19)$$

The boundary conditions for $r = R$ can be found from the fact that an atom from sublattice I on the boundary belongs simultaneously to an FM and to an AF phase, i.e. the logarithmic derivative of $\psi_1(\mathbf{r})$ must be continuous at $r = R$. Representing $\psi_1(\mathbf{r})$ as a spherical wave with real wave number k in the FM region and with an imaginary wave number iz outside it, we obtain from (5.2.18, 19) a transcendental equation for the energy of the system, coinciding with (5.2.1a, 3), if the depth of the potential well U is put equal to (5.2.14), and the expression

$$R_{\min} = \frac{\pi}{2} a [z(\sqrt{2S+1}-1)]^{-1/2} \quad (5.2.20)$$

is taken for R_{\min} . If we make use of formulae (5.2.14, 20) for U and R_{\min} , the condition for the existence of a ferron (5.2.5) and formulae (5.2.6) for its energy and its radius for $R \gg R_{\min}$ will remain in force. It follows from (5.2.5, 6) that for typical values of the parameters $B \sim 0.1$ eV, $S = 3$, $JS \sim 0.001-0.01$ eV the radius of an FM microregion is $\sim 2-3a$, this justifying the use of the continuous-medium approximation. The conditions for the existence of a ferron can easier be met with large S . Thus, for $W \sim 0.5$ eV they may materialize at $T_N < 40$ K, if $S = 7/2$, but only at $T_N < 8$ K, if $S = 1$.

In cases when the ratio JS/B is not as small as required for the radius of an FM microregion to exceed the lattice parameter, another approach should be chosen [70, 73]. If only the spin of the $\mathbf{g} = 0$ atom is reversed, we may still use the wave function (5.2.15), putting in it $R = 0$. Then the set of equations similar to (5.2.16, 17) will be written in the form ($\delta(\mathbf{g}, \mathbf{f})$ is the three-dimensional delta-function of a discrete argument assuming values 1 or 0):

$$z\lambda\psi(\mathbf{g}) = \sum_{\Delta} \psi(\mathbf{g} + \Delta) - \chi \sum_{\Delta} \psi(\mathbf{g} + \Delta) [\delta(\mathbf{g}, 0) + \delta(\mathbf{g}, -\Delta)], \quad (5.2.21)$$

$$\chi = \sqrt{2S+1} - 1, \quad \lambda = -E_e \sqrt{2S+1} / 6|B|.$$

Expanding $\psi(\mathbf{g})$ into the Fourier series

$$\psi(\mathbf{g}) = \frac{1}{\sqrt{N}} \sum_{\mathbf{k}} e^{-i\mathbf{k} \cdot \mathbf{g}} \psi_{\mathbf{k}},$$

we can rewrite equation (5.2.21) in the form

$$(\lambda - \gamma_{\mathbf{p}}) \psi_{\mathbf{p}} = \frac{\chi}{N} \sum_{\mathbf{k}} \gamma_{\mathbf{k}} \psi_{\mathbf{k}} + \frac{\chi \gamma_{\mathbf{p}}}{N} \sum_{\mathbf{k}} \psi_{\mathbf{k}}. \quad (5.2.22)$$

The condition for the existence of a solution of the integral equation (5.2.22) is of the form

$$[1 - \chi G_1(\lambda)]^2 = \chi^2 G_0(\lambda) G_2(\lambda), \quad (5.2.23)$$

where

$$G_n(\lambda) = \frac{a^3}{\pi^3} \int_0^{\pi/a} \frac{\gamma_{\mathbf{p}}^n d\mathbf{p}}{\lambda - \gamma_{\mathbf{p}}}. \quad (5.2.23a)$$

Equation (5.2.23a) enables Green's functions G_1 and G_2 to be expressed in terms of G_0

$$G_1 = \lambda G_0 - 1, \quad G_2 = \lambda G_1. \quad (5.2.24)$$

Then we can, using formulae (5.2.24), rewrite equation (5.2.23) in the form

$$1 + 1/2S = \lambda G_0(\lambda). \quad (5.2.25)$$

For small $\sqrt{\lambda - 1}$ the approximate solution of equation (5.2.25) is given by the expression

$$\sqrt{\lambda - 1} \simeq 0.4 [1 - 1/S]. \quad (5.2.26)$$

It follows from the equation (5.2.26) that, in particular, a ferron state of the type being considered is possible only if $S > 1$, and that its energy diminishes with an increase in S . In the limit $\sqrt{2S - 1} \gg 1$ we obtain from (5.2.25), as was to be expected, $E_e = -|B| \sqrt{z}$.

It should be pointed out that in [74] an attempt has been made to calculate the energy of a ferron with one deviated spin, the spin deviation angle being presumed to be less than π . However, this calculation cannot be accepted as a satisfactory one, there being two reasons: firstly, since the inequality $|B| \gg |A| S^2$ is always known to be satisfied, at least one spin must have been rotated through π . A much more typical situation is one with a great number of such spins ($\sim \frac{4\pi}{3} \left(\frac{R}{a}\right)^3$, where $R \sim 2-3a$). Secondly, even for one reversed spin the result of [74] based on a classical treatment of the spins is valid, as has already been noted in Sec. 3.5, only in the quite unrealistic limit $\sqrt{2S} \gg 1$.

The situation for $A < 0$ is drastically different from one consid-

ered above for $A > 0$. This is the outcome of the fact that for $A > 0$ the quasi-oscillator effective mass is of the order of the electron mass, whereas in the case $A < 0$ being considered now it is very large. This means that the electron may be presumed to be autolocalized even in the absence of an FM region. The reason that its formation may be energetically favoured is that, according to (3.5.18b), the effective Bloch integral in the FM phase is $\sqrt{2S}$ times greater than in the AF phase. But on the other hand for the ferron to be created, magnetic energy has to be spent to establish a local FM ordering, whereas no energy is required for quasi-oscillator-type motion. For this reason minimum carrier energy is attained when the latter is in a mixed ferron-quasi-oscillator state. This means that the electron is able to leave the FM region and move outside it like the quasi-oscillator. The only difference from the quasi-oscillator described in Sec. 5.1 is that the quasi-elastic force attracts the electron not to the central atom but to the boundary of the FM region. The relative weight of the ferron state in such a mixed state obviously grows with S [159]. For all spin magnitudes, the minimum radius of the FM region is the lattice constant.

Ferron-polaron States. The polarization of the ionic lattice of the crystal by the ferrons substantially improves their stability [359]. The coupling constant α of free electrons with optical phonons in semiconducting rare-earth or transition metal compounds is not large (2-3), i.e. the interaction may be described in terms of the perturbation theory (as discussed in Sec. 1.3, it is applicable up to $\alpha \simeq \simeq 6$). Hence, a free electron polarizes the lattice weakly, and the polaron shift of its energy $\alpha\omega$ (ω is the frequency of optical phonons) is small (~ 0.01 eV). However, an electron trapped by an FM region polarizes the lattice much more effectively: if the electron is practically confined in the region, the polarization energy shift E_p turns out to be of the order of e^2/ϵ^*R , where R is the radius of the FM region, e is the electron charge, $1/\epsilon^* = 1/\epsilon_\infty - 1/\epsilon_0$, ϵ_0 and ϵ_∞ being the static and the high-frequency dielectric constants of the crystal. In typical conditions E_p amounts to 0.2-0.3 eV, i.e. it is close to the difference in the minimum energies of the electron in the FM and the AF states. Consequently, such a state is in effect a mixed ferron-polaron state.

We consider here a ferron in a polarizable crystal whose conduction-bandwidth W is large as compared with the c - l exchange energy $AS/2$. The calculation is based on a method similar to one used by Pekar [60]. Such an approximation for bound polarons of an electron orbit radius not very large is valid even if α is of the order of unity [604]. The functional of the total energy of the system is of the form

$$E = \frac{1}{2m^*} \int (\nabla\psi)^2 d\mathbf{r} - \frac{AS}{2} \int_0^R \psi^2 d\mathbf{r} + E_M + E_P, \quad (5.2.27)$$

where $\psi(\mathbf{r})$ is the electron wave function, E_M is the energy required to establish a ferromagnetic microregion, m^* is the effective mass of a band electron. The expression for the polarization energy E_P is (see (1.3.2)):

$$E_P = -\frac{1}{2} \int \mathcal{P}_i \cdot \mathfrak{D} d\mathbf{r}, \quad \mathfrak{D} = -e\nabla \int \frac{|\psi(\mathbf{r}')|^2 d\mathbf{r}'}{|\mathbf{r} - \mathbf{r}'|}, \quad (5.2.28)$$

where \mathcal{P}_i is the lattice polarization, $\mathfrak{D}(\mathbf{r})$ is the electric induction vector.

The minimum value of the functional E yields the total energy of the system. To solve the problem, we make use of the variational principle, presuming an FM ordering to be established inside a sphere of radius R . The radius R plays the part of the variational parameter. The electron trial wave function ψ describes the ground state of an electron in a spherically-symmetrical potential well of radius R and constant depth $AS/2$. Thus, the wave function of an electron with an energy E_e is chosen in the form

$$\begin{aligned} \psi &= C_1 \frac{\sin kr}{r}, \quad k = \sqrt{2m^* \left(\frac{AS}{2} - |E_e| \right)} \quad (r < R), \\ \psi &= C_2 \frac{e^{-\kappa r}}{r}, \quad \kappa = \sqrt{2m^* |E_e|} \quad (r > R), \end{aligned} \quad (5.2.29)$$

where C_1 and C_2 are constants determined from matching conditions at the boundary (at $r = R$) and of normalization of the wave functions.

The maximum value $D_c = |\mathcal{P}|_{\max} S$ is obtained from the conditions that the energy E (5.2.3) and its derivative with respect to the radius R be zeros.

A numerical calculation has been carried out for europium chalcogenides: $\epsilon_0 = 9.4$, $\epsilon_\infty = 5$, $AS = 0.6$ eV, $W = 5$ eV, $a = 3 \times 10^{-8}$ cm, $\omega = 0.01$ eV, $\alpha = 4$. The electron effective mass is approximately equal to that of a free electron. In this case $|E_P| \gg \alpha\omega$, i.e. the energy of lattice polarization by a free electron can be neglected. For the maximum Néel temperature T_N^{\max} of a crystal in which the ferron is still stable at $T \ll T_N$ we obtain, taking into account (2.6.13), an estimate $T_N^{\max} \simeq 21$ K. In the absence of electron-phonon interaction $T_N^{\max} \simeq 9$ K, i.e. lattice polarization doubles the ferron stability. But at the same time it reduces the ferron moment.

One can also easily determine the maximum temperature up to which the ferron state is stable when ferrons are possible in the crystal, i.e. when the crystal Néel point T_N lies below the limiting value T_N^{\max} starting from which the ferrons exist at $T = 0$. At $T > T_N$ the free energy of the system is expressed by formula (5.2.27) in which in the term E_M the quantity $D(T)$ (5.2.12) has been substi-

tuted for D . We obtain from here that for the parameters cited above the temperature at which the ferron state is destroyed rises twice on account of the ferron being stabilized by lattice polarization and reaches 20 K. An attempt to improve the accuracy of the above calculation has been made in [536].

5.3. LOCALIZED FERRONS AND THEIR INFLUENCE ON MAGNETIC PROPERTIES OF ANTIFERROMAGNETS

The same reasons that make it possible for a free conduction electron in an AFS to establish an FM region and to become autolocalized in it make it possible for an electron localized on a donor to set up an FM region. This region should obviously take the shape of a sphere with the imperfection at its centre. Such states would naturally be termed *localized ferron states*. They can appreciably affect the magnetic properties of a crystal. Specifically, in case of large concentrations of imperfections the localized ferrons may result in a substantial increase in the initial magnetic susceptibility [195]. In the PM region they can even reverse the sign of the PM Curie point, making it positive.

In some instances the interaction between localized ferrons may produce a spontaneous magnetization in the crystal.

If the imperfection is an impurity atom, which substitutes a regular magnetic atom, there will be no symmetry with respect to variation of the direction of the ferron moment: in the ground state the ferron must be oriented in a definite direction with respect to the moment of the sublattice to which the imperfection belongs.

Unfortunately, the accuracy of the continuous-medium model used in Sec. 6.2 to calculate large ferron states is inadequate for determining the most favourable direction of the ferron moment possible. Still, in the small-ferron (only one reversed l -spin) limit it can be found immediately: the ferron moment should be collinear to the vector of antiferromagnetism \mathbf{l} (Fig. 2.4). From symmetry considerations one would expect this condition to remain in force for large ferrons as well. A field strong enough is required to break the coupling between the ferron moment and that of the sublattice. Only when such fields are attained will the moments of localized ferrons belonging to different sublattices point in the same direction. If the ferron moments are parallel to the antiferromagnetism vector, in weak field orthogonal to this vector their total moment will be proportional to the field. In case of a symmetrical arrangement of imperfections with respect to the sublattices (an anion vacancy), an arbitrarily small field at $T \rightarrow 0$ will be enough to orient all the ferron moments in the same direction.

Below we shall calculate the moment of a localized ferron for the case of wide bands $W \gg 4S$ in the assumption of an electron orbit

of a sufficiently large radius when the effective-mass method is applicable [195, 276]. The difference from the conventional problem of a hydrogen-like atom (Sec. 1.2) is in this case that the imperfection is enveloped in an FM region of radius R acting as a potential well of depth $AS/2$ for the electron. Accordingly, the electron Schrödinger equation takes the form

$$\left\{ -\frac{1}{2m^*} \Delta - \frac{e^2}{\epsilon_0 r} - \frac{AS}{2} \theta(R-r) - E_e \right\} \psi = 0, \quad (5.3.1)$$

where $\theta(x)$ is the Heaviside unity jump function, ϵ_0 is the crystal dielectric constant.

Although in principle a precise solution of equation (5.3.1) may be obtained, it will be more expedient for us to apply the variational principle. The trial wave function is chosen in the form

$$\psi = \left(\frac{y^3}{\pi a_B^3} \right)^{1/2} \exp \left\{ -\frac{yr}{a_B} \right\}, \quad a_B = \frac{\epsilon_0}{m^* e^2}, \quad (5.3.2)$$

where a_B is the Bohr orbit radius in the crystal, and y is the variational parameter.

Using formulae (5.3.1, 2), we obtain the following expression for the electron energy:

$$E_e = \left(\frac{y^2}{2} - y \right) \frac{e^2}{\epsilon_0 a_B} - \frac{AS}{2} \left\{ 1 - e^{-\frac{2yR}{a_B}} \left(1 + \frac{2R^2 y^2}{a_B^2} + \frac{2R}{a_B} y \right) \right\}, \quad (5.3.3)$$

which should be minimized in y . For $\exp \left(-\frac{2yR}{a_B} \right) \ll 1$ the approximate solution of the transcendental equation $dE_e/dy = 0$ can be found in an explicit form, and then we obtain for the equilibrium (for a specified R) electron energy

$$E_e = -\frac{e^2}{2a_B \epsilon_0} - \frac{AS}{2} + \frac{AS}{2} \left[1 + 2 \left(\frac{R^2}{a_B^2} + \frac{R}{a_B} \right) \right] \exp \left(-\frac{2R}{a_B} \right). \quad (5.3.4)$$

Making use of this formula and of the expression for the energy required to create an FM region (see (5.2.4)), we obtain for the radius of the latter an expression:

$$R = \frac{a_B}{2} \ln \left\{ \frac{AS}{2\pi D} \left(\frac{a}{a_B} \right)^3 \right\} \quad (5.3.5)$$

valid for $R > a_B$. Choosing the parameters $m^* = m_0$, $AS/2 = 0.3$ eV, $\epsilon_0 = 20$, $a = 5$ Å (so that $a_B = 10$ Å), we obtain for $D = 10^{-3}$ eV $R \simeq 1.2 a_B$, and in case of a metamagnet with $D = 10^{-5}$ eV the ra-

dus $R \approx 3.5 a_B$. In the first case the ferron moment is equal to about 60 and in the second case to about 1500 atomic moments S .

The presence of FM regions around the donors alters the nature of the interaction between the neighbouring unionized donors. Consider the case when the ferron moments are not bound to the sublattice moments. In nonmagnetic semiconductors two neighbouring donors form an analogue of the hydrogen molecule with a zero total electron spin, since this guarantees a gain in the electron exchange energy of the order of $Q^2 e^2 / a_B \epsilon_0$ where Q is the integral of overlapping of orbits of neighbouring donor atoms. Correspondingly, the average electron spin on each atom in the vicinity of donors will be zero. In an AFS such a state would not be an energetically-favoured one, since with the zero average electron spin on each magnetic atom it would not be possible to obtain a gain in the c - l exchange energy by setting up an FM energy region around the donors that could substantially exceed $Q^2 e^2 / a_B \epsilon_0$.

On the other hand, if the electron spins of neighbouring donors are parallel, and their FM regions do not overlap, the electron will gain in the c - l exchange energy not only in the microregion around its donor, but also in the microregion of the neighbouring donor, which when $R \gtrsim a_B$ the electron enters with a probability $\sim Q^2$. This additionally reduce its energy by the amount ASQ^2 , despite the fact that the energy of the exchange between the electrons rises by $\sim Q^2 e^2 / a_B \epsilon_0$. Therefore for $AS \gg e^2 / a_B \epsilon_0$ the state with a parallel orientation of the neighbouring ferron moments and spins of neighbouring donor electrons proves to be the most energetically-favoured one.

The reasons why the parallel orientation of the moments of neighbouring ferrons is energetically favoured at shorter distances between defects, when ferromagnetic regions of neighbouring donors overlap, are somewhat different. In this case the increase in the energy of the exchange between magnetic atoms following the substitution of an FM ordering for an AF one turns out to be less than in the case when the regions do not overlap. The savings in the energy of exchange interaction between magnetic atoms are the greater the closer are the donors. However, the parallel orientation of the c -electron spins increases their energy of exchange with each other. As before, the condition of the energy advantage of parallel orientation of atomic spins is expressed by the inequality $AS > e^2 / a_B \epsilon_0$. One can easily prove this to be true by considering the limit of distances between the donor atoms so small that the system turns into a helium-like atom. The energy of its singlet state $(1s)^2$ when there is no FM region is equal to $-2.9e^2 / a_B \epsilon_0$ [277]. On the other hand, the energy of the $(2s)(1s)$ state in the presence of an FM region and in conditions of applicability of formula (5.3.5) is equal to $-(2.2e^2 / a_B \epsilon_0 + AS)$, the inequality $AS > 0.7e^2 / a_B \epsilon_0$ guaranteeing the state $(2s)(1s)$ being energetically favoured.

It follows from the above that in the case of donor imperfections of the type of anion vacancies an increase in their concentration in an AFS may result in FM ordering of localized ferrons, since the crystal will partially go over to an FM state remaining an insulator. In anisotropic crystals this may be facilitated by magnetic dipole-dipole interaction between the ferrons. Moreover, if the radius of the FM region R is large as compared with that of the Bohr orbit a_B , the crystal as a whole can go over into an FM state without the donor electrons being delocalized, i.e. without a semimetal-type conductivity being induced in it. Indeed, according to the Mott criterion (1.6.1, 2), delocalization of electrons takes place only when the average separation between the donors $n^{-1/3}$ is less than Ca_B , where the numerical factor $C \sim 1$ is usually put equal to 4. Hence, for $2R > Ca_B$ there is a range of concentrations $2R > n^{-1/3} > Ca_B$ in which the electrons on localized impurity levels are responsible for the ferromagnetism of a doped AFS.

It follows from the above estimates of R obtained with formula (5.3.5) that such a situation is possible, for example, in metamagnets [276].

It is worth pointing out that some materials classified as FMS (e.g. EuB_6) can be synthesized only with deviations from stoichiometry. It is probable that the imperfection ferromagnetism described above is possible in such materials.

A peculiar situation is created when donor atoms are adsorbed on the surface of an AFS. The valence electron of each such adatom is drawn into the crystal and tends to set up an FM region around the adatom. As has already been discussed above, overlapping of FM regions of neighbouring atoms whose moments point in the same direction reduces the energy required for their creation. This results in a peculiar mechanism of attraction between the adatoms stemming from their tendency to merge their FM regions, which diminishes the exchange energy needed for their creation. In effect this is a novel mechanism of the chemical bond. It differs from conventional mechanisms in that the agglomeration of adatoms produced by it can contain an unlimited number of them, the spins of valence electrons of all adatoms being parallel [279, 280].

Let us now turn to calculating the contribution of localized ferrons to the magnetic susceptibility χ of a nondegenerate semiconductor when the interaction between the ferrons can be ignored [195]. The ferron moment is presumed for $\mathcal{H} \rightarrow 0$ to point in the direction of the vector of antiferromagnetism \mathbf{l} . The magnetic imperfection of the type being considered has a moment

$$M_F = \frac{8\pi}{3} S \left(\frac{R}{a} \right)^3. \quad (5.3.6)$$

For $\mathcal{H} \perp \mathbf{l}$ the magnetic moments of each sublattice deviate from their positions at $\mathcal{H} = 0$ in the direction of the applied field by the

angles $\theta_1(r)$ and $\theta_2(r)$, respectively (Fig. 2.4). The influence of imperfections on the magnetic moment of the crystal makes itself manifest not only on account of their abnormally great magnetic moments as compared to atomic ones, but also on account of abnormally great (as compared with an ideal lattice) deflection angles. To be definite, let the magnetic moment of the imperfection at $\mathbf{r} = 0$ be parallel to the moment of sublattice II. Within the framework of the continuous-medium approximation the energy E of a cubic crystal for small θ 's can be represented as a functional of the angles $\theta_1(r)$ and $\theta_2(r)$ sought as follows:

$$\begin{aligned}
 E &= E\{\lambda\} + E\{\mu\}, \quad \lambda = \theta_2 - \theta_1, \quad \mu = \theta_1 + \theta_2, \\
 E\{\lambda\} &= -\frac{S^2}{8} \int_{r, r_1 \geq R}^{\infty} \mathcal{K}(\mathbf{r} - \mathbf{r}_1) [\lambda(r) - \lambda(r_1)]^2 d\mathbf{r} d\mathbf{r}_1 \\
 &\quad + \frac{bS^2}{2} \int_{r \geq R}^{\infty} \lambda^2(r) d\mathbf{r} - \frac{\mathcal{H}M_F}{2} \lambda(R), \quad (5.3.7) \\
 E\{\mu\} &= -\frac{S^2}{8} \int_{r, r_1 \geq R}^{\infty} \mathcal{K}(\mathbf{r} - \mathbf{r}_1) [\mu(r) + \mu(r_1)]^2 d\mathbf{r} d\mathbf{r}_1 \\
 &\quad - S\mathcal{H} \int_{r \geq R}^{\infty} \mu(r) d\mathbf{r} - \frac{\mathcal{H}M_F}{2} \mu(R).
 \end{aligned}$$

Here the quantities $\mathcal{K}(r)$ and b describe the exchange interaction between atoms belonging to different sublattices and the anisotropic interaction that provides for the stability of the configuration being considered, respectively.

Expressions (5.3.7) are written in the assumption that the moments of all atoms in the ferromagnetic microregion $r < R$ deviate by the same angle $\theta_2(R)$, and that outside the microregion the interaction of the c -electron of the imperfection with the magnetic atoms can be neglected.

Suppose (subsequent calculation will substantiate it) that the quantity $\lambda(r)$ proportional to the projection of vector \mathbf{l} on the field direction is a slowly-varying function of the radius r . Taking into account that the exchange interaction length is small, we obtain the Euler equation for the functional $E(\lambda)$ in the form

$$\frac{1}{r^2} \frac{d}{dr} \left[r^2 \frac{d}{dr} \lambda(r) \right] - \kappa_1^2 \lambda(r) = 0, \quad (5.3.8)$$

where

$$\kappa_1 = \frac{4b}{|\mathcal{H}_1|}, \quad \mathcal{H}_1 = \frac{S^2}{3} \int_0^{\infty} \mathcal{K}(r) r^2 dr.$$

The boundary conditions for it can be obtained from the condition that the variations $\lambda(r)$ be arbitrary at $r = R$ and $r = \infty$:

$$r^2 \frac{d\lambda(r)}{dr} \Big|_{r=\infty} = 0, \quad r^2 \frac{d\lambda(r)}{dr} \Big|_{r=R} = -\frac{\mathcal{H}M_F}{2\pi |\mathcal{F}_1|}. \quad (5.3.9)$$

The solution of equation (5.3.8) with the boundary conditions (5.3.9) is given by the expression

$$\lambda(r) = \frac{\mathcal{H}M_F \exp\{-\alpha_1(r-R)\}}{2\pi |\mathcal{F}_1| [1 - \alpha_1 R] r}. \quad (5.3.10)$$

It will be evident from (5.3.10) that, to be able to consider the imperfections independently of one another as is being done here, one will have to meet the condition $\alpha_1 \gg n^{1/3}$, where n is the impurity concentration.

As to the function $\mu(r)$, it cannot generally be regarded as a slowly-varying function of r at distances of the order of the exchange interaction length, i.e. of the lattice parameter. This could cast doubt on the applicability of the phenomenological approach. However, it will be demonstrated below that the rapid variations of $\mu(r)$ can be ignored, and it may be presumed to be a constant. By varying the functional $E\{\mu\}$ (5.3.7), we obtain the following equation

$$\int_{r_1 \geq R}^{\infty} \mathcal{K}(r-r_1) [\theta(r) - \theta(r_1)] d\Omega dr_1 = -\frac{2\pi M_F}{R^2} \delta(r-R), \quad (5.3.11)$$

where

$$\theta(r) = \mu(r) - \frac{\mathcal{H}S}{2\pi}, \quad 4\mathcal{K} = \int \mathcal{K}_i(r) dr$$

$d\Omega$ is an element of the solid angle corresponding to the vector \mathbf{r} .

On account of the condition $R \gg a$ equation (5.3.11) can be approximated by the equation

$$\int_0^{\infty} \mathcal{F}(r-r_1) [\theta(r-R) + \theta(r_1-R)] dr_1 = -\frac{\pi M_F}{2\pi R^2} \delta(r),$$

$$\mathcal{F}(r-r_1) \approx R^2 \int \mathcal{K}(r-\mathbf{r}_1) d\Omega. \quad (5.3.12)$$

The kernel $\mathcal{F}(r)$ of the integral equation (5.3.12) rapidly decays at ranges of the order of a . Without jeopardizing the generality of the estimate obtained, one can conveniently approximate it by an exponent

$$\mathcal{F}(r) \approx K \exp\{-r/a_1\}. \quad (5.3.13)$$

The equivalence of the integral equation (5.3.12) with the kernel (5.3.13) and the following differential equation

$$\theta''(r+R) - \frac{2}{a_1^2} \theta(r+R) = - \frac{\mathcal{H}M_F}{2\pi R^2 a_1 K} \left[\delta''(r) - \frac{\delta(r)}{a_1^2} \right] \quad (5.3.14)$$

is established by checking directly.

The solution of equation (5.3.14) obtained by extending it to the region $r < 0$ and by making use of the Fourier transformation is of the form

$$\mu(r) = - \frac{\mathcal{H}M_F}{4\pi \sqrt{2} R^2 K a_1^2} \exp \left\{ - \frac{\sqrt{2}(r-R)}{a_1} \right\} + \frac{\mathcal{H}S}{|2\pi|}. \quad (5.3.15)$$

Hence, according to (5.3.15), $\mu(r)$ remains practically constant up to $r - R \sim a_1$, where it experiences a sharp discontinuity. However, it follows from the comparison of (5.3.15) and (5.3.10) that

$$\mu(R)/\lambda(R) \sim a/R \ll 1,$$

i.e. the contribution of $\mu(R)$ to $\theta_2(R)$ can be neglected as compared with that of $\lambda(R)$.

It follows from expression (5.3.15) and from the definition of μ that the magnetic moment of an AFS already in the immediate vicinity of the imperfection is equal to its value in the ideal crystal. Accordingly, the following expression for the transverse susceptibility of the imperfections being considered $\chi_{\perp F}$ is obtained (per unit volume):

$$\chi_{\perp F} \simeq M_F^2 n / 4\pi | \mathcal{Y}_1 | R (1 + \kappa R). \quad (5.3.16)$$

Comparing the result (5.3.16) with the expression for the susceptibility of an ideal antiferromagnet χ_{\perp} as determined from (5.3.15) for $M_F = 0$, we obtain $\chi_{\perp F} / \chi_{\perp} \sim R^3 n a^{-2}$. In actual conditions $\chi_{\perp F}$ may amount to several tens percent of χ_{\perp} . The linear growth of the total magnetic moment of ferrons with the field continues up to its critical value H_{LF} at which the moments of all ferrons become oriented in the direction of the field. According to formulae (5.3.10) and (5.3.15), the field $\mathcal{H}_{LF} \sim (aR)^2$ of the magnetic saturation field \mathcal{H}_F (2.3.6).

Experimental data in support of the existence of localized ferrons are presented in Sec. 7.5.

5.4. ELECTRICAL AND OPTICAL PROPERTIES

OF ANTIFERROMAGNETIC SEMICONDUCTORS (EXPERIMENT)

Ferrons. To illustrate the specific properties of AFS, it would be reasonable first to consider such materials as EuTe and EuSe, which from the crystallochemical point of view are analogues of the FMS EuO and EuS, and because of that all the difference in their behaviour from EuO and EuS is the result of AF ordering. Let us begin

with the anomalous dependence of the photoconductivity and the luminescence of the AFS EuSe and EuTe on the magnetic field not displayed by FMS.

By analyzing the data on the luminescence and the photoconductivity of EuSe and EuTe, Wachter [6] arrived at the conclusion that ferron states must exist in these materials. Normally strong luminescence is associated with the presence of imperfections that produce localized levels in the electron spectrum. But the luminescence of EuSe did not lose in intensity as the material was purified. At $T \gg T_N$ the magnetic field exercises a small effect on the luminescence,

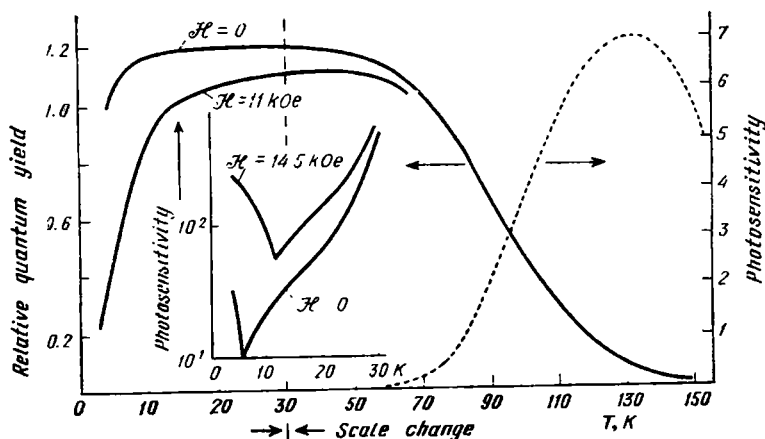


Fig. 5.4. Relative quantum yield of luminescence vs. temperature for EuSe in the absence of a field and in a field of 11 kOe (solid lines). Insert and dashed line—photosensitivity (in arbitrary units) [6]

but at 4.2 K a magnetic field of 11 kOe, which produces a magnetization amounting to 80% of the saturation value, reduces the integral luminescence 5 times, sharply increasing the photoconductivity (Fig. 5.4). This is proof that the magnetic field destroys localized levels that facilitated electron transitions in its absence. The ferron states are just such states that are not associated with any imperfections, exist at temperatures not too high and disappear in a magnetic field. Similar effects are observable in EuTe [6].

The ferron hypothesis also enables the nature of the spectral dependence of the luminescence of EuSe at 4.3 K without a magnetic field and in a field of 11 kOe depicted in Fig. 5.5 to be explained [6]. As seen from the figure, the field does not practically diminish the emission near the long-wave band edge, but reduces it by several orders of magnitude near the short-wave edge. The energies near the short-wave edge of the emission band (1.5–1.7 eV) are very close to

the frequencies of electron transitions from the ferron state to the upper levels of the valence band. Indeed, the optical absorption edge of EuSe at 4.3 K lies at about 1.75 eV (Fig. 4.2). The level of a large ferron lies approximately $AS/2$ lower than the conduction band bottom. The value of $AS/2$ for europium chalcogenides, according to experimental data on EuO, is almost equal to 0.26 eV [112]. Hence, the ferron level should lie at a distance of ~ 1.5 eV from the valence band maximum. Its considerable spreading can be explained by the ferron-hole interaction, by the formation of ferron complexes and by the effect of imperfections. Ferron level spreading also results from a spread in the shape and the dimensions of FM regions in

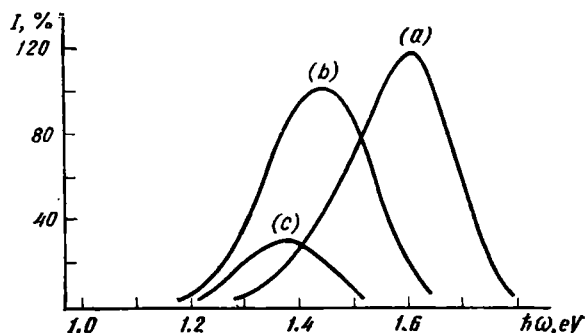


Fig. 5.5. Relative emission intensity spectrum for EuSe: (a) at 51 K; (b) at 4.3 K in the absence of a field; (c) at 4.3 K in a field of 11 kOe [6]

which the photoelectron is localized. It is the outcome of the circumstance that adequate time is required to establish such regions of optimum dimensions, and that the electron may go over from the ferron level to the valence band before this has been done.

As has been pointed out in Sec. 4.7, the valence band in EuO is little sensitive to the magnetic order. The same is to be expected in the case of EuSe. As to the ferron level, it disappears in sufficiently strong magnetic fields. The emission resulting from the ferron-valence band transitions disappears simultaneously. This corresponds to the behaviour of the short-wave emission band edge in the field depicted in Fig. 5.5.

The long-wave emission (1.2-1.3 eV) is obviously the result of different electron transitions involving impurity centres. Their weak sensitivity to the magnetic field can be explained by the electrons on impurity centres occupying localized ferron states. Because of that the application of a magnetic field, on the one hand, little affects the local magnetic ordering in the vicinity of such an imperfection, since this ordering is already an FM one. On the other hand, the localized level will not disappear, if not only the vicinity of the imper-

fection, but the crystal as a whole turns FM, because the electron will as before be trapped by the field of the imperfection.

The fact that in a magnetic field the emission maximum, same as the absorption edge (Fig. 4.2), shifts towards the long-wave side could also be a result of another luminescence mechanism: of the electron transitions from the conduction band to level in the vicinity of the valence band maximum little sensitive to the magnetic order. However, a more detailed analysis shows the experimental data [6] not to agree with such a mechanism: the effect of the magnetic field on the emission is much more pronounced than on the absorption. Indeed, the ratio of the shifts of the emission maximum and the absorption edge at 20, 10 and 4.3 K will be seen from Figs. 4.2 and 5.6 to be equal to 5.2 and 1.5, respectively. Moreover, such a mechanism of itself does not explain the sharp fall of the emission in the field.

The temperature shift of the emission maximum at $\mathcal{H} = 0$ also greatly exceeds the absorption edge shift. The increase in the frequency of the emitted light with the temperature can be explained by the dissociation of ferrons at high temperatures, this resulting in the rise of the levels from which the transitions to the valence band take place.

The localized ferrons are easier to observe than the free. The local magnetization in the vicinity of imperfections that have trapped charge carriers exists up to rather high temperatures. Proof of this are the results of [531]. In EuSe containing Se vacancies charge carriers have been excited by light, captured by traps and freed by the magnetic field that reduced the depth of traps. The measurements have been carried out in the temperature range from 20-70 K. Strong fields from 40 to 100 kOe reduce the activation energy from the zero-field value 0.17 eV to 0.011 eV. As has already been mentioned in Sec. 4.5, the reduction in the depth of localized levels by the field is a direct consequence of the existence of local magnetization around the imperfections at $\mathcal{H} = 0$. As discussed in Sec. 7.5, localized ferrons influence the PM Curie point very strongly.

Other Optical Properties. In contrast to FMS, there is no giant red shift of the absorption edge E_g in typical AFS. For instance, in EuTe ($E_g = 2.0$ eV) a blue shift is observed of only 0.03 eV. Still it is an order of magnitude greater than in nonmagnetic semiconductors. The magnetic field diminishes it. In fields exceeding 60 kOe

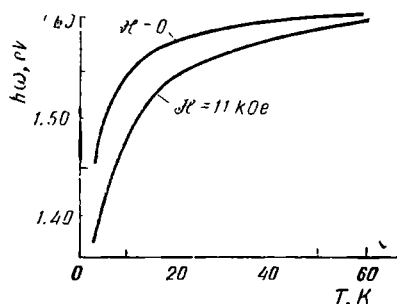


Fig. 5.6. Position of spectral emission maximum vs. temperature for EuSe [6]

the sign of the shift is reversed. The field-induced edge shift is at its maximum at Néel point where it displays a discontinuity [6] (Fig. 5.7).

The absorption edge vs. magnetic field dependence in EuTe at 1.7 K has been studied in [522]. However, it is difficult to gain any information about the energy spectrum of EuTe from these results, because the position of the absorption edge turned out to be greatly dependent on the orientation of the electric vector \mathbf{E} of the light with respect to the external magnetic field \mathcal{H} . The red shift E_g in the magnetic saturation field (~ 70 kOe) with respect to its position at $\mathcal{H} = 0$ amounts only to 0.035 eV for $\mathbf{E} \parallel \mathcal{H}$ and to 0.08 eV for

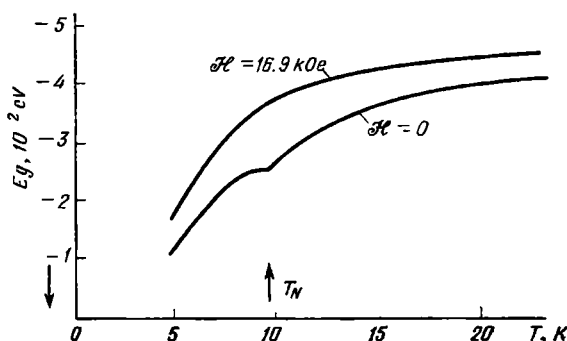


Fig. 5.7. Optical absorption edge vs. temperature for EuTe [6]

$\mathbf{E} \perp \mathcal{H}$. It is also difficult to understand why the red shift in EuTe is so small in comparison with that in other Eu chalcogenides (see Figs. 4.2 and 4.3). I am of the opinion that additional studies are necessary.

A blue shift of the absorption edge ~ 0.03 eV is observed also in the metamagnet Eu_3O_4 . However, in a field of 13 kOe the shift turns into a red one [526].

In the AFS CoO and MnS the blue shift is much greater: in the temperature range from $T \gg T_N$ to $T = 0$ is as high as 0.25 eV [250], i.e. of the same order of magnitude as in FMS, but of an opposite sign (Fig. 5.8).

According to theoretical results obtained above, the magnitude of the shift of the conduction band bottom in AFS with narrow energy bands is much greater than in the wide-band ones. Taking into account (5.1.18) and the results of Sec. 4.1, we can evaluate the former using the formula

$$\Delta E \approx \frac{W}{2} \left(\frac{1}{\sqrt{2}} - \frac{1}{\sqrt{2S+1}} \right). \quad (5.4.1)$$

If only one band should be held responsible for the entire absorption edge shift in CoO and MnS ($S = 5/2$), this would yield $W \sim 2$ eV. For such wide bands it is difficult to meet the condition $W \ll AS$. It is more probable that the large absorption edge shift is the result of a simultaneous shift of the narrow electron and hole bands. This

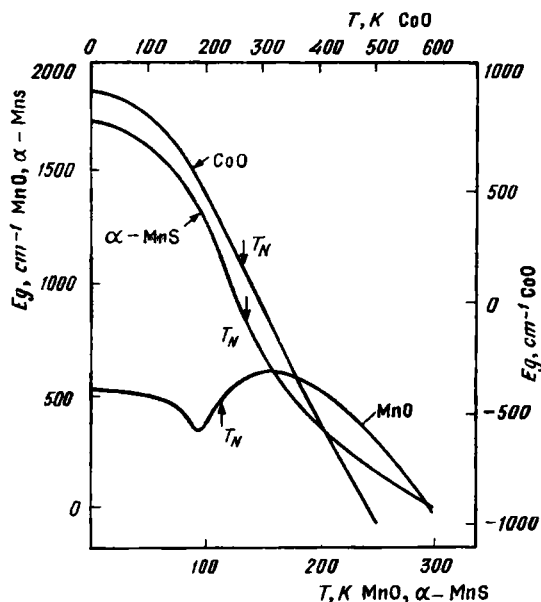
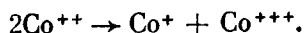


Fig. 5.8. Optical absorption edge vs. temperature for CoO, MnO and α -MnS [250]

means that both these bands are of the d -type, i.e. that an electron-hole pair is generated as a result of a reaction of the type



In [516] where a giant blue shift has also been observed in α -MnS, an attempt has been made to explain it as a result of the formation of a Kasuya magnetic exciton [88, 517] discussed in Sec. 4.6. A choice in favour of one of these points of view can be made, if the photoconductivity in α -MnS and kindred materials is studied (see Sec. 4.6.).

The small absorption edge shift in the AFS EuTe together with a large shift in kindred FMS is proof that in them the inequality $W \gg AS$ is satisfied. Indeed, according to (3.2.12) and (4.3.13), the blue shift in AFS should be $\simeq A^2 S^2 / 2W$. Were we in accordance with the shift in EuO, EuS and EuSe (Figs. 4.2, 4.3) to take the value of 0.25 eV for $AS/2$, we would obtain for the shift in EuTe equal to 0.03 eV the

bandwidth $W \simeq 3$ eV, which corresponds to an electron effective mass almost precisely equal to true mass.

However, there are nonferromagnetic semiconductors that display a red shift of the absorption edge. In the metamagnetic EuSe the red shift is chiefly observed above the Néel point, being practically nonexistent below it [6, 527]. A magnetic field of 14.5 kOe makes the crystal go over in the FM state, and the absorption edge behaves as in a typical FMS (Fig. 4.2). As was already discussed in Sec. 2.8, the red shift above T_N may be explained by the establishment of an FM short-range order. It should be noted that a small red shift should occur in the result of the establishment of a four-sublattice AF ordering. In fact, within the framework of the layered magnet model (Sec. 2.7) at $T = 0$ $S_z = \sqrt{2} S \cos\left(\frac{\pi}{4}g + \frac{\pi}{4}\right)$ for the ordering considered, g standing for the number of the FM plane. Taking this into

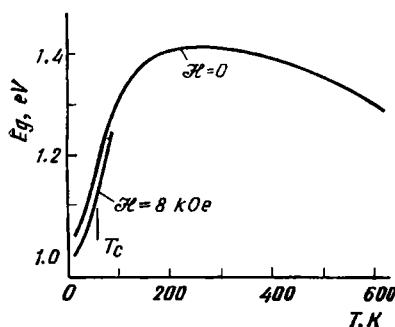


Fig. 5.9. Optical absorption edge vs. temperature for HgCr_2S_4 [161]

account and making use of the dispersion law (1.1.2) for electrons, one obtains from (4.3.1) and (4.3.12) that the red shift caused by the saturated four-sublattice ordering should be equal to $3A^2S^2/4W$, which amounts only to hundredths of an eV for typical values of W and AS . Still less it should be in the PM region.

A red shift is also observed in the HgCr_2S_4 crystal having the helicoidal ordering. Magnetic fields at which the helicoidal ordering is still preserved have a rather small influence on this shift (Fig. 5.9). It takes place both above and below the Néel point amounting altogether to 0.4 eV, i.e. it exceeds the red shift in most FMS. This is proof that the electron energy is determined not by the average, but by the local crystal moment. From the theoretical viewpoint, the red shift is a result of the conduction-band-bottom lowering with decreasing temperature. According to (3.2.6, 10), in a crystal with a helicoidal ordering for $4 | B | \gg AS$ the bottom sinks, if the heliocoid vector q does not exceed $q_0 = \sqrt{2m^*AS}$, since in this case the c -l shift at $T \rightarrow 0$ is about $AS/2$, at $T \rightarrow \infty$ it being of the order of A^2S^2/W . For a narrow-band semiconductor ($W \ll AS$), it follows from (3.2.10) and from the fact that at $T \rightarrow \infty$ the conduction band width is, according to (4.1.5), $\sqrt{2}$ times smaller than in the case of FM ordering that for the red shift to exist it suffices that the inequality $qa < 1$ be satisfied.

It is an interesting point that the absorption edge shift in MnO

is not monotonous (Fig. 5.8). In the PM region it is a blue one, but below the Néel point the absorption edge passes through a minimum.

The shift in a definite temperature interval above T_N being a red one, it corresponds to a short-range FM order. Hence one may deduce by analogy with EuSe that an "order-improper disorder" phase transition takes place in MnO (see Secs. 2.7, 2.8). Still more pronounced

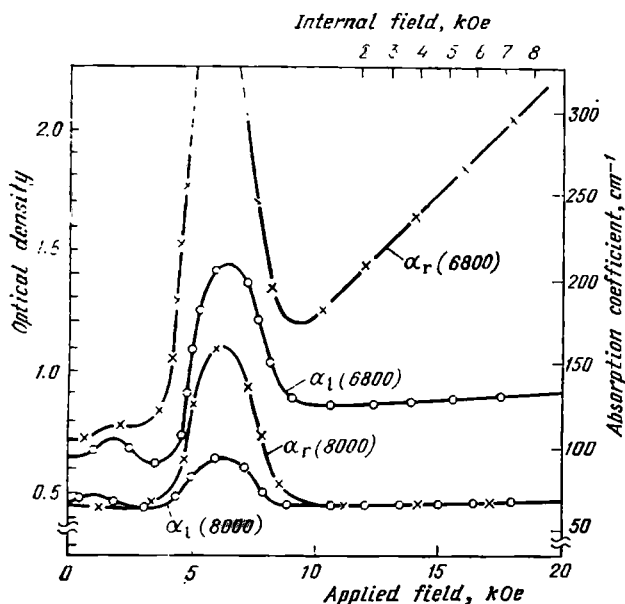


Fig. 5.10. Magnetic dichroism of EuSe at 4.2 K. α_r and α_l are absorption coefficients of clockwise- and anticlockwise-polarized light for the wavelengths of 6800 Å and 8000 Å [309]

is the minimum in the position of the optical absorption edge at T_N in the helicoidally-ordered ZnCr_2Se_4 [324].

The metamagnetic EuSe at 4.2 K displays magnetic dichroism, i.e. anticlockwise- and clockwise polarized light propagating along the magnetic field experiences different absorption. The absorption maximum is attained in a field of ~ 6 kOe, same as the dichroism maximum. The height of the maxima drops rapidly as the wavelength is increased (Fig. 5.10) [309]. This effect resembles the Faraday polarization plane rotation, the imaginary part of the dielectric function tensor being responsible for it (Appendix 11). The absorption peak is probably associated with the transition of the metamagnet to the FM state.

The Faraday spectrum of EuSe in weak fields has been studied in [472]. The peak at 2.6 eV exists only in the range from 1.5 to 4.6 K,

outside this range a shoulder replaces it. The type of the spectrum below 1.5 K is very similar to that of MnO.

The Faraday spectra of EuTe and EuSe at 3 K in fields of ~ 100 kOe when such materials are ferromagnetically-ordered display a maximum at $2.3\text{--}2.4\text{ eV}$ $2 \times 10^6\text{ deg}\cdot\text{cm}^{-1}$ high. The nature of the spectrum of EuTe alters in the region of smaller fields where the sublattice moments do not coincide in direction. The Faraday rotation θ monotonously diminishes with the field, but at a constant field smaller than the spin-flip field at 2.45 eV passes through a maximum as a function of the temperature. In high fields it grows monotonously as the temperature decreases. The Faraday rotation in EuSe does not attain saturation in fields of ~ 14 kOe. The saturation is attained in fields ~ 70 kOe, much higher than the fields at which the transition to the FM state takes place [519].

Among other magnetooptical effects, the studies of Raman scattering of light in EuSe and EuTe [434, 510, 511, 528, 529] deserve to be mentioned. In [329] the Faraday effect in NiO has been observed in very high fields (up to 1.6×10^6 Oe) at 300 K. It is nonlinear in the field and, having passed through a maximum $\sim 100\text{ deg}\cdot\text{cm}^{-1}$, changes sign at 10^6 Oe.

Electrical Properties. The resistivity peak at the critical point typical of FMS is usually nonexistent in AFS. The $\rho(T)$ curve frequently displays a kink at T_N of the type observed in EuTe (Fig. 7.17) [151] (the reasons for the resistivity remaining constant at $H \geq 39$ kOe will be discussed in Sec. 7.5). According to [533], the resistivity of FeO has a discontinuity of the temperature derivative of the type of $d\rho/dT \sim |T - T_N|^{-0.4}$ at the Néel point. In some cases the conductivity activation energy of nondegenerate AFS also changes at the Néel point, being lower at $T < T_N$ than at $T > T_N$ [154, 155]. For instance, in MnTe_2 the activation energy is 0.011 eV at $T < T_N$ and 0.039 eV at $T > T_N$ [154]. The same temperature dependence is displayed by the photoconductivity in EuTe (Fig. 4.16): it grows with the temperature both below and above the Néel point, but at the Néel point its activation energy rises abruptly from 2.9×10^{-1} to $3.7 \times 10^{-3}\text{ eV}$ [6]. However, it is still unclear, whether the increase in the activation energy as the Néel point is passed from the low-temperature side is a general rule.

The discontinuity in the temperature dependence of the resistivity in an AFS in the vicinity of T_N vanishes as the degree of the crystal imperfection increases. For example, a $d\rho/dT$ discontinuity of the same type as that of the specific heat has been observed in relatively pure MnTe_2 crystals at the Néel point. At the same time in very heavily-doped crystals a resistivity maximum appears in the vicinity of T_N instead, although it is much less pronounced than that in FMS in the vicinity of T_c (Fig. 5.11 [153]). However, the minimum of photoconductivity in EuSe near T_N (Fig. 5.4) cannot be explained

as the effect of crystal imperfections. As has been pointed out above, ferrons are apparently responsible for it.

A point worthy of note is that, in full accord with the theory [532] (Sec. 4.5), which in the PM region is equally applicable to FMS and AFS, in a definite temperature range above T_N and in weak magnetic fields a magnetoresistance of an anomalous (positive) sign has been observed in ZnCr_2Se_4 . In strong magnetic fields the sign of the magnetoresistance was a normal negative one [534]. The qualitative picture of the magnetoresistance behaviour is in this case the same as in degenerate MS (Fig. 7.28).

The peculiar electrical properties of NiO crystals have already been discussed in Sec. 1.3. According to data presented there, there are no reasons to presume that small polarons materialize in NiO, although an exponential temperature dependence of the conductivity is possible in compensated crystals, if the main contribution to the conductivity is that of carriers hopping over impurity levels. An additional proof that the width of the d -band in compounds of transition metals is as a rule too large for small polarons to exist in them are the experimental data on their absorption edge shift (Fig. 5.8) and estimates of the conduction-band width obtained from them.

According to results [78], if one determines the carrier concentration from the Hall effect using the relationship $R_H \sim 1/nec$, he will obtain that the hole mobility in CoO, although small ($\sim 0.1 \text{ cm}^2 \text{ V} \cdot \text{s}$), is little dependent on the temperature in the range of 300 to 1000 K, this being proof of the absence in such materials of small polarons.

Other electrical properties of NiO-type materials are also quite peculiar, and not all of them could as yet be explained. Thus, for example, the sign reversal of the Hall constant in NiO in the course of passage through the Néel point, resulting in it being of sign opposite to that of the thermoelectric power, still defies explanation [62].

It should be noted in conclusion that an attempt to evaluate the electron effective mass in EuSe from the polarizability of double-donor Se vacancies was made in [535]. But the value obtained $m^* = 0.28 m_0$ appears to be underestimated. In any case it does not agree with the localized level depth found in [531].

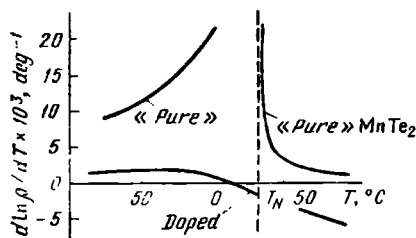


Fig. 5.11. Temperature coefficients of resistivity of a relatively pure and a heavily-doped MnTe_2 crystal in the vicinity of the Néel point [153]

5.5. EXCITON POLARONS AND TRANSFERONS IN MAGNETOEXCITONIC SEMICONDUCTORS

As has already been pointed out in Sec. 3.1, in some transition-element and rare-earth compounds the energy required to make a cation go over to a state with a spin of different magnitude is not large. In some cases such cations are nonmagnetic in the ground state, but upon excitation go over to a state with a nonzero spin S , e.g. with $S = 1$. Such an excitation may be interpreted as the creation on the cation of a triplet Frenkel exciton. Excitation of a cation can take place without a change in the magnitude of its spin as well, and in this case we may speak of the creation on the cation of a singlet Frenkel exciton. We shall term the materials in which the magnetic cations can easily be made go over to an excited state *magnetoexcitonic*. Co compounds, such as LaCoO_3 in which the energy of the creation of a triplet exciton involving the transition of a Co^{3+} ion from a nonmagnetic to a magnetic state is ~ 0.01 eV, may serve as an example of such materials [252, 253]. The creation of low-frequency Frenkel excitons on cations with a nonzero spin is also possible in principle.

Naturally, Frenkel excitons themselves cannot transport charges, but the interaction of conduction electrons with them may have a substantial effect on the latter. Various mechanisms of interaction between the electrons and Frenkel excitons producing carrier states of various types are possible. In this section we shall study states of carriers in the case when the dominant part is played by their interaction with Frenkel excitons whose appearance does not alter the atomic spin. More precisely, we shall deal with singlet excitons on diamagnetic atoms (with $S = 0$).

Exciton Polarons. If the dipole exciton transitions are allowed, the usual polarization electron-exciton interaction will result in the formation of exciton polarons, of quasi-particles of the same type as the polarons in ionic crystals [256]. When we have been discussing the polaron problem in Secs. 1.3, 1.4, we have pointed out that the polarization of the electron shells of ions adiabatically follows the motion of the conduction electron irrespective of its state. By force of this such a polarization cannot produce a potential well for the conduction electron, if the latter is localized somewhere in space. However, the electron polarization can follow the motion of the conduction electron adiabatically only if the characteristic electron frequencies of the inner shells are high as compared with the frequency of the motion of the conduction electron. In case of the low-frequency Frenkel excitons this condition is not met: an electron moving freely in the crystal flies past them at such a speed that its field does not manage to excite the excitons. If on the other

hand the electron is localized somewhere in space, it will polarize the inner partially-filled cation shells.

The substantial difference between the properties of conventional and exciton polarons is as follows. The exciton polarization is limited to the excitation of not more than one exciton on every cation. There are no similar limitations on the lattice polarization. The formal expression of this fact consists in the optical phonons obeying the Bose commutation rules with the excitons obeying the Pauli commutation rules. On account of this the results of the theory of conventional polarons cannot be automatically extended to exciton polarons.

In the dipole approximation the electron-exciton interaction Hamiltonian in the simplest form is given by expression (1.4.1) where b_q^* , b_q should be interpreted as exciton operators, and c_q

$$c_q = \frac{4\pi e^2 (\mathbf{q} \cdot \mathbf{d})}{\sqrt{N} \epsilon_\infty a^3 q^2}. \quad (5.5.1)$$

In formula (5.5.1) d represents the dipole moment for the exciton transition. The quantity

$$\alpha_{ex} = \frac{4\pi d^2 e^2}{a^3 \epsilon_\infty^2 \omega^2} \sqrt{2m^* \omega}, \quad (5.5.2)$$

where ω is the exciton frequency, serves as an analogue of the electron-phonon coupling constant. For $m^* = m_0$, $\epsilon_\infty = 10$, $a = 3 \text{ \AA}$, $\omega = 0.3 \text{ eV}$, $d = 0.5 \text{ \AA}$ it is equal to 4, i.e. can be sufficiently high.

For $\alpha < 1$ the number of virtual excitons accompanying the electron is not large. Because of that the non-Bose nature of the excitons is of little importance, and one may make use of formula (1.4.7) with c_q as determined from formula (5.5.1). However, even in such conditions the polaron shift of the exciton level may, because of the high exciton frequency, be very great: for the parameters specified $|E_p| = \alpha\omega = 1.2 \text{ eV}$.

The effect of the non-Bose nature of the excitons can be illustrated with the aid of the example of a small exciton polaron at $T = 0$. The Hamiltonian of the system takes the form $H = H_{ex} + H_B$ where the zeroth-approximation Hamiltonian H_{ex} is determined by the expression

$$\begin{aligned} H_{ex} &= \sum_{\mathbf{h}} b_{\mathbf{h}}^* b_{\mathbf{h}} + \sum_{\mathbf{h}, \mathbf{f}} c(\mathbf{h} - \mathbf{f}) (b_{\mathbf{h}}^* + b_{\mathbf{h}}) a_{\mathbf{f}}^* a_{\mathbf{f}}, \\ c(\mathbf{g}) &= \frac{1}{\sqrt{N}} \sum_{\mathbf{q}} c_{\mathbf{q}} e^{i\mathbf{q} \cdot \mathbf{g}}, \\ b_{\mathbf{h}} &= \frac{1}{\sqrt{N}} \sum_{\mathbf{k}} e^{-i\mathbf{k} \cdot \mathbf{h}} b_{\mathbf{k}}. \end{aligned} \quad (5.5.3)$$

The exciton operators corresponding to the same site obey the Fermi commutation rules, and those corresponding to different sites obey

the Bose rules. The Hamiltonian H_B (1.1.1) acts as a perturbation.

The zeroth-approximation Hamiltonian H_{ex} can be precisely diagonalized. The normalized eigenfunction of the ground state of atom \mathbf{h} depends on the number \mathbf{f} of the atom occupied by the conduction electron and is expressed in terms of the exciton vacuum wave function $|0\rangle_{ex}$ as follows

$$\psi_{\mathbf{f}}(\mathbf{h}) = [x_1(\mathbf{f} - \mathbf{h}) + x_2(\mathbf{f} - \mathbf{h}) b_{\mathbf{h}}^*] |0\rangle_{ex} \equiv B^*(\mathbf{h}|\mathbf{f}) |0\rangle_{ex}, \quad (5.5.4)$$

$$x_2/x_1 = 2c(\mathbf{f}) [\omega - \sqrt{\omega^2 + 4c^2(\mathbf{f})}]^{-1},$$

where $|0\rangle_{ex}$ is the exciton vacuum state.

The wave function of the system is represented in the form

$$\Phi_{\mathbf{k}} = \sum e^{i\mathbf{k} \cdot \mathbf{r}} a_{\mathbf{f}}^* |0\rangle \prod_{\mathbf{h}} B^*(\mathbf{h}|\mathbf{f}) |0\rangle_{ex}. \quad (5.5.5)$$

Then, using formulae (5.5.3-5) and (1.1.1), we obtain for the polarization energy E_P and the width of the polaron band W_P the following expressions

$$E_P = E_{PB} + \sum_{\mathbf{f}} \left\{ \left[\frac{\omega}{2} - \sqrt{\frac{\omega^2}{4} - c^2(\mathbf{f})} \right] - \frac{c^2(\mathbf{f})}{\omega} \right\}, \quad (5.5.6)$$

$$W_P = 2z |B| \exp \left\{ -\frac{1}{2} \sum_{\mathbf{f}} \{ [x_1(\mathbf{f}) - x_1(\mathbf{f} + \Delta)]^2 + [x_2(\mathbf{f}) - x_2(\mathbf{f} + \Delta)]^2 \} \right\}. \quad (5.5.7)$$

Here E_{PB} is the energy the polaron would have, should the exciton operators be of the Bose type (an analogue of (1.3.2)).

The non-Bose nature of the excitons will be seen from (5.5.6) to cause a decrease in the polarization energy, this decrease for typical parameter values amounting perhaps to several tenths of an eV. The exponential factor in (5.5.7) describes the decrease in the carrier band width on account of the polaron effect. Unfortunately, it has not been possible to establish a simple relationship between the Bose and the Pauli decrease.

Transferons. In addition to the polarization interaction between the electron and the excitons, a specific interaction associated with the motion of the electron in the crystal is also possible. It differs from the polarization interaction in that its nature is essentially a nonlocal one. Its origin can be explained with the help of a simple model [257, 258]. Let the crystal be made up of atoms having two electron levels: E_1 and $E_2 = E_1 + \omega$, and let the number of electrons be equal to that of atoms. We do not take into account the spin degeneracy of the electrons. In the ground state, owing to Coulomb repulsion, each electron is localized on its atom, as in the case of the Hubbard model for $W \ll U$ (Sec. 1.5), and occupies the level

E_1 with the minimum energy. The transition of the electron to the level E_2 on the same atom corresponds to creation on the atom of a Frenkel exciton. Such a system becomes conducting when an additional electron with an energy E_2 appears on one of the atoms (atom I in Fig. 5.12a). It can go over to the neighbouring atom II occupying there the same level E_2 (Fig. 5.12b). This corresponds to the conventional band mechanism of carrier motion.

But there is also another possibility for the transition of an excess electron from atom I to atom II : the electron occupying the level E_2 on atom I remains at rest, and the electron from the level E_1

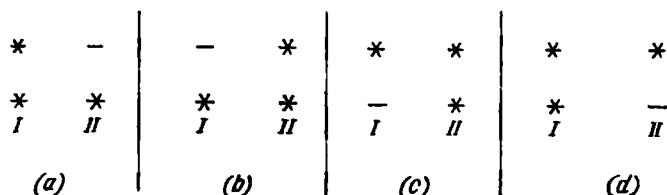


Fig. 5.12. Transferon electron-exciton interaction (asterisk denotes an electron)

makes the transition. In the result atom I , after an excess electron has left it, will be in an excited state (Fig. 5.12c). In the latter instance the situation is exactly the same as in the case of a spin-polaron moving in a narrow-band AFS, provided the c - l exchange integral is negative (Sec. 5.1). The corresponding terms in the Hamiltonian must have a structure similar to (3.5.19b).

Not only the reverse transition from state c (Fig. 5.12) to state a is possible, but also a transition to state d in which the excess electron and the exciton change places. In accordance with the afore-said, the Hamiltonian of the system assumes the form (its derivation from the conventional many-electron Hamiltonian is presented in [257, 258]):

$$\begin{aligned}
 H = & B \sum a_g^* a_{g+\Delta} + \omega \sum b_g^* b_g \\
 & + \mathcal{K} \sum (b_{g+\Delta}^* a_g^* a_{g-\Delta} + a_g^* a_{g+\Delta} b_g) + \mathcal{L} \sum a_{g+\Delta}^* b_g^* b_{g+\Delta} a_g \\
 & + V \left\{ \sum a_g^* a_g b_g^* b_g + \frac{1}{2} \sum b_g^* b_g^* b_g b_g \right\}. \quad (5.5.8)
 \end{aligned}$$

Here a_g^* , a_g and b_g^* , b_g are the creation and annihilation operators for the conduction electron (i.e. for the excess electron or an atom) and for the Frenkel exciton, respectively. The term proportional to V has been introduced into the Hamiltonian formally. It takes account of the prohibition for two quasi-particles (electrons or excitons) to occupy the same atom. In final calculation results one

will have to go over to the limit $V' \rightarrow \infty$ (this prohibition could be accounted for without the introduction of a term $\sim V'$ into the Hamiltonian by means of appropriate commutation rules between the operators [257]).

It is worth pointing out that the mechanism of electron-exciton interaction (5.5.8) is a more universal one than the polarization mechanism, since it operates in cases when dipole transitions inside atoms are forbidden, as well.

The Hamiltonian (5.5.8) is very complex, and it has been up to now only possible to find the energy spectrum of a charge carrier (a "transferon") only for two cases: (1) in the limit when the terms proportional to \mathcal{K} and \mathcal{L} can be regarded as a perturbation [258], (2) and in the opposite limiting case when the first term in it can be neglected, and the carrier motion corresponds to the quasi-oscillator type considered in Sec. 5.1.

5.6. FERRONS IN MAGNETIC SYSTEMS WITH EASILY VARIABLE ATOMIC MOMENTS

In many types of crystals the creation of a low-frequency Frenkel exciton is accompanied by changes in the atomic moment. In such crystals regions with enhanced magnetization can be produced not by means of a spin rotation of magnetic moments of constant magnitude (a situation discussed in Sec. 5.2), but by means of growth of the magnitude of moments themselves. On account of a small energy required to establish ferromagnetic microregions, ferron states become possible in such magnetoexcitonic crystals. Below we shall consider in detail two types of magnetoexcitonic semiconductors.

Crystals with a Diamagnetic Ground State of the Ions. In this case the ferrons appear in the result of the conduction electrons interacting with the triplet excitons born on diamagnetic atoms. The triplet excitons cannot be induced by the polarization of l -shells by the electron field or by the electron going over from atom to atom, because such mechanisms conserve the l -shell spin. Hence, the motion of the electron about the crystal cannot be accompanied by the creation and the annihilation of triplet excitons, i.e. the number of triplet excitons is a constant of motion. In other words, whereas an electron can interact with virtual singlet excitons, it cannot do so with the virtual triplet excitons.

The interaction of the electrons with the triplet excitons is in fact a c - l exchange with the magnetic atoms, which acquired a non-zero spin in the result of excitation. In case of an appropriate mutual orientation of the electron spin and that of a magnetic atom an attraction develops between them, and if it is strong enough, the exciton will be able to trap the electron. Moreover, same as in antiferromagnets, ferron states can form in magnetoexcitonic semi-

conductors [134]. Indeed, the creation of a triplet exciton or even of a complex of such excitons may prove energetically-favoured, if the energy spent on it will be compensated by the decrease in the electron energy in the result of its capture by excited atoms.

The dimensions of the complex should be determined from the condition that the total energy of the system be minimum. Here we have in mind that, for the minimum electron energy to be attained, the spins of all excited atoms will have to be parallel. Hence, in a magnetoexcitonic crystal the existence of FM regions capable of capturing electrons is possible.

In case of a sufficiently large microregion, the corresponding calculation almost precisely coincides with one carried out in Sec. 5.2. The quantity D in formulae (5.2.1-6) representing the energy spent to establish an FM ordering should be taken to mean the exciton frequency ω to which the energy of the direct exchange between the excited atoms with a $S = 1$ spin equal to $(-zJ/2)$ has been added. In case of a positive integral A of exchange between the electron and the triplet exciton, the depth of the potential well U is equal simply to A^2 , since $S = 1$, and the modulus of the same expression may be used for $A < 0$ when $W \gg AS$.

The situation is somewhat more complicated for $A < 0$ in the opposite limit of narrow bands, when the carrier in an FM region is in the spinpolaron state. According to (4.1.1), the energy of the electron-exciton exchange is in this case equal to $|A| (S + 1)/2$, so that in (5.2.1-6) we must put $U = |A|$. Strictly speaking, the energy-band width in the ferromagnetic region is $2S/(2S + 1) = 2/3$ times smaller than outside it. But in compliance with the condition $W \ll AS$ the electron is almost entirely concentrated in the FM microregion, and its energy depends very little on its effective mass m^* outside the potential well. Accordingly, we should substitute $(3/2) m^*$ for m^* in formulae (5.2.1-3).

A substantial difference between the narrow-band $W \ll AS$ magnetoexcitonic semiconductors and their AF analogues is that in the former the depth of the ferron well is determined not by the smaller, but by the larger of the quantities AS and W . Because of that, the energy spent to establish an FM region per atom being equal, the ferron states are much more favoured in magnetoexcitonic semiconductors than in AFS. In particular, since the c - l exchange energy may be as high as several eV, even in the case of the exciton frequency $\sim 10^{-2}$ eV as in Co compounds, ferrons having a moment of the order of 100 atomic moments are possible. Moreover, in case of narrow bands small (single-exciton) ferrons are possible, even if the exciton frequency is almost as high as AS , i.e. exceeds 1 eV.

In case of the spin of a magnetic atom being nonzero, the intensification of c - l exchange following the creation of an exciton is not

necessarily the result of an increase in the spin. It may be enough for the c - l integral to grow, with the spin remaining unchanged or even decreasing. In the latter case the autolocalization of the electron in an AFS is as before accompanied by the establishment of a region with enhanced magnetization, whereas in an FMS on the contrary a region with reduced magnetization is established. If the creation of an exciton does not alter the spin, in addition to the c - l exchange the polarization effects discussed in Sec. 5.5 should also be taken into account.

Singlet Magnets. Another class of materials in which exciton ferrons may materialize consists of semiconducting magnets with a singlet ground state of the ions ("singlet magnets"). As has been pointed out in Secs. 2.2 and 2.3, in them, on account of a strong effect of the magnetic anisotropy, the average value of the ionic moment projection $\langle J^z \rangle$ would have been zero, but for the exchange interaction of the ions with their neighbours resulting in a magnetic polarization. This makes for magnetic ordering with unsaturated atomic moments $\langle J^z \rangle$ ($0 < \langle J^z \rangle < J$) of some type or other to be established.

Even in case the ordering is of an FM type, the energy of the conduction electron is higher in a singlet magnet than in an FM with a saturated moment by the amount

$$U = \frac{A}{2} [J - \langle J^z \rangle]. \quad (5.6.1)$$

Accordingly, a gain in the energy of the system may be obtained by establishing a microregion with a saturated FM ordering and by localizing a conduction electron in it [420]. The creation of such a region is tantamount to the excitation of every atom in it to a state representing the superposition of all the components of a multiplet produced in the result of the splitting of an atomic level with the specified J by the crystal field. Of course, exciton ferrons are also possible in singlet AF, where a conduction electron simultaneously changes the orientation and the magnitude of atomic moments. Conditions favourable for their materialization may also exist in singlet magnets with an exchange between the ions and their neighbours so weak that no magnetic polarization takes place (i.e. $\langle J^z \rangle = 0$).

Below we shall present the calculation of exciton ferrons in a singlet magnet. It will be demonstrated that the ferrons can exist in a wide temperature range from $T = 0$ to the PM region.

First of all we shall have to estimate the free energy required to set up an FM microregion. The Hamiltonian (2.2.6) is represented in the form

$$H = H_{MF} + H_1, \quad (5.6.2)$$

where H_{MF} is the mean field Hamiltonian (2.3.8). The mean field in it \mathcal{H}_{MF} , in contrast to expression (2.3.7), is obtained by temperature averaging to the exciton operators over eigenstates of the Hamiltonian H_{MF} . The average magnetization $\langle J^z \rangle \equiv \mathcal{M}$ is determined from the self-consistency relation similar to (2.5.2) containing the Hamiltonian H_{MF} instead of H_e . Taking into account relation (2.3.10), we obtain the self-consistency equation in the form

$$\begin{aligned} 1 - \sqrt{1 - \left(\frac{\alpha \mathcal{M}}{c}\right)^2} &= \alpha \tanh \left\{ \sqrt{1 - \left(\frac{\alpha \mathcal{M}}{c}\right)^2} \frac{\omega}{2T} \right\}, \\ \alpha &= \frac{2\mathcal{K}c^2}{\omega}. \end{aligned} \quad (5.6.3)$$

The free energy is evaluated with the aid of the formula

$$\begin{aligned} F &= F_{MF} + \text{Sp} \{H_1 \exp(-H_{MF}/T)\} / \text{Sp} \exp(-H_{MF}/T), \\ F_{MF} &= -T \ln \text{Sp} \exp(-H_{MF}/T). \end{aligned} \quad (5.6.4)$$

From formulae (5.6.2, 4), (2.2.6) and (2.3.8) we obtain the expression for the free energy per atom

$$f = \frac{\omega}{2} - T \ln \left\{ 2 \cosh \left[\frac{\omega}{2T} \sqrt{1 - \left(\frac{\alpha \mathcal{M}}{c}\right)^2} \right] \right\} - \frac{\mathcal{K} \mathcal{M}^2}{2}. \quad (5.6.5)$$

The free energy spent per atom to set up a microregion with a saturated FM ordering is equal to

$$D = f - \omega_F, \quad \omega_F = e_F - \frac{\mathcal{K} J^2}{2}, \quad (5.6.6)$$

where e_F is the energy spent to make the ion go over to a state having the maximum moment projection $\langle J^z \rangle = J$. It corresponds to the multiplet centre and usually exceeds the minimum ion excitation energy ω about 1.5 times.

Formulae (5.2.1-6) remain in force for an exciton ferron in a singlet FM, but in them the depth of the potential well U and the magnetic energy losses D should be taken from (5.6.4, 6). They can be applied even in the vicinity of T_c , since in a singlet FM the degree of magnetic polarization of ions diminishes with rising temperature, and because of that the short-range magnetic order of which formula (5.6.1) takes no account is less important in them than in the Heisenberg FM.

The condition for the ferron state to be a thermodynamically-favoured one is written down in the form

$$D^* = \left[1 - \frac{\mathcal{M}}{J} \right]^{-\frac{5}{2}} D < 0.2W \left(\frac{AJ}{2W} \right)^{5/2} = D_c. \quad (5.6.7)$$

Fig. 5.13 depicts the results of numerical computation of D^* for certain values of ω_F/ω and for the following parameters: $W = 3$ eV, $AJ/2W = 0.1$, $c'J = 0.6$, $\alpha = 1.2$ (the moment at $T = 0$ corresponding to this α is equal to $0.55c$). For a specified value of ω , the autolocalized state of the electron in the region of enhanced

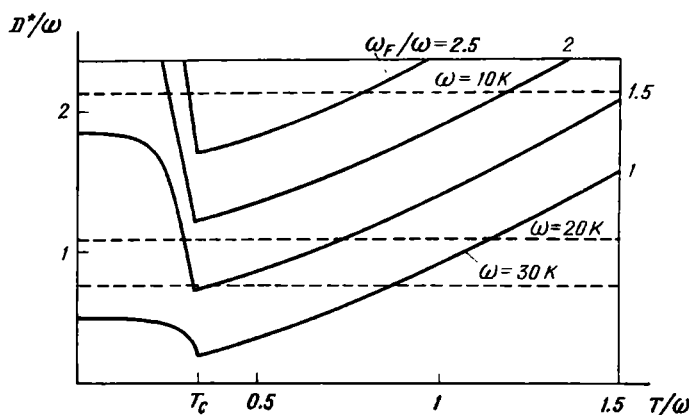


Fig. 5.13. Ferron states in a singlet ferromagnet

magnetization is stable when the appropriate curve lies below the dashed straight line D_c/ω . The Curie temperature has been determined from formula (5.6.3) from the condition that the magnetization be zero.

For $\omega_F/\omega = 1.5$ and $\omega = 10$ K the ferrons will be seen from this figure to be stable in a wide temperature range from $T = 0$ to the far PM region. However, already for $\omega = 20$ K the ferrons are stable only in the vicinity of T_c as in a Heisenberg magnet. A decrease in α from 1.2 to 1 (at this value there is, according to (2.3.11), no spontaneous magnetization in the crystal) greatly improves the stability of ferron states.

CHAPTER 6

INDIRECT EXCHANGE IN MAGNETIC SEMICONDUCTORS

6.1. INDIRECT EXCHANGE IN FERROMAGNETIC SEMICONDUCTORS

Chief Features. As has already been discussed in Sec. 3.2, the conduction-band bottom in a magnetic semiconductor lies lowest of all in case of the FM ordering. In semiconductors the conduction electrons occupy only the states lying in the vicinity of the band bottom, and when the latter sinks their energy decreases. Accordingly, they tend to establish the FM ordering (this is generally not applicable to metals in which the Fermi energy is large as compared to the c - l exchange energy, and the Fermi surface is intricately shaped*). If the concentration of electrons in a semiconductor is high enough, they can substantially affect the magnetic ordering in the crystal, and this is observed in degenerate semiconductors. In nondegenerate semiconductors the electron concentration is too small to exercise a noticeable effect on the magnetization of the crystal as a whole. However, localized c -electrons can substantially affect the local magnetic properties of the crystal in the vicinity of the imperfections that have trapped them.

In Sec. 3.3 we have presented the RKKY theory of indirect exchange based on the treatment of the c - l exchange as a small perturbation. The condition of its applicability is the smallness of the c - l exchange energy AS as compared with the Fermi energy μ of the carriers. But the inequality $\mu \gg AS$ as a rule does not hold in semiconductors. Indeed, if the conduction band is narrow ($W \ll AS$), the Fermi energy μ will be smaller in comparison with AS , i.e. the situation is directly opposite to that in metals. But even though the conduction band is wide ($W \gg AS$), even the weak inequality $\mu > AS$ will not hold as a rule, because of relatively low carrier concentrations in degenerate semiconductors ($v = n/N \ll 1$). Thus, if the effective carrier mass is equal to the true electron mass, for $AS = 0.5$ eV the Fermi energy becomes equal to AS only for a carrier concentration of 10^{21} cm $^{-3}$. Accordingly, a feature of paramount importance of the indirect exchange in magnetic semiconductors is that it cannot be described with the aid of the Heisenberg Hamiltonian: a Heisenberg Hamiltonian bilinear in

* This also does not apply to anomalous FMS with a blue absorption edge shift in which the conduction electrons tend to establish an AF ordering.

spins can be constructed from the c - l exchange Hamiltonian H_A (3.1.2) linear in spins only in the second order of the perturbation theory in H_A , and this requires that $AS\mu$ be small.

In some papers the RKKY theory is applied to magnetic semiconductors and not only to degenerate, but even to nondegenerate ones. It might seem that for degenerate semiconductors this could be justified by the smallness of $\frac{AS}{\mu}$ v. That in actual fact not this quantity, but $AS\mu$ serves as the small parameter in the RKKY theory, will be seen directly from formula (3.3.9). The term $H_{M\sigma}$ in (3.3.6) reduces to an expression bilinear in the spins, i.e. quadratic in \mathfrak{M} , only if the electron distribution function $n_{k\sigma}$ can be expanded in AS/μ . Qualitatively, the inapplicability of the RKKY theory for $\mu < AS$ will be evident, if the case of the ferromagnetic ordering at $T = 0$ is considered. For $A > 0$ the ground state of the system with the Hamiltonian (3.1.1) can be determined precisely. In it all the c -electrons have the same spin projection as the l -spins. This distinguishes it radically from the ground state of free electrons with unpolarized spins described by the Hamiltonian H_B . The former state cannot be obtained from the latter, which corresponds to the zeroth approximation of the RKKY theory, no matter what order of the perturbation theory in $AS\mu$ is employed.

Similarly, it can easily be demonstrated that for the perturbation theory to be applicable to nondegenerate semiconductors, AS/T will have to be small. It is not enough for the number of electrons per atom v to be small, and that consequently ASv/T be small. Indeed, in the RKKY theory the magnetic Hamiltonian constitutes a correction to the electron energy due to the c - l exchange. Since every c -electron interacts with the l -spins independently of the others, any order in H_A of the electron energy will contain terms proportional to their number. For this reason v does not enter the ratio of the correction of the subsequent order to that of the preceding one, and consequently cannot make this ratio small.

Magnon Frequencies. The approach employed below differs from the RKKY theory in that the essential part of the c - l exchange is taken into account already in the zeroth approximation. Such an approach enables the magnon spectrum at $T = 0$ to be determined. The inverse spin $1/2S$ [70, 89, 166] serves in this case as the small parameter. Averaging the Hamiltonians (4.1.2) and (4.2.4) over the electron variables, we obtain in the first order in this parameter:

in the case of narrow bands $W \ll AS$

$$\begin{aligned} \omega_q &\simeq \omega_q^0 + \mathcal{Y}_{\text{eff}}(1 - \gamma_q), \\ \mathcal{Y}_{\text{eff}} &= \frac{z|B|}{2SN} \sum_{\mathbf{k}} n_{\mathbf{k}} \gamma_{\mathbf{k}} \simeq \frac{z|B|}{2S} v, \end{aligned} \quad (6.1.1)$$

and in the case of wide bands $W \gg AS$

$$\omega_q \simeq \omega_q^0 + \frac{Avq^2}{2(q_0^2 + q^2)}, \quad (6.1.2)$$

respectively, where ω_q^0 is the magnon frequency in the absence of the indirect exchange (2.4.4), and $q_0^2 \simeq 2m^*AS$. When writing out (6.1.2), we took into account that the conduction electrons are completely spin-polarized.

Both expressions (6.1.1, 2) obviously satisfy the requirement stemming from the isotropy of the system: the magnon frequency for $q \rightarrow 0$ is proportional to q^2 , as should be the case for a Goldstone mode. This means that the law T^3 is valid for the variation of the magnetization with the temperature in full analogy to (2.4.8). The magnon frequency (6.1.2) turns zero for $q \rightarrow 0$, because of the presence of q_0^2 in the denominator, i.e. because the frequency is nonanalytic in the c - l exchange for $AS \ll W$. Hence, this property proves to be associated with the isotropy of the space causing the gap in the magnon spectrum to be absent.

At first glance it might appear strange that the magnon frequency for $W \ll AS$ (6.1.1) is independent of the c - l exchange constant A , despite the fact that the existence of the indirect exchange is a consequence of the c - l exchange. But the c - l exchange by itself cannot produce the indirect exchange, if the electron is bound to some atom and not allowed to go over to other atoms. Accordingly, the electron contribution to the magnon frequency should vanish for $B = 0$, and this is reflected in formula (6.1.1) valid in the first approximation in WAS . The omission from it of the c - l exchange integral is the result of the spinpolaron state of the electron: its spin is rigidly bound to the local moment irrespective of the angle it makes with the total moment of the crystal. For the same reason the integral A is omitted from formula (6.1.2) for $q^2 \ll q_0^2$, and then expression (6.1.2) turns into (6.1.1).

It follows from formulae (6.1.1, 2) that the effective exchange integral $\mathcal{Y}_{\text{eff}}(\mathbf{g}) = -\frac{1}{N} \sum_q \omega_q e^{-i\mathbf{q} \cdot \mathbf{g}}$ for $W \ll AS$ is nonzero only for the nearest neighbours, decaying exponentially for $W \gg AS$ at the distance q_0^{-1} . It does not display any Ruderman-Kittel-type oscillations. The magnon frequency grows with the growth in v in the region $v \ll 1$, i.e. the conduction electrons, as required, tend to uphold the FM ordering.

Paramagnetic Curie Point. Doping the crystal with a donor impurity also shifts the Curie point of the crystal. This shift in EuO and EuS can be as high as 100% [9]. Whereas the problem of the magnon spectrum of degenerate FMS can in principle be solved with any precision desired, it is much more difficult to establish the dependence of their Curie points on the concentration. It would

appear at first glance that the RKKY theory could be used to calculate T_c in case of wide bands, since near T_c the spin polarization of conduction electron vanishes, and the electron energy can be expanded in the small parameter ASW . In fact this is not so: the RKKY theory (Sec. 3.3) requires the use of plane waves with a fixed spin direction for the zeroth-approximation electron states. At the same time, as has been demonstrated in Sec. 4.3, such states decay rapidly in the vicinity of T_c and cannot be used as basis states for constructing the perturbation theory.

However, at $T \gg T_c$ the RKKY theory may be applied for evaluating the paramagnetic Curie point of wide-conduction-band semiconductors, since, if the inequality $AS \ll \sqrt{\mu W}$ is satisfied, the conduction electrons with a fixed quasi-momentum and spin direction will, according to (4.3.3., 12), be well-defined elementary excitations. In the mean field approximation (Sec. 2.5) the magnetization \mathfrak{M} , if the diagonal part of the c - l exchange energy \tilde{H}_{cd} (3.3.6) is taken into account, will be determined from the equation

$$\mathfrak{M} = \frac{S(S+1)}{3T} \left[H + zJ\mathfrak{M} + \frac{A}{2N} (n_{\uparrow} - n_{\downarrow}) \right], \quad (6.1.3')$$

$$n_{\sigma} = \sum_{\mathbf{k}} n(E_{\mathbf{k}} - A\mathfrak{M}\sigma)$$

(the term containing σH in the electron energy can be neglected, for it is small as compared with $A\mathfrak{M}$). For $A\mathfrak{M} \ll \mu$ the electron distribution function $n(E)$ can be expanded in a series in $A\mathfrak{M}/\mu$, and then equation (6.1.3') reduces to the Curie-Weiss law with the PM Curie point shifted with respect to one in formula (2.5.6) by the amount (compare with (2.5.6), (3.3.14))

$$\Delta\theta = \frac{A^2 S(S+1) v}{8\mu}. \quad (6.1.3)$$

The result (6.1.3) means that the indirect exchange via conduction electrons renormalizes the direct exchange integral by adding to it the indirect exchange integral $\mathcal{Y}_{\text{eff}}(0)$ (3.3.12). It is valid for fields small as compared with the field \mathcal{H}_P of the total spin polarization of conduction electrons as determined from the equation $A\mathfrak{M}(\mathcal{H}_P) = 2^{2/3}\mu$. The non-Heisenberg nature of the indirect exchange makes itself manifest in a θ vs. \mathcal{H} dependence, which becomes essential in higher fields. The result that θ must be a function of \mathcal{H} follows already from the fact that in fields greater than \mathcal{H}_P , but small as compared with the saturation field $\sim T$, the indirect exchange retains the exchange integral unchanged, but renormalizes the magnetic field. Indeed, according to (6.1.3') for $\mathcal{H}_P < \mathcal{H} \ll T$ the magnetization is equal to $\chi(0)\mathcal{H}'$ where $\chi(0)$ is the susceptibility of an undoped sample (2.5.6), and the renormalized field

\mathcal{H}' exceeds the true field \mathcal{H} by $4\pi/2$. Hence, χ and θ diminish as the field is increased, reaching for $\mathcal{H} = \mathcal{H}_p$ the same values as in a pure crystal. In the interval $\mathcal{H}_p < \mathcal{H} \ll T$ they are practically independent of the field.

From the physical standpoint the decrease in the effect the electrons exercise on the magnetic susceptibility with the increase in the magnetic field can be explained as follows. In weak fields the electron magnetization is linear in the field, and because of that the electron energy E_e is quadratic in the field. The contribution of the electrons to the magnetic susceptibility is proportional to $\partial^2 E_e / \partial H^2$ and because of this nonzero in weak fields. On the other hand, in case the electrons are completely spin-polarized, their moment is independent of the field (it is equal to $n/2$). Accordingly, their energy is linear in the field, provided that the magnetization of the crystal is linear, too. This is exactly the reason why the electron contribution to χ of the crystal vanishes, despite the fact that the electrons increase its magnetization in an external field.

Such an effect has been observed in heavily-doped EuSe crystals, which behave in the PM region as FMS. In a crystal with a carrier concentration of $6 \times 10^{15} \text{ cm}^{-3}$ the paramagnetic Curie temperature varies from 26 K in weak fields to 11 K in strong fields [336] (θ of a pure specimen is equal to 9 K). The same shift of θ is obtained also from formula (6.1.3), if the electron effective mass and the c - l energy are put at values typical for europium chalcogenides: $m^* = 1.5 m_0$, $AS = 0.5 \text{ eV}$.

Curie Point. To obtain an estimate of the Curie point, below we shall make use of the method of low-temperature expansions in which T_c is expressed in accordance with formula (2.5.11) in terms of magnon frequencies renormalized owing to the magnon-magnon interaction. The anharmonism of magnons resulting from the indirect exchange must be taken into account in several other problems as well. Let us obtain the expression for the magnon-magnon interaction Hamiltonian in the case of narrow bands $W \ll AS$. We shall take the Hamiltonian (Ap. I.16a) as the initial one (to be definite, we put $A > 0$). We shall make use of the Holstein-Primakoff transformation (2.4.1), retaining terms of the first order in b^*b/S . Substituting expressions (2.4.1) into H_- (Ap. I.16a) and going over from the site to the momentum representation, we obtain the effective Hamiltonian of the spinpolaron-magnon system up to terms of the order $1/S^2$, inclusive, in the form [176]

$$H = -\beta \sum \gamma_{\mathbf{k}} \alpha_{\mathbf{k}}^* \alpha_{\mathbf{k}} + \frac{\beta}{4SN} \sum \left[(\gamma_{\mathbf{k}} + \gamma_{\mathbf{k}'} - 2\gamma_{\mathbf{k}+\mathbf{q}}) \right. \\ \left. - \frac{1}{2S} \left(\frac{3}{4} \gamma_{\mathbf{k}} + \frac{3}{4} \gamma_{\mathbf{k}'} - 2\gamma_{\mathbf{k}+\mathbf{q}} \right) \right] b_{\mathbf{q}}^* b_{\mathbf{q}'} \alpha_{\mathbf{k}}^* \alpha_{\mathbf{k}'} \mathcal{L}(\mathbf{k} + \mathbf{q}, \mathbf{k}' - \mathbf{q})$$

$$-\frac{\beta}{16S^2N^2} \sum \left[\gamma_{\mathbf{k}+\mathbf{q}-\mathbf{q}'} - \frac{1}{2} \gamma_{\mathbf{k}'} \right. \\ \left. - \frac{1}{2} \gamma_{\mathbf{k}} \right] b_{\mathbf{q}}^* b_{\mathbf{p}}^* b_{\mathbf{p}'} b_{\mathbf{q}'} \alpha_{\mathbf{k}}^* \alpha_{\mathbf{k}'} \mathcal{Z}(\mathbf{k} + \mathbf{p} + \mathbf{q}, \mathbf{k}' - \mathbf{p}' + \mathbf{q}'), \quad (6.1.4)$$

where $\beta = z |B|$, $\mathcal{Z}(\mathbf{x}, \mathbf{y}) = 1$ when \mathbf{x} and \mathbf{y} are equal, or their difference is equal to an arbitrary reciprocal lattice vector, and $\mathcal{Z}(\mathbf{x}, \mathbf{y}) = 0$ otherwise.

As has been discussed in Sec. 3.3, the part of the magnetic Hamiltonian is played by the correction to the electron energy expressed in terms of spin operators. In the second order of the perturbation theory in $1/S$ we obtain from (6.1.4) an expression for the indirect exchange Hamiltonian (the Heisenberg Hamiltonian (2.4.9), (2.4.4') has been added to it):

$$H_M = \sum (\omega_{\mathbf{q}} + \Delta\omega_{\mathbf{q}}) b_{\mathbf{q}}^* b_{\mathbf{q}} \\ - \frac{1}{4SN} \sum \left\{ \mathcal{Y} (2\gamma_{\mathbf{q}-\mathbf{q}'} - \gamma_{\mathbf{q}} - \gamma_{\mathbf{q}'}) + \frac{\mathcal{Y}_{\text{eff}}}{2} (\gamma_{\mathbf{q}-\mathbf{q}'} - 1) \right. \\ \left. + \frac{\beta}{4S} Z_{\mathbf{qp}; \mathbf{p}'\mathbf{q}'} [1 - \delta(\mathbf{q}, \mathbf{q}')] \right\} b_{\mathbf{q}}^* b_{\mathbf{p}}^* b_{\mathbf{p}'} b_{\mathbf{q}'} \mathcal{Z}(\mathbf{p} - \mathbf{q}, \mathbf{p}' - \mathbf{q}'), \quad (6.1.5)$$

where we make use of the notation

$$Z_{\mathbf{qp}; \mathbf{p}'\mathbf{q}'} = \frac{1}{N} \sum_{\mathbf{k}\mathbf{k}'} \frac{(\gamma_{\mathbf{k}} + \gamma_{\mathbf{k}'} - 2\gamma_{\mathbf{p}+\mathbf{k}'}) (\gamma_{\mathbf{k}} + \gamma_{\mathbf{k}'} - 2\gamma_{\mathbf{q}+\mathbf{k}})}{\gamma_{\mathbf{k}'} - \gamma_{\mathbf{k}}} \\ \times n_{\mathbf{k}'} (1 - n_{\mathbf{k}}) \mathcal{Z}(\mathbf{q} + \mathbf{k}, \mathbf{q}' + \mathbf{k}'),$$

and where the correction $\Delta\omega_{\mathbf{q}}$ of the next order in $1/S$ to the frequency $\omega_{\mathbf{q}}$ is given by the expression

$$\Delta\omega_{\mathbf{q}} = -\frac{\mathcal{Y}_{\text{eff}}}{4S} \left[\frac{3}{2} - 2\gamma_{\mathbf{q}} \right] - \frac{\beta}{16S^2N} \sum_{\mathbf{p}} Z_{\mathbf{qp}; \mathbf{qp}}. \quad (6.1.6)$$

It follows from formula (6.1.6) that for $q \rightarrow 0$ this correction tends to zero, as should be the case in an isotropic system. There is no magnon damping in the $1/S^2$ approximation. Next, it follows from (6.1.5) and (6.1.1) that, although in the main approximation in $1/S$ the direct and the indirect exchange result in similar magnon dispersion laws, the structure of the anharmonic terms for these two mechanisms is quite different. This is the consequence of the non-Heisenberg exchange via the spinpolarons.

As has already been stated in Sec. 2.4, the renormalized magnon frequency $\omega_{\mathbf{q}}$ is determined by the derivative of the average energy $\langle H_M \rangle$ with respect to the occupation number $m_{\mathbf{q}}$ of the corresponding magnon state. Making use of formulae (6.1.1, 5, 6) and (2.4.10)

we obtain at $T \gg T_c/S$

$$\tilde{\omega}_q(T) = \left\{ \gamma \left[1 - \frac{T}{(\gamma + \gamma_{\text{eff}})S} \right] + \gamma_{\text{eff}} \left[1 - \frac{T\gamma_q}{8(\gamma + \gamma_{\text{eff}})S} \right] \right\} (1 - \gamma_q). \quad (6.1.7)$$

(In the calculations we have used the numerical value 1.5 for the Watson integral (2.4.8a). The distribution function of m_q was put equal to $T/\omega_q(0)$.)

The ratio of the temperature-dependent corrections to the magnon frequency due to the indirect exchange (the term $\sim T\gamma_{\text{eff}}$), and to the direct exchange (the term $\sim T\gamma$) will be seen from formula (6.1.7) to be smaller by an order of magnitude than $\gamma_{\text{eff}}/\gamma$ determining the contributions of these mechanisms to ω_q at $T=0$. Moreover, the former correction, in contrast to the latter, alternates in sign, so that it may be discarded when T_c is calculated from formula (2.5.11). In the result we obtain

$$T_c = \frac{T_c^0 (1 + \gamma_{\text{eff}}/\gamma)^2}{(1 - 3\gamma_{\text{eff}}/5\gamma)}, \quad (6.1.8)$$

where $T_c^0 \simeq 0.4 \gamma S$ is the Curie point of the crystal in the absence of charge carriers obtained in the same approximation.

In the case of wide-conduction-band semiconductors to take account of the magnon anharmonism resulting from the indirect exchange via the conduction electrons, one has to perform extremely cumbersome calculations leading to rather intractable expressions (the fourth approximation of the perturbation theory for a Hamiltonian of a complex structure). However, as in the case of narrow-band semiconductors, this anharmonism may be expected to be inessential for the estimate of T_c , and we may confine ourselves to calculating the effects of the anharmonism of the direct exchange (in any case, such an approach guarantees greater precision than a total neglect of anharmonism). The computation of T_c is carried out with the aid of formulae (2.5.11), (6.1.2) by using a quadratic approximation for the dispersion law for ω_q^0 (2.4.10). Correspondingly, the integration with respect to q is performed over the sphere of radius $K = (6\pi^2)^{1/3} a^{-1}$ whose volume coincides with that of the Brillouin zone. For the Curie point of a degenerate wide-band semiconductor we obtain the following expression [362]:

$$T_c = T_c^0 \left\{ 1 - \frac{Q^2}{K \sqrt{q_0^2 + Q^2}} \arctan \frac{K}{\sqrt{q_0^2 + Q^2}} \right\}^{-1}, \quad (6.1.9)$$

$$Q^2 = A \nu M(T_c), \quad M^{-1}(T) = \frac{\tilde{\gamma} a^2}{3}.$$

For small electron concentrations, when the inequality $Q^2 \ll q_0^2 \ll \ll K^2$ is valid, it follows from formula (6.1.9) that

$$\Delta T_c = T_c - T_c^0 = \left(\frac{\pi}{6}\right)^{\frac{2}{3}} \frac{ASv}{aq_0}. \quad (6.1.10)$$

Hence, for smallest v the shift in T_c is linear in the electron concentration. A noteworthy point is that, in contrast to the RKKY theory, it is nonanalytic in the c - l exchange ($\Delta T_c \sim \sqrt[3]{A}$). However, as the concentration continues to grow, the dependence of the shift on v becomes weaker. In the region $q_0^2 \ll Q^2 \ll K^2$ it is of a square-root type

$$\Delta T_c \simeq 0.4 \sqrt{T_c^0 ASv}. \quad (6.1.11)$$

The difference in the expressions for the shift of T_c (6.1.10) and (6.1.11) follows from the fact that in the region of applicability of the former the contribution of the direct exchange to the magnon frequency for all quasi-momenta exceeds that of the indirect exchange. On the other hand, in the region of applicability of the latter the dominant factor for small quasi-momenta is the direct exchange, and for large quasi-momenta the indirect exchange. In the case when the indirect exchange dominates for all quasi-momenta ($Q^2 \gg K^2 \gg q_0^2$), the expression valid for the shift of the Curie point is

$$\Delta T_c = \frac{ASv}{2} \quad (6.1.12)$$

(in this case it is more expedient to use (2.5.11) and (6.1.2) directly). The structure of formulae (6.1.11, 12) is such that they can be directly applied to any isotropic crystal.

The transition from the linear-type shift (6.1.10) to the square-root type (6.1.11) takes place at concentrations

$$v \sim \frac{zT_c^0}{SW}.$$

In EuO ($T_c^0 \simeq 7 \times 10^{-3}$ eV, $W \sim 5$ eV, $S = 7/2$) the nonlinear dependence starts already at concentrations $\sim 10^{19} \text{ cm}^{-3}$ ($v \sim 10^{-3}$). The dependence (6.1.12) sets in only at $ASv \gg T_c^0$, i.e. in EuO with $AS \simeq 0.5$ eV it takes place at $n > 10^{20} \text{ cm}^{-3}$, and then the rate of increase in the Curie point with the concentration rises until AS becomes equal to μ .

The theoretical results obtained above agree well with the experimental data reported in [112] in which the dependence of Curie point in degenerate EuO - Gd specimens on the electron density was studied (see Table III). Only quantities measured directly in experiment have been used to compute ΔT_c . The value of 0.52 eV determined in [112] from the red shift of the absorption edge ΔE_g in an undoped specimen was chosen for AS (the decrease in the red

Table III

n , 10 ¹⁹ cm ⁻³	v , 10 ⁻³	$\frac{AS}{\mu}$	ΔT_c (theor.), 10 ⁻⁴ eV	ΔT_c (exp.), 10 ⁻⁴ eV	$\Delta\theta$, 10 ⁻⁴ eV
6.6	2.2	10	9.8	9.5	18
16	5.3	6	16	12	24
60	20	2.3	> 29.4 < 52	40	38

shift with rising v noticed in [112] and interpreted erroneously there as the result of a decrease in the c - l exchange integral A , as demonstrated in Sec. 4.6, finds its explanation in an increase in the Fermi energy of charge carriers owing to their spin-polarization). For $v = 2 \times 10^{-2}$ the quantities K and Q are of the same order of magnitude, and formulae (6.1.12) and (6.1.11) valid for $Q^2 \gg K^2$ and $Q^2 \ll K^2$ yield only the upper and the lower estimate of ΔT_c , respectively. For lower concentrations, the computations have been performed with the aid of formula (6.1.11). Specimens with $v < 6 \times 10^{-4}$ have not been considered, since, according to [112], the carrier concentration in them is strongly temperature-dependent. At the same time the theory developed above presumes such a dependence to be absent. In addition to ΔT_c , the table contains $\Delta\theta$ obtained from formula (6.1.3). The Fermi energy $\mu = (3\pi^2 n)^{2/3}/2m^*$ has been calculated for the value of the conduction-electron effective mass $m^* = 9 \times 10^{-28}$ g obtained from an analysis of experimental data on $E_g(v)$ [112] in Sec. 4.6. The number of electrons v per a Eu^{++} ion has been obtained from the electron concentration n with account taken of the fact that in a EuO crystal with a NaCl structure the number of Eu^{++} ions per unit volume is $4a^{-3}$ (see Table I).

Within the framework of the RKKY theory, $\Delta\theta$ should have been equal to ΔT_c , since in Heisenberg magnets the true PM and the Curie temperature are almost equal (Sec. 2.5).

It follows from Table III that in fact the shift of the PM Curie temperature should exceed the shift of the true Curie temperature. However, with the rise in the electron concentration and consequently in the Fermi energy μ , the difference $\Delta\theta - \Delta T_c$ decreases. In the limit $\mu \gg AS$, when the indirect exchange turns into a Heisenberg one, it should vanish altogether in the approximation used. Since a ferromagnet behaves like a Heisenberg one at $n = 0$ as well, this difference as a function of the concentration should pass through a maximum.

In semiconductors with an intermediate degree of doping, which have a finite conductivity at $T = 0$ but display a high resistivity peak in the vicinity of T_c , the conduction electrons exercise practically no influence on the Curie point, for in the vicinity of the

Curie point they go over to states localized on the donors (Sec. 7.6). Trapped by the donors, the electrons can affect only the short-range, but not the long-range magnetic order. Above T_c the electrons again

become delocalized and should shift the PM Curie point in accordance with (6.1.3).

The maximum of $(\theta - T_c)$ as a function of the concentration n has been experimentally observed in $\text{Eu}_{1-x}\text{Gd}_x\text{S}$ [9]. The difference $(\theta - T_c)$ practically equal to zero at $x = 0$, at $x \sim 0.01$ rises to as much as 20 K, diminishing as x continues to increase (Fig. 6.1). Similar results have been obtained with $\text{Eu}_{1-x}\text{Gd}_x\text{O}$ [130]. It has been established by conductivity measurements that in the range of room temperatures for $x < 0.015$ the system behaves like an insulator, and for $x > 0.015$ as a semimetal. In both cases θ has been observed to exceed T_c (Fig. 6.2). In the region of metallic conductivity the Curie-Weiss

law holds up to a good accuracy, whereas at $x \sim 0.005$ deviations from this law have been observed (Fig. 6.3). It should be noted that

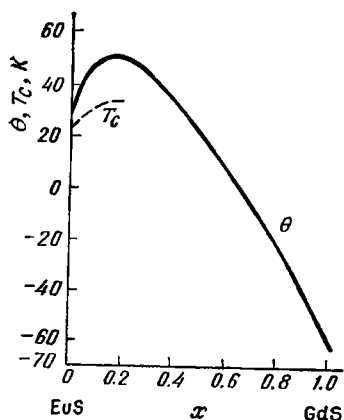


Fig. 6.1. Ferromagnetic and paramagnetic Curie points of $\text{Eu}_{1-x}\text{Gd}_x\text{S}$ [9]

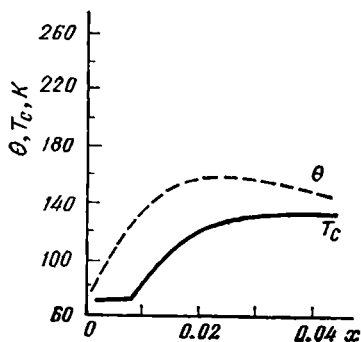


Fig. 6.2. Ferromagnetic and paramagnetic Curie points of $\text{Eu}_{1-x}\text{Gd}_x\text{O}$ [130]

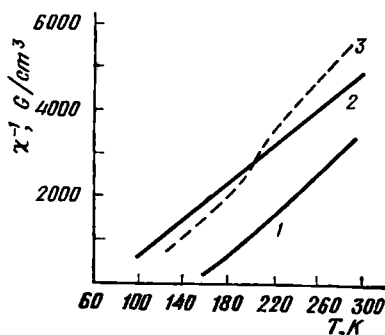


Fig. 6.3. Magnetic susceptibility vs. temperature for $\text{Eu}_{1-x}\text{Gd}_x\text{O}$ [130]:

1, $\text{Eu}_{0.97}\text{Gd}_{0.03}\text{O}$; 2, EuO ;
3, $\text{Eu}_{0.995}\text{Gd}_{0.005}\text{O}$

the total number of impurity atoms may greatly exceed that of conduction electrons since many impurities are in a nonactive state (e.g. forming clusters) and therefore do not contribute to the conduction electron density.

Usually the fact that θ exceeds T_c is explained as a result of the presence of localized ferrons in the crystal [115]. But there are none in degenerate crystals, because the donor electrons are delocalized. Next, deviations from the Curie-Weiss law should have been observed in the case of localized ferrons, because θ turns out to be temperature-dependent (Sec. 6.5). For this reason the experimental results [130] prove that the fact that θ exceeds T_c in degenerate semiconductors is associated not with the localized ferrons, but with the non-Heisenberg nature of the indirect exchange in MS. Additional proof of this is the considerable difference of the magnetization curve of a heavily-doped EuO specimen from the Brillouin curve typical of a pure EuO specimen [556].

One should remember that the indirect exchange via carriers is not the only mechanism by which the impurity effects the magnetic properties. Thus, at high impurity concentrations its effect on the superexchange becomes prominent. The record value of $T_c = 180$ K in EuO doped with Fe [430] is probably not associated with the indirect exchange.

6.2. HEAVILY-DOPED ANTIFERROMAGNETIC SEMICONDUCTORS

In heavily-doped AFS the indirect exchange via conduction electrons, which tends to establish the FM order, competes with the direct exchange between the magnetic atoms tending to establish the AF ordering.

Naturally, at sufficiently high concentrations, when the indirect exchange is predominant, an FM ordering should be established in the crystal. This has been observed, for example, in MnTe at a hole concentration of 10^{21} cm^{-3} [172]. In metamagnets the FM ordering is established at relatively low carrier concentrations, e.g. in EuSe it exists already at $n \sim 10^{18} - 10^{19} \text{ cm}^{-3}$, although in it the picture is complicated by an inhomogeneous magnetic state of the homogeneous crystal (Sec. 7.5). Below we shall consider the case when the crystal is in a homogeneous magnetic state, i.e. no ferrons are produced in it*. Although the electrons can produce spontaneous magnetization only if their concentration is high enough, above some critical value n_A , they can substantially affect the magnetization of the crystal when an external magnetic field is applied to it. In other words, for $n < n_A$ the electrons enhance the effect of the external field on the crystal.

Were the indirect exchange of the Heisenberg nature, the transition from the AF ordering to the FM one with rising carrier concentration would take place abruptly. However, as will be demonstrated

* The conditions for a homogeneous state are especially favourable in crystals with a layered AF ordering [198].

below, because of the non-Heisenberg nature of the exchange, there is a veritable concentration interval $[n_A, n_F]$ inside which neither the AF nor the FM state is stable [174, 175]. But an AFS begins to exhibit non-Heisenberg properties even before n_A is attained: its magnetic susceptibility in weak fields turns out to be much higher than in strong ones, whereas in a Heisenberg AF it should, according to (2.3.6), be constant [173, 174]. The non-Heisenberg nature of the indirect exchange also makes itself manifest in the magnon spectrum in a magnetic field.

Wide-band Semiconductors. Qualitatively, peculiar properties of wide-band AFS can be interpreted as follows. An external field by inducing a magnetization in an AFS induces thereby a mean crystal field $\mathcal{H}_M = A\mathcal{M}/2$, which acts on the conduction electron spins (\mathcal{M} is the atomic spin projection on the direction of the field). According to (2.3.6), it is $\sim AS/T_N$ times, i.e. by several orders of magnitude, higher than the external field, which induced it. Because of that even relatively small external fields induce a strong spin-polarization of conduction electrons, and in this sense we may speak of a giant Zeeman effect in an antiferromagnet [173, 259].

The fact that in an MS the Fermi energy μ is small as compared with AS results in a nonlinear magnetization vs. field dependence, whereas in undoped crystals it is linear (we ignore effects associated with the anisotropy). Namely, with increase in the field strength, the magnetic susceptibility decreases until the field reaches the value \mathcal{H}_P corresponding to complete electron polarization. In fields exceeding \mathcal{H}_P it becomes equal to the susceptibility of a pure crystal (2.3.6). According to the condition $\mu \ll AS$, the field \mathcal{H}_P is much smaller than the magnetic saturation field \mathcal{H}_F : it is determined from the condition of equality of the Fermi energy μ_P (1.7.1) and the energy of Zeeman splitting $A\mathcal{M}(\mathcal{H}_P)$ and consequently $\mathcal{M}(\mathcal{H}_P)$ is much smaller than $\mathcal{M}(\mathcal{H}_F) = S$. Hence, qualitatively, the magnetic susceptibility of a doped AFS behaves like that of an FMS at $T > T_c$ studied in Sec. 6.1.

The physical reasons for a nonlinear dependence of the moment of an AFS on the field are the same as in the case of an FMS: the non-Heisenberg nature of the indirect exchange via the conduction electrons. The tendency of the conduction electrons to establish an FM ordering makes itself manifest in different ways in different fields. At $\mathcal{H} \rightarrow 0$ the electrons renormalize the effective exchange integral, decreasing its absolute value. At $\mathcal{H} > \mathcal{H}_P$ they renormalize the magnetic field, shifting it by $A\mathcal{M}/2$ and leaving the exchange integral the same as in the case of their absence. For its part, the susceptibility is inversely-proportional to the effective exchange integral.

The relatively rapid rise in the magnetization M in weak fields, which subsequently slows down in stronger fields and becomes

linear (of the type depicted in Fig. 7.11), is usually associated with the existence of spontaneous magnetization in the crystal at $\mathcal{H} = 0$. Its value is determined by extrapolating the linear section of the M vs. H curve to the zero field. In particular, as demonstrated in Sec. 5.3, such a magnetization vs. field dependence should be observable in the presence of localized ferrons in the crystal (FM regions near nonionized donors). It follows from the results of this section that in heavily-doped AFS it should materialize in the absence of spontaneous magnetization of the crystal, too.

The existence of an instability interval $[n_A, n_F]$ can be explained as follows. In the Heisenberg model the exchange integral is by definition independent of crystal magnetization. The non-Heisenberg nature of the indirect exchange formally can be described by introducing a summary effective exchange integral $\tilde{\mathcal{Y}}(\mathfrak{M})$ dependent on the magnetization. As has already been pointed out, the effective integral must diminish with a rise in \mathfrak{M} (i.e. its modulus must grow). Hence it becomes clear why there is no abrupt change in the ordering from the AF to the FM with a rise in the concentration. The former loses its stability at the concentration n_A when $\tilde{\mathcal{Y}}(0)$ turns zero. But an FM state cannot be established at this concentration, because the integral $\tilde{\mathcal{Y}}(S)$ is smaller than $\tilde{\mathcal{Y}}(0)$, i.e. negative.

In order to establish the boundaries of the AF-FM transition interval, we must find the concentration at which the magnon frequencies in the AF and the FM states cease to be positively defined. The frequencies of AF magnons can be calculated with the aid of the perturbation theory in the c - l exchange. To this end the smallness of AS/W is a sufficient condition, since for $\mathfrak{M} = 0$ there is no need in expanding the electron occupation numbers in $A\mathfrak{M}/\mu$ (see the derivation of the effective RKKY-theory Hamiltonian in Sec. 3.3).

Hence the appropriate formula for the magnon frequencies in the AF state is (2.6.11) into which

$$\tilde{\mathcal{Y}}(\mathbf{q}) = \mathcal{Y}_{\mathbf{q}} + P_{\mathbf{q}}(0), \quad P_{\mathbf{q}}(0) = S\mathcal{Y}_{\text{eff}} \quad (6.2.1)$$

should be substituted for $\mathcal{Y}_{\mathbf{q}}$. Here the effective indirect-exchange integral \mathcal{Y}_{eff} coincides with expression (3.3.12). The factor $2S$ appears as a result of the Holstein-Primakoff transformation (2.4.1) (see also (6.2.18)).

The loss of stability begins when the magnon frequencies turn imaginary at quasi-momenta \mathbf{q} almost equal to 0 and Π , so that, in accordance with expression (6.2.1), the condition of stability of the AF state takes the form

$$\begin{aligned} \tilde{\mathcal{Y}}(\Pi) - \tilde{\mathcal{Y}}(0) &= 2|\mathcal{Y}| + P_{\Pi} - P_0(0) > 0, \\ \Pi &= \left(\frac{\pi}{a}, \frac{\pi}{a}, \frac{\pi}{a} \right). \end{aligned} \quad (6.2.2)$$

If $P_{\Pi} \sim A^2 S^2 / W$ is neglected, formula (6.2.2) yields the following relationship determining the maximum concentration n_A at which the AF state ceases to be stable:

$$2|\mathcal{Y}| = \frac{3A^2 S v_A}{9\mu_A}, \quad |\mu_A| = \frac{i(3\pi^2 n_A)^{2/3}}{2m^*}, \quad v_A = \frac{n_A}{N}. \quad (6.2.3)$$

The magnon frequencies in the FM state are given by expression (6.1.2), where the bare-magnon frequency ω_q^0 can be taken in the form (2.4.4) with a negative exchange integral \mathcal{Y} . Obviously, the first magnon frequency with a nonzero quasi-momentum to vanish with a rise in carrier concentration will be the one corresponding to the quasi-momentum Π . Taking into account the inequality $\frac{\pi}{a} \gg q_0 \sim \frac{1}{a} \sqrt{\frac{AS}{W}}$ from (6.1.2), we obtain that the FM ordering of a heavily-doped AFS ceases to be stable at concentrations lower than

$$v_F = \frac{54|\mathcal{Y}|}{A} = \frac{3}{4} \frac{AS v_A}{\mu_A} \quad \left(v_F = \frac{n_F}{N} \right). \quad (6.2.4)$$

The concentration v_F for $AS > \mu_A$ will indeed be seen from (6.2.4) to exceed v_A , and hence in the interval $[v_A, v_F]$ a state intermediate between FM and AF should be established. This interval is the wider the greater the ratio AS/μ_A , i.e. the more the indirect exchange in the AFS differs from the Heisenberg exchange occurring at small AS/μ_A .

In order to find the energy, the magnetic susceptibility and the magnon spectrum of an AFS in the presence of a field we may conveniently introduce local coordinate systems X_g, Y_g, Z_g for every atom g , so that the Z_g -axis would be directed along the moment of the sublattice to which the atom belongs. In the laboratory frame of reference the Z -axis points in the direction of the field at right angles to the AF vector. The Y -axes of all the coordinate systems coincide. Carrying out Holstein-Primakoff transformations (2.4.1) in every local frame of reference, we obtain

$$\begin{aligned} S_g^x &= \sqrt{\frac{S}{2}} (b_g + b_g^*) = S_g^x \cos \vartheta - S_g^z \sin \theta e^{i\Pi \cdot g}, \\ S_g^y &= i \sqrt{\frac{S}{2}} (b_g^* - b_g) = S_g^y, \\ S_g^z &= S - b_g^* b_g = S_g^x \sin \theta e^{i\Pi \cdot g} + S_g^z \cos \theta, \end{aligned} \quad (6.2.5)$$

where θ is the angle between the Z -axis and the sublattice moments. Taking into account formulae (6.2.5), we obtain the electron part of the Hamiltonian (3.1.1) in the form

$$\begin{aligned} H_0 &= \sum E_{\mathbf{k}\sigma} a_{\mathbf{k}\sigma}^* a_{\mathbf{k}\sigma} - \frac{AS_{\perp}}{2} \sum (a_{\mathbf{k}\uparrow}^* a_{\mathbf{k}+\Pi, \downarrow} + a_{\mathbf{k}\downarrow}^* a_{\mathbf{k}+\Pi, \uparrow}), \\ E_{\mathbf{k}\sigma} &= E_{\mathbf{k}} - A\mathfrak{M}\sigma, \quad \mathfrak{M} = S \cos \theta, \quad S_{\perp} = S \sin \theta. \end{aligned} \quad (6.2.6)$$

It is diagonalized in exactly the same way as in Sec. 3.2: we write down the equation of motion for Green's functions $\langle\langle a_{\mathbf{k}\uparrow} | a_{\mathbf{k}\uparrow}^* \rangle\rangle$ and for Green's function associated with it $\langle\langle a_{\mathbf{k}+\Pi, \downarrow} | a_{\mathbf{k}\uparrow}^* \rangle\rangle$ and from their poles find the energy spectrum. The expression for it is

$$E_{\mathbf{k}\pm} = \frac{E_{\mathbf{k}\uparrow} + E_{\mathbf{k}+\Pi, \downarrow}}{2} \pm \frac{1}{2} \sqrt{(E_{\mathbf{k}\uparrow} - E_{\mathbf{k}+\Pi, \downarrow})^2 + A^2 S_1^2}. \quad (6.2.7)$$

Retaining only the terms of not above the second order in AS/W , we obtain with the aid of formulae (6.2.6, 7) an expression for the ground state energy of the system

$$E_0(\theta) = \sum E_{\mathbf{k}\sigma} n_{\mathbf{k}\sigma} - \frac{SP_{\Pi}}{2} N \sin^2 \theta - \frac{\mathcal{Y}NS}{2} \cos 2\theta - \mathcal{H}SN \cos \theta, \quad (6.2.8)$$

where $n_{\mathbf{k}\sigma}$ is the Fermi electron distribution function at $T = 0$. When writing out (6.2.8), we took into account only the effect of the mean crystal field $AM/2$ on the electron spin, ignoring the direct effect on it of the magnetic field \mathcal{H} , since, as indicated above, \mathcal{H} is several orders of magnitude smaller than AM .

The equilibrium value of the angle θ can be found from the condition of the minimum energy $E_0(\theta)$ (6.2.8). When differentiating it, one must take account of the electron concentration n being constant, and this yields

$$\sum E_{\mathbf{k}\sigma} \frac{dn_{\mathbf{k}\sigma}}{d\theta} = \sum \mu \delta(\mu - E_{\mathbf{k}\sigma}) \frac{dE_{\mathbf{k}\sigma}}{d\theta} = \mu \frac{d}{d\theta} \sum n_{\mathbf{k}\sigma} = 0. \quad (6.2.9)$$

Taking into account relation (6.2.9), we obtain from formula (6.2.8) the following condition for the equilibrium of a magnet in an external field:

$$\tilde{\mathcal{Y}}(\mathcal{M}) = \mathcal{Y} + \frac{P_{\Pi} - P_0(\mathcal{M})}{2} = -\frac{\mathcal{H}}{2 \cos \theta}, \quad (6.2.10)$$

where we have introduced the notation

$$P_0(\mathcal{M}) = -\frac{AS}{2S\mathcal{M}} (v_{\uparrow} - v_{\downarrow}), \quad (6.2.11)$$

v_{\uparrow} and v_{\downarrow} are the numbers of conduction electrons per magnetic atom having spins up and down. For $v_{\downarrow} \neq 0$, they are determined from the condition that the chemical potential for the electrons with spins up be equal to that with spins down:

$$\frac{(6\pi^2)^{2/3}}{2m^*} (n_{\uparrow}^{2/3} - n_{\downarrow}^{2/3}) = AM. \quad (6.2.12)$$

The condition of equilibrium of a degenerate AFS in an external magnetic field (6.2.10) differs from the corresponding condition

for a Heisenberg AF (2.3.6) in that the quantity $\tilde{\mathcal{Y}}(\mathfrak{M})$ playing the part of the effective indirect exchange integral, for $\mu \leq AS$ itself depends on the magnetization \mathfrak{M} . For $\mu \gg AS$ this dependence may be neglected, and then both conditions will be equivalent.

Owing to the dependence of $\tilde{\mathcal{Y}}(\mathfrak{M})$ on the magnetization \mathfrak{M} , the dependence of the magnetic moment of the crystal on the external field turns out to be essentially nonlinear. For small fields for which the inequality $A\mathfrak{M} \ll \mu$ holds, the dependence of the magnetization on the field coincides with that predicted by the RKKY theory: the relationship connecting the initial magnetic susceptibility $\chi(\mathcal{H}=0)$ with that of a pure crystal χ_0 is as follows

$$\chi(\mathcal{H}=0) = \chi_0 \left[1 - \left(\frac{n}{n_A} \right)^{1/3} \right]^{-1}, \quad \chi_0 = \frac{S}{2|\mathcal{Y}|} \quad (6.2.13)$$

(the terms $\sim A^2S/W$ are small as compared with A^2S/μ and have been discarded for this reason).

If on the other hand $A\mathfrak{M}$ exceeds the Fermi energy of the electrons, i.e. a complete spin-polarization of the electrons is attained, it follows from expressions (6.2.10, 11) that the magnetic susceptibility in this range of fields coincides with χ_0 , and that the moment of the crystal is equal to

$$\mathfrak{M} = \chi_0 \left(\mathcal{H} + \frac{A\nu}{2} \right). \quad (6.2.14)$$

Putting $\mathfrak{M} = S$, we obtain from formula (6.2.14) the magnetic saturation field \mathcal{H}_F :

$$\mathcal{H}_F = 2|\mathcal{Y}| - \frac{A\nu}{2}. \quad (6.2.15)$$

The initial susceptibility of the crystal will be seen from formulae (6.2.13, 14) to exceed its value χ_0 in high fields the more the closer is the concentration to n_A . Should we extrapolate the magnetization (6.2.14) to $\mathcal{H} \rightarrow 0$, we would obtain the magnetization per atom equal to $\mathfrak{M}_{\text{eff}} = 1/2 \chi_0 \cdot 2$. It should however be emphasized that in this case such an extrapolation does not mean the actual existence of a spontaneous magnetization in the crystal at $\mathcal{H} = 0$.

At point ν_A as determined by relation (6.2.3) the initial susceptibility of an AFS becomes infinitely large. An increase in the concentration is accompanied by a decrease in the magnetic saturation field \mathcal{H}_F . The other boundary of the interval of intermediate structures ν_F can be determined by equating the field \mathcal{H}_F in equality (6.2.15) to zero, this yielding the result (6.2.4).

At concentrations below ν_A the magnetic susceptibility also displays a singularity at the field \mathcal{H}_P at which the electrons become completely spin-polarized. Making use of expressions (6.2.10), (6.2.12), we can easily establish its character. On the low-field

side of \mathcal{H}_P we obtain, retaining in (6.2.12) only the term $\sim v_{\downarrow}^{2/3} \ll 1$,

$$\begin{aligned} v_{\downarrow} &= v \left[\frac{A(\mathfrak{M}_P - \mathfrak{M})}{\mu_P} \right]^{3/2}, \quad \mu_P = 2^{2/3} \mu, \\ \mathcal{H}_P &= 2\mu_P |\mathcal{Y}| \left[1 - \frac{4}{3} \left(\frac{n}{4n_A} \right)^{1/3} \right] (AS)^{-1}, \end{aligned} \quad (6.2.16)$$

where \mathfrak{M}_P is the moment of the crystal in the field \mathcal{H}_P determined by the equality $\mu_P = A\mathfrak{M}_P$. Substituting (6.2.16) into (6.2.10), and differentiating the moment \mathfrak{M} with respect to \mathcal{H} , we obtain for the magnetic susceptibility on the low-field side of \mathcal{H}_P the expression

$$\chi = \chi_0 \left[1 + \frac{3ASv}{8|\mathcal{Y}|} \left(\frac{A}{\mu_P} \right)^{3/2} \sqrt{\mathfrak{M}_P - \mathfrak{M}} \right]. \quad (6.2.16a)$$

Hence, although the magnetic susceptibility itself is continuous at point \mathcal{H}_P , its backward derivative at \mathcal{H}_P becomes infinite, whereas its forward derivative remains constant ($\chi = \chi_0$) [173]. Such a behaviour corresponds to a phase transition of the "second-and-a-half" kind suggested by I.M. Lifshitz [260]. In actual systems this discontinuity should be somewhat blurred on account of the imperfections.

In principle, oscillations of the magnetic susceptibility are possible for the model being considered [173]. For them to materialize, the electron Fermi surface should be well-defined, so that the electron orbits would be quantized already in fields smaller than \mathcal{H}_P . This condition can be met in heavily-doped semiconductors only in favourable cases (a small effective mass etc.). Such oscillations belong to a quite different type than those of de Haas-van Alfvén type: firstly, the susceptibility in this case is paramagnetic and not diamagnetic and by 5-6 orders of magnitude greater than that of conduction electrons. Secondly, the chief contribution to the crystal moment is made not by the spins of conduction electrons, but by localized spins of magnetic atoms. From the physical standpoint the origin of these oscillations is associated with the redistribution of the electrons between states having opposite spin directions. By reason of the density of states in a quantizing field being nonanalytic in the field strength the electron occupation numbers are nonanalytic, too. As the Fermi level traverses the bottom of some Landau subband, the field derivative of the number of electrons in this subband, and consequently of the total number of electrons having a corresponding spin v_{σ} , experiences a discontinuity and subsequently returns to its original value. According to (6.2.10, 11), the susceptibility behaves in a similar manner. The signs of its jumps alternate, since the Fermi level successively traverses the subbands having spins down and up, the sign of the jump depending on the direction of the spin in the subband. The oscillations end as soon as the field reaches the value \mathcal{H}_P (6.2.16).

The magnon spectrum is sought in the form of a correction to the Hamiltonian (6.2.6) resulting from those terms in the Hamiltonian (3.1.1) transformed in accordance with (6.2.5), which contain magnon operators. Taking into account that, in compliance with (6.2.10), the terms proportional to b_{Π} vanish after they are summed with the corresponding terms from the direct exchange Hamiltonian (2.1.5), we obtain the electron perturbation Hamiltonian in the form

$$H = H_1 + H_2,$$

$$H_1 = -A \sqrt{\frac{S}{2N}} \sum \{ (s_{\sigma\sigma'}^-) b_{\mathbf{k}} + (s_{\sigma\sigma'}^+) b_{-\mathbf{k}}^* \} a_{\mathbf{p}\sigma}^* a_{\mathbf{p}+\mathbf{k}, \sigma'}, \quad (6.2.17)$$

$$H_2 = \frac{A}{N} \sum b_{\mathbf{k}}^* b_{\mathbf{k}'} \{ \sigma \cos \theta a_{\mathbf{p}\sigma}^* a_{\mathbf{p}-\mathbf{k}+\mathbf{k}', \sigma} + a_{\mathbf{p}\sigma}^* a_{\mathbf{p}+\Pi-\mathbf{k}+\mathbf{k}', -\sigma} \},$$

where $b_{\mathbf{k}}^*$, $b_{\mathbf{k}}$ are Fourier-transforms (2.4.3) of the operators $b_{\mathbf{g}}^*$, $b_{\mathbf{g}}$. In addition to the inequality $W \gg AS$, the inequality $2S \gg 1$ is also presumed to hold, so that the Hamiltonian H_1 is taken into account in the second order of the perturbation theory, and H_2 in the first. Carrying out calculations of the type performed in Sec. 3.3 and adding to the indirect exchange Hamiltonian thus obtained corresponding terms from the Hamiltonian (2.1.5) transformed in accordance with (6.2.5), we obtain finally a Hamiltonian of the form (2.6.5), differing from the latter only in the values of the coefficients $\mathcal{P}_{\mathbf{q}}$ and $\mathcal{C}_{\mathbf{q}}$. Accordingly, expression (2.6.11) in terms of these coefficients will be valid for the magnon spectrum. In this case it is deciphered as follows [327]:

$$\begin{aligned} \omega_{\mathbf{k}}^2 = & \{ \mathcal{Y} \cos(2\theta) (1 - \gamma_{\mathbf{k}}) + \mathcal{H} \cos \theta + R_{\Pi-\mathbf{k}} \sin^2 \theta \\ & + (P_{\mathbf{k}} - P_0) \cos^2 \theta - P_{\Pi} \sin^2 \theta \} \{ \mathcal{Y} (\cos 2\theta - \gamma_{\mathbf{k}}) \\ & + \mathcal{H} \cos \theta + P_{\mathbf{k}} - P_0 \cos^2 \theta - P_{\Pi} \sin^2 \theta \}, \end{aligned} \quad (6.2.18)$$

$$P_{\mathbf{k}} = \frac{A^2 S}{4N} \sum_{\mathbf{p}\sigma} \frac{n_{\mathbf{p}\sigma} - n_{\mathbf{p}+\mathbf{k}, -\sigma}}{E_{\mathbf{p}\sigma} - E_{\mathbf{p}+\mathbf{k}, -\sigma}}, \quad R_{\mathbf{k}} = \frac{A^2 S}{4N} \sum_{\mathbf{p}\sigma} \frac{n_{\mathbf{p}\sigma} - n_{\mathbf{p}+\mathbf{k}, \sigma}}{E_{\mathbf{p}\sigma} - E_{\mathbf{p}+\mathbf{k}, \sigma}},$$

where $E_{\mathbf{k}\sigma}$ is given by expression (6.2.6).

It follows from formula (6.2.18) that for $\mathcal{H} \ll \mathcal{H}_P$ the result for long-wave magnons coincides with that of the RKKY theory, i.e. the electrons renormalize the exchange integral in (6.2.1). For short-wave magnons results (6.2.18) and RKKY are greatly different. In particular, according to (6.2.18), in fields $\mathcal{H} \gg \mathcal{H}_P$, when the electrons are completely spin-polarized, for $k^2 \gg q_0^2 \cos^2 \theta$, the effect of the electrons makes itself manifest via the renormalization of the magnetic field in accordance with the relation (6.2.14) (i.e. they shift the field by $4v/2$, leaving the exchange integral unchanged as in an undoped AFS). In the RKKY theory only renormalization of the exchange integral occurs.

Narrow-band Semiconductors. Similar calculations can be carried out for the case of narrow-energy bands $AS \gg W$. We shall consider only the case $A > 0$ when even with an antiferromagnetic ordering the carrier effective mass is of the order of the band-electron mass (Sec. 5.1). First of all we shall find the carrier energy spectrum for an arbitrary angle 2θ between the sublattice moments. In the calculation it should be taken into account that the electron transitions from atom to atom generally alter the directions of the spins of magnetic atoms. The wave function of the system is sought in the form similar to (5.2.15). Since the spinpolaron operators have been introduced only for the angles $\theta = 0$ and $\pi/2$, it would be reasonable to return to the c -electron and the bare-spin operators by making use of expression (3.5.12) and introducing the operators $S_{\mathbf{g}}^-$ with the aid of equations (2.1.4)

$$\psi = \sum_{\mathbf{g}} \left\{ \Phi(\mathbf{g}, +) a^* (\mathbf{g} \uparrow_{\mathbf{g}}) + \frac{\Phi(\mathbf{g}, -)}{\sqrt{2S+1}} \times [a^* (\mathbf{g} \downarrow_{\mathbf{g}}) + a^* (\mathbf{g} \uparrow_{\mathbf{g}}) S_{\mathbf{g}}^-] \right\} |0\rangle_0. \quad (6.2.19)$$

Here $\Phi(\mathbf{g}, \pm)$ are unknown coefficients, $|0\rangle_0$ is the vacuum wave function for the conduction electron and for deviations of atomic spins from the directions of the moments of the sublattices to which these atoms belong (in other words, in a coordinate system with the $Z_{\mathbf{g}}$ -axis coinciding in direction with the moment of the sublattice to which the atom belongs $\langle 0 | S_{\mathbf{g}}^Z | 0 \rangle$ is equal to S). The electron spin indices $\uparrow_{\mathbf{g}}$ and $\downarrow_{\mathbf{g}}$ denote their spin projection on the $Z_{\mathbf{g}}$ -axis of the local coordinate system of the \mathbf{g} -atom.

The first term in expression (6.2.19) evidently corresponds to the state of an atom occupied by an electron with the maximum projection of their total spin on the direction of the moment of the sublattice to which the atom belongs, the second term corresponding to a state with a projection smaller by 1. The projections of spins of atoms, not occupied by electrons, on the direction of the moment of the appropriate lattice is always presumed to be maximum, this corresponding to the neglect of quasi-oscillator effects. Such neglect is justified by the results described in Sec. 5.1.

In the calculations we shall require rules for the transformation of electron operators from the \mathbf{g} -atom coordinate system to one of the $\mathbf{g} + \Delta$ -atom. They are obtained from formulae (3.5.1) by putting $\gamma_{\mathbf{g}} = \theta/2$ and, for example, $\nu_{\mathbf{g}} = \beta_{\mathbf{g}} = \pi/2$, $\delta_{\mathbf{g}} = \mu_{\mathbf{g}} = 0$:

$$a^* (\mathbf{g} + \Delta, \uparrow_{\mathbf{g}+\Delta}) = (\cos \theta) a^* (\mathbf{g} + \Delta, \uparrow_{\mathbf{g}}) + i (\sin \theta) a^* (\mathbf{g} + \Delta, \downarrow_{\mathbf{g}}), \quad (6.2.20)$$

$$a^* (\mathbf{g} + \Delta, \downarrow_{\mathbf{g}+\Delta}) = i (\sin \theta) a^* (\mathbf{g} + \Delta, \uparrow_{\mathbf{g}}) + (\cos \theta) a^* (\mathbf{g} + \Delta, \downarrow_{\mathbf{g}}).$$

The atoms can conveniently be attributed an "isotopic" spin with the +1 or the -1 values of its projection τ , depending on whether the atom belongs to the first or to the second sublattice. The coefficients $\Phi(g, \pm)$ of the wave function (6.2.19) are sought in the form

$$\Phi(g, \pm) = e^{ik \cdot g} \Phi(\tau_g, \pm). \quad (6.2.21)$$

The substitution of expressions (6.2.19-21) into the Hamiltonian (3.1.1) yields the following "bispinor" Schrödinger equation:

$$\begin{aligned} E\Phi(\tau, +) &= 6B(\cos\theta)\gamma_{\mathbf{k}}\Phi(-\tau, +) + \frac{i\tau 6B\gamma_{\mathbf{k}}\sin\theta}{2S+1}\Phi(-\tau, -). \\ E\Phi(\tau, -) &= \frac{i\tau 6B\gamma_{\mathbf{k}}\sin\theta}{\sqrt{2S+1}}\Phi(-\tau, +) + \frac{6B\gamma_{\mathbf{k}}\cos\theta}{2S+1}\Phi(-\tau, -). \end{aligned} \quad (6.2.22)$$

In writing out this equation we made use of the condition $|B| \gg |J|$.

The solution of equations (6.2.22) demonstrates that the energy spectrum of a spinpolaron consists of two bands with the dispersion laws

$$\begin{aligned} E_{\pm}(\mathbf{k}) &= -6B_{\pm}\gamma_{\mathbf{k}}, \quad \gamma_{\mathbf{k}} = \frac{1}{z} \sum_{\Delta} e^{ik \cdot \Delta}, \\ B_{\pm} &= \frac{|B|}{\sqrt{2S+1}} \{ \sqrt{1+y^2} \pm y \}, \quad y = \frac{\mathfrak{M}}{\sqrt{2S+1}}. \end{aligned} \quad (6.2.23)$$

In case of a complete antiferromagnetic ordering ($\theta = \pi/2$) both these bands coincide. However, as the magnetic moment grows, one of these bands begins to widen, and its bottom sinks. The other band on the contrary grows narrower, and its bottom rises. In the limit $\theta = 0$ the wider of the two corresponds to the state with the maximum spin of the crystal — the c -electron system, and the narrower to the spin less by a unit.

The expression for the ground state energy of the system is

$$\begin{aligned} E &= -3JS^2N \cos 2\theta - \mathcal{H}SN \cos \theta (1 + \nu/2S) \\ &+ \sum_{\mathbf{k}} [E_+(\mathbf{k})n_+(\mathbf{k}) + E_-(\mathbf{k})n_-(\mathbf{k})], \end{aligned} \quad (6.2.24)$$

where $n_{\pm}(\mathbf{k})$ is the Fermi distribution function for the carriers with an energy $E_{\pm}(\mathbf{k})$ at $T = 0$, $\nu = n/N$.

At $T = 0$ the condition for the independence of the number of carriers of the moment yields the equation:

$$\sum_{(\pm), \mathbf{k}} E_{\pm}(\mathbf{k}) \frac{d}{d\theta} n_{\pm}(\mathbf{k}) = \mu \frac{d}{d\theta} \sum_{\mathbf{k}} n_{\pm}(\mathbf{k}) = 0. \quad (6.2.25)$$

Taking into account (6.2.25), we write the condition of the minimum energy of the ground state (6.2.24) with respect to the angle θ

for $v \ll 1$ in the form

$$-12\mathfrak{M} - \mathcal{H} - 6 \left[v_+ \frac{d}{d\mathfrak{M}} B_+ + v_- \frac{d}{d\mathfrak{M}} B_- \right] = 0, \quad (6.2.26)$$

where the relative carrier concentrations in both bands are determined from the condition of equality of the chemical potentials in them, i.e.

$$B_+ [-6 + (6\pi^2 v_+)^{2/3}] = B_- [-6 + (6\pi^2 v_-)^{2/3}]. \quad (6.2.27)$$

For small \mathfrak{M} we obtain from formulae (6.2.27, 23) in the main order in the parameter $\mathcal{H} \gg 1$

$$v_+ = v_- \simeq v \left[\frac{3}{4} \mathcal{H} y - \frac{1}{32} \mathcal{H}^3 y^3 \right], \quad (6.2.28)$$

$$\mathcal{H}(v) = 12(3\pi^2 v)^{-2/3}. \quad (6.2.29)$$

Using formulae (6.2.26-29), one can easily find the susceptibility of the system. For $\mathcal{H} \rightarrow 0$ it is equal to

$$\chi = \chi_0 \left[1 - \frac{9}{4} \left| \frac{B}{\varepsilon} \right| (2S+1)^{-3/2} v \mathcal{H}(v) \right]^{-1},$$

$$\chi_0 = \frac{S}{2|\mathcal{Y}|}. \quad (6.2.30)$$

It turns into infinity at the boundary of stability of AF ordering v_A . According to formulae (6.2.30) and (6.2.29), we obtain for v_A the expression

$$v_A = \left(\frac{\pi}{4} \right)^4 \left[2 \left| \frac{\mathcal{Y}}{B} \right| (2S+1)^{3/2} \right]^3. \quad (6.2.31)$$

As the moment grows, the number of carriers in the upper band decreases, and starting from some critical value \mathfrak{M}_c all the carriers concentrate in the lower band. From this instant the expression for the magnetic susceptibility of the crystal reads

$$\chi = \chi_0 \left[1 - 3v \left| \frac{B}{\varepsilon} \right| S^2 (\mathfrak{M}^2 - 2S + 1)^{-3/2} \right]^{-1}. \quad (6.2.32)$$

For high magnetization the magnetic susceptibility will be seen from formula (6.2.32), in contrast to the case of wide bands $W \gg AS$, not to coincide with the susceptibility of the undoped crystal χ_0 and to be a nonlinear function of the magnetization. Still, in this case it remains smaller than the initial susceptibility (6.2.30), too, since, according to (6.2.29), $\mathcal{H} \gg 1$. At fields corresponding to \mathfrak{M}_c the crystal also displays the phase transition of the second-and-a-half kind in the magnetic field with an infinite jump of the derivative of the susceptibility with respect to the field strength.

For the magnetic saturation field we obtain from formulae (6.2.26) and (6.2.23) the equation

$$\mathcal{H}_F = 2|\mathcal{Y}| - \frac{6v|B|}{S+1}. \quad (6.2.33)$$

Equating it to zero, we obtain the boundary of stability of the FM state

$$v_F = \frac{2|J|S(S+1)}{|B|}. \quad (6.2.34)$$

The concentration v_F in the limit $S \gg 1$ coincides with that for which the frequencies of FM magnons (6.1.1) in case of a negative direct exchange integral J vanish (in the limit $WAS \rightarrow 0$ this takes place simultaneously for all q 's). Since the small quantity J/B enters v_F (6.2.34) linearly and v_A (6.2.31) in the cubic power, the concentration v_F is higher than v_A .

Numerical estimates of the boundary concentrations n_A and n_F with the aid of (6.2.3, 4) or (6.2.31, 34) yield for typical parameter values $T_N \sim 10^{-3}$ eV, $\min\{AS, W\} \sim 0.1$ eV values of n_F of the order of 10^{20} - 10^{21} cm $^{-3}$ and values of n_A lower by one or two orders of magnitude.

The Problem of Structures Intermediate between the Ferromagnetic and the Antiferromagnetic. As has been already demonstrated in this section, there is an interval of concentrations $[n_A, n_F]$ inside which both the AF and the FM ordering are absolutely unstable in a heavily-doped AFS. This means that in the interval specified there is even no relative energy minimum to correspond to them. In principle, as the concentration rises inside this interval, a continuous transition from the AF to the FM can take place. At the boundary points of the interval n_A and n_F changes in the symmetry of the system take place. Accordingly, such points may be regarded as points of the concentration phase transitions of the second kind. They differ from normal phase transitions not only in that they occur in an ensemble of specimens having different electron concentrations, but also in that they can take place at $T = 0$ in the absence of parameter fluctuations.

The state materializing inside the interval $[n_A, n_F]$ should be intermediate between the FM and the AF, i.e. in any case it can be characterized by a spontaneous magnetization \mathfrak{M} appearing at point n_A and attaining saturation at point n_F . Some of its properties can be obtained from a phenomenological analysis of the problem even without going into details of the structure of the intermediate state.

In the absence of any special symmetry properties of the crystal the energy of the system $E(n)$ must be an even function of the magnetic moment \mathfrak{M} . By complete analogy with the Landau theory of phase transitions (Sec. 2.5), this energy for small \mathfrak{M} and in the case of a negligible magnetic anisotropy should be given by expression (2.5.12), where the coefficients \mathcal{A} and \mathcal{B} should be presumed to depend on the electron concentration, and Φ_0 should be interpreted as the energy of the system in the antiferromagnetic state.

Consider the behaviour of E as a function of n at $\mathcal{H} = 0$. For small n 's the crystal should be antiferromagnetic and by force of it \mathcal{A} should be positive. For large n 's the indirect exchange should be the predominant mechanism, and therefore \mathcal{A} should be negative. Hence, there should be a critical concentration n_A at which the coefficient $\mathcal{A}(n)$ would vanish. For a positive coefficient $\mathcal{B}(n_A)$ it follows from the condition for a minimum free energy that for concentration $n > n_A$ the crystal must have a nonzero moment. Presuming that in the vicinity of n_A $\mathcal{A}(n_A)$ is proportional to $n - n_A$, we obtain from expressions (2.5.12, 13) that for small $n - n_A$ the moment is a function of this difference of the type $\mathfrak{M} \sim \sqrt{n - n_A}$.

In the vicinity of n_F we should carry out the expansion in the "demagnetization" $\mathfrak{N} = S - \mathfrak{M}$. Since at $\mathcal{H} = 0$ the system in addition to the demagnetization vector is characterized by another vector, that of the total moment, we can construct a scalar linear in \mathfrak{N} . Accordingly, at $\mathcal{H} = 0$, too, the expansion of the energy begins with a term linear in \mathfrak{N} :

$$E(n, \mathfrak{N}) = E_F(n) + \mathcal{F}_1(n) \mathfrak{N} + \mathcal{F}_2(n) \mathfrak{N}^2 - (S - \mathfrak{N}) \mathcal{H}, \quad (6.2.35)$$

where E_F is the energy in the FM state. The ideas expressed above concerning the concentration phase transition are easily generalized to include this case. In particular, if the coefficient \mathcal{F}_1 is proportional to $n_F - n$ in the vicinity of the phase transition point from the intermediate to the FM state n_F , the demagnetization \mathfrak{N} will also be proportional to this difference.

Let us analyze the dependence of the magnetization of the intermediate state in the external magnetic field. It follows from (2.5.12, 13) that for small \mathfrak{N} the increment $\Delta \mathfrak{M}$ is connected with the spontaneous magnetization by means of relations

$$\begin{aligned} \Delta \mathfrak{M} &= \frac{\mathcal{H}}{8\mathfrak{M}^2 \mathcal{B}} & \mathcal{H} \ll |\mathcal{A}| \mathfrak{M}, \\ \Delta \mathfrak{M} &= \sqrt[3]{\frac{\mathcal{H}}{\mathcal{B}}} & |\mathcal{H}| \gg |\mathcal{A}| \mathfrak{M}. \end{aligned} \quad (6.2.36)$$

The initial magnetic susceptibility will be seen from formula (6.2.36) to be proportional to \mathfrak{M}^{-2} for small \mathfrak{M} 's, but to be independent of the initial magnetization in high fields. At high magnetization levels the state of the crystal in the field is determined by a linear relationship between the field and the moment

$$\mathfrak{N} = \frac{|\mathcal{B}_1| - \mathcal{H}}{2\mathcal{B}_2}$$

(it makes sense for fields for which $\mathfrak{N} \geq 0$).

To establish the detailed nature of the intermediate state, we should note that, according to formulae (6.1.1, 2, 5, 6), in the region $n > n_F$ the magnon frequency with $q = \Pi$ vanishes first

as the carrier concentration decreases. Then, in accordance with the Landau-Lifshitz theory of phase transitions, the structure at n smaller than n_F should be one with a nonzero moment whose period is twice that of the period of the FM structure. It may be interpreted as follows: were we to reduce the concentration n below n_F , the magnon frequencies with $\mathbf{q} = \Pi$ would become negative, and their generation would become energetically favoured. This generation is limited by the magnon anharmonism, since the magnon-magnon interaction raises the energy of the system. Consequently its minimum is attained at a finite magnon concentration.

Indeed, the energy of the system in the vicinity of the point n_F can be represented as the function of the number of magnons Q in the form

$$E_Q = \omega_\Pi Q + CQ^2/2,$$

where the term quadratic in Q describes their mutual interaction. At n exceeding n_F the frequency ω_Π is positive, and the energy has a minimum at $Q = 0$, i.e. in the FM state with a saturated moment. At n less than n_F in the case of a negative anharmonism constant C there is nothing to limit the magnon generation, and a state greatly different from the ferromagnetic should be stable. For a positive C the energy minimum is attained with the magnon number equal to $|\omega_\Pi/C|$ tending to zero for n tending to n_F from the low-density side. Hence, the intermediate state represents a Bose-Einstein condensate of magnons with the quasi-momentum $\Pi = (\frac{\pi}{a}, \frac{\pi}{a}, \frac{\pi}{a})$.

The appearance of a spin wave with a quasi-momentum Π means that the situation repeats itself along every coordinate axis with a period of 2π : $\pi/a = 2a$, that is the period of the intermediate structure is twice that of the ferromagnetic. The moment of the structure is nonzero and equal to $S(1 - Q/N)$ per atom.

In principle, various two-sublattice states having a nonzero moment are possible. The simplest of them is the canted AF state (Fig. 2.4) the possibility of whose existence in semiconductors for $n < n_F$ has first been suggested in [74]*. It differs in principle from one caused by relativistic effects (Sec. 2.3) in that it is possible in crystals of any symmetry (formally, the "relativistic" canted structure is associated with the presence of a term $\sim \mathbf{l}\mathbf{m}$ in the expression for the energy and the "nonrelativistic" discussed here with an anomalous smallness of the coefficient in (2.5.12) multiplying \mathbf{m}^2), where \mathbf{l} and \mathbf{m} are the AF and FM vectors (Fig. 2.4).

* This problem has been considered in [74] not quite correctly, because the carrier-band-width in the AF state has been presumed to be zero. This led to an erroneous conclusion that such an ordering is possible for n arbitrarily small.

There is also another possibility. The crystal splits up into two crystallographically equivalent sublattices with unequal, but collinear moments (a FIM-type ordering) [176]. In the case of a canted antiferromagnet (CAF) the AF vector \mathbf{l} (the difference between the sublattice moments) is orthogonal and in the case of FIM parallel to the crystal moment. Other two-sublattice magnetic structures with a nonzero moment are also possible.

The fact that CAF ordering is energetically favoured in the interval $[n_A, n_F]$ as compared with FM and AF orderings has been proved in [173-175] both for narrow- and for wide-band semiconductors. Formally, the characteristics of CAF ordering can be obtained from equations (6.2.10) and (6.2.26). In the interval $[n_A, n_F]$ and in the absence of an external field they have solutions corresponding to a nonzero moment and yield results in qualitative agreement with the above-mentioned phenomenological ones. But despite the fact that these equations have been obtained from the condition that the energy be minimum with respect to the moment, this is not sufficient to guarantee the stability of the states described by them. In fact, the above-mentioned condition guarantees only the stability of the CAF state with respect to long-wave fluctuations, since an increase or a decrease of the moment as compared with its equilibrium value is tantamount to the appearance of a fluctuation with an infinitely great wavelength. But the CAF state can be unstable with respect to short-wave fluctuations.

The analysis of this problem in the case of wide-band semiconductors is facilitated by expression (6.2.18) for the magnon spectrum in the interval $[n_A, n_F]$ being valid also for a CAF ordering in the absence of a magnetic field. For $n > 1.7 n_A$, when all the electrons are spin-polarized, it assumes the form for short-wave magnons

$$\omega_{\mathbf{k}} = |\gamma| \frac{|\Pi - \mathbf{k}|}{\sqrt{3}} \left[1 - \left(\frac{n}{4n_A} \right)^{1/3} \right]^{1/2} \left(1 - \frac{n^2}{n_F^2} \right) \quad (6.2.37)$$

(when deducing (6.2.37), one should take into account that the Fermi energy of the electrons is multiplied by $2^{2/3}$ as a result of their spin polarization).

According to formula (6.2.37), for $n_F > 4n_A$ the frequencies of short-wave magnons in the interval $n_F > n > 4n_A$ are imaginary, i.e. this state does not correspond to an energy minimum at all, this minimum being attained in some other state. For $n \leq 4n_A$ a relative energy minimum corresponds to the CAF state. However, it follows from considerations of continuity that in the vicinity of $4n_A$ it is not a profound one, lying above the principal minimum. Accordingly even for $n \leq 4n_A$ the stability of CAF ordering is not guaranteed.

It will be demonstrated in Sec. 7.4 that the concentration $4n_A$ from which the CAF state initially becomes unstable is close to

that at which the instability of the homogeneous state against infinitesimal electron density fluctuations appears. This indicates that the state corresponding to the minimum energy is one with an inhomogeneous distribution of the electron density and of the magnetization.

However, for $n_F < 4n_A$ the necessary conditions of stability of the CAF ordering are satisfied in the entire range of concentrations. This inequality also guarantees the stability of the ordering for small electron density fluctuations (Sec. 7.4).

In the opposite limit of narrow-band semiconductors $W \ll AS$ the CAF ordering in case of small carrier concentrations is unstable for small charge density fluctuations (Sec. 7.4). As to the experimental data on the CAF ordering of the type considered above, up to now it has been discovered only in metal alloys (GdMg with a CsCl structure and others [442]). In doped AFS it has as yet not been observed. Attempts to interpret the available data on their properties in terms of a CAF ordering have proved unsuccessful (see Sec. 7.5).

Conduction electrons can also transform a semiconductor with a helicoidal magnetic ordering into one with an FM ordering [263]. If the period of the helicoid in the insulating state is large enough, such a transition takes place smoothly as the charge carrier concentration rises. In the opposite case the transition takes place via some intermediate state. A state with an FM helical-type ordering (i.e. with a nonzero projection of the moment on the helicoid axis) whose particular case is the CAF ordering discussed above can play the part of such a state. However, although a proof that the FM helix is energetically favoured as compared with the normal one in some concentration range is contained in [263], the question of its stability remains unanswered. It has also been demonstrated in [263] that doping of an FMS increases the thickness of domain walls (Appendix III).

6.3. PHOTOFERROMAGNETISM

Indirect Exchange via Photoelectrons. The fact that conduction electrons tend to establish the FM ordering suggests that by exciting charge carriers by light it is possible to raise the Curie point of an FMS and to transform an AFS into an FMS*. However, to shift T_c by as little as 1 K, photoelectron concentrations $\sim 10^{19} \text{ cm}^{-3}$ (see Table III) are needed, which are unobtainable in real conditions. Accordingly, the generation of photoelectrons by light will

* This idea has first been advanced in [561, 562]. However, the effect has been estimated with the aid of the RKKY theory, which is inapplicable for MS. Because of that the effect has been overestimated by many orders of magnitude in [561, 562].

hardly be able to shift the Curie point appreciably. Moreover, the absorption of light of necessity heats the crystal causing the magnetic ordering to be destroyed, i.e. lowering T_c . Photoferromagnetism can be observed in dynamic conditions that preclude thermal effects, e.g. in conditions when the crystal is illuminated with short pulses with a small repetition rate. In stationary conditions it can be observed probably only in thin specimens whose small thickness makes for good cooling.

The same holds for AFS: to transform them completely into FMS, carrier concentrations $n_F \sim T_N^3 / 4Sa^3$ are needed. For $T_N \sim 10$ K n_F should be of the order of 10^{20} cm^{-3} , so that such a complete FM \rightarrow AF transformation can hardly be realized. The aforesaid does not concern metamagnets, since in them the energy per atom spent to replace the AF ordering is much less than T_N , being of the order of $\mathcal{H}_c S$, where \mathcal{H}_c is the critical field at which the jump from the AF to the FM state takes place (see Fig. 2.6). For $\mathcal{H}_c \simeq 3 \times 10^3$ Oe, $S = 7/2$ (as in EuSe) the concentration n_F turns out to be of the order of 10^{18} – 10^{19} cm^{-3} , this being also hardly attainable in experiment. However, EuSe possesses a remarkable property that distinguishes it from other metamagnets: at 4.2 K fields < 200 Oe transform it from the AF to the FIM state with an unsaturated moment $\mathcal{M}_0 = S/3$. This makes experimental observation of the light-induced transition to the FIM state possible, for only concentrations $\sim 10^{17} \text{ cm}^{-3}$ that can additionally be reduced by the application of a field \mathcal{H} weaker than \mathcal{H}_c are needed for it [398].

It should also be kept in mind that the photoelectrons in an AFS can go over to ferron states. Hence, if the electron concentration is insufficient for an FM ordering to be established throughout the crystal, it can be established in separate microregions of the crystal. This is apparently what has been observed in the studies of magneto-optical phenomena in EuSe (see Sec. 5.3). At high electron concentrations several individual FM microregions may merge to form a united region. Its stability will be higher, if not only photoelectrons, but photoholes are also localized in it to make it as a whole electro-neutral. The problem of regions of a normally-unstable phase produced in the result of joint localization in them of photoelectrons and photoholes was first solved in [415], which reported the studies of the effects of light on the phase transition in a ferroelectric semiconductor. It has been specifically demonstrated there that the dimensions of such regions are determined by the diffusion length of nonequilibrium charge carriers. Those results are easily applied to cover the case of magnetic semiconductors [599].

Irrespective of whether photoferrons form in an AFS or not, the free electrons that have not gone over to ferron states can produce in AFS a two-sublattice structure with a nonzero moment discussed in the preceding section, which is far easier attainable than the

FM structure. In cases when the photoelectron temperature T_{ph} and their concentration at small magnetizations \mathfrak{M} can be regarded as independent of \mathfrak{M} the expansion in the magnetization of the type (2.5.12) for the energy of the magnetic subsystem retains its validity. For it to be applicable, the energy of the c - l shift A \mathfrak{M} must be small as compared with T_{ph} (see Sec. 6.1).

Since the direct l - l exchange tends to establish an AF ordering, and the indirect exchange via c -electrons an FM one, the coefficient in \mathcal{A} in the equation (2.5.12) represents the difference between two terms the first of which is proportional to $T_N N$, and the second to $A^2 S^2 n / T_{ph}$ (the latter expression is a correction to the c -electron energy of the second order in the c - l exchange). Hence, the critical photoelectron concentration n_A at which the nonmagnetized state becomes unstable, i.e. for which the coefficient \mathcal{A} in (2.5.12) turns zero, is of the order of $T_N T_{ph} (AS)^{-2} a^{-3}$. It is difficult to obtain a numerical estimate of n_A , because the photoelectron temperature is not known. At room temperatures it usually coincides with the lattice temperature, but at low temperatures it can appreciably exceed the latter. If we presume that $T_{ph} \sim T_N$, we shall obtain that for $T_N \sim 10^{-3} AS$ the concentration n_A should be of the order of 10^{16} - 10^{17} cm^{-3} . Such photoelectron concentrations are attainable in experiment, which may be not the case for concentrations needed for complete AF \rightarrow FM transformation. In [398] the above consideration has been generalized to include the case of a photoelectron concentration heavily dependent on the magnetization.

A detailed analysis of light-induced phase transitions was given in [563]. The specific property of such transitions is that they take place in thermodynamically nonequilibrium conditions, i.e. when the energy of the absorbed light is dissipated. For this reason the free energy cannot be used to describe such transitions, and one is not entitled to speak about the discontinuities of its derivatives, e.g. of the specific heat, at the transition point. Nonequilibrium phenomena are characterized by the entropy production rate \dot{S} . It is \dot{S} and its derivatives that should display discontinuities at the point of phase transition.

To describe nonequilibrium phase transitions, some quantity is introduced whose stationary value is obtained by minimizing it as a function of the magnetization. The entropy production rate is proportional to the derivative of this quantity with respect to the light frequency, and because of that it received the name of the synergetic potential. In the mean field approximation a Landau-Lifshitz-type expansion (2.5.12) is obtained for it in the vicinity of the Curie point. The phase transition type is determined by the sign of the coefficient multiplying \mathfrak{M}^4 . Calculations show that for a realistic absorption coefficient vs. light frequency dependence the FM-PM transition can both be continuous and abrupt. Abrupt phase

transitions must take place when the light frequency is close to the absorption edge. In principle the frequency may even be less than the band-gap in the PM state, but must, of course, exceed it in the FM state.

Naturally, in the course of an abrupt phase transition the entropy production rate itself experiences a discontinuity. On the other hand, in case of a continuous phase transition we obtain in the mean field approximation that the discontinuities must be experienced by the derivatives of S with respect to the temperature, the frequency and the intensity of light. The same is true of the corresponding derivatives of the photoelectron concentration.

It was stated in [266] that the illumination of EuSe-type materials can produce photoheterojunctions. Indeed, the intensity of light diminishes as it penetrates the bulk of the crystal owing to absorption. Whereas near the surface the light generates so many carriers that an FM or a FIM ordering can be established, in the bulk its intensity will not be high enough for that. In the result a boundary between the magnetized and the nonmagnetized portions of the crystal is produced. Since the conduction-band bottom in the phase with a nonzero magnetization M lies AM^2 lower than in the nonmagnetized, a voltage is set up between them.

In principle, photoferromagnetism not associated with the charge carriers generation is possible, when a light-induced increase in the degree of FM ordering should take place even in the region of optical transparency of the crystal [399, 414]. It is caused by virtual transitions of the electrons from the valence to the conduction band. The virtual conduction electrons produced in the result differ sharply from the actual: no energy of the light is spent to produce them, and they cannot transport a charge over the crystal. In fact, the term "virtual electrons" describes the changes in the valence-band states caused by the light-induced admixture of conduction-band states. But the electrons residing in the valence band before the illumination will remain in it, although the band itself will be changed by the light.

If the valence-band states are constructed chiefly of p -orbits of nonmagnetic anions, and the conduction-band states of external orbits of magnetic cations, the admixture of the latter to the former will greatly enhance the exchange between the valence-band electrons and the l -spins of internal cation shells. Depending on the orientation of the electron spin with respect to the crystal moment, the enhancement of the exchange may either increase or decrease the electron energy. Should the degree of the admixture be independent of the orientation of the electron spin, the total change in the energy of the exchange of the electrons from the completely-filled valence band with the l -spins would have been zero, since a decrease in the energy of the electrons having a certain spin projection would be

compensated by an increase in the energy of the electrons having an opposite spin projection. Accordingly, light would not be able to alter the magnetic state of the crystal.

However in an FMS the degree of admixture depends on the spin orientation. Indeed, it is the greater the less is the separation between the valence-band top and the conduction-band bottom. The latter for its part is spin-split so that the bottom of one of the subbands lies AS lower than that of the other (the exchange between the valence-band electrons and the l -spins presumed to be weak, its splitting can be ignored). This means that we may speak of virtual electrons as being spin-polarized, with virtual electrons with such a spin projection being predominant, which enables a gain in the c - l exchange to be obtained. Hence, in an FMS light induces changes in the exchange between the valence-band electrons and l -spins resulting in an enhanced stability of FM ordering.

Estimates [414] show that for typical parameter values, if the light frequency is close to the absorption edge, light with an electric field intensity of $\sim 10^6$ V cm can cause a T_c shift of several tenths of a degree or even of several degrees. It should only be kept in mind that the ferromagnetic effect via actual electrons coexists with that via virtual electrons. Even if the light frequency is below the absorption edge, the photocarriers may be produced by many-photon processes, which are rather intense at high light intensities. If on the other hand the light frequency is above the absorption edge, the real single-photon electron transitions are possible only between such valence- and conduction-band states for which the momentum and the energy conservation laws are simultaneously satisfied, only virtual transitions being possible between other states. The contributions of the real and the virtual transitions can be separated by making use of the difference in the corresponding magnetization decay times.

Real and virtual photoelectrons may produce magnetization in other types of crystals as well, e.g. in magnetoexcitonic crystals or in singlet magnets [567]. But in addition to a direct effect on the exchange, other mechanisms of light-induced effects on magnetization are also possible. Namely, a circularly-polarized light by generating carriers with a definite spin projection changes the domain structure of an FMS, increasing the volume of domains having a certain spin projection and decreasing that with the opposite [566, 565].

Experimental Studies. Photoferromagnetic effect has been observed in experiments with EuS films illuminated by a laser with a high-frequency modulation of the illuminating beam, enabling the effect to be separated from highly-inertial thermal effects caused by the heating of the illuminated crystal [407, 412, 413]. The increase

in the magnetization of a crystal has been observed directly, when a specimen placed in a constant magnetic field of 1.2 kOe has been illuminated. The magnetization of a specimen illuminated with an unpolarized light changes with the modulation frequency of the illuminating beam ($\omega \sim 3$ MHz). It is accompanied by a change in the magnetic flux flowing in a measuring coil, thereby inducing an emf. Whether an increase or a decrease of the magnetization takes place upon illumination, is established from the phase shift of the emf with respect to the alternating component of the light flux. At a density of excitation by the pumping light of $10^{25} \text{ cm}^{-3} \text{ s}^{-1}$ and at a temperature of the specimen of 12 K the relative increase in the magnetization amounted to 1%. Since the specimen is in a magnetic field that suppresses its domain structure, the change in the magnetization can take place only in the result of an enhancement in the exchange between the magnetic atoms. In the case being considered it corresponds to a rise in T_c of 0.1 K [413].

This conclusion is supported by optical measurements. The specimen is illuminated simultaneously with a laser beam and with a test beam of a fixed wavelength sufficiently close to the absorption edge. An increase in the magnetization of the sample shifts the absorption edge to lower frequencies, causing an increase in the absorption of the test light. On the contrary, a decrease in the magnetization reduces its absorption. It has been discovered that for modulation frequencies ω of the laser beam less than 1 MHz the time-dependent component of the absorption is out of phase with that of the modulation of the pumping light. But starting from a frequency ~ 1 MHz, the oscillations of the pumping light and of the absorption begin to be in-phase. This proves that at low frequencies the oscillations of the magnetizations are determined by the oscillations of the temperature of the specimen. However, at high frequencies the temperature of the specimen is unable to follow the pumping intensity, and the time-dependent magnetization is determined by the light-induced modulation of the exchange interaction between the magnetic atoms [412]. Another indication of this is the appearance of optical dichroism ($\sim 10^{-2}\%$) induced by a circularly-polarized light in a demagnetized specimen at temperatures below T_c [407].

Unfortunately, photoelectric phenomena accompanying the photoferromagnetic phenomena have not been studied in the papers cited above. Accordingly, it cannot even be asserted with any certainty that the magnetization of EuS has been caused by photoelectrons. It has been stated in the papers referred to that the light-induced shift in T_c corresponds to photoelectron concentrations $\sim 10^{18} \text{ cm}^{-3}$. However, the reality of such high concentrations is open to doubt: it is not known, whether they are attainable even in best photoconductors, whereas the specimens of EuS studied were highly imperfect (thin films), and the measurements have been carried out close

enough to T_c . At the same time the nonequilibrium carrier lifetime normally displays a very profound minimum in the vicinity of T_c (see Sec. 4.7).

On the other hand recently a light-induced reconstruction of the magnetic structure of the AFS ErCrO_3 has been discovered, which takes place without the participation of photoelectrons [568-570] so that the photoconductivity mechanism of phase transitions considered in this section is not the only one possible.

Much greater influence of light on the magnetic properties of FMS has been discovered in the studies of the magnetic susceptibility $\mu(\omega)$ in an alternating magnetic field first in a ferromagnetic yttrium-iron garnet doped with Si [408, 411] and subsequently [409] in $\text{Cd}_{1-x}\text{Ga}_x\text{Cr}_2\text{Se}_4$. In the latter case it has been established that the illumination of the crystal with $x = 0.015$ with a white light from a conventional incandescent lamp practically instantly reduces the susceptibility of the

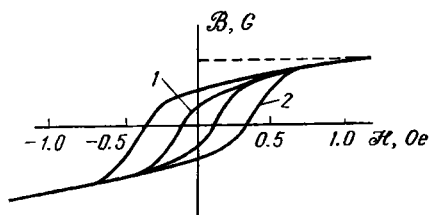


Fig. 6.4. Dynamic hysteresis loops of CdCr_2Se_4 at a frequency of 50 Hz at 77 K: 1, in darkness; 2, when illuminated with white light of 5 mW/cm² intensity [410]

crystal at a frequency of ~ 10 kHz by a half. After the illumination has been switched off, the susceptibility slowly returns to its original value with a relaxation time of ~ 1 min. As the temperature is lowered, the relative variation of the light-induced alternating magnetization and the relaxation time grow. They are also functions of the illumination intensity (with an increase in the latter the light-induced susceptibility decreases somewhat).

Further studies of the high-frequency photoferromagnetic effect have been reported in [140, 169, 410, 600]. Fig. 6.4 depicts the extension of the magnetic hysteresis loop in CdCr_2Se_4 at a frequency of 50 Hz at 77 K [410]. There is no doubt that the effect is a result of the light-induced photoelectrons or imperfections affecting the motion of the domain walls. The opinion has been expressed in [600] that such influence is exercised via photoinduced Cr^{4+} ions, which increase the local magnetic anisotropy. This explanation seems not very convincing. On account of a great thickness of the domain walls in CdCr_2Se_4 , such imperfections are most probably not point defects, but extended defects such as dislocations occupied by photoelectrons. Such photoelectrons effecting an indirect exchange between the atoms in the vicinity of the dislocation and thereby enhancing the FM coupling between them, turn the dislocation into a potential barrier for the domain wall. The same is true of two-dimensional defects of the grain boundary type.

6.4. SUBSURFACE MAGNETISM

It is a well-known fact that the magnetic properties of the crystal surface are generally different from those of its bulk. Even if the Heisenberg exchange integral on the surface is the same as in the bulk, already the change in the coordination number of surface atoms as compared with that of the atoms in the bulk will cause a change in the properties of the surface of an insulating crystal as compared with those of its bulk. More realistic models should also account for the change in the exchange integral on the surface [557, 572-578]. As a result, the surface layer of a Heisenberg FM can at finite temperatures be magnetized more or less than the bulk. In the latter case, according to [572, 574], the FM ordering on the surface may be replaced by an AF or a CAF.

In semiconductors there is an additional mechanism that may bring about an appreciable change in the magnetic properties of the surface.

Very often for various reasons a charge carrier depletion or enrichment layer is produced close to the surface of a semiconductor. The intensity of the indirect exchange via the charge carriers in this layer is not the same as in the bulk, and because of that the surface magnetic properties are not the same as the bulk.

The thickness and the charge of the surface layer are determined by the state of the surface, e.g. by the chemical adsorption of various substances, by the degree of its imperfection etc. But these quantities can also be varied by an external electric field*. The electric field in a specimen being studied is set up by making it a capacitor plate. To obtain high fields, a high-dielectric-constant insulator is placed between the plates. If the field points so that it decreases the carrier concentration on the surface, a field of sufficient intensity will produce a layer free of charge carriers. Its thickness l_e , according to [273], is connected with the induction on the interface of the dielectric by means of a relationship easily obtained by solving the Poisson equation

$$l_e = \frac{\mathcal{Z}}{4\pi en}.$$

For a charge carrier concentration of 10^{18} cm^{-3} and an induction of 10^6 V cm the thickness l_e is of the order of 10^{-6} cm . Obviously, only the direct exchange (more precisely superexchange) between magnetic atoms is possible in the carrier depletion layer.

In case of a field pointing in the opposite direction a layer enriched with carriers is formed on the surface. As has been pointed out in [274] its thickness l_i is almost equal to the screening length r_s ,

* The variation of the surface magnetization induced by an electric field is a particular case of the magnetoelectric effect (see Sec. 7.1).

(1.7.10), and the carrier concentration in it n_s is connected with the bulk concentration n by means of the relationship

$$\frac{n_s}{n} = \left[1 + \frac{5\mathcal{Z}^2}{16\pi\epsilon_0\mu n} \right]^{3/5}.$$

As has been pointed out in [274], values of induction of the order of 10^8 V/cm are attainable in practice. For $\epsilon_0 = 10$, a bulk carrier concentration $n = 10^{19}$ cm $^{-3}$ and $\mu = 0.1$ eV, the concentration on the surface is about 30 times that in the bulk. The screening length is in this case equal to $3 \cdot 10^{-7}$ cm, i.e. to about ten lattice parameters.

First of all let us discuss the effect of the charging of the surface relative to the bulk on the surface properties of heavily-doped FMS. When surface magnons in Heisenberg magnets are studied, it is usually presumed that the existence of a surface either has no effect on the value of the exchange integral [271] or results only in changes in a monoatomic surface layer [272]. The charging of the surface relative to the bulk may produce a magnon branch of a type quite different from those considered in [271]. [272], since in this case the length at which the effective exchange integral changes is great as compared with the lattice parameter a .

Such quasi-surface magnons in a highly-doped FMS have been considered in [166, 170]. For $W \ll AS$ the indirect exchange Hamiltonian is obtained in the first approximation in $1/S$ from (3.5.18) by averaging over the electron variables. Applying the condition of a slow rate of spatial variation of the electron density, we can substitute the local electron density $v(\mathbf{g})$ for average values of the type of $\langle \alpha_{\mathbf{g}}^* \alpha_{\mathbf{g}+\Delta} \rangle$. The direct exchange Hamiltonian \mathcal{J} (2.4.2) is added to the indirect exchange Hamiltonian:

$$\begin{aligned} \mathcal{H} &= \frac{S}{2} \sum_{\mathbf{g}, \Delta} \mathcal{J} \left(\mathbf{g}_z + \frac{\Delta_z}{2} \right) (b_{\mathbf{g}}^* b_{\mathbf{g}} + b_{\mathbf{g}+\Delta}^* b_{\mathbf{g}+\Delta} - b_{\mathbf{g}}^* b_{\mathbf{g}+\Delta} - b_{\mathbf{g}+\Delta}^* b_{\mathbf{g}}), \\ \mathcal{J} \left(\mathbf{g}_z + \frac{\Delta_z}{2} \right) &= \mathcal{J} + \mathcal{J}_{\text{eff}}(\mathbf{g}_z, \mathbf{g}_z + \Delta_z), \quad (6.4.1) \\ \mathcal{J}_{\text{eff}}(\mathbf{g}, \mathbf{g} + \Delta) &= \frac{|B|}{2S^2} \langle \alpha_{\mathbf{g}}^* \alpha_{\mathbf{g}+\Delta} \rangle \approx \frac{|B|}{2S^2} v(\mathbf{g}). \end{aligned}$$

By applying the transformation of magnon operators of the type of (1.2.4)

$$B_{\mathbf{g}} = \sum \psi_{\mathbf{k}}(\mathbf{g}_z) \exp \{ i(k_x g_x + k_y g_y) \}$$

we obtain a one-dimensional Schrödinger equation for the wave function $\psi_{\mathbf{k}}$ of the z -coordinate with the z -axis orthogonal to the surface. It also depends on the quasi-momentum along the surface as a parameter. In the Wentzel-Kramers-Brillouin (WKB) approximation the solution of the Schrödinger equation can be represented

as a magnon band that bends and changes its width as it approaches the surface (Fig. 6.5, where $J(z)$ is the effective exchange integral that takes into account both direct and indirect exchanges). The corresponding picture differs from that of bent electron bands in that the latter retain their width. It will be seen from the figure that there are quasi-surface magnons for which the surface itself is classically inaccessible (i.e. their amplitude is exponentially small not only in the bulk, but also on the surface).

Thus, an external field by changing the carrier concentration distribution in the crystal and thereby its magnon spectrum is able

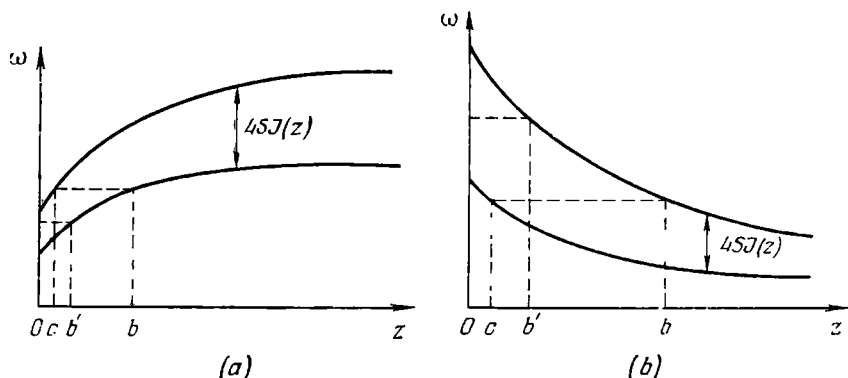


Fig. 6.5. Quasi-surface magnons in a degenerate ferromagnetic semiconductor: (a) in case of a deficiency in conduction electrons in the subsurface layer; (b) in case of their excess

at finite temperatures to cause noticeable changes in the magnetization of thin specimens. For example, if the Curie point of an undoped specimen T_c^0 is appreciably below T_c , in the interval $T_c^0 < T < T_c$ its moment will be diminished by the field owing to the demagnetization of the depletion layer whose thickness is l . By contrast, at $T > T_c$ the field can induce magnetization in the layer enriched with electrons.

Experimental data obtained for EuO [171, 152, 559] are proof of the influence exercised by the indirect exchange on the magnetization of the surface of an FMS. Judging by the polarization of neutrons and of photoelectrons, the magnetization of the surface is appreciably lower than that of the crystal bulk, this effect appearing even at temperatures much below the Curie point*. The magnetization of the surface of crystals containing several percent La or Gd proved to be much greater than in pure specimens, this being an

* A paramagnetic surface layer could not be discovered in experiments on cold emission from EuS [421, 558].

indication of an enhancement of FM coupling on the surface owing to conduction electrons produced by doping. Doping can also affect photoemission by charging the surface relative to the bulk [560]. The surface paramagnetism also vanished in the result of chemisorption of Cs on the surface of EuO [275]. This can be explained by the fact that the adsorbed Cs atoms behave like surface donors. Their valence electrons are drawn into the crystal and delocalized, being concentrated near the surface. By force of this they carry out the FM indirect exchange between the subsurface ions enhancing the FM coupling between them.

The charging of the surface can have a considerable effect also on the surface properties of heavily-doped AFS. In particular, even if the bulk carrier concentration is below the critical n_A at which the AF ordering becomes unstable, it may exceed it on the surface and may even exceed the concentration n_F at which the FM ordering becomes stable. Thus, an electric field of a sufficiently high intensity can transform the surface of an AFS into an FM state, the bulk remaining AF [166]. As is well known, in two-dimensional systems only anisotropy can stabilize magnetic ordering at finite temperatures.

In contrast to a thin film of the same thickness, the magnetic ordering in a surface layer should exist at $T \neq 0$ even in the absence of magnetic anisotropy. Indeed, only surface magnons could be dangerous for the FM ordering, since the p^{-2} -type divergence of their distribution function is not compensated by the small volume element of the phase space turning zero proportionally with p at $p \rightarrow 0$, where p is the surface quasi-momentum. However, the penetration of surface magnon into the bulk at $p \rightarrow 0$ increases at a rate not slower than $1/p$. This is enough for the stability of a surface FM at finite temperatures.

Indeed, at great distances from the surface the magnetic Hamiltonian coincides with the Hamiltonian of an ideal AF, i.e. the magnon frequency is determined by (2.6.11), (2.4.4)

$$\omega = 2 |J| S \sqrt{1 - \frac{1}{9} (\cos p_x a + \cos p_y a + \cos ka)^2}.$$

In case of surface magnons k is imaginary. From the condition that the magnon frequency be real it follows that for $p = \sqrt{p_x^2 + p_y^2}$ tending to zero the inverse penetration length k must also tend to zero, i.e. that $k \sim p^m$ ($m \geq 1$). The magnitude Hamiltonian of the crystal can be diagonalized by the canonical transformation of the operators of the spin deviations from the spin equilibrium positions as determined by the quasi-classical method

$$b_g = \sum_{\lambda} \{u_{\lambda}(g) b_{\lambda} + v_{\lambda}(g) b_{\lambda}^*\}.$$

In the surface FM layer coefficients $v_\lambda(g)$ can be put equal to zero, so that the average demagnetization of an atom of this layer will be given by the expression

$$\mathfrak{N}_g = \sum_\lambda |u_\lambda(g)|^2 \left\{ \exp\left(\frac{\omega_\lambda}{T}\right) - 1 \right\}^{-1}. \quad (6.4.2)$$

As has already been pointed out above, the quantity $|u_{pk}(z)|$ corresponding to surface magnons for large z 's is proportional to e^{-kz} . Then it follows from the normalization conditions that for $1/k \gg l$ the order of magnitude of this quantity on the surface is $\sqrt{k N_s}$, where N_s is the number of atoms on the surface. Hence, the "dangerous" portion of the integral (6.4.2) corresponding to the surface magnons converges: if the quadratic dependence of the frequency on p is taken into account, the integrand will be proportional to $p^{m-2} \leq p^{-1}$ and not to p^{-2} as in the case of a thin film. This means that the coupling existing between the spin deviations on the surface and in the bulk stabilizes the FM layer.

The surface concentration can be increased by an external electric field, i.e. this field can transform the surface of an AFS into the FM state.

6.5. THE EFFECT OF ELECTROACTIVE IMPERFECTIONS ON THE MAGNETIC PROPERTIES OF SEMICONDUCTORS AND THE TEMPERATURE-INDUCED SHIFT OF DONOR LEVELS

Localized Magnons. As has already been pointed out, in nondegenerate MS the conduction electron concentration is too small to affect the magnetic ordering of the crystal as a whole. However, electrons localized on donors create high local electron densities and thereby appreciably affect the local magnetic properties in the vicinity of the donors. In fact, we are entitled to speak of the indirect exchange in the vicinity of the donor via the electron localized on it. In an FM crystal this intensifies the coupling between the atoms in the vicinity of a donor, and accordingly discrete levels with frequencies ω_d above the maximum magnon frequency ω_H of an ideal crystal may appear in the magnon spectrum [116, 89, 90]. The corresponding spin waves are characterized by an exponential decay of their amplitudes with the distance from the imperfection.

Such discrete levels are produced only when the FM coupling between magnetic atoms via the donor electron is strong enough. As this coupling becomes weaker, the frequency ω_d approaches the frequency ω_H , and the radius of the localized magnon state grows. At a definite critical value of the indirect exchange constant, when ω_d becomes equal to ω_H the localized magnon level vanishes (when

ω_d coincides with ω_{Π} , the radius of the localized state becomes infinitely large).

The disappearance of discrete levels near the top of the magnon band ω_{Π} does not mean that the imperfection no longer influences the magnon spectrum: it as before increases the density of states $g_m(\omega)$ of high-frequency magnons, however this time not above, but below the top of the band. The density of states of long-wave magnons decreases correspondingly. The growth of $g_m(\omega)$ below ω_{Π} is conventionally interpreted as the appearance there of a resonance level. The difference between the latter and a discrete level is that the discontinuity corresponding to a discrete level is a delta-type discontinuity in the density of states $g_m(\omega) \sim \delta(\omega - \omega_d)$, whereas a density peak of finite width corresponds to a resonance level. The latter circumstance reflects the fact that a resonance state is not an eigenstate of the system. Therefore there is no definite energy to correspond to it. Qualitatively, it can be interpreted as follows: an imperfection may trap a magnon, but if the energy of the trapped magnon lies inside the energy band of free magnons, the localized magnon can, retaining its energy, go over to the free state. The energy level of a localized magnon broadens owing to the lifetime of the magnon in the localized state being finite. Originally the discrete and resonance magnon levels have been studied in [270, 269, 242] within the framework of the Heisenberg model.

The mathematical analysis of the problems can be carried out easiest of all in the case of narrow bands $W \ll AS$ by making use of the Hamiltonian of the type (6.4.1). If the electron can with an appreciable probability reside only on the imperfection and on atoms belonging to the first coordination sphere of the latter, and if the imperfection has the same spin as the regular atoms, the indirect exchange via a spinpolaron will change the effective exchange integral of the imperfection with its neighbours by the amount

$$J_{\text{eff}} = \frac{|B|}{2S^2} \langle \alpha_0^* \alpha_{\Delta} \rangle \quad (6.5.1)$$

(the indices 0 and Δ denote the imperfection and its nearest neighbours, respectively). Hence, the effective indirect exchange Hamiltonian with account taken of the symmetry of the wave function of a localized spinpolaron will assume the form

$$H_d = JS \sum_{g\Delta} (b_g^* b_g - b_g^* b_{g+\Delta}) + \Delta JS \sum_{\Delta} (b_0^* b_0 + b_{\Delta}^* b_{\Delta} - b_{\Delta}^* b_0 - b_0^* b_{\Delta}), \quad (6.5.2)$$

where ΔJ includes in addition to J_{eff} also the change in the direct exchange integral introduced by the imperfection.

The problem of the magnon spectrum in the presence of a local perturbation in the Hamiltonian (the last term in H_d) can be solved precisely by making use of ideas contained in papers by I. M. Lifshitz [268]. To this end a transformation to the Fourier-components of magnon operators is carried out in H_d (2.4.3), and an equation of motion for Green's function $\langle\langle b_{\mathbf{k}} | b_{\mathbf{q}}^* \rangle\rangle$ is written down

$$(\omega - \omega_{\mathbf{k}}) \langle\langle b_{\mathbf{k}} | b_{\mathbf{q}}^* \rangle\rangle = \delta_{\mathbf{k}\mathbf{q}} + \frac{\Delta\mathcal{Y}}{N} \sum_{\mathbf{k}'} V_{\mathbf{k}\mathbf{k}'} \langle\langle b_{\mathbf{k}'} | b_{\mathbf{q}}^* \rangle\rangle, \quad (6.5.3)$$

where

$$\begin{aligned} \Delta\mathcal{Y} &= 6\Delta\mathcal{J}S, \quad \varphi_{\mathbf{q}} = \mathcal{Y}(1 - \gamma_{\mathbf{q}}), \\ V_{\mathbf{k}\mathbf{k}'} &= (1 + \gamma_{\mathbf{k}-\mathbf{k}'} - \gamma_{\mathbf{k}} - \gamma_{\mathbf{k}'}) \\ &= \frac{1}{3} \sum_{i=x, y, z} [(1 - \cos k_i a)(1 - \cos k'_i a) + \sin k_i a \sin k'_i a] \end{aligned}$$

(the lattice is presumed to be a simple cube).

The equation (6.5.3) with respect to Green's function is obviously an integral equation with a six-fold degenerate kernel. It is solved by usual methods. We introduce the quantities

$$\mathcal{X}_i = \sum_{\mathbf{k}'} (1 - \cos k'_i a) \langle\langle b_{\mathbf{k}'} | b_{\mathbf{q}}^* \rangle\rangle, \quad \mathcal{Y}_i = \sum_{\mathbf{k}'} \sin k'_i a \langle\langle b_{\mathbf{k}'} | b_{\mathbf{q}}^* \rangle\rangle. \quad (6.5.4)$$

For them we obtain from formula (6.5.3) the following equations

$$\mathcal{X}_i [1 - \Delta\mathcal{Y}G_d] - \Delta\mathcal{Y}G_{nd} \sum_{j \neq i} \mathcal{X}_j = \frac{(1 - \cos q_i a)}{\omega - \omega_{\mathbf{q}}}, \quad (6.5.5)$$

$$\mathcal{Y}_i [1 - \Delta\mathcal{Y}G_s] = \frac{\sin q_i a}{\omega - \omega_{\mathbf{q}}}, \quad (6.5.6)$$

where we make use of the notation

$$\begin{aligned} G_d &= \frac{1}{3N} \sum_{\mathbf{k}} \frac{(1 - \cos k_x a)^2}{\omega - \omega_{\mathbf{k}}}, \\ G_{nd} &= \frac{1}{3N} \sum_{\mathbf{k}} \frac{(1 - \cos k_x a)(1 - \cos k_y a)}{\omega - \omega_{\mathbf{k}}}, \\ G_s &= \frac{1}{3N} \sum_{\mathbf{k}} \frac{\sin^2 k_x a}{\omega - \omega_{\mathbf{k}}}. \end{aligned}$$

According to (6.5.3-6), in addition to the poles corresponding to magnons in an ideal crystal, Green's functions $\langle\langle b_{\mathbf{k}} | b_{\mathbf{q}}^* \rangle\rangle$ have new poles due to the presence of the imperfection (the poles of \mathcal{X}_i and \mathcal{Y}_i). They correspond to discrete or resonance magnon levels. According to (6.5.5, 6), the equations to determine them are of the form:

$$1 - \Delta\mathcal{Y}G_s = 0 \quad (6.5.7)$$

(a three-fold degenerate level),

$$1 - \Delta\gamma (G_d + 2G_{nd}) = 0$$

(a nondegenerate level),

$$1 - \Delta\gamma (G_d - G_{nd}) = 0$$

(a doubly-degenerate level).

The density of magnon states $g_m(\omega)$ is obtained from the Fourier-transforms of Green's function with the aid of the well-known formula [242]

$$g_m(\omega) = \frac{1}{\pi N} \sum \text{Im} \langle \langle b_{\mathbf{q}} | b_{\mathbf{q}}^* \rangle \rangle,$$

where Green's function $\langle \langle b_{\mathbf{q}} | b_{\mathbf{q}}^* \rangle \rangle$ is determined by equations (6.5.3-6). The general expression for it is very cumbersome, but it is greatly simplified in the long-wave limit [242]:

$$g_m(\omega) \simeq \left\{ 1 - \frac{N_d}{N} \frac{3\Delta\gamma}{\gamma - 0.2\Delta\gamma} \right\} g_m^0(\omega), \quad (6.5.8)$$

$$g_m^0 = \sum_{\mathbf{k}} \delta(\omega - \omega_{\mathbf{k}}),$$

where N_d is the number of electrons on the donor impurities in the crystal, $g_m^0(\omega)$ is the density of states in the ideal crystal. For $\Delta\gamma > 0$ the value of g_m will be seen from (6.5.8) to be lower than g_m^0 . This is the consequence of the imperfection redistributing the magnon levels over the energies without altering their total number. Accordingly the increase in the density of states in the short-wave part of the spectrum caused by the imperfections is compensated by an appropriate decrease in the long-wave part.

Localized magnons can appear also when the radius of the electron orbit substantially exceeds the lattice parameter. Such a situation is quite common in wide-conduction-band semiconductors. In this case the expression for the indirect exchange Hamiltonian in the main approximation in the c - l exchange is (4.5.13a). Carrying out in it a transformation to magnon operators by using formulae (2.4.1), we obtain for the energetically-favoured electron spin direction a magnon Hamiltonian of the following form [49]:

$$H_d = \frac{A}{2} \sum w_{\mathbf{g}} w_{\mathbf{f}} (b_{\mathbf{g}}^* b_{\mathbf{g}} - b_{\mathbf{g}}^* b_{\mathbf{f}}) + \gamma S \sum (b_{\mathbf{g}}^* b_{\mathbf{g}} - b_{\mathbf{g}}^* b_{\mathbf{g}+\Delta}). \quad (6.5.9)$$

To diagonalize it, we carry out the canonical transformation of magnon operators

$$b_{\mathbf{i}} = \sum_{\mathbf{g}} c_{\mathbf{g}\mathbf{i}} b_{\mathbf{g}}$$

thus obtaining the wave equation

$$\gamma S \sum_{\Delta} (c_{\mathbf{g}} - c_{\mathbf{g}+\Delta}) + \frac{A}{2} \sum_{\mathbf{f}} w_{\mathbf{g}} w_{\mathbf{f}} (c_{\mathbf{g}} - c_{\mathbf{f}}) = \omega c_{\mathbf{g}}. \quad (6.5.10)$$

We shall be interested in magnon levels near the magnon-band top. This chief contribution to their wave functions is from the Fourier-transforms with wave vectors approximately equal to $\Pi = \left(\frac{\pi}{a}, \frac{\pi}{a}, \frac{\pi}{a}\right)$. Making use for the magnons of the effective mass method (Sec. 1.2), we represent the coefficients c_g in the form

$$c_g = \varphi(g) \exp(i\Pi \cdot g), \quad (6.5.11)$$

where $\varphi(g)$ is a slowly-changing function of the magnetic atom g coordinate. Expanding formally $\varphi(g + \Delta)$ in Δ we obtain from formulae (6.5.10, 11)

$$\frac{1}{2M} \Delta \varphi(g) + \frac{A}{2} w_g \varphi(g) - \frac{A}{2} w_g e^{-i\Pi \cdot g} \sum_f w_f \varphi(f) e^{i\Pi \cdot f} = (\omega - 2\gamma) \varphi(g), \quad (6.5.12)$$

where the expression for the magnon effective mass is (2.4.5).

Note first of all that the last term in the left-hand part of equation (6.5.12) can be discarded, for in the sum over f the slowly-changing coordinate function $w_f \varphi(f)$ is multiplied by a rapidly oscillating factor. Next, the expression for ω_g in the hydrogen-like model of a donor is

$$w_g = \frac{1}{\pi} \left(\frac{a}{a_B} \right)^3 \exp \left(-\frac{2g}{a_B} \right), \quad (6.5.13)$$

where a_B is the radius of the electron orbit. If the signs of all the terms in (6.5.13) are reversed, the corresponding problem will be identical to that of a particle trapped in a potential well whose solution is well-known (see [401]). Making use of it, we obtain the condition for the existence of at least one discrete level above the magnon band

$$\frac{A(S+1)}{T_c} > 18 \left(\frac{a_B}{a} \right). \quad (6.5.14)$$

Hence, for specified AS and T_c it is the more difficult to satisfy the condition for the existence of localized magnon levels in the vicinity of a donor imperfection the greater the radius of the donor orbit. This result was to be expected: as is known from quantum mechanics, for a potential well of a depth V to produce a discrete level, $V a_B^2$ must exceed some critical value [75]. At the same time in the case being considered $V \sim \frac{A}{a_B^3}$ and for large a_B this condition cannot be met. For $AS \simeq 0.5$ eV, $a_B \simeq 4a$ local magnons are possible in all semiconductors with a T_c below 70 K.

For the second magnon level to appear, the inequality should be satisfied

$$\frac{A(S+1)}{T_c} > 76 \left(\frac{a_B}{a} \right). \quad (6.5.15)$$

For the parameters specified above, the second magnon level is possible only, if $T_c < 20$ K. Hence, one may conclude, in particular, that large-radius donor states produced by doping EuO with gadolinium can result only in one discrete magnon level appearing per every donor atom.

There are no such localized magnons in degenerate semiconductors, but to make up for this spatial fluctuations of electron density produce a tail of magnon states lying above the magnon-band top $\omega_m \equiv \omega_{\Pi}(n)$ [310]. (This tail is obviously an analogue of the electron-density tail in the band-gap (Sec. 1.7).) The density of states in this tail can be found by making use of the quasi-classical approximation. In this case it is justified, because near the band top the magnon wavelength is small as compared with the characteristic electron density variation length (i.e. the screening length).

To begin with, we must express the magnon frequency $\omega_q(\mathbf{r})$ regarded as a function of the local electron density $n(\mathbf{r})$ in terms of the electrostatic potential fluctuation $\varphi(\mathbf{r})$. It is associated with the electron density fluctuation by means of a relationship resulting from the condition that the electrochemical potential of the system (1.7.5) remains constant. Hence, making use of relation (6.1.1, 2) and (1.7.6), we may express the magnon frequency in the form

$$\omega_q(\mathbf{r}) = \bar{\omega}_q + C_q \varphi(\mathbf{r}), \quad C_q = \frac{3e}{2\mu} [\bar{\omega}_q - \omega_q^0], \quad (6.5.16)$$

where $\bar{\omega}_q$ is the magnon frequency corresponding to the average electron density n . By definition of the density of states

$$g_m(\omega) = \frac{1}{N} \sum_q \int_{-\infty}^{\infty} \delta(\omega - \bar{\omega}_q - C_q \varphi) P(\varphi) d\varphi, \quad (6.5.17)$$

where, according to formula (1.7.13), the potential distribution function is a Gaussian one

$$P(\varphi) = \frac{e}{\sqrt{\pi} E_f} \exp\{-e^2 \varphi^2 / E_f^2\} \quad (6.5.18)$$

(E_f is the mean-square fluctuation potential).

It follows from formulae (6.5.17, 18) that the magnon density of states in the tail decreases with the distance from the band top as

$$g_m \sim \exp\{-e^2(\omega - \omega_m)^2 / E_f^2 C_{\Pi}^2\}. \quad (6.5.19)$$

As will be demonstrated in Secs. 7.3, 7.4, at finite temperatures $\tilde{\varepsilon}_0 = \varepsilon_0(1 - \Gamma_0)$, where Γ_0 (see 7.3.12-15 below) rises with the

temperature, should be substituted for ϵ_0 in the definition of E_f (1.7.14). Accordingly, the magnon density of states in the tail should grow with rising temperature. From the physical point of view this is a result of an increase in the electron density fluctuations. The magnetization in the vicinity of the donors is greater than at a distance from them, because the electron density is higher near the donors, and hence the FM coupling is stronger. But the electrons tend to accumulate in regions of maximum magnetization, and accordingly their density in the vicinity of the donor grows as the temperature rises.

Temperature-induced Shift of Donor Levels. In what follows we intend to demonstrate that the temperature-induced shift of electron levels can be expressed in terms of the magnon density of states calculated with account taken of the effect exercised on it by the electrons. This circumstance facilitates the calculation of the temperature dependence of the donor levels. By way of an example we shall consider narrow-band semiconductors. The indirect exchange Hamiltonian is given by the correction to the spinpolaron energy of the first order in $1/2S$, i.e. the structure of the full Hamiltonian is that of (6.4.1) with the effective indirect exchange integral

$$J_{\mathbf{g}\mathbf{g}'}(\mathbf{g}, \mathbf{g} + \Delta) = \frac{1}{2S^2} \frac{|B|}{2S^2} \langle \alpha_{\mathbf{g}}^* \alpha_{\mathbf{g}+\Delta} \rangle = \frac{|B|}{2S^2} \sum_v \psi_v^*(\mathbf{g}) \psi_v(\mathbf{g} + \Delta) n_v^0, \quad (6.5.20)$$

where $n_v^0 = 0, 1$ are the numbers of spinpolarons in the v -th eigenstate of the Hamiltonian $H_0 = H_d - H_B$ of spinpolarons not interacting with the magnons, where H_d and H_B are given by (1.2.3) and (1.1.1) respectively and $\psi_v(\mathbf{g})$ are coefficients of the canonical transformation (1.2.4) that diagonalizes the Hamiltonian H_0 .

The effective exchange Hamiltonian will be seen from formula (6.5.20) to be a functional of the spinpolaron occupation numbers. The character of the magnon spectrum changes as the spinpolaron state changes. For instance, the transition of a spinpolaron from a donor level to the conduction band results in the disappearance of localized magnons. The dependence of the magnon spectrum on the state of the spinpolarons can be accounted for, if the magnon density of states is regarded as a functional of the spinpolaron occupation numbers.

To find the average spinpolaron occupation numbers n_v , we apply the method of the nonequilibrium thermodynamic potential [246]: we write the thermodynamic potential $\Omega = E - TS_T - \mu n$ regarded as a functional of the occupation numbers $n(\epsilon)$ and $m(\epsilon)$ of spinpolaron and magnon states, respectively, and minimize it with respect to these numbers. Taking into account the familiar expressions for the entropy S_T of the fermions and bosons, we obtain

it in the form

$$\begin{aligned}\Omega\{n, m\} = & \int (\varepsilon - \mu) n(\varepsilon) g_e(\varepsilon) d\varepsilon + \int d\omega \omega g_m[\omega, \{n\}] \\ & + T \int d\varepsilon g_e(\varepsilon) \{n \ln n + (1-n) \ln(1-n)\} \\ & - T \int d\omega g_m[\omega, \{n\}] \{m \ln m + (1-m) \ln(1-m)\}. \quad (6.5.21)\end{aligned}$$

Minimizing the functional (6.5.21) in the occupation numbers, we obtain their average values: the magnon distribution function is obtained in the usual Bose form, and the fermion one in the Fermi form, but with a renormalized energy

$$\tilde{E}_v = E_v - \delta F_m\{n\} / \delta n(E_v), \quad (6.5.22)$$

where F_m is the magnon free energy, a functional of the fermion distribution function:

$$F_m\{n\} = T \int d\omega g_m[\omega, \{n\}] \ln \left(1 - e^{-\frac{\omega}{T}}\right). \quad (6.5.23)$$

The second term in formula (6.5.22) is none other than the fermion mass operator. Its structure resembles that of the mass operator in the Fermi-liquid theory (4.5.4). Expression (6.5.22) is valid in all cases when the fermion damping is either absent or small. In particular, for free spinpolarons ($v \rightarrow k$) it yields the result (4.1.3), which can be easily ascertained, if use is made of expression (6.5.8) for the magnon density of states g_m with account taken of the frequency shift caused by the indirect exchange (6.1.1).

If we presume Δ_j in (6.5.2, 8) to coincide with J_{eff} , we making use of expressions (6.5.22, 23) and (6.5.8) will obtain the following result for the shift of the donor level at $T \ll \psi$ ($v \rightarrow L$):

$$\Delta E_L = -\frac{\delta F_m}{\delta n_L} = -\frac{\zeta(5/2)}{2\pi^{3/2}} \frac{J_{\text{eff}} T^{5/2}}{J \pm 0.2 J_{\text{eff}} (J S)^{3/2}}, \quad (6.5.24)$$

where $\zeta(x)$ is Riemann's zeta-function. Comparing ΔE_L with the shift of free spinpolaron levels ΔE_c (4.1.3) and taking account of expression (6.5.1) for the effective exchange integral, we obtain

$$\frac{\Delta E_L}{\Delta E_c} < \psi_L(0) \psi_L(\Delta) \leq \frac{1}{2\sqrt{z}}, \quad (6.5.25)$$

i.e. indeed a localized level shifts with the temperature much more slowly than the conduction-band bottom.

The Effect of Imperfections on the Paramagnetic Susceptibility. The FM ordering is retained up to much higher temperatures in the vicinity of nonionized donors than on the average in the crystal as a whole. In the result magnetic clusters are produced around the

imperfections, which are similar to those in AFS considered in [195] (Sec. 5.3). They may be called localized ferrons, too. They can greatly raise the PM susceptibility of the crystal. In [88] this has been interpreted as an increase in the PM Curie temperature θ with the FM Curie temperature T_c remaining unchanged. The reason for the rise in θ is that, according to (2.5.6), every moment determining the crystal magnetization makes a contribution to the susceptibility χ proportional to its square. A cluster consisting of \mathcal{N} atoms and having a moment $\mathcal{K} = \mathcal{N}S$ makes a contribution to the susceptibility χ (2.5.6) proportional to $\mathcal{N}^2 S^2$, whereas the same atoms not united in a cluster would make a contribution \mathcal{N} times smaller. Accordingly, if the cluster is sufficiently large, the imperfections will exercise an appreciable effect on the magnetization even if their concentration is not very high.

(One can easily obtain an estimate for the maximum contribution χ_d of donors to the susceptibility of a nondegenerate FMS, when the donor concentration satisfies the condition $n^{1/3} a_B < C$ ($C \simeq 1/4$; see (1.6.2)). The radius of the sphere inside which a donor electron maintains an FM ordering can naturally be assumed to be close to that of the electron orbit a_B , i.e. $\mathcal{N} \simeq 4 (a_B/a)^3$. Hence, χ_d is proportional to $n\mathcal{N}^2$ not exceeding $\mathcal{N}a^{-3} 16$. At the same time the susceptibility of a pure crystal χ_0 is proportional to a^{-3} , i.e. χ_d/χ_0 in a nondegenerate semiconductor may be as high as $\sim 0.05 \mathcal{N}$. When the number of atoms in a cluster exceeds 20, the contribution of the imperfections to the susceptibility may exceed the susceptibility of the undoped crystal (a similar situation exists in the case of a donor impurity in an antiferromagnet at $T = 0$ (see Sec. 5.3).

As the temperature rises, the moment of the cluster decreases and χ_d falls correspondingly. The calculation of the cluster moment is especially simplified, when the intensity of the indirect exchange via a c -electron greatly exceeds that of the direct exchange, and when one can assume the electron to occupy all the \mathcal{N} atoms belonging to the cluster with an equal probability $w = 1/\mathcal{N}$. Then the eigenvalues of the Hamiltonian (4.5.13a) will be proportional to the eigenvalues of the cluster moment \mathcal{K} . The latter assume all integral values between \mathcal{K}_{\min} and \mathcal{K}_{\max} , where the minimum cluster moment \mathcal{K}_{\min} is equal to 0 for an even \mathcal{N} and S for an odd \mathcal{N} , with the maximum moment \mathcal{K}_{\max} being equal to $\mathcal{N}S$. The average cluster moment is given by the expression

$$\mathcal{K}(T) = 2\mathcal{N}T \frac{d}{dA} \ln \sum_{\mathcal{K}} (2\mathcal{K} + 1) \mathcal{F}(\mathcal{K}) \exp \left\{ \frac{A\mathcal{K}}{2\mathcal{N}T} \right\}, \quad (6.5.26)$$

where $\mathcal{F}(\mathcal{K})$ is the number of ways in which one can construct the moment of \mathcal{K} from \mathcal{N} moments of S (see Sec. 4.5).

Up to now we have been dealing with singly-charged donors. In the case of doubly-charged donors with spins of both electrons

parallel (e.g. in the $(1s)$ and $(2s)$ states) the situation qualitatively remains unchanged: the indirect exchange via the donor electrons enhances the FM coupling between the atoms in the vicinity of the donor. If the electron spins are antiparallel, this statement is generally not true. In particular, if the donor is in the $(1s)^2$ state, the indirect exchange on the contrary weakens the FM coupling.

Indeed, the indirect exchange integral in this case does not contain terms of the first order in A , since opposite signs correspond to the opposite c -spin projections in the Hamiltonian H_{M1} (4.5.13a). On the contrary, the Heisenberg term H_{M2} (4.5.13b) is doubled as a result of summation over the two spin projections. The conclusion that in this case the indirect exchange is antiferromagnetic is based on the following considerations. The Hamiltonian H_{M2} is none other than the second-approximation correction to the energy of the ground state of the electron E_{1s} . It follows from (4.5.13b) that the indirect exchange energy cannot be positive. (The situation is quite common in quantum mechanics.) On the other hand from the condition of orthonormality of the functions ψ_μ (g)

$$\sum_g \psi_g^*(g) \psi_\mu(g) = \delta_{\nu\mu} \quad (6.5.27)$$

it follows that in case of an FM ordering the indirect exchange energy (4.5.13b) is zero. Hence, it attains its maximum in this case. At the same time it attains its minimum in case of such a magnetic ordering when there is no direction the projection of all the spins onto which is nonzero.

The weakening of FM coupling between the l -spins in the vicinity of doubly-charged donors in the $(1s)^2$ state should result in a decrease in the magnetic susceptibility of the crystal. This should also accompany the doping of anomalous FMS displaying a blue shift of the absorption edge (Sec. 4.2) with singly-charged donors, if the donor level lies sufficiently close to the conduction band. Indeed, the energy of the donor electron same as that of the conduction electron should be maximum in case of an FM ordering, and because of that the electron should tend to destroy it [384].

At present extensive experimental data have accumulated in support of a drastic increase in θ following the doping of FMS with donor impurities [9]. In particular, results on EuO depicted in Fig. 6.3 serve to illustrate this point. It follows from them that for a Gd concentration of 0.5% when, according to [130], the crystal is a poor conductor, its magnetic susceptibility at $T < 200$ K exceeds that of an undoped crystal, approaching it as the temperature rises. However, the reason why at $T > 200$ K the susceptibility of a doped specimen is lower than that of an undoped one is not clear. Possibly it may be explained by the presence of oxygen vacancies acting as double donors.

As was already pointed out, in the $(1s)^2$ state they diminish χ . Localized ferrons are possible in AFS as well (Sec. 5.3). In the same way as they raise the effective PM Curie point of an FMS, they must raise it in an AFS. Specifically, at sufficiently high imperfection concentrations θ may even become positive, and this has been observed for example in iodine-doped EuTe crystals: in the range of concentrations where the conductivity of the crystal retained its semiconducting nature θ reached 12 K, whereas in an undoped EuTe it was equal to -5 K [106].

In contrast to the rest of FMS, CdCr_2S_4 displaying an anomalous sign of the temperature-induced shift of the absorption edge also displays an anomalous sign of the variation of χ following its doping with the singly-charged donor impurity Ga: it decreases instead of increasing it [202]. This agrees with the theoretical considerations presented above.

Finally, we would like to point out specific magnetic properties of compensated semiconductors: the doping of EuO + Eu with the acceptor impurity Ag (0.57% by weight) or with Cu (0.75%), while decreasing the conductivity, simultaneously raises both θ and T_c to 150 K [430]. The effect remains unexplained as yet. It should be noted that it resembles the rise in T_c of EuO due to Fe doping, when T_c reaches 180 K [430].

Inversion of Energy Terms of a Doubly-charged Donor. In contrast to a nonmagnetic semiconductor in which the ground state of a doubly-charged donor is always $(1s)^2$, in an FMS it may be the $(1s)(2s)$ state. The explanation is that the enhancement of the orbital energy E_{12} resulting from the transition of one of the electrons from the $(1s)$ to the $(2s)$ state can be made up for by the gain in the c - l exchange energy $A\mathcal{L}$ achieved when the spins of both electrons are parallel to the crystal moment in case of $A > 0$ or antiparallel to it in case of $A < 0$. Here the local crystal moment is determined by the equality

$$\mathcal{L} = \frac{1}{2} \left\langle \sum_{\mathbf{g}} [|\psi_{1s}(\mathbf{g})|^2 + |\psi_{2s}(\mathbf{g})|^2] \mathbf{S}_{\mathbf{g}} \right\rangle,$$

where the angular brackets symbolize averaging over the temperature. Obviously, at $T = 0$ the moment \mathcal{L} will be equal to the atomic spin S , but as the temperature rises it will diminish. Accordingly, at a temperature T_i as determined by the equality $A\mathcal{L}(T_i) \simeq E_{12}$ the nonionized donors must go over from the $(1s)(2s)$ state with parallel spins to the $(1s)^2$ state with antiparallel spins. In the result of the inversion the local magnetization in the vicinity of the donor drops sharply. Hence, the inversion resembles a phase transition of the first kind in a system of \mathcal{N}_2 atoms over which the electron in the $2s$ state is spread [386].

Since the local magnetization is destroyed much more slowly than the average crystal magnetization, and since besides it is sustained by the indirect exchange via donor electrons in the $(1s)(2s)$ state, the inversion should take place at temperatures close to the Curie point T_c or even at much higher temperatures. If the s -electrons are in the $(1s)^2$ state, the atomic spins in the vicinity of the imperfection may be presumed to be completely disordered. Below the intensity of the indirect exchange in the $(1s)(2s)$ state will be presumed to be considerably higher than that of the direct exchange, so that the condition $4.2\mathfrak{N}_2 \geq T$ will be satisfied. Then the atomic spins enclosed in the $2s$ -orbit can be presumed to be similarly oriented. In the above case the free energy of the donor may be represented in the form (see (2.5.2))

$$F_d = -T \ln \left\{ \left[Z_s \left(\frac{\mathcal{H}}{T} \right)^{\mathfrak{N}_2} + \exp \left(\frac{\Delta}{T} \right) Z_{\mathfrak{N}_2 S} \left(\frac{\mathcal{H}}{T} \right) \right] \right\}, \quad (6.5.28)$$

where $\Delta = AS - E_{12}$ is the energy of the $(1s)(2s) \rightarrow (1s)^2$ transition at $T = 0$.

It follows from (6.5.28) that at $\mathcal{H} = 0$ the contribution of a donor to the specific heat $C_d = -T \partial^2 F_d / \partial T^2$ passes through a $\sim \mathfrak{N}_2^2$ high maximum at the inversion temperature $T_i \simeq \Delta \mathfrak{N}_2 \ln(2S - 1)$. The relative width of the specific heat peak $\delta T / T_i \sim 1/\mathfrak{N}_2$. In respect of the specific heat the term inversion imitates a phase transition of the second kind with a critical exponent α equal to 2 (see Sec. 2.5), although in fact it constitutes a phase transition of the first kind in a system of finite dimensions.

Repeating the arguments contained in the preceding item, we find that the relative width of the peak of the specific heat of imperfections in a nondegenerate semiconductor may be as high as $0.05\mathfrak{N}_2$, i.e. that the peak may be quite noticeable. The term inversion also affects the conductivity: the conductivity activation energy diminishes with rising temperature after the passage of T_i .

The inversion of donor terms may exercise a considerable influence on the magnetic properties of the crystal, and vice versa, the external magnetic field may itself greatly affect the inversion. The former makes itself manifest, for example, in a drastic reduction in the contribution of the donors to the magnetic susceptibility of the crystal, because of the $(1s)(2s) \rightarrow (1s)^2$ transition. The latter for its part results in field-induced $(1s)^2 \rightarrow (1s)(2s)$ transitions at temperatures above T_i . It follows from (6.5.28) that a field $\mathcal{H}_i \sim \sim T_i / \mathfrak{N}_2 S$ is required for such a transition at temperatures exceeding T_i by the amount $\delta T \sim T_i / \mathfrak{N}_2$, i.e. immediately above the specific heat peak.

The susceptibility of the imperfections $\chi_d = -\partial^2 F_d / \partial \mathcal{H}^2$ at $\mathfrak{N}_2 S \mathcal{H}_i \ll T_i$ rises monotonously with the field, its value for \mathcal{H} exceeding \mathcal{H}_i being \mathfrak{N}_2 times higher than for \mathcal{H} below it. At $\mathfrak{N}_2 S \mathcal{H}_i \gg$

$\gg T_i$, the susceptibility as a function of the field behaves differently, passing through a maximum at $\mathcal{H} = \mathcal{H}_i$. The value of χ at point \mathcal{H}_i is approximately \mathfrak{N}_2 times higher than at $\mathcal{H} \ll \mathcal{H}_i$. Such a transition possibly explains the jump in the magnetization in CdCr_2Se_4 crystals containing selenium vacancies, which takes place in fields ~ 10 kOe [402].

To avoid misunderstanding, we would like to emphasize that the inversion of terms is a possible, but not an inevitable, phenomenon. Indeed, the considerations, which resulted in formula (4.5.3), point to the conclusion that even at $T \rightarrow \infty$ the magnitude of the c - l shift in the $(1s)(2s)$ state is approximately equal to

$$E_{cl}(\infty) = -\frac{AS}{2} \left(\frac{1}{\sqrt{\mathfrak{N}_1}} + \frac{1}{\sqrt{\mathfrak{N}_2}} \right), \quad (6.5.29)$$

where \mathfrak{N}_1 and \mathfrak{N}_2 are numbers of atoms in the region of localization of $1s$ - and $2s$ -electrons. This quantity may be quite high and actually may exceed E_{12} , i.e. the $(1s)(2s)$ state may retain its stability up to the highest temperatures. For instance, if we presume the $1s$ - and $2s$ -electrons in EuO to occupy $\mathfrak{N}_1 = 6$ Eu^{++} ions nearest to an oxygen vacancy and $\mathfrak{N}_2 = 8$ next-nearest Eu^{++} ions, $E_{cl}(\infty)$ in EuO , according to (6.5.29), must be as high as $0.4 AS$. The term inversion in the vicinity of the Curie point is even less probable: at $T_c = 0.01$ eV and for $AS = 0.5$ eV the average c - l exchange energy, according to (6.5.26), is equal to $0.9 AS$.

CHAPTER 7

COLLECTIVE FERRON STATES AND ELECTRICAL PROPERTIES OF DEGENERATE SEMICONDUCTORS

7.1. MAGNETOELECTRIC EFFECT IN DEGENERATE SEMICONDUCTORS

Electric Field Response Functions. Quite essential information about cooperative phenomena in degenerate magnetic semiconductors is provided by response functions to an external electric field. In contrast to nonmagnetic materials, where the response of the system is described only by means of the dielectric function $\epsilon(\mathbf{q}, \omega)$, magnetic systems should be described in addition by functions of magnetic response to the electric field, since the latter generally alters their magnetic ordering. For instance, it is a well-known fact that a uniform electric field induces the magnetization of AF insulators with special symmetry properties (Cr_2O_3 , etc.) [264, 395, 396]. In case of an MS to talk about the magnetoelectric effect caused by a uniform electric field is senseless, because the field is screened by the conduction electrons. However, a magnetoelectric effect in a nonuniform field is possible in them, no special crystal symmetry being required for it.

The reason for the existence of a magnetoelectric effect in this case is that the field produces a redistribution of charge carriers in the crystal, thereby changing the local intensity of the indirect exchange, and this must affect the state of the spin system. To describe it, we ought to specify all the spin correlation functions of all possible orders. Since all of them are altered by the electric field, in principle there should be an infinite set of magnetic response functions to this field.

On the other hand, the state of conduction electrons in the crystal not only affects the state of the spins, but in its turn is a function of the latter. Therefore, if we are confronted with a problem how to study the effect of an external electric field $\Phi(\mathbf{q}, \omega)$ on the electrons in an MS, we must take into account that it not only induces an internal electric field $\varphi(\mathbf{q}, \omega)$, but also alters the state of the magnetic system. The effective field acting on the electron is made up of two fields: the internal electric field $\varphi(\mathbf{q}, \omega) = \epsilon^{-1}(\mathbf{q}, \omega) \times \Phi(\mathbf{q}, \omega)$ induced in the crystal by an external field and of the field describing the changes in the exchange interaction between the electron and the magnetic atoms brought about by the electric field. In the simplest case when the energy of this interaction is equal to $(-A\mathbf{R}\sigma)$, and the variation of the magnetization component

induced by the external field is related to its magnitude by means of the linear expression

$$\mathfrak{M}(\mathbf{q}, \omega) = \lambda(\mathbf{q}, \omega) \Phi(\mathbf{q}, \omega), \quad (7.1.1)$$

the effective field $\tilde{\varphi}_\sigma(\mathbf{q}, \omega)$ acting on the electron with a spin projection σ is equal to

$$\tilde{e}\varphi_\sigma(\mathbf{q}, \omega) = e\varphi(\mathbf{q}, \omega) - A\mathfrak{M}(\mathbf{q}, \omega) \sigma \equiv \tilde{\varepsilon}^{-1}_\sigma(\mathbf{q}, \omega) \Phi(\mathbf{q}, \omega), \quad (7.1.2)$$

where we have introduced the notation for the spin-dependent dielectric constant

$$\tilde{\varepsilon}^{-1}_\sigma(\mathbf{q}, \omega) = \varepsilon^{-1}(\mathbf{q}, \omega) - A\sigma\lambda(\mathbf{q}, \omega)/e \quad (7.1.3)$$

The physical meaning of $\varepsilon(\mathbf{q}, \omega)$ and $\tilde{\varepsilon}_\sigma(\mathbf{q}, \omega)$ is quite different: the former characterizes the internal field in the medium that acts on a test spinless particle, whereas the latter characterizes the field that acts on the conduction electron. From this it follows specifically that the field acting on the ions of the magnetic semiconductor is not the same as that acting on the electrons.

Hence, to describe the state of the electron, we must in addition to the diagonal response function $\varepsilon(\mathbf{q}, \omega)$ also know the off-diagonal $\lambda(\mathbf{q}, \omega)$ as determined by relation (7.1.1)*. The off-diagonal response function was first introduced in [50] for FM metals. In the case of an FMS the effective field acting on the electron is described by a more complex expression, since even for $W \gg AS$ formula (4.2.1) has a limited sphere of applicability. However, for them, too, we may introduce the effective dielectric function $\tilde{\varepsilon}(\mathbf{q}, \omega)$ using a method described below [52, 310].

Formula (7.1.3) satisfactorily describes the physical situation in the PM region or in an AFS placed in a magnetic field, since in such cases the long-wave fluctuations of the magnetic moment for which according to Secs. 4.2 and 4.3 equation (7.1.2) is invalid—are inessential. In the absence of a magnetic field the effect of an electric field on the state of the electron in an AFS or a PMS makes itself manifest only via spin correlation functions of higher orders starting from the binary, but the electron energy is relatively little dependent on them (in higher orders in AS/W). The vicinity of the Curie point of an FMS, where such dependence is abnormally strong, forms an exception to this rule, but it will not be considered here.

At finite frequencies ω greatly exceeding the frequency of spin motion $\sim \gamma$ the state of the latter is unable to follow the field, and for this reason the field does not change the magnetization. Correspondingly, the off-diagonal response function $\lambda(\mathbf{q}, \omega)$ should

* It would be natural to term it magnetoelectric response function.

diminish rapidly as the frequency rises. Since the effect described above is especially prominent in the statical case, only the latter will be considered below.

Paramagnetic Region. To clarify the situation, we shall first present a simplified derivation of statical response functions in the long-wave limit $q \ll k_F$ for a wide-conduction-band semiconductor $W \gg AS$ at temperatures high above the magnetic ordering point [440]. The magnetic field will be assumed to be so strong that the electrons are completely spin-polarized, i.e. $AM > \mu_P$. At each point a c - l exchange field

$$V(\mathbf{r}) = -\frac{AM(\mathbf{r})}{2} \quad (7.1.4)$$

acts on the electron. The local magnetization $M(\mathbf{r})$ ($0 < M < S$) is connected with the external field and the electron density via the relationship that follows from formula (6.1.3')

$$M(\mathbf{r}) = \frac{S(S+1)}{3(T-\theta)} \left\{ \mathcal{H} + \frac{A}{2} v(\mathbf{r}) \right\}, \quad (7.1.5)$$

where θ is the PM Curie point of the undoped crystal. Expression (7.1.4) should be included into the effective field $e\varphi(\mathbf{r})$ that acts on the electron, i.e. the quantity

$$e\tilde{\varphi}(\mathbf{r}) = e\varphi(\mathbf{r}) - \frac{A}{2} [M(\mathbf{r}) - \bar{M}], \quad (7.1.6)$$

where \bar{M} is the mean magnetization, should be substituted for $e\varphi(\mathbf{r})$ in the condition for a constant electrochemical potential μ (1.7.5).

Then by linearizing the expression

$$\mu_P(\mathbf{r}) = \frac{[6\pi^2 n(\mathbf{r})]^{2/3}}{2m^*} = \mu_P - e\varphi(\mathbf{r}) - \frac{A}{2} [M(\mathbf{r}) - \bar{M}], \quad (7.1.7)$$

with account taken of equation (7.1.5) we obtain for the density and potential Fourier transforms the relation

$$n(\mathbf{q}) = -\frac{3en\varphi(\mathbf{q})}{2\mu_P(1-\Gamma_0)}, \quad \mu_P = \frac{(6\pi^2 n)^{2/3}}{2m^*} = 2^{2/3}\mu, \quad (7.1.8)$$

where we have introduced the notation

$$\Gamma_0 = \frac{A^2 S(S+1)v}{8\mu_P(T-\theta)} = \left(\frac{n}{4n_D} \right)^{\frac{1}{3}}, \quad n_D^{\frac{1}{3}} = \frac{2(3\pi^2)^{\frac{2}{3}} W(T-\theta)}{3A^2 S(S+1)a} \quad (7.1.9)$$

(we made use of the relationship between the bandwidth and the effective mass (1.1.5)). The meaning of $n_D(T)$ is that of an electron concentration at which the paramagnetic Curie point $\theta + \Delta\theta$ attains the value of T . $\Delta\theta$ is the shift of θ caused by doping the specimen, as determined by formula (6.1.3).

The dielectric function of the medium $\varepsilon(\mathbf{q})$ is expressed in terms of $n(\mathbf{q})$ and $\varphi(\mathbf{q})$ with the aid of the Poisson equation (1.7.8). Making use of equality (7.1.8), we obtain from it that the dielectric function is given by expression (1.7.9) in which the parameter κ^2 should be replaced by

$$\kappa_D^2 = \frac{\kappa_P^2}{1 - \Gamma_0}, \quad \kappa_P^2 = 2^{-\frac{2}{3}} \kappa^2, \quad (7.1.10)$$

where κ is the inverse Thomas-Fermi screening length (1.7.10) (the factor $2^{-\frac{2}{3}}$ appears in the result of electron spin polarization).

The proportionality factor $\lambda(\mathbf{q})$ between the magnetization $\mathfrak{M}(\mathbf{q})$ and the external field $\Phi(\mathbf{q})$ is found using relations (7.1.5, 8-10):

$$\lambda(\mathbf{q}) = - \frac{2e\Gamma_0}{A(1 - \Gamma_0)\varepsilon}. \quad (7.1.11)$$

We obtain from formulae (1.7.9), (7.1.3, 10, 11) for the effective dielectric function $\tilde{\varepsilon} \equiv \tilde{\varepsilon}_\uparrow$ corresponding to $\sigma = 1/2$

$$\tilde{\varepsilon}(\mathbf{q}) = \varepsilon_0 [(1 - \Gamma_0) + \kappa_P^2/q^2]. \quad (7.1.12)$$

As seen from expressions (7.1.10, 12), the quantities $\varepsilon(\mathbf{q})$ and $\tilde{\varepsilon}(\mathbf{q})$ differ from the corresponding quantity (1.7.9), which characterizes the field in a nonmagnetic crystal, in that it contains the feed-back function Γ_0 introduced in [51]. Its appearance is the result of the existence of a positive feed-back between the magnetic moment and electric field in the crystal. Indeed, for example, the field of an ionized donor increases the electron concentration in its vicinity, thereby intensifying FM coupling between the atoms and increasing the magnetization. In accordance with formula (7.1.4), it diminishes the electron energy in the vicinity of the donor, and because of that there is an additional incentive for the electrons to get nearer to the donor etc. As seen from formulae (7.1.10, 12), although the feed-back reduces the electrostatic field of the imperfection ($\varepsilon(\mathbf{q})$ grows with Γ_0 , which should be less than unity to ensure that $\varepsilon(\mathbf{q})$ is positive) it enhances the effective field produced by the imperfection and acting on the electrons ($\tilde{\varepsilon}(\mathbf{q})$ diminishes as Γ_0 increases).

The calculation of response functions for weak magnetic fields is carried out in exactly the same fashion. For $A\mathfrak{M} \ll \mu$ the calculation yields expression (1.7.9), where the quantity

$$\kappa_D^2 = \kappa^2 \left\{ 1 + \frac{A^2 \mathfrak{M}^2}{16\mu^2} \frac{\left[2 \left(\frac{n}{n_D} \right)^{\frac{1}{3}} - 1 \right]}{\left[1 - \left(\frac{n}{n_D} \right)^{\frac{1}{3}} \right]} \right\} \quad (7.1.13)$$

takes the place of κ^2 . The magnetization $\mathfrak{M} = \chi \mathcal{H}$ in (7.1.13) is expressed in terms of the magnetic susceptibility χ (2.5.6) in which the PM Curie point θ is displaced owing to the indirect exchange via conduction electrons by the amount $\Delta\theta$ (6.1.3) with respect to (2.5.6, 3).

The off-diagonal response function $\lambda(\mathbf{q})$ is given by the expression

$$\lambda(\mathbf{q}) = -\frac{e^2 \mathfrak{M}}{z(\mathbf{q}) \mu} \left[\left(\frac{n_D}{n} \right)^{\frac{1}{3}} - 1 \right]^{-1}. \quad (7.1.14)$$

The condition for the applicability of formulae (7.1.13, 14) is the inequality $n < n_D$ satisfied at high enough temperatures.

In very strong magnetic fields the linear relationship between the field and the magnetization of the type (7.1.5) ceases to be valid. Instead we may use the equations of the self-consistent field theory (Sec. 2.5)

$$\mathfrak{M}(\mathbf{r}) = B_S \left\{ \frac{1}{T} \left[\mathcal{H} + z \int \mathfrak{M}(\mathbf{r}) - \frac{A}{2} v(\mathbf{r}) \right] \right\}, \quad (7.1.15)$$

where the Brillouin function B_S is determined by formula (2.5.2) (the complete spin polarization of the electrons is taken into account). By simply reformulating the derivation presented above, we arrive at the following expression for the feed-back function

$$\Gamma_0 = \frac{3A^2 B'_S v}{8\mu (T - z \int B'_S)}, \quad (7.1.16)$$

whose particular case is formula (7.1.9) (B'_S is the derivative of the Brillouin function with respect to its argument for $\mathfrak{M}(\mathbf{r}) = \mathfrak{M}$ and $v(\mathbf{r}) = v$).

Singlet Magnets. Similar calculations can be performed for unsaturated FM with ions in the singlet ground state, provided their conduction electrons are completely spin-polarized. Neglecting the direct exchange between the magnetic atoms as described by the Hamiltonian (2.2.6), we may represent the c - l model Hamiltonian in the case being considered as follows

$$H = \omega \sum b_g^* b_g - A \sum [(\langle 0 | \mathbf{J}_g | 1 \rangle \cdot \mathbf{s}_{g0}) b_g^* a_{g0}^* a_{g0} + \text{c.c.}] + B \sum a_{g0}^* a_{g+\Delta 0}. \quad (7.1.17)$$

For the sake of simplicity we presume the ionic level $|1\rangle$, nearest to the ground level $|0\rangle$, to be also a singlet one. Then the magnetization at $T = 0$ in the self-consistent field approximation will be determined from the equation

$$H_{MF} = \omega b^* b - \frac{Acv}{2} (b^* + b), \quad c = \langle 0 | \mathbf{J}^z | 1 \rangle. \quad (7.1.18)$$

This yields

$$\mathfrak{M} = c(b + b^*) = \frac{\gamma v c}{1 - \frac{\gamma^2 v^2}{\omega^2 + 4}}, \quad \gamma = \frac{Ac}{2}. \quad (7.1.19)$$

Making use of formulae (7.1.4, 19) and employing a method similar to one employed above in this section, we obtain the following expression for the feed-back function Γ_0 [420]

$$\Gamma_0 = \frac{3}{8\mu v} \frac{(\gamma v \omega)^2}{[\gamma^2 v^2 + \omega^2/4]^{3/2}}. \quad (7.1.20)$$

For $c < J$ at sufficiently high carrier concentrations it may become necessary to take into account higher multiplet components. This enables the above calculations to be extended to cover the case of magnetization approaching the maximum.

7.2. ELECTRIC FIELD RESPONSE FUNCTIONS OF AN ANTIFERROMAGNET AT $T = 0$

The qualitative dependence of the electric field response functions of an AFS on the magnetic field at the absolute zero is generally similar to that in the paramagnetic region [199, 331]. Below we shall obtain response functions for the case of classically large spins without making any assumptions as to the smallness of q in comparison with k_F . Taking into account the inhomogeneity introduced by the electric field, we obtain for the spin projections the expressions

$$\begin{aligned} S_g &= (S e^{i\Pi \cdot g} \sin \theta_g, 0, S \cos \theta_g), \\ \Pi &= \left(\frac{\pi}{a}, \frac{\pi}{a}, \frac{\pi}{a} \right), \end{aligned} \quad (7.2.1)$$

where the angles $\theta_g = \theta + \delta_g$ are approximately equal to the angle θ determined from the condition that the energy be minimum in the absence of a field.

As usual, we start from the c - l model Hamiltonian (3.1.1), to which we must add terms describing the interaction of the electrons with the external electric field $\Phi(\mathbf{q})$ and the electron-electron interaction. Taking into account that the order of magnitude of the angles δ_g is that of Φ we may conveniently represent the Hamiltonian in the form of an expansion in the powers of Φ

$$H = H_0 + H_1 + H_2 + O(\Phi^3). \quad (7.2.2)$$

The expression for the term H_0 is (6.2.6) to which we must add the energy of the interaction of the spins with one another and with the magnetic field pointing along the Z -axis (the last two terms in expression (6.2.8)). The angle θ is obtained from the condition for the minimum energy (6.2.10). The Hamiltonian H_1 is given by

the expression (it does not contain terms with $q = 0$):

$$H_1 = \frac{e}{\varepsilon_0} \sum \varphi_q \rho_{-q\sigma} + \frac{2\pi e^2}{\varepsilon_0} \sum \frac{\rho_q \rho_{-q}}{q^2} + AS \sin \theta \sum \sigma \delta_q \rho_{-q\sigma} - \frac{AS}{2} \cos \theta \sum \delta_q (a_{k\uparrow}^* a_{k+\pi-q\downarrow} + a_{k\downarrow}^* a_{k+\pi-q\uparrow}), \quad (7.2.3)$$

where δ_q are Fourier transforms of the angles δ_g :

$$\delta_g = \sum_q e^{iq \cdot g} \delta_q, \quad \rho_{q\sigma} = \sum_p a_{p\sigma}^* a_{p-q, \sigma}, \quad \rho_q = \sum_{\sigma} \rho_{q\sigma}. \quad (7.2.4)$$

The Hamiltonian H_2 is a collection of terms proportional to δ^2 :

$$H_2 = \frac{\mathcal{H} SN \cos 2\theta}{2} \sum_q (1 + \gamma_q) |\delta_q|^2 + \frac{SN \cos \theta}{2} \left[\mathcal{H} + \frac{A(v_{\uparrow} - v_{\downarrow})}{2} \right] \sum_q |\delta_q|^2. \quad (7.2.5)$$

The parameters δ_q contained in the Hamiltonian should be chosen so as to obtain the minimum energy of the system E_{Φ} in the magnetic field, i.e. from the condition

$$\frac{\partial E_{\Phi}}{\partial \delta_q} = 0. \quad (7.2.6)$$

Instead of calculating the energy as a function of δ_q it is much more convenient to make use of the familiar formula

$$\frac{\partial E_{\Phi}}{\partial \delta_q} = \left\langle \frac{\partial H}{\partial \delta_q} \right\rangle_{\Phi}, \quad (7.2.7)$$

where the angular brackets $\langle \dots \rangle_{\Phi}$ denote quantum mechanical averaging over the corresponding state of the system in the field. For $qa \ll 1$, making use of the condition of equilibrium (6.2.10), we obtain from formulae (7.2.3-7) the following expression for δ_q :

$$\delta_q = - \frac{A}{2 | \mathcal{H} | N \sin \theta} \sum_{\sigma} \sigma \langle \rho_{q\sigma} \rangle_{\Phi}. \quad (7.2.8)$$

When calculating δ_q the last term in (7.2.3) is not taken into account since it connects the electron states with a difference in the energy equal to W , and for this reason its contribution is of the next order in AS/W .

The relationship between the density fluctuations $\langle \rho_{q\sigma} \rangle_{\Phi}$ and the potential can be established by calculating the correlation functions $\langle a_{p\sigma}^* a_{p-q, \sigma} \rangle_{\Phi}$. This can be done by applying the method of equations of motion. The state being steady, the correlation

functions are independent of time. Making use of the equation

$$i \frac{d}{dt} \langle a_{p\sigma}^* a_{p-q, \sigma} \rangle \Phi = \langle [H_1 a_{p\sigma}^* a_{p-q, \sigma}] \rangle \Phi, \quad (7.2.9)$$

we obtain with the aid of formulae (7.2.2, 3):

$$\begin{aligned} (E_{p-q, \sigma} - E_{p\sigma}) \langle a_{p\sigma}^* a_{p-q, \sigma} \rangle \Phi \\ + [e\Phi(\mathbf{q}) + AS \sin \theta \delta_q] \langle a_{p\sigma}^* a_{p\sigma} - a_{p-q, \sigma}^* a_{p-q, \sigma} \rangle \Phi \\ + \frac{4\pi e^2}{\epsilon_0 q^2} \langle \rho_q (a_{p\sigma}^* a_{p\sigma} - a_{p-q, \sigma}^* a_{p-q, \sigma}) \rangle \Phi = 0. \end{aligned} \quad (7.2.9')$$

When writing the equations of motion, we have for reasons stated above discarded the contribution of the last term in H_1 (7.2.3). Next, in the random phase approximation we can decouple higher correlation functions, retaining only the terms with singularities at small momentum transfer [311]:

$$\langle \rho_q a_{p\sigma}^* a_{p\sigma} \rangle \Phi \simeq n_{p\sigma} n(\mathbf{q}), \quad n(\mathbf{q}) = \langle \rho_q \rangle \Phi, \quad (7.2.10)$$

where the quantity $n_{p\sigma}$ denotes in the linear approximation in Φ the mean occupation number of the electron states in the absence of an external field. In the same way in a linear approximation in Φ we can carry out the averaging over the zero-field state in the term before the last in (7.2.9'). Let us also take into account that, by definition, the internal electric field $\varphi(\mathbf{q})$ in the medium is connected with the external field $\Phi(\mathbf{q})$ by means of the relationship

$$\varphi(\mathbf{q}) \equiv \frac{\Phi(\mathbf{q})}{\kappa(\mathbf{q})} = \Phi(\mathbf{q}) + \frac{4\pi en(\mathbf{q})}{\epsilon_0 q^2}. \quad (7.2.11)$$

From expressions (7.2.9-11) we obtain by summing the correlation functions over the momentum \mathbf{p}

$$\langle \rho_q a_{p\sigma}^* a_{p\sigma} \rangle \Phi = -\Pi_{q\sigma}^0 \left[\frac{e\varphi(\mathbf{q})}{\epsilon(\mathbf{q})} + AS \sin \theta \delta_q \right], \quad (7.2.12)$$

$$\Pi_{q, \sigma}^0 = - \sum_{\mathbf{p}} \frac{n_{p\sigma} - n_{p-q, \sigma}}{E_{p\sigma} - E_{p-q, \sigma}}. \quad (7.2.13)$$

The angle δ_q itself is expressed in terms of the electron density $\langle \rho_q \rangle \Phi$ by equation (7.2.8).

Finding the mean density $n(\mathbf{q}) = \sum_{\sigma} \langle \rho_q a_{p\sigma}^* a_{p\sigma} \rangle \Phi$ from (7.2.12) and making use of the Poisson equation (1.7.8), we obtain the expression for the dielectric function

$$\begin{aligned} \epsilon(\mathbf{q}) = \epsilon_0 + \frac{4\pi e^2}{q^2} \Pi_q^0 \left[1 + \frac{A^2 S (\Delta H_q)^2}{8 |Z| N \Pi_{q, \sigma}^0 Z_q} \right], \\ Z_q = 1 - \frac{A^2 S \Pi_q^0}{8 |Z| N}, \end{aligned} \quad (7.2.14)$$

where we make use of the notation

$$\Pi_q^0 = \Pi_{q\uparrow}^0 + \Pi_{q\downarrow}^0, \quad \Delta\Pi_q^0 = \Pi_{q\uparrow}^0 - \Pi_{q\downarrow}^0.$$

The off-diagonal response function $\lambda(q)$ is found from the condition that the moment induced by the electric field be equal to

$$\mathfrak{M}_g = S [\cos \theta_g - \cos \theta] = -S \sin \theta \delta_g. \quad (7.2.15)$$

Hence, taking into account equality (7.2.8), the Poisson equation (1.7.8) and the expression for $\varepsilon(q)$ (7.2.14), we obtain:

$$\lambda(q) = -\frac{eAS\Delta\Pi_q^0}{4N|\mathcal{H}|\varepsilon(q)Z_q}. \quad (7.2.16)$$

In the long-wave limit $q \ll k_F$ expressions (7.2.14, 16) yield results different from (7.1.9-14) in that the concentration n_A (6.2.3) at which the ferromagnetic ordering becomes unstable takes the place of n_D . The magnetization in the corresponding formulae must be expressed in terms of the initial magnetic susceptibility of the antiferromagnet χ ($\mathcal{H} = 0$) (6.2.13). It should be pointed out that for $n = n_A$ the expressions for the functions $\varepsilon(q)$ and $\lambda(q)$ of the type (7.1.13, 14) are inapplicable in finite fields \mathcal{H} because χ diverges.

In the case of a narrow-band crystal one manages to obtain only the long-wave asymptotic behaviour of the response functions. To this end it suffices to notice that the spinpolaron energy depends on the magnetization \mathfrak{M} chiefly via the position of the bottom of the spinpolaron band as determined by the quantity $-zB_-(\mathfrak{M})$, where $B_{\pm}(\mathfrak{M})$ is the effective Bloch integral (6.2.23). Then the result (1.7.9, 10) with an effective mass appropriately defined (i.e. multiplied $\sqrt{2S+1}$ times) will remain valid for $\mathfrak{M} = 0$ in this case as well. In case of \mathfrak{M} high enough, presuming only one spinpolaron band to be occupied, we can easily generalize the calculations of Sec. 1.7 by introducing into (1.7.6) instead of φ the potential

$$\tilde{\varphi}(\mathbf{r}) = e\varphi(\mathbf{r}) - z[B_+(\mathfrak{M}(\mathbf{r})) - B_+(\mathfrak{M})], \quad (7.2.17)$$

where \mathfrak{M} is the mean magnetization. Then we obtain for the dielectric function the equations (1.7.9), (7.1.10), where Γ_0 is given by formula

$$\Gamma_0 = \frac{3}{2} \frac{n}{\mu_P(n)} z \frac{d}{d\mathfrak{M}} B_+(\mathfrak{M}) \frac{d\mathfrak{M}}{dn}, \quad (7.2.18)$$

$$\mu_P(n) = (6\pi^2)^{2/3} B_+(\mathfrak{M}) v^{2/3},$$

and \mathfrak{M} is connected with n by relation (6.2.26). According to (6.2.26, 27), the magnitude of the magnetization \mathfrak{M}_c for which all the carriers assemble in one band is small: $\mathfrak{M}_c \simeq 2Sv^{2/3}$.

7.3. ELECTRIC FIELD RESPONSE FUNCTION OF FERROMAGNETS IN THE SPIN-WAVE REGION

To obtain response functions to an external electric field of an arbitrary degree of inhomogeneity for an FMS in the spin-wave region we have to use a much more sophisticated mathematical apparatus than one used in the preceding sections [51, 52, 310] (see also [416]).

We shall carry out the calculations for the case of wide bands $W \gg .1S$ in the assumption of a complete spin polarization of the electrons ($\mu_P < .1S$). We shall start with the Hamiltonian (4.2.4) to which a term describing electron-electron interaction

$$H = \sum E_{\mathbf{k}} a_{\mathbf{k}}^* a_{\mathbf{k}} + \sum C_{\mathbf{k}\Gamma} a_{\mathbf{k}}^* a_{\mathbf{k}-\Gamma} b_{\mathbf{q}}^* b_{\mathbf{q}+\Gamma} + \sum \omega_{\mathbf{q}}^0 b_{\mathbf{q}}^* b_{\mathbf{q}} + \frac{2\pi e^2}{\epsilon_0} \sum q^{-2} \rho_{\mathbf{q}} \rho_{-\mathbf{q}} \quad (7.3.1)$$

has been added (the spin index has been omitted). In the Hamiltonian (7.3.1) we have discarded small terms $\sim e^2$ obtained in the result of the canonical transformation (1.4.2-4), (4.2.3) (this transformation of the Hamiltonian (3.1.1) serves to introduce dressed magnons).

The calculations are based on the familiar expression for the dielectric function in terms of the Fourier transform of a double-time Green's function [312]:

$$\frac{1}{\epsilon(\mathbf{q}, \omega)} = \epsilon_0 + \frac{4\pi e^2}{q^2} \langle\langle \rho_{\mathbf{q}} | \rho_{-\mathbf{q}} \rangle\rangle. \quad (7.3.2)$$

We may conveniently use the method of temperature Green's functions [295]. Introduce a temperature analogue of Green's function, which enters expression (7.3.2)

$$K(\mathbf{q}, i\omega_n) = - \int_0^\beta \exp(i\omega_n \tau) \langle \hat{T} \tilde{\rho}_{\mathbf{q}}(\tau) \tilde{\rho}_{-\mathbf{q}}(0) \rangle, \quad (7.3.3)$$

where $\beta = 1/T$, $\omega_n = 2\pi nT$ ($n = 0, 1, \dots$), \hat{T} is the imaginary-time-ordering operator, $\tilde{\rho}_{\mathbf{q}}(\tau)$ is the operator of electron density fluctuations in the Heisenberg representation for the imaginary time.

When drawing diagrams, we shall make use of the modified chain approximation of all the diagrams containing electron-electron vertices: we shall select only those that have a singularity at small momentum transfers (this is known to correspond to the

random phase approximation [295]). Hence, Green's function sought is represented by a sum of chain-like diagrams

$$\begin{aligned} K(\mathbf{q}, i\omega_n) = & \text{shaded loop} + \text{shaded loop} \text{---} \text{undulation} \text{---} \text{shaded loop} \\ & + \text{shaded loop} \text{---} \text{undulation} \text{---} \text{shaded loop} \text{---} \text{undulation} \text{---} \text{shaded loop} + \dots \end{aligned} \quad (7.3.4)$$

where the shaded loop $\Pi(\mathbf{q}, i\omega_n)$ is a block not containing Coulomb vertices $4\pi e^2/\epsilon_0 q^2$ denoted by an undulation. Summing the geometric progression (7.3.4), we obtain the expression for Green's function sought

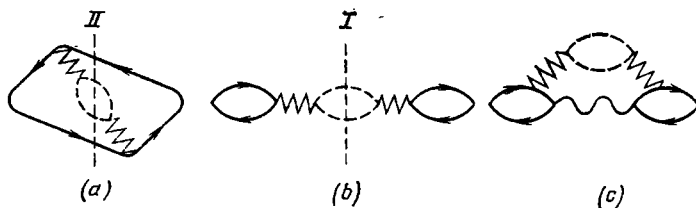
$$K(\mathbf{q}, i\omega_n) = \Pi(\mathbf{q}, i\omega_n) \left[1 + \frac{4\pi e^2}{\epsilon_0 q^2} \Pi(\mathbf{q}, i\omega_n) \right]^{-1}. \quad (7.3.5)$$

Therefore, according to formulae (7.3.3, 5), if we take into account the definition of the retarded Green's function (3.2.4), we shall obtain for the dielectric function $\epsilon(\mathbf{q}, \omega)$ the expression

$$\epsilon(\mathbf{q}, \omega) = \epsilon_0 + \frac{4\pi e^2}{\epsilon_0 q^2} \Pi(\mathbf{q}, \omega), \quad (7.3.6)$$

where $\Pi(\mathbf{q}, \omega)$ is the analytic continuation of $\Pi(\mathbf{q}, i\omega_n)$ from the upper half-plane to the real semiaxis $\omega \geq 0$.

Some of the diagrams for the polarization operator $\Pi(\mathbf{q}, i\omega_n)$ are depicted below:



Solid and dashed lines depict Green's functions for a free electron $G_p(i\epsilon_n) = (i\epsilon_n - E_p + \mu)^{-1}$ and a free magnon $D(i\omega_m) = (i\omega_m - \omega_q)^{-1}$ respectively. The saw-toothed line depicts electron-magnon interaction. According to (7.3.1), two electron and two magnon lines meet at every electron-magnon vertex, and the multiplier corresponding to such a vertex is C_{qgr} . Other rules for constructing the diagrams are the same as in [295] ($\epsilon_n = \pi(2n+1)T$ etc.).

The diagonal part of the electron-magnon interaction Hamiltonian in (7.3.1) is taken into account, as usual, by shifting of the bare-electron energy and the bare-magnon frequency in expressions G_p and D_q in accordance with formulae (4.2.5) and (6.1.2). An essential point is that the renormalized magnon frequency ω_q^0 remains small as compared with the c - l exchange integral A ($\omega_q^0 - \omega_q \leq 4v^2$, where v is the number of conduction electrons per atom), and that accordingly $AS \gg T_c$.

When calculating the polarization operator, we should select the leading diagrams whose contributions are of the order of AS/T_c and higher. Such are the diagrams in which it is possible to separate portions containing only magnon loops. Such diagrams have at least one cross-section between two electron-magnon vertices across which the energy is transported solely by magnons, e.g. diagram *b*, so that the corresponding energy denominator is of the form $i\omega_n + \omega_p - \omega_{n-q}$, i.e. is $\sim T_c S$ for $\omega_n = 0$. The addition of a magnon loop to the original fermion loop results in the appearance on the diagram of yet another fermion loop identical with the original (diagram *b*), which for small q 's is of the order of v/μ . On the whole, for small momenta q the first-order correction in the electron-magnon interaction, if one takes into account that C_{kqr} is proportional to A , turns out at $T_c S < T < T_c$ to be of the order of $(\frac{AS}{T_c})^2 \frac{Tv}{\mu}$ times the zero-order polarization operator (the bare-fermion loop), i.e. can even exceed the latter*.

At the same time the inclusion of the electron-magnon interaction into the polarization loop (diagram *a*) does not result in the appearance of cross-sections the energy transport through which is carried out solely by the magnons. Since the electron energy is high as compared with the magnon, joint transport of energy by the electrons and the magnons produces an energy denominator $\sim W \gg T_c$, e.g. in cross-section *II* between two electron-magnon vertices, i.e. the contribution of diagram *a* is small as compared with that of diagram *b*. A similar reason enables diagram *c*, in which the electron-magnon interaction connects two polarization loops, to be also discarded.

By virtue of the foregoing, in the static case $i\omega_n = 0$ each simple polarization loop should be modified by summing up an infinite sequence of diagrams. Each of them is obtained from the previous by adding one magnon and one fermion loop connected with one another by an electron-magnon interaction line. The result of this summation can be represented with the aid of the renormalized

* For finite frequencies $\omega \gg T_c$ such diagrams are $(T_c/\omega)^2$ times smaller than for $\omega = 0$, and because of that they can be neglected.

for $\lambda(\mathbf{q}) = \lambda(\mathbf{q}, 0)$ the following result:

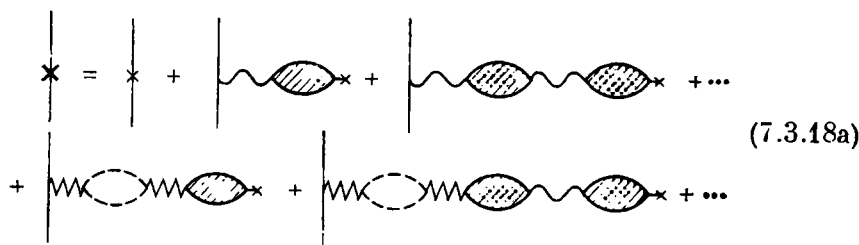
$$\lambda(\mathbf{q}) = -\frac{4\Gamma(\mathbf{q})}{A} \left[1 - \Gamma(\mathbf{q}) - \frac{4\pi e^2}{\varepsilon_0 q^2} \Pi^0(\mathbf{q}) \right]^{-1} \quad (7.3.17)$$

(the general expression for $\lambda(\mathbf{q})$ is presented in [51]).

To find the effective dielectric function $\tilde{\varepsilon}(\mathbf{q})$ that describes the effect of the external electric field on the electron not only via the electric field set up by it in the medium, but via the changes in the magnetization induced by it, it suffices to analyze the interaction between the electron and a charged impurity atom. To this end consider diagrams for the off-diagonal single-electron Green's function [310]

$$\mathcal{G}'_{\mathbf{k}\mathbf{k}'}(i\varepsilon_n) = - \int_0^{\beta} \exp(i\varepsilon_n \tau) \langle \hat{T} \tilde{a}_{\mathbf{k}'}(\tau) a_{\mathbf{k}}^*(0) \rangle \quad (7.3.18)$$

taking account of the interaction between the electron and the impurity atom. In compliance with the condition of heavy doping $\mu \gg e^2 n^{1/3} / \varepsilon$, we need only consider diagrams with one impurity vertex. Since the scattering probability is proportional to $|\langle a_{\mathbf{k}'}(t) a_{\mathbf{k}}^* \rangle|^2$, such an approach is equivalent to the Born approximation. Two classes of such diagrams are depicted below (the interaction with the charge of the impurity atom is shown in the first line and with its magnetic moment in the second):



$$(7.3.18a)$$

A fine cross denotes the unrenormalized potential of the impurity atom $\Phi(\mathbf{q}) = \frac{4\pi e}{\varepsilon_0 q^2}$, and the solid one the renormalized potential $\tilde{\varphi}(\mathbf{q})$. By summing diagrams (7.3.18a), we obtain the following expression for the effective potential of the interaction between the electron and the impurity atom:

$$\tilde{\varphi}(\mathbf{q}) = \frac{4\pi e}{q^2 \tilde{\varepsilon}(\mathbf{q})}, \quad \tilde{\varepsilon}(\mathbf{q}) = \varepsilon(\mathbf{q}) [1 - \Gamma(\mathbf{q})]. \quad (7.3.19)$$

Expression (7.3.19) in the long-wave limit will obviously correspond to (7.1.12).

Similar results have been obtained for the case of narrow bands [182]. In the long-wave limit they are represented by expressions (1.7.9), (7.1.10) with the feed-back function $\Gamma_0(T)$ equal to

$$\Gamma_0 = \frac{3}{2} \frac{n}{\mu_P} z \frac{d}{dn} |\tilde{B}|. \quad (7.3.20)$$

Expression (7.3.20) is obtained in the same way as (7.2.18), only instead of $B(\mathfrak{M})$ in formula (7.2.17) one should use the effective Bloch integral \tilde{B} (4.1.3). Making use of the dispersion law for magnons (6.1.1), we obtain at $T \gg \omega$ from (7.3.20):

$$\Gamma_0 = \frac{3T}{2v\mu_P} \left(\frac{\mathcal{Y}_{\text{eff}}}{\mathcal{Y} + \mathcal{Y}_{\text{eff}}} \right)^2. \quad (7.3.21)$$

The result (7.3.21) in the $\mathcal{Y} \ll \mathcal{Y}_{\text{eff}}$ limit coincides with the result (7.3.15) obtained for wide-band FMS.

7.4. SCREENED POTENTIAL AND INSTABILITY OF UNIFORM STATE OF MAGNETIC SEMICONDUCTORS

Screening in Ferromagnetic Semiconductors. The physical meaning of the results obtained in Secs. 7.1-7.3 becomes more clear if they are used to calculate the screening potential of a point charge at sufficiently great ranges $r > k_F^{-1}$ [51, 52]. First of all we shall consider the case of an FMS in the spin-wave region. Making use of formulae (1.7.10, 11) and of expressions (7.3.9) and (7.3.11) for the long-wave asymptotic behaviour of $\Pi(\mathbf{q})$ and $\Gamma(\mathbf{q})$, we obtain that at temperatures low enough, when Γ_0 is much smaller than 1, the interaction with the magnons reduces the screening length in comparison with its value κ_P^{-1} at $T = 0$ according to the law

$$r_s(T) = \kappa_P^{-1} \sqrt{1 - \Gamma_0(T)}. \quad (7.4.1)$$

As the temperature rises, and $\Gamma_0 \rightarrow 1$, the term of the next order in q^2 should be taken into account in expressions for the dielectric function (7.3.6, 9). Calculations show the changing nature of the screened potential for $|1 - \Gamma_0| \ll 1$: the pole of $\varepsilon^{-1}(q)$ moves away from the imaginary axis, and the screened potential (1.7.11) turns into an oscillating function

$$\varphi(r) = \frac{e}{\varepsilon_0 r} \exp\{-\alpha_+ r\} \left[\cos \alpha_- r + \frac{\xi(1 - \Gamma_0) \sin \alpha_- r}{\sqrt{2\alpha_+ \alpha_-}} \right], \quad (7.4.2)$$

$$\alpha_{\pm} = \frac{1}{2} \sqrt{2\kappa_P \xi \pm (1 - \Gamma_0) \xi^2}. \quad (7.4.3)$$

The condition of heavy doping $\kappa_P \ll k_F < \xi$ is taken into account when writing (7.4.2).

The potential begins to oscillate starting from the temperature T_- determined by the equality

$$T_{\mp} = \left[1 \mp \frac{2\kappa_P}{\xi} \right] Q^{-1}. \quad (7.4.4)$$

As the temperature continues to rise, the screening length having passed a minimum at T_- in accordance with (7.4.2, 3), again grows and tends to infinity at T_+ also determined by equality (7.4.4) (the pole of $\varepsilon^{-1}(q)$ goes over to the real axis). The amplitude of the oscillations of the potential also becomes infinite at point T_+ .

From the point of view of physics, the temperature anomalies in the behaviour of the screened potential are associated with the positive feed-back between the local magnetization and the local electron density. Indeed, the electron energy is at its minimum at such points of the crystal where the degree of FM order is greatest. For this reason the conduction electrons tend to assemble at such points. On the other hand, as the electrons carry out the indirect exchange between the magnetic atoms, which tends to establish an FM order, its degree rises as n grows. This facilitates a further increase in the electron concentration at this point. Hence, we may speak of a specific attraction between the electrons via magnons, resulting from the joint suppression of the magnons by the electrons [52]. Such an attraction via real magnons differs basically from the one via virtual phonons that results in superconductivity.

In the vicinity of a donor the electron concentration is higher than away from it. Accordingly, the degree of FM order is higher there, too, i.e. an additional force appears attracting electrons to the donor. At first it results in a decrease in the screening length with rising temperature. However, at $T > T_-$ this attraction becomes so strong that at short ranges from the impurity even an overcompensation of the screened charge by the electrons takes place. The extra charge of the latter must also be screened, and it, too, turns out to be overcompensated. This causes the potential to oscillate. At $T > T_+$ the attraction via the magnons becomes so strong that a uniform state of the system becomes unstable against infinitesimal fluctuations. (It is presumed that $T_+ < T_c$.)

Similar behaviour is exhibited by the effective field $\tilde{\varphi}(r)$ as well. It follows from formulae (7.3.19) and (1.7.9, 10) that taking into account the feed-back function at $T < T_-$ is equivalent to the renormalization of the statical dielectric constant (the substitution of $\tilde{\varepsilon}_0 = \varepsilon_0(1 - \Gamma_0)$ for ε_0). Hence, the formula for the potential $\tilde{\varphi}$ will be simply (1.7.11) with a renormalized dielectric constant. The fact that it is smaller than ε_0 means that on account of the magnetic moment induced by the charge the interaction of the electron with this charge became stronger.

In the range $[T_-, T_+]$ the effective potential behaves in a way similar to the electrostatic $q(r)$ (7.4.2): it decays exponentially with the distance, oscillating in the process, and diverges at T_+ .

It is worth noting that, whereas at $T = 0$ the condition of applicability of the approximation employed above coincides with equality (1.7.3), at higher temperatures it should be replaced by

$$e^2 n^{1/3} / \tilde{\epsilon}_0 \ll \mu, \quad (7.4.5)$$

whose left-hand side grows with rising temperature. At T_- relation (7.4.5), according to (7.4.4, 7.3.11), takes the form (it is presumed that $q_0 \geq k_F$):

$$\sqrt{\frac{e^2 n^{1/3}}{\epsilon_0}} \ll \sqrt{\mu}, \quad (7.4.6)$$

i.e. in principle it can still be satisfied. However, as T_- is approached, the charge carrier scattering by fluctuations of the impurity potential becomes so intense that electron damping exceeds their kinetic energy. Because of that it is not possible within the framework of the approximation used to consider the point of absolute instability T_- itself and its vicinity for a heavily-doped semiconductor correctly.

The Problem of Stability of a Uniform State of a Ferromagnet. Useful information can be gained, if one analyzes the nature of the transition in a model system in which the donor charge is assumed to be distributed uniformly over the crystal. Such an analysis can be carried out with the aid of the results obtained above [52]. Namely, we shall have to consider the stability of a uniform state of the system against infinitesimal fluctuations. Since there are no spatial magnetization fluctuations in the case of a uniform state, inequality (1.7.3) continues to act as the condition of applicability of the results obtained above. The stability of the system is analyzed by studying the free energy of the system:

$$\begin{aligned} F &= F_k + F_m + F_Q + F_t + F_\Phi - \frac{AS}{2} n, \\ F_k &= \frac{3(6\pi^2)^{2/3}}{10m^*} \int n^{5/3}(\mathbf{r}) d\mathbf{r}, \\ F_Q &= \frac{e^2}{2\epsilon_0} \int \frac{[n(\mathbf{r}) - n][n(\mathbf{r}') - n]}{|\mathbf{r} - \mathbf{r}'|} d\mathbf{r} d\mathbf{r}', \\ F_\Phi &= \frac{e}{\epsilon_0} \int n(\mathbf{r}) \Phi(\mathbf{r}) d\mathbf{r}, \\ F_m &= T \sum_q \int d\mathbf{r} \ln \left\{ 1 - \exp \left(- \frac{\omega_q(n)}{T} \right) \right\}. \end{aligned} \quad (7.4.7)$$

The meaning of the terms in expression (7.4.7) is as follows: F_k is the kinetic energy, F_Q is the energy of Coulomb interaction,

F_Φ is the energy of interaction of the electrons with the external field. We neglect the contribution of thermal excitations to the electron free energy, since it is of the order of $(T/\mu)^2 \ll 1$. The magnon free energy F_m takes account of the indirect exchange via the conduction electrons, i.e. we use expression (6.1.2) for the magnon frequencies. Thereby, in accordance with formula (6.5.22) we also account for the temperature renormalization of the electron spectrum.

The term F_i whose structure is as yet to be defined, describes the correction to the free energy resulting from a small inhomogeneity of the electron gas. In order to solve the problem we have set ourselves, we expand the free energy in a series in electron density fluctuations $\delta n(\mathbf{r})$ up to terms of the fourth order inclusive. Since the fluctuations are presumed to vary slowly in space, the density of the inhomogeneity term F_i can be assumed to be proportional to $(\nabla n)^2$. Hence, F_i contributes only to terms of the second order in the fluctuations, and the latter can be expressed in terms of the dielectric function of the system. To this end note that formula (7.4.7) leads to the equality

$$\mu = \frac{\delta F}{\delta n(\mathbf{r})} = \int K(\mathbf{r} - \mathbf{r}') \delta n(\mathbf{r}') d\mathbf{r}' - e\varphi(\mathbf{r}) + O(\delta n^3), \quad (7.4.8)$$

where

$$K(\mathbf{r} - \mathbf{r}') = \frac{\delta^2}{\delta n(\mathbf{r}) \delta n(\mathbf{r}')} (F_k + F_m + F_i) |_{\delta n=0},$$

$\varphi(\mathbf{r})$ is the field in the medium as determined by formula (7.2.11). The free energy of the system in the absence of an external field is expressed in terms of the same quantity $K(\mathbf{r} - \mathbf{r}')$ in the second order in fluctuations:

$$F = \text{const} + \frac{1}{2} \int \left[K(\mathbf{r} - \mathbf{r}') + \frac{e^2}{\varepsilon_0 |\mathbf{r} - \mathbf{r}'|} \right] \delta n(\mathbf{r}) \delta n(\mathbf{r}') d\mathbf{r} d\mathbf{r}'. \quad (7.4.9)$$

Using the Fourier transformation of the fluctuations and taking into account the definition of the dielectric function $\varepsilon(\mathbf{q}) = \Phi(\mathbf{q})/\varphi(\mathbf{q})$, we obtain from formulae (7.4.8, 9), (1.7.9)

$$K(\mathbf{q}) = \int e^{i\mathbf{q} \cdot \mathbf{r}} K(\mathbf{r}) d\mathbf{r} = \frac{4\pi e^2}{q^2} [\varepsilon(\mathbf{q}) - \varepsilon_0]^{-1}. \quad (7.4.10)$$

Formulae (7.4.9, 10) generalize the results of [267] for the case when the electron gas, while still almost completely degenerate, interacts with another subsystem whose state is strongly temperature-dependent.

The terms of the fourth order in the fluctuations are obtained directly from formula (7.4.7) by expanding $F_k + F_m$ (there is no contribution from other terms). Then we obtain for the variation of the free energy $F(\mathbf{q})$ produced by the fluctuation with the wave

vector \mathbf{q} (cf. (7.3.6)):

$$F(\mathbf{q}) = \frac{\varepsilon(\mathbf{q})}{\varepsilon_0 \Pi(\mathbf{q})} |n(\mathbf{q})|^2 + \mathcal{E}_4 |n(\mathbf{q})|^4,$$

$$\mathcal{E}_4 = \frac{8}{27} \frac{\mu_P}{n^3} - 6T \sum_{\mathbf{q}} \left[\frac{Aa^3 q^2}{2\omega_{\mathbf{q}}(q_0^2 + q^2)} \right], \quad (T > T_c(S)). \quad (7.4.11)$$

The necessary condition for the stability of a uniform state is the positive sign of the term in (7.4.11) quadratic in the fluctuations, this requiring that the expression $\varepsilon(\mathbf{q}) [\varepsilon(\mathbf{q}) - \varepsilon_0]^{-1}$ be positive for all \mathbf{q} 's. This condition will obviously be met if all the $\varepsilon(\mathbf{q})$ lie outside the interval $[0, \varepsilon_0]$ either exceeding ε_0 or being less than zero. The latter case is also quite real: a situation is possible in FMS when some Fourier transforms $\varepsilon(\mathbf{q})$ are negative, others exceeding ε_0 , so that there is no \mathbf{q} for which $\varepsilon(\mathbf{q})$ could find itself inside the interval $[0, \varepsilon_0]$. Therefore, the necessary condition for the stability of a uniform state will be satisfied as before.

Indeed, if at low temperatures all $\varepsilon(\mathbf{q})$, according to (7.3.6, 9, 11, 13) exceed ε_0 , then at temperatures above Q^{-1} determined by the equality $\Gamma(0) = 1$ the long-wave components of $\varepsilon(\mathbf{q})$ become negative. The behaviour of $\varepsilon(\mathbf{q})$ at $T > Q^{-1}$ is determined by the fact that $\Gamma(\mathbf{q})$ (7.3.11) diminishes as q grows. For this reason the

difference $1 - \Gamma(\mathbf{q})$ is negative only for $q < q_i$, where q_i is determined from the equality $\Gamma(q_i) = 1$. For $q > q_i$ this difference is positive. This is true also of $\varepsilon(\mathbf{q})$, which exceeds ε_0 for all $q > q_i$ (Fig. 7.1). In the interval $[0, q_i]$ the dielectric function tends to minus infinity as both boundaries of the interval are approached. Therefore it should pass through a maximum inside this interval. This maximum rises with rising temperature, reaching the value $\varepsilon = 0$ at the temperature T_+ . At $T > T_+$ the lower portion of ε vs. q curve intercepts the axis, i.e. a uniform state becomes absolutely unstable. As has already been pointed out, screening disappears at the same temperature T_+ (7.4.4).

At $T < T_+$ a uniform state of the system is, according to (7.4.11), stable against small fluctuations, even if some components of $\varepsilon(\mathbf{q})$ are negative. The physics of it is that the field acting in reality on the electrons is not $\Phi(\mathbf{q})/\varepsilon(\mathbf{q})$, but $\Phi(\mathbf{q})/\tilde{\varepsilon}(\mathbf{q})$. The effective

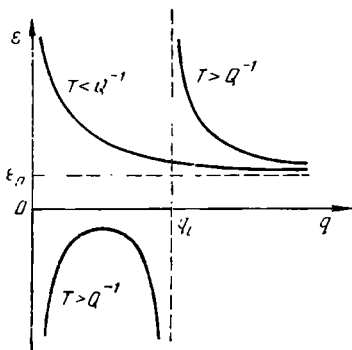


Fig. 7.1. Spatial dispersion of static dielectric function of a degenerate ferromagnetic semiconductor

dielectric function $\tilde{\epsilon}(\mathbf{q})$ (7.3.19), in contrast to $\epsilon(\mathbf{q})$, remains positively determined in the temperature range $[Q^{-1}, T_+]$ on whose right-hand boundary it vanishes for the first time (for the same value of q as $\epsilon(\mathbf{q})$ to which it is proportional). On the other hand, making use of formulae (7.3.6, 9, 19) we easily find that the quantity $\epsilon(\mathbf{q})/\Pi(\mathbf{q})$ in the expansion (7.4.11) is equal to $\tilde{\epsilon}(\mathbf{q})\Pi^0(\mathbf{q})$, with the bare polarization operator $\Pi^0(\mathbf{q})$ being, in contrast to $\Pi(\mathbf{q})$, always positive. It will be clear from this that the stability of the system being considered is guaranteed by the positive sign of $\tilde{\epsilon}(\mathbf{q})$ and not of $\epsilon(\mathbf{q})$.

The above consideration dealt only with the stability of the electron gas, the problem of the stability of the crystal lattice

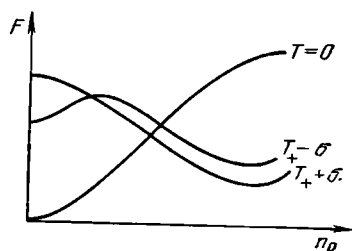


Fig. 7.2. Free energy of a degenerate ferromagnetic semiconductor as a function of the magnitude of electron density fluctuations n_p

remaining outside its scope. The stability of the lattice of ionic crystals is enforced both by long-range electrostatic forces and by short-range chemical bond forces. At the same time the true and not the effective electrostatic field $\Phi(\mathbf{q})/\epsilon(\mathbf{q})$ acts on its ions. Accordingly we may not *a priori* discount the possibility that after $\epsilon(\mathbf{q})$ has ceased to be positively determined the crystal lattice will become unstable.

Naturally, the stability of the electron system against small fluctuations analyzed above is no guarantee of its stability against large fluctuations. It means only that there is a minimum of the free energy to correspond to a uniform state of the system, however, it may be not the absolute minimum, but only a relative one. In this case the uniform state will be metastable. The temperature T_+ will be the point of a second-kind phase transition only if the absolute minimum of F corresponds to the uniform state at $T < T_+$. Otherwise the phase transition from the uniform to the nonuniform state will be a transition of the first kind.

The nature of the phase transition can be determined unambiguously only if the coefficient \mathcal{E}_4 in expression (7.4.11) is negative. In that case the transition will necessarily be of the first kind and must take place at some temperature T_1 below T_+ . Indeed, at $T = T_+ - \delta$ ($\delta \rightarrow 0$) there is even no relative minimum of the free energy to correspond to the uniform state. It follows from the negative sign of \mathcal{E}_4 that a minimum should be attained for sufficiently large fluctuations (Fig. 7.2). At $T = T_+ - \delta$ there is a minimum of F to correspond to the uniform state, but from considerations

of continuity it follows that it is very shallow and of necessity must be above the principal minimum whose position remains practically unchanged in case of small temperature variations. On the other hand at $T = 0$ the absolute minimum of F corresponds to the uniform state. Hence inside the interval $[0, T_+]$ there must lie a point T_1 at which minima corresponding to the uniform and nonuniform states lie at the same level. If the point T_1 is distant enough from T_+ , and if the condition (7.4.5) is satisfied at T_1 , this means that the phase transition not only in the model being considered, but also in the actual heavily-doped semiconductor will necessarily be of the first kind. Estimates made with the aid of formulae (7.4.11) and (6.1.2) demonstrate that the coefficient \mathcal{C}_4 will be negative, if

$$v > T_c^0 SW, \quad (7.4.12)$$

where T_c^0 is the Curie point of the undoped crystal.

For positive \mathcal{C}_4 the nature of the phase transition cannot be established using above treatment. But for v so small that \mathcal{C}_4 is positive a phase transition may prove to be impossible at all. (At small electron concentrations their effect is inadequate to make a uniform state unstable.) If a phase transition of the second kind is at all possible, a heterogenous structure with the wave vector $\sim \sqrt{\kappa_P \epsilon}$ for which $\epsilon(\mathbf{q})$ first vanishes must be established at point T_+ . Actually, such a state corresponds to a superposition of the charge density and the spin wave having equal periods incommensurate with the lattice parameter. Such "incommensurate" structures may materialize not only in MS, but in other materials as well, especially in the quasi-one-dimensional and quasi-two-dimensional. At high temperatures the nonuniform state of the model system must become unstable, since at $T \rightarrow \infty$ the free energy of the magnetic subsystem $F_M = -T N \ln(2S + 1)$ is independent of the electron density, and because of that does not decrease as its distribution becomes nonuniform. This means that spin and charge density waves present at lower temperatures should vanish as temperature increases, and the crystal should go over to the uniform state again. In other words, the nonuniform state should be reentrant.

The following remark should be made concerning the stability of a uniform state of an FMS at $T > T_c$. In the absence of a magnetic field such a state is of necessity stable against small fluctuations. It can be easily seen, if one takes into account that the dielectric function in the absence of magnetization is determined by a conventional expression (1.7.9). The physical explanation for this has just been given: an infinitesimal fluctuation is unable to produce local magnetization, and accordingly there is no reason why the free energy should decrease owing to this fluctuation. But this is not the case with strong fluctuations. If the uniform state has lost

its stability below T_c , it must continue to be unstable in some temperature interval above T_c as well. In other words, inside this interval a highly heterogeneous state of the crystal corresponds to the absolute minimum of F .

A uniform state at $T > T_c$ does not lose its relative stability even when a magnetic field is switched on, although for $\mathcal{H} \neq 0$ a local increase in the electron density, same as at $T < T_c$ is accompanied by a local increase in the magnetization. To convince oneself, it suffices to note that the feed-back function Γ_0 (7.1.9) cannot exceed unity. Indeed, n_D is determined by the equality $T = \theta + \Delta\theta(n_D)$, which is equivalent to (7.1.9). In the PM region the Curie point of a doped crystal must lie below T . Since the shift of $\Delta\theta(n)$ (6.1.3) grows with n , it follows from the aforesaid that n is always smaller than n_D . However, the uniform state may prove unstable against large fluctuations for $\mathcal{H} \neq 0$ as well. Similar considerations are valid for the ground state of an AFS with $n < n_A$. Note that a uniform state of an FMS may be unstable also when $\mu \gg AS$ [317].

Screened Potential in Paramagnetic and Antiferromagnetic Systems. Qualitatively, the behaviour of heavily-doped MS without a spontaneous magnetization in an electric field is equally independent of their specific nature, i.e. whether they are AFS or FMS above T_c . In the absence of a magnetic field, variations in the electron density caused by a weak electric field do not produce spontaneous magnetization. Therefore, such materials react on the electric field like nonmagnetic semiconductors, i.e. for $W \gg AS$ the expression for the screened potential of a point charge is the conventional one (1.7.11). The magnetic field changes the screening length. In cases when the interdependence between the local electron density and the magnetization can be neglected the expression for the screening length remains as before κ^{-1} (1.7.10). The kinetic energy of electrons in this expression grows with the field owing to the growth of the degree of spin polarization of the electrons. In the field \mathcal{H}_p in which the electrons become completely spin-polarized the kinetic energy increases $2^{2/3}$ times ($\mu_p = 2^{2/3}\mu$) after which it ceases to be dependent on \mathcal{H} . Because of an increase in the Fermi energy, the screening length grows in field weaker than \mathcal{H}_p . For $\mathcal{H} = \mathcal{H}_p$ it is $2^{1/3}$ times greater than for $\mathcal{H} = 0$. For fields stronger than \mathcal{H}_p it is independent of the field.

The behaviour of the screening length in a magnetic field turns out to be much more intricate when the interdependence between the electron density and the magnetization is taken into account. As in the case of FMS at $T < T_c$ there is an attraction between the electrons resulting from their joint participation in the establishment of a magnetization. This produces a tendency for the screening length to diminish with growing fields opposite to that produced

by the kinetic energy increasing with the field. Which of the two tendencies proves to be dominant will depend on the electron concentration.

In case of an AFS at $T = 0$, the feed-back function Γ_0 does not attain values sufficient for the screened charge to be over-compensated, so that oscillations of the screened potential do not set in even at the point n_A , where the stability of the AF state is no longer maintained. For all $n \leq n_A$, the Debye character of the screened potential (1.7.11) is retained.

It follows from formulae (7.1.10) and (7.1.13) with n_D replacing n_A that for $n < n_A/8$ the screening length always increases with an increase in the magnetic field, and that for $n > n_A/5$ it always decreases. In the intermediate region $[n_A/8, n_A/5]$ it displays a non-monotonous behaviour: at first it decreases with the field and subsequently grows. In fields exceeding the conduction-electron-spin-polarization field \mathcal{H}_P it ceases to be dependent on the field. The reason for this is in fact evident from formula (6.2.14), which describes the dependence of the magnetization on the field and on the carrier concentration: the variation of the magnetization caused by electron density fluctuations is independent of the field when $\mathcal{H} > \mathcal{H}_P$. The same is true of paramagnetic semiconductors up to the substitution of n_D for n_A .

Formulae (7.2.14, 16) remain valid for a canted AF structure, as well (Sec. 6.2), if the latter indeed can be established for $n > n_A$ in the absence of a magnetic field. At the point n_A itself the screening length must experience a jump. Indeed, for n smaller than n_A $\Delta\Pi_q = 0$ for $\mathcal{H} = 0$, and because of that the expression in square brackets in (7.2.14) is equal to unity. For n exceeding n_A (i.e. for $n = n_A + \delta$) $\Delta\Pi_q$ is proportional to magnetization, i.e. to $\sqrt{n - n_A}$, the quantity Z_0 with account taken of (6.2.3) being proportional to $n - n_A$. Hence, when n tends to n_A from the $n > n_A$ side, the ratio of $(\Delta\Pi_0)^2$ to Z_0 remains finite, and the expression in square brackets in (7.2.14) is not equal to unity. A more accurate consideration shows that, as the concentration passes n_A , the screening length in the canted AF phase turns out to be twice less than in the collinear AF phase. The off-diagonal response function $\lambda(\mathbf{q})$ in (7.2.16), which is equal to zero for $n = n_A - \delta$ and for $n = n_A + \delta$ behaves like $q^2 (n - n_A)^{-1/2}$, should display a still stronger singularity at n_A .

The existence of a jump in the screening length follows also from the simple phenomenological theory (see Sec. 6.2). At point n_A the quantity $d^2E/dn^2 = d\mu/dn$ must experience a discontinuity. According to (1.7.10) specifically $d\mu/dn$ determines the screening length. Since in the course of the transition to the canted state $d\mu/dn$ decreases by $(dA/dn)^2/2\mathcal{E}$, the screening length must also diminish.

It is however worth pointing out that, as point n_A is approached, the range of electric fields for which the linear response theory is applicable becomes narrower degenerating into a point at n . Accordingly, the singularities of the response functions at point n_A should be interpreted in the sense that first we must make the electric field tend to zero and only afterwards make the difference $n - n_A$ tend to zero.

The Problem of Stability of Intermediate Structures. As has already been pointed out in Sec. 6.2, an energy minimum corresponds to a canted AF ordering only when $n < 4n_A$. When $n > 4n_A$, the magnon frequencies cease to be positively-determined. Making use of formula (7.2.14), one will easily see that, as the concentration $4n_A$ is approached, the Debye screening law is replaced by an oscillating one of the type of (7.4.2). However, for $n < 4n_A$ canted AF ordering remains stable against small electron density fluctuations. It follows from formulae (7.4.11), (7.2.14, 16) that instability sets in at the concentration n_i determined by the equality

$$\left(\frac{n_i}{N_A}\right)^{1/2} = 2^{2/3} \left(1 + \frac{\omega_L}{2^{5/2}\mu}\right), \quad \omega_L = \left(\frac{6\pi e^2 n}{\varepsilon_0 m^*}\right)^{1/2}. \quad (7.4.13)$$

According to the condition of heavy doping (1.7.3), it is very close to $4n_A$. This suggests that in the range $n_A < n < 4n_A$, too, the absolute minimum of the energy of the system corresponds to a nonuniform state in case the inequality $4n_A > n_F$ is not satisfied.

In the case of a narrow-band AFS the problem whether a canted AF state is possible in it is solved by means of an analysis of its stability against small density fluctuations. One may easily obtain an estimate of Γ_0 (7.2.18) for the case when all the spinpolarons are in the lowest of the bands (6.2.23). In typical cases, according to (6.2.31, 34), $n_A \ll n_F$. If (6.2.23) is taken into account, $\frac{dB_+(\mathfrak{M})}{d\mathfrak{M}} \frac{d\mathfrak{M}}{dn} \simeq \simeq \frac{|B|}{n_F}$ is obtained for $n \gg n_A$. Next, the electron spinpolaron energy, according to this equality, is equal approximately to

$$\mu = (6\pi^2 v)^{2/3} B_+(\mathfrak{M}) \simeq (6\pi^2 v)^{2/3} |B| \frac{n}{n_F}. \quad (7.4.14)$$

With account taken of these estimates we obtain for $n \gg n_A$

$$\Gamma_0 \simeq (2v^{2/3})^{-1} \quad \text{for } \mathfrak{M} \gg \sqrt{2S+1}. \quad (7.4.15a)$$

In a similar way we may find an estimate for Γ_0 for $n - n_A \ll n_A$ as well

$$\Gamma_0 \simeq 2^{-2/3} (2S+1) (v/v_A) \quad \text{for } \mathfrak{M} \ll \sqrt{2S+1}. \quad (7.4.15b)$$

Hence, when $v < 0.3$, Γ_0 exceeds 1.

According to formulae (7.4.11, 15a) and (7.3.6, 9), for $\mathfrak{M} \gg \sqrt{2S+1}$ in the long-wave limit $q < k_F$ the variation of energy

caused by fluctuating electron density is proportional to

$$\frac{4\pi e^2}{\epsilon_0 q^2} - \frac{\mu}{3n v^{2/3}}. \quad (7.4.16)$$

Taking into account inequality (1.7.3), we find that the first term in (7.4.16) for $q \sim k_F$ is small as compared with the second, this inequality being very strong owing to v being small. A similar result is obtained for $\mathfrak{M} \ll \sqrt{2S-1}$ as well. Hence, CAF ordering is absolutely unstable against electron density fluctuations, if they reduce the energy of the system. This result has been obtained for a crystal with an AF ordering of the staggered type in conditions of validity of the inequality $n_A \ll n_F$ and of the strong degeneracy condition. Other cases (for example, layered antiferromagnets) require special treatment.

The problem of stability of a uniform state of unsaturated FMS with a singlet ionic state belongs to the same class. It follows from formula (7.1.20) that their feed-back function Γ_0 passes through a maximum at $v = \omega (4\sqrt{2\gamma})^{-1}$ where it reaches the value

$$\Gamma_0^{\max} \simeq 0.56 \frac{\gamma}{\mu}. \quad (7.4.17)$$

According to (7.1.19), the magnetization at such parameter values is equal to 0.3 c . Were we to use the following parameter values: $\gamma = 0.1$ eV, $m^* = m$ and $n \sim 10^{19} \text{ cm}^{-3}$ (the corresponding optimum frequency $\omega = 4\sqrt{2\gamma}v$ is of the order of several degrees Kelvin) to estimate Γ_0 , we would obtain for Γ_0^{\max} the value above 1. It follows from the aforesaid that the possibility for Γ_0 to exceed 1 is an evidence that the uniform state of a singlet magnet tends to be unstable.

7.5. NONUNIFORM STATES OF ANTIFERROMAGNETIC AND MAGNETOEXCITONIC SEMICONDUCTORS

Theory. Nonmagnetic semiconductors are subdivided into the lightly- and the heavily-doped, depending on their electric properties at $T \rightarrow 0$, the conductivity of the former tending to zero, whereas that of the latter remaining finite. The conductivity of lightly-doped crystals is the result of thermal ionization of donors (or acceptors). The situation in case of AFS is rather more complex. The thermally-excited electron of a donor in a lightly-doped semiconductor may be self-trapped in the FM microregion it itself has created, and because of that will be unable to take part in the charge transport processes (Sec. 5.2). Hence, the breaking of the bond between an electron and a positively-charged imperfection is not of itself tantamount to the appearance of a free charge carrier.

In degenerate semiconductors the electrons leave the donors already in the ground state of the crystal (the delocalization of donor electrons involving the creation of an impurity band merged with the conduction band). However, for exactly the same reasons as in a lightly-doped AFS, in a heavily-doped AFS self-trapping of charge carriers is also possible turning it into an insulator at $T = 0$. Therefore, one can judge whether a semiconductor is degenerate or not only from the magnitude and the temperature dependence of its conductivity at temperatures appreciably exceeding the Néel point, when self-trapping of electrons in FM microregions is no longer possible.

Self-trapping in a degenerate AFS means that its ground state ceases to be a magnetically uniform one: the crystal splits up into FM and AF parts with all the conduction electrons concentrating in the former. In principle, the energy gained in the result of electrons being self-trapped in an FM microregion can be calculated by presuming each electron to be self-trapped independently of the others, as described in Sec. 5.2. However, a situation may turn out to be still more favourable when several FM microregions merge to form a single region. The fact that it contains simultaneously several conduction electrons raises the Coulomb energy of the system and the kinetic energy of the self-trapped electrons, but this is made up by a reduction of magnetic energy spent to create the FM phase. The detailed structure of the self-trapped state is determined from the condition that the total energy of the system be minimum [197, 46]. Such a state may be termed the collective ferron one unlike ferron states discussed in Secs. 5.2-5.4.

The calculations presented below show that for relatively low carrier concentrations (at which however the semiconductor remains degenerate) it is energetically favoured for only one electron to reside in each FM microregion. The number and size of FM microregions grow with the concentration, and so does the number of trapped electrons in each microregion. Were it not for fluctuations of the imperfection potential, we would be justified in speaking of FM microregions containing trapped conduction electrons being of a spherical shape and forming a periodic structure inside the insulating AF matrix (Fig. 7.3a). Since the conduction electrons are localized each in its own FM sphere and cannot leave it, such a system is an insulator (two-phase insulating state)*.

* In an ideal crystal FM droplets acted upon by an external field would be able to move across the crystal, i.e. a current would flow in the crystal. Actually, because of the fluctuations of the impurity potential, the FM droplets are pinned down in the most energetically-favoured positions (an analogue of pinning of charge-density waves). However, external fields strong enough can pull the FM droplets out of the potential wells, and the droplets will begin to move, i.e. the break-down of the crystal will occur.

Starting from some critical concentration n_T , the FM spheres begin to make contact with each other. From this instant (the "percolation threshold") the two-phase conducting state with AF spheres forming a periodic structure inside a conducting FM matrix (Fig. 7.3b) becomes more energetically-favoured. Hence, at the concentration n_T the ground state of the crystal should change from the insulating to the conducting. In fact, conduction electrons, locked inside FM droplets at $n < n_T$, in case of the opposite sign of this inequality are free to move over the crystal by-passing the

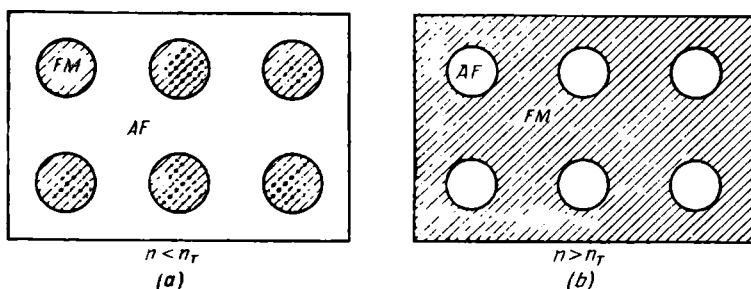


Fig. 7.3. Two-phase states of a degenerate antiferromagnetic semiconductor: (a) insulating; (b) conducting. The ferromagnetic part of the crystal is shaded, the antiferromagnetic is not

insulating AF droplets. The nonuniform state continues to be energetically-favoured also inside a definite interval of concentrations exceeding the value n_F starting from which the crystal in a uniform state would be completely FM (Sec. 6.2). Such a state, in contrast to the ferron states, would merit the term antiferrom. The fact that it is energetically-favoured follows from the partial restoration of AF ordering producing a gain in the energy of the direct exchange between magnetic atoms exceeding the loss in the *c*-electron energy.

Materials with $n < n_T$ and $n > n_T$ should exhibit a qualitatively different dependence of the conductivity on the temperature and the magnetic field. As the temperature is raised, the magnetic ordering is destroyed, and the crystal becomes magnetically-uniform. Because of that there are no longer any reasons for the electrons to be accumulated in some part of the crystal, and they spread out over the entire crystal. A strong enough magnetic field, which turns the whole crystal into an FM state, also makes it magnetically-uniform. At $n < n_T$ the transition to the magnetically-uniform state should be accompanied by the transition from the insulating to the conducting state, because the electrons formerly trapped in droplets isolated from each other now are able to travel across the whole crystal from one electrode to the other. In the case $n > n_T$,

on the other hand, the electrons are able to move freely in the crystal, by-passing inclusions of the AF phase, also in the magnetically-nonuniform state. For this reason by turning a crystal into a magnetically-uniform state by raising its temperature or applying a magnetic field, a relatively small effect on its conductivity should be obtained.

Everything said above is directly applicable to magnetoexcitonic semiconductors.

The calculations are carried out in the assumption of the heavy doping condition (1.7.3) being satisfied. This enables the spatial fluctuations of the donor potential to be neglected, and their charge is presumed to be uniformly distributed over the crystal. Because of an essential nonlinearity of the problem, a variational procedure will be used to solve it. All the conduction electrons are presumed to be concentrated in the ferromagnetic portion of the crystal (this will be substantiated below). As to the geometry of nonuniform states, only configurations depicted in Fig. 7.3 will be considered (a higher energy corresponds to alternating FM and AF layers [197, 46]). The ratio $x = V_A/V_F$ of the volumes of the AF and FM phases and the radius R of the spherical inclusion of the alien phase in the dominant phase (an FM sphere in Fig. 7.3a and an AF one in Fig. 7.3b) serve as variational parameters.

The assumption that the crystal splits up into regions with an FM and AF ordering and not into regions with an intermediate ordering of the type of canted AF is justified on account of the instability of the intermediate state for the transition to a nonuniform state proved in the preceding section. If the inequality $n_F \gg \gg n_A$ is satisfied, this alone is an ample reason for the electron concentration in the FM portion of the crystal, which should be above n_F , to be of necessity greater than their concentration in the AF portion, which is lower than n_A .

A point of principal importance in the solution of the problem is that the surface energy of the boundary separating the FM and the AF phase must be introduced correctly. It would be a mistake to use a concentration-independent quantity as the surface tension coefficient α_s as was done in [540] when a similar problem was solved for elevated temperatures. In effect, such a quantity is nothing but the coefficient of surface tension between the FM and the AF phase in the absence of conduction electrons. At the same time the coefficient α_s is meaningful only for phases that can coexist: by definition, it is equal to the derivative of the Gibbs free energy of the system with respect to the area of the interface calculated at a pressure and a temperature connected with one another by the condition of coexistence of the phases. The positive sign of α_s is guaranteed by the very fact of the coexistence of the phases [246]. However, in the absence of conduction electrons the FM and the AF

phase cannot coexist. Hence, there is neither a theoretical nor an experimental procedure to determine an α_s independent of n .

The part of the surface energy dependent on the electron concentration is played by the energy of quantization of electron motion in regions of finite dimensions. Since by limiting the electron motion to the FM portion of the crystal we raise the electron energy, this is a guarantee of the positive sign of the effective surface energy E_s . In the quasi-classical approximation the surface energy is easily found by making use of the expansion of the electron density of states in the inverse product of the Fermi momentum times the characteristic dimension of the system. In the first order in this product, according to the results of [334], when calculating the electron energy, we should substitute

$$\tilde{g}_e(E) = g_e(E) \left[1 - \frac{\pi}{4 \sqrt{2m^*E}} \frac{S_F}{V_F} \right] \quad (7.5.1)$$

for the density of states for the free electron $g_e(E)$ (1.2.10) (less the spin factor 2, because the electrons are spin-polarized). In (7.5.1) S_F is the area of the interface between the FM and the AF portion of the crystal (the external surface of the crystal need not be taken into account, since its area is much smaller than S_F). The first term in (7.5.1) yields the conventional bulk energy E_V , and the second the surface energy E_s .

In the nearest-neighbour approximation the exchange interaction between magnetic atoms does not contribute to the surface energy: the increase in the exchange energy is completely determined by the number of reversed spins, i.e. only by the volume of the FM region, but not by its shape.

In compliance with the condition (1.7.3), the electron density n_x is presumed to be constant in the ferromagnetic portion of the crystal. As there are no electrons in the AF portion of the crystal, it is related to the mean electron density in the crystal n by means of the expression $n_x = n(1-x)$ (x is the ratio of the volumes of the AF and the FM portions). Taking this into account and making use of expression (7.5.1), we obtain for the energy per unit volume

$$E = E_V + E_s + E_Q + E_M, \quad (7.5.2)$$

$$E_V = \frac{3}{5} \mu_P(n) n (1-x)^{2/3}, \quad \mu_P(n) = \frac{(6\pi^2 n)^{2/3}}{2m^*}, \quad (7.5.3)$$

$$E_s = \beta \left(\frac{\pi}{6} \right)^{1/3} \frac{5}{16} \frac{E_V}{n^{1/3} (1+x)^{1/3} R}, \quad (7.5.3a)$$

where $\beta = 3$ for FM spheres and $\beta = 3x$ for AF spheres.

The Coulomb energy E_Q is calculated by dividing the crystal into Wigner cells, i.e. into spheres enveloping the inclusions of an alien phase drawn so as to make the total charge inside the sphere

vanish. In the main approximation in $(Rn^{-1/3})^{-1}$ the expression for the Coulomb energy is

for FM spheres

$$E_Q = \frac{2\pi}{5\epsilon_0} n^2 e^2 R^2 [2x + 3 - 3(1+x)^{2/3}], \quad (7.5.4a)$$

for AF spheres

$$E_Q = \frac{2\pi}{5\epsilon_0} n^2 e^2 R^2 x [3x + 2 - 3x^{1/3}(1+x)^{2/3}]. \quad (7.5.4b)$$

The magnetic energy E_M and the magnetic moment \mathfrak{M} (per atom) are represented in the form:

$$E_M = - \left[\frac{AS}{2} n - \frac{|\mathcal{Y}|S}{(1-x)a^3} + \frac{\mathcal{H}^2 S x}{4|\mathcal{Y}|a^3(1-x)} + \frac{\mathcal{H}S}{(1-x)a^3} \right]. \quad (7.5.5)$$

$$\mathfrak{M} = \frac{S}{1+x} \left[1 + \frac{\mathcal{H}x}{2|\mathcal{Y}|} \right]. \quad (7.5.6)$$

The equilibrium values of the parameters x and R are found from the equations

$$\partial E / \partial R = 0, \quad \partial E / \partial x = 0.$$

It follows from equations (7.5.2-5) that only the effective surface energy E_S and the Coulomb energy E_Q are sensitive to the geometry of the FM portion of the specimen. By minimizing the sum $Q = E_S + E_Q$ in R for a fixed x , we obtain the following expressions:

for FM spheres

$$Q_F/n \simeq 1.2\gamma [2x + 3 - 3(1+x)^{2/3}]^{1/3} (1-x)^{2/9}. \quad (7.5.7a)$$

for AF spheres

$$Q_A/n \simeq 1.2\gamma x [3x + 2 - 3x^{1/3}(1+x)^{2/3}]^{1/3} (1+x)^{2/9}. \quad (7.5.7b)$$

Here we make use of the notation

$$\gamma = [\mu_B^2(n) e^2 n^{1/3} / \epsilon_0]^{1/3}.$$

Expressions (7.5.7) enables us to determine the precise geometry that guarantees the minimum energy of the system. It should be kept in mind that the Wigner cell method is not very accurate when the volume of the matrix is considerably less than that of the droplets inside which another type of magnetic ordering exists. For this reason expression (7.5.7a) yields a reliable value for Q_F only for large enough x , whereas the expression (7.5.7b) for Q_A only for small enough x . (It should be recalled that, according to its definition, x is the ratio of volumes of AF and FM parts of the crystal.)

For small concentrations $n \ll n_F$ x must be large, and because of that, according to (7.5.2-7), the minimum energy is attained when spherical FM domains form inside an AF matrix. At concentrations

n exceeding $n_F x$ must be small. Hence, the minimum energy is attained when spherical AF domains form inside an FM matrix.

By analyzing equations (7.5.2-7), we are able to establish that within the framework of the model employed nonuniform states will be more energetically-favoured than the uniform for arbitrarily small carrier concentrations n , if the inequality

$$\frac{AS}{2} > 2^{5/3} \left[\frac{2}{5} \mu_P(n_F) + \gamma(n_F) \right] \quad (7.5.8)$$

is satisfied. (The criterion (7.5.8) is established by calculating the energy of the state with FM droplets in the limit $x^{1/3} \gg 1$ for $\mathcal{H} = 0$.) Of course, it is practically meaningful only up to concentrations at which $\mu > e^2 n^{1/3} \varepsilon_0$. At lower concentrations spatial fluctuations of the impurity potential result in conduction electron transitions to impurity bound states.

From the high-concentration side the region of existence of nonuniform states is limited by the maximum concentration obtained from the condition $\partial E / \partial x = 0$ for $x = 0$. Taking into account definitions (7.5.2, 5.7b), we obtain it in the form:

$$0.4\mu_P(n_h) + 1.5\gamma(n_h) = \frac{|Z|S}{n_h a^3} \left[1 - \frac{\mathcal{H}}{2|Z|} \right]^2. \quad (7.5.9)$$

It follows from formulae (7.5.9) and (6.2.4) that for $\mathcal{H} = 0$

$$\frac{n_h}{n_F} \geq \left(\frac{AS}{1.6\mu_P(n_F)} \right)^{2/5} > 1,$$

i.e. that in the range $[n_F, n_h]$ antiferromagnetic states are indeed possible.

As the concentration n_h is approached from the low-concentration side, the fraction x of the volume occupied by the AF phase tends to zero (we would like to remind the reader that $V_A = \frac{x}{1-x}$), but the radius of each AF droplet remains finite tending to

$$R_h = \left(\frac{5\varepsilon_0\mu_P(n_h)}{16\pi e^2 n_h^{1/3}} \right)^{1/3} n_h^{-1/3}. \quad (7.5.10)$$

The critical concentration may turn out to be less if the condition of the complete spin polarization of the electrons has been violated.

Let us now discuss the validity of the assumption of a total absence of conduction electrons in the AF portion of the crystal. To this end it suffices to find the variation of the energy of the system following the transfer of a small number of electrons δn from the FM portion to the AF portion of the crystal. In the first order in δn the geometric parameters of the system R and x can be presumed to coincide with those for $\delta n = 0$, since, according to the condition that the energy be minimum with respect to R and x , the correction to the energy resulting from their variation $\delta R, \delta x \sim \delta n$ turns out

to be of the order of $(\delta R)^2$ or $(\delta x)^2$, i.e. $(\delta n)^2$. In that case the electron concentration in the FM portion will be equal to

$$\tilde{n}_x = \tilde{n}(1+x), \quad \tilde{n} = n \left(1 - \frac{\delta n}{n} V_A\right). \quad (7.5.11)$$

Substituting \tilde{n} (7.5.11) into formulae (7.5.2-7) for n , expanding the corresponding expressions in δn and taking into account that in the AF phase the electron energy is higher than in the FM phase by the amount U equal to $AS/2$ for $AS \ll W$ and to expression (5.2.14) for $AS \gg W$, we obtain the following expression for the variation of the energy:

$$\delta E = V_A \left[-\frac{5}{3} \frac{E_V}{n} - \frac{14}{9} \frac{Q}{n} + U \right] \delta n + O(\delta n^{2/3}). \quad (7.5.12)$$

Hence, for $\mu \ll U$ the correction δE is positive, and therefore there are no electrons in the AF portion of the crystal.

We shall undertake numerical calculations for parameter values corresponding in the orders of magnitude to those of rare-earth compounds of the type of EuTe: the energy $| \mathcal{H} | S = 10^{-3}$ eV, $S = 7/2$, $AS/2 = 0.5$ eV, $\epsilon_0 = 20$, $a^{-3} = 4 \times 10^{22}$ cm $^{-3}$, the effective mass is equal to the true mass ($W \simeq 4$ eV). It will be demonstrated below that for such parameters the conditions of applicability of the quasi-classical approximation are well satisfied in a wide enough concentration range. Calculations have also been carried out for the case of a narrow-band ($AS \gg W$) semiconductor. The following parameters have been presumed: $| \mathcal{H} | S = 4 \times 10^{-3}$ eV, $W \simeq 0.7$ eV, other parameters remaining unchanged.

Numerical results for the first set of parameters corresponding to a wide-band semiconductor are depicted in Fig. 7.4. In addition Fig. 7.5 depicts the field-dependence of the magnetization of a wide-band semiconductor. The gain ΔE in the energy of a nonuniform state as compared with that of a uniform state (AF for $n < n_A$ (6.2.3), canted AF for $n_A < n < n_F$ or FM for $n > n_F$ (6.2.4)) is at its maximum when the concentrations are small. It can be as high as 0.15 eV for $n = 2 \times 10^{19}$ cm $^{-3}$ and vanishes for $n_h = 2 \times 10^{20}$ cm $^{-3}$.

The region of stability of nonuniform states will be seen from Fig. 7.4 to be wider than the interval $[n_A, n_F]$. The concentration n_T separates the two-phase insulating state of the crystal from the two-phase conducting state. Below n_T the FM portion of the crystal is multiply connected, i.e. consists of individual FM spheres separated by regions of the AF phase. All the electrons are confined to the FM droplets, and because of that can take no part in the charge transport. Actually, in the immediate proximity to n_T the electric conductivity turns out to be nonzero, since the electrons can cross

from one FM droplet to another by tunnelling through the thin anti-ferromagnetic region separating them. Above n_T the FM portion of the crystal is singly connected, i.e. an electron can travel across the whole crystal without leaving this portion. In such a state the conductivity of the crystal is close to that it had in the uniform state, i.e. it is of the order of magnitude typical of heavily-doped semiconductors (10^1 - 10^3 Ohm $^{-1}$ cm $^{-1}$).

In a magnetic field the magnetization of the specimen increases with the field both on account of magnetization of the AF portion of

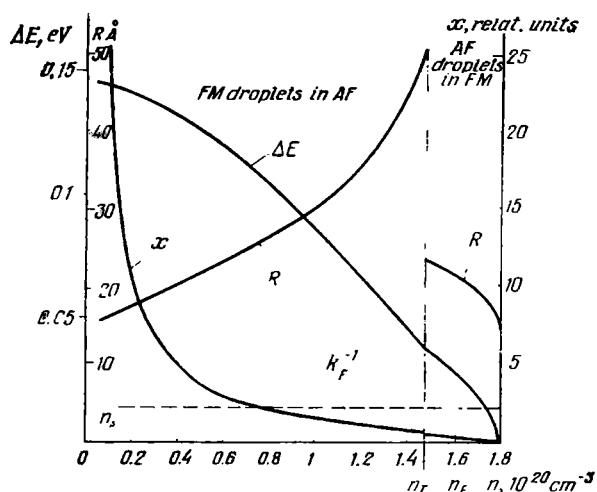


Fig. 7.4. The radius R of ferromagnetic ($n < n_T$) and of anti-ferromagnetic ($n > n_T$) droplets, the relative increase in carrier concentration in the ferromagnetic part of the crystal x and the inverse Fermi momentum in it $k_F^{-1}(n_x) = (1+x)^{1/3} k_F(n)$ as functions of the average carrier concentration n

the specimen and on account of the increase in the dimensions of the FM portion. For this reason the rate of growth of the moment with the field is higher in this case than in the undoped AFS, and in high fields the moment displays an essentially nonlinear field dependence (Fig. 7.5). Crystals residing in the absence of a magnetic field in a two-phase insulating state can be induced by a field to go over into a two-phase conducting state. A small jump on the curves 2, 3, 4 in Fig. 7.5 corresponds to the fields at which such a transition takes place. Its small magnitude is proof of the compatibility of the approximations employed on both sides of the percolation point n_T where the topology changes.

Note that for $n > 4n_A$ when, according to (7.4.13), the uniform canted state is unstable against infinitesimal electron density fluctuations, it cannot be stabilized by a magnetic field. Indeed, the ener-

gy of interaction of the electrons with the field is a function only of their total number, and because of that does not change in the result of fluctuations that change the local electron density, but not their total number. This probably explains the result depicted in Fig. 7.5: a transition to the uniform state takes place only after a complete FM ordering has been established.

However, for $n < 1n_A$ a magnetic field can in principle induce a transition from a two-phase insulating state to the canted conducting state, i.e. cooperative ferron states can be destroyed by the field like the individual ferron states (Sec. 5.2), by-passing the two-phase conducting state.

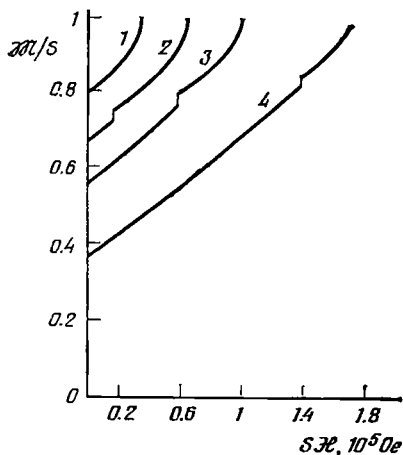


Fig. 7.5. Magnetization of a crystal vs. field. The insulating two-phase state is to the left of the discontinuity points, the conducting to the right. Concentration n assumes the values: 1, 1.6; 2, 1.4; 3, 1.2; 4, $0.8 \times 10^{20} \text{ cm}^{-3}$

However, for $n = 2 \times 10^{19} \text{ cm}^{-3}$ ($R = 16 \text{ \AA}$, $x = 8$) n_d is equal only to 3, i.e. the initial assumption about a large number of electrons in a droplet serving as the basis of the above quasi-classical calculations is at the limit

A problem of interest is that of the nature of variation of cooperative ferron states following the variation of the electron concentration. According to data presented in Fig. 7.4, for $n = n_T = 1.45 \times 10^{20} \text{ cm}^{-3}$ the radius of a ferromagnetic droplet $R = 50 \text{ \AA}$, $x \approx 0.5$, so that the number of electrons in a droplet is $n_d = \frac{4\pi}{3} n R^3 (1+x) = 100$.

However, for $n = 2 \times 10^{19} \text{ cm}^{-3}$ ($R = 16 \text{ \AA}$, $x = 8$) n_d is equal only to 3, i.e. the initial assumption about a large number of electrons in a droplet serving as the basis of the above quasi-classical calculations is at the limit

of its applicability in this range of concentrations. In the case of a narrow-band semiconductor the cooperative nature of ferron states is much less pronounced: even for $n = n_T = 10^{21} \text{ cm}^{-3}$ the mean number of electrons in a droplet is only 6, and for $n = 6 \times 10^{20} \text{ cm}^{-3}$ it drops to 1.5.

Note that the Fermi energy μ corresponding to concentrations n at which the number of electrons in a droplet n_d is of the order of unity is comparable to $e^2 n^{1/3} / \epsilon_0^*$. At the same time large numbers of electrons in a droplet correspond to concentrations at which the condi-

* This result can also be obtained in an analytical form for n so small that $x^{1/3} \gg 1$. It follows from the inequality $n_d \ll \left(\frac{12|S|}{W} \right)^{2/5} \left(\frac{\epsilon_0 W a}{e^2} \right)$ valid in the limit specified.

tion of high doping (1.7.3) is well satisfied. Hence, FM droplets containing large numbers of electrons are possible only in very highly-doped semiconductors where the Coulomb repulsion between the electrons plays a much smaller part than in semiconductors with an intermediate doping level (i.e. for which $\mu \sim e^2 n^{1/3} / \epsilon_0$).

Clearly, if every FM microregion contains one electron, it is energetically-favoured for each such complex to be localized near a charged donor forming a localized ferron (Sec. 5.3). However, in this case, too, insulator-metal transitions induced by a magnetic field or by elevated temperatures are possible. As has already been pointed out in Sec. 1.6, when the number of donors is very small, every electron is localized on its own impurity atom at $T = 0$. As the number of donors increases, so does the overlapping of the electron orbits of neighbouring donors, and at some critical concentration n_c the donor electrons become delocalized forming an impurity band, which possibly merges with the conduction band.

In an AFS every electron of a donor creates an FM microregion around its donor in which it itself becomes trapped (Sec. 5.3). Were we by applying a magnetic field to make an AFS go over to the FM state, the radius of the electron orbit should increase, since in the FM state the electron is attracted to the donor only by the charge of the latter, whereas in the AF state it is attracted additionally by the FM microregion around the donor. Hence it will be clear that the critical concentration n_{cF} in the FM state is lower than n_{cA} in the AF state. If the donor concentration is intermediate between n_{cF} and n_{cA} , in the antiferromagnetic state every electron will be localized on its donor. However, after the crystal was made go over by the application of a field to the FM state, the electrons should become delocalized, i.e. the magnetic field should cause an insulator-metal transition. The same must take place as the temperature is raised with the result that the FM region around a donor is destroyed, and hence the radius of its orbit grows. Thus, the qualitative properties of a semiconductor with the concentration $n_{cF} < n < n_{cA}$ are similar to those in the case of cooperative autolocalization of electrons in FM droplets.

Should we presume the delocalization of donor electrons to take place at equal ratios of the electron orbit radius to the mean spacing between the donors, we would obtain the following relationship between the critical concentrations n_{cF} and n_{cA} :

$$n_{cA} y^3 = n_{cF},$$

where y is determined from the energy minimum (5.3.3). For $n < n_{cF}$ a crystal containing localized ferrons behaves like a conventional impurity semiconductor, i.e. the free carrier concentration at $T = 0$ is zero, growing exponentially with the temperature.

As the temperature is raised, such a growth continues also after the ferromagnetic ordering around the donors has been destroyed.

Experiment. There is an adequate amount of experimental data in support of the existence of nonuniform FM-AF states in highly-doped AFS. First of all it concerns the results of research on the magnetic and the electric properties of the LaMnO_3 compound with a layered AF ordering. In normal conditions only Mn^{3+} ions are present in it. However, doping with Ca, Sr or heat treatment in an oxygen atmosphere produces Mn^{4+} ions in the result of which the crystal acquires a spontaneous magnetization [177, 332] (Fig. 7.6). This

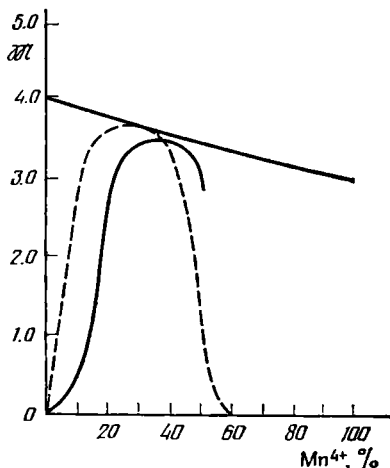


Fig. 7.6. Magnetization vs. concentration of Mn^{4+} ions for $\text{La}_{1-x}\text{Ca}_x\text{MnO}_3$. Solid line from data of [177], dashed line from [332]. Straight line, top, is the maximum magnetization for the specified composition (M in Bohr magnetons per Mn ion)

can be destroyed by creating oxygen vacancies and reducing the number of Mn^{4+} ions [585, 586]. For small concentrations n (Mn^{4+}) the magnetization grows with n and attains the maximum value for the specified n in the region of the relative amount of Mn^{4+} $n \sim 30\%$ (perfect FM ordering) after which it starts falling again. For example, intrinsic CaMnO_3 containing Mn ions only in the form of Mn^{4+} is non-ferromagnetic. In the range of smaller concentrations of Mn^{4+} the neutron scattering spectra at 4.2 K represent a superposition of spectra corresponding to the AF and FM order [177]. Fig. 7.7 depicts the spectrum of a specimen with $\sim 18\%$ Mn^{4+} . AF peaks are shaded, other peaks being FM.

In principle, such spectra may be associated both with the two-phase FM-AF state of the specimen and with the single-phase two-sublattice one having a nonzero moment. A unique choice between the two is made possible by studying the spectra as functions of the magnetic field [177]. In case the field is directed along the neutron scattering vector \mathbf{q} , FM peaks must become lower (vanishing altogether in the high-field limit), since the intensity of ferromagnetic scattering is proportional to $[1 - (\mathbf{q} \cdot \mathbf{m})^2]$, where \mathbf{m} is the unit vector pointing in the direction of the moment [99].

On the other hand, the intensity of AF scattering is proportional to $[1 - (\mathbf{q} \cdot \mathbf{l})^2]$, where \mathbf{l} is the unit AF vector (pointing in the direction of the difference between the sublattice moments (see Fig. 2.4)).

In the case of a two-phase system with the \mathbf{l} and the \mathbf{m} vectors not interconnected, a weak magnetic field $\mathcal{H}_A < \mathcal{H} < \sqrt{\mathcal{H}_A T_N}$ will rotate only the magnetism vector \mathbf{m} , not affecting the AF vector \mathbf{l} (Sec. 2.3), i.e. the AF scattering will remain unchanged. On the other hand in the case of a one-phase system, the vector \mathbf{l} will rotate together with the vector \mathbf{m} , and because of that in case of a FIM ordering ($\mathbf{m} \parallel \mathbf{l}$) AF scattering should be less and in case of a canted AF ordering ($\mathbf{m} \perp \mathbf{l}$) more intense.

Fig. 7.7 shows clearly that a field of 4.5 kOe reduces FM scattering by more than a half and has no effect whatsoever on the AF scattering. Hence, one may conclude that the crystal is in a two-phase

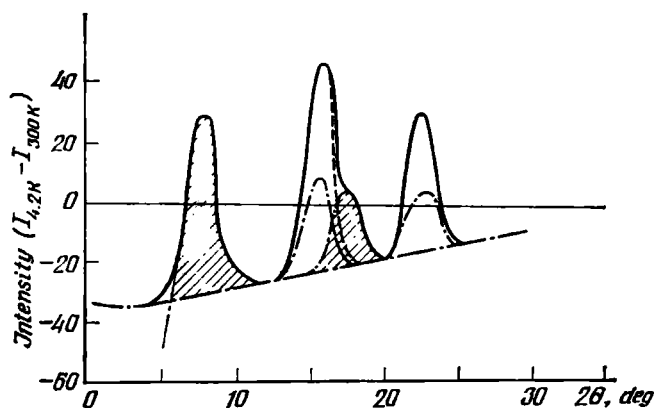


Fig. 7.7. Neutron scattering intensity vs. scattering angle 2θ in $\text{La}_{1-x}\text{Ca}_x\text{MnO}_3$ with 18% Mn^{4+} at 4.2 K less the intensity at 300 K (in arbitrary units). Shaded peaks are antiferromagnetic, unshaded—ferromagnetic. Dashed lines depict the same spectrum in a 4.5 kOe field [177]

state, and that the hypothesis advanced by de Gennes [74] that the results of [177] can be interpreted in terms of a canted AF ordering is in contradiction with the above results.

It has been demonstrated by X-ray studies that, despite magnetic heterogeneity, the specimens studied are homogeneous from the crystallographic viewpoint. Besides, the formation of FM regions in the crystal cannot be explained by fluctuations in the distribution of Mn^{4+} ions over the crystal producing complexes consisting of such ions in certain parts of the crystal. Indeed, the exchange interaction between the Mn^{4+} ions is of the AF type, proof of this being the antiferromagnetism of the CaMnO_3 system.

Similarly, the appearance of a Mn^{4+} ion is not always tantamount to the appearance of a mobile hole, CaMnO_3 being an insulator. Research on the electric properties of doped CaMnO_3 [332, 333] demon-

strates that crystals displaying pure FM ordering (30-40% Mn^{4+}), according to Fig. 7.6, also have a high metallic conductivity. The conductivity of two-phase specimens with a small relative volume of FM parts ($\sim 10\%$ Sr, i.e. the same amount of Mn^{4+}) is very small at low temperatures, growing exponentially with the temperature even at such temperatures at which the FM phase has already been destroyed (Fig. 7.8 [333]) (arrows indicate Curie points). The fact that at

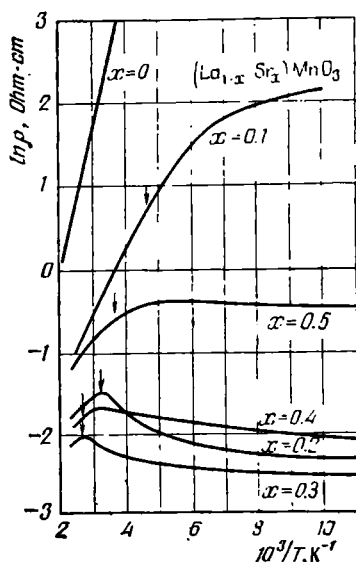


Fig. 7.8. Resistivity vs. temperature for $\text{La}_{1-x}\text{Sr}_x\text{MnO}_3$ [332, 333]

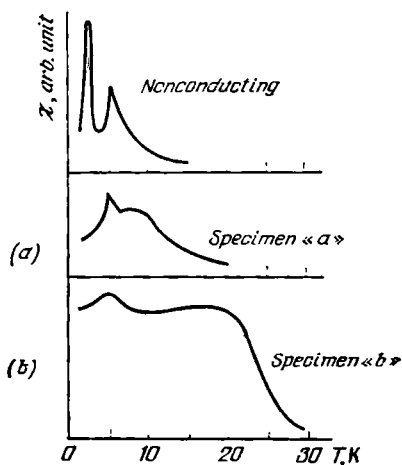


Fig. 7.9. Initial magnetic susceptibility of a stoichiometric and a nonstoichiometric (with excess of Eu) specimens of EuSe with carrier concentrations at 300 K:

(a) $6 \times 10^{18} \text{ cm}^{-3}$; (b) $3.5 \times 10^{19} \text{ cm}^{-3}$ [315]

sufficiently high temperatures the conductivity does not turn into the metallic speaks in favour of the existence of localized ferrons in such materials. But the main portion of a two-phase specimen with 20% Mn^{4+} is, according to Fig. 7.6, FM. Its high conductivity (Fig. 7.8) proves that it is in a state of the type shown in Fig. 7.3b.

Still more impressive is the experimental verification of the existence of cooperative ferron states in degenerate EuSe and EuTe obtained by magnetic, optical and electric measurements. The former provide proof of the coexistence of AF and FM phases in such crystals at low temperatures. The presence of an AF phase is estab-

lished on the grounds of a magnetic susceptibility peak in very weak fields ($\mathcal{H} \rightarrow 0$). In all cases the Néel point is the same as in an undoped crystal [168, 106, 315, 38], this being proof that there are no conduction electrons in the AF portion of the crystal (otherwise they would lower T_N because of indirect exchange via them). Fig. 7.9 depicts the susceptibility of a stoichiometric specimen of EuSe and a nonstoichiometric one containing excess of Eu [315]. They all display a peak at $T_N = 4.6$ K (the peak of χ in a stoichiometric specimen at 2.8 K is associated with a low-temperature phase tran-

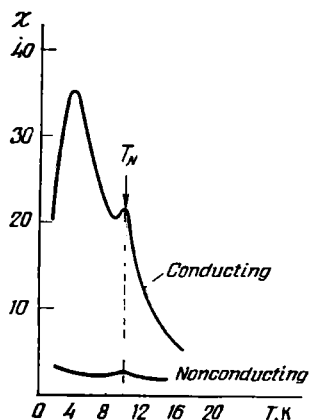


Fig. 7.10. Initial magnetic susceptibility of an undoped and an iodine-doped EuTe specimen with a carrier concentration of $\sim 10^{19}$ cm $^{-3}$ at 77 K (e.m. units/g·kOe) [38]

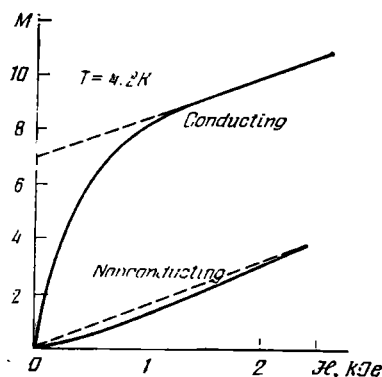


Fig. 7.11. Magnetization vs. field at 4.2 K for the same EuTe specimen as in Fig. 7.10. Dashed lines are magnetization lines in high fields extrapolated to $\mathcal{H} = 0$ (M in e.m. units/g) [38]

sition and has nothing to do with the phenomenon being discussed. As was pointed out in Sec. 2.8 there is no such transition in imperfect crystals). EuTe doped with I behaves similarly [38] (Fig. 7.10). Doping with I also does not change the value of $\chi(\mathcal{H})$ in EuTe at a fixed temperature, provided the field is not too low (then χ is independent of \mathcal{H} , Fig. 7.11 [38], Fig. 7.12 [106]). This means that a doped crystal contains regions of the antiferromagnetic phase with precisely the same properties as in an undoped crystal.

However, in weak fields the behaviour of doped specimens is essentially different from that of the undoped: they exhibit a sharp rise in the magnetization M whose magnitude grows with the electron concentration n . The rise in the magnetization of EuTe in fields ~ 100 Oe too small to change noticeably the angle between the sublattice moments of the antiferromagnet can be explained

only as the result of the orientation by the field of "ready-made" magnetic moments of a magnitude large enough. Judging by the fact that the linear dependence of M on \mathcal{H} at 4.2 K starts already in low fields ~ 1 kOe (Fig. 7.11), the contribution of "ready-made" moments already attains saturation in such fields. This means that the crystal contains regions with saturated FM ordering, since their spontaneous magnetization does not change in higher fields. The magnitude of the total spontaneous magnetic moment is evaluated from the start of the knee on the $M(\mathcal{H})$ curve or by extrapolating the high-field magnetization to $\mathcal{H} = 0$. It should be pointed out that a rise

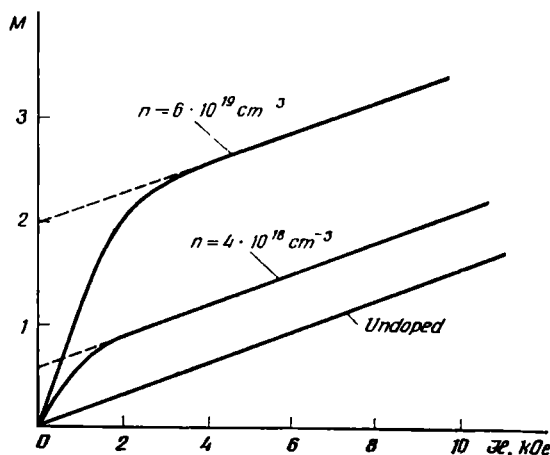


Fig. 7.12. Magnetization vs. field at 8 K for an undoped and an iodine-doped EuTe specimens with high-temperature carrier concentrations of 4×10^{18} and $6 \times 10^{19} \text{ cm}^{-3}$ (M in arbitrary units) [106]

in magnetization in weak fields has been observed also in such LaMnO_3 specimens whose neutronographic spectra represent a superposition of the FM and AF peaks [177].

After the rise in magnetization of a doped specimen the rate of its subsequent increase with the field turns out to be the same as in an undoped AFS, this being proof of the absence of electrons in the AF portion of the crystal. This rise cannot be explained as the effect of the conduction electrons on the magnetic susceptibility of the crystal (Sec. 6.2), since the EuTe crystals investigated are nonconducting at $T \rightarrow 0$. The possibility that a crystal, although possessing a spontaneous magnetization, resides in a uniform magnetic state is ruled out on account of the Faraday effect data in the region of optical frequencies obtained with the same specimens: doping of EuTe produces a very large Faraday rotation independent of the frequency of the light, which is typical of ferromagnets. Its magnitude in

the range of fields where the magnetization is a linear function of the field (Fig. 7.12) depends very little on the field (Fig. 7.13). In a uniformly-magnetized specimen the rotation would have been proportional to its magnetization. The Faraday rotation will be seen from Fig. 7.14 to become very small at temperatures above 40 K. The rise in the magnetization on the $M(H)$ curves disappears simultaneously.

Another evidence in favour of the magnetic heterogeneity of doped EuTe crystals is the depolarization of polarized light propagating

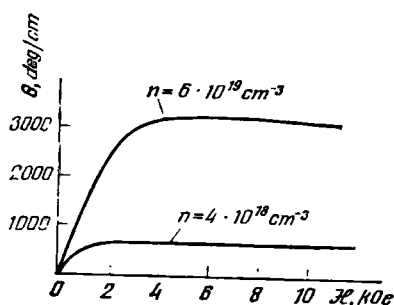


Fig. 7.13. Frequency-independent Faraday rotation as a function of the field at 8 K for the same EuTe specimens as in Fig. 7.12 (there is no rotation in the undoped specimen) [106, 313]

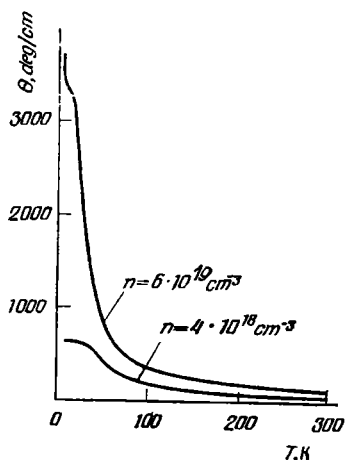


Fig. 7.14. Frequency-independent Faraday rotation vs. temperature in a 10 kOe field for the same EuTe specimens as in Figs. 7.12, 7.13

in the direction of the 3 kOe magnetic field applied to the specimen [313]. When the beam is at right angles to the field, there is no depolarization, but with such an arrangement there is no Faraday effect either (Appendix II). For this reason the depolarization of light can be naturally explained as the result of the Faraday magnetic rotation produced by magnetized sections of the crystal, which do not constitute an ideally-periodic structure, and whose dimensions fluctuate. The deviations from the periodicity must be a consequence of the random potential of the impurity atoms.

In EuSe the direct observation of FM microregions using the magnetization vs. field dependence is handicapped because the material experiences abrupt transitions to the FIM and FM states in weak fields (see Sec. 2.7). However, EuSe specimens with maximum doping display no metamagnetic properties, and their magnetization

curve is of the same type as that of EuTe [315]. This follows from the graph in Fig. 7.15, representing the magnetization vs. field dependence for a highly-conducting specimen (specimen "b", see Fig. 7.9) at 4.2 K.

The existence of a region with a spontaneous magnetization in doped EuSe specimens can be established easier using the temperature dependence of χ for $T \rightarrow 0$ (Fig. 7.9). The doped specimens in contrast to the undoped display a susceptibility shoulder above the Néel point the more pronounced and the more displaced to the high-temperature side the greater the carrier concentration. It appears in the result of formation of ferromagnetic regions as the temperature is

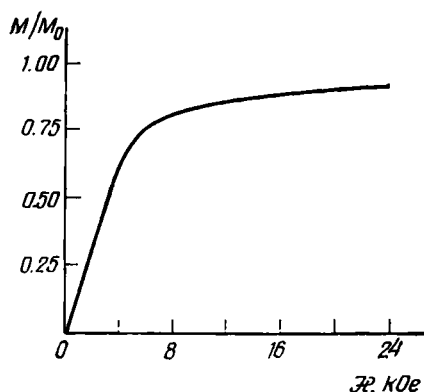


Fig. 7.15. Magnetization vs. field for a high-conductivity EuSe specimen (specimen "b" of Fig. 7.9) at 4.2 K [315]

lowered and brings about a drastic increase in the initial susceptibility of the crystal tantamount to the rise in the magnetization in weak fields. Indeed, direct studies of the temperature dependence of the magnetization in the specimen "b" demonstrate that the spontaneous magnetization in it appears simultaneously with the appearance of the susceptibility shoulder at 21 K [315].

We would like to point out that the nonlinear magnetization vs. field dependence of the highly-conducting "b" specimen cannot be explained on the basis of a uniform AFS with a non-Heisenberg indirect exchange via conduction electrons (Sec. 6.2). Firstly, it has a singularity of the susceptibility typical of the Néel point at exactly the same place as an undoped specimen. Should there be electrons in the AF portion of the specimen, the Néel point would lie lower. Secondly, the shoulder lies considerably above T_N , i.e. the rise in the magnetization in weak fields is not associated with AF ordering. Results of electrical measurements demonstrate that the FM-AF state can be both insulating and conducting. In the former case the crystal can be made conducting by destroying its two-phase structure with the aid of a magnetic field or by raising its temperature. This is seen especially clearly on the example of EuSe where the part of donor impurity is played by anion vacancies [315]. Consider two specimens "b" and "a" (Fig. 7.16) whose carrier concentrations at $T = 300$ K are $3.5 \times 10^{19} \text{ cm}^{-3}$ and $7.8 \times 10^{18} \text{ cm}^{-3}$ respectively. The difference in their conductivities is only an order of magnitude at 70 K, the ratio between their concentrations being 4.5 to 1. How-

ever, at 1.6 K the conductivity of the former is almost equal to its high-temperature value, whereas that of the latter it is 8 orders of magnitude lower. A noteworthy point is that the transition of the specimen "a" to the insulating state takes place simultaneously with the appearance of a spontaneous magnetization in it, as evidenced by magnetic measurements (a shoulder on the $\chi(T)$ curve, Fig. 7.9, of the specimen "a" having almost the same high-temperature carrier concentration as in Fig. 7.16a).

The 10 kOe magnetic field that induces the transition of the AF EuSe in an FM state at 1.6 K reduces the resistance of the specimen "a" by an enormous amount—by 9 orders of magnitude, whereas the resistance of the high-conductivity "b" specimen changes little in this magnetic field. The resistance of the specimen "b" turns out to be more sensitive to the field in the vicinity of the Curie point ~ 20 K: the resistivity peak in the vicinity of T_c is greatly reduced by the field, this being typical of FMS (Sec. 7.7). This is additional proof that all electrons are concentrated in the FM portion of the crystal.

The FM phase will be seen from Fig. 7.15 to occupy in the specimen "b" over 0.6 of the volume of the crystal. It is impossible to evaluate its volume reliably in the specimen "a". By comparing the heights of the shoulders of the "a" and "b" specimens (Fig. 7.9) we see only that this volume is small.

Hence, the data referred to is proof that the FM portion of the specimen "b" is singly-connected (Fig. 7.3b) and of the specimen "a" multiply-connected (Fig. 7.3a). In the former case the conduction electrons, being concentrated in the FM portion of the crystal, are able to propagate freely in it, and because of that the conductivity of the crystal is high. In the latter case, at $T \rightarrow 0$, they are confined to isolated droplets, and because of that are able to participate in the charge transport only after those droplets have been destroyed by a magnetic field or by rising temperature.

A two-phase conducting state has not been observed in EuTe. The temperature dependence of the resistance of a specimen in a two-phase insulating state is qualitatively the same as that of the EuSe specimen "a". At low temperatures the resistance is high, and as the temperature rises its decrease of two orders of magnitude occurs simultaneously with the destruction of the spontaneous magnetization (Fig. 7.17). Above 77 K its temperature dependence is weak [38]. A high magnetic field reduces the low-temperature resistance to its high-temperature value, probably in the result of the destruction of the two-phase insulating state. It should be remembered that the strength of the magnetization saturation field for pure EuTe is about 70 kOe. For doped specimens it is still smaller due to the FM indirect exchange via conduction electrons. Thus, an 84 kOe field is adequate to ensure that the specimens studied in [38] are in a homogeneous FM state.

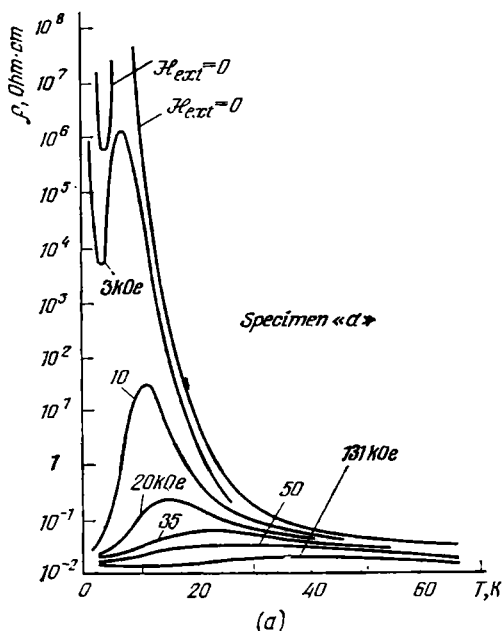
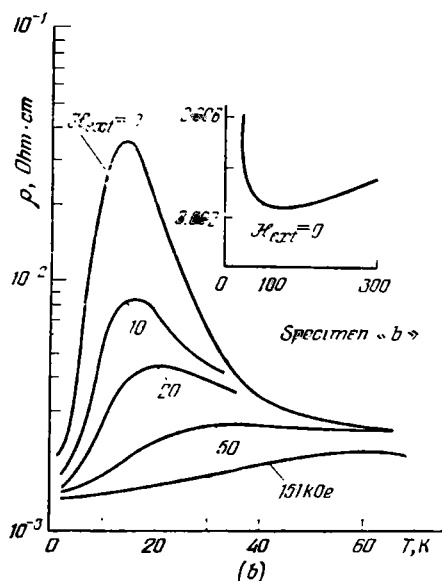


Fig. 7.16. Resistivity in the absence of a field and in fields of 3, 10, 20, 35, 50, at 297 K: (a) $7.8 \times 10^{11} \text{ cm}^{-3}$, (b) $3.5 \times 10^{19} \text{ cm}^{-3}$ [315]

Crystals with $n < n_T$ exhibit a finite conductivity owing to the thermal excitation of the electrons from the FM droplets into the AF portion of the crystal. The reason why the temperature dependence of the resistance of the specimen "a" of EuSe (Fig. 7.16a) is not monotonous is the same as in the case of nondegenerate FMS (Sec. 4.5): as in FMS, the conduction-band bottom in EuSe shifts upwards as the temperature is raised above T_N (Fig. 4.2). Accordingly, the energy of electron excitation from an FM droplet to the conducting state grows with the temperature, if the latter is low enough. In EuTe whose conduction band displays a small temperature-induced shift of the opposite sign (Fig. 5.7) the resistivity falls monotonously as the temperature is raised (Fig. 7.17).

An interesting point is that at 4.2 K weak fields ~ 100 Oe are able to reduce the resistivity of some EuTe specimens several times [38]. This effect can be explained by electrons tunnelling from one ferromagnetic droplet to another. A weak magnetic field orients random moments of different droplets in one direction, thereby increasing the probability of the electron transition from one droplet to another (Fig. 7.18). (The situation is quite similar to that discussed



131 and 151 kOe vs. temperature for EuSe specimens with carrier concentrations

in Sec. 3.5 apart from that the conduction electrons are localized inside the FM droplets and not on separate atoms.)

Comparing the results of calculations for parameters close to those of EuTe (Fig. 7.4) with experimental results, we see them to agree not only qualitatively, but quantitatively as well. According to data [106], the ratio between volumes of AF and FM portions of the crystal corresponding to a high-temperature electron concentration of $6 \times 10^{19} \text{ cm}^{-3}$ is $x = 5$, whereas the theoretical value is $x = 3$. If this value is evaluated from data [38] for a specimen with $n = 10^{19} \text{ cm}^{-3}$ (Fig. 7.11), $x = 20$ will be obtained. Corresponding to this x is, according to Fig. 7.4, $n = 2 \times 10^{19} \text{ cm}^{-3}$ (in this case the calculations are not very accurate, because the number of electrons in a ferromagnetic droplet is only about ~ 3).

In order to establish the details of the structure of a nonuniform FM-AF state, we may use the Faraday depolarization of light discovered in [106, 313]. The latter can be described in terms of light scattering by ferromagnetic regions accompanied by a change in the polarization [330]. In the presence of a long-range order in the arrangement of the droplets the light scattering by them in a magnetic

field that perfectly orients the moments would be characterized by infinitely-high peaks in the direction of the reciprocal vectors of the structure. Actually, however, because of fluctuation of the impurity atom potential the long-range order should vanish, although the short-range order should generally be maintained, because the fluctuating potential is a small perturbation in heavily-doped semiconduc-

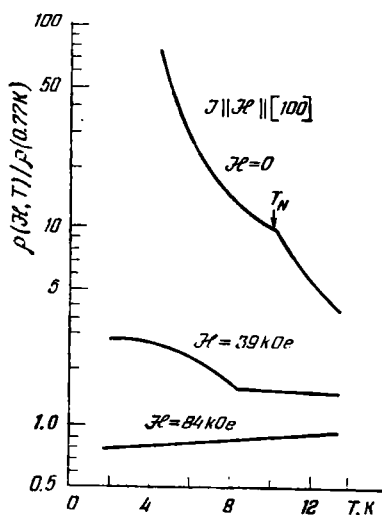


Fig. 7.17. Resistivity vs. temperature for a degenerate EuTe specimen (same as in Figs. 7.10, 7.11) [38]

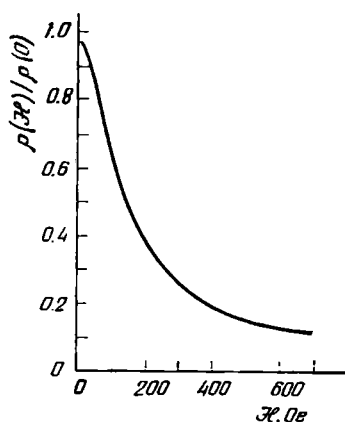


Fig. 7.18. Magnetoresistance of a degenerate EuTe specimen at 4.2 K, $\rho(0) \simeq 0.3$ Ohm-cm (same as in Figs. 7.10, 7.11, 7.17) [38]

tors. In that case the peaks will spread, and their height will become proportional to the number N_c of droplets contained in a short-range order region.

If the wave length of the light in the crystal λ exceeds the dimensions of the short-range order region, the expressions for the lengths b_H and b_0 at which the depolarization of light in an orienting field H and in the absence of such, respectively, takes place will be [330]:

$$b_H \simeq \frac{0.3 \cdot b_0}{N_c}, \quad b_0 \simeq \frac{1.5 \pi \lambda^2}{4 \pi^2 R^3 \theta_F^2}.$$

Thus, from b_H and b_0 one can determine both the dimensions of the ferromagnetic droplets and the short-range order parameter N_c . Unfortunately, [313] presents only a qualitative description of the phenomenon, and on account of this only very rough estimates of the respective quantities can be obtained. Since there was no zero-field depolarization, N_c should be no less than 100. For the Faraday rota-

tion θ_F we may put 10^5 deg/cm (such values have been obtained for EuTe made to go over to the FM state by a field [326]). For a depolarization length $b_{\text{ex}} \sim 1 \text{ cm}$ the radius R should be smaller than 60 \AA .

The dimension of an FM region containing one conduction electron could serve as the lower estimate of R . Concentrations of conduction electrons should naturally be determined from high-temperature data. Both references [106] and [38] yield very similar results $R \simeq 10\text{--}12 \text{ \AA}$. The theoretical value $R = 25 \text{ \AA}$ lies between the above estimates of 10 \AA and 60 \AA .

Results similar to those described above have also been obtained for Gd_2S_3 with an excess of Gd, where not only the insulating, but also the conducting FM-AF state has been observed [328]. A two-phase AF-FM state may also be possible in $\text{GdN}_{1-x}\text{O}_x$ with x in the vicinity of 0.04. For example, the composition with $x = 0.04$ is a degenerate antiferromagnetic semiconductor with a high number of conduction electrons per atom $v = 0.073$. Its Néel point of 40 K coincides with that of pure GdN, but the semiconductor also displays a spontaneous magnetization [594]. But this point needs further investigations.

7.6. NONUNIFORM STATES OF HEISENBERG AND SINGLET FERROMAGNETIC SEMICONDUCTORS, AND THE METAL-INSULATOR PHASE TRANSITION

Extremely interesting effects have been observed in the course of experimental research on the strongly-degenerate FMS. As the temperature is raised, EuO crystals containing oxygen vacancies in a definite range of concentrations display a transition from a semimetallic to an insulating state. The transition temperature ($\sim 50 \text{ K}$) is appreciably lower than the Curie point [108, 109, 121, 185-188] (curve 2 in Fig. 7.19 [109] and Fig. 7.20 [121]). As a result of this transition the resistivity of the crystal increases by over 13 orders of magnitude. This transition differs essentially from the insulator-metal transitions in V_2O_5 -type crystals, firstly because of a conductivity jump of a giant magnitude (in the latter case it does not exceed 8 orders of magnitude), and secondly because of the inversion of the conducting and the insulating phase about the transition point. (In this case the conducting phase is the low-temperature one.)

In the insulating phase the resistivity drops exponentially with the temperature, its activation energy at $T \gg T_c$ being equal to 0.3 eV. In external magnetic fields the transition point shifts to higher temperatures, with the $\rho(T)$ curve becoming less steep (Fig. 7.20). However, even in fields of 140 kOe the resistivity rises in the interval from 70 to 120 K by 6 orders of magnitude [121]. The

data about the nature of the dependence of the activation energy on T and on \mathcal{H} [185, 108, 189] is presently controversial. It will be seen from Fig. 7.19 that there is no metal-insulator transition in specimens having greater low-temperature conductivities. According to [121], it is observed at $n \sim 1\text{--}2 \times 10^{19} \text{ cm}^{-3}$, but disappears already at $n \sim 3 \times 10^{19} \text{ cm}^{-3}$. The fact that this transition is sensitive to the electron concentration speaks of its cooperative nature.

In specimens displaying a metal-insulator phase transition the Curie point is not displaced with respect to that of an undoped cry-

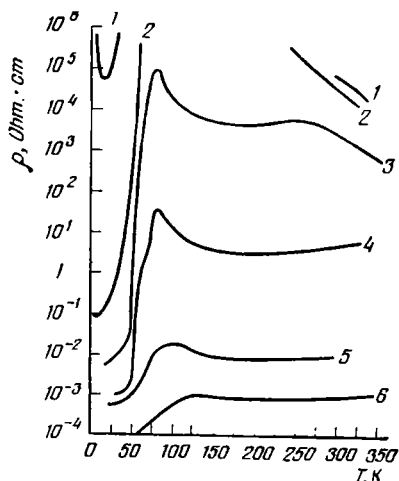


Fig. 7.19. Resistivity vs. temperature for several EuO specimens containing oxygen vacancies [109]

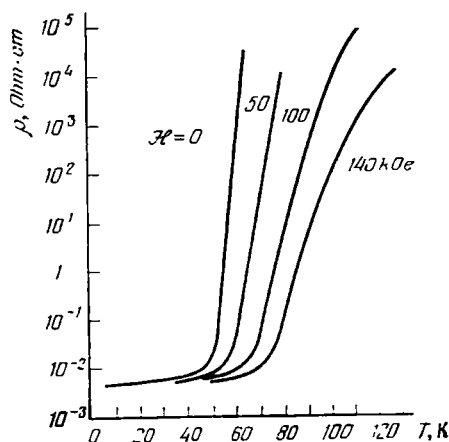


Fig. 7.20. Effect of a magnetic field on the metal-insulator transition in EuO containing oxygen vacancies [121]

stal. But it is greatly displaced in specimens containing larger carrier concentrations, which do not go over into the insulating state (cf. Sec. 6.4). In the absence of this transition, a resistivity peak with a clearly-defined structure typical of FMS is observable somewhat above T_c , the relative height of the peak diminishing as the concentration rises. Optical properties of EuO + Eu crystals have been studied in [201], and the photoconductivity of crystals displaying an insulator-metal transition in [587].

In contrast to EuO, EuS crystals containing excess of Eu do not experience a transition to the insulating state, although in this case, too, a sharp resistivity peak is observable in the region of T_c . However, according to [190, 122], they display an additional singularity of the resistivity of the type that should be observable in the course of a transition of an FMS to a nonuniform state. Fig. 7.21 shows that, as the temperature rises, a rapid increase in the resistivity by about

an order of magnitude takes place close to 8 K, but no corresponding decrease in the resistivity takes place as the temperature drops again (the dashed line in Fig. 7.21). The high-resistivity state is metastable and decays in several minutes, its rate of decay diminishing with time. The metastable state can also be destroyed by a magnetic field of several kOe, the decrease in the resistivity being accompanied by a decrease in the Hall constant $\sim 1/n$ (Fig. 7.22). The effect

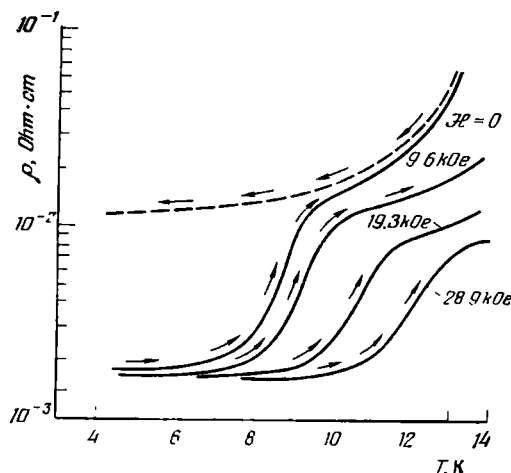


Fig. 7.21. Thermal hysteresis of EuS crystals containing excess of Eu [190, 122]

is mainly the result of the variation of carrier concentration, but it has been impossible to determine its value.

It would be natural, if one tried to associate the resistivity jump in heavily-doped semiconductors with their transition to a nonuniform state. Specifically, it would enable the possibility of the high-resistivity metastable state in EuS below 8 K to be explained, since, according to the results of Sec. 7.4, the phase transition from a uniform to a nonuniform state may be of the first kind, and the nonuniform state can exist below the transition point as a supercooled state.

The nonuniform state of a degenerate FMS differs in essence from that of an AFS: it has no regions in which the conduction electron concentration turns zero. This follows from the results of numerical computations carried out in the preceding section for the states of the type considered and for parameters lying inside an extensive range. (The chief difference in the computations is that in the case of an AFS we have to substitute the free energy (7.4.7) for the energy E_M (7.5.2) of creation of the FM phase.) Because of that the transition of a heavily-doped uniform semiconductor to a nonuniform state does not turn it into an insulator, and this is just what has

been observed in EuS. Assessing the temperature of absolute instability T_+ (7.4.4) for $AS/2 = 0.5$ eV, $N = 10^{22}$ cm $^{-3}$, $n = 0.8 \times 10^{20}$ cm $^{-3}$, $\epsilon_0 = 20$, $S = 7/2$, $W \simeq 4$ eV, we obtain 9×10^{-4} eV, this being close to the temperature at which the resistivity jump in EuS takes place. More favourable are the conditions for the appearance of a nonuniform state inside the subsurface layer of FMS.

This state can be governed by an external electric field changing the carrier density in the surface layer [588].

Some authors believe that an insulating nonuniform state of nondegenerate FMS is possible in which many-electron droplets exist in regions of enhanced degree of FM ordering [540, 544]. But this result obtained in [540] is a direct consequence of an incorrect treatment of the surface energy of these droplets. (It is introduced as a constant, which does not depend on n . As was pointed out in Sec. 7.5, such an assumption is inadequate.) The numerical value for the surface tension used in [540] was taken at random. As to [544], only two- and three-electron, but not really many-electron droplets were

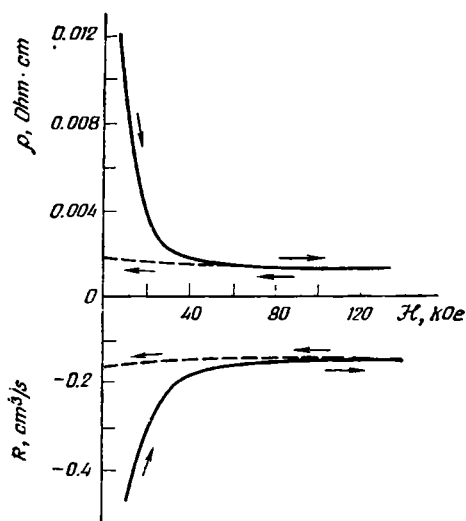


Fig. 7.22. Hysteresis of resistivity ρ and Hall constant R of the same EuS specimen as in Fig. 7.21 in a magnetic field ($T = 4.2$ K)

calculated in this paper (two-electron droplets were previously treated in [583]). Remarks made in Sec. 5.2 concerning calculations of one-electron ferrons in the mean field approximation by the same authors [206, 426] are valid for two- and three-electron ferrons, too. As was shown in Sec. 7.5, because of Coulomb interaction the number of electrons inside an FM droplet diminishes with the total electron concentration. Thus, in my opinion, it is much more difficult to meet the conditions for the existence of many-electron droplets in nondegenerate FMS than in degenerate ones. Meanwhile it has still to be proved that it is even possible to satisfy the conditions for the existence of one-electron ferrons at realistic parameter values.

In order to explain the transition to the insulating state observed in EuO, one has to take account of the impurity atom potential, which begins to play an appreciable role when $\mu \sim e^2 n^{1/3} \epsilon_0$. The qualitative treatment [196, 90] presented below demonstrates that

such a transition is possible at concentrations only slightly higher than n_c at which donor electron delocalization takes place in the ground state of the crystal (Sec. 1.6). (The difference between a doped FMS and a nonmagnetic semiconductor is that the electrons of the former are spin-polarized, and because of that the values of n_c are probably different in both cases.)

Consider first the case of singly-charged donors. The specific properties of a phase transition to a cooperative ferron state at concentrations only slightly exceeding n_c are determined by the impurity atom screened potential at $T = 0$ being "almost adequate" to trap an electron. It becomes adequate at finite temperatures, since the potential of exchange forces produced by excess magnetization appearing in the vicinity of a donor is added to the electrostatic potential. The magnetization appears because of a higher conduction-electron concentration near the donor and of a consequent enhanced effectiveness of the indirect exchange, which tends to maintain ferromagnetic ordering. As has been stated in Sec. 7.3, formally this can be accounted for by substituting the effective dielectric function $\epsilon_0(1 - QT)$ for ϵ_0 . Hence, the radius of the Bohr orbit a_B proportional to ϵ_0 diminishes as the temperature rises*. Whereas at $T = 0$ the product $a_B n^{1/3}$ was greater than the critical value C starting from which the electrons become delocalized, $a_B n^{1/3}$ may become less than C as the temperature rises. Then the donor electrons must become localized.

The above consideration is unsatisfactory in that it takes no account of the enhanced magnetic order in the vicinity of a donor on which an electron is localized. A more rigorous proof of the existence of the metal-insulator transition is also available [196, 90].

As in the case of $n \gg n_c$ (see Sec. 7.4), we may expect the phase transition to be of the first order. This is confirmed by experiment (see Fig. 7.19): the resistivity jump is sharp, although it is somewhat blurred owing to the random impurity distribution. That is why the transition is studied by comparing the free energies of the insulating and conducting states. As has already been pointed out, only the free magnon energy F_m constitutes the temperature-dependent portion of F . Because of the impurity potential fluctuations, the electron density is nonuniformly distributed in space. If the Bohr radius of an electron on a donor is large enough, the electron density even in an insulating state will vary slowly in space. This is still more true of a conducting state. For this reason in the range $T_c'S < T < T_c$, when only short-wave magnons are of essential importance, the Wentzel-Kramers-Brillouin approximation will be applicable to them, i.e. their frequencies ω_q may be presumed to depend on r .

* In some cases the true drop in ϵ_0 with rising temperature caused by the widening gap between the valence and the conduction band (see Chapter 4) may also prove important.

Their free energy F_m , when (7.4.7) is taken into account, can be represented in the form

$$F_m \simeq \frac{T}{(2\pi)^3} \left\{ \int d\mathbf{q} \ln \left(\frac{\bar{\omega}_{\mathbf{q}}}{T} \right) - \frac{A^2 v^2 \mathcal{Z}^2 \mathcal{G}}{8} \right\}, \quad (7.6.1)$$

$$\mathcal{Z}^2 = \int d\mathbf{r} \left[\frac{v(\mathbf{r}) - v}{v} \right]^2, \quad \mathcal{G} = \int \frac{d\mathbf{q}}{\omega_{\mathbf{q}}^2} \left[\frac{q^2}{q_0^2 - q^2} \right]^2,$$

where $\omega_{\mathbf{q}}$ is the frequency corresponding to the mean electron density v . When writing down (7.6.1), we presume the spatial dispersion of magnon frequencies to be small.

Since the density dispersion \mathcal{Z}^2 in the insulating state is greater than in the conducting, all the other quantities in (7.6.1) being identical, it is clear that, as the temperature rises, the free energy of the former diminishes at a greater rate than of the latter (Fig. 7.23). This is because in the insulating state the magnetic ordering in region of higher electron concentrations is destroyed more slowly than in the conducting state. The difference ΔF in the magnetic free energies F_m of the conducting and insulating states passes through a maximum in the region of T_c where the magnetic

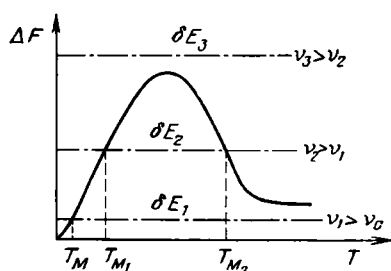


Fig. 7.23. Energy diagram of a metal-insulator transition

ordering in the conducting state is completely destroyed and in the insulating state is still maintained in the vicinity of the donors. As the temperature continues to rise, it, too, begins to be destroyed, and ΔF diminishes accordingly. However, $\Delta F(\infty)$ remains finite at $T \rightarrow \infty$ for the very reason for which the depth of the local levels remains greater than at $T = 0$: the spin of a localized electron adjusts itself to the fluctuating local magnetic moment (see Sec. 4.5). The conclusions remain in force also when the Bohr orbit radius is small [90]. $\Delta F(\infty)$ will obviously be the greater the smaller the radius of the orbit of the localized electron.

In case of a pronounced difference between the electron density distribution in the conducting and insulating states, ΔF for $v - v_c \ll v_c$ will depend little on v . Unfortunately, little is known at present about the difference $\delta E(v)$ between the energies of the insulating and conducting state. It is obvious however that it must rise with the rise in $v - v_c$. Hence, depending on the magnitude of this difference, three types of situations are feasible (Fig. 7.23):

(1) for very small $v - v_c$ the straight line δE_1 intersects the curve ΔF (i.e. the free energies of the conducting and the insulating state

become equal) only at one point T_M . This means that the crystal after having gone over to the insulating state remains in it up to the maximum temperatures;

(2) for greater $v - v_c$ the lines δE_2 and ΔF have two points of intersection T_{M1} and T_{M2} , i.e. a reverse transition to the conducting state takes place after the initial transition to the insulating state, this being manifest by a sharp resistivity peak between T_{M1} and T_{M2} ;

(3) for still greater v the lines δE_3 and ΔF do not intersect, i.e. no transition to the insulating state takes place at all.

Evidently, the smaller is $\Delta F(\infty)$ the narrower is the concentration interval inside which a transition to the insulating state takes place, and the more difficult is to observe this transition. Taking into account what was said in Sec. 4.5, we obtain that $\Delta F(\infty)$ should be of the order of $AS(a a_B)^{3/2}$. Hence, $\Delta F(\infty)$ diminishes as the radius of the orbit of the impurity state a_B increases and its depth diminishes. This is perhaps the reason why no metal-insulator transition is observed in crystals doped only with Gd: the donor levels of Gd are very shallow (Sec. 4.6). (According to [112], the doping of EuO with Gd produces oxygen vacancies in the crystal, and in this case a metal-insulator transition does take place. However, by annealing the crystal in an atmosphere of Eu vapours this transition is made to disappear.)

The theory developed above can be directly applied to doubly charged donors such as oxygen vacancies in EuO, provided they remain inside the entire temperature range of interest in a magnetic state of the (1s) (2s) type (see Sec. 6.5). Of paramount importance is the circumstance that r_2 , the radius of the (2s)-orbit, greatly exceeds, r_1 , the radius of the (1s)-orbit (within the framework of the helium-like model, four times, since the 1s-electron moves in the donor field unscreened by the 2s-electron, and the 2s-electron in the donor field half-screened by the 1s-electron [277]). Since it is much more easy to satisfy the delocalization conditions for the 2s-electrons than for the 1s-electrons, the metal-insulator transition must be the result of a cooperative autolocalization of 2s-electrons taking place without any change in the state of 1s-electrons.

In addition to the ferron mechanism, there is another possible mechanism of the metal-insulator transition: the transition can be the result of inversion of terms of doubly-charged donors (1s) (2s) \rightarrow (1s)², which can take place as the temperature is raised owing to the decrease in the local magnetization in the vicinity of the donors (Sec. 6.5). The cause of the transition is the obvious circumstance that an inversion sharply reduces the overlapping of the electron orbits of neighbouring donor atoms [385]. Actually, a very similar idea has been advanced in [335], but the authors failed to distinguish between the mean and the local magnetization, and because of that some of the results of [335] need be revised.

The inversion mechanism qualitatively yields the same dependences of the effect on the concentration as the ferron mechanism. Suppose for the sake of simplicity that the constant C in the Mott criterion (1.6.2) is the same for donors with paired and unpaired electrons. Then, depending on the donor concentration, three cases are feasible:

(1) If the Mott delocalization criterion is satisfied for 1s-electrons ($n^{1/3}r_1 > C$), it will be still more so for 2s-electrons, and the system will be in a conducting state at all temperatures.

(2) If the concentration lies inside the limits $n^{1/3}r_2 > C > n^{1/3}r_1$ at high temperatures, the system will be in an insulating state. However, as the temperature drops as soon as the term inversion takes place, the delocalization conditions will be met, and the system will become conducting.

(3) Finally, if the delocalization conditions are not satisfied even for 2s-electrons, the system will remain an insulator at all temperatures ($n^{1/3}r_2 < C$).

It is necessary to emphasize that a specific feature of all the theories developed above is the treatment of the metal-insulator transition as of a cooperative phenomenon, because only such an approach enables its dependence on the donor concentration to be explained. Some authors attempted to interpret this effect, ignoring its cooperative nature. For example, an attempt was made to explain it by bound "magnetic polarons" (i.e. ferrons), ignoring the interaction between them [188]. As was shown in Sec. 4.5, such an approach makes it possible to explain the resistivity peak close to T_c in non-degenerate FMS. But it is inadequate for the treatment of the metal-insulator transition. Mechanisms of this transition resembling the one suggested in [196, 90] are advanced in subsequent papers, for example in [589-591]. But unlike [196, 90], they gave no explanation for the fact that, on temperature increase, the transition from the conducting to the insulating state is not accompanied by a reverse one. Arguments presented in them suggested rather that the reverse transition was inevitable.

Formerly an opinion was sometimes voiced that, as the temperature is lowered, the conduction-band bottom sinks, and the local level remains where it has been, so that eventually it finds itself inside the conduction band, and the system becomes conducting. Such a hypothesis not only is incapable of explaining the experimentally observed dependence of the properties of crystals on the donor concentration (the metal-insulator transition takes place only in a very narrow concentration interval), but also is in contradiction with quantum mechanics: in the Coulomb field of a donor there is always a localized level lying below the continuous spectrum.

An experimental criterion to decide, which of the two mechanisms described above operates in EuO containing oxygen vacancies,

is provided by the nature of the dependence of the paramagnetic susceptibility of the crystal on the donor concentration. As has been already indicated in Sec. 6.5, donors in the $(1s)(2s)$ state increase and in the $(1s)^2$ state decrease χ . The available experimental data [188] suggest an increase in the magnetic susceptibility of EuO when oxygen vacancies are produced in it. Hence, they serve as proof that above the insulator-metal transition point the donors are in the $(1s)(2s)$ state, i.e. that the transition is not associated with the donor term inversion. It is worth pointing out that another evidence of the stability of the $(1s)(2s)$ state are the results of calculation of the c - l shift in EuO in the vicinity of T_c carried out in Sec. 6.5 under certain probably reasonable assumptions about the nature of the $1s$ and the $2s$ states: it is only 10% less than at $T = 0$.

There are experimental data [592] according to which the transition from the high-conductivity to the insulating state also takes place in CdCr_2Se_4 doped by In. As In is a singly-charged donor impurity, this fact supports the cooperative ferron mechanism of the metal-insulator transition in FMS. But more detailed study of this phenomenon in CdCr_2Se_4 is necessary.

The ideas of cooperative ferron states in FMS developed above enable also anomalous properties of singlet FM with unsaturated moments of the type of HoN to be explained. It was discovered in them that small-angle neutron scattering appearing above the Curie point rises monotonously as the temperature is lowered, i.e. that it behaves in a similar fashion to the scattering by the long order appearing at the Curie point [424]. Such a behaviour of small-angle scattering sharply distinguishes HoN from conventional FM in which it passes through a maximum at T_c (Fig. 7.24).

The presence of an abnormally high background scattering forces the authors of [424] to the conclusion that it represents a superposition of high-index peaks of scattering by the long-range magnetic order. To obtain a satisfactory agreement with the experiment, they had to presume that an extremely complex magnetic structure with a nonzero total moment materializes in HoN (the directions of atomic spins change abruptly every 7 lattice parameters). There are no answers in [424] to the questions why such a structure appears in

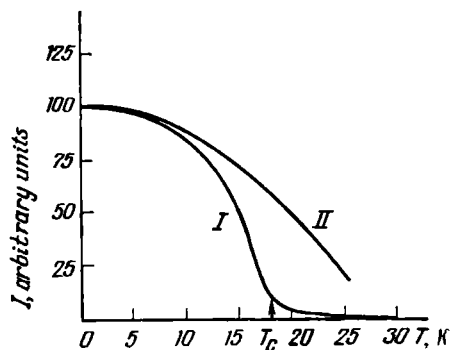


Fig. 7.24. Neutron scattering intensity vs. temperature in HoN: I, magnetic peak; II, small-angle scattering [424]

very simple crystals (of the NaCl type), and why small-angle scattering begins at temperatures higher than the Curie point.

We can offer an alternative explanation based on the fact that the materials of the type of HoN, being highly nonstoichiometric, are degenerate semiconductors [425]. Since the FM ordering in them is unsaturated, cooperative autolocalization of electrons in regions of enhanced FM order is possible in them. Since the charge carrier concentration in them may exceed 10^{21} cm^{-3} , their Fermi energy generally exceeds the c - l exchange energy. For this reason, in contrast to the ferron states in AFS discussed in the preceding section, a localization of only a certain part of the conduction electrons in regions with an enhanced magnetization takes place, and the crystal remains conductive [420].

If we presume the small-angle scattering to be caused by regions with enhanced magnetization, we will be able to present a natural explanation, why it begins already at temperatures appreciably above

T_c and grows as the temperature continues to fall. Indeed, microregions with an enhanced magnetization may have an ordering temperature (it is at the same time the temperature of their formation) higher than T_c of the crystal, since they have a higher concentration of conduction electrons, indirect exchange via which enhances FM coupling between the atomic l -moments. As the temperature falls, the number and the volume of such regions should grow, and with the intensity of small-angle scattering of neutrons. The absence of a critical scattering peak is probably associated with specific properties of singlet magnets whose atomic moments in the vicinity of T_c are small.

Evidence in favour of this interpretation is provided by the result (7.4.17) on the basis of which we concluded in Sec. 7.4 that the uniform state of the materials being discussed may be unstable. The possibility of the existence of regions with an enhanced degree of FM order in a wide range of temperatures from $T = 0$ to the PM region is substantiated by numerical calculations carried out in Sec. 6.2 for the particular case when each such region contains one electron.

7.7. TRANSPORT PHENOMENA IN DEGENERATE MAGNETIC SEMICONDUCTORS

Resistivity. Typical of the resistivity of heavily doped n -type FMS are the regularities depicted in Fig. 7.19. Of the specimens shown in the figure, the heavily-doped are those, which have a semimetal-type conductivity at $T \rightarrow 0$. As the temperature is raised, all of them in some degree or other display a growth in the resistivity, which passes through a maximum in the vicinity of the Curie point. The resistivity peak is the less pronounced the higher the conduc-

tivity of the crystal at $T=0$, i.e. the higher the carrier concentration. Whereas a degenerate semiconductor with the minimum conductivity experiences even a metal-insulator transition, a crystal with the maximum conductivity has practically no resistivity peak, although its high-temperature conductivity turns out to be almost by an order of magnitude lower than the low-temperature.

The cause of the transition to the insulating state has already been revealed in the preceding section. The high peak at the Curie point, when the resistivity exceeds its high-temperature value by several

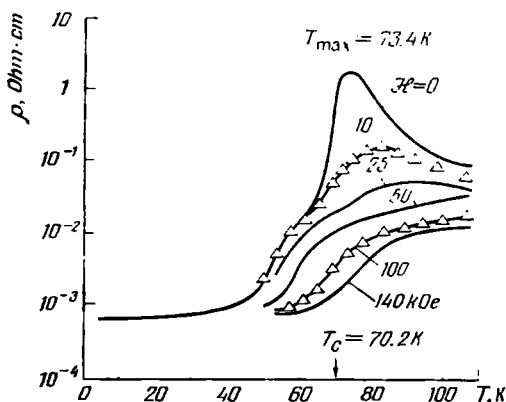


Fig. 7.25. Resistivity vs. temperature for EuO containing excess of Eu. Electron concentration is equal to $3.4 \times 10^{19} \text{ cm}^{-3}$ at 4.2 K and $5.5 \times 10^{18} \text{ cm}^{-3}$ at 298 K, mobility is equal to 290 and $19 \text{ cm}^2/\text{V}\cdot\text{s}$, respectively [121]

orders of magnitude (e.g., in Fig. 7.25 [121], Fig. 7.26 [141]), can be interpreted as two successive transitions: a metal-insulator and a reverse.

It is quite clear that such a peak cannot be explained simply by the increase in electron scattering by the imperfections or by fluctuations of the magnetic order in the vicinity of T_c . Indeed, scattering causes the appearance of an uncertainty in the electron energy $\sim 1/\tau_l$, where τ_l is the electron lifetime in a state with a definite momentum. It is in any case less than the transport relaxation time τ (1.7.16) since $\tau_l^{-1} = \sum_{\mathbf{k}} W_{\mathbf{k}\mathbf{k}'}$. If the electron concentration is presumed to be

constant, the peak value τ_l^{-1} will exceed the Fermi energy μ by several orders of magnitude, i.e. the concept of a free electron scattered by imperfections will become meaningless. Hence it is clear that we shall have to take into account the changes in the carrier concentration owing to the transition of electrons to localized states.

A quantitative theory of transport phenomena can be developed only for cases for which inequality (7.4.5) is satisfied. However, it may yield some qualitative results, which remain valid even when this inequality is violated, and which at any rate enable the experimental results to be explained. We may reasonably start with the case of an FMS in the spin-wave region. Here the increase of the re-

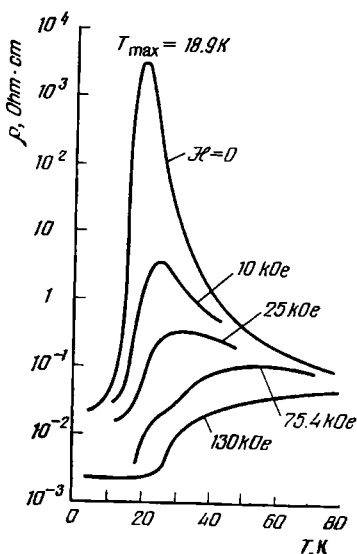


Fig. 7.26. Resistivity vs. temperature for a EuS specimen containing excess of Eu [141]

sistivity with the temperature is usually explained as the result of enhanced scattering of carriers by the spin waves. It will be demonstrated below that actually this increase is the result of specific interaction between the carriers and the imperfections, and that this explains the strong dependence of the resistivity on the concentration of the imperfections.

The difference between the heavily-doped magnetic and nonmagnetic semiconductors is that in the former not only spatial fluctuations of the electrostatic impurity potential exercise an influence on the state and the transport of charge carriers, but also magnetization fluctuations that accompany them. In case of an FMS at temperatures $T < T_-$ when the conventional Debye screening law (1.7.11) remains valid, their total effect is accounted for by substituting the renormalized

dielectric constant $\tilde{\epsilon}_0$ (7.3.19) for the bare ϵ_0 . Since $\tilde{\epsilon}_0$ is temperature-dependent, such electron characteristics as the density of states, carrier relaxation times for scattering by imperfections turn out, according to formulae (1.7.14), (1.7.18), to be temperature-dependent. In particular, it follows from formulae (1.7.13, 14), (7.3.13) that in the interval $T_c S \ll T \ll T_c$ the density of states in the tail of the conduction band grows exponentially with the temperature. The number of electrons in the tail, i.e. in localized states, grows accordingly as the temperature rises, thus diminishing the number of charge carriers.

As a result of substitution of ϵ_0 for $\tilde{\epsilon}_0$ the relaxation time for the electron scattering by the imperfections $\tilde{\tau}_h(T)$ at finite temperatures is expressed with a logarithmic accuracy in terms of the relaxa-

tion time τ_k (1.7.18) at $T = 0$ by the expression [310]

$$\tilde{\tau}_k(T) = (1 - \Gamma_0)^2 \tau_k. \quad (7.7.1)$$

According to (7.7.1), (7.3.13), the scattering by imperfections in the interval $T_c \leq T < T_c$ linearly rises with the temperature, the temperature-dependent part of the resistivity ρ_d due to the imperfections behaving similarly. The resistivity ρ_m caused by the scattering of carriers by magnons inside this interval is quadratic in T (4.4.7). In order to compare the temperature-induced growth of the resistivity due to the imperfections $\Delta\rho_d = \rho_d(T) - \rho_d(0)$, we may conveniently express the relaxation time for scattering by magnons (4.4.3) in terms of Γ_0 (7.3.10). Then, neglecting the temperature dependence of the carrier concentration, we obtain from (7.7.1) and (4.4.3)

$$\frac{\Delta\rho_d}{\rho_m} \leq \frac{2}{3\pi^2} \frac{e^2 m^*}{\epsilon_0^2 T} \ln \eta \sim \left(\frac{e^2}{\epsilon_0 a} \right)^2 \frac{1}{WT}. \quad (7.7.2)$$

It follows from (7.7.2) that for typical parameter values (the width of the conduction band W of the order of several eV, $e^2 \epsilon_0 a$ of the order of several tenths of an eV) $\Delta\rho_d$ in an FMS having a Curie point below 100 K exceeds ρ_m , i.e. in degenerate semiconductors not the magnons, but the imperfections are responsible for the growth of resistivity with the temperature. In FMS with high T_c the magnons contribute appreciably to the resistivity only at temperatures close enough to T_c . According to (7.7.1), in the region of the linear Γ_0 vs. T dependence ($\Gamma_0 \propto QT$ (7.3.13)), the temperature coefficient of resistivity $\frac{1}{\rho} d\rho/dT$ is equal to $2Q$. Making use of parameters corresponding to EuO ($AS \sim 0.3$ eV, $W \sim 4$ eV, $\epsilon_0 S \sim 0.02$ eV), we obtain from (7.3.15) that the theoretical value of the temperature coefficient for a specimen with $n = 3.4 \times 10^{19}$ cm $^{-3}$ is of the same order of magnitude as the experimental value estimated from Fig. 7.25.

It follows from formulae (7.3.15) that in the region of large $v \gg T_c AS$ the feedback function Γ_0 decreases as the carrier concentration rises. Thus, at a specified temperature the effective dielectric constant $\tilde{\epsilon}_0$ is the larger the higher the carrier concentration. Correspondingly, the increase in the resistivity, as T_c is approached from the low-temperature side, caused by increased scattering by the imperfections and by the transition of the carriers to localized states, turns out to be the more rapid the lower the carrier concentration.

For $v \ll T_c AS$, Γ_0 decreases slowly as the concentration decreases, but for real crystals the condition of applicability of the Born approximation (7.4.5) is not satisfied in this region, and accordingly one cannot insist that the temperature dependence of the resistivity should become weaker. In particular, if the decrease in Γ_0 with v

starts only in the vicinity of the critical concentration for the delocalization of the donor electrons v_c , in accordance with the results of Sec. 7.6, a sharp strengthening of the temperature dependence of the resistivity—a metal-insulator transition depicted in Fig. 7.19—will take place instead of its weakening.

In the high-temperature limit both the scattering by the imperfections and the PM scattering by spin fluctuations are temperature independent. In accordance with (1.7.18) and (4.4.8), the ratio of the relaxation times τ_m and τ_d corresponding to scattering by spins and by imperfections is equal approximately to

$$\frac{\tau_m}{\tau_d} = \frac{\rho_d}{\rho_m} \simeq v^{-1/3} \ln \eta \left(\frac{e^2}{a\varepsilon_0 AS} \right)^2. \quad (7.7.3)$$

It follows from (7.7.3) that, if the condition of applicability of formula (1.7.18), i.e. the inequality $\eta \gg 1$, and the smallness of concentration in typical conditions ($AS \sim 0.5$ eV, $\varepsilon_0 \sim 10$ -20) are taken into account, the dominant part at high temperatures can be played by the scattering of the electrons by the imperfections. Although at $T \rightarrow \infty$ $\tilde{\varepsilon}_0$ coincides with ε_0 , the electrons are however spin depolarized, i.e. their Fermi energy is $2^{2/3}$ times lower than at $T = 0$ (see (1.7.1)). For this reason the high-temperature scattering of the electrons by impurities, according to formula (1.7.18), turns out to be up to logarithmic accuracy 2 times stronger than at $T = 0$. This together with paramagnetic scattering explains why high-temperature resistivity $\rho(\infty)$ is several times higher than at $T = 0$. Nevertheless the electron mobility in degenerate FMS may be large enough: in EuO it is about $300 \text{ cm}^2/\text{V}\cdot\text{s}$ [121] and in HgCr_2Se_4 it reaches even $1000 \text{ cm}^2/\text{V}\cdot\text{s}$ [555].

For the electron scattering by imperfections to cause maximum resistivity in the region of T_c , it is necessary that $\rho(T_c)$ should exceed not only $\rho(0)$, but $\rho(\infty)$ as well. If we take into account that $\rho(\infty)/\rho(0)$ should exceed 2, we obtain from (7.7.1) that to this end $\Gamma_0(T_c)$ should exceed 0.3. At the same time, as has been already pointed out, the feed-back function Γ_0 rapidly decreases as n rises. For this reason at high concentrations the scattering by imperfections does not cause a resistivity maximum near the Curie point. The experimental fact that there is no resistivity peak at all at high concentrations is an evidence that it is the result only of the action of imperfections, but not of the critical magnetization fluctuations. This agrees with the fact that there is also no photoresistance peak in pure EuO crystals at the Curie point (Sec. 4.7).

Magnetoresistance. Another characteristic feature of n -type FMS is a giant negative magnetoresistance (Figs. 7.25-7.27). It is especially high in the vicinity of T_c . Magnetic fields of an adequate intensity are even able to cut off the zero-field resistivity maximum at T_c in those samples where it occurs. According to [121], whereas

the metal-insulator transition is the result only practically of a change in the concentration, the resistivity peak in EuO at high n is caused simultaneously by minimum concentration and by maximum scattering. To suppress the concentration minimum, fields of the order of several kOe are adequate, but maximum scattering is suppressed only by very high fields. However, on account of the

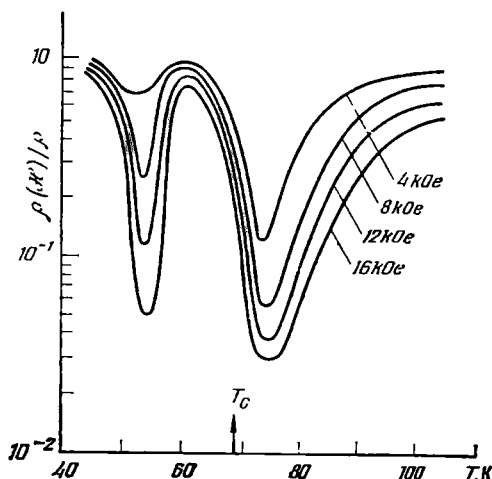


Fig. 7.27. Relative magnetoresistance of a EuO specimen containing excess of Eu [109]

inapplicability of conventional transport theory in the vicinity of T_c this conclusion cannot be regarded as a well-founded one.

According to [109], in some EuO specimens containing oxygen vacancies a maximum of the negative magnetoresistance well below T_c is observed in addition to one in the vicinity of T_c (Fig. 7.27). The reason for this phenomenon is not clear.

Whereas at $T \lesssim T_c$ the magnetoresistance is negative, in the paramagnetic regions heavily-doped FMS display a positive magnetoresistance in some temperature and field interval whose magnitude is 3 to 4 orders higher than in nonmagnetic semiconductors and is independent of the orientation of the magnetic field. Such a magnetoresistance has been observed in EuS [83] and in CdCr_2Se_4 [316] as well as in heavily-doped AFS EuTe [83] and EuSe [315], which, if one judges by the positive sign of their PM point, behave as FM at elevated temperatures. Fig. 7.28 depicts a typical dependence of the magnetoresistance on the field in EuSe with $n = 3.5 \times 10^{19} \text{ cm}^{-3}$ (data of [315]). As will be seen from the figure, the magnetoresistance after passing through a maximum begins falling, becoming nega-

tive in fields strong enough. As the temperature rises, the magnetoresistance maximum shifts to higher fields (Fig. 7.29).

The height of the maximum at first grows with the temperature, but subsequently begins to diminish, and at high enough temperatures the magnetoresistance becomes negative. The temperature interval inside which the magnetoresistance is positive widens as the carrier concentration increases (Fig. 7.30).

The usual explanation for the negative magnetoresistance is that the magnetic field reduces magnetization fluctuations, which in turn

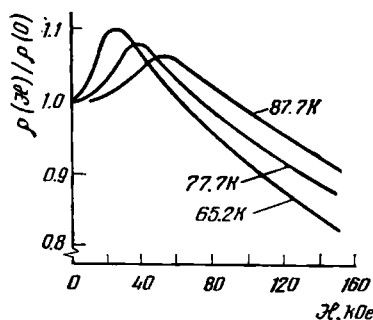


Fig. 7.28. Magnetoresistance of EuSe containing excess of Eu as a function of the field at three temperatures; $n = 3.5 \times 10^{19} \text{ cm}^{-3}$ [315]

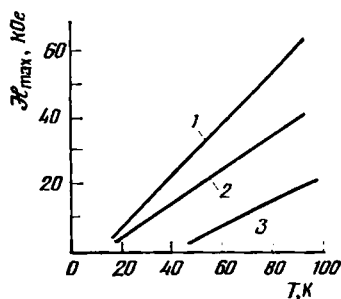


Fig. 7.29. Field of maximum magnetoresistance vs. temperature for degenerate *n*-type EuS and EuTe semiconductors:

1, EuTe, $n = 2.6 \times 10^{19} \text{ cm}^{-3}$; 2, EuTe, $n = 8.4 \times 10^{18} \text{ cm}^{-3}$; 3, EuS, $n = 1.3 \times 10^{19} \text{ cm}^{-3}$ [315]

causes a decrease in carrier scattering by these fluctuations. There is no doubt that this mechanism is responsible for the growth of mobility in magnetic fields in nondegenerate semiconductors. But it is unsuitable for the interpretation of the positive magnetoresistance in the PM region. On the other hand, as has been demonstrated above, in degenerate semiconductors the dominant part is played by impurity scattering. Hence, one should seek to explain the anomalies of the magnetoresistance of degenerate MS as a consequence of the influence of the magnetic field on the spatial fluctuations of magnetization caused by those impurities.

The magnetic field can both diminish and enhance such fluctuations. The former takes, for example, place when the magnetization in regions with higher electron concentrations practically reaches the maximum value, and the only thing the field can do is to raise the magnetization of the regions with lower electron concentration to its level, i.e. to diminish the fluctuations. In the opposite limit when there is no magnetization at $\mathcal{H} = 0$, the field induces a mag

netization, which fluctuates together with the electron density, i.e. the field enhances magnetization fluctuations.

Besides, the field enhances the degree of electron spin-polarization, in case it has not been maximum at $\tilde{\mathcal{H}} = 0$. This raises the kinetic energy of the electrons, reducing, according to (1.7.18), their scattering by imperfections. If the field reduces the fluctuations, both factors will operate in the same direction and produce a negative magnetoresistance. However, if the field enhances the fluctuations, the competition of the two factors may produce both a positive and a negative magnetoresistance, depending on n , \mathcal{H} and T .

A quantitative theory of negative magnetoresistance in FMS at $T < T_c$ can be developed for cases

when formula (1.7.18) with $\tilde{\epsilon}_0$ substituted for ϵ_0 is valid. The magnetic field is taken into account by shifting the magnon frequencies in the expression for $\Gamma(\mathbf{q})$ (7.3.10)

by the amount $\tilde{\mathcal{H}}$. It will be seen from formula (7.3.10) that for $\tilde{\mathcal{H}} \gg T$ the feed-back function Γ tends to zero, and the resistance consequently tends to its lowest value attainable at $T = 0$. For small \mathcal{H} $\Gamma_0(\mathcal{H})$ can be expanded in

$$\Gamma_0(\tilde{\mathcal{H}}) = \Gamma_0 - C\mathcal{H}, \quad C \sim \frac{S}{T_c} \Gamma_0. \quad (7.7.4)$$

Substituting $\Gamma_0(\tilde{\mathcal{H}})$ (7.7.4) into (7.7.1), we obtain the following expression for the magnetoresistance

$$\frac{\Delta\rho}{\rho} = \frac{\rho(\tilde{\mathcal{H}})}{\rho(0)} - 1 = -\frac{2\mathcal{H}C}{1-\Gamma_0}. \quad (7.7.5)$$

As seen from (7.7.5), the negative magnetoresistance caused by impurity scattering is linear in the field and grows with the temperature, because of the growth of Γ_0 . The qualitative dependence of the magnetoresistance on the impurity concentration is the same as that of the temperature coefficient of resistivity: outside the region $ASv \ll T_c^2$ the magnetoresistance decreases as the concentration rises. Hence, the higher is the resistivity peak near T_c the greater can it be reduced by the field, this being just what is observed in experiment.

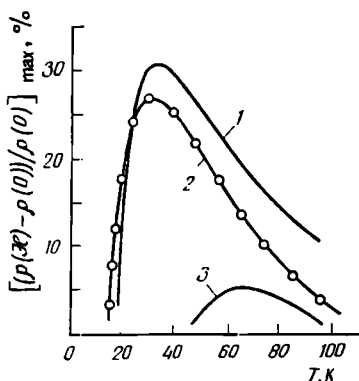


Fig. 7.30. Maximum magnetoresistance vs. temperature for degenerate EuS and EuTe semiconductors. Curves 1, 2, 3 are the same as in Fig. 7.29

At $T > T_c$ the magnetic field may enhance the impurity scattering. Formally this is associated with the feed-back function Γ_0 , equal to zero at $\mathcal{H} = 0$, becoming nonzero in the field, i.e. with the decrease in the effective dielectric constant $\tilde{\epsilon}_0$ in the field. The aforesaid remains valid for AFS as well. If the electron spin polarization is taken into account, the conductivity of crystals magnetized by an external field will be described by the expression [167, 440, 199]:

$$\sigma(\mathcal{H}) = \frac{e^2}{m^*} [n_{\uparrow} \tau_{\uparrow}(\mu_{\uparrow}) + n_{\downarrow} \tau_{\downarrow}(\mu_{\downarrow})], \quad (7.7.6)$$

where μ_{σ} is the kinetic energy of electrons with the spin projection σ . The relaxation time for the impurity scattering is calculated by making use of expression (7.1.2), where Φ is taken to mean the Coulomb field of the impurity, and of expressions (7.1.10, 11, 13-16) (for an antiferromagnet n_A (6.2.3) should be substituted for n_D (7.1.9)). In the Born approximation up to a logarithmic accuracy we obtain that the magnetoresistance associated with impurity scattering is equal to

$$\frac{\rho(\mathcal{H}) - \rho(0)}{\rho(0)} = - \left(\frac{3A\mathfrak{M}}{4\mu} \right)^2 \left\{ 1 - \frac{4}{3} \left[\left(\frac{n^*}{n} \right)^{1/3} - 1 \right]^{-1} + \frac{1}{3} \left[\left(\frac{n^*}{n} \right)^{1/3} - 1 \right]^{-2} \right\} \quad (7.7.7)$$

in fields \mathcal{H} small as compared with the field \mathcal{H}_P of complete electron spin-polarization, and to

$$\frac{\rho(\mathcal{H}) - \rho(0)}{\rho(0)} = \frac{1}{2} [1 - \Gamma_0]^2 - 1 \quad (7.7.8)$$

in strong enough fields $\mathcal{H} < \mathcal{H}_P$, when the electrons are completely spin-polarized. Here n^* is equal to n_A for AFS and n_D for PMS. At $T > T_c$ expression (7.1.16) for Γ_0 dependent on \mathcal{H} should generally be used in formula (7.7.8). However in the range of fields exceeding \mathcal{H}_P , but small compared with the saturation field ($\sim T$), the expression for Γ_0 is (7.1.9), i.e. it is practically independent of the field.

The qualitative behaviour of the magnetoresistance as a function of the field proves rather complicated.

(1) In the range $n < 0.1n^*$ the magnetoresistance (7.7.7, 8) is negative in all fields.

(2) In the interval between $0.1n^*$ and $0.125n^*$ the magnetoresistance is negative for $\mathcal{H} \ll \mathcal{H}_P$, but becomes positive as \mathcal{H} approaches \mathcal{H}_P . The difference between the behaviour in very weak fields and in stronger fields is the result of the impurity scattering of electrons from the less occupied spin subband at $\mathcal{H} < \mathcal{H}_P$ being not enhanced, but on the contrary, reduced by the magnetization fluctuations induced by the field in the vicinity of the impurities (this follows from (7.1.2, 3)).

(3) For $n > 0.125n^*$ the magnetoresistance is positive already in the weakest fields (Fig. 7.31).

In very strong fields the magnetoresistance is negative for all concentrations, but the change of its sign takes place differently in an antiferromagnet and a paramagnet. In the former the magnetoresistance for $\mathcal{H} \geq \mathcal{H}_F$ is independent of the field and changes its sign abruptly as the magnetic saturation field \mathcal{H}_F is attained. The

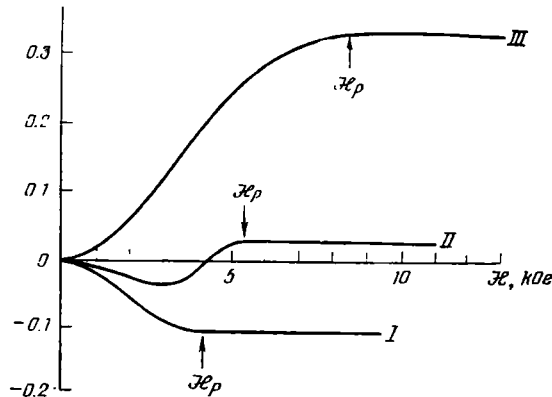


Fig. 7.31. Theoretical magnetoresistance vs. field curves for degenerate anti-ferromagnets at $T = 0$ and for ferromagnets at $T > T_c$: I, $n < 0.1n_L$; II, $0.1n_L < n < 0.125n_L$; III, $0.125n_L < n$. Field scale corresponds to EuTe at $T = 0$

independence of the resistivity of the field in the range $[\mathcal{H}_p, \mathcal{H}_F]$ is the result of the variation of electron density δn in the vicinity of the impurity causing, according to (6.2.14), a variation of the magnetization $\delta \mathcal{M} = \delta n A S \frac{1}{2} \left| \frac{\mathcal{H}}{N} \right|$ independent of the field. At $\mathcal{H} > \mathcal{H}_F$ the magnetization fluctuations vanish, and the effect of the field on electron transport phenomena makes itself felt only via the growth of their kinetic energy because of spin polarization. This effect, as has already been established, produces a negative magnetoresistance. Its magnitude can be determined from formula (7.7.8) by putting in it $\Gamma_0 = 0$: the resistivity is twice less than at $\mathcal{H} = 0$.

In the case of a PM the feed-back function Γ_0 , according to (7.1.16), decays with the field. Accordingly, starting from a definite field the magnetoresistance changes sign. Consequently, it must pass through a maximum at some value of the field not far from \mathcal{H}_p . Since the magnetic susceptibility in compliance with the Curie-Weiss law decreases as the temperature rises, higher fields are required to cause the complete spin polarization of the electrons. Therefore the field at which the magnetoresistance passes through its maximum grows correspondingly (see Fig. 7.23).

The dependence of the sign of the magnetoresistance on n/n_D at $T > T_c$ can easily be translated into the language of the temperature dependence, if one notes that for a fixed concentration n the value n_D rises with the temperature (see 7.1.9), while the ratio n/n_D cannot exceed unity by virtue of the physical meaning of n_D (see Sec. 7.4). Within the framework of the approximation employed, at high temperatures, when $n < 0.1n_D$, the magnetoresistance is negative, but can become positive at $n > 0.1n_D$. As the temperature continues to fall, it can again become negative in the vicinity of the Curie point.

The width of the interval in which the magnetoresistance is positive is proportional to carrier concentration. Accordingly, at a constant temperature the magnetoresistance will be the higher the higher the carrier concentration. All these corollaries of formulae (7.7.8) and (7.1.9) agree with experiment (Fig. 7.24).

If the paramagnetic scattering by spin fluctuations is comparable to the impurity scattering, the temperature interval in which the magnetoresistance is positive becomes narrower.

When the paramagnetic scattering is the dominant mechanism, the magnetoresistance is always negative. Qualitatively, its field-dependence at $T \gg T_c$ can be understood, if one analyzes formula (4.4.15). As \mathcal{H}_p is reached, the scattering by spin fluctuations, if the change in the Fermi momentum of the carriers is taken into account, decreases $3 \times 2^{-1/3}$ times. Afterwards it decreases slowly with the field up to fields $\sim T$, becoming $\sim \exp(-\mathcal{H}/T)$ for $\mathcal{H} \gg T$. Since PM scattering diminishes in a field, and the impurity scattering for $n > 0.1n_D$ grows, the latter mechanism may become predominant in strong enough fields $\mathcal{H} \gg \mathcal{H}_p$, even if in the absence of a magnetic field the impurity and the PM scattering have been comparable. In [593] it has been demonstrated that the theory developed above is in excellent agreement with data on Gd_2S_3 .

APPENDIX I. SPINPOLARON HAMILTONIAN
IN THE GENERAL CASE

This Appendix is a logical conclusion of Sec. 3.5. In order to construct a spinpolaron Hamiltonian in case of an arbitrary spin configuration, all atoms are attributed equal effective spins, the difference in real spins of atoms with or without an electron being accounted for by the structure of the Hamiltonian. In [70] the spin S of free atoms not occupied by electrons has been chosen as such an "effective" spin. The effective spin thus introduced coincides with the true spin of free atoms, and has no actual physical meaning for atoms housing an electron. However, all physical quantities can be readily expressed in terms of the effective spin by applying familiar rules (here is the simplest example: for $A < 0$ when the true spin of an atom with an electron on it is equal to $S - 1/2$, the projection of its true spin $T_{\mathbf{g}}^z$ is connected with the projection of its effective spin $S_{\mathbf{g}}^z$ by means of the equality $T_{\mathbf{g}}^z = S_{\mathbf{g}}^z - 1/2$). The magnon operators introduced in Sec. 3.5 can be regarded as those obtained from the effective spin operators by employing the Holstein-Primakoff relations, i.e. the effective spin is a direct generalization of such operators.

In order to introduce the effective spin, we alter the description of an atom carrying an electron: instead of the projection of its total momentum M we shall use one of the two values of the projection of the "intrinsic" atomic spin possible for a specified M . Namely, we put $M = m - 1/2$ for the $\psi_{\mathbf{g}M}^-$ (3.5.13) state and $M = m + 1/2$ for the $\psi_{\mathbf{g}M}^+$ (3.5.12) state, where the new index of state m can assume $2S + 1$ different values.

In the first instance the number of allowed values of m will obviously exceed the number of allowed values of M by unity. Actually, the extra degree of freedom is a fictitious one, because when $m = -S$, (i.e. $M = -S - 1/2$) the wave function $\psi_{\mathbf{g}(-S-1/2)}^-$ vanishes. In the second instance the number of allowed values of m is one less than that of M . The fact that we failed to take into account the state with $M = -S - 1/2$ can have any noticeable effect on the result, only if the following conditions are simultaneously met:

- (1) the c - l exchange must be ferromagnetic;
- (2) the temperature must be comparable with the Curie point or higher;

(3) the spin S must not be large (the relative weight of the neglected state, when the above conditions are met, is equal to $\frac{1}{2}(S+1)$). We shall indicate in the end of the section how it should be taken into account in case it is necessary.

Expressions (3.5.12, 13) can be rewritten with account taken of the changes in the indices by introducing the operators increasing or decreasing spin projection $S^\pm = S^x \pm iS^y$ and by making use of the designations S_{g0}^z instead of m for the indices of states

$$\psi_{gM}^\pm \equiv \psi_g^\pm(S_{g0}^z) = A_{g\pm}^*(S_{g0}^z) \delta(S_g^z, S_{g0}^z) |0\rangle, \quad (\text{Ap.I.1})$$

where

$$A_{g+}^*(S_{g0}^z) = \frac{1}{\sqrt{2S+1}} \left\{ \sqrt{S - S_{g0}^z + 1} a_{g+}^* + \frac{a_{g+}^* S_g^+}{\sqrt{S - S_{g0}^z + 1}} \right\},$$

$$A_{g-}^*(S_{g0}^z) = \frac{1}{\sqrt{2S+1}} \left\{ \sqrt{S + S_{g0}^z} a_{g-}^* - \frac{a_{g-}^* S_g^-}{\sqrt{S - S_{g0}^z}} \right\}.$$

When writing down relation (Ap. I.1), we made use of equalities (2.1.3, 4).

Since we are not interested here in the interaction between the carriers, we may confine ourselves to considering the single-electron problem. To go over to the spinpolaron representation, expand the eigenfunction of the Hamiltonian (3.1.1, 2) into eigenfunctions of the Hamiltonian H_A . Since the electron interacts only with the atom it occupies, these functions in the single-electron case can be written down in the form

$$\psi_{gMg}^\pm \prod_{f \neq g} \delta(S_f^z, S_{f0}^z). \quad (\text{Ap.I.2})$$

The set of functions (Ap. I.2) is obviously complete in the space of functions dependent on the coordinate g of the electron, on its spin and on the spins of all magnetic atoms. As has already been pointed out above, we shall not make a great mistake by omitting functions of the type of $\psi_{g, -S-1/2}^\pm \prod_{f \neq g} \delta(S_f^z, S_{f0}^z)$. Accordingly, the above

expansion, when formulae (Ap. I.1) are taken into account, can be represented in the form

$$\psi = \sum c_g^\mu(S_0^z) \chi_g^\mu(S_0^z), \quad (\text{Ap.I.3})$$

$$\chi_g^\mu(S_0^z) = A_{g\mu}^*(S_{g0}^z) |0\rangle |S_0^z\rangle, \quad (\text{Ap.I.4})$$

where μ assumes the values $+$ or $-$, S_0^z is the set of S_{f0}^z , and the use has been made of the notation

$$|S_0^z\rangle = \prod_f \delta(S_f^z, S_{f0}^z). \quad (\text{Ap.I.5})$$

Formulae (Ap. I.3) is a sum over all the values of g , μ and S_{i0}^z . Because of the delta-like nature of the basis functions $\chi_g^\mu(S_0^z)$, $c_g^\mu(S_0^z)$ has the meaning of the envelope of the wave function.

By substituting the expansion (Ap. I.3) into the Hamiltonian (3.1.1, 2), we are able to obtain the wave equation in a matrix form

$$c_g^{(-)}(S_1^z) \left[\frac{A(S+1)}{2} - E \right] = \sum_{f\mu S_0^z} c_f^\mu(S_0^z) [\chi_g^{(-)}(S_1^z), (H_B + H_M) \chi_f^\mu(S_0^z)], \quad (\text{Ap.I.6})$$

$$c_g^{(+)}(S_1^z) \left[-\frac{AS}{2} - E \right] = \sum_{f\mu S_0^z} c_f^\mu(S_0^z) [\chi_g^{(+)}(S_1^z), (H_B + H_M) \chi_f^\mu(S_0^z)]. \quad (\text{Ap.I.7})$$

In writing the set of equations (Ap. I.6, 7) we made use of expression (3.4.9) for the eigenvalues of the c - l exchange Hamiltonian.

The transformation from (Ap. I.6, 7) to a wave equation in an operator form is accomplished by introducing the operators S_{g0} acting in the space of functions of the indices of state S_{g0}^z in the same way as the corresponding operators S_g act in the space of functions of the true variables S_g^z . The transformation procedure to the energy operator will be illustrated with the aid of the example of the first term in the right-hand side of equations (Ap. I.6). Namely, we calculate the expression

$$\sum_{S_1^z} c_f^{(-)}(S_1^z) [\chi_g^{(-)}(S_1^z), H_B \chi_f^{(-)}(S_0^z)] \equiv \mathcal{X}_1 - \mathcal{X}_2. \quad (\text{Ap.I.8})$$

Taking into account expressions (3.1.4) and (Ap. I.3-5) and the orthonormality of the set of functions $|S_0^z\rangle$, we obtain

$$\begin{aligned} \mathcal{X}_1 &= \frac{B}{2S+1} \sum_{S_0^z \Delta} | \overline{(S - S_{g1}^z)(S - S_{g+\Delta, 0}^z)} \langle S_1^z | S_0^z \rangle c_{g+\Delta}^{(-)}(S_0^z) \\ &= \frac{B}{2S-1} \sum_{\Delta} | \overline{(S - S_{g1}^z)(S - S_{g+\Delta, 1}^z)} \rangle c_{g+\Delta}^{(-)}(S_1^z), \end{aligned} \quad (\text{Ap.I.9})$$

since

$$\langle S_1^z | S_0^z \rangle = \prod_f \sum_{S_f^z} \delta(S_f^z, S_{f1}^z) \delta(S_f^z, S_{f0}^z) = \prod_f \delta(S_{f0}^z, S_{f1}^z). \quad (\text{Ap.I.10})$$

When calculating \mathcal{X}_2 , we employ a useful relation

$$S^- \delta(S^z, S_0^z) = S^+ \delta(S^z, S_0^z) \quad (\text{Ap.I.11})$$

and its conjugate, obtaining with account taken of (Ap. I.10)

$$\begin{aligned}
 x_2 &= \frac{B}{2S+1} \sum_{S_0^z \Delta} \frac{\langle S_1^z | S_g^+ S_{g+\Delta}^- | S_0^z \rangle c_{g+\Delta}^{(-)}(S_0^z)}{\sqrt{(S+S_g^z)(S+S_{g+\Delta}^z, 0)}} \\
 &= \frac{B}{(2S+1) \sqrt{S+S_g^z}} \sum_{S_0^z \Delta} \frac{[S_{g0}^- S_{g+\Delta}^+, 0] \langle S_1^z | S_0^z \rangle c_{g+\Delta}^{(-)}(S_0^z)}{\sqrt{S-S_{g-\Delta}^z, 0}} \\
 &= \frac{B}{(2S+1) \sqrt{S+S_g^z}} \sum_{\Delta} S_{g1}^+ S_{g+\Delta, 1}^- \sum_{S_0^z} \frac{\langle S_1^z | S_0^z \rangle c_{g+\Delta}^{(-)}(S_0^z)}{\sqrt{S+S_{g+\Delta}^z, 0}} \\
 &= \frac{B}{2S+1} \sum_{\Delta} \frac{1}{\sqrt{S+S_g^z}} S_{g1}^+ S_{g+\Delta, 1}^- \frac{c_{g+\Delta}^{(-)}(S_1^z)}{\sqrt{S+S_{g-\Delta}^z, 1}}. \quad (\text{Ap.I.12})
 \end{aligned}$$

As a result of these and of similar calculations equations (Ap. I.6, 7) assume the following form (the index "1" of the spin operators has been omitted):

$$\begin{aligned}
 \left\{ E - \frac{A(S+1)}{2} - H_M \right\} c_g^{(-)}(S^z) \\
 = B \sum_{\Delta} F^{(-)}(S_g, S_{g+\Delta}) c_{g+\Delta}^{(-)}(S^z) - B \sum_{\Delta} G(S_g, S_{g+\Delta}) c_{g-\Delta}^{(-)}(S^z), \\
 \quad (\text{Ap.I.13})
 \end{aligned}$$

$$\begin{aligned}
 \left\{ E + \frac{AS}{2} - H_M \right\} c_g^{(+)}(S^z) \\
 = B \sum_{\Delta} F^{(+)}(S_g, S_{g+\Delta}) c_{g-\Delta}^{(+)}(S^z) + B \sum_{\Delta} G^*(S_{g-\Delta}, S_g) c_{g+\Delta}^{(+)}(S^z), \\
 \quad (\text{Ap.I.14})
 \end{aligned}$$

where the notation is used

$$\begin{aligned}
 F^{(-)}(S_g, S_{g+\Delta}) &= \frac{1}{2S+1} \left\{ \sqrt{(S+S_g^z)(S+S_{g+\Delta}^z)} - \frac{1}{\sqrt{S+S_g^z}} S_g^- S_{g+\Delta}^- \sqrt{\frac{1}{S+S_{g+\Delta}^z}} \right\}, \\
 F^{(+)}(S_g, S_{g+\Delta}) &= \frac{1}{2S+1} \left\{ \sqrt{(S+S_g^z-1)(S+S_{g+\Delta}^z-1)} \right. \\
 &\quad \left. + \frac{1}{\sqrt{S+S_g^z-1}} S_g^- S_{g+\Delta}^+ \sqrt{\frac{1}{S+S_{g+\Delta}^z-1}} \right\}, \quad (\text{Ap.I.15}) \\
 G(S_g, S_{g+\Delta}) &= \frac{1}{2S+1} \left\{ \sqrt{S+S_g^z} S_{g+\Delta}^+ \sqrt{\frac{1}{S+S_{g+\Delta}^z+1}} \right. \\
 &\quad \left. - \frac{1}{\sqrt{S+S_g^z}} S_g^+ \sqrt{S+S_{g+\Delta}^z+1} \right\}.
 \end{aligned}$$

In equations (Ap. I.13-14) the terms describing the variation of the Hamiltonian H_M on account of the presence of conduction electrons have been omitted, because they are of the order of J/B with respect to terms retained in it. The terms omitted here are cited in [71].

The form of equations (Ap. I.14, 15) makes it possible to write the Hamiltonian of the system being considered in its final form

$$H = H_{\dots} + H_{\dots} + H_{\dots} + H_M, \quad (\text{Ap.I.16})$$

$$H_{>} = -\frac{AS}{2} \sum \alpha_{g,>}^* \alpha_{g,>} + B \sum F^{(+)}(S_g, S_{g+\Delta}) \alpha_{g,>}^* \alpha_{g+\Delta,>}, \quad (\text{Ap.I.16a})$$

$$H_{<} = \frac{A(S+1)}{2} \sum \alpha_{g,<}^* \alpha_{g,<} + B \sum F^{(-)}(S_g, S_{g+\Delta}) \alpha_{g,<}^* \alpha_{g+\Delta,<}, \quad (\text{Ap.I.16b})$$

$$H_{\dots} = B \sum G(S_g, S_{g+\Delta}) \alpha_{g,<}^* \alpha_{g+\Delta,>} + \text{c.c.}, \quad (\text{Ap.I.16c})$$

where $\alpha_{g,>}^*$, $\alpha_{g,>}$ are the operators of creation and of annihilation of a spinpolaron on the g -atom, if the total spin of the atom and the electron localized on it is equal to $S - 1/2$, and $\alpha_{g,<}^*$, $\alpha_{g,<}$ are similar terms for the case when the total spin is $S + 1/2$. The commutation relations connecting the spin operators may obviously be assumed to be of the Fermi type. The problem is discussed in more detail in [71].

The equivalence of the Hamiltonian (Ap. I.16) and the Hamiltonian present in the wave equation (Ap. I.13, 14) is easily proved by applying H (Ap. I.16) to the single-electron wave function of the system represented in terms of spinpolaron operators in the form

$$\psi = \sum c_{g\mu}^\mu (S^z) \alpha_{g\mu}^* |0\rangle, \quad (\text{Ap.I.17})$$

where $|0\rangle$ is the vacuum function of the spinpolaron.

It will be seen from expression (Ap. I.16) that in the first order in WAS the Hamiltonians H_{\dots} and H_{\dots} can be considered independently of one another. By making use of the Holstein-Primakoff transformations (2.4.1), we are able to obtain from the Hamiltonians H_{\dots} and H_{\dots} (Ap. I.16a, b) the corresponding Hamiltonians (3.5.18a, b) in the spin-wave approximation.

In case of $A > 0$, choosing the effective spin equal to that of a free atom S , we lose one of the states of the atom occupied by an electron, because its multiplicity is greater than that of the free atom. At low-level excitations of a ferromagnetic crystal or at high spin values this circumstance may be ignored, but in some cases one has to take into account all possible states. Below we shall construct

a spinpolaron Hamiltonian that takes account of all the states of atoms occupied by electrons. To this end we must choose the magnitude of the spin of an atom occupied by an electron $T = S + 1/2$ as an effective spin and regard the electron creation and annihilation operators in (3.1.2) as the operators of the annihilation and creation of a hole on the same atom, respectively. Here the part of the integral of exchange between the hole and the atomic spin will be played by the quantity $(-A)$, i.e. the problem reduces to the one already discussed up to the substitution of the "antispinpolaron" operators for the spinpolaron operators in the Hamiltonian $H_{<}$. Returning to spinpolaron operators conjugate to those of the antispinpolaron and making use of the commutation relations for the spin components (2.1.2), we obtain from $H_{<}$ (Ap. I.16)

$$H_{>} = -\frac{AS}{2} \sum \alpha_{g,>}^* \alpha_{g,>} - \frac{B}{2S+1} \sum \left\{ V \frac{1}{(T \pm T_g^z)(T \pm T_{g-\Delta}^z)} + \frac{1}{\sqrt{T \pm T_g^z - 1}} T_g^- T_{g-\Delta}^- \frac{1}{\sqrt{T - T_{g-\Delta}^z - 1}} \right\} \alpha_{g,>}^* \alpha_{g,>} \quad (\text{Ap. I.18})$$

Here T_g^z , T_g^\pm have the meaning of appropriate projections of the g -atom spin, which coincides with the true one only if there is an electron on the atom. In case of its absence T_g^z is by $1/2$ larger than the actual atomic spin projection. Hence, the states of atoms unoccupied by electrons with $T_g^z = -(S + 1/2)$ are nonphysical states, this being automatically accounted for by the structure of Hamiltonian (Ap. I.18). Indeed, the effective Bloch integral (i.e. the coefficient in front of $\alpha_{g,>}^* \alpha_{g+\Delta,>}$) vanishes for $T_g^z = -(S + 1/2)$.

Compare now the classical Hamiltonians $H_{>}$ and $H_{<}$ (3.5.3) obtained below with the Hamiltonians $H_{>}$ and $H_{<}$, respectively, in the large spin limit. Substituting into the latter the components of the vector \mathbf{S}_g expressed in terms of the angles θ_g and φ_g we obtain that the canonical transformation

$$\alpha_{g\uparrow}^* = \exp \left\{ -\frac{i\varphi_g}{2} \right\} \alpha_{g,>}^*,$$

$$\alpha_{g\downarrow}^* = \exp \left\{ \frac{i\varphi_g}{2} \right\} \alpha_{g,<}^*,$$

transforms the Hamiltonian $H_{>}$ into $H_{<}$ and the Hamiltonian $H_{<}$ into $H_{>}$. This proves the equivalence of these Hamiltonians.

It is an interesting point that $F^{(1)}$ in (Ap. I.16b) for $S = 1/2$ is independent of the spin configuration. Hence, the case $S = 1/2$, $A < 0$ is a unique instance when the electron energy does not diminish in the course of FM ordering, although it does not grow as well. However, when we take into account the terms of the following order in W/AS , we obtain that FM ordering in this case, too, minimizes the charge carrier energy.

The procedure developed above enables the equivalence of the polar model of a magnetic semiconductor and the particular case of the c - l model with $S = 1/2$, $|A| S \gg W$, $A < 0$ to be proved. The Shubin-Vonsovsky polar model [42] has very much in common with that of Hubbard. In particular, in it, with the number of electrons being equal to that of atoms, every electron in the limit of strong Coulomb repulsion acting between the electrons is localized on its own atom. However, in contrast to the Hubbard model, the polar model also accounts for the direct exchange between the neighbouring atoms.

We shall presume for the sake of simplicity that the dominant part is played by the direct exchange between the electrons of neighbouring atoms, and that the contribution to the exchange of the virtual transitions of electrons to neighbouring atoms can be neglected. We shall also presume the number of electrons to be by one greater than the number of atoms, i.e. that every atom but one is occupied by an electron, one atom being occupied by two electrons. Since the Coulomb energy does not change as a result of the transitions of the extra electron from atom to atom, it need not be written out, and the Hamiltonian (1.5.1) can be represented in the following form

$$H_{dd} = B' \sum P a_{g\sigma}^* a_{g+\Delta, \sigma} P - \frac{1}{8} \sum \mathcal{J}(\mathbf{g}-\mathbf{f}) P a_{g\sigma}^* a_{f\sigma} a_{f\sigma}^* a_{g\sigma} P \quad (\text{Ap.I.19})$$

(the contributions of other terms are of higher orders in the overlapping of the orbits of neighbouring atoms and are not taken into account because of it). The symbol P denotes the operator of projection into the subspace of such functions that describe the occupation of one of the atoms by two electrons and of the rest by one electron each (only one charge carrier is presumed to exist in the crystal).

The wave function of the system being considered is represented in the form

$$\psi = \sum_{\{\sigma_f\}} c_{\mathbf{g}}(\{\sigma_f\}_{\mathbf{g}}) a_{\mathbf{g}\uparrow}^* a_{\mathbf{g}\downarrow}^* \prod_{f \neq \mathbf{g}} a_{f\sigma_f}^* |0\rangle, \quad (\text{Ap.I.20})$$

where $|0\rangle$ is the vacuum function, $\{\sigma_f\}_{\mathbf{g}_1 \dots \mathbf{g}_n}$ is a set of all indices of σ_f except $\sigma_{\mathbf{g}_1} \dots \sigma_{\mathbf{g}_n}$. Making use of expressions (Ap. I.19, 20) and (2.1.3), we can obtain the following representation for the wave equation

$$i \frac{\partial}{\partial t} c_{\mathbf{g}}(\{\sigma_f\}_{\mathbf{g}}) = B' \sum_{\Delta \tau_{\mathbf{g}}} c_{\mathbf{g}+\Delta}(\tau_{\mathbf{g}}, \{\sigma_f\}_{\mathbf{g}, \mathbf{g}+\Delta}) \delta(\tau_{\mathbf{g}}, \sigma_{\mathbf{g}+\Delta}) - \sum_{\mathbf{h}, \mathbf{l} \neq \mathbf{g}} \sum_{\tau_1 \tau_{\mathbf{h}}} \mathcal{J}(\mathbf{h}-\mathbf{l}) (s_{\sigma_1 \tau_1} \cdot s_{\sigma_{\mathbf{h}} \tau_{\mathbf{h}}}) c_{\mathbf{g}}(\tau_1, \tau_{\mathbf{h}}, \{\sigma_f\}_{\mathbf{h}, \mathbf{g}}). \quad (\text{Ap.I.21})$$

On the other hand within the framework of the c - l model the wave equation can be obtained in the form (Ap. I.21) by making use of the Hamiltonian $H_c + H_M$ (Ap. I.16) and of the wave function (Ap. I.17) with $c_g^{++} = 0$ and by putting $B' = B/2$. Hence, the c - l model is applicable also in cases when l -electrons act as charge carriers in magnetic semiconductors.

APPENDIX II. SPONTANEOUS HALL AND FARADAY EFFECTS

Hall Effect. Whereas in nonmagnetic materials the Hall and the Faraday effect are produced only in external magnetic fields, in FM they exist also in the absence of a magnetic field (spontaneous Hall and Faraday effects). The mean field acting on an electron in a medium is equal to the magnetic induction $\mathfrak{B} = \mathfrak{H} - 4\pi\mathbf{M}$ [264], i.e. in FM in the absence of an external field it is proportional to the magnetic moment per unit volume $M = \mathfrak{M}'a^3$. The part of the Hall potential proportional to \mathfrak{B} is conventionally termed in magnets normal Hall effect. However, the actual field acting on an electron differs from the mean magnetic field \mathfrak{B} . This produces an additional contribution to the Hall potential, which received the name of anomalous Hall effect: because of the presence of two pseudovectors \mathfrak{B} and \mathbf{M} in the system, the linear relationship between the electric field in the medium \mathcal{E} and the current \mathbf{j} is established by the expression

$$\mathcal{E} = \sigma^{-1}\mathbf{j} + R[\mathfrak{B} \times \mathbf{j}] + R_A[\mathbf{M} \times \mathbf{j}], \quad \mathbf{M} = \mathfrak{M}'a^3, \quad (\text{Ap. II.1})$$

where R and R_A are termed constants of the normal and the anomalous Hall effect, respectively. To make the comparison of the magnitudes of the normal and the anomalous Hall effect more convenient, the latter can be characterized by the magnitude of the equivalent field $\mathcal{B}_A = R_A M / R$ for which the normal Hall effect coincides in magnitude with the anomalous (for $\mathfrak{B} = 0$) [363].

As to the origin of the anomalous Hall effect, it cannot be the result of the c - l exchange acting on the c -spins without affecting the orbital motion of the c -electrons. It can be caused only by spin-orbital interaction. The Hamiltonian H_{S_0} (2.2.2) that describes it consists of two terms. The first corresponds to the interaction of the orbit of an electron with its own spin, and the second—with the spins of all other electrons. Since we are not interested in the interaction of the conduction electron spins with the orbits of electrons of partially-filled shells, we shall in future consider the orbital motion only of conduction electrons. The second term in (2.2.2) permits of a simple physical interpretation: it corresponds to the Lorentz force acting on a conduction electron, because the l -spin located at point

\mathbf{g} , being a magnetic dipole, sets up at point \mathbf{r} a magnetic field

$$\mathcal{H}_{\mathbf{g}}(\mathbf{r}) = -2\mu_B \nabla \{[\mathbf{S}_{\mathbf{g}} \cdot (\mathbf{r} - \mathbf{g})][|\mathbf{r} - \mathbf{g}|^3]\}. \quad (\text{Ap. II.2})$$

At $T = 0$ there should be no anomalous Hall effect. Indeed, because of the absence of thermal vibrations, the atoms form an ideal periodic structure. By reason of this the force ∇U , which enters the expression for the energy of interaction of a c -orbit with its own spin, has the periodicity of the lattice, i.e. its quasi-momentum remains a well-defined quantum number, and no deviation of the electron in its rectilinear motion takes place. On the other hand, according to (Ap. II.2), in case of the ideal ferromagnetic ordering the mean magnetic field with which the l -spins act on a c -electron is equal to $4\pi\mathbf{M}$ [360] and therefore is part of the induction \mathbf{B} to which the normal Hall effect is proportional. As for the deviations of this field from the mean value, they have the periodicity of the lattice and for reasons stated above cannot produce a Hall effect.

At finite temperature the Hall effect is nonzero. Below we shall examine in detail the contribution to it of the interaction of a c -electron orbit with the spins of l -atoms, which is of greatest importance in lightly-doped magnetic semiconductors. The Hamiltonian H_{S_0} is linear in the magnetic moment of the crystal. Since the effect being considered is also linear in the magnetization of the crystal, the Hamiltonian H_{S_0} can enter the expression for the Hall field only linearly. On the other hand the effect is associated with thermal magnetization fluctuations, and if simply averaged over them will disappear. To obtain a nonzero result, the spin-orbital interaction must interfere with the isotropic c - l interaction, which is a function of the same fluctuations. The resultant effect is linear in the unit vector directed along the preferred direction, i.e. the magnetic moment, but nonlinear in the fluctuations, and because of it remains finite after being averaged over them.

Since the effect is associated with the fluctuations of the magnetization, it would be natural to interpret it in terms of electron scattering by them. We should deal with two scattering mechanisms: with the c - l exchange mechanism and the spin-orbital. In the Born approximation each of these mechanisms operates independently of the other, and to obtain their interference, we must go beyond this approximation. In the result we obtain that the scattering probability becomes anisotropic: the frequency of electron transitions to states with a definite direction of the momentum becomes greater than that of transitions to states with an opposite direction of the momentum. This direction is orthogonal to the applied electric field and to the spontaneous moment of the crystal. The flow of particles in this direction is prevented by the appearance of a transverse Hall field that compensates the scattering anisotropy.

The calculation of the anomalous Hall effect is appreciably facilitated by the possibility of using the effective mass approximation (Sec. 4.2) [363]. Going over with the aid of formulae (2.4.1) from the l -spin to magnon operators and from the coordinate representation for the c -electrons to that of secondary quantization, we obtain from the second term in (2.2.2) the Hamiltonian of interaction of the c -orbit with the l -spins in the following form:

$$\begin{aligned} \tilde{H}_{S0} &= \frac{2e\mu_B}{m_0 c} \sum \mathcal{H}_{\mathbf{g}\mathbf{g}'\mathbf{f}} a_{\mathbf{g}}^* b_{\mathbf{f}}^* b_{\mathbf{f}}, \\ \mathcal{H}_{\mathbf{g}\mathbf{g}'\mathbf{f}} &= \int \varphi_{\mathbf{g}}^*(\mathbf{r}) |\mathbf{r} - \mathbf{f}|^{-3} [(\mathbf{r} - \mathbf{f}) \times \hat{\mathbf{p}}]_z \varphi_{\mathbf{g}'}(\mathbf{r}) d\mathbf{r}, \end{aligned} \quad (\text{Ap. II.3})$$

where $\varphi_{\mathbf{g}}(\mathbf{r})$ is a Wannier function; the spin indices in the c -electron operators have been omitted, since all the electron spins are presumed to be similarly oriented. The terms linear in the l -magnon operators in the Hamiltonian (Ap. II.3) have been discarded, because they contribute to the effect only in higher approximations in $1/S$ (when a transformation from the bare l -magnons to the dressed magnons is performed, see Sec. 4.2).

The most significant interaction of the c -electron will be seen from formula (Ap. II.3) to be that with remote l -spins. Taking into account that the overlapping of the Wannier functions $\varphi_{\mathbf{g}}$ and $\varphi_{\mathbf{g}'}$ decays rapidly with the separation $|\mathbf{g} - \mathbf{g}'|$, we can represent the coefficient $\mathcal{H}_{\mathbf{g}\mathbf{g}'\mathbf{f}}$ in the form

$$\mathcal{H}_{\mathbf{g}\mathbf{g}'\mathbf{f}} \simeq m_0 |\mathbf{g} - \mathbf{f}|^{-3} [(\mathbf{g} - \mathbf{f}) \times \mathbf{v}(\mathbf{g} - \mathbf{g}')], \quad \mathbf{v}_{\mathbf{k}} = \frac{\hbar}{m} e^{i\mathbf{k} \cdot \mathbf{h}} \mathbf{v}(\mathbf{h})$$

where $\mathbf{v}(\mathbf{g} - \mathbf{g}')$ are matrix elements of the velocity operator in the Wannier functions. Carrying out the Fourier transformation (1.4.3) of the operators and making use of the formula $\mathbf{v}_{\mathbf{k}} = \nabla_{\mathbf{k}} E_{\mathbf{k}}$ and of (1.4.4), we reduce the Hamiltonian H_{S0} (Ap. II.3) to the form

$$\begin{aligned} \tilde{H}_{S0} &= -\frac{i}{N} \sum \mathcal{Z}(\mathbf{k}, \mathbf{k}') a_{\mathbf{k}}^* a_{\mathbf{k}'} b_{\mathbf{q}'}^* b_{\mathbf{q}} \mathcal{Z}(\mathbf{k} - \mathbf{q}, \mathbf{k} - \mathbf{q}'), \\ \mathcal{Z}(\mathbf{k}, \mathbf{k}') &= -\frac{\lambda |\mathbf{k} \times \mathbf{k}'|_z}{|\mathbf{k} - \mathbf{k}'|^2}, \quad \lambda = \frac{16\pi\mu_B^2}{a^3} \left(\frac{m_0}{m^*} \right), \end{aligned} \quad (\text{Ap. II.3}')$$

where the symbol $\mathcal{Z}(\mathbf{x}, \mathbf{y})$ expresses the quasi-momentum conservation law. In the main order in $1/S$ we may think the true magnon operators to be present in formula (Ap. II.3').

The usual method when considering the anomalous Hall effect is to write a chain of equations of motion for the density matrix [148, 321, 149]. This in effect provides a rigorous foundation for the approach to the problem, which appears natural from the physical point of view: it is necessary to solve a conventional Boltzmann equation

that takes account of the anisotropy of electron scattering

$$W_{\mathbf{k}, \mathbf{k}-\mathbf{r}} = \sum_{\mathbf{q}} \bar{W}_{\mathbf{k}\mathbf{q}; \mathbf{k}+\mathbf{r}, \mathbf{q}-\mathbf{r}},$$

where $\bar{W}_{\mathbf{k}\mathbf{q}; \mathbf{k}+\mathbf{r}, \mathbf{q}-\mathbf{r}}$ is the probability averaged over the magnons of scattering of an electron with the momentum $\mathbf{k} + \mathbf{r}$ by a magnon with the momentum $\mathbf{q} - \mathbf{r}$ involving the momentum transfer $2\mathbf{r}$.

Taking into account the first post-Born terms, we obtain for the transition probability [75]

$$W_{fi} = 2\pi \left| V_{fi} + \sum_v \frac{V_{fv} V_{vi}}{\omega_{iv} + i\eta} \right|^2 \delta(\omega_{if}), \quad (\text{Ap. II.4})$$

$$\omega_{\alpha\beta} = E_{\alpha} - E_{\beta}, \quad \eta \rightarrow 0,$$

where i, v, f are the indices of the initial, the intermediate and the final state, the excitation Hamiltonian V corresponds to the sum of the c - l exchange (4.2.4) and the c - l spin orbital Hamiltonian (Ap. II.3'). Since the coefficients of the former are real, and those of latter are imaginary, it is represented by a sum $V = V' + iV''$. In the first approximation in V'' we obtain from expression (Ap. II.4):

$$W_{fi} = W_{fi}^0 + W_{fi}^1, \quad W_{fi}^0 = 2\pi |V'_{fi}|^2 \delta(\omega_{fi}),$$

$$W_{fi}^1 = (2\pi)^2 \delta(\omega_{fi}) \left\{ V'_{fi} \sum_v (V''_{fv} V'_{vi}) \right.$$

$$\left. + V''_{fv} V'_{vi} \delta(\omega_{iv}) + V'_{fi} \sum_v V'_{fv} V'_{vi} \delta(\omega_{iv}) \right\}. \quad (\text{Ap. II.5})$$

The terms of higher orders in V'' in expression (Ap. II.5) have been dropped. The quantities $\bar{W}_{\mathbf{k}\mathbf{q}; \mathbf{k}+\mathbf{r}, \mathbf{q}-\mathbf{r}}$ are calculated by using formulae (Ap. II.5) in the main approximation in the ratio of electron momentum to the magnon momentum, which, according to Sec. 4.4, is small. In this approximation the coefficients $C_{\mathbf{q}} \equiv C_{0\mathbf{q}0}$ in the Hamiltonian V' are substituted for $C_{\mathbf{k}\mathbf{q}\mathbf{r}}$, and magnon occupation numbers $m_{\mathbf{q}}$ for $m_{\mathbf{q}+\mathbf{k}}$. We also take into account that the scattering of electrons by magnons may be regarded as elastic. Then we obtain for the anisotropic portion $W_{\mathbf{k}\mathbf{p}}^1$ of the scattering probability after summing over all the magnon momenta

$$W_{\mathbf{k}\mathbf{p}}^1 = \sum_{\mathbf{q}} \bar{W}_{\mathbf{k}, \mathbf{q}; \mathbf{p}, \mathbf{k}+\mathbf{q}-\mathbf{p}}^1 = \left(\frac{2\pi}{N} \right)^2 \mathcal{L} \sum_{\mathbf{l}} [\mathcal{K}(\mathbf{k}, \mathbf{p})$$

$$+ \mathcal{K}(\mathbf{l}, \mathbf{p}) + \mathcal{K}(\mathbf{k}, \mathbf{l}) \delta(\omega_{\mathbf{k}, \mathbf{l}}) \delta(\omega_{\mathbf{p}, \mathbf{k}}), \quad (\text{Ap. II.6})$$

$$\mathcal{L} = \frac{\pi^2 A^2 \lambda}{4N} \sum_{\mathbf{q}} m_{\mathbf{q}} (1 + m_{\mathbf{q}}) (1 + 2m_{\mathbf{q}}) C_{\mathbf{q}}^2.$$

The contribution of two last terms in expression (Ap. II.6) will easily be seen to vanish in the result of summing over \mathbf{l} . For example,

the second term vanishes, because

$$\sum_{\mathbf{l}} \frac{|\mathbf{l} \times \mathbf{p}|_z}{|\mathbf{l} - \mathbf{p}|^2} \delta(\omega_{\mathbf{pl}}) = \sum_{\mathbf{l}} \frac{\mathbf{l} \cdot \mathbf{p} \times \mathbf{b}_z}{2(p^2 - \mathbf{p} \cdot \mathbf{l})} \delta\left(\frac{p^2 - l^2}{2m^*}\right), \quad (\text{Ap. II.6}')$$

where \mathbf{b}_z is a unit vector pointing along the Z-axis. Indeed, the numerator of (Ap. II.6') is odd with respect to the components of the vector \mathbf{l} orthogonal to the vector \mathbf{p} , there being no such components in the denominator, and the argument of the delta-function being even in them.

The Boltzmann equation in the case being considered takes the form

$$e(\mathbf{v}_{\mathbf{k}} \cdot \mathcal{E}) \frac{\partial n_{\mathbf{k}}}{\partial E} = \sum_{\mathbf{p}} \{W_{\mathbf{p}\mathbf{k}}^0 + W_{\mathbf{p}\mathbf{k}}^1\} (f_{\mathbf{p}} - f_{\mathbf{k}}). \quad (\text{Ap. II.7})$$

The field applied to the crystal is presumed to point along the X-axis. Since the moment points along the Z-axis, a field is established in the crystal directed along the Y-axis and proportional to the small anisotropic part of the scattering probability W^1 . The solution of equation (Ap. II.7) is sought in the form of an expansion

$$f_{\mathbf{k}} = n_{\mathbf{k}} + (\psi_x k_x + \psi_y k_y) \frac{\partial n_{\mathbf{k}}}{\partial E}, \quad (\text{Ap. II.8})$$

the quantity ψ_y being also presumed small.

In the zeroth approximation equation (Ap. II.7) coincides with (4.4.1), and the expression for ψ_x is

$$\psi_x = - \frac{e \mathcal{E}_x \tau_{\mathbf{k}}}{m^*} \quad (\text{Ap. II.9})$$

with the relaxation time as determined by equality (4.4.3).

In the first approximation we obtain from expressions (Ap. II.7-9)

$$e k_y \mathcal{E}_y = - \psi_y k_y m^* \tau_{\mathbf{k}}^{-1} - e \mathcal{E}_x \tau_{\mathbf{k}} \sum_{\mathbf{p}} W'_{\mathbf{kp}} (p_x - k_x). \quad (\text{Ap. II.10})$$

It follows from expression (Ap. II.6) that the integral on the right-hand side of (Ap. II.10) vanishes for $k_y = 0$, but remains finite for $k_x = 0$. Accordingly, we obtain for it the estimate

$$\frac{1}{N} \sum W'_{\mathbf{kp}} (p_x - k_x) \sim \mathcal{L} g_{\mathbf{k}}^2 k_y \alpha, \quad g_{\mathbf{k}} \equiv g_e(E_{\mathbf{k}}), \quad (\text{Ap. II.11})$$

where g_e is the electron density of states (1.2.10), and $\alpha \sim 1$.

Expressing ψ_y in terms of the field \mathcal{E}_y and equating the current in the direction of the Y-axis to zero

$$\frac{e}{m^*} \sum_{\mathbf{k}} \psi_y(\mathbf{k}) k_y^2 \frac{\partial f_{\mathbf{k}}^0}{\partial E} = 0, \quad (\text{Ap. II.12})$$

we obtain the expression for the anomalous Hall field \mathcal{E}_y . In accordance with the definition of the constant of the anomalous Hall effect (Ap. II.1), it is expressed in terms of the Hall field by the relation

$$R_A = \mathcal{E}_y / \mathcal{E}_x \sigma M, \quad (\text{Ap. II.13})$$

where σ is the conductivity of the crystal

$$\sigma = -\frac{e^2}{(m^*)^2} \sum k_x^2 \tau_k \frac{\partial f_k^0}{\partial E} \equiv \frac{ne^2 \langle \tau \rangle}{m^*}. \quad (\text{Ap. II.14})$$

This constant, according to formulae (Ap. II.10-14), is equal to

$$R_A = \frac{\alpha \mathcal{L} e^2}{M \sigma^2 (m^*)^2} \sum k_y^2 \tau_k^2 \frac{\partial f_k^0}{\partial E} g_k^2 \equiv -\frac{\alpha \mathcal{L} m^*}{M e^2 n} \frac{\langle \tau^2 g_e^2 \rangle}{\langle \tau^2 \rangle}, \quad (\text{Ap. II.15})$$

where the definition of the averaged values $\langle \tau \rangle$ etc. will be obvious from formulae (Ap. II.14, 15) themselves.

To obtain an expression for the equivalent field \mathcal{H}_A from formula (Ap. II.15), one should make use of the expression for the constant of the normal Hall effect [214]:

$$R = R_0 \frac{\langle \tau^2 \rangle}{\langle \tau \rangle^2}, \quad R_0 = 1/nec, \quad (\text{Ap. II.15}')$$

$$\frac{\mathcal{H}_A}{\mathcal{H}_0} = \frac{16\pi^2}{S} \alpha \frac{\langle \tau^2 g_e^2 \rangle}{\langle \tau^2 \rangle} \frac{1}{N} \frac{d^2}{d\beta^2} \sum_q C_q^2 \frac{m_q}{\omega_q^2}, \quad (\text{Ap. II.16})$$

where

$$\mathcal{H}_0 = \frac{8\pi\mu_B S}{a^3}, \quad \beta = \frac{1}{T}.$$

The anomalous Hall field \mathcal{H}_A will be seen from formula (Ap. II.16) to be zero at $T = 0$, but to rise rather rapidly with the temperature. For $2S \gg 1$ inside the limits of applicability of the spin-wave approximation the effect is especially large in the region $T > T_c$, where it grows with the temperature as T^3 for degenerate and as T^4 for nondegenerate semiconductors. For $W \gg AS$ we obtain from formula (Ap. II.16) the following estimate (\bar{E}_k is the mean kinetic electron energy)

$$\mathcal{H}_A / \mathcal{H}_0 \sim 10 \sqrt{\frac{AS}{W}} \frac{\bar{E}_k}{W} \left(\frac{T}{T_c} \right)^3, \quad T_c \simeq \frac{T_c S}{3}. \quad (\text{Ap. II.17})$$

In the opposite limit of narrow bands $W \ll AS$ it follows from formula (Ap. II.16) that

$$\frac{\mathcal{H}_A}{\mathcal{H}_0} \sim 10 \frac{\bar{E}_k}{W} \left(\frac{T}{T_c} \right)^3. \quad (\text{Ap. II.17}')$$

The field \mathcal{H}_0 is by definition the induction in a fully magnetized ferromagnet, so that $\mathcal{H}_A / \mathcal{H}_0$ is actually the ratio of the anomalous and normal Hall voltage in a vanishing external field. The role of

the anomalous Hall effect will be seen from formula (Ap. II.17) to increase with the growth of the mean electron kinetic energy \bar{E}_k . Whereas in metals the parameter $\bar{E}_k W$ is of the order of unity, in semiconductors it is small. Because of that the anomalous Hall effect should be much less pronounced in semiconductors than in metals. The presence of the parameter $\bar{E}_k W$ in formula (Ap. II.17) reflects the physical fact that the electron wavelength in a semiconductor is great, and because of that an almost complete averaging of the fluctuations takes place over it, so that the electron on the whole responds only to the mean field $\bar{\mathcal{H}}$. For this reason the normal Hall effect is as a rule dominant in semiconductors.

Choosing for the purpose of evaluation the parameters corresponding to those of europium chalcogenides: $S = 7/2$, $W = 4$ eV, $AS = 0.5$ eV, we obtain, according to (Ap. II.17), that even as T_c is approached the anomalous Hall effect in semiconductors with $T_c \sim 10$ -100 K remains negligibly small as compared with the normal. In degenerate semiconductors, according to (Ap. II.17), the anomalous Hall effect caused by the electron-magnon scattering becomes noticeable only at carrier concentrations $n \sim 10^{21}$ cm $^{-3}$. This estimate is in accord with the experimental fact that no anomalous Hall effect is observed in EuO and EuS with smaller carrier concentrations [119-122]. According to (Ap. II.17), the conditions for the observation of the anomalous Hall effect are to some extent more favourable in narrow-band semiconductors. The problem of the magnitude of this effect in the immediate vicinity of the Curie point has at present found no solution.

In heavily-doped semiconductors spatial fluctuations of the electrostatic field of imperfections due to the random nature of their distribution should also make their contribution to the anomalous Hall effect. The calculations of [364] for the case of FM metals with delocalized d -electrons can be automatically adapted to this case, the only difference being that the vector of the relative magnetization \mathbf{M}/M in the averaged first term of (2.2.2) must be replaced by the vector of the relative magnetization of the c -electrons \mathbf{M}_I/M_I (we could also introduce into expression (Ap. II.1) a term in the form of $[\mathbf{j} \times \mathbf{M}_I]$, but since the vectors \mathbf{M} and \mathbf{M}_I are collinear, it may be regarded as accounted for by the corresponding renormalization of the constant R_A).

According to [364], such an effect is nonzero in the third order in the electrostatic potential of the imperfections, if the matrix elements of the potential are calculated in the wave functions of the zeroth approximation that includes the spin-orbital interaction. Since the latter in the case of nondegenerate electron bands is itself calculated in the first order of the perturbation theory, the effect will be obtained only in the fourth order of the perturbation theory, if

the usual Bloch functions with a fixed spin direction are chosen as the unperturbed electron states. Thus, the relative contribution of imperfection scattering to the anomalous Hall effect may be expected to be much less than to the resistivity (the latter, same as the magnon, corresponds to the second order of the perturbation theory). However, it is hardly possible to obtain reliable estimates of the anomalous Hall effect due to imperfection scattering, since we have to know the detailed pattern of the crystal lattice potential and the structure of the energy bands.

Faraday Rotation. The spontaneous Faraday rotation of the plane of polarization of light at finite frequencies is an analogue of the spontaneous Hall effect. From phenomenological considerations of the type which resulted in formula (Ap. II.1), it follows that the vectors of the magnetic and the electric induction are related to vectors of corresponding field strengths by the expressions

$$\begin{aligned}\mathbf{B} &= \mu \mathcal{H} + i [\mathcal{H} \times \mathcal{G}_m] \equiv \hat{\mu} \mathcal{H}, \\ \mathbf{D} &= \varepsilon \mathcal{E} + i [\mathcal{E} \times \mathcal{G}_e] \equiv \hat{\varepsilon} \mathcal{E},\end{aligned}\quad (\text{Ap. II.18})$$

where \mathcal{G}_m , \mathcal{G}_e are vectors proportional to the magnetization. The second terms in expressions (Ap. II.18) are imaginary, because the components of the magnetic permeability μ and dielectric permittivity $\hat{\varepsilon}$ tensors must satisfy the Onsager relations of the type

$$\varepsilon_{ij}(\omega, \mathcal{H}) = \varepsilon_{ji}(\omega, -\mathcal{H}). \quad (\text{Ap. II.19})$$

The spontaneous Faraday effect consists in the rotation of the polarization plane of light propagating in the direction of the crystal magnetic moment. Indeed, oscillations along two axes orthogonal to each other and to the moment, according to formulae (Ap. II.18) and (Ap. II.19), are interconnected. Because of that the original direction of oscillations cannot be maintained in the course of the wave propagating in the crystal. Since the Maxwell equations reduce to a second-order differential equation with respect to spatial and temporal derivatives of the field, two waves propagating in the specified direction correspond to every frequency. In the isotropic case they constitute an arbitrary pair of plane waves with mutually orthogonal polarization planes. In case the medium has a preferential axis, and the wave propagates in its direction, it follows from the cylindrical symmetry of the problem that only clockwise- and anticlockwise-polarized oscillations, which have the same symmetry, can be the eigenoscillations of such a system. Two different refractions indices n_+ and n_- correspond to them.

Any plane wave can be represented as a superposition of two circularly-polarized waves rotating in opposite directions. Since they propagate in the crystal with different velocities $v_{\pm} = c n_{\pm}$, the polarization plane of a plane wave incident on the crystal changes

as the wave propagates in it. The angle of rotation per unit length is given by the expression

$$\theta_F = \frac{\omega}{2c} (n_+ - n_-). \quad (\text{Ap. II.20})$$

In the ultrahigh-frequency band the difference between n_+ and n_- is determined by the magnetic gyration vector \mathcal{G}_m . The electric gyration vector \mathcal{G}_e can be put equal to zero [42]. Then the refraction indices will be given by expressions whose structure follows from simple physical considerations

$$n_{\pm} = \sqrt{(1 + 4\pi\chi_{\pm}) \varepsilon}, \quad \chi_{\pm} = \frac{\chi_{\perp}}{1 \mp \omega/\omega_{\mathcal{H}}}, \quad (\text{Ap. II.21})$$

where $\chi_{\mp} = \chi_{xx} \pm i\chi_{xy}$ are the magnetic susceptibilities of the crystal for anticlockwise- and clockwise-polarized waves propagating along the Z-axis to which the crystal moment \mathbf{M} ($4\pi\chi_{xy} = i\mathcal{G}_m$) is parallel. By reason of the magnetic field of the waves being orthogonal to the crystal moment, χ_{xy} are proportional to the transverse susceptibility $\chi_{\perp} = M'\mathcal{H}$, where \mathcal{H} is the external static field along the crystal moment (this expression of χ_{\perp} follows from the fact that for a small variation of the field $\delta\mathcal{H}$ orthogonal to \mathcal{H} the moment rotates through the angle $\delta\mathcal{H}/\mathcal{H}$ without changing its magnitude). The nature of the frequency dependence of χ_{\pm} is determined from the condition that they have a pole at the frequency of the ferromagnetic resonance. This resonance sets in when the frequency of electromagnetic waves coincides with the frequency of an infinitely long-wave magnon equal to \mathcal{H} . The difference in frequencies of the clockwise- and anticlockwise-polarized waves is also taken into account.

It follows from formulae (Ap. II.20, 21) that for $\omega \gg \mathcal{H}$ the Faraday rotation is frequency-independent. This is a property typical of long-wave Faraday rotation in FM.

In the optical frequency band quantum-mechanical effects become of essential importance. In the presence of optical absorption the effect of magnetization on the optical properties of the crystal makes itself manifest not only by means of Faraday rotation of the polarization plane, but also by means of optical dichroism (the dependence of the light absorption coefficient on the polarization). Despite the fact that, according to [314], in the optical band as well such effects may in a considerable degree be determined by the magnetic gyration vector, the high-frequency magnetic susceptibility is quite often nearing unity. Accordingly, the chief part in the optical band is usually played by the electric gyration vector $\mathcal{G}_e = -i\varepsilon_{xy}$. Correspondingly the difference between the squares of the refraction indices $n_+^2 - n_-^2 = 2\mathcal{G}_e$.

The effect of the magnetization on the optical properties of a crystal is the result of spin-orbital interaction. In contrast to the

Hall effect, the Faraday effect is generally not associated with conduction electrons already present in the crystal or appearing in the result of photoexcitation, despite the fact that in heavily-doped semiconductors conduction electrons can make some contribution to it. In principle, one can without difficulty obtain a general quantum-mechanical expression for the tensor of the high-frequency dielectric polarizability. However, because of the complex structure of the electron spectrum, it is hardly possible to use this expression for a quantitative description of the effect. That is why, we shall consider below a simplified model, which will enable us to establish the main regularities of the phenomenon. It corresponds to the Faraday rotation caused by electron transitions inside the l -shell (the creation and annihilation of Frenkel excitons on magnetic atoms).

The crystal is presumed to be built of identical single-electron atoms. The exchange interaction between the electrons establishes a ferromagnetic ordering. Every atom has two levels: a lower s -type and a higher p -type. The spin-orbital interaction in the atom is described by a Hamiltonian in the form of $\lambda (\mathbf{L} \cdot \mathbf{s})$, where \mathbf{L} is the orbital angular momentum operator of the electron, \mathbf{s} , as before, being its spin operator. Such a Hamiltonian is obtained by averaging the first term in formula (2.2.2) over the orbital state of the electron [75]. Taking into account that in the FM state spins of all electrons point in the direction of the Z -axis, we write the Hamiltonian of every atom in the form

$$H = E_s a_s^* a_s + E_p \sum_{i=x, y, z} a_i^* a_i - \frac{i\lambda}{2} (a_x^* a_y - a_y^* a_x) \quad (\text{Ap.II.22})$$

(the spin index is omitted, the wave functions of p -level are presumed to be polarized along the coordinate axes:

$$\psi_z = \psi_0, \quad \psi_x = 2^{-1/2} (\psi_1 + \psi_{-1}), \quad \psi_y = -i2^{-1/2} (\psi_1 - \psi_{-1}),$$

where ψ_m are wave functions with definite values $m = 0, \pm 1$ of the projection of the orbital angular momentum L^z).

In accordance with the general theory of linear response to an external excitation [312], the atom polarizability tensor is expressed in terms of the retarded Green's function constructed of dipole moment projection operators P_i :

$$\alpha_{ij} = - \langle \langle P_i | P_j \rangle \rangle_\omega, \quad P_i = er (a_s^* a_i + a_i^* a_s), \quad (\text{Ap.II.23})$$

where r is the matrix element of the coordinate r_i in functions ψ_s and ψ_i . The equations of motion for Green's functions present in

expression (Ap. II.23) are written down as follows (see Sec. 3.2)

$$\begin{aligned}
 (\omega - \nu) \langle \langle a_x^* a_x | a_y^* a_s \rangle \rangle &= -\frac{i\lambda}{2} \langle \langle a_x^* a_y | a_y^* a_s \rangle \rangle, \\
 (\omega + \nu) \langle \langle a_x^* a_s | a_y^* a_y \rangle \rangle &= \frac{i\lambda}{2} \langle \langle a_y^* a_s | a_s^* a_y \rangle \rangle, \\
 (\omega - \nu) \langle \langle a_s^* a_y | a_y^* a_s \rangle \rangle &= 1 + O(\lambda), \\
 (\omega + \nu) \langle \langle a_y^* a_s | a_s^* a_y \rangle \rangle &= -1 + O(\lambda), \\
 \nu &= E_p - E_s.
 \end{aligned}
 \tag{Ap.II.24}$$

The following expressions for the polarizability tensor components are obtained from them in the main order in λ :

$$\alpha_{xy} = \frac{\lambda \omega \alpha_{xx}}{\nu^2 - \omega^2}, \quad \alpha_{xx} = \frac{2e^2 r^2 \nu}{\nu^2 - \omega^2}. \tag{Ap.II.25}$$

The tensor is related to the dielectric function tensor by the expression

$$\varepsilon_{ij} = \delta_{ij} - 4\pi \alpha_{ij} a^{-3}.$$

It follows from expression (Ap. II.25) that the Faraday rotation proportional to $\text{Re } \alpha_{xy}$ passes through a maximum near the resonance frequency $\omega = \nu$. The optical dichroism also appears at this frequency. The difference between the absorption coefficient of the clockwise- and anticlockwise-polarized waves is proportional to $\text{Im } \alpha_{xy}$. In contrast to the diagonal polarizability, the off-diagonal does not change signs after passing through the resonance.

In the model analyzed above every magnetic atom causes spontaneous Faraday rotation independently of the others. The role of FM ordering is to make every atom rotate the polarization plane in the same direction. It is obvious that at finite temperatures the resultant Faraday rotation should be proportional to the average magnetization.

APPENDIX III. EFFECT OF INDIRECT EXCHANGE ON HELICOIDAL ORDERING AND ON THE STRUCTURE OF DOMAIN WALLS IN FERROMAGNETS

As a rule, helicoidal ordering is the result of anisotropy of the exchange interaction in a low-symmetry crystal, but sometimes it is also possible in isotropic materials, e.g. in some magnetic semiconductors with a cubic symmetry (in chrome spinels HgCr_2S_4 , ZnCr_2Se_4 , etc.).

This section is intended to elucidate the nature of magnetic ordering in such materials in the presence of conduction electrons [263].

We shall analyze uniform magnetic structures in a magnetic semiconductor with anisotropic exchange made up of layers of magnetic atoms ferromagnetically ordered inside each layer, taking into account the direct exchange between the nearest and next-nearest neighbours and the indirect exchange via conduction electrons (helicoidal ordering in the absence of electrons has been considered in Sec. 3.2).

It will be demonstrated that, if the moments of the layers form a simple helix, its gradual transformation into the FM ordered structure in the course of an increase in carrier concentration is possible only if the period of the helix is large. In the opposite case an intermediate state may be formed, which is in principle impossible in the Heisenberg model. An FM helicoid whose particular case is the CAF structure considered in Sec. 6.2 may be such a state.

For $W \gg AS$, a qualitative understanding of these results may be gained from the fact that, according to formula (3.2.6), for small helicoid vectors the conduction electron aligns its spin in the direction of the local magnetic moment and because of it gains almost fully in the c - I exchange energy. It will be clear from this that, if the helicoid vector q is small, the introduction of electrons into the conduction band should result not in a magnetization of the crystal, but only in a decrease in the magnitude of q . However, for $q > q_0$ a dependence of the energy on the helicoid period appears only in the second order in AS IV, whereas on the magnetization already in the first. For this reason, beginning from a definite carrier concentration, a smaller energy will correspond to the magnetized state (to the FM helicoid) than to a simple spiral. The helicoid period corresponding to minimum energy must also obviously change with the appearance of the electrons, but comparatively little.

A domain wall in an FMS can also be regarded as a helicoidal-type ordering. The presence of conduction electrons makes the wall thicker in the same way as it makes the helicoid vector shorter.

To establish the nature of magnetic ordering at not too high conduction electron concentrations, let us analyze how FM ordering loses its stability when the carrier concentration is decreased. To this end find the conditions under which the magnon frequencies with a nonzero momentum vanish. As in (2.3.2), we shall take into account the direct exchange between two coordination spheres. The electron dispersion law will be used in the form of (1.1.1). Since the direct exchange between the layers is nonferromagnetic, the frequency ω_q for a specified q will be minimum, if the vector q points in the direction of the helicoid axis c . For such $q \parallel c$ we obtain from (2.4.4) and (4.2.4) up to terms $\sim \mu/AS \ll 1$:

$$\omega_q = \mathcal{Y}_1(1 - \cos aq) + \mathcal{Y}_2(1 - \cos 2aq) + \frac{2\alpha(1 - \cos aq)|B|v}{S(2\alpha + (1 - \cos aq))} = \frac{4|\mathcal{Y}_2||B|(1 - \cos aq)}{AS + 2|B|(1 - \cos aq)}$$

$$\times \left\{ \left[2 \sin^2 \frac{aq}{2} - \left(\frac{\gamma_1}{4\gamma_2} + 1 - \alpha \right) \right]^2 - \left(\frac{\gamma_1}{4\gamma_2} + 1 + \alpha \right)^2 + \frac{Av}{4|\gamma|} \right\}, \quad (\text{Ap. III.1})$$

$$\alpha = \frac{AS}{4|B|}, \quad \gamma_i = 2S\mathcal{J}_i.$$

As seen from formula (Ap. III.1), the sign of ω_q coincides with that of the factor in braces, and the frequency to vanish first is one that corresponds to the minimum of this factor. Accordingly, one may conveniently consider three regions of parameter variation separately.

1. Consider first the case when $\gamma_1/4\gamma_2 - 1 > \alpha$. Here the first to vanish is the magnon frequency with $q = q_1 = \pi a$ at $v = v_{cM1} = \frac{4|\gamma_1|}{A}$. This result means that at $v < v_{cM1}$ the FM state is unstable for the formation of an AF structure with a long-range order. Note that in Case 1 the crystal is an antiferromagnet in the absence of conduction electrons. This situation is similar to the one discussed in Sec. 6.2: at $v < v_{cM1}$ a two-sublattice intermediate state may be one of the possibilities to materialize.

2. If $\left| \frac{\gamma_1}{4\gamma_2} - \alpha \right| < 1$, the first to vanish will be the frequency with $q = q_2 = \frac{1}{a} \arccos \left(\alpha - \frac{\gamma_1}{4\gamma_2} \right)$ at a concentration $v_{cM2} = \frac{4|\gamma_2|}{A} \times \left(\frac{\gamma_1}{4\gamma_2} + 1 + \alpha \right)^2$. Here at $v = 0$ a simple spiral with a small enough period $aq = \arccos \left(-\frac{\gamma_1}{4\gamma_2} \right) > 2 \arcsin \sqrt{\frac{\alpha}{2}}$ or (in a small region of parameter variation $0 < \frac{\gamma_1}{4\gamma_2} - 1 < \alpha$) an AF ordering corresponds to the minimum energy.

3. In case $1 - \frac{\gamma_1}{4\gamma_2} < \alpha$, the first to become negative will be the frequencies of the longest-wave magnons at $v < v_{cM3} = -\frac{(\gamma_1 + 4\gamma_2)S}{|B|}$. At $v = 0$ the structure corresponding to this case is a helicoidal one with a great period $aq < 2 \arcsin \sqrt{\frac{\alpha}{2}}$. Note that for a fixed parameter γ_2 , the following inequalities will hold for the critical concentrations v_{cMi} , which depend on the ratio γ_1/γ_2 :

$$v_{cM1} \geq \frac{16|\gamma_2|}{A} \geq v_{cM2} \geq \frac{16|\gamma_2|\alpha^2}{A} > v_{cM3}.$$

Hence it follows that for an energy of magnetic ordering of an equal order of magnitude it is much easier to make, with the aid of conduction electrons, a crystal with a helicoidal ordering go over to the FM state than one with an AF ordering.

As has already been pointed out in Sec. 6.2, if the frequency of the magnon having the momentum q is the first to vanish, the concentration transition of the second kind must result in a structure with the same wave vector being established. We shall confine ourselves to the consideration of the simplest structures with an appropriate periodicity and at the same time possessing a nonzero moment, i.e. of FM spirals. However, it is possible that the true energy minimum will correspond to more complex structures of the same symmetry.

Within the framework of the variational principle utilized below, the substitution of classical vectors with the components

$$S_g = S (\sin \theta \cos qg_z, \sin \theta \sin qg_z, \cos \theta) \quad (\text{Ap.III.2})$$

for the operators of the g atom spin corresponds to a definite choice of the trial function in which the parameters of the ferromagnetic helicoid q and θ play the part of variational parameters. The structure is determined from the condition that the total energy of the system obtained from the Hamiltonian (3.1.1) with account taken of relations (Ap. III.2) be minimum with respect to q and θ

$$\begin{aligned} E = E_e + E_M = \sum_k E_{k\pm} \theta (\mu - \tilde{E}_{k\pm}) \\ - (\psi_1 \cos aq + \psi_2 \cos 2aq) \frac{NS \sin^2 \theta}{2} \\ - (\psi_1 + \psi_2) NS \cos^2 (\theta/2). \quad (\text{Ap.III.3}) \end{aligned}$$

The expression for the electron energy in the case of a ferromagnetic helicoid is easily obtained by generalizing (3.2.6)

$$\begin{aligned} \tilde{E}_{k\pm} = \frac{E_k - E_{k-q}}{2} \\ \pm \frac{1}{2} \sqrt{(E_k - E_{k+q} - AS \cos \theta)^2 - (AS \sin \theta)^2}. \quad (\text{Ap.III.4}) \end{aligned}$$

If the state of the system is close to the FM ($\sin \theta \ll 1$), the electrons for all q 's fill one subband, and in calculations all the carriers may be presumed to occupy the band bottom (the kinetic energy $(3/5) \mu n$ is in this case presumed to be a constant, since the appropriate corrections are small, $\mu/AS \ll 1$), i.e.

$$\frac{E_e}{N} = \frac{1}{N} \sum_k E_{k\pm} \theta (\mu - \tilde{E}_{k\pm}) \simeq \text{const} - v_z |B|. \quad (\text{Ap.III.4'})$$

The expansion of the energy (Ap. III.3) in the powers of the small parameter $y = \sin \theta$ in this case takes the form, with account taken of (Ap. III.4) and (1.1.1):

$$\frac{E}{N} = \text{const} + \frac{S\omega_q y^2}{2} - \frac{|B| v \alpha^4}{4} \\ \times \left[\frac{2}{\alpha(s^2 + \alpha)^2} - \frac{1}{\alpha^3} - \frac{1}{(s^2 + \alpha)^3} + \frac{s^2 c^2}{(s^2 + \alpha)^4} \right] y^4, \quad (\text{Ap. III.5}) \\ s = \sin aq/2, \quad c = \cos aq/2.$$

Note that for $y = 0$ the energy cannot be a function of q , since this ordering is purely of the FM type. Therefore const in (Ap. III.5) is independent of y .

Since for $v_{\mathcal{M}i} > v$ the FM ordering, because of the negative sign of ω_{q_i} , is replaced by an ordering with $q \sim q_i$, the energy (Ap. III.5) is conveniently represented in the form of a power expansion for $\frac{v_{\mathcal{M}i} - v}{v} \ll 1$:

$$\frac{E}{N} = \text{const} + \mathcal{A}_0(q_i) y^2 + \mathcal{A}_2(q_i) (q - q_i)^2 y^2 \\ - \mathcal{C}_0(q_i) y^4 - \mathcal{C}_1(q_i) (q - q_i) y^4. \quad (\text{Ap. III.6})$$

Note that the term $\sim y^2$ linear in $(q - q_i)$ is not present, because the vector \mathbf{q}_i has been selected from the condition that the frequency ω_{q_i} (Ap. III.4) be minimum. We do not present the detailed expressions for the coefficients \mathcal{A} , \mathcal{C} etc., because only the signs of these coefficients are of any importance for the study of the phase transition.

Consider first Case 3, when the frequencies of the longest-wave magnons are the first to become negative. Here we should put $q_i = 0$ in formula (Ap. III.6). Besides, here we will have to take into account the next term $\sim y^6$:

$$\frac{E}{N} = \text{const} + \mathcal{A}_2 q^2 y^2 + \mathcal{A}_4 q^4 y^2 + \mathcal{C}_4 q^4 y^4 - \mathcal{G}_2 q^2 y^6 \dots \quad (\text{Ap. III.7})$$

Here $\mathcal{A}_4 > 0$, $\mathcal{C}_4 > 0$, $\mathcal{G}_2 > 0$, $\mathcal{A}_2 \sim v - v_{\mathcal{M}3}$. Since the coefficients \mathcal{A}_4 , \mathcal{C}_4 , \mathcal{G}_2 are generally not small, the terms containing higher powers of y and q can be neglected as compared with those written out in (Ap. III.7).

Making use of expansion (Ap. III.7), one may easily see that for $v < v_{\mathcal{M}3}$ there is no energy minimum with a small $y = \sin \theta$, since for any fixed value $qy \neq 0$ the energy (Ap. III.7) is a monotonous function of y . Indeed, putting $q^2 y^2 = d$, we can rewrite the expression for the energy in the form

$$E_d \sim \text{const} + \frac{\mathcal{A}_4 d^2}{y^2} - \mathcal{G}_2 d \cdot y^4.$$

From it follows immediately that the derivative $\frac{\partial E_d}{\partial(y^2)}$ is negative. For this reason a gradual transition of the complete FM ordering to an FM helicoidal one is impossible in Case 3.

Note now that for small $\cos \theta$ only one electron subband is filled in this case, and we may discard corrections $\sim \mu/AS$ and ignore the dependence of the kinetic energy on q and θ .

Substituting expression (Ap. III.4) with account taken of the terms $\sim \cos^2 \theta$ into formula (Ap. III.3), we may easily demonstrate that in the total energy the coefficient multiplying $\cos^2 \theta$ will be positive for all $v < v_{cH3}$. This means that in Case 3 a concentration-induced phase transition of the second kind to an FM helicoidal ordering is impossible not only from the FM state, but also from a simple helicoidal ordering, and that in the expression for the energy (Ap. III.3) we may put $\cos \theta = 0$:

$$\frac{E}{N} = \frac{\mathcal{V}_1 S}{2} \cos aq - \frac{\mathcal{V}_2 S}{2} \cos 2aq - 2 |B| v \cos \frac{aq}{2} + \text{const.} \quad (\text{Ap. III.8})$$

Expanding (Ap. III.8) into a series in the powers of q , we see that the coefficient in front of y^2 is proportional to $v - v_{cH3}$, and the one in front of q^4 is positive. In accordance with the Landau theory of phase transitions of the second kind, a concentration-induced phase transition from the FM state to the simple helicoidal ordering takes place at $v = v_{cH3}$. At $v < v_{cH3}$ its period is a function of the concentration

$$a^2 q^2 = \frac{8 |B| (v - v_{cH3})}{S | \mathcal{V}_1 + 20 \mathcal{V}_2 |}. \quad (\text{Ap. III.9})$$

It is worth pointing out that in actual materials the long-range dipole-dipole interaction makes an FM ordering of the entire crystal unfavourable, and it splits into FM domains. That is why, the phase transition from a helicoidal ordering should be calculated with account taken of the factors that determine the parameters of the domain structure, so that formula (Ap. III.9) is meaningful only if the period of the helicoid is much smaller than that of the domain structure.

In Case 2 at $v < v_{cH2}$ the ordering corresponding to the minimum energy (Ap. III.6) is one of the FM helicoid type. Indeed, for $q_2 < \frac{\pi}{a}$ it follows from formula (Ap. III.5) that in formula (Ap. III.6) the expansion coefficients are $\mathcal{A}_0 \sim v - v_{cH2}$, $\mathcal{A}_2 > 0$, $\mathcal{V}_0 > 0$, $\mathcal{V}_1 > 0$. For the parameters q and θ corresponding to the minimum E this leads at $v \ll v_{cH2}$ to relations typical of phase transitions of the

second kind $\sin \theta \sim (1 - v/v_{0M2})^{1/2}$ and $q - q_2 \sim -(1 - v/v_{0M2})$. As the concentration continues to decrease, starting from some definite value v_A , the minimum energy begins to correspond to helicoidal ordering without a magnetic moment. The following expression is obtained for the concentration v_A

$$v_A = \frac{S | \mathcal{Y}_1 + 4\mathcal{Y}_2 c^2 | s^2 (1 + \alpha^2 s^{-2})}{3\alpha^2 B^2 (1 - \alpha^2 c^2 s^{-4})} \mu(v_A). \quad (\text{Ap.III.10})$$

It can be demonstrated that at $v = v_A(q_A)$ a phase transition of the second kind from a simple spiral to the FM ordering takes place with $\cos \theta \sim [v - v_A(q_A)]$ and $q - q_A \sim v - v_A(q_A)$, where q_A practically coincides with q for $v = 0$. To obtain an estimate, put $|B| = 0.5$ eV, $\alpha = 1/5$, $|\mathcal{Y}_2| S = 30$ K, and the period of the helicoidal ordering equal to six lattice parameters (i.e. $s = \frac{1}{2}(1 + \frac{\mathcal{Y}_1}{4\mathcal{Y}_2}) = 1/2$). Should we presume $\sim 10^{22}$ magnetic atoms to be in a cubic centimetre, we would obtain from (Ap. III.10) $n_A \sim 10^{19} \text{ cm}^{-3}$.

Naturally the aforesaid should not be taken to mean that there will be necessarily an FM spiral when $v > v_A$. Same as in the case of a CAF, it may prove unstable with respect to short-wave magnons. However, the fact established in Sec. 6.2 that for definite parameter values the necessary conditions for the stability of an FM spiral with $q = \pi/a$ can be satisfied justifies the assertion that such conditions can also be met for $q < \pi/a$.

Similarly we can also analyze the effect of electrons on the domain wall in FMS. The spin ordering in it may be presumed to be helicoidal with a small wave vector $q(z)$ slowly varying along the z axis normal to domain boundaries. Therefore, we may use expression (3.2.8) for the energy of an electron in the domain wall in the quasi-classical approximation in the limit $a^2 q^2 \ll AS/4 |B|$:

$$\tilde{E}_p \simeq -\frac{AS}{2} + \frac{|B| a^2 q^2(z)}{4}. \quad (\text{Ap.III.11})$$

Since the electron energy is a function of the coordinates, the electron density in the domain wall is also a function of coordinates. From expression (Ap. III.11) we obtain, taking into account the inequality $\mu < AS$ and the electric neutrality of the wall as a whole, that up to terms of the second order in the deviation of the electron density from its mean value the contribution of the electrons to the energy of the wall is given by the expression

$$\sum_e \int \sigma_e dz = \frac{1}{4} |B| v \int q^2(z) dz + O(v^{5/3}), \quad (\text{Ap.III.12})$$

where σ_e is the electron energy density.

According to formula (2.3.2) and the relation $\theta(z) = q(z)a$, the contribution of the direct exchange to the energy of the wall has

the same structure as Σ_e (Ap. III.12)

$$\sum_M = \int \sigma_M dz = \frac{\mathcal{I} S^2}{a} \int q^2(z) dz \quad (\text{Ap. III.13})$$

(the factor a^{-3} appears when summing over the atoms is replaced by integration).

The quantities (Ap. III.12) and (Ap. III.13) add up, whence, according to [264], it follows that the appearance of electrons in the conduction band results in an increase in the wall thickness δ . The relative increase in the thickness of the domain wall is described by the expression

$$\frac{\delta(v)}{\delta(0)} = \left[1 + \frac{|B|v}{4\gamma S^2} \right]^{1/2}. \quad (\text{Ap. III.14})$$

According to formula (Ap. III.14), the contribution of the electrons is independent of the c - l exchange energy AS , but is proportional to the width of the electron band, i.e. inside the domain wall the electron resides in the spinpolaron state. Putting $W = 12 |B| = 3$ eV, $T_c^0 = 2\gamma S(S+1) = 20$ K, we obtain that the wall thickness doubles when $v \sim 2 \times 10^{-2}$ ($n \sim 10^{20} \text{ cm}^{-3}$).

REFERENCES

1. Will G., Pickart S., Alperin H., Natans R., *J. Phys. Chem. Sol.*, **24**, 1679 (1963).
2. Fischer P., Hälgl W., Schwob P., Vogt O., von Wartburg W., *Phys. kondens. Mat.*, **9**, 249 (1969).
3. Schwob P., Vogt O., *Phys. Lett.*, **22**, 374 (1966).
4. Busch G., Wachter P., *Phys. kondens. Mat.*, **5**, 232 (1966).
5. Sclar N., *J. Appl. Phys.*, **35**, 1534 (1964).
6. Wachter P., *CRC Crit. Rev. in Sol. State Sci.*, **3**, 189 (1972).
7. Griessen R., Landolt M., Ott H., *Sol. State Com.*, **9**, 2219 (1971).
8. Holtzberg F., McGuire T., Methfessel S., Suits J., *J. Appl. Phys.*, **35**, 1033 (1964).
9. Methfessel S., Mattis D., "Magnetic Semiconductors". Handbuch der Physik, herausgegeben von S. Flügge, Bd. XVIII/1, Springer, Berlin/New York, 1968.
10. Tsubokawa I., *J. Phys. Soc. Japan*, **15**, 1664 (1960).
11. Matthias B., Bosorth R., van Vleck J., *Phys. Rev. Lett.*, **7**, 160 (1961).
12. Halperin B., Rice T., *Sol. State Phys.*, **21**, 115 (1968).
13. Holmes L., Schubert M., *J. Appl. Phys.*, **37**, 968 (1966).
14. Samokhvalov A.A., Volkenshtein N.V., Zotov T.D. et al., *ZhETF*, **54**, 1341 (1968).
15. Morozov Yu.N., Thesis, UGU, Sverdlovsk, 1972 (in Russian).
16. Goodenough J., "Magnetism and the Chemical Bond", Interscience Publ., New York/London, 1963.
17. Wollan E., *Phys. Rev.*, **117**, 387 (1960).
18. Bachmann R., Lee K., Geballe T., Menth A., *J. Appl. Phys.*, **41**, 1431 (1970).
19. Poderno M., Poczaynicki S., Stalinski B., *Phys. State Sol.*, **24**, K73 (1967).
20. Miedema A., Wielinga R., Huiskamp W., *Physica*, **31**, 1585 (1965).
21. Wood D., Dalton N., *Proc. Phys. Soc.*, **87**, 755 (1966).
22. Hulliger F., Vogt O., *Sol. State Com.*, **8**, 771 (1971).
23. Matthias B., *Phys. Lett. A*, **27**, 511 (1968).
24. Wood V., *Phys. Lett. A*, **37**, 357 (1971).
25. Catanese C., Meissner H., *Phys. Rev. B*, **8**, 2060 (1973).
26. Verreault R., *Phys. kond. Mat.*, **14**, 37 (1971).
27. Shafer M., McGuire T., Suits Y., *Phys. Rev. Lett.*, **11**, 251 (1963).
28. Kaldis E., Streit P., Wachter P., *J. Phys. Chem. Sol.*, **32**, 159 (1971).
29. Hulliger F., Vogt O., *Helv. Phys. Acta*, **39**, 199 (1966).
30. Kaldis E., Streit P., Vassani S., Wachter P., *J. Phys., Chem. Sol.*, **35**, 231 (1974).
31. De Jongh L., Miedema A., *Advances in Phys.*, **23**, 104 (1974).
32. De Jongh L., van Amstel W., Miedema A., *Physica*, **58**, 277 (1972).
33. Arend H., Schoenes Y., Wachter P., *Proc. 12th Intern. Conf. Semiconductor Physics*, Stuttgart, 1974.
34. Heller P., Benedeck G., *Phys. Rev. Lett.*, **8**, 428 (1962).
35. Menyuk N., Dwight K., Reed T., *Phys. Rev. B*, **3**, 1689 (1971).

36. Huang C., Pindack R., Ho Y., *Sol. State Com.*, **14**, 559 (1974).
37. Hughes R., Everett G., Lawson A., *Phys. Rev. B*, **9**, 2394 (1974).
38. Oliveira N.Jr., Foner S., Shapira Y., Reed T., *Phys. Rev. B*, **5**, 2634 (1972). Shapira Y., Foner S., Oliveira N.Jr., Reed T., *ibid.*, 2647.
39. Matveev V.M., Nagaev E.L., *FTT*, **14**, 492 (1972).
40. Matveev V.M., *FTT*, **16**, 1635 (1974).
41. Karimov Yu.S., Vol'pin M.E., Novikov Yu.N., *ZhETF (Pis'ma)*, **14**, 217 (1971).
42. Vonsovsky S.V., "Magnetizm" (Magnetism) Nauka, Moscow, 1971 (in Russian).
43. Hubbard I., *Proc. Roy. Soc.*, **A277**, 237 (1964).
44. De Gennes P., *Compt. rend.*, **247**, 1836 (1958).
45. Nagaev E.L., *FTT*, **13**, 1163 (1971).
46. Kashin V.A., Nagaev E.L., *ZhETF*, **66**, 2105 (1974).
47. Bloch C., Balian R., *Ann. Phys.*, **60**, 401 (1970).
48. Nagaev E.L., *FTT*, **13**, 891 (1971).
49. Nagaev E.L., *ZhETF*, **74**, 1375 (1978).
50. Kim D., Schwartz B., Pruddance H., *Phys. Rev. B*, **7**, 205 (1973).
51. Nagaev E.L., Grigin A.P., *Phys. State Sol. b*, **65**, 457 (1974).
52. Nagaev E.L., Grigin A.P., *ZhETF (Pis'ma)*, **20**, 650 (1974).
53. Nagaev E.L., *FTT*, **12**, 2137 (1970).
54. Mattis D., "The Theory of Magnetism", Harper & Row, New York, 1965.
55. Jamashita J., Kurosawa T., *Phys. Chem. Sol.*, **5**, 34 (1958).
56. Holstein T., *Ann. Phys.*, **8**, 325, 342 (1959).
57. Nagaev E.L., *FTT*, **3**, 2567 (1961); **4**, 2201 (1962).
58. Lang I.G., Firsov Yu.A., *ZhETF*, **43**, 1843 (1962).
59. Heikes R., Johnston W., *J. Chem. Phys.*, **26**, 582 (1957).
60. Pekar S.I., "Issledovaniya po elektronnoy teorii kristallov" (Studies in the Electron Theory of Crystals), Gostekhizdat, Moscow/Leningrad, 1951 (in Russian).
61. Belov K.P., Svirina E.P., *UFN*, **96**, 21 (1968).
62. Bosman A., Van Daal H., Knuvers G., *Phys. Lett.*, **9**, 372 (1965).
63. Spear W., Tannhauser D., *Phys. Rev. B*, **7**, 831 (1973).
64. Zubarev D.N., *UFN*, **71**, 71 (1960).
65. Falicov L., Kimball J., *Phys. Rev. Lett.*, **22**, 997 (1969).
66. Kasuya A., Tachiki M., *Phys. Rev. B*, **8**, 5298 (1973).
67. Elliott R., Wedgwood F., *Proc. Phys. Soc.*, **81**, 846 (1963); **84**, 63 (1964).
68. Zener C., *Phys. Rev.*, **82**, 403 (1951).
69. Anderson P., Hasegawa H., *Phys. Rev.*, **100**, 675 (1955).
70. Nagaev E.L., *ZhETF*, **56**, 1013 (1969).
71. Nagaev E.L., *FMM*, **29**, 905 (1970).
72. Nagaev E.L., Sokolova E.B., *FTT*, **16**, 1293 (1974).
73. Nagaev E.L., *Phys. State Sol. b*, **65**, 11 (1974).
74. De Gennes P., *Phys. Rev.*, **118**, 141 (1960).
75. Landau L.D., Lifshitz E.M., "Kvantovaya mekhanika" (Quantum Mechanics), Fizmatgiz, Moscow, 1963 (in Russian).
76. Nagaev E.L., *ZhETF*, **58**, 1269 (1970).
77. Izyumov Yu.A., Medvedev M.V., *ZhETF*, **59**, 553 (1970).
78. Zhuze V.P., Shelykh A.I., *FTT*, **8**, 629 (1966).
79. Wolfram T., Callaway J., *Phys. Rev.*, **127**, 1606 (1962); **130**, 46 (1963).
80. Dyson F., *Phys. Rev.*, **102**, 1217, 1230 (1956).
81. Vaks V.G., Larkin A.I., Pikin S.A., *ZhETF*, **53**, 1281 (1967).
82. Nagaev E.L., Grigin A.P., *Sol. State Com.*, **15**, 1267 (1974).
83. Shapira Y., Kautz R., Reed T., *Phys. Lett. A*, **47**, 39 (1974).
84. Makhotkin V.E., Shabunina G.G., Aminov T.P. *et al.*, *FTT*, **16**, 3141 (1974).
85. Busch G., Junod P., Wachter P., *Phys. Lett.*, **12**, 11 (1964).
86. Arai T., Wakaki M., Onari S. *et al.*, *J. Phys. Soc. Jap.*, **34**, 68 (1973).

87. Rys F., Helman I., Baltensperger W., *Phys. kond. Mat.*, **6**, 105 (1967).
88. Yanase A., Kasuya T., *J. Phys. Soc. Jap.*, **25**, 1025 (1968).
89. Grigin A.P., Nagaev E.L., *TMF*, **18**, 393 (1974).
90. Grigin A.P., Nagaev E.L., *Phys. State Sol. b*, **61**, 65 (1974).
91. Nagaev E.L., *FTT*, **9**, 2469 (1967).
92. Dzyaloshinsky I.E., *ZhETF*, **47**, 336 (1964).
93. Nagaev E.L., Zil'bervarg V.E., *Sol. State Com.*, **16**, 823 (1975).
Nagaev E.L., Zil'bervarg V.E., *FTT*, **16**, 1261 (1975).
94. Nagaev E.L., *Sol. State Com.*, **15**, 109 (1974).
95. Kambara T., Tanabe I., *J. Phys. Soc. Jap.*, **28**, 628 (1970).
96. Adler D., Brooks H., *Phys. Rev.*, **155**, 826 (1967).
97. Sokoloff J., *Phys. Rev. B*, **2**, 3707 (1970); **3**, 3826 (1971).
98. Roulet B., Fisher M., Doniach S., *Phys. Rev. B*, **7**, 403 (1973).
99. Izyumov Yu.A., Ozerov R.P., "Magnitnaya neitronografiya" (Magnetic Neutronography), Nauka, Moscow, 1966 (in Russian).
100. Ahn K., Shafer M., *J. Appl. Phys.*, **41**, 1260 (1970).
101. Schoenes J., Wachter P., Rys F., *Sol. State Com.*, **15**, 1891 (1974).
102. Tu K., Ahn K., Suits J., *IEEE Trans. on Magnetics*, **8**, 651 (1972).
103. Buckwald R., Hirsch A., *Sol. State Com.*, **17**, 621 (1975).
104. Gor'kov L.P., Mnatsakanov T.T., *ZhETF*, **63**, 684 (1972).
105. Menth A., Bühler E., *Bull. Am. Phys. Soc.*, **15**, 577 (1970).
106. Vitins J., Wachter P., *Sol. State Com.*, **13**, 1273 (1973).
107. Amith A., Gunsalus G.L., *J. Appl. Phys.*, **40**, 1020 (1969).
108. Penny T., Shafer M., Torrance J., *Phys. Rev. B*, **5**, 3669 (1972).
109. Oliver M.R., Kafalas J., Dimmock J., Reed T., *Phys. Rev. Lett.*, **24**, 1064 (1970).
110. Samokhvalov A.A., in: "Redkozemel'nye magnitnye poluprovodniki" (Rare-earth Magnetic Semiconductors), ed. by V.P. Zhuze, Nauka, Leningrad, 1977 (in Russian).
111. Kaldis E., Schoenes J., Wachter P., *ALP Conf. Proc.*, **5**, 269 (1971).
112. Schoenes J., Wachter P., *Phys. Rev. B*, **9**, 3097 (1974).
113. Lehmann H., *Phys. Rev.*, **163**, 488 (1967).
114. Negovetić I., Konstantinović I., *Sol. State Com.*, **13**, 249 (1973).
115. Janase A., Kasuya T., *J. Phys. Soc. Jap.*, **25**, 1025 (1968).
116. Nagaev E.L., *FTT*, **11**, 3428 (1969).
117. Haas C., *IBM J. Res. Develop.*, **14**, 282 (1970).
118. Balberg I., Pinch H., *Phys. Rev. Lett.*, **28**, 909 (1972).
119. Kajita K., Masumi T., Reed T., *Proc. ICM-73**, vol. 5, Nauka, Moscow, 1974, p. 143.
120. Von Molnar S., Kasuya T., *Phys. Rev. Lett.*, **21**, 1757 (1968).
121. Shapira Y., Foner S., Reed T., *Phys. Rev. B*, **8**, 2299 (1973).
122. Shapira Y., Reed T., *Phys. Rev. B*, **5**, 4877 (1972).
123. Axe J., *J. Phys. Chem. Sol.*, **30**, 1403 (1969).
124. Campbell T., Lawson A., *J. Phys. Chem. Sol.*, **30**, 775 (1969).
125. Haas C., *CRC Crit. Rev. Sol. State Sci.*, **1**, 47 (1970).
126. White R., *Phys. Rev. Lett.*, **23**, 858 (1969).
127. Wittekoek S., Bongers P., *Sol. State Com.*, **7**, 1719 (1969).
128. Methfessel S., *Zs. angew. Phys.*, **18**, 414 (1965).
129. Holtzberg F., McGuire T., Methfessel S., Suits J., *Phys. Rev. Lett.*, **13**, 18 (1964).
130. Samokhvalov A.A., Arbuzova T.I., Simonova M.I., Fal'kovskaya L.D., *FTT*, **15**, 3690 (1973).
131. Kajita K., Masumi T., *J. Phys. Soc. Jap.*, **31**, 946 (1971).
132. Kajita K., Masumi T., *Appl. Phys. Lett.*, **21**, 332 (1972).
133. Kajita K., Masumi T., *Sol. State Com.*, **8**, 1039 (1970).
134. Nagaev E.L., *ZhETF*, **59**, 1215 (1970).

* ICM-73, International Conference on Magnetism, Moscow, 1973.

135. Amith A., Berger S., *J. Appl. Phys.*, **42**, 1472 (1971).
136. Sato K., Teranishi T., *J. Phys. Soc. Jap.*, **29**, 523 (1970).
137. Larsen P., *Proc. ICM-73*, vol. 5, Nauka, Moscow, 1974, p. 485.
138. Belov K.P., Korolyova L.I., Batorova S.D. *et al.*, *ZhETF (Pis'ma)*, **20**, 191 (1974).
139. Aminov T.G., Veselago V.G. *et al.*, *FTT*, **16**, 1673 (1974).
140. Anzina L.V., Veselago V.G., Vigeleva E.S. *et al.*, *Proc. ICM-73*, vol. 5, Nauka, Moscow, 1974, p. 480 (in Russian).
141. Haas C., *Phys. Rev.*, **168**, 531 (1968).
142. Grigin A.P., Kozlov V.A., Nagaev E.L., *FTT*, **16**, 2808 (1974).
143. Lazarev G.L., Nagaev E.L., in: "Struktura i svoistva ferritov" (Structure and Properties of Ferrites). Nauka i tekhnika, Minsk, 1974, p. 5 (in Russian).
144. Grigin A.P., Nagaev E.L., *ZhETF (Pis'ma)*, **16**, 438 (1972).
145. De Gennes P., Friedel J., *J. Phys. Chem. Sol.*, **4**, 71 (1958).
146. Fisher M., Langer J., *Phys. Rev. Lett.*, **20**, 665 (1968).
147. Kasuya T., Kondo A., *Sol. State Com.*, **14**, 249, 253 (1974).
148. Kohn W., Luttinger J., *Phys. Rev.*, **108**, 590 (1957).
149. Irkhin Yu. P., Shavrov V.G., *ZhETF*, **42**, 1233 (1962).
150. Nagaev E.L., Kozlov V.A., *FTT*, **17**, 991 (1975).
151. Shapira Y., Foner S., Oliveira N.Jr., Reed T., *Phys. Rev. B*, **5**, 2647 (1972).
152. Sattler K., Siegmann H., *Proc. ICM-73*, vol. 5, Nauka, Moscow, 1974, p. 139.
153. Avdeyev B.V., Krashenin Yu.P., *FTT*, **15**, 3044 (1973).
154. Sawaoka A., Miyahara S., *J. Phys. Soc. Jap.*, **20**, 2087 (1965).
155. Bruck A., Tannhauser D., *J. Appl. Phys.*, **38**, 2520 (1967).
156. Handley S., Bradberry G., *Phys. Lett. A*, **40**, 277 (1972).
157. Bulayevsky L.N., Nagaev E.L., Khomsky D.I., *ZhETF*, **54**, 1562 (1968).
158. Nagaev E.L., *ZhETF*, **58**, 1269 (1970).
159. Nagaev E.L., *FTT*, **13**, 958 (1971).
160. Brinkman W., Rice T., *Phys. Rev. B*, **2**, 1324 (1970).
161. Lehmann H., Harbeke G., *Phys. Rev. B*, **1**, 319 (1970).
162. Von Molnar S., Methfessel S., *J. Appl. Phys.*, **38**, 959 (1967).
163. Nagaev E.L., *UFN*, **117**, 437 (1975).
164. Nagaev E.L., in: "Redkozemel'nye poluprovodniki" (Rare-earth Semiconductors), ed. by V.P. Zhurav, Nauka, Leningrad, 1977 (in Russian).
165. Fujii J., Shirane G., Yamada Y., *Phys. Rev. B*, **11**, 2036 (1975).
166. Nagaev E.L., *FTT*, **11**, 2779 (1969).
167. Nagaev E.L., *FTT*, **12**, 2137 (1970).
168. Vitins J., Wachter P., *Phys. Rev. B*, **12**, 3829 (1975).
169. Veselago V.G., Vigeleva E.S., Vinogradova G.I. *et al.*, *ZhETF (Pis'ma)*, **15**, 316 (1972).
170. Zil'berverg V.E., Nagaev E.L., *FTT*, **15**, 1585 (1973).
171. Sattler K., Siegmann H., *Phys. Rev. Lett.*, **29**, 1565 (1972).
172. Cochrane R., Hedgcock F., Ström-Olsen J., *Phys. Rev. B*, **8**, 4262 (1974).
173. Nagaev E.L., *FTT*, **13**, 1321 (1971).
174. Nagaev E.L., *FTT*, **14**, 773 (1972).
175. Nagaev E.L., *ZhETF*, **57**, 1274 (1969).
176. Nagaev E.L., *FTT*, **12**, 1109 (1970).
177. Wollan E., Koehler W., *Phys. Rev.*, **100**, 545 (1955).
178. Jarrett H., Cloud W., Bouchard R. *et al.*, *Phys. Rev. Lett.*, **21**, 617 (1968).
179. Leroux-Hugon P., *Phys. Rev. Lett.*, **29**, 939 (1972).
180. Balkarey Yu.I., *FTT*, **16**, 1369 (1974).
181. Lascaray J., Merle P., Mathieu H. *et al.*, *Phys. Rev. B*, **16**, 358 (1977).
182. Zil'berverg V.E., Nagaev E.L., *FTT*, **16**, 2834 (1974).
183. Bonch-Bruевич V.L., in: "Fizika tverdogo tela" (Solid-state Physics), VINITI, Moscow, 1965 (in Russian).
184. Efros A.L., *UFN*, **111**, 451 (1973).

185. Oliver M., Kafalas J., Dimmock J., Reed T., *Phys. Rev. Lett.*, **24**, 106 (1970).
186. Petrick G., von Molnar S., Penney T., *Phys. Rev. Lett.*, **26**, 885 (1970).
187. Von Molnar S., Shafer M., *J. Appl. Phys.*, **41**, 1093 (1970).
188. Torrance J., Shafer M., McGuire T., *Phys. Rev. Lett.*, **29**, 1168 (1972).
189. Shapira Y., Foner S., Aggarwal R., Reed T., *Phys. Rev. B*, **8**, 2316 (1973).
- Shapira Y., Foner S., Reed T. *et al.*, *Phys. Lett. A*, **41**, 471 (1972).
190. Shapira Y., Reed T., *Phys. Lett. A*, **36**, 105 (1971).
191. Shapira Y., Reed T., *Phys. Rev. B*, **5**, 4877 (1972).
192. Wachter P., *Phys. Lett. A*, **41**, 391 (1972).
193. Lidorenko N.S., Kreshchishina L.T., Nagaev E.L., *FTT*, **14**, 613 (1972).
194. Nagaev E.L., *ZhETF (Pis'ma)*, **6**, 484 (1967).
195. Nagaev E.L., *ZhETF*, **54**, 228 (1968).
196. Nagaev E.L., Grigin A.P., *Phys. Lett. A*, **38**, 469 (1972).
197. Nagaev E.L., *ZhETF (Pis'ma)*, **16**, 558 (1972).
198. Lazarev G.L., Matveev V.M., Nagaev E.L., *FTT*, **17**, 1955 (1975).
199. Kashin V.A., Nagaev E.L., *ZhETF (Pis'ma)*, **21**, 126 (1975).
200. Lazarev G.L., Nagaev E.L., *FTT*, **15**, 1635 (1973).
201. Von Molnar S., Methfessel S., *J. Appl. Phys.*, **38**, 959 (1967).
202. Belov K.P., Batorova S.P., Korolyova L.I., Shalimova M.A., *ZhETF (Pis'ma)*, **26**, 68 (1977).
203. Akhiezer A.I., Baryakhtar V.G., Peletminsky S.V., "Spinovye volny" (Spin Waves), Nauka, Moscow, 1967 (in Russian).
204. Kasuya T., *Sol. State Com.*, **8**, 1635 (1970).
205. Umehara M., Kasaya T., *J. Phys. Soc. Jap.*, **33**, 602 (1972).
206. Kasuya T., Yanase A., Takedo T., *Sol. State Com.*, **8**, 1543 (1970).
207. Yanase A., *Int. J. Mag.*, **2**, 99 (1972).
208. Kasuya T., Yanase A., Takedo T., *Sol. State Com.*, **8**, 1551 (1970).
209. Kübler J., *Zs. Phys.*, **250**, 324 (1972).
210. Aronov A.G., Kudinov E.K., *ZhETF*, **65**, 1344 (1968).
211. Plumier R., *J. Appl. Phys.*, **27**, 964 (1966).
212. Bogolyubov N.N., "Lektsii z kvantovoy statistiki" (Lectures on Quantum Statistics), Radyanska shkola, Kiev, 1949 (in Ukrainian).
213. Kohn W., *Phys. Rev. A*, **133**, 171 (1964).
214. Anselm A.I., "Introduction to Semiconductor Theory", Mir Publishers, Moscow, 1981.
215. Tyablikov S.V., "Metody kvantovoi teorii magnetizma" (Methods of Quantum Theory of Magnetism), Nauka, Moscow, 1965 (in Russian).
216. Turov E.A. "Fizicheskiye svoystva magnitoporyadochennykh kristallov" (Physical Properties of Magnetically-ordered Crystals), Izd. AN SSSR, Moscow, 1963.
217. Luttinger J., *Phys. Rev.*, **81**, 1015 (1951).
218. Smart J., "Effective Field Theories of Magnetism", Saunder, Philadelphia/London, 1966.
219. Borovik-Romanov A.S., Orlova N.P., *ZhETF*, **31**, 579 (1956).
220. Dzyaloshinsky I.E., *ZhETF*, **32**, 1547 (1957); **33**, 1454 (1958).
221. Balberg J., *Phys. Lett. A*, **58**, 203 (1976).
222. Stephenson R., Wood P., *J. Phys. C*, **3**, 90 (1970).
223. Von Molnar S., Lawson A., *Phys. Rev. A*, **139**, 1598 (1965).
224. Dillon J., Olsen C., *Phys. Rev. A*, **135**, 434 (1964).
225. Als-Nielsen J., Dietrich O., Kunnmann W., Passel L., *Phys. Rev. Lett.*, **27**, 741 (1971).
226. Salamon H., *Sol. State Com.*, **13**, 1741 (1973).
227. Lederman F., Salamon M., *Phys. Rev. B*, **9**, 2981 (1974).
228. Hulliger F., Vogt O., *Phys. Lett.*, **17**, 238 (1965).
229. Hirakawa K., Ikeda H., *J. Phys. Soc. Jap.*, **35**, 1328 (1973).
230. Kubo H., *J. Phys. Soc. Jap.*, **36**, 675 (1974).
231. Ohhashi K., Tsujikawa J., *J. Phys. Soc. Jap.*, **37**, 63 (1974).

232. Dixon G., *Phys. Rev. B*, **8**, 3206 (1973).
233. Litvin D., *Phys. Lett. B*, **44**, 487 (1973).
234. German K., Maier K., Strauss E., *Sol. State Com.*, **14**, 1309 (1974).
235. Ruderman M., Kittel C., *Phys. Rev.*, **96**, 99 (1954).
236. Yosida K., *Phys. Rev.*, **106**, 893 (1957).
237. Kasuya T., *Prog. Theor. Phys.*, **16**, 45 (1956).
238. Bloembergen N., Rowland T., *Phys. Rev.*, **97**, 1679 (1955).
239. Matveev V.M., Nagaev E.L., *FTT*, **15**, 2874 (1973).
240. Kramers H., *Physica*, **1**, 184 (1934).
241. Callen E., *Phys. Rev. Lett.*, **20**, 2045 (1968).
242. Izyumov Yu.A., Medvedev M.V., "Teoriya magnitouporyadochennykh kristallov s primesyami" (Theory of Magnetically-ordered Crystals with Impurities), Nauka, Moscow, 1970 (in Russian).
243. Izyumov Yu.A., Kassan-Ogly F.A., Skryabin Yu.N., "Polevye metody v teorii ferromagnetizma" (Field Methods in the Theory of Ferromagnetism), Nauka, Moscow, 1974 (in Russian).
244. Fröhlich H., *Phys. Rev.*, **79**, 845 (1950).
245. Bairamov A.I., Gurevich A.G., Emiryani L.M., Parfenova N.N., *Phys. Lett. A*, **62**, 242 (1977).
246. Landau L.D., Lifshitz E.M., "Statisticheskaya fizika" (Statistical Physics), Nauka, Moscow, 1964 (in Russian).
247. Lifshitz I.M., *Adv. Phys.*, **13**, 483 (1964).
248. Van Houten S., *J. Phys. Chem. Sol.*, **17**, 7 (1960).
249. Salyganov V.I., Shil'nikov Yu.R., Yakovlev Yu.M. *et al.*, *FTT*, **16**, 3174 (1974).
250. Chou H., Fan H., *Phys. Rev. B*, **10**, 901 (1974).
251. Bloch D., Maury R., Vetter C., Yelon W., *Phys. Lett. A*, **49**, 354 (1974).
252. Johnker G., *Phil. Res. Rep.*, **24**, 1 (1969).
253. Bhide V., Rajoria D., Reddy Y. *et al.*, *Phys. Rev. Lett.*, **28**, 1133 (1972).
254. Menth A., Buehler E., Geballe T., *Phys. Rev. Lett.*, **22**, 295 (1969).
255. Mehran F., Torrance J., Holtzberg F., *Phys. Rev. B*, **8**, 1268 (1973).
256. Nagaev E. L., *ZhETF*, **57**, 469 (1969).
257. Nagaev E.L., *TMF*, **14**, 91 (1973).
258. Nagaev E.L., Sokolova E.B., *Phys. Stat. Sol. b*, **64**, 411 (1974).
259. Nagaev E.L., Polnikov V.G., *ZhETF (Pis'ma)*, **15**, 48 (1972).
260. Lifshitz I.M., Kaganov M.I., *UFN*, **78**, 411 (1962).
261. Tyablikov S.V., *ZhETF*, **21**, 377 (1951).
262. Frönlich N., Pelzer H., Zienau S., *Phil. Mag.*, **41**, 221 (1950).
263. Matveev V.M., Nagaev E.L., *ZhETF*, **69**, 2151 (1975).
264. Landau L.D., Lifsnitz E.M., "Electrodynamics of Continuous Media", Pergamon Press, Oxford/New York, 1960.
265. Matveev V.M., Nagaev E.L., *FTT*, **17**, 2483 (1975).
266. Lidorenko N.S., Matveev V.M., Nagaev E.L., *DAN SSSR*, **230**, 1085 (1976).
267. Hohenberg P., Kohn W., *Phys. Rev. B*, **136**, 864 (1964).
268. Lifshitz I.M., *ZhETF*, **17**, 1017, 1076 (1947).
269. Wolfram T., Callaway J., *Phys. Rev.*, **130**, 2207 (1963).
270. Bonch-Bruевич V.L., *FMM*, **2**, 215 (1956).
271. Wallis R., Maradudin A., Ipatova I., Klochikchin A., *Sol. State Com.*, **5**, 89 (1967).
272. Filippov B.N., *FTT*, **9**, 1339 (1967).
273. Pikus G.E., "Osnovy teorii poluprovodnikovyykh priborov" (Fundamentals of Theory of Semiconductor Devices), Nauka, Moscow, 1965 (in Russian).
274. Sandomirsky V.B., *ZhETF (Pis'ma)*, **2**, 396 (1965).
275. Meier F., Pierce D., Sattler K., *Sol. State Com.*, **16**, 401 (1975).
276. Nagaev E.L., *FTT*, **13**, 891 (1971).
277. Gombás P., "Theorie und Lösungsmethoden des Mehrteilchenproblems der Wellenmechanik", Birkhäuser, Basel, 1950.

278. Mott N., Davis E., "Electronic Processes in Non-Crystalline Materials", Clarendon Press, Oxford, 1971.
279. Nagaev E.L., Lazarev G.L., *ZhFKh*, **50**, 1781 (1976).
280. Nagaev E.L., Lazarev G.L., *Surf. Sci.*, **54**, 1, (1976).
281. Landau L.D., *Sov. Phys.*, **3**, 664 (1933).
282. Feynman R., Hibbs A., "Quantum Mechanics and Path Integrals", McGraw-Hill, New York, 1965.
283. Bogolyubov N.N., *Ukr. matem. zhurn.*, **2**, 3 (1950).
284. Tyablikov S.V., *ZhETF*, **21**, 377 (1951).
285. Schultz T., *Phys. Rev.*, **116**, 526 (1959).
286. Ziman J., "Electrons and Phonons", Clarendon Press, Oxford, 1960.
287. Balberg J., Pankove J., *Phys. Rev. Lett.*, **27**, 596 (1971).
288. Evans M., Warming E., Hutchings M., Stringfellow M., *Sol. State Com.*, **12**, 795 (1973).
289. Varma C., *Rev. Mod. Phys.*, **48**, 219 (1976).
290. Kittel C., "Quantum Theory of Solids", Wiley, New York/London, 1963.
291. Ikezawa M., Suzuki T., *J. Phys. Soc. Jap.*, **35**, 1556 (1973).
292. Bogomolov V.N., Kudinov E.K., Firsov Yu.A., *FTT*, **9**, 2077 (1967).
293. Fröhlich H., *Proc. Roy. Soc. A.*, **215**, 291 (1952).
294. Bohn H., Zinn W., Dorner B., Kollmar A., *Phys. Rev. B*, **22**, 5447 (1980).
295. Abrikosov A.A., Gor'kov A.P., Dzyaloshinsky I.E., "Metody kvantovoy teorii polya v statisticheskoy fizike" (Methods of Quantum Field Theory in Statistical Physics), Fizmatgiz, Moscow, 1962 (in Russian).
296. Anderson P., *Phys. Rev.*, **109**, 1492 (1958).
297. Kane E., *Phys. Rev.*, **131**, 79 (1963).
298. Morigaki K., Onda M., *J. Phys. Soc. Jap.*, **36**, 1049 (1974).
299. Endo H., Eatah A., Wright J., Cusack N., *J. Phys. Soc. Jap.*, **34**, 666 (1973).
300. Phelps D., Avri R., Flynn C., *Phys. Rev. Lett.*, **34**, 23 (1974).
301. Jayaraman A., Narayanamurti V., Bucher E., Maines R., *Phys. Rev. Lett.*, **25**, 1430 (1970).
302. McWhan D., Rice T., *Phys. Rev. Lett.*, **22**, 887 (1969).
303. McWhan D., Marezio M., Remeika J., Dernier P., *Phys. Rev. B*, **10**, 490 (1974).
304. Kawai N., Mochizuki Shesuke, *Sol. State Com.*, **9**, 1393 (1971).
305. Jayaraman A., *Phys. Rev. Lett.*, **29**, 1674 (1972).
306. Tonkov E.Yu., Aptekar' I.L., *FTT*, **14**, 1507 (1974).
307. Sleight A., Gillson I., Weiher I., Bindloss W., *Sol. State Com.*, **14**, 357 (1974).
308. Kaldis E., Wachter P., *Sol. State Com.*, **11**, 907 (1972).
309. Suits J., Argyle B., Freiser M., *Phys. Rev. Lett.*, **15**, 822 (1965).
310. Grigin A.P., Nagaev E.L., *FTT*, **17**, 2614 (1975).
311. Pines D., "Elementary Excitations in Solids", Benjamin, New York/Amsterdam, 1964.
312. Zubarev D.N., "Neravnovesnaya statisticheskaya termodinamika" (Non-equilibrium Statistical Thermodynamics), Nauka, Moscow, 1971 (in Russian).
313. Vitins J., Wachter P., *Proc. ICM-73*, vol. 1(2), Nauka, Moscow, 1974, p. 140.
314. Krinchik G.S., Chetkin M.V., *UFN*, **98**, 4 (1969).
315. Shapira Y., Foner S., Oliveira N.Jr., *Phys. Rev. B*, **10**, 4765 (1974).
316. Belov K.P., Korolyova L.I., Batorova S.D. et al., *ZhETF (Pis'ma)*, **22**, 304 (1975).
317. Drakin A.E., Nagaev E.L., *FNT*, **4**, 320 (1978).
318. Matveev V.M., Nagaev E.L., *Phys. Lett. A*, **42**, 88 (1972).
319. Nagaev E.L., *ZhETF*, **59**, 1218 (1970).
320. Coutinho Filho M.D., Miranda L.C.M., Rezende S.R., *Phys. State Sol. b*, **57**, 85 (1973); **65**, 689 (1974); **66**, 395 (1974).

321. Kagan Yu., Maksimov L.A., *FTT*, **7**, 530 (1965).
322. Bongers P., Haas C., van Run A., Zanmarchi G., *J. Appl. Phys.*, **40**, 958 (1969).
323. Lehmann H., Harbeke G., *J. Appl. Phys.*, **38**, 946 (1967).
324. Buseh G., Magyar B., Wachter P., *Phys. Lett.*, **23**, 438 (1966).
325. Harbeke G., Pinch H., *Phys. Rev. Lett.*, **17**, 1090 (1966).
326. Sato K., Teranishi T., *J. Phys. Soc. Jap.*, **29**, 523 (1970).
327. Kashin V.A., Nagaev E.L., Pishchalko V.D., *FTT*, **18**, 1091 (1976).
328. Andrianov D.G., Drozdov S.A., Lazareva G.V. et al., *FNT*, **3**, 497 (1977).
329. Pavlovsky A.I., Druzhinin V.V., Tatsenko O.M., Pisarev R.V., *ZhETF (Pis'ma)*, **20**, 561 (1974).
330. Nagaev E.L., Sokolova E.B., *FTT*, **21**, 13-26 (1979).
331. Kashin V.A., Nagaev E.L., *FNT*, **2**, 1530 (1976).
332. Jonker C., Van Santen J., *Physica*, **160**, 337 (1950); **19**, 120 (1953).
333. Volger J., *Physica*, **20**, 49 (1954).
334. Balian R., Bloch C., *Ann. Phys.*, **60**, 401 (1970).
335. Von Molnar S., Kasuya T., *Proc. 11th Intern. Conf. Physics of Semicond.*, Cambridge, Mass., 1970, p. 233.
336. Shapira Y., Kautz R., *Phys. Rev. B*, **10**, 4781 (1974).
337. De Gennes P., *Compt. rend.*, **247**, 1836 (1958).
338. Irkhin Yu.P., *ZhETF*, **50**, 379 (1966).
339. Liu S., *Phys. Rev.*, **121**, 451 (1961).
340. Levanyuk A.P., *ZhETF*, **36**, 810 (1959).
341. Ginzburg V.L., *FTT*, **2**, 2031 (1960).
342. Braut R., "Phase Transitions", Univ. of Brussels, New York/Amsterdam, 1965.
343. Dzyaloshinsky I.E., *ZhETF*, **46**, 1420 (1964).
344. Fisher M., "The Nature of Critical Points", Univ. of Colorado Press, Colo., 1965.
345. Domb C., Sykes M., *Phys. Rev.*, **128**, 168 (1962).
346. Bean C., Rodbell D., *Phys. Rev.*, **126**, 104 (1962).
347. Vonsovsky S.V., *DAN SSSR*, **27**, 550 (1940).
348. Vonsovsky S.V., *Izv. AN SSSR, ser. fiz.*, **11**, 485 (1947).
349. Patashinsky A.Z., Pokrovsky V.L., "Fluktuatsionnaya teoriya fazovykh perekhodov" (Fluctuation Theory of Phase Transitions), Nauka, Moscow, 1975 (in Russian).
350. Fisher M., in: "Critical Phenomena", Proc. Int. School Phys. "Enrico Fermi", Varenna, 1970.
351. Kadanoff L., in: "Critical Phenomena", Proc. Int. School Phys. "Enrico Fermi", Varenna, 1970.
352. Belov K.P., Tret'yakov Yu.D., Gordeyev I.V. et al., in: "Ferromagnitnye khal'kogenidnye shpineli" (Ferromagnetic Chalcogenide Spinels), ed. by K.P. Belov, Yu.D. Tret'yakov, Izd. MGU, Moscow, 1975 (in Russian).
353. Herring C., *Phys. Rev.*, **96**, 1163 (1954).
354. Kozlov V.A., Nagaev E.L., *ZhETF (Pis'ma)*, **13**, 639 (1972).
355. Kopylov V.N., Mezhev-Deglin L.P., *ZhETF (Pis'ma)*, **15**, 269 (1972).
356. Gomes M., Miranda L., *Phys. Rev.*, **B**, **12**, 3788 (1975).
357. Borukhovich A.S., Marunya M.S., Lobachevskaya N.I. et al., *FTT*, **16**, 2084 (1974).
358. Druzhinin V.V., Pavlovsky A.I., Samokhvalov A.A., Tatsenko O.M., *ZhETF (Pis'ma)*, **23**, 259 (1976).
359. Lakhno V.D., Nagaev E.L., *FTT*, **18**, 3429 (1976).
360. Kittel C., *Phys. Rev. Lett.*, **10**, 339 (1963).
361. Belov K.P., Korolyova L.I., Tovmasyan L.N. et al., *FTT*, **19**, 622 (1977).
362. Nagaev E.L., Sokolova E.B., *FTT*, **19**, 533 (1977).
363. Nagaev E.L., Sokolova E.B., *FTT*, **19**, 732 (1977).
364. Luttinger J.M., *Phys. Rev.*, **112**, 739 (1958).
365. Hessler J.P., *Phys. Rev. B*, **8**, 3151 (1973).

366. Taylor K., Darby K., "Physics of Rare-earth Solids", Chapman & Hall, London, 1972.
367. Birgeneau R.J., Als-Nielsen J., Bucher E., *Phys. Rev. B*, **6**, 2724 (1972).
368. Lea K.R., Leask M.J.M., Wolf W.P., *J. Phys. Chem. Sol.*, **23**, 1381 (1962).
369. Bucher E., Andres K., di Salvo F.J. *et al.*, *Phys. Rev. B*, **11**, 500 (1975).
370. Schrödinger E., *Proc. Roy. Irish Acad.*, **41A**, 39 (1941).
371. Trammel G., *J. Appl. Phys.*, **31**, 362S (1960).
372. Trammel G., *Phys. Rev.*, **131**, 932 (1963).
373. Bleaney B., *Proc. Roy. Soc. A*, **276**, 19 (1963).
374. Huang C., Ho J., *Phys. Rev. A*, **12**, 5255 (1975).
375. Belov K.P., Korolyova L.I., Shalimova M.A. *et al.*, *FTT*, **17**, 3156 (1975).
376. Bloch D., Hermann-Konzaud D., Vettier C. *et al.*, *Phys. Rev. Lett.*, **35**, 963 (1975).
377. Brazovsky S.A., Dzyaloshinsky I.E., *ZhETF (Pis'ma)*, **21**, 360 (1975).
378. Brazovsky S.A., Dzyaloshinsky I.E., Kukharensko B.G., *ZhETF*, **70**, 2257 (1976).
379. Bak P., Krinsky S., Mukamel D., *Phys. Rev. Lett.*, **36**, 52 (1976).
380. Zil'bervarg V.E., Nagaev E.L., *FTT*, **18**, 1583 (1976).
381. Richard T.G., Geldart D.J.W., *Phys. Rev. Lett.*, **30**, 290 (1973).
382. Geldart D.J.W., Richard T.G., *Phys. Rev. B*, **12**, 5175 (1975).
383. Binder K., Meissner G., Mais H., *Phys. Rev. B*, **13**, 4890 (1976).
384. Nagaev E.L., *ZhETF (Pis'ma)*, **25**, 87 (1977).
385. Nagaev E.L., Sokolova E.B., *ZhETF (Pis'ma)*, **24**, 543 (1976).
386. Kovalenko A.A., Nagaev E.L., *FTT*, **20**, 2325 (1978).
387. Vitins J., Wachter D., *Phys. Lett. A*, **58**, 275 (1976).
388. Mitani T., Koda T., *Phys. Rev. B*, **12**, 2311 (1975).
389. Belov K.P., "Ferrity v sil'nykh magnitnykh polyakh" (Ferrites in Strong Magnetic Fields), Nauka, Moscow, 1972 (in Russian).
390. Korenblit I.Ya., Tankhilevich B.G., *ZhETF (Pis'ma)*, **24**, 598 (1976).
391. Kun'kova Z.E., Aminov T.G., Golik L.L. *et al.*, *FTT*, **18**, 2083 (1976).
392. Golik L.L., Elinson M.I., Kun'kova Z.E., *et al.*, *Microelektronika*, **6**, 201 (1977).
393. Desfours J., Nadai J., Averous M., Godard G., *Sol. State Com.*, **20**, 691 (1976).
394. Golik L.L., Novikov L.N., Elinson M.I. *et al.*, *FTT*, **18**, 3700 (1976).
395. Dzyaloshinsky I.E., *ZhETF*, **37**, 881 (1959).
396. Astrov D.N., *ZhETF*, **38**, 984 (1960).
397. Hastings J.M., Corliss L.M., *Phys. Rev. B*, **14**, 1995 (1976).
398. Matveev V.M., Nagaev E.L., *FTT*, **17**, 2483 (1975).
399. Lakhno V.D., Nagaev E.L., *FTT*, **20**, 82 (1978).
400. Batlogg B., Kaldis E., Schlegel A., Wachter P., *Phys. Rev. B*, **14**, 553 (1976).
401. Calogero F., "Variable Phase Approach to Potential Scattering", Academic Press, New York/London, 1967.
402. Belov K.P., Korolyova L.I., Shalimova M.A. *et al.*, *ZhETF*, **72**, 1995 (1977).
403. Akimitsu J., Siratori K., Shirane G., *J. Phys. Soc. Jap.* **44**, 172 (1978).
404. Kittel C., *Phys. Rev.*, **120**, 335 (1960).
405. Busch G., Schwob P., Vogt O., *Phys. Lett.*, **20**, 602 (1966).
406. Nagaev E.L., Sokolova E.B., in: "Fazovyie perekhody metall-dielektrik" (Metal-dielectric Phase Transitions), Izd. LGU, Lvov, 1977 (in Russian).
407. Afanas'yev M.M., Kompan M.E., Merkulov I.A., *ZhETF*, **71**, 2068 (1976).
408. Teale R.W., Temple D.W., *Phys. Rev. Lett.*, **19**, 904 (1967).
409. Lems W., Rijnierse P.J., Bongers P.F., Enz. U., *Phys. Rev. Lett.*, **21**, 1643 (1968).
410. Anzina L.V., Veselago V.G., Rudov S.G., *ZhETF (Pis'ma)*, **23**, 520 (1976).
411. Antonini B., Paoletti A., Paroll P. *et al.*, *Phys. Rev. B*, **12**, 3840 (1975).

412. Afanas'yev M.M., Kompan M.E., Merkulov I.A., *ZhETF (Pis'ma)*, **23**, 621 (1976).
413. Afanas'yev M.M., Kompan M.E., Merkulov I.A., *ZhETF (Pis'ma)*, **2**, 982 (1976).
414. Lakhno V.D., Nagaev E.L., *ZhETF*, **74**, 2123 (1978).
415. Larkin A.I., Khmel'nitsky D.E., *ZhETF*, **55**, 2345 (1968).
416. Genkin G.M., *ZhETF*, **71**, 2278 (1976).
417. Passell L., Dietrich O.W., Als-Nielsen J., *Phys. Rev. B*, **14**, 4897 (1976).
418. Als-Nielsen J., Dietrich O.W., Passell L., *Phys. Rev. B*, **14**, 4908 (1976).
419. Dietrich O.W., Als-Nielsen J., Passell L., *Phys. Rev. B*, **14**, 4923 (1976).
420. Zatsarinny O.I., Nagaev E.L., *ZhETF (Pis'ma)*, **25**, 505 (1977).
421. Kisker E., Baum G., Mahan A.H. *et al.*, *Phys. Rev. Lett.*, **36**, 982 (1976).
422. Kornblit A., Ahlers G., *Phys. Rev. B*, **11**, 2678 (1975).
423. Konstantinović J., Babić B., *Sol. State Com.*, **18**, 701 (1976).
424. Child H.R., Wilkinson M.K., Cable J.W. *et al.*, *Phys. Rev.*, **131**, 22 (1963).
425. Sclar N., *J. Appl. Phys.*, **35**, 1534 (1964).
426. Krivoglaз M.A., *FTT*, **11**, 2230 (1969).
427. Krivoglaз M.A., Trushchenko A.A., *FTT*, **11**, 3119 (1969).
427. Vol'sky E.P., "Fazovye perekhody metall-dielektrikov oksislakh perekhodnykh metallo" (Metal-dielectric Phase Transitions in Transition Metal Oxides). Preprint IFM UNTs AN SSSR, 1974 (in Russian).
428. Matveev V.M., *ZhETF*, **65**, 1626 (1973).
429. Salyganov V.I., Yakovlev Yu.M., Shil'nikov Yu.R., *ZhETF (Pis'ma)*, **18**, 366 (1973).
430. Lee K., Suits J., *Phys. Lett. A*, **34**, 141 (1971).
431. Korenblit I.Ya., Tankhilevich B.G., *ZhETF*, **73**, 2231 (1977).
432. Bass F.G., Oleynik I.N., *FTT*, **18**, 2334 (1976).
433. Bass F.G., Oleynik I.N., *FTT*, **19**, 2047 (1977).
434. Schlegel A., Wachter P., *Sol. State Com.*, **13**, 1865 (1973).
435. Silberstein R., Tekippe V., Dresselhaus M., *Phys. Rev. B*, **16**, 2728 (1977).
436. Koshizuka N., Yokoyama Y., Tsushima T., *Sol. State Com.*, **23**, 967 (1977).
437. Safran S., Dresselhaus G., Lax B., *Phys. Rev. B*, **16**, 2749 (1977).
438. Gurevich A.G., Yakovlev Yu.M., Karpovich V.I. *et al.*, *Proc. ICM-73*, vol. 5, Nauka, Moscow, 1974, p. 469 (in Russian).
439. Karpovich V.I., Gurevich A.G., *FTT*, **17**, 247 (1975).
440. Zil'berverg V.E., Nagaev E.L., *FTT*, **18**, 2499 (1976).
441. Phillips J., *Solid State Phys.*, **18**, 55 (1966).
442. Nagaev E.L., *UFN*, **136**, 61 (1982).
443. Kittel C., *Phys. Rev.*, **120**, 335 (1960).
444. Matveev V.M., *ZhETF*, **63**, 1626 (1973).
445. Chen H., Levy P., *Phys. Rev. Lett.*, **27**, 1383 (1971).
446. Nauciel-Bloch M. *et al.*, *Phys. Rev. B*, **5**, 4603 (1972).
447. Nagaev E.L., Kovalenko A.A., *ZhETF*, **79**, 907 (1980).
448. Grunberg P., Metawe F., *Phys. Rev. Lett.*, **39**, 1561 (1977).
449. Mayr C. *et al.*, *J. Magn. Magn. Mat.*, **13**, 177 (1979).
450. Guy C. *et al.*, *Sol. State Com.*, **33**, 1055 (1980).
451. Hulliger F., *Mat. Res. Bull.*, **14**, 259 (1979).
452. Schwob P., Vogt O., *Phys. Lett. A*, **22**, 374 (1966); *ibid.*, **24**, 242 (1967).
453. McWhan D., Souers P., Jura G., *Phys. Rev.*, **143**, 385 (1966).
454. Sokolova G.K. *et al.*, *ZhETF*, **49**, 452 (1965).
455. Stevenson R., Robinson M., *Can. J. Phys.*, **43**, 1744 (1965).
456. Shapira Y. *et al.*, *Phys. Rev. B*, **14**, 3007 (1976).
457. Day P., *Accounts Chem. Res.*, **12**, 236 (1979).
458. Bohn D. *et al.*, *Phys. Rev. B*, **22**, 5447 (1980).
459. Kornblit A., Ahlers G., Buehler E., *Phys. Rev. B*, **17**, 282 (1978).
460. Dunlap R., Gottlieb A., *Phys. Rev. B*, **22**, 3422 (1980).
461. Mook H., *Phys. Rev. Lett.*, **46**, 508 (1981).
462. Kondal S., Seehra M., *Phys. Rev. B*, **22**, 5482 (1980).

463. Kötztler J., von Philipsborn H., *Phys. Rev. Lett.*, **40**, 790 (1978).
464. Kötztler J., Scheite W., *Phys. Lett. A*, **72**, 473 (1979).
465. Berzhansky V.N., Ivanov V.I., Gavrichkov S.A., *FTT*, **21**, 2858 (1979).
466. Kato J. *et al.*, *J. Phys. Soc. Jap.*, **47**, 1367 (1979).
467. Streit P., Everett G., *Phys. Rev. B*, **21**, 169 (1980).
468. Johanson W., McCollum D., *Phys. Rev. B*, **21**, 2435 (1980).
469. Ma S., "Modern Theory of Critical Phenomena", Benjamin, London, 1976.
470. Hasting J. *et al.*, *Phys. Rev. B*, **22**, 1327 (1980).
471. Petrich Y., Kasuya T., *Sol. State Com.*, **8**, 1625 (1970).
472. Schoenes J., Wachter P., *Phys. Lett. A*, **61**, 68 (1977).
473. Kuznia C., Kneer G., *Phys. Lett. A*, **27**, 664 (1968).
474. Everett G., Jones R., *Phys. Rev. B*, **4**, 1561 (1971).
475. Harris E., Owen J., *Phys. Rev. Lett.*, **11**, 9 (1963).
476. Huang N., Orbach L., *Phys. Rev. Lett.*, **12**, 275 (1964).
477. De Seze L., *J. Phys. C*, **10**, L353 (1977).
478. Aharony A., *J. Phys. C*, **11**, L457 (1978).
479. Villain J., *Z. Phys. B*, **33**, 31 (1979).
480. Maletta H., Felsch W., *Phys. Rev. B*, **20**, 1245 (1979).
481. Murani A., *Phys. Rev. Lett.*, **37**, 450 (1976).
482. Néel L., *Compt. rend.*, **228**, 664 (1949).
483. Nagata S. *et al.*, *Phys. Rev. B*, **22**, 3331 (1980).
484. Galazka R., Nagata S., Keesom P., *ibid.*, 3344.
485. Ferré J. *et al.*, *J. Phys. C*, **13**, 3697 (1980).
486. Von Löhnysen H., *Phys. Rev. B*, **22**, 273 (1980).
487. Maletta H., Convert P., *Phys. Rev. Lett.*, **42**, 108 (1979).
488. Hauser J., *Phys. Rev. B*, **22**, 2554 (1980).
489. Belov K.P., Korolyova L.I. *et al.*, *ZhETF (Pis'ma)*, **31**, 96 (1980).
490. Korolyova L.I., Nagaev E.L., Tsvetkova N.A., *ZhETF*, **79**, 600 (1980).
491. Westerholt R., Scheer T., Methfessel S., *J. Magn. Magn. Mat.*, **15-18**, 823 (1980).
492. Alexander S., Helman J., Balberg J., *Phys. Rev. B*, **13**, 304 (1976).
493. Balberg J., Helman J., *Phys. Rev. B*, **18**, 303 (1978).
494. Kasuya T., Kondon A., *Sol. State Com.*, **14**, 249, 253 (1974).
495. Ausloos M., Durczewski R., *Phys. Rev. B*, **22**, 2439 (1980).
496. Hauser J., *Phys. Rev. B*, **22**, 2554 (1980).
497. Görlich E. *et al.*, *Phys. State Sol. b*, **64**, K147 (1974).
498. Chien C., Greedan J., *Phys. Lett. A*, **36**, 197 (1971).
499. Hiev M., Arai T., *Sol. State Com.*, **31**, 79 (1979).
500. Wagner V., Mitlehrer H., Geick R., *Opt. Com.*, **2**, 429 (1971).
501. Lee T., *J. Appl. Phys.*, **42**, 1441 (1971).
502. Merlin K. *et al.*, *Sol. State Com.*, **22**, 609 (1977).
503. Balberg J., Maman A., *Phys. Rev. B*, **16**, 4535 (1977).
504. Battlog B., Zvara M., Wachter P., *Sol. State Com.*, **28**, 567 (1979).
505. Hulin D., Benoit à la Guillome C., *Sol. State Com.*, **25**, 235 (1979).
506. Yao S. *et al.*, *Phys. Rev. Lett.*, **46**, 558 (1981).
507. Lascaray J. *et al.*, *Phys. Rev. B*, **18**, 358 (1977).
508. Isikawa Y. *et al.*, *Sol. State Com.*, **22**, 577 (1977).
509. Koshizuka N., Ushioda S., Tsushima T., *Phys. Rev. B*, **21**, 1316 (1980).
510. Safran S. *et al.*, *Sol. State Com.*, **29**, 339 (1979).
511. Silberstein R., *Phys. Rev. B*, **22**, 4791 (1980).
512. Vitins J., Wachter P., *Phys. Rev. B*, **15**, 3225 (1977).
513. Novikov L.N. *et al.*, *FTT*, **22**, 3032 (1980).
514. Tarascon J. *et al.*, *Sol. State Com.*, **37**, 133 (1981).
515. Ito T., Ito K., Oka M., *Jap. J. Appl. Phys.*, **17**, 371 (1978).
516. Terasawa H. *et al.*, *J. Phys. C*, **13**, 5615 (1980).
517. Kasuya T., Yanase A., *Rev. Mod. Phys.*, **40**, 684 (1968).
518. Yanase A., Kasuya T., *J. Appl. Phys.*, **39**, 430 (1968).
519. Schoenes J., Wachter P., *Physica B*, **89**, 155 (1977).

520. Belov K.P. *et al.*, "Magnitnye poluprovodniki—khal'kogenidnye shpineli" (Magnetic Semiconductors—Chalcogenide Spinels), Izd. MGU, Moscow, 1981 (in Russian).
521. Wiedenmann A. *et al.*, *Sol. State Com.*, **38**, 129, (1981).
522. Schmutz L., Dresselhaus G. *et al.*, *Sol. State Com.*, **28**, 597 (1978).
523. Tholence J., *J. Appl. Phys.*, **50**, 7359 (1979).
524. Tholence J. *et al.*, *ibid.*, 7350.
525. Wiedenmann A. *et al.*, *Sol. State Com.*, **39**, 801 (1981).
526. Batlogg B. *et al.*, *Phys. Rev. B*, **12**, 3940 (1975).
527. Batlogg B., Wachter P., *Sol. State Com.*, **24**, 569 (1977).
528. Silberstein R. *et al.*, *Sol. State Com.*, **18**, 1173 (1976).
529. Osaka Y., Sakai Y., Tachiki M., *Sol. State Com.*, **23**, 589 (1977).
530. Balberg J., Maman A., Alexander S., *Sol. State Com.*, **22**, 701 (1977).
531. Yamada K., Heleskivi I., Salin A., *Sol. State Com.*, **37**, 957 (1981).
532. Kovalenko A.A., Nagaev E.L., *FTT*, **21**, 1075 (1979).
533. Balberg I., Alexander S., Helman J., *Phys. Rev. Lett.*, **33**, 836 (1974).
534. Belov K.P., Korolyova L.I. *et al.*, *FNT*, **6**, 738 (1980).
535. Kuivalainen P. *et al.*, *Sol. State Com.*, **32**, 691 (1979).
536. Umehara M., *J. Phys. Soc. Jap.*, **50**, 1082 (1981).
537. Hihara T., Kojima K., Kamigaishi T., *J. Phys. Soc. Jap.*, **50**, 1499 (1981).
538. Kojima K. *et al.*, *J. Phys. Soc. Jap.*, **49**, 2419 (1980).
539. Podel'shchikov A.I., Nagaev E.L., *FTT*, **23**, 859 (1981).
540. Krivoglaz M.A., *ZhETF*, **63**, 671 (1972).
541. Sakai O., Yanase A., Kasuya T., *J. Phys. Soc. Jap.*, **42**, 596 (1977).
542. Auslender M., Bebenin N., *Phys. Lett. A*, **81**, 297 (1981).
543. Kalashnikov V.P., Bebenin N.G., *FTT*, **21**, 2360 (1979).
544. Kasuya T., *Sol. State Com.*, **18**, 51 (1976).
545. Egorov B.V., Krivoglaz M.A., *FTT*, **21**, 1426 (1979).
546. Kambara T., Oguchi T., Gondaira K., *J. Phys. C*, **13**, 1493 (1980).
547. Oguchi T., Kambara T., Gondaira K., *Phys. Rev. B*, **22**, 872 (1980).
548. Almeida N., Miranda L., *Phys. Lett. A*, **81**, 78 (1981).
549. Tholence J., Tournier R., *J. de Phys.*, **35**, C4-229 (1974).
550. Beck P., *Metal Transact.*, **2**, 2015 (1971).
551. Wohlfarth E., *Physica*, **86-88B+C**, 852 (1977).
552. Volkonskaya T.I. *et al.*, *FTT*, **21**, 631 (1979).
553. Gibart P. *et al.*, *J. de Phys.*, **41**, C5-157 (1980).
554. Selmi A., Gibart P., Goldstein L., *J. Magn. Magn. Mat.*, **15-18**, 1285 (1980).
555. Selmi A., Gibart P., Weill G., *Phys. State Sol.*, **a**, **64**, 665 (1981).
556. Mauger A. *et al.*, *J. de Phys.*, **39**, 1125 (1978).
557. Mills D., *Phys. Rev. B*, **3**, 3887 (1971).
558. Kisker E., Mahan A., Reihl B., *Phys. Lett. A*, **62**, 261 (1977).
559. Meier F., Zürcher P., *J. Magn. Magn. Mat.*, **15-18**, 1083 (1980).
560. Vigren D., *Phys. Rev. Lett.*, **41**, 194 (1978).
561. Berdyshev A.A., *FTT*, **4**, 1382 (1962).
562. Karpenko B.V., Berdyshev A.A., *FTT*, **5**, 3397 (1963).
563. Nagaev E.L., *ZhETF*, **80**, 2346 (1981).
564. Rosenbaum T. *et al.*, *Phys. Rev. Lett.*, **45**, 1723 (1980).
565. Genkin G.M., Tokman G.M., *ZhETF (Pis'ma)*, **45**, 1723 (1981).
566. Merkulov I.A., Samsonidze G.G., *FTT*, **22**, 2437 (1980).
567. Nagaev E.L., Sokolova E.B., *ZhETF (Pis'ma)*, **28**, 105 (1978).
568. Golovenchitz E.I., Laykhtman B.D., Sanina V.A., *ZhETF (Pis'ma)*, **31**, 243 (1980).
569. Golovenchitz E.I., Sanina V.A., Shaplygina T.A., *ZhETF*, **80**, 1911 (1981).
570. Rurita S. *et al.*, *Sol. State Com.*, **38**, 235 (1981).
571. Doroshenko R.A. *et al.*, *FTT*, **21**, 2193 (1979).
572. Demangeat C., Mills D., *Phys. Rev. B*, **16**, 2321 (1977).
573. Kaganov M.I., *ZhETF*, **62**, 1196 (1972).

574. Trullinger S., Mills D., *Sol. State Com.*, **12**, 819 (1973).
575. Weiner R., *Phys. Rev. Lett.*, **31**, 1588 (1973).
576. Weiner R., *Phys. Rev. B*, **8**, 4427 (1973).
577. Kaganov M.I., Omel'yanchuk A.M., *ZhETF*, **61**, 679 (1971).
578. Kumar P., Maki K., *Phys. Rev. B*, **13**, 2011 (1976).
579. Auslender M.I., Katznel'son M.I., *TMF*, **43**, 261 (1980).
580. Katznel'son M.I., Vonsovsky S.V., *FTT*, **21**, 2384 (1979).
581. Auslender M.I., Katznel'son M.I., Vonsovsky S.V., *J. Magn. Magn. Mat.*, **15-18**, part II, 906 (1980).
582. Lakhno V.D., Nagaev E.L., *ZhETF*, **77**, 1407 (1979).
583. Krivoglaz M.A., *UFN*, **111**, 617 (1973).
584. Egorov B.V., Krivoglaz M.A., *FTT*, **21**, 481 (1979).
585. Tamura S., Kuriyama M., *Phys. Lett. A*, **70**, 469 (1979).
586. Tamura S., *Phys. Lett. A*, **78**, 401 (1980).
587. Desfours J. et al., *Sol. State Com.*, **20**, 691 (1976).
588. Baru V.G., Grekov E.V., *FTT*, **22**, 802 (1980).
589. Leroux-Hugon P., *Phys. Rev. Lett.*, **29**, 939 (1972).
590. Kübler J., Vigren D., *Phys. Rev. B*, **11**, 4440 (1975).
591. Mauger A., Godart C., *Sol. State Com.*, **35**, 785 (1980).
592. Belov K.P., Korolyova L.I., Tovmasyan L.N., *FNT*, **4**, 725 (1978).
593. Andrianov D.G., Drozdov S.A., Lazareva G.V., *FTT*, **21**, 2179 (1979).
594. Wachter P., Kaldis E., *Sol. State Com.*, **34**, 241 (1980).
595. Callen H., De Moura M., *J. Magn. Magn. Mat.*, **7**, 58 (1978).
596. De Moura M., Callen H., *Physica B*, **86-88B**, 132 (1977).
597. Callen H., de Moura M., *Phys. Rev. B*, **16**, 4121 (1977).
598. Bass F.G., Oleynik I.N., *FTT*, **20**, 25 (1978).
599. Baru V.G., Grekov E.V., Sukhanov A.A., *FTT*, **17**, 948 (1975).
600. Doroshenko R.A. et al., *FTT*, **21**, 2193 (1979).
601. Khomsky D.I., *UFN*, **129**, 443 (1979).
602. Jaccarino V. et al., *Phys. Rev.*, **160**, 467 (1967).
603. Takahashi Y., Moriya T., *J. Phys. Soc. Jap.*, **46**, 1451 (1979).
604. Takegahara K., Kasuya T., *J. Phys. Soc. Jap.*, **39**, 1292 (1975).
605. Maletta H., *J. Magn. Magn. Mat.*, **24**, 179 (1981).
606. Bak P., Rasmussen F., *Phys. Rev. B*, **23**, 4538 (1981).
607. Edwards S., Anderson P., *J. Phys. F*, **5**, 965 (1975).
608. Solin N.I. et al., *FTT*, **18**, 2014 (1976).
609. Samokhvalov A.A. et al., *ZhETF (Pis'ma)*, **28**, 413 (1978).
610. Samokhvalov A.A. et al., *ZhETF (Pis'ma)*, **30**, 658 (1979).
611. Samokhvalov A.A. et al., *FTT*, **22**, 1193 (1980).
612. Thöni W., Wachter P., *Phys. Rev. B*, **19**, 247 (1979).
613. Schobinger-Pagamantellos P. et al., *Sol. State Com.*, **39**, 759 (1981).
614. Andres K. et al., *Sol. State Com.*, **27**, 825 (1978).
615. Haen P. et al., *Phys. Rev. Lett.*, **43**, 304 (1979).
616. Battlog B. et al., *Phys. Rev. Lett.*, **42**, 278 (1979).
617. Campagna M., in: "Photoemission in Solids", ed. by L. Ley and M. Cardona, Springer, Berlin, 1979.
618. Anderson P., *Solid State Phys.*, **14**, 99 (1965).
619. Shastri B., Mattis D., *Phys. Rev. B*, **24**, 5340 (1981).
620. Rangette A. et al., *Sol. State Com.*, **12**, 171 (1973).

ABBREVIATIONS FOR SOVIET JOURNALS:

<i>FTT</i>	Fizika tverdogo tela (Solid State Physics)
<i>ZhETF</i>	Zhurnal eksperimental'noy i teoreticheskoy fiziki (Journal of Experimental and Theoretical Physics)
<i>ZhETF (Pis'ma)</i>	JETP Letters
<i>UFN</i>	Uspekhi fizicheskikh nauk (Advances in Physical Sciences)
<i>FMM</i>	Fizika metallov i metallovedenie (Physics of Metals and Metals Science)
<i>TMF</i>	Teoreticheskaya i matematicheskaya fizika (Theoretical and Mathematical Physics)
<i>ZhFKh</i>	Zhurnal fizicheskoy khimii (Journal of Physical Chemistry)
<i>FNT</i>	Fizika nizkikh temperatur (Low-temperature Physics)
<i>ZhTF (Pis'ma)</i>	Zhurnal tekhnicheskoy fiziki (Pis'ma) (Journal of Technical Physics. Letters)

- Anderson localization, 26, 193
- Antiferromagnets, 193, 307
- Autolocalization of conduction electrons, heterophase, 7, 8, 15, 193

- Band-gap of FMS vs. pressure, 170

- Canted AF ordering, 13, 14, 78, 254-256, 304, 305
- Carrier density in FMS, 157-162
- Charge carriers in narrow-band MS, 10, 97-99, 116-133, 189-192, 249-252, 264, 273, 288, 304, 305, 312
- Charge density waves, 8, 301
- Critical magnetic properties, 70-74, 82, 85, 86, 89, 93
- Critical scattering of charge carriers, 12, 150-153
- Curie point of degenerate FMS, 237-241

- Dichroism, magnetic, 219
- Dielectric constant of degenerate MS, effective, 272, 281, 283, 294, 299, 300, 338-340
- Dielectric function of degenerate FMS, negative, 299
- Domain walls in degenerate FMS, 370, 371
- Double exchange, 118, 119
- Doubly-charged donors in FMS, inversion of energy terms, 272-279, 333, 334

- Excitons, magnetic, 100, 174, 176, 217
- Exciton polarons, 222-224

- Faraday depolarization of light in degenerate AFS, 321, 325-327
- Faraday rotation, 7, 171-174, 219, 220, 321, 361-364
- Ferrites, 7, 92
- Ferrons in AFS,
 - collective, 17, 305-327
 - free, 193-198, 200-204, 212-215, 257
 - localized, 206-212
 - surface, 200
- Ferrons in FMS, 18, 19, 198-200, 329, 330
- Ferrons in magnetoexcitonic semiconductors, 226-228, 305-316
- Ferrons in singlet magnets, 20, 228-230, 335, 336
- Ferron-polaron states, 204-206
- Ferron-quasi-oscillator states, 203, 204

- Hall effect, anomalous, 182, 183, 354-361
- Heating of charge carriers by electrical field, 157, 184
- Helicoidal ordering, its influence on conduction electrons, 11, 102-105, 189, 218, 219, 221, 256, 364-370
- Heterophase AF-FM state of degenerate AFS,
 - conducting, 307, 314
 - insulating, 306, 316
- Hubbard model, 35-38, 189

- Impurity conductivity, hopping, 167
 Instability, magnetoelectric,
 in degenerate FMS, 18, 296, 299-302
 in degenerate canted AFS, 304, 305
 Insulator-metal transition, 39-49
 in degenerate AFS, 16, 17, 306, 307, 324, 325
 in degenerate FMS, 19, 327-335

 Luminescence of MS, 175, 213-215

 Magnetoelectric effect in degenerate MS, 14, 263, 280
 Magnetoelectric response functions, 280-284, 288, 293, 294
 Magnetoresistance,
 negative, 7, 9, 153-155, 183, 184, 322-324, 340-342, 346
 positive, 153, 183, 184, 342-346
 Magnon drag, 156
 Magnon generation by charge carriers, 157
 Magnons,
 localized, 267-273
 magnetostatic, 86
 subsurface, 264-265
 surface, 263
 virtual, 268
 Mass, effective, of electron, 23, 179, 180, 221
 of magnon, 67, 147
 Metamagnets, 64, 79, 90, 91, 92, 196, 209, 216
 Mixed valency, 41-44, 92
 Mobility of charge carriers in FMS, 12, 19, 181, 182, 185, 186, 221, 340
 Mott criterion of electron delocalization, 40, 209, 315, 334

 Optical absorption, shift of the edge,
 blue, 9, 139, 171, 177, 178, 215-217
 in heavily-doped FMS, 178, 179
 red, 7, 9, 11, 12, 91, 132, 133, 137, 138, 168-171, 177, 218, 219, 324
 structure of spectra, 167

 Paramagnetic Curie point of degenerate FMS, 234, 240, 241, 282, 335, 341
 of nondegenerate MS, 274-277
 Paramagnons, 85
 Phase transitions, magnetic, of the first kind,
 light-induced, 258-260, 262
 order-order, 78, 79, 89, 90
 order-proper disorder, 81, 93
 order-improper disorder, 81, 82, 90, 91-93, 219
 Polarons in MS, 29-31
 large, 29, 32-33
 small, 8, 27, 28, 30, 31, 34, 221
 Photoconductivity of MS, 175, 184-187, 213-215
 Photoferromagnetism, static, 15, 258-262
 high-frequency, 262
 Photoheterojunction, 259
 Photomagnetization by circularly-polarized light, 260

 Quasi-oscillators, 190-192, 203, 204

 Raman scattering, 175, 220
 Resistivity of FMS, peak at T_c , 9, 12, 19, 150-153, 159, 180, 181, 337-341
 of AMS, 220, 221, 318, 322-324
 RKKY theory of indirect exchange, 105-109
 its inapplicability to MS, 231, 232

 Scattering of charge carriers,
 by localized ferrons, 164-166
 by magnons, 147, 148

 Non-Heisenberg exchange, 13, 14, 55, 78-81, 109-111, 163, 164
 magnetic structures in EuSe, 79, 80, 89-92

- Scattering of charge carriers,
 impurity magnetoelectric, 19, 338-340
 paramagnetic, 149, 150
- Screening of an electrical charge,
 in degenerate FMS, 50, 51, 295-297
 in degenerate AMS and PMS, 302-304
- Singlet magnets, 58, 65, 66, 228-230, 284
- Spin density waves, 8, 301
- Spin glasses, semiconducting, 93-95
- Spinpolaron, narrow-band, 10, 12, 122-127, 128-133, 232, 235-237
 wide-band, 134-137, 148, 233
- Spinpolaron vector, 104, 136, 189, 195
- Surface layer, paramagnetic, 265, 266
- Surface magnetism, 15, 263-267
- Susceptibility, paramagnetic of impure crystals, 274-277
- Temperature shift of the conduction band in FMS, 132, 137, 139, 145, 146
 of impurity levels, 158-164, 273-274
- Thermopower, 155, 181
- Transferons, 224-226
- Trapping of charge carriers,
 by magnetization fluctuations, 144, 193, 199
 by localized ferrons, 166, 167, 187
- Valence band built from *p*-anion orbitals, 176
- Tail of density of states, electron, 51, 144, 167, 168, 170
 magnon, 272
- Zeeman splitting, giant in AFS, 242
 spontaneous, 134, 139, 144, 145

TO THE READER

Mir Publishers would be grateful for your comments on the content, translation and design of this book. We would also be pleased to receive any other suggestions you may wish to make.

Our address is: Mir Publishers,
2 Pervy Rizhsky Pereulok,
I-110, GSP, Moscow, 129820,
USSR

Printed in the Union of Soviet Socialist Republics

ALSO FROM MIR PUBLISHERS

Laser Physics

L. TARASOV, Cand. Sc. (Phys.-Math.)

This book aims at bringing the reader up-to-date with the latest achievements and trends in the physics of laser processes, as well as at providing sufficient information so that the reader can then independently make use of the specialized literature in this field. It describes the present state of affairs in the development of laser technology from the point of view of research as well as applications in various branches of industry.

The three main aspects considered in this book are: methods for obtaining inverted active media, generation of radiation field in a resonator, and the dynamics of laser processes. A systematic description has been given of the methods, approaches and approximations used in the laser theory. Intended for scientists and engineers engaged in laser research, this book can also be quite useful for students and teachers in universities.

An Introduction to Statistical Physics

A. VASILYEV, D. Sc. (Phys.-Math.)

Based on lectures read by the author to students of the department of engineering-electronics at the Moscow Power Engineering Institute for a number of years, the present book treats statistical physics with an accent placed on its application to fields associated with electronics. In these and similar fields, acquaintance with the fundamentals of statistical physics of non-equilibrium states (kinetics) is very important because a foundation is set up helping to master special subjects dealing in some way or other with the flow of an electric current in gases, semiconductors, and metals.

In acquainting the reader with the basic methods and concepts of statistical physics, the author illustrates all the material with examples, following the well justified principle: from concrete to abstract, from simple to complicated material.

The book is intended for students of higher educational institutions who have completed a course in mathematics and general physics.

A Survey of Semiconductor Radiation Techniques

Edited by L. SMIRNOV, D. Sc. (Phys.-Math.)

This book has been written for two sorts of people primarily. The first group includes the engineers, technicians, and research workers who are entering upon active work of exploration of new areas of semiconductor technology. The second type of person for whom the book is intended is the college student or post-graduate who may use the book as a source of general information about the subject.

The book supplies a specific information on radiation defects in semiconductors and discusses, with reliance on particular examples, the feasibility of employment of said defects for technological purposes. Ample space is given in this book to treatment of the problems relating to radiation control. Point defects, disordered regions, disordered and amorphous layers obtained as a result of irradiation of semiconductor materials, the properties and stability of such defects, doping by ion implantation and nuclear transmutation, ionic and radiation-enhanced diffusion are the topics taken up by this book.

